Sarine Markossian • Abigail Grossman • Hannah Baskir • Michelle Arkin
Douglas Auld • Christopher Austin • Jonathan Baell • Kyle Brimacombe
Thomas D.Y. Chung • Nathan P. Coussens • Jayme L. Dahlin
Viswanath Devanarayan • Timothy L. Foley • Marcie Glicksman
Kirill Gorshkov • Stefan Grotegut • Matthew D. Hall • Samuel Hoare
James Inglese • Philip W. Iversen • Madhu Lal-Nag • Zhuyin Li
Jason R. Manro • James McGee • Allison Norvil • Mackenzie Pearson
Terry Riss • Peter Saradjian • G. Sitta Sittampalam
Michael A. Tarselli • O. Joseph Trask, Jr. • Jeffrey R. Weidner
Mary Jo Wildey • Kelli Wilson • Menghang Xia • Xin Xu

Assay Guidance Manual

Last Updated: 52, 2.02

Eli Lilly & Company and the National Center for Advancing Translational Sciences
Bethesda (MD)

Halozyme EX2083 (part 1 of 6)
Merck v. Halozyme
PGR2025-00039

Eli Lilly & Company and the National Center for Advancing Translational Sciences, Bethesda (MD)

All Assay Guidance Manual content, except where otherwise noted, is licensed under a Creative Commons Attribution-NonCommercial-ShareAlike 3.0 Unported license (CC BY-NC-SA 3.0), which permits copying, distribution, transmission, and adaptation of the work, provided the original work is properly cited and not used for commercial purposes. Any altered, transformed, or adapted form of the work may only be distributed under the same or similar license to this one.

Previous Editors: Bruce Bejcek, Jose M.M. Caaveiro, Neely Gal-Edd, Steven D. Kahl, Stephen C. Kales, Susan Kirshner, Vance P. Lemmon, Owen McManus, Lisa Minor, Andrew Napper, Henrike Nelsen, John M. Peltier, Yueming Wang

Contact Information: sarine.markossian@nih.gov

The Assay Guidance Manual is supported by the Intramural Research Program of the National Center for Advancing Translational Sciences at the National Institutes of Health (ZIA TR000340). The contributions of the NIH author(s) were made as part of their official duties as NIH federal employees, are in compliance with agency policy requirements, and are considered Works of the United States Government. However, the findings and conclusions presented in these chapters are those of the author(s) and do not necessarily reflect the views of the NIH or the U.S. Department of Health and Human Services.

NLM Citation: Markossian S, Grossman A, Baskir H, et al., editors. Assay Guidance Manual [Internet]. Bethesda (MD): Eli Lilly & Company and the National Center for Advancing Translational Sciences; 2004-.

This eBook is a comprehensive, crucial resource for investigators optimizing assays to evaluate collections of molecules with the overall goal of developing probes that modulate the activity of biological targets, pathways or cellular phenotypes. Such probes might be candidates for further optimization and investigation in drug discovery and development.

Originally written as a guide for therapeutic project teams within a major pharmaceutical company, this manual has been adapted to provide guidelines for scientists in academic, non-profit, government and industrial research laboratories to develop assay formats compatible with High Throughput Screening (HTS) and Structure Activity Relationship (SAR) measurements of new and known molecular entities. Topics addressed in this manual include:

- Descriptions of assay formats that are compatible with HTS and determination of SAR
- Selection and development of optimal assay reagents
- Optimizations and troubleshooting for assay protocols with respect to sensitivity, dynamic range, signal intensity and stability
- Adaptations of assays for automation and scaling to microtiter plate formats
- Instrumentation
- Sources of assay artifacts and interferences
- Statistical validation of assay performance parameters
- Secondary assays for chemical probe validation and SAR refinement
- Data standards for reporting the results of screening and SAR assays
- *In vivo* assay development and validation
- Assay development and validation for siRNA-based high-throughput screens

The National Center for Advancing Translational Sciences (NCATS) manages the content of the Assay Guidance Manual with input from industry, academia and government experts. More than 100 authors from around the globe have contributed content to this free resource, which is updated quarterly with contributions by experienced scientists from multiple disciplines working in drug discovery and development worldwide.

For more information about the Assay Guidance Manual and related training opportunities, visit https://ncats.nih.gov/expertise/preclinical/agm.

Editors

Sarine Markossian, Editor-in-Chief
National Center for Advancing Translational Sciences, National Institutes of Health

Abigail Grossman, Managing Editor
National Center for Advancing Translational Sciences, National Institutes of Health

Hannah Baskir, Scientific Program Manager
National Center for Advancing Translational Sciences, National Institutes of Health

Associate Editors

Michelle Arkin
University of California, San Francisco

Douglas Auld
Novartis Institutes for Biomedical Research

Christopher Austin
GSK plc

Jonathan Baell
Lyterian Therapeutics

Kyle Brimacombe
National Center for Advancing Translational Sciences, National Institutes of Health

Thomas D.Y. Chung
Sanford Burnham Prebys Medical Discovery Institute

Nathan P. Coussens
Frederick National Laboratory for Cancer Research

Jayme L. Dahlin
Agios Pharmaceuticals

Viswanath Devanarayan
Eisai, Inc

Timothy L. Foley
Pfizer Inc

Marcie Glicksman
EnClear Therapies

Kirill Gorshkov
Bristol Myers Squibb

Stefan Grotegut

Eli Lilly and Company

Matthew D. Hall
National Center for Advancing Translational Sciences, National Institutes of Health

Samuel Hoare
Pharmechanics, LLC

James Inglese
National Center for Advancing Translational Sciences, National Institutes of Health

Philip W. Iversen
Luther College

Madhu Lal-Nag
InSphero AG

Zhuyin Li
Bristol Myers Squibb

Jason R. Manro
Eli Lilly and Company

James McGee
Eli Lilly and Company (Retired)

Allison Norvil
Eli Lilly and Company

Mackenzie Pearson
Eli Lilly and Company

Terry Riss
Promega Corporation

Peter Saradjian
Beth Israel Deaconess Medical Center

G. Sitta Sittampalam
NewFoundMed

Michael A. Tarselli
Amazon Web Services

O. Joseph Trask, Jr.
Revvity, Inc.

Jeffrey R. Weidner
QualSci Consulting, LLC

Mary Jo Wildey

Merck & Co., Inc. (Retired)

Kelli Wilson
National Center for Advancing Translational Sciences, National Institutes of Health

Menghang Xia
National Center for Advancing Translational Sciences, National Institutes of Health

Xin Xu
National Center for Advancing Translational Sciences, National Institutes of Health

Table of Contents

New in Assay Guidance Manual xi

Preface xiii
G. Sitta Sittampalam and Nathan P. Coussens

Acknowledgements xix

Considerations for Early Phase Drug Discovery 1
Thomas D.Y. Chung, Nathan P. Coussens, G. Sitta Sittampalam, and Yueming Wang

Early Drug Discovery and Development Guidelines: For Academic Researchers, Collaborators, and Start-up Companies 3
Jeffrey Strovel, Sitta Sittampalam, Nathan P. Coussens, Michael Hughes, James Inglese, Andrew Kurtz, Ali Andalibi, Lavonne Patton, Chris Austin, Michael Baltezor, Michael Beckloff, Michael Weingarten, and Scott Weir

***In Vitro* Biochemical Assays** 39
Nathan P. Coussens, Timothy L. Foley, Sam R.J. Hoare, James McGee, and G. Sitta Sittampalam

Analyzing Kinetic Binding Data 41
Sam R.J. Hoare

Validating Identity, Mass Purity and Enzymatic Purity of Enzyme Preparations 81
John E Scott and Kevin P Williams

Basics of Enzymatic Assays for HTS 93
Harold B. Brooks, Sandaruwan Geeganage, Steven D. Kahl, Chahrzad Montrose, Sitta Sittampalam, Michelle C. Smith, and Jeffrey R. Weidner

Mechanism of Action Assays for Enzymes 105
John Strelow, Walthere Dewe, Phillip W Iversen, Harold B Brooks, Jeffrey A Radding, James McGee, and Jeffrey Weidner

Assay Development for Protein Kinase Enzymes 127
J. Fraser Glickman

Receptor Binding Assays for HTS and Drug Discovery 145
Douglas S Auld, Mark W. Farmen, Steven D. Kahl, Aidas Kriauciunas, Kevin L. McKnight, Chahrzad Montrose, and Jeffrey R. Weidner

Protease Assays 187
Guofeng Zhang

Inhibition of Protein-Protein Interactions: Non-Cellular Assay Formats 199
Michelle R. Arkin, Marcie A. Glicksman, Haian Fu, Jonathan J. Havel, and Yuhong Du

Immunoassay Methods 223
Karen L. Cox, Viswanath Devanarayan, Aidas Kriauciunas, Joseph Manetta, Chahrzad Montrose, and Sitta Sittampalam

GTPγS Binding Assays 263
Neil W. DeLapp, Wendy H. Gough, Steven D. Kahl, Amy C. Porter, and Todd R. Wiernicki

Histone Acetyltransferase Assays in Drug and Chemical Probe Discovery 275
Sanket Gadhia, Jonathan H. Shrimp, Jordan L. Meier, James E. McGee, and Jayme L. Dahlin

***In Vitro* Cell Based Assays** 317
Marcie Glicksman, Zhuyin Li, Sarine Markossian, Terry Riss, G. Sitta Sittampalam, O. Joseph Trask, Jr., and Yueming Wang

Machine Learning and Assay Development for Image-based Phenotypic Profiling of Drug Treatments 319
Jonathan Z. Sexton, Reid Fursmidt, Matthew J. O'Meara, Wienand Omta, Arvind Rao, David A. Egan, and Steven A. Haney

Biosensor Assays for Measuring the Kinetics of G-Protein and Arrestin-Mediated Signaling in Live Cells 369
Sam R.J. Hoare and Thomas E. Hughes

Cell Viability Assays 403
Terry L Riss, Richard A Moravec, Andrew L Niles, Sarah Duellman, Hélène A Benink, Tracy J Worzella, and Lisa Minor

Cytotoxicity Assays: *In Vitro* Methods to Measure Dead Cells 429
Terry Riss, Andrew Niles, Rich Moravec, Natashia Karassina, and Jolanta Vidugiriene

Apoptosis Marker Assays for HTS 445
Terry L. Riss, Martha A. O'Brien, Richard A. Moravec, Kevin Kupcho, and Andrew L. Niles

Pluripotent Stem Cell Culture Scale-Out 463
Debra L. Johnson, Robert Scott, and Rhonda Newman

Authentication of Human and Mouse Cell Lines by Short Tandem Repeat (STR) DNA Genotype Analysis 489
Jamie L. Almeida and Christopher T. Korch

In vitro 3D Spheroids and Microtissues: ATP-based Cell Viability and Toxicity Assays 543
Monika Kijanska and Jens Kelm

Cell-Based RNAi Assay Development for HTS 557
Scott Martin, Gene Buehler, Kok Long Ang, Farhana Feroze, Gopinath Ganji, and Yue Li

FLIPR™ Assays for GPCR and Ion Channel Targets 581
Michelle R. Arkin, Patrick R. Connor, Renee Emkey, Kim E. Garbison, Beverly A. Heinz, Todd R. Wiernicki, Paul A. Johnston, Ramani A. Kandasamy, Nancy B. Rankl, and Sitta Sittampalam

Ion Channel Screening 615
Owen B McManus, Maria L Garcia, David Weaver, Melanie Bryant, Steven Titus, and James B Herrington

Automated Electrophysiology Assays 639
Birgit T. Priest, Rok Cerne, Michael J. Krambis, William A. Schmalhofer, Mark Wakulchik, Benjamin Wilenkin, and Kevin D. Burris

Assay Development Guidelines for Image-Based High Content Screening, High Content Analysis and High Content Imaging: Image-Based High Content Screening and Analysis 683
William Buchser, Mark Collins, Tina Garyantes, Rajarshi Guha, Steven Haney, Vance Lemmon, Zhuyin Li, and O. Joseph Trask

Advanced Assay Development Guidelines for Image-Based High Content Screening and Analysis 747
Mark-Anthony Bray and Anne Carpenter; Imaging Platform, Broad Institute of MIT and Harvard

Nuclear Factor Kappa B (NF-κB) Translocation Assay Development and Validation for High Content Screening: NF-κB Translocation Assay Development and Validation for High Content Screening 775
O. Joseph Trask, Jr

High Content Screening with Primary Neurons 815
Hassan Al-Ali, Murray Blackmore, John L Bixby, and Vance P. Lemmon

Phospho-ERK Assays 847
Kim E. Garbison, Beverly A. Heinz, Mary E. Lajiness, Jeffrey R. Weidner, and G. Sitta Sittampalam

IP-3/IP-1 Assays 853
Kim E. Garbison, Beverly A. Heinz, and Mary E. Lajiness

Cardiomyocyte Impedance Assays 859
Sarah D. Lamore, Clay W Scott, and Matthew F. Peters

Screening for Target Engagement using the Cellular Thermal Shift Assay - CETSA 873
Hanna Axelsson, Helena Almqvist, Brinton Seashore-Ludlow, and Thomas Lundbäck

Measurement of cAMP for $G_{\alpha s}$- and $G_{\alpha i}$ Protein-Coupled Receptors (GPCRs) 899
Tao Wang, Zhuyin Li, Mary Ellen Cvijic, Litao Zhang, and Chi Shing Sum

Measurement of β-Arrestin Recruitment for GPCR Targets 919
Tao Wang, Zhuyin Li, Mary Ellen Cvijic, Carol Krause, Litao Zhang, and Chi Shing Sum

Genome Editing Using Engineered Nucleases and Their Use in Genomic Screening 931
Joana R. Costa, Bruce E. Bejcek, James E. McGee, Adam I. Fogel, Kyle R. Brimacombe, and Robin Ketteler

Inhibition of Protein-Protein Interactions: Cell-Based Assays 955
Mark Wade, Jacqui Méndez, Nathan P. Coussens, Michelle R. Arkin, and Marcie A. Glicksman

Pharmacological Characterization of GPCR Agonists, Antagonists, Allosteric Modulators and Biased Ligands from HTS Hits to Lead Optimization 983
Chi Shing Sum, Brian J. Murphy, Zhuyin Li, Tao Wang, Litao Zhang, and Mary Ellen Cvijic

In Vivo Assay Guidelines 1011
Viswanath Devanarayan and Philip W. Iversen

In Vivo Assay Guidelines 1013
Joseph Haas, Jason Manro, Harlan Shannon, Wes Anderson, Joe Brozinick, Arunava Chakravartty, Mark Chambers, Jian Du, Brian Eastwood, Joe Heuer, Stephen Iturria, Philip Iversen, Dwayne Johnson, Kirk Johnson, Michael O'Neill, Hui-Rong Qian, Dana Sindelar, and Kjell Svensson

In Vivo Receptor Occupancy in Rodents by LC-MS/MS 1053
Cynthia D. Jesudason, Susan DuBois, Megan Johnson, Vanessa N. Barth, and Anne B. Need

Assay Artifacts and Interferences 1065
Nathan P. Coussens and Jayme L. Dahlin

Interference and Artifacts in High-content Screening 1067
Jayme L. Dahlin, David A. Close, Paul A. Johnston, Steven A. Haney, Steven A Titus, Bridget K. Wagner, and O. Joseph Trask

Compound-Mediated Assay Interferences in Homogeneous Proximity Assays 1105
Nathan P. Coussens, Douglas Auld, Philippe Roby, Jarrod Walsh, Jonathan B. Baell, Stephen Kales, Kamyar Hadian, and Jayme L. Dahlin

Assay Interference by Chemical Reactivity 1155
Jayme L. Dahlin, Jonathan Baell, and Michael A. Walters

Interference with Fluorescence and Absorbance 1189
Anton Simeonov and Mindy I. Davis

Interferences with Luciferase Reporter Enzymes 1201
Douglas S. Auld and James Inglese

Assay Interference by Aggregation 1215
Douglas S. Auld, James Inglese, and Jayme L. Dahlin

Assay Validation, Operations and Quality Control 1241
Viswanath Devanarayan, Philip W. Iversen, Jeffrey R. Weidner, and Mary Jo Wildey

Basic Guidelines for Reporting Non-Clinical Data 1243
Jayme L. Dahlin, G. Sitta Sittampalam, Nathan P. Coussens, Viswanath Devanarayan, Jeffrey R. Weidner, Philip W. Iversen, Joseph V. Haas, Duane D. Bronson, O. Joseph Trask, Jr., Todd R. Wiernicki, and Steven D. Kahl

Development and Applications of the Bioassay Ontology (BAO) to Describe and Categorize High-Throughput Assays: Development and Applications of the BAO to Describe and Categorize High-Throughput Assays 1291
Uma D. Vempati and Stephan C. Schürer

Data Standardization for Results Management 1317
Robert M. Campbell, Julia Dymshitz, Brian J. Eastwood, Renee Emkey, David P. Greenen, Julia M. Heerding, Dwayne Johnson, Thomas H. Large, Thomas Littlejohn, Chahrzad Montrose, Suzanne E. Nutter, Barry D. Sawyer, Sandra K. Sigmund, Martin Smith, Jeffrey R. Weidner, and Richard W. Zink

HTS Assay Validation 1335
Philip W. Iversen, Benoit Beck, Yun-Fei Chen, Walthere Dere, Viswanath Devanarayan, Brian J Eastwood, Mark W. Farmen, Stephen J. Iturria, Chahrzad Montrose, Roger A. Moore, Jeffrey R. Weidner, and G. Sitta Sittampalam

Assay Operations for SAR Support 1361
Benoit Beck, Yun-Fei Chen, Walthere Dere, Viswanath Devanarayan, Brian J. Eastwood, Mark W. Farmen, Stephen J. Iturria, Phillip W. Iversen, Steven D. Kahl, Roger A. Moore, Barry D. Sawyer, and Jeffrey Weidner

Minimum Significant Ratio – A Statistic to Assess Assay Variability 1375
Joseph V. Haas, Brian J. Eastwood, Philip W. Iversen, Viswanath Devanarayan, and Jeffrey R. Weidner

Assay Technologies 1389
Marcie Glicksman, James McGee, Owen McManus, and G. Sitta Sittampalam

HPLC-MS/MS for Hit Generation 1391
Stefan Jon Thibodeaux, David A Yurek, and James E McGee

Impedance-Based Technologies 1409
Kim E. Garbison, Beverly A. Heinz, Mary E. Lajiness, Jeffrey R. Weidner, and G. Sitta Sittampalam

Instrumentation 1417
Nathan P. Coussens, Sarine Markossian, and G. Sitta Sittampalam

Microplate Selection and Recommended Practices in High-throughput Screening and Quantitative Biology 1419
Douglas S. Auld, Ph.D., Peter A. Coassin, B.S., Nathan P. Coussens, Ph.D., Paul Hensley, Carleen Klumpp-Thomas, Sam Michael, G. Sitta Sittampalam, Ph.D., O. Joseph Trask, B.S., Bridget K. Wagner, Ph.D., Jeffrey R. Weidner, Ph.D., Mary Jo Wildey, Ph.D., and Jayme L. Dahlin, M.D., Ph.D.

Basics of Assay Equipment and Instrumentation for High Throughput Screening 1467
Eric Jones, Sam Michael, and G. Sitta Sittampalam

Calculations and Instrumentation used for Radioligand Binding Assays 1493
Steven D. Kahl, G. Sitta Sittampalam, and Jeffrey Weidner

Pharmacokinetics and Drug Metabolism 1511
Thomas D.Y. Chung and Xin Xu

In Vitro and *In Vivo* Assessment of ADME and PK Properties During Lead Selection and Lead Optimization – Guidelines, Benchmarks and Rules of Thumb: In Vitro / In Vivo Assessment of ADME and PK Properties During Lead Selection / Optimization 1513
Thomas D.Y. Chung, David B. Terry, and Layton H. Smith

Glossary 1527
Nathan P. Coussens, Sarine Markossian, G. Sitta Sittampalam, and Jeffrey R. Weidner

Glossary of Quantitative Biology Terms 1529
Viswanath Devanarayan, Barry D. Sawyer, Chahrzad Montrose, Dwayne Johnson, David P. Greenen, Sitta Sittampalam, Terry Riss, and Lisa Minor

New in Assay Guidance Manual

New Chapters

Interference and Artifacts in High-content Screening 28 May 2025

Machine Learning and Assay Development for Image-based Phenotypic Profiling of Drug Treatments 15 Mar 2023

Authentication of Human and Mouse Cell Lines by Short Tandem Repeat (STR) DNA Genotype Analysis 17 Jan 2023

Biosensor Assays for Measuring the Kinetics of G-Protein and Arrestin-Mediated Signaling in Live Cells 01 Sep 2021

Apoptosis Marker Assays for HTS 01 Jul 2021

Recently Updated Chapters

Immunoassay Methods 08 Jul 2019

Receptor Binding Assays for HTS and Drug Discovery 01 Jul 2018

Histone Acetyltransferase Assays in Drug and Chemical Probe Discovery 01 Jul 2018

Interference with Fluorescence and Absorbance 01 Jul 2018

Interferences with Luciferase Reporter Enzymes 01 Jul 2018

Preface

G. Sitta Sittampalam, PhD[1] and Nathan P. Coussens, PhD[1]

Created: May 1, 2012; Updated: March 31, 2017.

Introduction to the Assay Guidance Manual

The Assay Guidance Manual (AGM) provides guidance on developing robust *in vitro* and *in vivo* assays for biological targets, pathways, and cellular phenotypes in the context of drug discovery and development. The proper development and implementation of such assays is critical for an appropriate evaluation of chemical compounds, probes, or siRNA collections. Chemical probes can be candidates for further optimization and development as potential therapeutics, which might require multiple variations of these assays, reagents, and analytical processes.

This manual began as the *Guidelines for Screening* in 1995 at Eli Lilly & Company and Sphinx Pharmaceuticals. With contributions from well over 100 drug discovery scientists, the manual grew substantially and was named the *Quantitative Biology Manual* in the late 1990s. Internally, the *Quantitative Biology Manual* provided valuable reference and training materials for the scientists. As the NIH Molecular Libraries and Imaging Roadmap program developed in 2003, discussions between Jim Inglese, PhD, Doug Auld, PhD, and Chris Austin, MD, at the NIH and the management at Eli Lilly and Sphinx Pharmaceuticals resulted in an agreement to publish this manual on the NIH Chemical Genomics Center (NCGC) website. The goals were to share best practices in quantitative biology and the development of robust assay methods throughout the drug discovery community in addition to enhancing academic-industrial collaborations in translational biology and medicine.

The AGM requires regular updates and the addition of new content as drug discovery technologies, assay methodologies, and best practices continue to evolve and improve. To accomplish this efficiently, the AGM was published as an eBook on the National Library of Medicine/National Center for Biotechnology Information (NLM/NCBI) website. The eBook format has several advantages: (a) it is freely available to a worldwide audience, (b) AGM chapters have PMCID citations for contributing authors, and (c) high quality is maintained by a centralized submission process that accommodates updates and edits to chapters. The current eBook is an updated version of the original manual published by NCGC, which encompassed 18 chapters. The first eBook edition of the AGM, published on May 1, 2012, included three new chapters. Content is added to address emerging technologies and translational processes, and reflect best practices in assay development and validation amidst the rapidly changing drug discovery landscape. The AGM is sponsored by the National Center for Advancing Translational Sciences (NCATS) and is managed by an editorial board with members from industry, academia, and other translational research laboratories who have extensive experience (>20 years) in drug discovery and development. Our thanks and gratitude goes to the past and present editorial board members for having been diligent and committed during the past 14 years in bringing this endeavor together.

Originally written as a guide for therapeutic project teams within a major pharmaceutical company, this manual has been adapted to provide guidelines for scientists in academic, nonprofit, government, and industrial research laboratories. The scope encompasses the development of biologically, physiologically, and pharmacologically relevant assay formats compatible with high-throughput screening (HTS) and structure activity relationship (SAR) assessments of new and known molecular entities. Topics addressed in this manual include:

a. Descriptions of assay formats that are compatible with HTS and determination of SAR
b. Selection and development of optimal assay reagents
c. Optimizations for assay protocols with respect to sensitivity, dynamic range, signal intensity and stability

Author Affiliation: 1 National Center for Advancing Translational Sciences, National Institutes of Health.

d. Adaptations of assays for automation and scaling to microtiter plate formats
e. Statistical validation of assay performance parameters
f. Secondary assays for chemical probe validation and SAR refinement
g. Data standards for reporting the results of screening and SAR assays
h. *In vivo* assay development and validation
i. Assay development and validation for siRNA-based high-throughput screens

General Definition of Biological Assays

An assay is an analytical measurement procedure defined by a set of reagents that produces a detectable signal, allowing a biological process to be quantified. In general, the quality of an assay is defined by the robustness and reproducibility of this signal in the absence of any test compounds or in the presence of inactive compounds. Assay quality depends on the type of signal measured (absorbance, fluorescence, luminescence, radioactivity, etc.), reagents, reaction conditions, analytical and automation instrumentation, as well as statistical models for the data analysis. Subsequently, the quality of a high-throughput screen is defined by the behavior of a given assay utilized to screen a collection of compounds. These two general concepts, assay quality and the quality of data collected for predictive analysis of biological and pharmacological activities, are discussed with specific examples in the AGM chapters.

In practice, assays developed for HTS and SAR measurements can be roughly characterized as cell-free (biochemical) or cell-based procedures. The choice of either a biochemical or cell-based assay along with the particular assay format is ultimately a balancing act. On one side of the fulcrum is the need to ensure that the measured signal is capable of providing data that is biologically relevant. On the other side is the requirement for an assay to yield robust data in microtiter plate formats where typically 10^5 to 10^6 samples are screened during an HTS operation.

General Concepts in Assay Development and Validation

The investigator must validate a biological assay system and methodology by proceeding through a series of steps along the pathway to HTS and SAR. *The overall objective of any assay validation procedure is to demonstrate that the assay is acceptable for its intended purpose*. As mentioned above, the purpose can be to determine the biological and/or pharmacological activities of new chemical entities on pathways involved in normal and disease processes. The acceptability of an assay begins with its design, construction, and execution in automated or semi-automated procedures, which can significantly affect its performance and robustness.

The assay development and validation cycle is a process with multiple validation steps (Figure 1). Successful completion of assay validation increases the likelihood of success in a drug discovery or chemical probe development program. During the design phase, assay conditions and procedures are selected to minimize the impact of potential sources of invalidity on the measurement of an analyte or biological endpoint in targeted sample matrices or test solutions. False positive and false negative hit rates are related to the selectivity and sensitivity of an assay, respectively. Additionally, technology-related artifacts, such as interference with the reporter system, also contribute to invalid results. Many other variables including assay automation, pipetting, reagent stability, quantities of available reagent, and data analysis models impact the overall validity of an assay.

There are three fundamental areas in assay development and validation: (a) pre-study (pre-screen) validation, (b) in-study (in-screen) validation, and (c) cross-validation or assay transfer validation. These stages encompass the systematic scientific steps within the assay development and validation cycle. Rigorous validation is critical considering that assays are expected to perform robustly over several years during preclinical development.

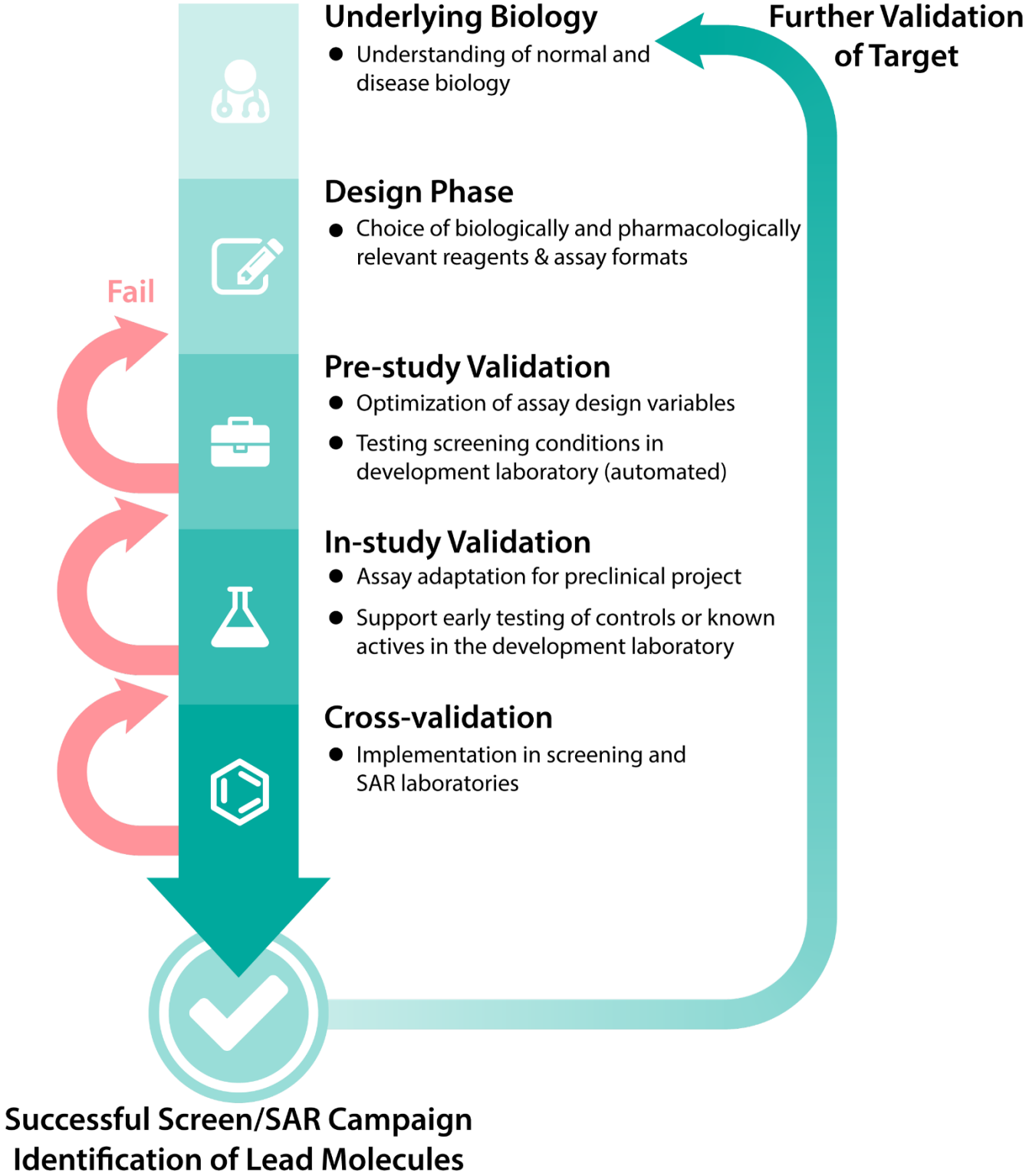

Figure 1. The Assay Development and Validation Cycle. The cycle begins in the design phase, which is followed by multiple validation steps that are executed at different stages throughout the assay life cycle, including: pre-study (pre-screen) validation, in-study (in-screen) validation, and cross-validation (assay transfer validation). Failure to validate the assay in any of these steps requires either addressing the deficiency or developing a new assay that meets the validation requirements (figure by Kyle Brimacombe).

Pre-study Validation

The investigator is faced with a number of choices with respect to the assay format and design. For many well-characterized target classes there are a number of assays and commercially available kits. At this stage the choice of an assay format is made. Close attention must be paid to factors such as the selection of reagents with appropriate biological relevance (e.g. cell type, enzyme-substrate combination, form of enzyme/protein target, readout labels, etc.), specificity, and stability. The choice of detection is also made at this stage. If fluorescent labels are chosen, careful attention must be paid to the wavelength to ensure low interference by test compounds, compatibility with microtiter plate plastics, and the availability of appropriate filters for the plate readers. Validation of assay performance should proceed smoothly if high-quality reagents and procedures are chosen. Assessment of assay performance requires appropriate statistical analysis of confirmatory data using appropriate reagents, assay conditions and control compounds. The assessment is made from planned experiments and the analytical results must satisfy predefined acceptance criteria. If control compounds or reagents are available, the assay sensitivity and pharmacology is evaluated. The HTS Assay Validation chapter illustrates common procedures for compound evaluation using dose-response curves. Several examples of assay design and optimization are given for well-studied target classes in other chapters of the AGM.

In-study Validation

In-study validation is needed to verify that an assay remains acceptable during its *routine use*. For assays to be conducted in automated (larger compound screening, HTS), or even semi-automated (a series of compounds during SAR) modes, the assay must be adapted to microtiter plate volumes that are standard in preclinical screening laboratories. Therefore, plate acceptance testing is required where the assay is run in several microtiter plates (at least 96-well plates). From this data, statistical measures of assay performance, such as Z-factors, are calculated. Some assays might require additional experiments to validate the automation and scale-up that might not have been addressed in earlier stages. The plates should contain appropriate maximum and minimum control samples to serve as quality controls for each run and indicate the assay performance. If positive and negative control compounds are available, they can be used to establish maximum and minimum (or basal) signals as appropriate. This will allow the investigator to identify procedural errors and to evaluate stability of the assay over time. Examining a randomly selected subset of test compounds at multiple concentrations monitors parallelism of test and standard curve samples. The HTS Assay Validation chapter illustrates the procedures typically used to evaluate assay performance in microtiter plates and some of the common artifacts that are observed.

Cross-validation

Cross-validation is required if an assay is transferred from the individual investigator's team to a high-throughput screening center or other laboratories collaborating on the project. More broadly, this procedure can be used at any stage to verify that an acceptable level of agreement exists in analytical results *before* and *after* procedural changes to an assay (reagents, instrumentation, personnel, lab location, etc.), as well as between results from two or more assays or laboratories. Typically, each laboratory performs the assay with a subset of compounds using the same well-documented protocols, and the agreement in results is compared to *predefined criteria* that specify the allowable performance of the assay during transfer. Considerations for adapting assays to automated robotic screening protocols are also discussed in the chapters of this manual. Note that the modification of assays to miniaturized 384- and 1536-well microtiter plate formats, which minimize costly reagent use and increase throughput, is not trivial. These formats should be rigorously validated before changing the assay operation from a 96-well format to higher density plates, because the assumption that a reduction in volume will not affect the results is not valid. Note that this might happen inadvertently if assay methods are transferred to collaborators and remote labs.

Critical Path

The entire compound development program, whether intended for chemical probe or drug discovery efforts, encompasses a series of assays which have been subjected to the process described above. These assays are set in place to answer key questions along the path of development to identify compounds with desired properties. For example, assays acting as "counter-screens" can serve to identify direct interference with the detection technology. Orthogonal assays serve to provide additional evidence for targeted activity. Selectivity assays can provide information on the general specificity of a compound or compound series. Biophysical assays can be used to confirm direct binding of a compound to the target. Cell-based assays can be implemented to measure efficacy of a compound in disease-relevant cell types with specific biomarkers. *In vivo* assays can serve as models of the disease, while proof-of-concept clinical assays serve as a measure of efficacy in humans. Placing the right assays at the appropriate points will define the success of a program and the chosen configuration of these assays is referred to as the "critical path".

Additional References

1. Smith WC, Sittampalam GS. Conceptual and statistical issues in the validation of analytic dilution assays for pharmaceutical applications. J Biopharm Stat. 1998;8(4):509–32.doi: 10.1080/10543409808835257. PubMed PMID: 9855031.
2. Findlay JW, Smith WC, Lee JW, Nordblom GD, Das I, DeSilva BS, et al. Validation of immunoassays for bioanalysis: a pharmaceutical industry perspective. J Pharm Biomed Anal. 2000;21(6):1249–73. PubMed PMID: 10708409.
3. Inglese J, Johnson RL, Simeonov A, Xia M, Zheng W, Austin CP, et al. High-throughput screening assays for the identification of chemical probes. Nat Chem Biol. 2007;3(8):466–79.doi: 10.1038/nchembio.2007.17. PubMed PMID: 17637779.
4. Thorne N, Auld DS, Inglese J. Apparent activity in high-throughput screening: origins of compound-dependent assay interference. Curr Opin Chem Biol. 2010;14(3):315-24. doi: 10.1016/j.cbpa.2010.03.020. PubMed PMID: 20417149; PubMed Central PMCID: PMCPMC2878863.
5. Dahlin JL, Inglese J, Walters MA. Mitigating risk in academic preclinical drug discovery. Nat Rev Drug Discov. 2015;14(4):279–94.doi: 10.1038/nrd4578. PubMed PMID: 25829283.

Acknowledgements

We would like to thank our collaborators at the National Library of Medicine/National Center for Biotechnology Information (NLM/NCBI), who have been very helpful in the transition of the Assay Guidance Manual from the wiki format to the Bookshelf in 2012, and for their continued efforts in keeping the manual updated. Special thanks go to NCBI Director David Lipman and Jim Ostell, Chief, Information Engineering Branch at NCBI, and to the Bookshelf and PubMed Central development teams, especially Marilu Hoeppner and Sam Grammer.

Considerations for Early Phase Drug Discovery

Thomas D.Y. Chung, Nathan P. Coussens, G. Sitta Sittampalam, and Yueming Wang

Early Drug Discovery and Development Guidelines: For Academic Researchers, Collaborators, and Start-up Companies

Jeffrey Strovel,[1] Sitta Sittampalam,[2] Nathan P. Coussens,[2] Michael Hughes,[3] James Inglese,[2] Andrew Kurtz,[4] Ali Andalibi,[4] Lavonne Patton,[5] Chris Austin,[6] Michael Baltezor,[3] Michael Beckloff,[5] Michael Weingarten,[4] and Scott Weir[3]

Created: May 1, 2012; Updated: July 1, 2016.

Abstract

Setting up drug discovery and development programs in academic, non-profit and other life science research companies requires careful planning. This chapter contains guidelines to develop therapeutic hypotheses, target and pathway validation, proof of concept criteria and generalized cost analyses at various stages of early drug discovery. Various decision points in developing a New Chemical Entity (NCE), description of the exploratory Investigational New Drug (IND) and orphan drug designation, drug repurposing and drug delivery technologies are also described and geared toward those who intend to develop new drug discovery and development programs.

Note: The estimates and discussions below are modeled for an oncology drug New Molecular Entity (NME) and repurposed drugs. For other disease indications these estimates might be significantly higher or lower.

Background

Medical innovation in America today calls for new collaboration models that span government, academia, industry and disease philanthropy. Barriers to translation and ultimate commercialization will be lowered by bringing best practices from industry into academic settings, and not only by training a new generation of 'translational' scientists prepared to move a therapeutic idea forward into proof of concept in humans, but also by developing a new cadre of investigators skilled in regulatory science.

As universities begin to focus on commercializing research, there is an evolving paradigm for drug discovery and early development focused innovation within the academic enterprise. The innovation process -- moving from basic research to invention and to commercialization and application -- will remain a complex and costly journey. New funding mechanisms, the importance of collaborations within and among institutions, the essential underpinnings of public-private partnerships that involve some or all sectors, the focus of the new field of regulatory science, and new appropriate bridges between federal health and regulatory agencies all come to bear in this endeavor.

We developed these guidelines to assist academic researchers, collaborators and start-up companies in advancing new therapies from the discovery phase into early drug development, including evaluation of therapies in human and/or clinical proof of concept. This chapter outlines necessary steps required to identify and properly validate drug targets, define the utility of employing probes in the early discovery phase, medicinal chemistry, lead optimization, and preclinical proof of concept strategies, as well as address drug delivery needs through preclinical proof of concept. Once a development candidate has been identified, the guidelines provide an overview of human and/or clinical proof of concept enabling studies required by regulatory agencies prior to initiation of clinical trials. Additionally, the guidelines help to ensure quality project plans are developed and

Author Affiliations: 1 ConverGene, LLC, Gaithersburg, MD. 2 National Center for Advancing Translational Sciences (NCATS), National Institutes for Health (NIH), Bethesda, MD. 3 Institute for Advancing Medical Innovation, University of Kansas, Lawrence, KS. 4 Small Business Innovation Research, National Cancer Institute, Washington, DC. 5 Beckloff Associates, Inc. Overland Park, KS. 6 NIH Chemical Genomics Center, Bethesda, MD.

projects are advanced consistently. We also outline the expected intellectual property required at key decision points and the process by which decisions may be taken to move a project forward.

Purpose

The purpose of this chapter is to define:

- Three practical drug discovery and early development paths to advancing new cancer therapies to early stage clinical trials, including:
  1. Discovery and early development of a New Chemical Entity (NCE)
  2. Discovery of new, beneficial activity currently marketed drugs possess against novel drug targets, also referred to as "drug repurposing"
  3. Application of novel platform technology to the development of improved delivery of currently marketed drugs
- Within each of the three strategies, decision points have been identified along the commercial value chain and the following concepts have been addressed:
  - Key data required at each decision point, targets and expectations required to support further development
  - An estimate of the financial resources needed to generate the data at each decision point
  - Opportunities available to outsource activities to optimally leverage strengths within the institution
  - Integration of these activities with the intellectual property management process potential decision points which:
    - Offer opportunities to initiate meaningful discussions with regulatory agencies to define requirements for advancement of new cancer therapies to human evaluation
    - Afford opportunities to license technologies to university start-up, biotechnology and major pharmaceutical companies
    - Define potential role(s) the National Institutes of Health SBIR programs may play in advancing new cancer therapies along the drug discovery and early development path

Scope

The scope of drug discovery and early drug development within the scope of these guidelines spans **target identification through human (Phase I) and/or clinical (Phase IIa) proof of concept.** This chapter describes an approach to drug discovery and development for the treatment, prevention, and control of cancer. The guidelines and decision points described herein may serve as the foundation for collaborative projects with other organizations in multiple therapeutic areas.

Assumptions

1. These guidelines are being written with target identification as the initial decision point, although the process outlined here applies to a project initiated at any of the subsequent points.
2. The final decision point referenced in this chapter is human and/or clinical proof of concept. Although the process for new drug approval is reasonably well defined, it is very resource intensive and beyond the focus of most government, academic, and disease philanthropy organizations conducting drug discovery and early drug development activities.
3. The decision points in this chapter are specific to the development of a drug for the treatment of relapsed or refractory late stage cancer patients. Many of the same criteria apply to the development of drugs intended for other indications and therapeutic areas, but each disease should be approached with a logical customization of this plan. Development of compounds for the prevention and control of cancer would follow a more conservative pathway as the benefit/risk evaluation for these compounds would be

different. When considering prevention of a disease one is typically treating patients at risk, but before the disease has developed in individuals that are otherwise healthy. The development criteria for these types of compounds would be more rigorous initially and would typically include a full nonclinical development program to support the human studies. Similarly, compounds being developed to control cancer suggest that the patients may have a prolonged life expectation such that long term toxicity must be fully evaluated before exposing a large patient population to the compound. **The emphasis of the current chapter is on the development of compounds for the treatment of late stage cancer patients.**

4. Human and/or clinical proof of concept strategies will differ depending upon the intent of the product (treatment, prevention, or control). The concepts and strategies described in this chapter can be modified for the development of a drug for prevention or control of multiple diseaes.
5. The cost estimates and decision points are specific to the development of a small molecule drug. Development of large molecules will require the evaluation of additional criteria and may be very specific to the nature of the molecule under development.
6. This plan is written to describe the resources required at each decision point and does not presume that licensing will occur only at the final decision point. It is incumbent upon the stakeholders involved to decide the optimal point at which the technology should move outside their institution.
7. The plan described here does not assume that the entire infrastructure necessary to generate the data underlying each decision criterion is available at any single institution. The estimates of financial resource requirements are based on an assumption that these services can be purchased from an organization (or funded through a collaborator) with the necessary equipment, instrumentation, and trained personnel to conduct the studies.
8. The costs associated with the tasks in the development plan are based on the experiences of the authors. It is reasonable to assume that variability in the costs and duration of specific data-generating activities will depend upon the nature of the target and molecule under development.

Definitions

At Risk Initiation – The decision by the project team to begin activities that do not directly support the next unmet decision point, but will instead support a subsequent decision point. *At Risk Initiation* is sometimes recommended to decrease the overall development time.

Commercialization Point – In this context, the authors use the term to describe the point at which a commercial entity is involved to participate in the development of the drug product. This most commonly occurs through a direct licensing arrangement between the university and an organization with the resources to continue the development of the product.

Counter-screen – A screen performed in parallel with or after the primary screen. The assay used in the counter-screen is developed to identify compounds that have the potential to interfere with the assay used in the primary screen (the primary assay). Counter-screens can also be used to eliminate compounds that possess undesirable properties, for example, a counter-screen for cytotoxicity (1).

Cumulative Cost – This describes the total expenditure by the project team from project initiation to the point at which the project is either completed or terminated.

Decision Point[1] – The latest moment at which a predetermined course of action is initiated. Project advancement based on decision points balances the need to conserve scarce development resources with the requirement to develop the technology to a commercialization point as quickly as possible. Failure to meet the criteria listed for the following decision points will lead to a *No Go* recommendation.

[1] Behind each Decision Point are detailed decision-making criteria defined in detail later in this chapter

False positive – Generally related to the "specificity" of an assay. In screening, a compound may be active in an assay but inactive toward the biological target of interest. For this chapter, this does not include activity due to spurious, non-reproducible activity (such as lint in a sample that causes light-scatter or spurious fluorescence and other detection related artifacts). Compound interference that is reproducible is a common cause of false positives, or target-independent activity (1).

Go Decision – The project conforms to key specifications and criteria and will continue to the next decision point.

High-Throughput Screen (HTS) – A large-scale automated experiment in which large libraries (collections) of compounds are tested for activity against a biological target or pathway. It can also be referred to as a "screen" for short (1).

Hits – A term for putative activity observed during the primary high-throughput screen, usually defined by percent activity relative to control compounds (1).

Chemical Lead Compound – A member of a biologically and pharmacologically active compound series with desired potency, selectivity, pharmacokinetic, pharmacodynamic and toxicity properties that can advance to IND-enabling studies for clinical candidate selection.

Incremental Cost – A term used to describe the additional cost of activities that support decision criteria for any given decision point, independent of other activities that may have been completed or initiated to support decision criteria for any other decision point.

Library – A collection of compounds that meet the criteria for screening against disease targets or pathways of interest (1).

New Chemical Entity (NCE) – A molecule emerging from the discovery process that has not previously been evaluated in clinical trials.

No Go Decision – The project does not conform to key specifications and criteria and will not continue.

Off-Target Activity – Compound activity that is not directed toward the biological target of interest but can give a positive read-out, and thus can be classified as an active in the assay (1).

Orthogonal Assay – An assay performed following (or in parallel to) the primary assay to differentiate between compounds that generate false positives from those compounds that are genuinely active against the target (1).

Primary Assay – The assay used for the high-throughput screen (1).

Qualified Task – A task that should be considered, but not necessarily required to be completed at a suggested point in the project plan. The decision is usually guided by factors outside the scope of this chapter. Such tasks will be denoted in this chapter by enclosing the name of the tasks in parentheses in the Gantt chart, e.g. (qualified task).

Secondary Assay – An assay used to test the activity of compounds found active in the primary screen (and orthogonal assay) using robust assays of relevant biology. Ideally, these are of at least medium-throughput to allow establishment of structure-activity relationships between the primary and secondary assays and establish a biologically plausible mechanism of action (1).

Section 1 Discovery and Development of New Chemical Entities

The Gantt chart (Table 1) illustrates the scope of this chapter. The left-hand portion of the chart includes the name of each decision point as well as the incremental cost for the activities that support that task. The black bars on the right-hand portion of the chart represent the duration of the summary task (combined criteria) to

support a decision point as well as the *cumulative cost* for the project at the completion of that activity. A similar layout applies to each of the subsequent figures; however, the intent of these figures is to articulate the activities that underlie each decision point.

The submission of regulatory documents, for the purpose of this example, reflects the preparation of an Investigational New Drug (IND) application in Common Technical Document (CTD) format. The CTD format is required for preparation of regulatory documents in Europe (according to the Investigational Medicinal Product Dossier [IMPD]), Canada for investigational applications (Clinical Trial Application) and is accepted by the United States Food and Drug Administration (FDA) for INDs. The CTD format is required for electronic CTD (eCTD) submissions. The advantages of the CTD are that it facilitates global harmonization and lays the foundation upon which the marketing application can be prepared. The sections of the CTD are prepared early in development (at the IND stage) and are then updated, as needed, until submission of the marketing application.

Table 1: Composite Gantt Chart Roll-up Representing Target ID through Clinical POC

		Year 1				Year 2				Year 3				Year 4				Year 5				Year 6				Year 7				Year 8				Year 9			
Task Name	Cost	Q1	Q2	Q3	Q4	Q1	Q2	Q3	Q4	Q1	Q2	Q3	Q4	Q1	Q2	Q3	Q4	Q1	Q2	Q3	Q4	Q1	Q2	Q3	Q4	Q1	Q2	Q3	Q4	Q1	Q2	Q3	Q4	Q1	Q2	Q3	Q4
#1 Target Identification	**$200,000**	**$200,000**																																			
#2 Target Validation	**$268,500**			**$468,500**																																	
#3 Identification of Actives	**$472,500**					**$941,000**																															
#4 Confirmation of Hits	**$522,000**							**$1,463,000**																													
#5 Identification of Chemical Lead	**$353,300**											**$1,816,300**																									
#6 Selection of Optimized Chemical Lead	**$302,500**													**$2,118,800**																							
#7 Selection of a Development Candidate	**$275,000**															**$2,393,800**																					
#8 Pre-IND Meeting with FDA	**$37,000**																	**$2,430,800**																			
#9 File IND	**$780,000**																	**$3,210,800**																			
#10 Human Proof of Concept	**$1,000,000**																					**$4,210,800**															
#11 Clinical Proof of Concept	**$5,000,000**																									**$9,210,800**											

Decision Point #1 - Target Identification

Target-based drug discovery begins with identifying the function of a possible therapeutic target and its role in the disease (2). There are two criteria that justify advancement of a project beyond target identification. These are:

- Previously published (peer-reviewed) data on a particular disease target pathway or target, OR
- Evidence of new biology that modulates a disease pathway or target of interest

Resource requirements to support this initial stage of drug discovery can vary widely as the novelty of the target increases. In general, the effort required to elucidate new biology can be significant. Most projects will begin with these data in hand, whether from a new or existing biology. We estimate that an additional investment might be needed to support the target identification data that might already exist (Table 2). However, as reflected in Table 2, if additional target validation activities proceed *at risk*, the total cost of the project at a "No Go" decision will reach approximately $468,500 (estimated).

Table 2: Target Identification and Target Validation

		Year 1				Year 2			
Task Name	Cost	Q1	Q2	Q3	Q4	Q1	Q2	Q3	Q4
#1 Target Identification	**$200,000**	**$200,000**							
Previously published data on disease target	**$1,000**								
New biology that modulates a disease	**$199,000**								
#2 Target Validation	**$268,500**			**$468,500**					
Known molecules modulate target	**$100,000**								
Type of target has a history of success	**$1,000**								
Genetic confirmation	**$80,000**								
Availability of known animal models	**$7,500**								
Low throughput target validation assay that represents biology	**$70,000**								
Intellectual property of the target	**$7,500**								
Marketability of the target	**$2,500**								
#3 Identification of Actives	**$472,500**					**$941,000**			

Decision Point #2 - Target Validation

Target validation requires a demonstration that a molecular target is directly involved in a disease process, and that modulation of the target is likely to have a therapeutic effect (2). There are seven criteria for evaluation prior to advancement beyond target validation. These are:

- Known molecules modulate the target
- Type of target has a history of success (e.g. Ion channel, GCPR, nuclear receptor, transcription factor, cell cycle, enzyme, etc.)
- Genetic confirmation (e.g. Knock-out, siRNA, shRNA, SNP, known mutations, etc.)
- Availability of known animal models
- Low-throughput target validation assay that represents biology
- Intellectual property of the target
- Market potential of the disease/target space

The advancement criteria supporting target validation can usually be completed in approximately 12 months by performing most activities in parallel. In an effort to reduce the overall development timeline, we recommend starting target validation activities *at risk* (prior to a "Go" decision on target identification). Table 2 illustrates the dependencies between the criteria supporting the first two decision points. The incremental cost of the activities supporting decision-making criteria for target validation is approximately $268,500. However, a decision to initiate target validation prior to completion of target initiation (recommended) and subsequent initiation of identification of actives *at risk* would lead to a total project cost (estimate) of $941,000 if a "No Go" decision were reached at the conclusion of target validation.

Decision Point #3 - Identification of Actives

An active is defined as a molecule that shows significant biological activity in a validated screening assay that represents the disease biology and physiology. By satisfying the advancement criteria listed below for identification of actives, the project team will begin to define new composition of matter by linking a chemical structure to modulation of the target. There are five (or six if invention disclosure occurs at this stage) criteria for evaluation at the identification of actives decision point. These are:

- Acquisition of screening reagents
- Primary HTS assay development and validation
- Compound library available to screen
- Actives criteria defined
- Perform high-throughput screen
- (Composition of Matter invention disclosure)

The advancement criteria supporting identification of actives can be completed in approximately 12 months in most cases by performing activities in parallel. Table 3 illustrates the dependencies and timing associated with a decision to begin activities supporting confirmation of hits prior to a "Go" decision on decision point #3. The incremental cost associated with decision point #3 is estimated to be $472,500 (assuming the assay is transferred and validated without difficulty). The accumulated project cost associated with a "No Go" decision at this point is estimated to be $1.46 million. This assumes an *at risk* initiation of activities supporting decision point #4.

Table 3: Identification of Actives

		Year 1				Year 2				Year 3			
Task Name	Cost	Q1	Q2	Q3	Q4	Q1	Q2	Q3	Q4	Q1	Q2	Q3	Q4
#2 Target Validation	**$268,500**			**$468,500**									
#3 Identification of Actives	**$472,500**					**$941,000**							
Acquisition of screening reagents	**$100,000**												
Primary HTS assay development and validation	**$150,000**												
Compound library available to screen	**$150,000**												
Actives criteria defined	**$2,500**												
Perform high-throughput screen	**$70,000**												
(Composition of Matter invention disclosure)	**Variable**												
#4 Confirmation of Hits	**$522,000**							**$1,463,000**					

Decision Point #4 - Confirmation of Hits

A hit is defined as consistent activity of a molecule (with confirmed purity and identity) in a biochemical and/or cell based secondary assay. Additionally, this is the point at which the project team will make an assessment of

the molecular class of each of the hits. There are six (or seven if initial invention disclosure occurs at this stage) criteria for evaluation at the confirmation of hits decision point. These are:

- Confirmation based on repeat assay, Concentration Response Curve (CRC)
- Secondary assays for specificity, selectivity, and mechanisms
- Confirmed identity and purity
- Cell-based assay confirmation of biochemical assay when appropriate
- Druggability of the chemical class (reactivity, stability, solubility, synthetic feasibility)
- Chemical Intellectual Property (IP)
- (Composition of Matter invention disclosure)

The advancement criteria supporting decision point #4 can usually be completed in approximately 18 months, depending upon the existence of cell-based assays for confirmation. If the assays need to be developed or validated at the screening lab, we recommend starting that activity *at risk* concurrent with the CRC and mechanistic assays. Table 4 represents the dependencies and timing associated with the decision to begin activities supporting confirmation of hits prior to a "Go" decision on decision point #3. The incremental cost of confirmation of hits is $522,000. The accumulated project cost at a "No Go" decision on decision point #4 can be as high as $1.8 million if a proceed *at risk* decision is made on identification of a chemical lead (decision point #5).

Table 4: Confirmation of Hits

		Year 2				Year 3				Year 4			
Task Name	Cost	Q1	Q2	Q3	Q4	Q1	Q2	Q3	Q4	Q1	Q2	Q3	Q4
#3 Identification of Actives	**$472,500**	**$941,000**											
#4 Confirmation of Hits	**$522,000**			**$1,463,000**									
Confirmation based on repeat assay, Concentration Response Curve (CRC)	**$50,000**												
Secondary assays for specificity, selectivity, and mechanisms	**$400,000**												
Confirmed identity and purity	**$10,000**												
Cell-based assay confirmation of biochemical assay when appropriate	**$50,000**												
Druggability of the chemical class (reactivity, stability, solubility, synthetic feasibility)	**$2,000**												
Chemical Intellectual Property (IP) (prior art search, med chemist driven)	**$10,000**												
(Composition of Matter invention disclosure)	**Variable**												
#5 Identification of Chemical Lead	**$353,300**							**$1,816,300**					

Decision Point #5 - Identification of Chemical Lead

A chemical lead is defined as a synthetically feasible, stable, and drug-like molecule active in primary and secondary assays with acceptable *specificity* and *selectivity* for the target. This requires definition of the Structure-Activity Relationship (SAR) as well as determination of synthetic feasibility and preliminary evidence of *in vivo* efficacy and target engagement ***(Note: projects at this stage might be eligible for Phase I SBIR)***. Characteristics of a chemical lead are:

- SAR defined
- Drugability (preliminary toxicity, hERG, Ames)

- Synthetic feasibility
- Select mechanistic assays
- *In vitro* assessment of drug resistance and efflux potential
- Evidence of *in vivo* efficacy of chemical class
- PK/Toxicity of chemical class known based on preliminary toxicity or *in silico* studies

In order to decrease the number of compounds that fail in the drug development process, a druggability assessment is often conducted. This assessment is important in transforming a compound from a lead molecule into a drug. For a compound to be considered druggable it should have the potential to bind to a specific target; however, also important is the compound's pharmacokinetic profile regarding absorption, distribution, metabolism, and excretion. Other assays will evaluate the potential toxicity of the compound in screens such as the Ames test and cytotoxicity assay. When compounds are being developed for indications where the predicted patient survival is limited to a few years, it is important to note that a positive result in the cytotoxicity assays would not necessarily limit the development of the compound and other drugability factors (such as the pharmacokinetic profile) would be more relevant for determining the potential for development.

The advancement criteria supporting decision point #5 will most likely be completed in approximately 12-18 months due to the concurrent activities. We recommend that SAR and drugability assessments begin *at risk* prior to a "Go" on confirmation of hits. Synthetic feasibility and PK assessment will begin at the completion of decision point #4. The cost of performing the recommended activities to support identification of a chemical lead is estimated to be $353,300 (Table 5). The accumulated project costs at the completion of decision point #5 are estimated to be $2.1 million including costs associated with *at risk* initiation of activities to support decision point #6.

Table 5: Identification of a Chemical Lead

		Year 2				Year 3				Year 4			
Task Name	Cost	Q1	Q2	Q3	Q4	Q1	Q2	Q3	Q4	Q1	Q2	Q3	Q4
#4 Confirmation of Hits	**$522,000**			**$1,463,000**									
#5 Identification of Chemical Lead	**$353,300**							**$1,816,300**					
SAR Defined	**$167,900**												
Specificity	**$20,000**												
Selectivity	**$40,000**												
Drugability	**$107,900**												
Solubility	**$10,000**												
Permeability n=50	**$15,000**												
Metabolic stability n=30 (human, murine, rat)	**$40,000**												
In vitro toxicology n=5	**$25,000**												
hERG (QT prolongation) n=10	**$7,500**												
Mini Ames (mutagenicity) n=3	**$5,400**												
Cytotoxicity assays n=3	**$5,000**												
Synthetic feasibility	**$6,500**												
Number of steps	**$2,500**												
Occupational health (starting materials and reagents)	**$2,500**												
Cost	**$1,000**												
Availability of starting materials and reagents	**$500**												

Table 5 continued from previous page.

		Year 2				Year 3				Year 4			
Task Name	Cost	Q1	Q2	Q3	Q4	Q1	Q2	Q3	Q4	Q1	Q2	Q3	Q4
Select mechanistic assays n=10	**$25,000**												
No relative drug resistance issues n=10	**$6,000**												
Evidence of *in vivo* efficacy of chemical class (PD Study)	**$10,000**												
PK feasibility of chemical class	**$10,000**												
Provisional application -composition of matter	**$20,000**												
#6 Selection of Optimized Chemical Lead	**$302,500**									**$2,118,800**			

Decision Point #6 - Selection of Optimized Chemical Lead

An optimized chemical lead is a molecule that will enter IND-enabling GLP studies and GMP supplies will be produced for clinical trials. We will describe the activities that support GLP and GMP development in the next section. This section focuses on the decision process to identify those molecules (**Note: projects at this stage may be eligible for Phase II SBIR**). Criteria for selecting optimized candidates are listed below**:**

- Acceptable *in vivo* PK and toxicity
- Feasible formulation
- *In vivo* preclinical efficacy (properly powered)
- Dose Range Finding (DRF) pilot toxicology
- Process chemistry assessment of scale up feasibility
- Regulatory and marketing assessments

The advancement criteria supporting decision point #6 can be completed in approximately 12-15 months. As indicated above, we recommend commencing activities to support selection of an optimized chemical lead prior to a "Go" decision on decision point #5. In particular, the project team should place emphasis on 6.3 (*in vivo* preclinical efficacy). A strong lead will have clearly defined pharmacodynamic endpoints at the preclinical stage and will set the stage for strong indicators of efficacy at decision point #11 (clinical proof of concept). The cost of performing the recommended activities to support decision point #6 is estimated to be $302,500 (Table 6). The accumulated project costs at the completion of decision point #6 are estimated to be $2.4 million, including costs associated with *at risk initiation* of activities to support decision point #7.

Table 6: Selection of an Optimized Chemical Lead

		Year 3				Year 4				Year 5			
Task Name	Cost	Q1	Q2	Q3	Q4	Q1	Q2	Q3	Q4	Q1	Q2	Q3	Q4
#5 Identification of Chemical Lead	**$353,300**			**$1,816,300**									
#6 Selection of Optimized Chemical Lead	**$302,500**					**$2,118,800**							
Acceptable *in vivo* PK	**$32,500**												
Route of administration	**$10,000**												
Bioavailability	**$7,500**												
Clearance	**$7,500**												
Drug distribution	**$7,500**												
Feasible formulation	**$15,000**												
In vivo preclinical efficacy (properly powered)	**$165,000**												

Table 6 continued from previous page.

		Year 3				Year 4				Year 5			
Task Name	Cost	Q1	Q2	Q3	Q4	Q1	Q2	Q3	Q4	Q1	Q2	Q3	Q4
Tumor size and volume	**$40,000**												
Biomarkers	**$25,000**												
Survival	**$30,000**												
Target validation	**$30,000**												
Dose frequencey	**$40,000**												
Dose Range Finding (DRF) pilot toxicology	**$40,000**												
Process chemistry assessment of scale up feasibility	**$50,000**												
Regulatory and marketing assessments	**Variable**												
#7 Selection of a Development Candidate	**$275,000**							**$2,393,800**					

Decision Point #7 - Selection of a Development Candidate

A development candidate is a molecule for which the intent is to begin Phase I evaluation. Prior to submission of an IND, the project team must evaluate the likelihood of successfully completing the IND-enabling work that will be required as part of the regulatory application for first in human testing. Prior to decision point #7, many projects will advance as many as 7-10 molecules. Typically, most pharma and biotech companies will select a single development candidate with one designated backup. Here, we recommend that the anointed "Development Candidate" be the molecule that rates the best on the six criteria below. In many cases, a Pre-IND meeting with the regulatory agency might be considered. A failure to address all of these by any molecule should warrant a "No Go" decision by the project team. The following criteria should be minimally met for a development candidate:

- Acceptable PK (with a validated bioanalytical method)
- Demonstrated *in vivo* efficacy/activity
- Acceptable safety margin (toxicity in rodents or dogs when appropriate)
- Feasibility of GMP manufacture
- Acceptable drug interaction profile
- Well-developed clinical endpoints

The advancement criteria supporting decision point #7 are estimated to be completed in 12 months, but may be compressed to as little as 6 months. The primary rate limit among the decision criteria is the determination of the safety margin, as this can be affected by the formulation and dosing strategies selected earlier. In this case, the authors have presented a project that includes a 7-day repeat dose in rodents to demonstrate an acceptable safety margin. The incremental costs of activities to support the selection of a development candidate (as shown) are estimated to be approximately $275,000. The accumulated project cost at this point is approximately $2.4 million to complete decision points #6, #7, and the FDA Pre-IND meeting (Table 7). If the development plan requires a longer toxicology study at this point, costs can be higher (approximately $190,000 for a 14-day repeat dose study in rats and $225,000 in dogs).

Table 7: Selection of a Development Candidate

		Year 4				Year 5			
Task Name	Cost	Q1	Q2	Q3	Q4	Q1	Q2	Q3	Q4
#6 Selection of Optimized Chemical Lead	**$302,500**	**$2,118,800**							
#7 Selection of a Development Candidate	**$275,000**			**$2,393,800**					

Table 7 continued from previous page.

		Year 4				Year 5			
Task Name	Cost	Q1	Q2	Q3	Q4	Q1	Q2	Q3	Q4
Acceptable PK (with a validated bioanalytical method)	**$30,000**								
Well-developed clinical endpoints	**$40,000**								
Demonstrated *in vivo* efficacy/activity	**$50,000**								
Acceptable safety margin (toxicity in rodents or dogs when appropriate)	**$125,000**								
GMP manufacture feasibility	**$25,000**								
Acceptable drug interaction profile	**$5,000**								
#8 Pre-IND Meeting with FDA (for non-oncology projects only)	**$37,000**					**$2,430,800**			

Decision Point #8 - Pre-IND Meeting with the FDA

Pre-IND advice from the FDA may be requested for issues related to the data needed to support the rationale for testing a drug in humans; the design of nonclinical pharmacology, toxicology, and drug activity studies, including design and potential uses of any proposed treatment studies in animal models; data requirements for an IND application; initial drug development plans, and regulatory requirements for demonstrating safety and efficacy (1). We recommend that this meeting take place after the initiation, but before the completion of tasks to support decision point #7 (selection of a development candidate). The feedback from the FDA might necessitate adjustments to the project plan. Making these changes prior to candidate selection will save time and money. Pre-IND preparation will require the following:

- Prepare pre-IND meeting request to the FDA, including specific questions
- Prepare pre-IND meeting package, which includes adequate information for the FDA to address the specific questions (clinical plan, safety assessments summary, CMC plan, etc.)
- Prepare the team for the pre-IND meeting
- Conduct pre-IND meeting with the FDA
- Adjust project plan to address the FDA comments
- Target product profile

The advancement criteria supporting decision point #8 should be completed in 12 months. We recommend preparing the pre-IND meeting request approximately 3 to 6 months prior to selection of a development candidate (provided that the data supporting that decision point are promising). The cost of performing the recommended activities to support pre-IND preparation #8 is estimated to be $37,000.

Decision Point #9 - Preparation and Submission of an IND Application

The decision to submit an IND application presupposes that all of the components of the application have been addressed. The largest expense associated with preparation of the IND is related to the CMC activities (manufacture and release of GMP clinical supplies). A “Go” decision is contingent upon all of the requirements for the IND having been addressed and that the regulatory agency agrees with the clinical plan. (Note: projects at this stage may be eligible for SBIR BRIDGE awards). The following criteria should be addressed in addition to addressing comments from the pre-IND meeting:

- Well-developed clinical plan
- Acceptable clinical dosage form
- Acceptable preclinical drug safety profile
- Clear IND regulatory path

- Human Proof of Concept (HPOC)/Clinical Proof of Concept (CPOC) plan is acceptable to regulatory agency (pre-IND meeting)
- Reevaluate IP positions

The advancement criteria supporting decision point #9 are estimated to be completed in 12 months, but might be compressed to as little as 6 months if necessary. We recommend initiating "*at risk*" as long as there is confidence that a qualified development candidate is emerging before completion of decision point #7 and the plan remains largely unaltered after the pre-IND meeting (decision point #8). The incremental costs of completing decision point #9 are estimated to be $780,000. The accumulated project cost at this point will be approximately $3.2 million (Table 8).

Table 8: Submit IND Application

		Year 5			
Task Name	Cost	Q1	Q2	Q3	Q4
#8 Pre-IND Meeting with FDA (for non-oncology projects only)	**$37,000**	**$2,430,800**			
#9 File IND	**$780,000**	**$3,210,800**			
Acceptable clinical dosage form	**$360,000**				
Delivery, reconstitution, practicality	**$30,000**				
stability (at least one year)	**$80,000**				
GMP quality	**$250,000**				
Acceptible preclinical drug safety profile	**$350,000**				
Safety index (receptor profiling, safety panels)	**$30,000**				
Dose response (PK)	**$20,000**				
Safety pharmacology	**$300,000**				
Clear IND regulatory path	**$30,000**				
HPOC/CPOC plan is acceptible to regulatory agency	**$40,000**				

Decision Point #10 - Human Proof of Concept

Most successful Phase I trials in oncology require 12-21 months for completion, due to very restrictive enrollment criteria in these studies in some cases. There is no "*at risk*" initiation of Phase I; therefore, the timeline cannot be shortened in that manner. The most important factors in determining the length of a Phase I study are a logically written clinical protocol and an available patient population. A "Go" decision clearly rests on the safety of the drug, but many project teams will decide not to proceed if there is not at least some preliminary indication of efficacy during Phase I (decision point #10, below). Proceeding to Phase II trials will depend on:

- IND clearance
- Acceptable Maximum Tolerated Dose (MTD)
- Acceptable Dose Response (DR)
- Evidence of human pharmacology
- Healthy volunteer relevance

We estimate the incremental cost of an oncology Phase I study will be approximately $1 million. This can increase significantly if additional patients are required to demonstrate MTD, DR, pharmacology and/or efficacy. Our estimate is based on a 25 patient (outpatient) study completed in 18 months. The accumulated project cost at completion of decision point #10 will be approximately $4.2 million (Table 9).

Table 9: Human Proof of Concept

		Year 5				Year 6				Year 7			
Task Name	Cost	Q1	Q2	Q3	Q4	Q1	Q2	Q3	Q4	Q1	Q2	Q3	Q4
#9 File IND	**$780,000**	**$3,210,800**											
#10 Human Proof of Concept	**$1,000,000**					**$4,210,800**							
IND/CTA clearance	**$242,500**												
Acceptable Maximum Tolerated Dose (MTD)	**$242,500**												
Acceptable Dose Response (DR)	**$242,500**												
Evidence of human pharmacology	**$242,500**												
Healthy volunteer relevance	**$30,000**												

Decision Point #11: Clinical Proof of Concept

With acceptable Dose Ranging and Maximum Tolerable Dose having been defined during Phase I, in Phase II the project team will attempt to statistically demonstrate efficacy. More specifically, the outcome of Phase II should reliably predict the likelihood of success in Phase III randomized trials.

- Meeting the IND objectives
- Acceptable human PK/PD profile
- Evidence of human pharmacology
- Safety and tolerance assessments

We estimate the incremental cost of an oncology Phase IIa study will be approximately $5.0 million (Table 10). This cost is largely dependent on the number of patients required and the number of centers involved. Our estimate is based on 150 outpatients with studies completed in 24 months. The accumulated project cost at the completion of decision point #11 will be approximately $9.2 million (Table 10).

Table 10: Decision Point #11 in Detail

		Year 6				Year 7				Year 8				Year 9			
Task Name	Cost	Q1	Q2	Q3	Q4	Q1	Q2	Q3	Q4	Q1	Q2	Q3	Q4	Q1	Q2	Q3	Q4
#10 Human Proof of Concept	**$1,000,000**	**$4,210,800**															
#11 Clinical Proof of Concept (n=2)	**$5,000,000**							**$9,210,800**									
IND/CTA clearance	**$500,000**																
Acceptable PK/PD profile	**$500,000**																
Evidence of pharmacology	**$2,500,000**																
Efficacy	**$1,250,000**																
Direct and indirect biomarkers	**$1,250,000**																
Safety and tolerance assessments	**$1,500,000**																

Section 2. Repurposing of Marketed Drugs

Drug repurposing and rediscovery development projects frequently seek to employ the 505(b)(2) drug development strategy. This strategy leverages studies conducted and data generated by the innovator firm that is available in the published literature, in product monographs, or product labeling. Improving the quality of drug development plans will reduce the time of 505(b)(2) development cycles, and reduce the time and effort required by the FDA during the NDA review process. Drug repurposing projects seek a new indication in a different

patient population and perhaps a different formulated drug product than what is currently described on the product label. By leveraging existing nonclinical data and clinical safety experience, sponsors have the opportunity to design and execute novel, innovative clinical trials to characterize safety and efficacy in a different patient population. The decision points for drug repurposing are summarized in Table 11.

Table 11: Summary of Decision Points for Drug Repurposing

		Year 1												Year 2											
Decision Points	Cost	M1	M2	M3	M4	M5	M6	M7	M8	M9	M10	M11	M12	M13	M14	M15	M16	M17	M18	M19	M20	M21	M22	M23	M24
#1 Identification of Actives	**$500,000**	**$500,000**																							
#2 Confirmation of Hits	**$205,000**			**$705,000**																					
#3 Initial Gap Analysis/ Development Plan	**$250,000**							**$955,000**																	
#4 Clinical Formulation Development	**$100,000**							**$1,055,000**																	
#5 Preclinical Safety Data Package	**$800,000**									**$1,855,000**															
#6 Clinical Supplies Manufacture	**$500,000**											**$2,355,000**													
#7 IND Preparation and Submission	**$500,000**														**$2,855,000**										
#8 Human Proof of Concept	**$1,000,000**														**$3,855,000**										

Decision Point #1: Identification of Actives

For drug repurposing, actives are identified as follows (Table 12):

- Acquisition of Active Pharmaceutical Ingredients (API) for screening
- Primary HTS assay development, validation
- Actives criteria defined
- Perform HTS
- (Submit invention disclosure and consider use patent)

Table 12: Identification of Actives

		Year 1											
Decision Point	Cost	M1	M2	M3	M4	M5	M6	M7	M8	M9	M10	M11	M12
#1 Identification of Actives	**$500,000**	**$500,000**											
Acquisition of Active Pharmaceutical Ingredients (API) for screening	**Variable**												
Primary HTS assay development, validation	**Variable**												
Actives criteria defined	**Variable**												
Perform high-throughput screen	**Variable**												
(Submit invention disclosure and consider use patent)	**Variable**												
#2 Confirmation of Hits	**$205,000**			**$705,000**									

Decision Point #2: Confirmation of Hits

Hits are confirmed as follows for a drug repurposing project (Table 13):

- Confirmation based on repeat assay, CRC
- Secondary assays for specificity, selectivity, and mechanisms
- Cell-based assay confirmation of biochemical assay when appropriate
- (Submit invention disclosure and consider use patent)

Table 13: Confirmation of Hits

		Year 1											
Decision Point	Cost	M1	M2	M3	M4	M5	M6	M7	M8	M9	M10	M11	M12
#1 Identification of Actives	**$500,000**	**$500,000**											
#2 Confirmation of Hits	**$205,000**			**$705,000**									
Confirmation based on repeat assay, concentration response curve (CRC)	**Variable**												
Secondary assays for specificity, selectivity, and mechanisms	**Variable**												
Cell-based assay confirmation of biochemical assay when appropriate	**Variable**												
(Submit invention disclosure and consider use patent)	**Variable**												
#3 Initial Gap Analysis/Development Plan	**$250,000**							**$955,000**					

Decision Point #3: Gap Analysis/Development Plan

When considering the 505(b)(2) NDA approach, it is important to understand what information is available to support the proposed indication and what additional information might be needed. **The development path is dependent upon the proposed indication, change in formulation, route, and dosing regimen.** The gap analysis/development plan that is prepared will take this information into account in order to determine what studies might be needed prior to submission of an IND and initiating first-in-man studies. A thorough search of the literature is important in order to capture information available to satisfy the data requirements for the IND. Any gaps identified would need to be filled with studies conducted by the sponsor. A pre-IND meeting with the FDA will allow the sponsor to present their plan to the FDA and gain acceptance prior to submission of the IND and conducting the first-in-man study (Table 14).

- CMC program strategy
- Preclinical program strategy
- Clinical proof of concept strategy
- Draft clinical protocol design
- Pre-IND meeting with the FDA
- Commercialization/marketing strategy and target product profile

Table 14: Gap Analysis/Development Plan

		Year 1											
Decision Point	Cost	M1	M2	M3	M4	M5	M6	M7	M8	M9	M10	M11	M12
#2 Confirmation of Hits	**$205,000**			**$705,000**									
#3 Initial Gap Analysis/Development Plan	**$250,000**							**$955,000**					
CMC program strategy	**Variable**												
Preclinical program strategy	**Variable**												
Clinical proof of concept strategy	**Variable**												
Draft clinical protocol design	**Variable**												
Pre-IND meeting with FDA	**Variable**												
Commercialization/marketing strategy and target product profile	**Variable**												
#4 Clinical Formulation Development	**$100,000**							**$1,055,000**					

Decision Point #4: Clinical Formulation Development

The clinical formulation development will include the following (Table 15):

- Prototype development
- Analytical methods development
- Prototype stability
- Prototype selection
- Clinical supplies release specification
- (Submit invention disclosure on novel formulation)

Table 15: Clinical Formulation Development

		Year 1											
Decision Point	Cost	M1	M2	M3	M4	M5	M6	M7	M8	M9	M10	M11	M12
#3 Final Development Plan	**$250,000**							**$955,000**					

Table 15 continued from previous page.

		Year 1											
Decision Point	Cost	M1	M2	M3	M4	M5	M6	M7	M8	M9	M10	M11	M12
#4 Clinical Formulation Development	**$100,000**							**$1,055,000**					
Prototype development	**Variable**												
Analytical methods development	**Variable**												
Prototype stability	**Variable**												
Prototype selection	**Variable**												
Clinical supplies release specification	**Variable**												
(Submit invention disclosure on novel formulation)	**Variable**												
#5 Preclinical Safety Data Package	**$800,000**									**$1,855,000**			

Decision Point #5: Preclinical Safety Data Package

Preparation of the gap analysis/development plan will identify any additional studies that might be needed to support the development of the compound for the new indication. Based on this assessment, as well as the intended patient population, the types of studies that will be needed to support the clinical program will be determined. It is possible that a pharmacokinetic study evaluating exposure would be an appropriate bridge to the available data in the literature (Table 16).

- Preclinical oral formulation development
- Bioanalytical method development
- Qualify GLP test article
- Transfer plasma assay to GLP laboratory
- ICH S7a (Safety Pharmacology) & S7b (Cardiac Tox) core battery of tests
- Toxicology bridging study
- PK/PD/Tox studies if formulation & route of administration is different

Table 16: Preclinical Safety Data Package

		Year 1												Year 2											
Decision Point	Cost	M1	M2	M3	M4	M5	M6	M7	M8	M9	M10	M11	M12	M13	M14	M15	M16	M17	M18	M19	M20	M21	M22	M23	M24
#4 Clinical Formulation Development	**$100,000**							**$1,055,000**																	
#5 Preclinical Safety Data Package	**$800,000**									**$1,855,000**															
Preclinical oral formulation development	**Variable**																								
Bioanalytical method development	**Variable**																								
Qualify GLP test article	**Variable**																								
Transfer plasma assay to GLP laboratory	**Variable**																								
ICH S7a (Safety Pharmacology) & S7b (Cardiac Tox) core battery of tests	**Variable**																								
Toxicology bridging study	**Variable**																								
PK/PD/Tox studies if formulation & route of administration is different	**Variable**																								
#6 Clinical Supplies Manufacture	**$500,000**											**$2,355,000**													

Decision Point #6: Clinical Supplies Manufacture

Clinical supplies will need to be manufactured. The list below provides some of the considerations that need to be made for manufacturing clinical supplies (Table 17):

- Select cGMP supplier and transfer manufacturing process
- Cleaning validation development
- Scale-up lead formulation at GMP facility
- Clinical label design
- Manufacture clinical supplies

Table 17: Clinical Supplies Manufacture

		Year 1												Year 2											
Decision Point	Cost	M1	M2	M3	M4	M5	M6	M7	M8	M9	M10	M11	M12	M13	M14	M15	M16	M17	M18	M19	M20	M21	M22	M23	M24
#5 Preclinical Safety Data Package	**$800,000**									**$1,855,000**															
#6 Clinical Supplies Manufacture	**$500,000**											**$2,355,000**													
Select cGMP supplier and transfer manufacturing process	**Variable**																								
Cleaning validation development	**Variable**																								
Scale-up lead formulation at GMP facility	**Variable**																								
Clinical label design	**Variable**																								
Manufacture clinical supplies	**Variable**																								

Decision Point #7: IND Preparation and Submission

Following the pre-IND meeting with the FDA, and conducting any additional studies, the IND is prepared in common technical document format to support the clinical protocol. The IND is prepared in 5 separate modules that include administrative information, summaries (CMC, nonclinical, clinical), quality data (CMC), nonclinical study reports and literature, and clinical study reports and literature (Table 18). Following submission of the IND to the FDA, there is a 30-day review period during which the FDA may ask for additional data or clarity on the information submitted. If after 30-days the FDA has communicated that there is no objection to the proposed clinical study, the IND is considered active and the clinical study can commence.

- Investigator's brochure preparation
- Protocol preparation and submission to IRB
- IND preparation and submission

Table 18: IND Preparation and Submission

		Year 1												Year 2											
Decision Point	Cost	M1	M2	M3	M4	M5	M6	M7	M8	M9	M10	M11	M12	M13	M14	M15	M16	M17	M18	M19	M20	M21	M22	M23	M24
#6 Clinical Supplies Manufacture	**$500,000**											**$2,355,000**													
#7 IND Preparation and Submission	**$500,000**														**$2,855,000**										
Investigator's brochure preparation	**Variable**																								
Protocol preparation and submission to IRB	**Variable**																								
IND preparation and submission	**Variable**																								

Decision Point #8: Human Proof of Concept

Human proof of concept may commence following successful submission of an IND (i.e. and IND that has not been placed on 'clinical hold'). The list below provides some information concerning human proof of concept (Table 19):

- IND Clearance
- Acceptable MTD
- Acceptable DR
- Evidence of human pharmacology

Table 19: Human Proof of Concept

		Year 2											
Decision Point	**Cost**	**M13**	**M14**	**M15**	**M16**	**M17**	**M18**	**M19**	**M20**	**M21**	**M22**	**M23**	**M24**
#7 IND Preparation and Submission	**$500,000**		**$2,855,000**										
#8 Human Proof of Concept	**$1,000,000**		**$3,855,000**										
IND Clearance	**Variable**												
Acceptable Maximum Tolerated Dose (MTD)	**Variable**												
Acceptable Dose Response (DR)	**Variable**												
Evidence of human pharmacology	**Variable**												

Section 3. Development of Drug Delivery Platform Technology

Historically about 40% of NCEs identified as possessing promise for development, based on drug-like qualities, progress to evaluation in humans. Of those that do make it into clinical trials, about 9 out of 10 fail. In many cases, innovative drug delivery technology can provide a "second chance" for promising compounds that have consumed precious drug-discovery resources, but were abandoned in early clinical trials due to unfavorable side-effect profiles. As one analyst observed, "pharmaceutical companies are sitting on abandoned goldmines that should be reopened and excavated again using the previously underutilized or unavailable picks and shovels developed by the drug delivery industry" (SW Warburg Dillon Read). Although this statement was made more than 10 years ago, it continues to apply.

Beyond enablement of new drugs, innovative approaches to drug delivery also hold potential to enhance marketed drugs (e.g., through improvement in convenience, tolerability, safety, and/or efficacy); expand their use (e.g., through broader labeling in the same therapeutic area and/or increased patient acceptance/compliance); or transform them by enabling their suitability for use in other therapeutic areas. These opportunities contribute enormously to the potential for value creation in the drug delivery field. Table 20 summarizes the decision points for the development of drug delivery platform technology.

Table 20: Summary of Decision Points for Drug Delivery Platform Technology

		Year 1				Year 2				Year 3				Year 4				Year 5				Year 6			
Decision Point	Cost	Q1	Q2	Q3	Q4	Q1	Q2	Q3	Q4	Q1	Q2	Q3	Q4	Q1	Q2	Q3	Q4	Q1	Q2	Q3	Q4	Q1	Q2	Q3	Q4
#1 Clinical Formulation Development	**$250,000**	**$250,000**																							

Table 20 continued from previous page.

		Year 1				Year 2				Year 3				Year 4				Year 5				Year 6			
Decision Point	Cost	Q1	Q2	Q3	Q4	Q1	Q2	Q3	Q4	Q1	Q2	Q3	Q4	Q1	Q2	Q3	Q4	Q1	Q2	Q3	Q4	Q1	Q2	Q3	Q4
#2 Development Plan	**$300,000**			**$550,000**																					
#3 Clinical Supplies Manufacture	**$500,000**				**$1,050,000**																				
#4 Preclinical Safety Data Package	**$800,000**						**$1,850,000**																		
#5 IND Preparation and Submission	**$500,000**										**$2,350,000**														
#6 Human Proof of Concept	**$1,000,000**											**$3,350,000**													
#7 Clinical Proof of Concept	**$2,500,000**															**$5,850,000**									

Decision Point #1: Clinical Formulation Development

- Prototype development
- Analytical methods development
- Prototype stability
- Prototype selection
- Clinical supplies release specification
- (Submit invention disclosure on novel formulation)

See Table 21 for a schematic representation of the time and costs associated with development at this stage.

Table 21: Clinical Formulation Development

		Year 1			
Decision Point	Cost	Q1	Q2	Q3	Q4
#1 Clinical Formulation Development	**$250,000**	**$250,000**			
Prototype development	**Variable**				
Analytical methods development	**Variable**				
Prototype stability	**Variable**				
Prototype selection	**Variable**				
Clinical supplies release specification	**Variable**				
(Submit invention disclosure on novel formulation)	**Variable**				
#2 Development Plan	**$300,000**			**$550,000**	

Decision Point #2: Development Plan

Preparation of a development plan allows the sponsor to evaluate the available information regarding the compound of interest (whether at the development stage or a previously marketed compound) to understand what information might be available to support the proposed indication and what additional information may be needed. The development path is dependent upon the proposed indication, change in formulation, route, and dosing regimen. The development plan that is prepared will take this information into account in order to determine what information or additional studies might be needed prior to submission of an IND and initiating first-in-man studies. A thorough search of the literature is important in order to capture available information to satisfy the data requirements for the IND. Any gaps identified would need to be filled with studies conducted by the sponsor. A pre-IND meeting with the FDA will allow the sponsor to present their plan to the FDA and gain acceptance (de-risk the program) prior to submission of the IND and conducting the first-in-man study (Table 22).

- CMC program strategy
- Preclinical program strategy
- Clinical proof of concept strategy
- Draft clinical protocol design
- Pre-IND meeting with the FDA

Table 22: Development Plan

		Year 1				Year 2			
Decision Point	Cost	Q1	Q2	Q3	Q4	Q1	Q2	Q3	Q4
#1 Clinical Formulation Development	**$250,000**	**$250,000**							
#2 Development Plan	**$300,000**			**$550,000**					
CMC program strategy	**Variable**								
Preclinical program strategy	**Variable**								
Clinical proof of concept strategy	**Variable**								
Draft clinical protocol design	**Variable**								
Pre-IND meeting with FDA	**Variable**								
#3 Clinical Supplies Manufacture	**$500,000**				**$1,050,000**				

Decision Point #3: Clinical Supplies Manufacture

- Select cGMP supplier and transfer manufacturing process
- Cleaning validation development
- Scale up lead formulation at GMP facility
- Clinical label design
- Manufacture clinical supplies

See Table 23 for a schematic representation of the time and costs associated with development at this stage.

Table 23: Clinical Supplies Manufacture

		Year 1				Year 2				Year 3			
Decision Point	Cost	Q1	Q2	Q3	Q4	Q1	Q2	Q3	Q4	Q1	Q2	Q3	Q4
#2 Development Plan	**$300,000**			**$550,000**									
#3 Clinical Supplies Manufacture	**$500,000**				**$1,050,000**								

Table 23 continued from previous page.

		Year 1				Year 2				Year 3			
Decision Point	Cost	Q1	Q2	Q3	Q4	Q1	Q2	Q3	Q4	Q1	Q2	Q3	Q4
Select cGMP supplier and transfer manufacturing process	**Variable**												
Cleaning validation development	**Variable**												
Scale up lead formulation at GMP facility	**Variable**												
Clinical label design	**Variable**												
Manufacture clinical supplies	**Variable**												
#4 Preclinical Safety Data Package	**$800,000**						**$1,850,000**						

Decision Point #4: Preclinical Safety Package

Preparation of the gap analysis/development plan will identify any additional studies that might be needed to support the development of the new delivery platform for the compound. Based on this assessment, as well as the intended patient population, the types of studies that will be needed to support the clinical program will be determined. It is possible that a pharmacokinetic study evaluating exposure would be an appropriate bridge to the available data in the literature (Table 24).

- Preclinical oral formulation development
- Bioanalytical method development
- Qualify GLP test article
- Transfer drug exposure/bioavailability assays to GLP laboratory
- ICH S7a (Safety Pharmacology) & S7b (Cardiac Tox) core battery of tests
- Toxicology bridging study

Table 24: Preclinical Safety Package

		Year 1				Year 2				Year 3			
Decision Point	Cost	Q1	Q2	Q3	Q4	Q1	Q2	Q3	Q4	Q1	Q2	Q3	Q4
#3 Clinical Supplies Manufacture	**$500,000**				**$1,050,000**								
#4 Preclinical Safety Data Package	**$800,000**						**$1,850,000**						
Preclinical oral formulation development	**Variable**												
Bioanalytical method development	**Variable**												
Qualify GLP test article	**Variable**												
Transfer drug exposure/bioavailability assays to GLP laboratory	**Variable**												
ICH S7a (Safety Pharmacology) & S7b (Cardiac Tox) core battery of tests	**Variable**												
Toxicology bridging study	**Variable**												
#5 IND Preparation and Submission	**$500,000**										**$2,350,000**		

Decision Point #5: IND Preparation and Submission

Following the pre-IND meeting with the FDA and conducting any additional studies, the IND is prepared in common technical document format to support the clinical protocol. The IND is prepared in 5 separate modules, which include administrative information, summaries (CMC, nonclinical, clinical), quality data (CMC), nonclinical study reports and literature, and clinical study reports and literature. Following submission of the IND to the FDA, there is a 30-day review period during which the FDA might ask for additional data or

clarity on the information submitted. If after 30-days the FDA has communicated that there is no objection to the proposed clinical study, the IND is considered active and the clinical study can commence (Table 25).

- Investigator's brochure preparation
- Protocol preparation and submission to IRB
- IND preparation and submission

Table 25: IND Preparation and Submission

		Year 2				Year 3			
Decision Point	Cost	Q1	Q2	Q3	Q4	Q1	Q2	Q3	Q4
#4 Preclinical Safety Data Package	**$800,000**		**$1,850,000**						
#5 IND Preparation and Submission	**$500,000**						**$2,350,000**		
Investigator's brochure preparation	**Variable**								
Protocol preparation and submission to IRB	**Variable**								
IND preparation and submission	**Variable**								

Decision Point #6: Human Proof of Concept

Human proof of concept may commence following successful submission of an IND (i.e. and IND that has not been placed on 'clinical hold'). The list below provides some information concerning human proof of concept (Table 26):

- IND Clearance
- Acceptable MTD
- Acceptable DR
- Evidence of human pharmacology

Table 26: Human Proof of Concept

		Year 3				Year 4			
Decision Point	Cost	Q1	Q2	Q3	Q4	Q1	Q2	Q3	Q4
#5 IND Preparation and Submission	**$500,000**		**$2,350,000**						
#6 Human Proof of Concept	**$1,000,000**		**$3,350,000**						
IND clearance	**Variable**								
Acceptable Maximum Tolerated Dose (MTD)	**Variable**								
Acceptable Dose Response (DR)	**Variable**								
Evidence of human pharmacology	**Variable**								

Decision Point #7: Clinical Proof of Concept

With acceptable DR and MTD having been defined during Phase I, in Phase II the project team will attempt to statistically demonstrate efficacy. More specifically, the outcome of Phase II should reliably predict the likelihood of success in Phase III randomized trials (Table 27).

- IND Clearance
- Acceptable PK/PD profile
- Efficacy
- Direct and indirect biomarkers
- Safety and tolerance assessments

Table 27: Clinical Proof of Concept

		Year 3				Year 4				Year 5				Year 6			
Decision Point	Cost	Q1	Q2	Q3	Q4	Q1	Q2	Q3	Q4	Q1	Q2	Q3	Q4	Q1	Q2	Q3	Q4
#6 Human Proof of Concept	**$1,000,000**		**$3,350,000**														
#7 Clinical Proof of Concept	**$2,500,000**							**$5,850,000**									
IND clearance	**Variable**																
Acceptable PK/PD profile	**Variable**																
Efficacy	**Variable**																
Direct and indirect biomarkers	**Variable**																
Safety and tolerance assessments	**Variable**																

Section 4. Alternative NCE Strategy: Exploratory IND

The plans outlined previously in these guidelines describe advancement of novel drugs as well as repurposed or reformulated, marketed drug products to human and/or clinical proof of concept trials using the traditional or conventional early drug development, IND approach. This section of the guidelines outlines an alternative approach to accelerating novel drugs and imaging molecules to humans employing a Phase 0, exploratory IND strategy (exploratory IND). The exploratory IND strategy was first issued in the form of draft guidance in April, 2005. Following a great deal of feedback from the public and private sectors, the final guidance was published in January, 2006.

Phase 0 describes clinical trials that occur very early in the Phase I stage of drug development. Phase 0 trials limit drug exposure to humans (up to 7 days) and have no therapeutic intent. Phase 0 studies are viewed by the FDA and National Cancer Institute (NCI) as important tools for accelerating novel drugs to the clinic. There is some flexibility in data requirements for an exploratory IND. These requirements are dependent on the goals of the investigation (e.g., receptor occupancy, pharmacokinetics, human biomarker validation), the clinical testing approach, and anticipated risks.

Exploratory IND studies provide the sponsor with an opportunity to evaluate up to five chemical entities (optimized chemical lead candidates) or formulations at once. When an optimized chemical lead candidate or formulation is selected, the exploratory IND is then closed, and subsequent drug development proceeds along the traditional IND pathway. **This approach allows one, when applicable, to characterize the human pharmacokinetics and target interaction of chemical lead candidates. Exploratory IND goals are typically to:**

- Characterize the relationship between mechanism of action and treatment of the disease; in other words, to validate proposed drug targets in humans
- Characterize the human pharmacokinetics
- Select the most promising chemical lead candidate from a group of optimized chemical lead candidates (note that the chemical lead candidates do not necessarily have the same chemical scaffold origins)
- Explore the bio-distribution of chemical lead candidates employing imaging strategies (e.g., PET studies)

Exploratory IND studies are broadly described as “microdosing” studies and clinical studies attempting to demonstrate a pharmacologic effect. Exploratory IND or Phase 0 strategies must be discussed with the relevant regulatory agency before implementation. These studies are described below.

Microdosing studies are intended to characterize the pharmacokinetics of chemical lead candidates or the imaging of specific human drug targets. Microdosing studies are not intended to produce a pharmacologic effect. Doses are limited to less than 1/100th of the dose predicted (based on preclinical data) to produce a

pharmacologic effect in humans, **or a dose of less than 100 µg/subject, whichever is less.** Exploratory IND-enabling preclinical safety requirements for microdosing studies are substantially less than the conventional IND approach. In the US, a single dose, single species toxicity study employing the clinical route of administration is required. Animals are observed for 14 days following administration of the single dose. Routine toxicology endpoints are collected. The objective of this toxicology study is to identify the minimally toxic dose, or alternatively, demonstrate a large margin of safety (e.g., 100x). Genotoxicity studies are not required. The EMEA, in contrast to the FDA, requires toxicology studies employing two routes of administration, intravenous and the clinical route, prior to initiating microdosing studies. Genotoxicity studies (bacterial mutation and micronucleus) are required. Exploratory IND workshops have discussed or proposed the allowance of up to five microdoses administered to each subject participating in an exploratory IND study, provided each dose does not exceed 1/100th the NOAEL or 1/100th of the anticipated pharmacologically active dose, or the total dose administered is less than 100 mcg, whichever is less. In this case, doses would be separated by a washout period of at least six pharmacokinetic terminal half-lives. Fourteen-day repeat toxicology studies encompassing the predicted therapeutic dose range (but less than the MTD) have also been proposed to support expanded dosing in microdosing studies.

Exploratory IND clinical trials designed to produce a pharmacologic effect were proposed by PhRMA in May 2004, based on a retrospective analysis of 106 drugs that supported the accelerated preclinical safety-testing paradigm. In Phase 0 studies designed to produce a pharmacologic effect, up to five compounds can be studied. The compounds must have a common drug target, but do not necessarily have to be structurally related. Healthy volunteers or minimally ill patients may receive up to 7 repeated doses in the clinic. The goal is to achieve a pharmacologic response but not define the MTD. Preclinical safety requirements are greater compared to microdosing studies. Fourteen-day repeat toxicology studies are required and conducted in rodents (i.e., rats), with full clinical and histopathology evaluation. In addition, a full safety pharmacology battery, as described by ICH S7a, is required. In other words, untoward pharmacologic effects on the cardiovascular, respiratory, and central nervous systems are characterized prior to Phase 0. In addition, genotoxicity studies employing bacterial mutation and micronucleus assays are required. In addition to the 14-day rodent toxicology study, a repeat dose study in a non-rodent specie (typically dog) is conducted at the rat NOAEL dose. The duration of the non-rodent repeat dose study is equivalent to the duration of dosing planned for the Phase 0 trial. If toxicity is observed in the non-rodent specie at the rat NOAEL, the chemical lead candidate will not proceed to Phase 0. The starting dose for Phase 0 studies is defined typically as 1/50th the rat NOAEL, based on a per meter squared basis. Dose escalation in these studies is terminated when: 1) a pharmacologic effect or target modulation is observed, 2) a dose equivalent (e.g., scaled to humans on a per meter squared basis) to one-fourth the rat NOAEL, or 3) human systemic exposure reflected as AUC reaches ½ the AUC observed in the rat or dog in the 14-day repeat toxicology studies, whichever is less.

Early phase clinical trials with terminally ill patients without therapeutic options, involving potentially promising drugs for life threatening diseases, may be studied under limited (e.g., up to 3 days dosing) conditions employing a facilitated IND strategy. As with the Phase 0 strategies described above, it is imperative that this approach be defined in partnership with the FDA prior to implementation.

The reduced preclinical safety requirements are scaled to the goals, duration and scope of Phase 0 studies. Phase 0 strategies have merit when the initial clinical experience is not driven by toxicity, when pharmacokinetics are a primary determinant in selection from a group of chemical lead candidates (and a bioanalytical method is available to quantify drug concentrations at microdoses), when pharmacodynamic endpoints in surrogate (e.g., blood) or tumor tissue is of primary interest, or to assess PK/PD relationships (e.g., receptor occupancy studies employing PET scanning).

PhRMA conducted a pharmaceutical industry survey in 2007 to characterize the industry's perspective on the current and future utility of exploratory IND studies (3). Of the 16 firms who provided survey responses, 56%

indicated they had either executed or were planning to execute exploratory IND development strategies. The authors concluded that the merits of exploratory INDs continue to be debated, however, this approach provides a valuable option to advancing drugs to the clinic.

There are limitations to the exploratory IND approach. Doses employed in Phase 0 studies might not be predictive of doses over the human dose range (up to the maximum tolerated dose). Phase 0 studies in patients raises ethical issues compared to conventional Phase I, in that escalation into a pharmacologically active dose range might not be possible under the exploratory IND guidance. The Phase 0 strategy is designed to kill drugs early that are likely to fail based on PK or PK/PD. Should Phase 0 lead to a "Go" decision, however, a conventional IND is required for subsequent clinical trials, adding cost and time. **Perhaps one of the most compelling arguments for employing an exploratory IND strategy is in the context of characterizing tissue distribution (e.g., receptor occupancy following PET studies) after microdosing.**

Section 5. Orphan Drug Designation

Development programs for cancer drugs are often much more complex as compared to drugs used to treat many other indications. This complexity often results in extended development and approval timelines. In addition, oncology patient populations are often much smaller by comparison to other more prevalent indications. These factors (e.g., limited patent life and smaller patient populations) often complicate commercialization strategies and can, ultimately, make it more difficult to provide patient access to important new therapies.

To help manage and **expedite the commercialization of drugs used to treat rare diseases, including many cancers,** the Orphan Drug Act was signed into law in 1983. This law provides incentives to help sponsors and investigators develop new therapies for diseases and conditions of less than 200,000 cases per year allowing for more realistic commercialization.

The specific incentives for orphan-designated drugs are as follows:

- Seven years of exclusive marketing rights to the sponsor of a designated orphan drug product for the designated indication once approval to market has been received from the FDA
- A credit against tax for qualified clinical research expenses incurred in developing a designated orphan product
- Eligibility to apply for specific orphan drug grants

A sponsor may request orphan drug designation for:

- A previously unapproved drug
- A new indication for a marketed drug
- A drug that already has orphan drug status—if the sponsor is able to provide valid evidence that their drug may be clinically superior to the first drug

A sponsor, investigator, or an individual may apply for orphan drug designation prior to establishing an active clinical program or can apply at any stage of development (e.g., Phase 1 – 3). If orphan drug designation is granted, clinical studies to support the proposed indication are required. A drug is not given orphan drug status and, thus marketing exclusivity, until the FDA approves a marketing application. Orphan drug status is granted to the first sponsor to obtain FDA approval and not necessarily the sponsor originally submitting the orphan drug designation request.

There is no formal application for an orphan drug designation. However, the regulations (e.g., 21 CRF 316) identify the components to be included. **An orphan drug designation request is typically a five- to ten-page document** with appropriate literature references appended to support the prevalence statements of less than 200,000 cases/year. The orphan drug designation request generally includes:

- The specific rare disease or condition for which orphan drug designation is being requested
- Sponsor contact, drug names, and sources
- A description of the rare disease or condition with a medically plausible rationale for any patient subset type of approach
- A description of the drug and the scientific rationale for the use of the drug for the rare disease or condition
- A summary of the regulatory status and marketing history of the drug
- Documentation (for a treatment indication for the disease or condition) that the drug will affect fewer than 200,000 people in the United States (prevalence)
- Documentation (for a prevention indication [or a vaccine or diagnostic drug] for the disease or condition) that the drug will affect fewer than 200,000 people in the United States per year (incidence)
- Alternatively, a rationale may be provided for why there is no reasonable expectation that costs of research and development of the drug for the indication can be recovered by sales of the drug in the United States

Following receipt of the request, the FDA Office of Orphan Product Development (OOPD) will provide an acknowledgment of receipt of the orphan drug designation request. The official response will typically be provided within 1 to 3 months following submission. Upon notification of granting an orphan drug designation, the name of the sponsor and the proposed rare disease or condition will be published in the federal register as part of public record. The complete orphan drug designation request is placed in the public domain once the drug has received marketing approval in accordance with the Freedom of Information Act.

Finally, the sponsor of an orphan designated drug must provide annual updates that contain a brief summary of any ongoing or completed nonclinical or clinical studies, a description of the investigational plan for the coming year, any anticipated difficulties in development, testing, and marketing, and a brief discussion of any changes that may affect the orphan drug status of the product

Conclusion

While many authors have described the general guidelines for drug development (4,5, etc.), no one has outlined the process of developing drugs in an academic setting. It is well known that the propensity for late stage failures has lead to a dramatic increase in the overall cost of drug development over the last 15 years. It is also commonly accepted that the best way to prevent late stage failures is by increasing scientific rigor in the discovery, preclinical, and early clinical stages. Where many authors present drug discovery as a single monolithic process, we intend to reflect here that there are multiple decision points contained within this process.

An alternative approach is the exploratory IND (Phase 0) under which the endpoint is proof of principle demonstration of target inhibition (6). This potentially paradigm-shifting approach might dramatically improve the probability of late stage success and may offer additional opportunities for academic medical centers to become involved in drug discovery and development.

References

Literature Cited

1. Pre-IND Consultation Program. US Food and Drug Administration. [Online] [Cited: August 17, 2010.] Available at: http://www.fda.gov/Drugs/DevelopmentApprovalProcess/HowDrugsareDevelopedandApproved/ApprovalApplications/InvestigationalNewDrugINDApplication/Overview/default.htm.
2. Apparent activity in high-throughput screening: origins of compound-depedent assay interference. Thorne N, et al. 2010, Curr Opin Chem Biol, p. doi:10.1016/j.cbpa.2010.03.020.

3. Karara AH, Edeki T, McLeod J, et al. PhRMA survey on the conduct of first-in-human clinical trials under exploratory investigational new drug applications. J Clin Pharmacol. 2010;50:380–391. PubMed PMID: 20097935.
4. The price of innovation: new estimates of drug development costs. DiMasi, J.A., Hansen, R.W., and Grabowski, H.G. 2003, Journal of Health Economics, pp. 151-185.
5. Mehta, Shreefal S. Commercializing Successful Biomedical Technologies. Cambridge : Cambridge University Press, 2008.
6. Phase 0 Clinical Trails in Cancer Drug Development: From FDA Guidance to Clinical Practice. Kinders, Robert, et al. 2007, Molecular Interventions, pp. 325-334.

Additional References

Eckstein, Jens. *ISOA/ARF Drug Development Tutorial.*

In Vitro Biochemical Assays

Nathan P. Coussens, Timothy L. Foley, Sam R.J. Hoare, James McGee, and G. Sitta Sittampalam

Analyzing Kinetic Binding Data

Sam R.J. Hoare[1]

Created: April 1, 2021.

Abstract

Biological and therapeutic agents exert their actions by interacting with specific molecular targets. This process of ligand binding takes time, for the ligand to associate with the target, forming the target-ligand complex, and for the complex to break down. These processes are quantified by the association and dissociation rate constants. Knowledge of these rates can be important in the optimization of new therapeutics and in understanding the biological behavior of target proteins. Experimentally the rates are determined by measuring the time course of test compound binding to the target, directly or indirectly. This chapter describes how to analyze these time course data to determine the binding kinetic rate constant values. Data are analyzed by curve fitting using familiar nonlinear regression data analysis programs (exemplified here with Prism from GraphPad Software). The concepts are introduced using simple, direct target-ligand binding assays. Recently, indirect competition binding methods have become popular for evaluating binding kinetics of the large numbers of compounds encountered in drug discovery. Data analysis for this "Competition kinetics" approach is presented using a step-by-step guide, together with instruction on troubleshooting, limits of sensitivity and experimental artifacts. More complex scenarios are then introduced, including multistep binding interactions and the use of functional assays to quantify ligand binding kinetics. By describing how to quantify ligand binding kinetics and interpret the data, this chapter enables investigators to evaluate the role of the temporal dimension of binding activity to their targets of interest.

Introduction

Therapeutic molecules exert their action by interacting with specific molecular targets. The first step in this binding process is the association of the drug ligand molecule with the target. Once bound, the ligand can then dissociate from the target (assuming the ligand binds reversibly and not covalently). These processes take time. This temporal dimension is referred to as binding kinetics or binding dynamics (1,2). The time it takes for a ligand to associate with the target is governed by the association rate, which is the rate of ligand recognition by the target. The time it takes the ligand to dissociate is determined by the dissociation rate, which quantifies the stability of the target-ligand complex. These principles are shown using animations of the binding process in the following video.

Author Affiliation: 1 Pharmechanics, LLC; Email: sam.hoare@pharmechanics.com.

Corresponding author.

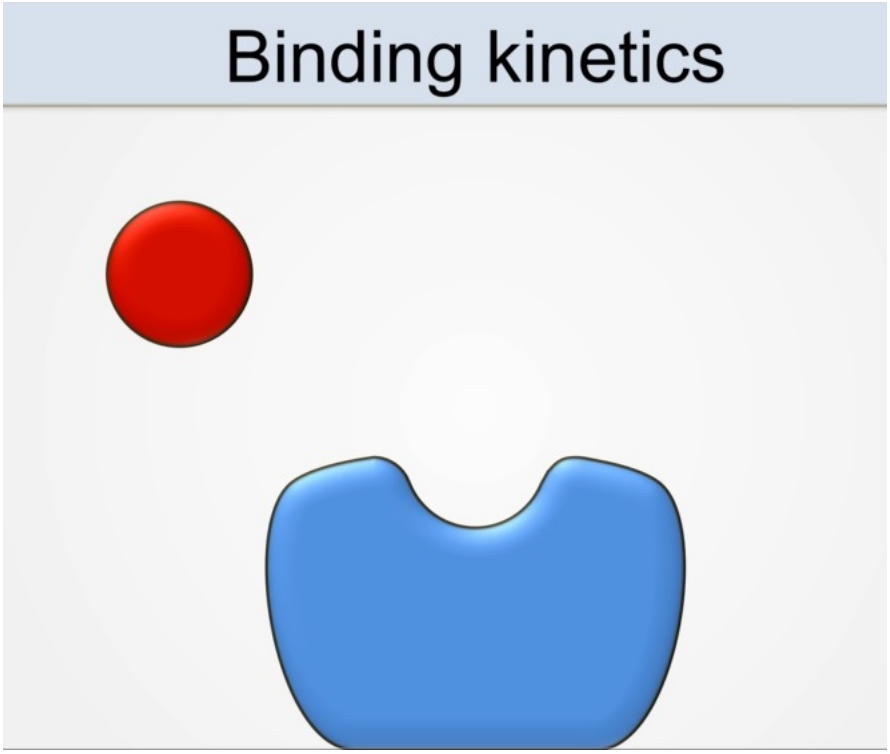

Video 1. Binding kinetics animation.
Download video

The binding rates are fundamental properties of the drug-target interaction. They can impact the therapeutic action and side effect profile of the ligand, as described in numerous recent reviews (1-16). They also impact quantification of other drug parameters, such as affinity, resulting in erroneous estimates of activity if the rates are not considered appropriately (17-19). Useful introductory webinars are available here and here.

The purpose of this chapter is to describe how to measure the kinetics of target-ligand interaction, specifically how to analyze binding kinetic data to measure the binding rate constants. Step-by-step analysis guides are provided, for the popular curve fitting program Prism (GraphPad Software, Inc). It is assumed the investigator has in hand an assay for measuring ligand binding. (Binding assay methods, briefly summarized in Basic Principles of Ligand Binding Kinetics and Table 1, are extensively reviewed in refs (15,16,20-22).) The chapter is organized as follows.

- **Basic principles of ligand binding kinetics.**
- **Kinetic analysis methods for direct target-ligand binding assays.** Applicable to targets where technology is available to directly measure target-ligand interaction.
- **Competition kinetics: Quantifying kinetics by competition against a tracer ligand.** Often it isn't feasible to measure ligand binding directly. Instead, competition binding approaches are employed where test ligand binding is assessed by inhibition of labeled "Tracer" ligand binding. This competition method can be used to quantify binding kinetics.
- **Compound washout method**. An indirect method popular for kinase enzymes is the compound washout method, in which target and compound are pre-incubated, then compound washed out, and compound dissociation recorded by its ability to slow association of a tracer ligand.
- **Complex binding mechanisms.** Sometimes the ligand binding mechanism is complex, for example involving multiple conformational states of the target. These more complex binding mechanisms and methods to measure their kinetics are introduced here.

- **Binding kinetics from functional assays.** For some targets, only a functional assay is available (e.g. enzyme catalysis or receptor signaling) and in this section methods to measure ligand binding kinetics in these assays are introduced.
- **Appendix**. Theoretical description of target-ligand binding and the equations used to analyze the data.

Table 1. Assays for measuring target-ligand interactions and their suitability for kinetic analysis

Assay modality	Continuous read?	Notes	References
Binding assay			
Fluorescent ligand binding	Yes	Ideal technology for kinetics, particularly new resonance energy transfer technologies.	(7,15,28,29)
Surface plasmon resonance (SPR)	Yes	Usually requires purified protein, or solubilized membrane targets.	(27)
Calorimetry	Yes	Usually requires purified protein.	(30)
Radioligand binding - filtration	No	Established methodology but endpoint format cumbersome for kinetics.	(22)
Radioligand binding – Scintillation Proximity Assay (SPA)	Yes	SPA modality enables continuous read capability for radioligand binding, though long read times can reduce sensitivity.	(22)
Functional assay			
Enzyme assays	Yes	For inhibitors, e.g. jump dilution method.	(31-34)
Cell signaling assays	Yes	For inhibitors. A short response time is desirable.	(35-39)

Basic Principles of Ligand Binding Kinetics

Most drugs bind their target by the classic bimolecular interaction. A single ligand molecule binds to a single site on the target, in a single step, as illustrated in Figure 1. The association step is governed by a rate constant called the association rate constant, denoted by the parameter k_1. The binding is reversible and the rate of breakdown of the complex is governed by a rate constant termed the dissociation rate constant, denoted by k_2. The process is shown in the video Binding kinetics animation (video 1). The interaction can be written schematically as:

$$R + L \underset{k_2}{\overset{k_1}{\rightleftharpoons}} RL$$

where R is the target, L the ligand, and RL the target-ligand complex.

The appearance of this mechanism in binding data is shown in Figure 2, where the time courses of association and dissociation are presented, and also in the video Binding kinetics animation (video 1). The y axis is the concentration of target-ligand complexes. In the association time course data, following mixture of target and ligand, the amount of the target-ligand complex rises rapidly at the beginning (Figure 2A). The increase then slows down and then the level of binding approaches a plateau. This plateau represents the equilibrium level of binding (also referred to as binding at steady state). This curve shape is called an association exponential curve. Dissociation of the target-ligand population over time is shown in Figure 2B. Decline of the population is rapid at first, then slows, then approaches zero at which point all the complexes have broken down. The dissociation curve follows the classic exponential decay curve, familiar in radioactive decay.

Unfortunately, the rate terms used to quantify kinetics are not intuitive for the uninitiated investigator. The units of the association rate constant are molar$^{-1}t^{-1}$ and of the dissociation rate constant t^{-1} (where t is time, in

minutes or seconds). The larger the rate constant value, the more rapid the binding event (association or dissociation). In an attempt to make the dissociation data easier to interpret, dissociation is often quantified as the residence time (RT), which is the reciprocal of k_2, i.e. 1 / k_2. Alternatively, sometimes dissociation is quantified as the half-time, which is 0.693 / k_2. These parameters give an estimate of the stability of the target-ligand complex, and so are more intuitive. However, the RT concept can give the misleading impression that every individual target-ligand complex in the population breaks down at this time. This is not the case. Dissociation is a random process (formally, a stochastic process) where an individual complex among the population can break down more rapidly or more slowly than the RT. The RT is an average of the population, formally the time at which the 63rd percentile of the population of targets breaks down. Detailed reviews on the mechanics of the association and dissociation process are available (20,23-26).

The rate constants are related to the binding affinity, i.e. the concentration of ligand required to occupy 50% of the targetss at equilibrium. The equilibrium constant (K_d), a measure of affinity, is related to the rate constants as follows:

$$K_d = \frac{k_2}{k_1}$$

This relationship allows an alternative method for measuring affinity, rather than the standard method of titrating the ligand concentration and incubating until equilibrium is reached. Instead, the affinity is determined by measuring the association and dissociation rates (as described below) and affinity then calculated using the equation. This method is used routinely in surface plasmon resonance (SPR) binding assays (27).

Kinetic Analysis Methods for Direct Target-Ligand Binding Assays

The goal is to measure the association rate constant k_1 and dissociation rate constant k_2. Here we measure the rate constants when an assay is available to directly quantify interaction of the ligand of interest with the target. A very broad array of assay technologies is available for measuring ligand binding and for the purposes of this chapter it is assumed the investigator has selected an appropriate binding assay for their target of interest. The methods and their suitability for kinetics are summarized in Table 1. The reader is referred to recent comprehensive reviews on binding assays ideally suited for kinetic measurements (15,16,20,21). The ideal assay permits serial reading of the binding reaction vessel, the “Real-time” continuous read modality, that enables multiple time point measurements in the same assay plate. Less ideal are end-point assays requiring a separate plate for each time point. Fluorescence or bioluminescence resonance energy transfer technologies are particularly useful for the continuous read modality (7,15,28,29).

The type of data analyzed is specific binding, i.e. the ligand binding signal that is specific to the target. This involves subtracting nonspecific binding (to other components in the assay and assay surfaces) from the total ligand binding signal. It is best practice to do this for each time point of the time course, in case there is a slight drift of the nonspecific binding signal over time. Ideally nonspecific binding will remain constant over time. If there is a major drift of nonspecific binding this can indicate technical issues with the assay that need to be resolved, e.g. photobleaching of fluorescent ligands.

Association Rate Constant from a Direct Target-Ligand Binding Assay

The association rate constant is measured using a target-ligand association assay. Ligand and target are combined and then binding of the target-ligand complex is measured at various time points (Figure 3). The resulting association curve conforms to an exponential association curve, as described above. Multiple concentrations of tracer are tested in the experiment and the data are analyzed in a two-step process. First, the time course data are fit to an exponential equation. This yields a parameter called the observed association rate, a

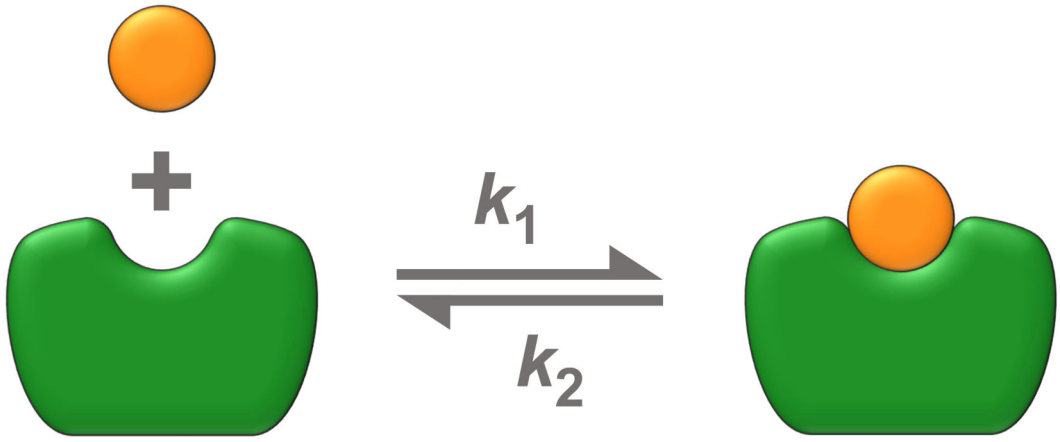

Figure 1. Simple bimolecular target-ligand binding interaction. Target (in green) interacts reversibly with ligand (orange). The rate of association, forming the target-ligand complex, is determined by the association rate constant, k_1. The complex can then dissociate, defined by the dissociation rate constant, k_2.

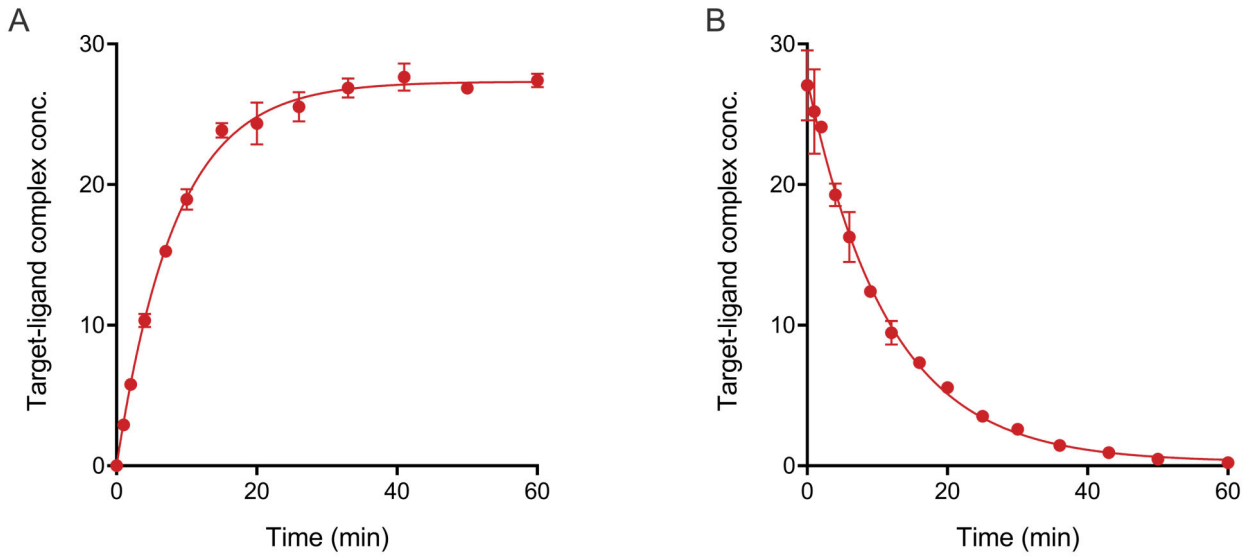

Figure 2. Time course data for target-ligand association (A) and dissociation (B). Curves are fits to exponential equations (A, Eq. 1; B, Eq. 2). Data points are the mean ± SEM of two technical replicates.

separate value for each ligand concentration. Second, the observed association rate is plotted against the ligand concentration. The data are then fit by linear regression. k_1 is then determined, as the gradient of the line.

The assay setup considerations are detailed in Box 1. Enough time points should be collected to properly define the curve, particularly the rise phase and plateau. Some iteration will likely be required to identify the optimal range of time points to satisfy these criteria. The concentration of tracer should span at least a 10-fold range with concentrations above and below the K_d. Precise ligand serial dilution is required, i.e. there should be minimal loss of ligand to surfaces on serial dilution. This is particularly important for high-affinity ligands where the concentration in the experiment is in the low nM or pM range. The concentration of ligand bound at the plateau of the time course should ideally be less than 10% of the total ligand concentration, as described in (22) ("Zone A") although < 20% is acceptable. It is possible to analyze data when a substantial fraction of the ligand is bound

by the target but this requires a different analysis (see, for example, Eq. 11 in ref. (40)). The tracer and target must be stable over the duration of the experiment.

Representative data for the association experiment are shown in Figure 3, for six concentrations of ligand. Note that as the concentration of ligand increases, the rate of association increases. This is evident visually by the steepness of the initial part of the time course increasing as the ligand concentration increases (Figure 3A). This is because association is driven by mass action; the more ligand, the faster the target becomes occupied. Now we proceed with the data analysis. The first step is to fit the time course data to the appropriate exponential equation. The equation used is the association exponential equation, which emerges from the underlying theory of target-ligand binding kinetics described in the Appendix. This equation is Eq. 1:

$$[\mathrm{RL}] = [\mathrm{RL}]_{t(inf)} \times \left(1 - e^{-k_{obs}t}\right) \quad \text{Eq. 1}$$

where [RL] is the concentration of target-ligand complex (the y axis value), t the time (the x axis value), and $[\mathrm{RL}]_{t(inf)}$the concentration of target-ligand complex at the plateau, i.e. at infinite time. k_{obs} is a parameter termed the observed rate constant. It is the observed rate of association of ligand with target at the concentration of ligand tested. It is important to stress that k_{obs} is not the same as the association rate constant, k_1. k_{obs} is related to k_1, as described below.

The time course data can be analyzed using commercially-available software, including Prism from GraphPad Software, Inc., XLfit from ID Business Solutions Ltd., and SigmaPlot from Systat Software, Inc. Eq. 1 is built into these programs. Here we show how to analyze these data using Prism (Version 8 is used but the equations are available in all previous versions). A step-by-step guide is shown in the supplementary file "Association data analysis." The procedure employs nonlinear regression to fit the time course data to the exponential association equation (Eq. 1). Data for each concentration of ligand is fit to the equation, yielding a k_{obs} value for each concentration (Figure 3A). The built-in equation in Prism is called, "One-phase association."(41) Note this equation is formatted slightly differently from Eq. 1. (Y0 in the Prism equation is binding at $t = 0$ (constrained to be zero), Span is equivalent to $[\mathrm{RL}]_{t(inf)}$, and K is equivalent to k_{obs} (41)).

The second step is the determination of k_1. This is done by plotting the k_{obs} values versus the concentration of ligand (Figure 3B). The data are then fit by linear regression to determine the slope and intercept of the line (as detailed in the supplementary file "Association data analysis"). The k_1 value is the gradient of the line. Applying this analysis to the data in Figure 3 gives a k_1 value of 1.0×10^7 $\mathrm{M^{-1}min^{-1}}$. This analysis assumes the experiment works ideally. Box 2 details troubleshooting tips when the data do not conform to the ideal.

The underlying theory of this second step is the equation defining the observed association rate. This equation, derived in the Appendix, is:

$$k_{obs} = [\mathrm{L}]k_1 + k_2$$

This is a straight line equation of the form $y = mx + c$, where the gradient m is equal to k_1. This equation also indicates something interesting. The dissociation rate constant k_2 can in principle, also be estimated from this analysis – visual inspection of the equations indicates it is the y intercept of the straight line equation. However, this approach is not advised for measuring k_2 – it is better to measure this parameter directly using a dissociation experiment, as described next.

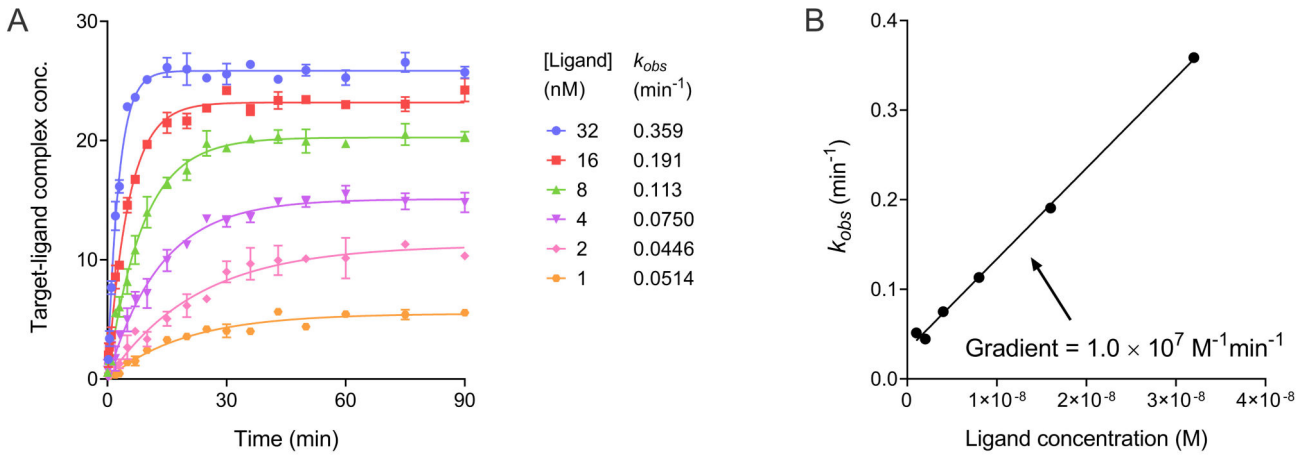

Figure 3. Measurement of k_1, the association rate constant, in a direct target-ligand binding assay. k_1 is determined in a two-step process. First, as shown in panel A, the time course of formation of the target-ligand complex is measured for multiple concentrations of ligand (see Box 1 for conditions). These data are then fit by nonlinear regression to the association exponential equation (Eq. 1) as detailed in the step-by-step guide "Association data analysis" in supplementary files. This analysis yields a fitted value of k_{obs}, the observed association rate, for each concentration of ligand. These k_{obs} values are shown on the legend in panel A. In the second part of the analysis, shown in panel B, the k_{obs} values are plotted against the ligand concentration. These data are then fit to the straight line equation. The gradient of this line is k_1 (1.0×10^7 $M^{-1}min^{-1}$). Data points in Panel A are the mean ± SEM of two technical replicates.

Box 1: Association rate constant assay considerations.

Time point range

Enough time points should be taken to define the curve. Ideally at least six time points on the initial rise phase of the association curve should be taken, and at least six after the midpoint of the curve. The time points should extend long enough to properly define the plateau of the curve. Some iteration will likely be required to identify the optimal range of time points to satisfy these criteria. The time range is dependent on the type of target and the investigator is advised to examine the literature on other targets in the class in selecting the initial time range.

Ligand concentration range

At least six concentrations are recommended that ideally span at least a 10-fold range: two concentrations below the K_d concentration, the K_d concentration itself, and three concentrations above the K_d. Representative data are shown in Figure 3, for a ligand with K_d of 4 nM, employing ligand concentrations of 1, 2, 4, 8, 16 and 32 nM.

Target concentration

The target concentration should be low enough that < 20% of the ligand added is bound by the target at equilibrium (i.e. at the plateau of the time course). Ideally < 10% should be bound but this is not always practical because sufficient target-ligand complex is required to minimize variability.

Stability

The target and ligand should be stable for the duration of the time course. For fluorescent ligands, this requires minimal photobleaching upon the repeated excitation of the fluorophore in continuous-read mode.

Box 2 Troubleshooting the association rate constant measurement.

k_{obs} vs ligand concentration graph is not linear

Imprecise serial dilution of ligand. Use low-binding surface plasticware and an ideal solvent (e.g. DMSO for small molecules) rather than assay buffer for serial dilution. If a radioligand is being used, count the dose to determine the concentration precisely.

Binding mechanism does not conform to the simple single-site binding interaction. Particularly evident if the k_{obs} vs [L] plot is a hyperbola (see graph at bottom right). Use alternative, appropriate equation for the binding mechanism (see Complex Binding Mechanisms), e.g. the post-binding conformational change model – see ref. (42).

Time course curve not fit well by association exponential equation

Instability of ligand and/or target, evident by fading time course (see below, left graph). Check stability of ligand and target. Add protease inhibitors, reduce temperature.

Binding mechanism does not conform to the simple single-site binding interaction. Evident by two phase time course (see below, center graph) and rise-and-fall curve shape. Often observed in whole-cell assays where targets are susceptible to a series of kinetic regulation events. Use membranes for membrane-associated targets (e.g. GPCRs) or purified proteins (e.g. kinases) to minimize regulation events and simplify the binding kinetics. If complex binding curves result from complex binding mechanism, use alternative, appropriate equation (Complex Binding Mechanisms).

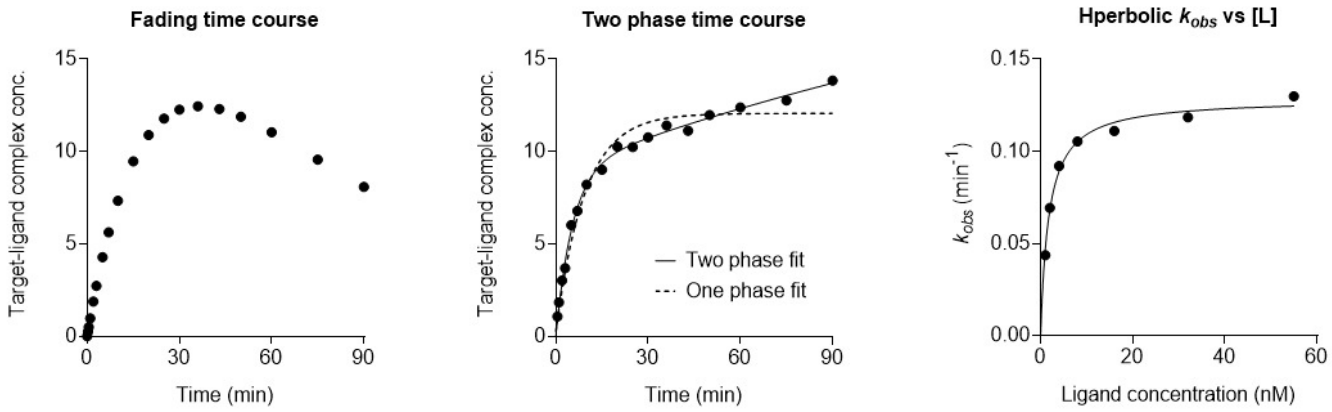

Dissociation Rate Constant from a Direct Target-Ligand Binding Assay

Measuring dissociation of ligand from a target requires a two-step assay. First, the target-ligand complex needs to form. Ligand and target are incubated together for a sufficient time, usually until equilibrium has been approached (the plateau of the association curve). In the next phase, the dissociation of ligand from the target is measured. This is initiated by an experimental intervention that stops association of the ligand with the target. With association blocked, the only process that takes place is dissociation. This results in a decrease of the target-ligand complex concentration over time (Figure 2B). In this way, the rate of dissociation can be quantified. This is usually done for a single concentration of ligand, at a concentration suitable to obtain sufficient signal, typically 3-fold the K_d concentration.

The intervention that initiates the dissociation phase is of two types: 1) If the ligand is labeled, an excess of unlabeled ligand is added. The excess prevents association by out-competing the labeled ligand for binding to

the target. The concentration of unlabeled ligand used is 100-300-fold the IC_{50} for the ligand in a competition binding assay versus the labeled ligand. 2) Washout of the labeled ligand. With one exception, this method is not recommended because it is challenging to determine that the labeled ligand has been completely washed out, especially in cell membrane-based binding assays employing hydrophobic ligands. The exception is SPR assays, in which washing of the surface is a continuous default process in the assay modality (27). In SPR assays, dissociation is initiated by the washout method.

Representative data are shown in Figure 2B. These binding data are specific tracer binding, i.e. data from which nonspecific binding has been subtracted. (It is good practice to measure and subtract nonspecific binding at each time point.) After the dissociation phase is initiated, the target binding signal declines, with the shape of the decline being the exponential decay curve (Figure 2B). After sufficient time, the specific binding signal declines to zero, i.e. all the target-ligand complexes dissociate (see Box 3 for when the signal does not decline to zero). It is desirable to determine the level of binding immediately before the initiation of the dissociation phase, if possible (giving the binding level at $t = 0$ of the dissociation phase).

The data analysis is simpler than that for association, requiring only a single step. All that is required is fitting the data to an exponential decay equation by nonlinear regression. The equation is Eq. 2, derived in the Appendix:

$$[\mathrm{RL}] = \left[\mathrm{RL}\right]_{t0} \times e^{-k_2 t} \qquad \text{Eq. 2}$$

where $[\mathrm{RL}]_{t0}$ is the concentration of target-ligand complexes immediately before initiation of the dissociation phase (the $t = 0$ binding level) and k_2 the dissociation rate constant. Analyzing the data in Figure 2 gives a k_2 value of 0.086 min^{-1}. This corresponds to a RT of 1 / 0.086 = 12 min. The binding data used in the analysis is target-specific binding, as described above. This analysis can be done in commercially available software; Eq. 2 or an analogous equation is built into these programs. A step-by-step guide using Prism is provided in the supplementary file "Dissociation data analysis." The built-in equation in Prism is called, "One-phase decay." (43) Note this equation is formatted slightly differently from Eq. 2. It includes a baseline term called "Plateau" which is binding at infinite time (which is assumed to be zero in Eq. 2). The rate term is called "K," which is equivalent to k_2. Troubleshooting the analysis is presented in Box 3.

Box 3 Troubleshooting dissociation rate constant measurement.

Time course curve not fit well by exponential decay equation

A two-phase time course (see below, left graph) can indicate the binding mechanism does not conform to the simple single-site binding interaction. Use alternative, appropriate equation for the binding mechanism (see Complex Binding Mechanisms).

Dissociation curve plateaus above zero

Often observed for GPCR agonist ligands where the binding does not decay to zero. This indicates a long-lived receptor state, usually the G-protein-coupled state. Either GTP or GTPγS can be added to uncouple the receptor from the G-protein (44).

A compartment is present which the unlabeled ligand cannot access, or from which the labeled ligand cannot be washed out. This is occasionally observed in whole cell and membrane binding assays and can be resolved by adding a small amount of membrane permeabilizing agent (e.g. 50 μg/ml saponin).

The binding mechanism does not conform to the simple single-site binding interaction. In this case, use an alternative, appropriate equation for the binding mechanism (see Complex Binding Mechanisms).

Box 3 continues on next page...

Box 3 continued from previous page.

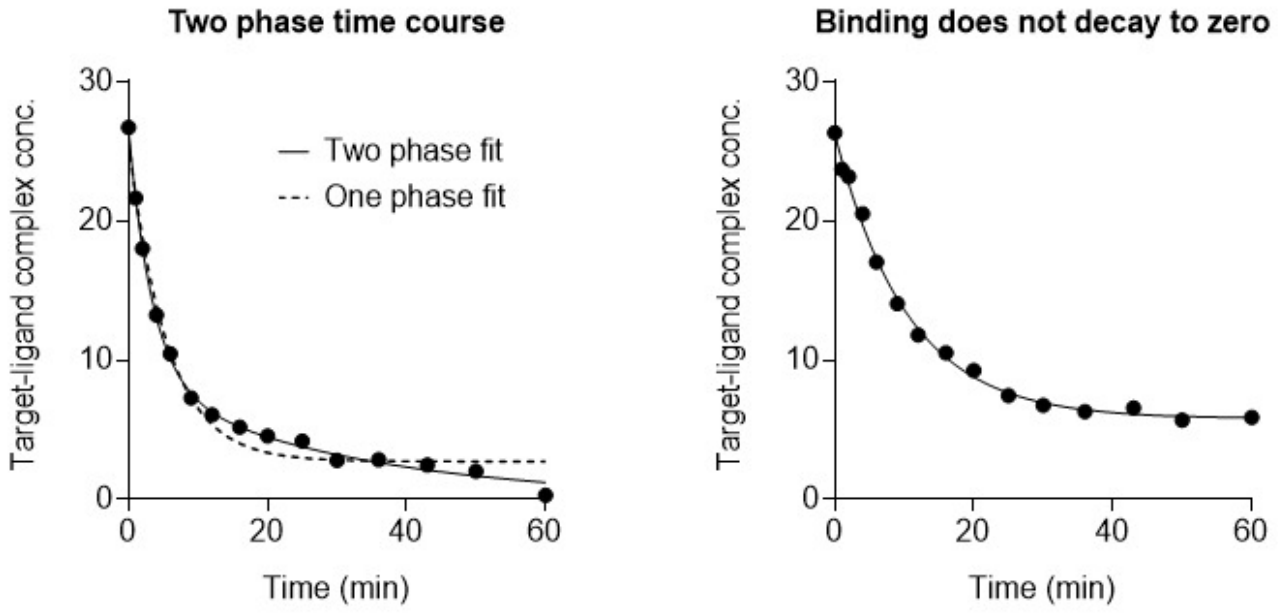

Competition Kinetics: Quantifying Kinetics by Competition Against a Tracer Ligand

Introduction

The sections above assume a direct method for measuring ligand binding to the target. However, this is usually not the case and instead a competition assay is used, particularly in lead optimization campaigns when large numbers of compounds are being tested. Competition assays are the familiar method for measuring ligand binding of unlabeled compounds (22). An unlabeled test ligand is incubated at various concentrations in competition with a tracer ligand for binding to the target. The test ligand inhibits tracer ligand binding and from this inhibition the binding of the test ligand can be determined. This method is used to measure affinity (K_i) (22) and is familiar to most investigators. Fortunately, the same approach can be used to measure the kinetics of the unlabeled test compound (association and dissociation rate constants) (Figure 4). This method is called "kinetics of competitive binding" or "competition kinetics" and the original papers describing it are refs. (18,19). The competition assay is run in kinetic mode; multiple concentrations of compound are tested at multiple time points (Figs. 5 and 6). The data are then fit to an equation by nonlinear regression, in a program like Prism. The analysis provides estimates of the association and dissociation rate constants of the test ligand. Two recent papers have provided a detailed description and evaluation of this method and its sensitivity limits (45,46). For examples of the method's application see refs. (7,45,49,50)

The binding mechanism is shown in Figure 4. Unlabeled test ligand competitively inhibits tracer ligand binding to the target. Both ligands bind reversibly in a simple one-step bimolecular interaction. The rate constants are termed, by convention, k_1 and k_2 for the tracer association and dissociation rate constant, respectively, with the corresponding terms being k_3 and k_4 for the unlabeled test ligand.

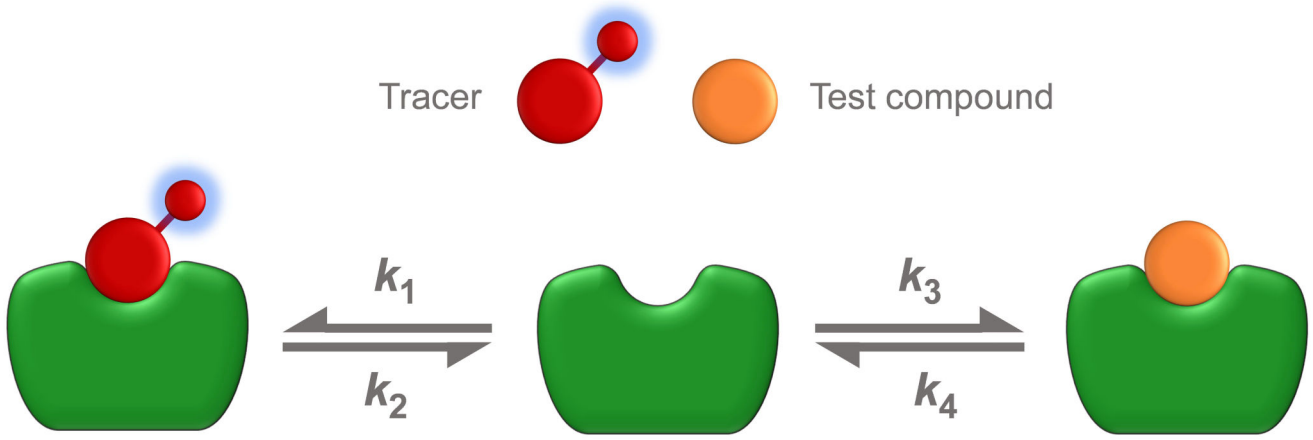

Figure 4. Competition kinetics for two ligands binding to the same binding site on the target. The target (in green) interacts reversibly with two ligands – a labeled tracer ligand in red and the test compound, which is unlabeled, in orange. k_1 and k_2 are the association and dissociation rate constants of the tracer, respectively, and k_3 and k_4 are the corresponding parameters for the test compound. k_3 and k_4 can be determined from a kinetic competition binding assay measuring inhibition of tracer binding by test compound at various time points (Figs. 5 and 6).

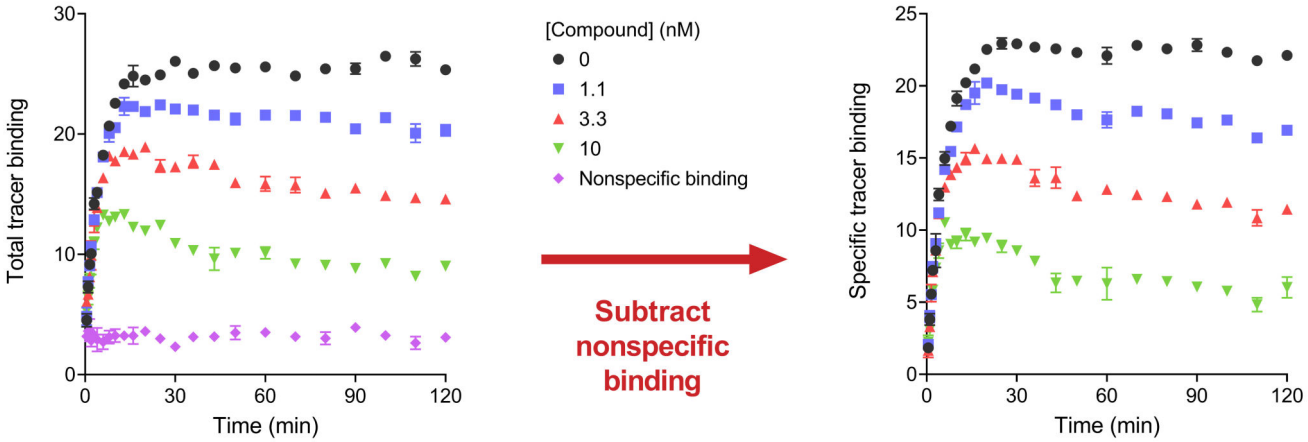

Figure 5. Raw data for competition kinetics assay. The y axis is binding of the labeled tracer ligand. Five conditions are measured, as shown in the left-hand graph. This graph shows total tracer binding data (total binding). The first step in the analysis is transformation to specific binding (i.e. target-specific tracer binding) – this is done by subtracting the nonspecific binding value at each time point. This yields the specific binding data in the right-hand graph. In this example, the average of the technical replicates for nonspecific binding was used and data points are the mean ± SEM of two technical replicates.

Assay Setup

The typical assay consists of five conditions (Box 4). Three concentrations of test compound are competed against the tracer ligand. There are two controls - tracer binding in the absence of test ligand, and nonspecific binding (measured at all time points) (Figure 5). The compound concentration range should span at least 25-75% inhibition of tracer binding at equilibrium. Consequently, a preliminary experiment needs to be done, an equilibrium binding assay to determine the IC_{50} of the test ligand. With the IC_{50} in hand, the ligand concentrations for the kinetic assay can be calculated. For three concentrations, the following calculation is used

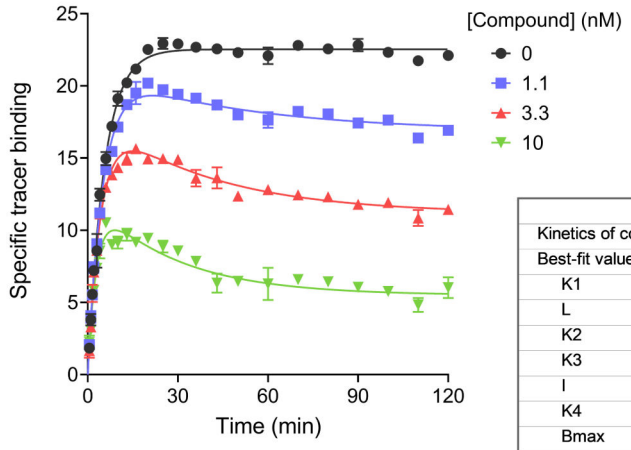

	1.1	3.3	10	Global (shared)
Kinetics of competitive binding				
Best-fit values				
K1	= 22342191	= 22342191	= 22342191	
L	= 6.000	= 6.000	= 6.000	
K2	= 0.05000	= 0.05000	= 0.05000	
K3	19072618	19072618	19072618	19072618
I	= 1.100	= 3.300	= 10.00	
K4	0.01663	0.01663	0.01663	0.01663
Bmax	31.06	31.06	31.06	31.06
Goodness of Fit				
Degrees of Freedom				141
R squared	0.9910	0.9809	0.8990	0.9879

Figure 6. Competition kinetics data analysis: curve fits and results table. The graph shows specific binding of the tracer over time, in the presence of three concentrations of the unlabeled test compound, and in the absence of test compound ("0"). The data are fit to the competition kinetics equation using Prism, as detailed in the supplementary file "Competition kinetics analysis". The table shows the results of the analysis – the fitted parameter values k_3, k_4 and B_{max}, and the goodness of fit parameter R squared (the correlation coefficient). Note the analysis globally fits all three concentration simultaneously, giving global fitted values of the parameters (red box). The fitted value of k_3 is 1.9×10^7 $M^{-1}min^{-1}$ and of k_4 is 0.017 min^{-1}.

25% inhibition – use 0.33-fold the IC_{50} concentration

50% - IC_{50} concentration

75% - 3-fold the IC_{50}.

So if the IC_{50} is 10 nM, the concentrations will be 3.3, 10 and 30 nM.

The compound serial dilution needs to be precise. The kinetic analysis is particularly unforgiving of imprecise dilution, i.e. the concentration in the assay being different from that predicted by the serial dilution calculation. Use of low-binding plasticware is recommended, and serial dilution in the ideal solvent for the ligand is required (e.g. DMSO for small molecules).

The concentration of tracer now needs to be selected. As a rule of thumb, a concentration 3-fold the K_d concentration is ideal. The tracer concentration selection is affected by three considerations. First, sufficient signal is required for sufficient robustness of detection of the binding signal. Second, the speed of the association needs to be controlled. Speed of association is dependent on ligand concentration, as described in Association Rate Constant from a Direct Target-Ligand Binding Assay and shown in Figure 3. If the concentration is too high, the association will be too rapid for there to be sufficient data points on the early part of the curve, necessary to robustly quantify the kinetics. If the concentration is too low, the association will take too long to measure. Ideally the concentration should allow at least four time points before the half-time of tracer association and at least 12 after, within the constraints of the workflow and instrumentation. Third, "Zone A" needs to be satisfied – the ligand concentration needs to be high enough that at most 20% of the tracer ligand is bound at the end of the experiment (i.e. at the plateau). This criterion also applies to the unlabeled ligand (see Box 5, "Troubleshooting the competition kinetics assay").

Next, the duration of the time course needs to be selected. At least four time points should be included before the half-time of the control association curve (absence of unlabeled compound). Then at least 12 time points

after the half-time should be included. The last time point recommended in exploratory experiments is two hours. This will give sufficient time to quantify RTs of up to an hour. Longer RTs require longer time courses to quantify accurately (45,46). As a rough rule of thumb, the time course duration should be at least double the RT of the unlabeled compound. In Box 4, time points are presented that provide a guide for pilot experiments. A large number of time points is recommended to accurately quantify the rates. For this reason, continuous-read assay modalities such as fluorescent ligand binding are ideal (7,15,28,29).

Box 4 Experimental setup for unlabeled ligand competition kinetics assay.

Conditions

1. Control (tracer only, no unlabeled compound)
2. Unlabeled compound, 0.33-fold the ligand IC_{50} in an equilibrium competition assay
3. Unlabeled compound, at the IC_{50} concentration
4. Unlabeled compound, at 3-fold the IC_{50} concentration
5. Nonspecific binding – high concentration of unlabeled ligand

Time points

- At least 4 time points before the half-time of the tracer-only association curve and at least 12 after.
- Last time point at 2 hours for pilot assays.
- Example range: (min): 0.5, 1, 1.5, 2, 3, 4, 6, 8, 10, 13, 16, 20, 25, 30, 36, 43, 50, 60, 70, 80, 90, 100, 110, 120

Tracer concentration

- 3-fold the tracer K_d as rule of thumb
- Adjust if necessary so that association is not too fast to violate time point criteria above, within the constraints of workflow and instrumentation.
- Ensure at most 20% of the added ligand is bound by the target (ideally < 10%, “Zone A”).

Box 5 Troubleshooting the competition kinetics assay.

Poor global fit to the equation – some concentrations fit well, others don’t, as follows:

Box 5 continues on next page...

Box 5 continued from previous page.

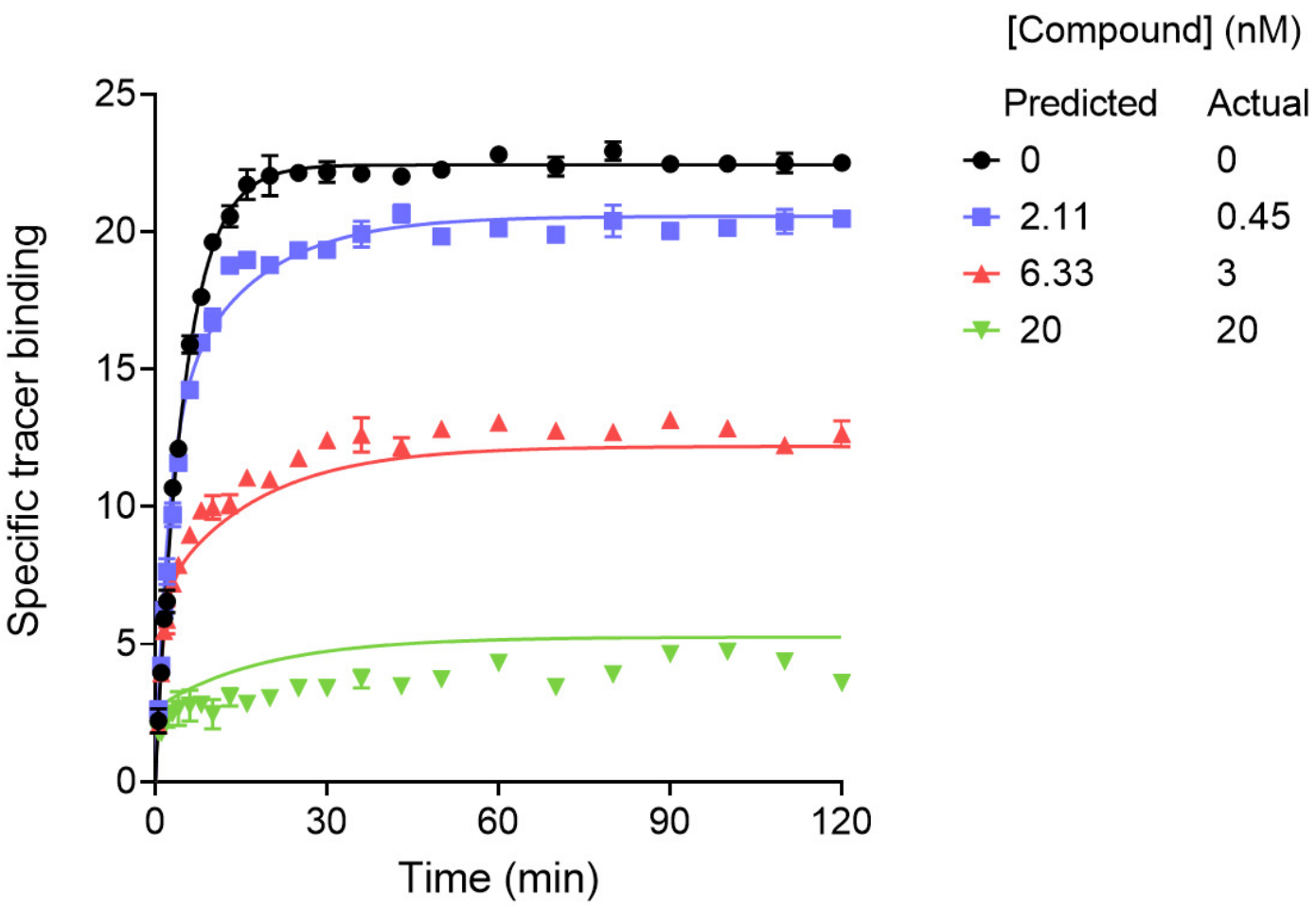

This pattern can result from imprecise serial dilution, specifically loss of compound on serial dilution. The legend above shows the predicted concentration (based on serial dilution) and actual concentration in the well. Very high affinity compounds can show this behavior because the concentration in the assay is so low. Use low-binding plasticware and ideal diluent for the compound. This pattern can also result from the target concentration being out of "Zone A", i.e. the target being at sufficient concentration that it depletes the compound concentration. Reduce the target concentration or increase tracer and compound concentrations.

Unrealistically high k_3 and k_4 values

Box 5 continues on next page...

Box 5 continued from previous page.

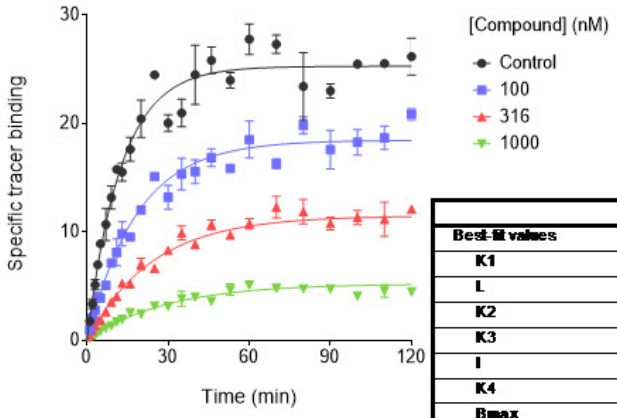

	100	316	1000	Global (shared)
Best-fit values				
K1	= 49415829	= 49415829	= 49415829	
L	= 1.000	= 1.000	= 1.000	
K2	= 0.03000	= 0.03000	= 0.03000	
K3	= 1903019176632	= 1903019176632	= 1903019176632	= 1903019176632
I	= 100.0	= 316.0	= 1000	
K4	= 184032	= 184032	= 184032	= 184032
Bmax	4123	4123	4123	4123
Goodness of Fit				
Degrees of Freedom				141
R squared	0.9559	0.9626	0.9369	0.9749

Note the very large k_3 and k_4 values in the data table. This results when dissociation of test compound is very rapid – see refs. (45,46). This can be solved by analyzing with an equation that assumes rapid dissociation and fits the equilibrium binding affinity (K_i) instead of the rates (51,52) – see Rapid Dissociation of Unlabeled Compound.

Data Analysis

The goal of the data analysis is determination of k_3 and k_4, the association and dissociation rate constant of the unlabeled test compound. The analysis proceeds in a series of steps:

1. Subtraction of nonspecific binding.
2. Fitting the control curve to determine k_1.
3. Fitting the test compound curves to determine k_3 and k_4.

The first step is the subtraction of nonspecific binding from the total binding signal and this is shown in Figure 5. Nonspecific binding at a given time point is subtracted from the total binding value at that time point, giving the target-specific binding value.

The resulting specific binding data are now analyzed by nonlinear regression. For the analysis to work, certain parameter values need to be determined first. Specifically, k_1 and k_2 (the association and dissociation rate constants of the tracer, respectively). k_2 is determined in a dissociation experiment which is run separately, and is usually determined in the characterization of the tracer (see Dissociation Rate Constant from a Direct Target-Ligand Binding Assay). k_1 is handled differently. The k_1 value is determined within the experiment, from the control (tracer binding without unlabeled compound). This is done as follows. The control curve data are fitted to the following equation (Eq. 3):

$$[\mathrm{RL}] = \frac{B_{max}[\mathrm{L}]k_1}{[\mathrm{L}]k_1 + k_2} \times \left(1 - e^{-([\mathrm{L}]k_1 + k_2)t}\right) \quad \text{Eq. 3}$$

This equation is built into Prism, named "Association kinetics - One conc. of hot." (47) A step-by-step guide on how to use it is provided in the supplementary file "Competition kinetics analysis". k_1 and B_{max} are fitted in the analysis and [L] and k_2 are entered as constants (note the Prism equation uses slightly different terminology - k_1 is termed Kon, k_2 is Koff, and [L] is Hotnm (47)). B_{max} is the total concentration of targets in the units used on

the y axis (e.g. cpm or dpm for a radioligand binding assay). [L] is the concentration of tracer ligand, in molar concentration for Eq. 3 and entered as nM concentration for the Prism equation.

Now we are ready to analyze the test compound curves to determine k_3 and k_4. This has been streamlined in Prism so that the user operates the analysis in the same was as other more familiar curve-fitting procedures (like dose-response analysis). The equation is complex (Eq. 4 shown at the end of this section) but has been pre-loaded into Prism (48) so the user simply selects it as the equation option and runs the analysis. There is one additional dimension to the data analysis. All the compound curves are analyzed simultaneously. This is done in Prism by labeling the column header in the data table with the compound concentration (48). Other programs that can handle this three-dimensional nonlinear regression are SigmaPlot and XLfit.

A step-by-step guide to the fitting procedure is shown in the supplementary file, "Competition kinetics analysis." The output is the fitted value of k_3 and k_4, the association and dissociation rate constants of the unlabeled compound, and B_{max}, the total number of ligand binding sites. A representative graph showing the curve fits and fitted values is shown in Figure 6. The fitted value of k_3 is 1.9×10^7 $M^{-1}min^{-1}$ and of k_4 is 0.017 min^{-1}. The RT ($1 / k_4$) is then 59 min.

The equation for the analysis is Eq. 4 (18,19):

$$[RL] = \frac{B_{max}[L]k_1}{K_F - K_S}\left[\frac{k_4(K_F - K_S)}{K_F K_S} + \frac{k_4 - K_F}{K_F}e^{-K_F t} - \frac{k_4 - K_S}{K_S}e^{-K_S t}\right] \quad \text{Eq. 4}$$

where,

$$K_F = 0.5\left\{K_A + K_B + \sqrt{(K_A - K_B)^2 + 4[L][I]k_1k_3}\right\}$$
$$K_S = 0.5\left\{K_A + K_B - \sqrt{(K_A - K_B)^2 + 4[L][I]k_1k_3}\right\}$$
$$K_A = [L]k_1 + k_2$$
$$K_B = [I]k_3 + k_4$$

The fitted parameters are k_3, k_4 and B_{max}. The parameters fixed at constant values in the analysis are [L], [I], k_1 and k_2. [I] is the inhibitor concentration in molar concentration for Eq. 4 and entered as nM concentration in Prism. The parameters K_F, K_S, K_A and K_B are combinations of the other parameters, introduced to simplify writing of the equation into curve-fitting programs.

Shape of the Curves Can Diagnose the Residence Time of the Test Compound

An interesting observation is immediately obvious on inspecting the data in Figure 6 – the curves are of an unusual shape. There is an overshoot of the tracer binding curve in the presence of compound, before the curve returns to a plateau value. This phenomenon arises when the RT of the test compound is longer than that of the tracer (18,19,45,46). More generally, the shape of the curve can diagnose the RT of the test compound, relative to the RT of the tracer. This is shown in Figure 7. Competition kinetics data are shown for compounds with a range of RTs, from 300 min to 3 min. The tracer RT is 67 min. It can be seen that when the compound RT is longer than the tracer RT, the overshoot phenomenon occurs (Figure 7A, 300 min and 7B, 100 min). The longer the RT, the more pronounced the overshoot (compare Figure 7A and B). When the compound RT is slightly shorter than the tracer RT (30 min, Figure 7C), a biphasic curve is evident – there is an initial rapid burst of binding followed by a shallower phase as the curve approaches the plateau. When the compound RT is short relative to the tracer (10 min and 3 min) the curve resembles a monophasic curve, similar in shape but different in dimensions to the control curve (Figure 7D,E).

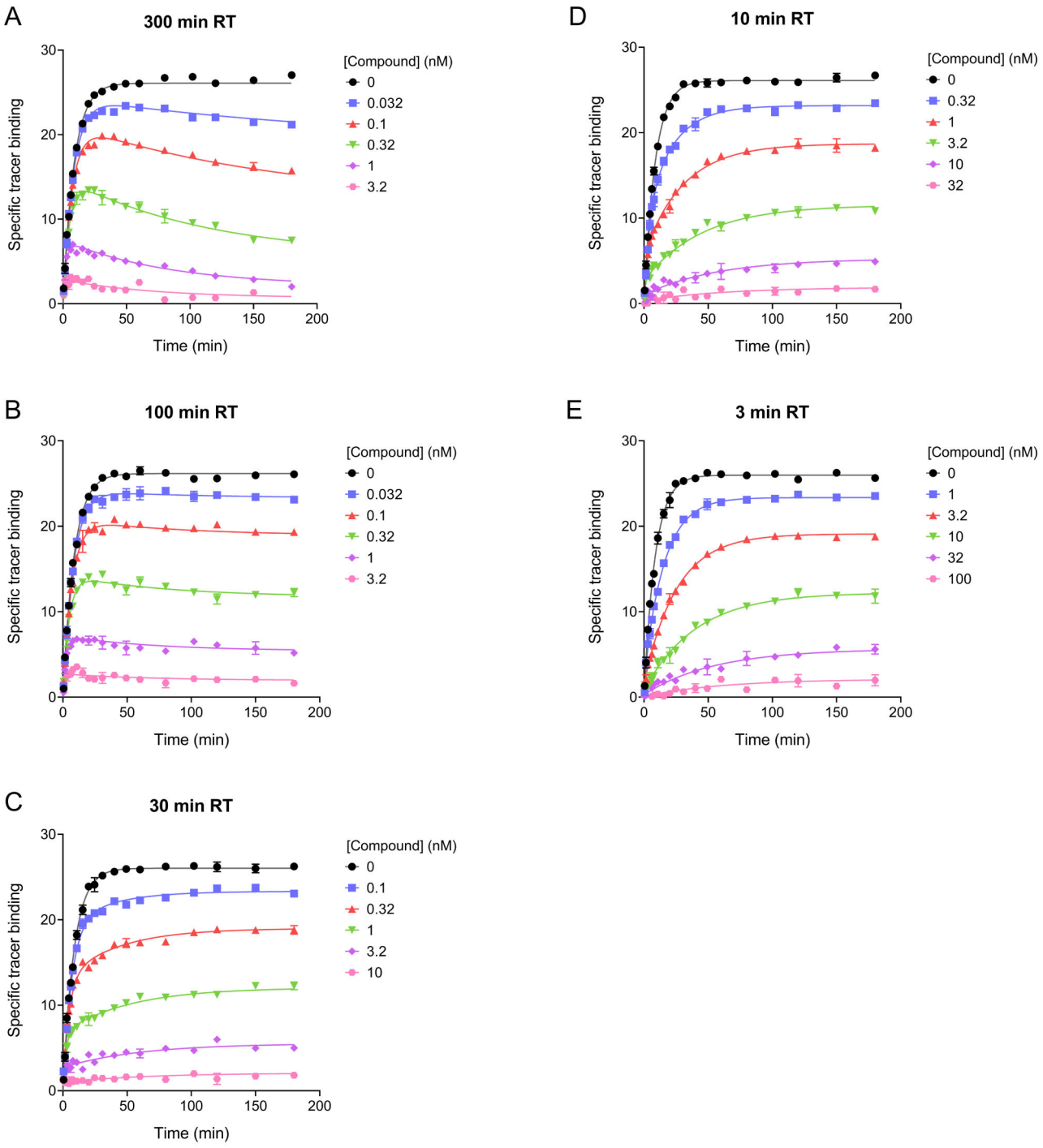

Figure 7. Curve shapes in competition kinetics assays. The curve shape is dependent on the RT of the test compound relative to the RT of the tracer. The tracer RT in this example is 67 min. When the compound RT is longer than the tracer RT, the overshoot phenomenon is evident – the curve peaks then declines to a plateau (300 min (A) and 100 min (B)). The longer the RT, the greater the overshoot (compare A with B). When the compound RT is slightly shorter than the tracer RT, a biphasic curve is evident (C, 30 min), where there is an initial rapid rise of tracer binding followed by a slower approach to the plateau. When the compound RT is short relative to the tracer, the curve appears monophasic (10 and 3 min, D and E). Data points are the mean ± SEM of two technical replicates.

Limits of Sensitivity

Like any other assay, there are limits to the sensitivity of the competition kinetics approach, specifically for quantifying the RT. This has been emphasized in two recent studies (45,46). If the RT is too short or too long, the analysis is unable to provide a realistic estimate of k_4. (Typically a short RT value in this context is less than 1 min and a long value > 3 hr.) Under these conditions, a false fit can result – the program is able to fit a curve, but the parameters are physically meaningless. Consequently, it is important for investigators not to take the fitted values at face value but rather to consider them within the limits of sensitivity of the analysis. Fortunately, intuition is a good guide in most cases. For example, if dissociation of a test compound is rapid, a high-frequency of reads and an early first read time is necessary; in other words, detecting rapid dissociation requires rapid sampling of the binding reaction (45,46). Reciprocally, detecting slow dissociation requires the duration of the assay to be long (45,46).

The limits of sensitivity were recently evaluated by simulation – Monte Carlo analysis was used to simulate virtual experiments under a variety of conditions. The reader is referred to refs (45,46) for a comprehensive evaluation. In this chapter, two examples are presented to show what the data look like when the limits of sensitivity are breached. The examples were constructed using the easy-to-follow methods described in the supplementary information of ref. (45), which investigators can use to evaluate their own systems. Here a best-case assay technology scenario is assumed, where there are no major limitations on sampling frequency, initial read time, or signal stability (for example, a resonance energy transfer continuous read assay with autoinjectors and a stable signal; see refs. (45,46) for the impact of these technical limitations).

Figure 8 shows a limit of sensitivity issue for long RT compounds. This simulation shows the effect of the assay run time (total observation time) on estimating the dissociation rate of a compound with a long RT (6 hr). If the run time is too short, the dissociation rate of the compound is poorly estimated (more precisely, the fitted k_4 value is highly variable between experimental runs). This is shown by the large range of fitted k_4 values in Figure 8A for a run time of 1 hr. Increasing the run time to 3 hr dramatically reduces the variability and increasing to 9 hr produces a further, slight improvement (Figure 8A). The reason for the variability is obvious when the curves are examined (compare Fig 8 panel B with panels C and D). At 1 hr, the curve shape is poorly defined – the binding is still coming down from the peak and most of the curve is missing. It takes until 3 hr for binding to come down to the plateau, and up to 9 hr for the curve to be fully defined. For a more detailed description, see Figure 2 of ref. (46). Improvements in estimating long RT values can also be obtained by using tracers with longer RTs (46).

Figure 9 shows a limit of sensitivity problem for short RT compounds. The simulation shows the effect of read frequency (the time interval between measurements of binding) on estimating the dissociation rate of a compound with a short RT (10 sec). If read frequency is too long (1 min), the dissociation rate is poorly estimated by the analysis, evident by the large spread of k_4 values in Figure 9A. This can be overcome by increasing the read frequency. Increasing to 10 seconds substantially reduces the variability, and increasing to 1 sec provides highly reproducible estimates of k_4 (Figure 9A). This makes intuitive sense – detecting events on the order of seconds is unlikely to be reliable with measurements separated by minutes. Simulations have also shown the first time point to be critical – if there is a delay between adding the target to the well and the first measurement, k_4 can be poorly estimated for rapidly-dissociating compounds (45). For this reason, autoinjectors on the reader are advised for quantifying short RTs.

Adaptations of the Method

The competition kinetics equation makes several assumptions regarding the binding mechanism and experimental setup that are not always applicable and/or desirable. To accommodate adaptations, new equations have been derived that investigators can use to analyze their data.

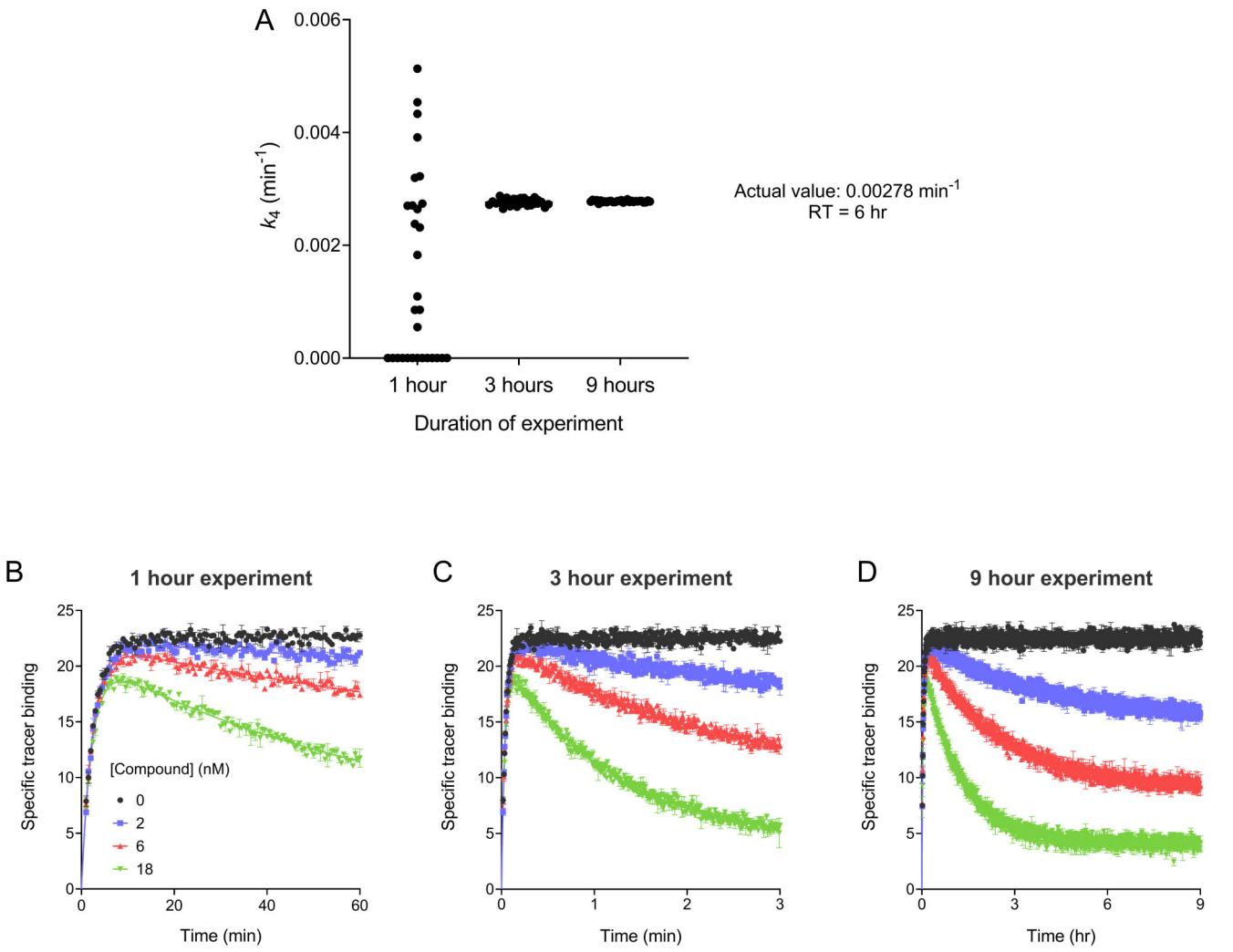

Figure 8. Sensitivity limits of a competition kinetics assay for detecting a long residence time: Effect of experiment run time. Simulated data show that if the incubation time is too short, residence time is poorly estimated by the method (45,46). Repeated experimental runs (30 in total) were simulated using the Monte Carlo method for a test compound with a RT of 6 hr, as described in the supplementary information of ref. (45). This was done for 3 experiment run times – 1, 3 and 9 hr. A) Fitted test compound dissociation rate constant. With a 1 hr run time, the k_4 estimates vary dramatically from experiment-to-experiment (note the values that are close to zero – in these experiments, the fitted value hit the constraint limit ($k_4 > 0$)). Increasing the run time to 3 and 9 hr dramatically increases the reliability of the fit, evident from the much smaller spread of k_4 values. B-D) Representative time course traces for 1, 3 and 9 hr run times. Simulation parameters were: k_1, 1×10^8 M^{-1}min^{-1}; k_2, 0.1 min^{-1}; k_3, 2.78×10^6 M^{-1}min^{-1}; k_4, 0.00278 min^{-1}; L, 3 nM; I, 2, 6 and 18 nM; B_{max}, 30; first time point, 30 sec; read frequency, 30 sec; 2 technical replicates; Gaussian absolute random scatter with SD of 0.5. Data based on Figure 2 of ref. (46).

Rapid Dissociation of Unlabeled Compound

Sometimes the dissociation of test compound is too rapid for the method to quantify k_4 reliably, within the constraints of the assay design (see "Limits of sensitivity" above). This can result in a false-fit to the data – the curve-fitting algorithm will fit a curve, but the parameter values are physically unrealistic. This is shown in Box 5 (bottom graph and table). When engaged in an SAR campaign, there is no data output from the experiment for these compounds, which can be inconvenient, for example when tabulating activity. To solve this problem, an equation has been derived that returns the value of the equilibrium binding affinity of such rapidly-dissociating compounds (51) (see Appendix, Adaptation for Rapidly-Dissociating Compounds). This is achievable because

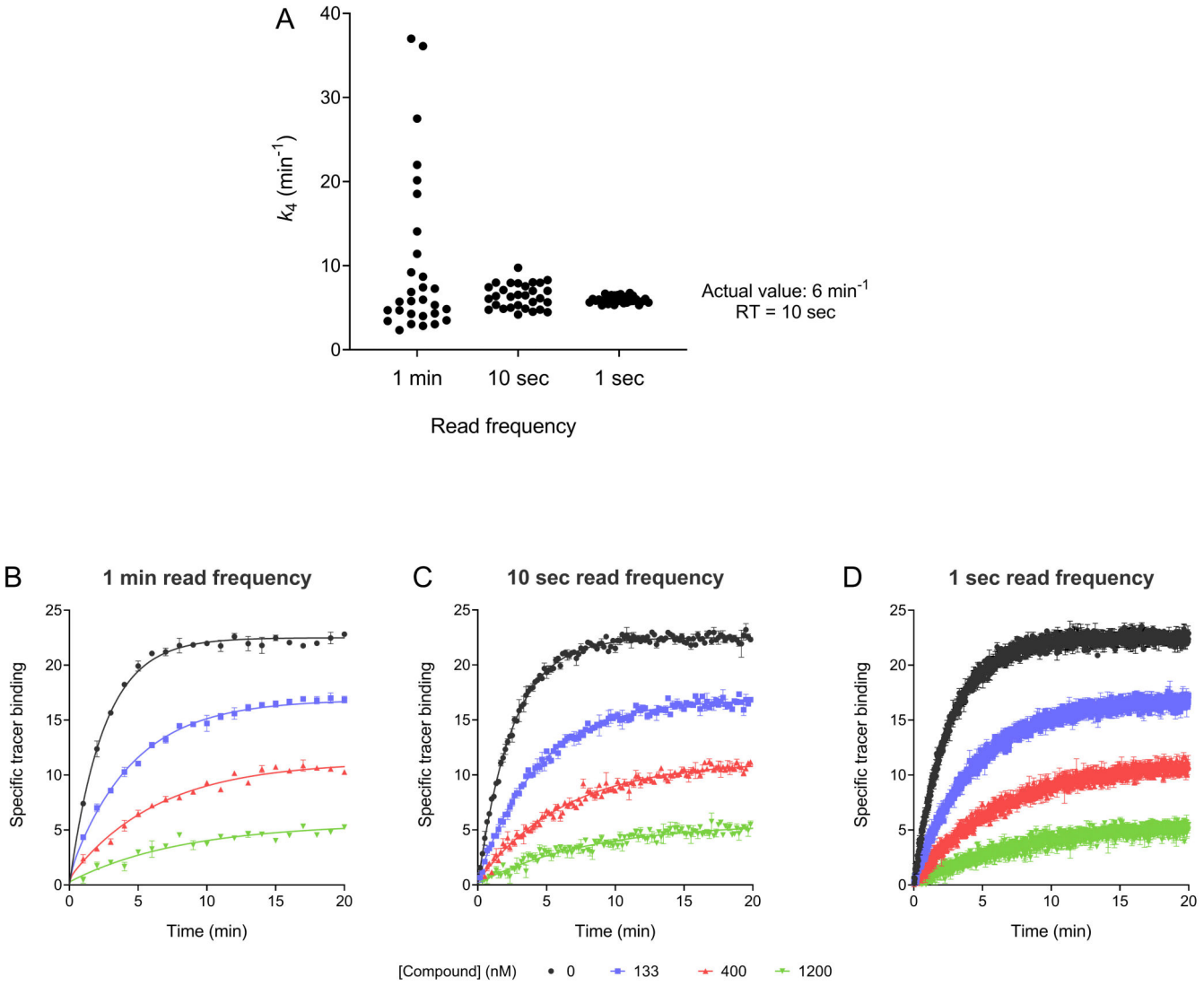

Figure 9. Sensitivity limits of a competition kinetics assay for detecting a short residence time: Effect of read frequency / measuring interval. Simulated data show that, to accurately measure short residence times, the read frequency needs to be high (45,46). Repeated experimental runs (30) were simulated using the Monte Carlo method for a test compound with a RT of 10 sec, as described in the supplementary information of ref. (45). This was done for 3 read frequencies – 1 min, 10 sec and 1 sec. A) Fitted test compound dissociation rate constant. With a 1 min read frequency, the k_4 estimates vary dramatically from experiment-to-experiment. Increasing the read frequency to 10 sec and 1 sec dramatically increases the reliability of the fit, evident from the much smaller spread of k_4 values. B-D) Representative time course traces for the different read frequencies. Simulation parameters were: k_1, 1×10^8 M^{-1}min^{-1}; k_2, 0.1 min^{-1}; k_3, 6×10^7 M^{-1}min^{-1}; k_4, 6 min^{-1}; L, 3 nM; I, 133, 400 and 1200 nM; B_{max}, 30; last time point, 20 min; 2 technical replicates; Gaussian absolute random scatter with SD of 0.5. Data based on Figure 3 of ref. (46).

the compound can be assumed to be at equilibrium with the unbound targets immediately after the target is added and throughout the time course of the experiment.

The experiment is run identically to the competition kinetics assay but a different equation is used to analyze the data (51,52). A step-by-step guide for running the analysis is provided in the supplementary file, "Rapid competitor data analysis." The first step in the analysis is to determine the k_1 value of the tracer, and this is done as described above (Data Analysis). The next step is to analyze the test compound data with the equation (Eq. 5 below). Unfortunately, this equation is not built-in to commercial curve-fitting software so it must be loaded in

as a user-defined equation. Fortunately, a simple way of doing this is available in Prism. The user downloads a Prism file containing the equation (Custom equations for binding kinetics) and then with a couple of mouse clicks loads the equation into the library on their computer. This is explained in the supplementary file "Loading equations into Prism from a file."

The analysis is run in the same way as the competition kinetics analysis, just with a different equation. Data for all concentrations of compound are analyzed simultaneously, giving a global fit that provides an estimate of the equilibrium binding affinity of the unlabeled compound for the target (K_i). The equation is Eq. 5 (51,52):

$$[RL]_t = \frac{B_{max}[L]k_1(1-\rho_I)}{k_{obs}}\left(1 - e^{-k_{obs}t}\right) \quad \text{Eq. 5}$$

where,

$$\rho_I = \frac{[I]}{K_i + [I]}$$
$$k_{obs} = [L]k_1(1-\rho_I) + k_2$$

(Note ρ_I and k_{obs} are composite parameters introduced to simplify writing of the equation into curve-fitting programs.) The fitted values are K_i and B_{max} and the following parameters are entered as fixed, constant values - [L], [I], k_1 and k_2.

Pre-incubating With Test Compound

The order of reagent addition is constrained in the original competition kinetics method. The target must be exposed simultaneously to the labeled tracer and unlabeled test ligands, i.e. the target is added last to the assay (18,19). This is not always feasible within the workflow of the experiment. For example, when using plated cells it is difficult to expose the cells to both ligands at the same time – this requires ligands to be mixed together before adding to the assay. Instead, for convenience, usually the test compound is added first, pre-incubated with the cells, then the tracer ligand is added.

An equation has been derived to handle pre-incubation of target with unlabeled compound before application of tracer (Figure 10, Eq. 6, see Pre-incubating with Test Compound) (53,54). The equation is a close analogue of the competition kinetics equation and is used in the same way, yielding fitted values of k_3 and k_4, the binding rate constants of test compound. To employ it in Prism, investigators are recommended to use the "Competition kinetics analysis" guide in supplementary files and substitute the competition kinetics equation with the "[Pharmechanics] Kinetics of competitive binding: Competitor pre-incubation" equation (this is a custom equation, available from the supplementary file "Custom equations for binding kinetics", loaded as described in "Loading equations into Prism from a file"). The x axis values are the time points after the pre-incubation, i.e. after the tracer is added. The equation contains one extra variable, the pre-incubation time with compound, termed "PIT" which is in the same units as the x axis values.

Pre-incubating with Tracer

An alternative way of setting up the assay is to pre-incubate target with tracer to allow target-tracer complexes to form, followed by addition of unlabeled test compound. An equation has been derived to analyze these data (Eq. 7, see Pre-incubating with Tracer) and its application detailed in ref. (53). The equation is available in the supplementary file "Custom equations for binding kinetics", where it is named "[Pharmechanics] Kinetics of competitive binding: Labeled ligand pre-incubation."

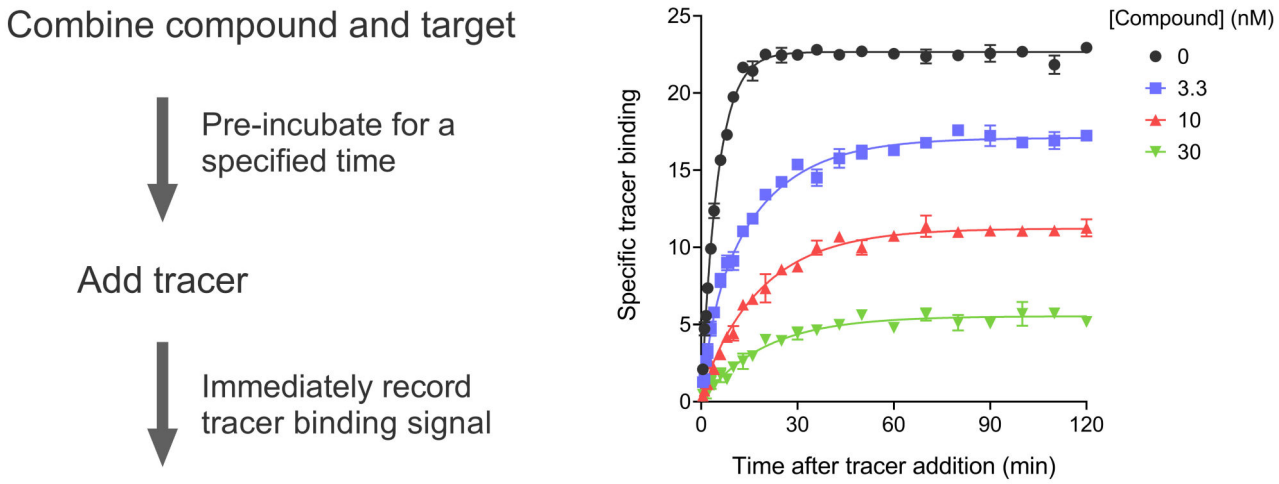

Figure 10. Compound pre-incubation competition kinetics method and analysis. Often it is desirable to pre-incubate compound with target before adding tracer in a binding assay, for example when using plated cells. An equation is available to analyze these data to determine the binding kinetic rates of test compound. In the experimental protocol (left), compound is added to target and the two are incubated for a specified time period. Tracer is then added, and tracer binding to the target recorded. Three concentrations of compound are tested, as described for the original competition kinetics method (Competition Kinetics Introduction). Data (right) are analyzed as for the original method (see supplementary file "Competition kinetics analysis") except a different equation us used that takes into account the pre-incubation. This equation is available in the supplementary file "Custom equations for binding kinetics", where it is named "[Pharmechanics] Kinetics of competitive binding: Competitor pre-incubation." It can be loaded as described in "Loading equations into Prism from a file." The equation contains an extra term, the pre-incubation time ("PIT"), entered as a constant in units the same as the x axis units. The analysis yields fitted values of k_3 and k_4, the binding rate constants of test compound. In this experiment, the fitted value of k_3 is 2.0×10^7 $M^{-1}min^{-1}$ and of k_4 is 0.049 min^{-1}. Data points are the mean ± SEM of two technical replicates.

Compound Washout Method

Introduction

A popular method for measuring unlabeled compound RT is the washout method, frequently employed for kinase enzyme targets. A detailed description of the experimental method is provided in ref. (55) and the procedure is shown in Figure 11. The target and the unlabeled test compound are incubated together to form the target-compound complex, in a pre-incubation step. Next, a wash step is performed to remove the free (unbound) test compound from the assay. At the end of the wash step, there is compound bound to the target and, ideally, no unbound compound. Immediately following the wash step, tracer ligand is added and the tracer binding to the target is recorded (Figure 11). As a control, tracer binding is measured in a sample where vehicle instead of compound is applied in the pre-incubation step.

This assay indirectly quantifies test compound dissociation from the target, by its ability to inhibit tracer binding. The test compound first has to dissociate from the target before the tracer can bind and this results in a delay in the association of the tracer (Figs. 11 and 12) (56-58). The extent of the delay is dependent on the dissociation rate of the test compound. If dissociation is slow, it takes a long time for the targets to become free of the compound, slowing association of the tracer (Figure 12B). By contrast, if dissociation is rapid, target becomes available quickly and there is little slowing of tracer association (Figure 12A). In the literature, the data are usually evaluated qualitatively. However, an equation is available to quantitatively analyze the data, to determine the RT value of test compound (56) (Eq. 8, see Washout Kinetics Method Equation). Applying the equation is described in Data Analysis to Quantify the Compound Residence Time below and the

supplementary file, "Washout method analysis". A useful, comprehensive application of the analysis is provided in ref. (58).

Experimental Considerations

Technically, the experiment must be performed carefully for the method to provide unambiguous results on the dissociation rate of the compound. It is essential that the unbound compound be thoroughly removed during the wash step; any remaining compound sufficient to occupy the target will block tracer binding by simple equilibrium competition. Note some free compound molecules will be in the well during the tracer incubation owing to breakdown of the target-compound complex. This concentration will be too low to significantly occupy the target if Zone A (minimal compound depletion by target) is satisfied. If there is sufficient free compound remaining in the tracer incubation step owing to incomplete washout, it will slow association of the tracer (59). This can give the false appearance of a long RT compound (Figure 13). This requires the washout method to be carefully considered, particularly for drug-like small molecules which tend to be hydrophobic and difficult to remove, especially from cells (59). If possible, a sample of the assay medium after washing should be removed and the presence of any remaining compound evaluated by testing the medium in a binding assay. Another check is the shape of the tracer binding curve – if test compound has been effectively removed, the curve will eventually reach the same level of binding as the control (no compound in pre-incubation), assuming compound dissociation is not too slow. If significant compound remains after the wash step, the curve will plateau below the no-compound control, as a result of equilibrium competition between residual compound and the tracer (Figure 13) (59).

In the pre-incubation step, a concentration of compound sufficient to occupy no more than 80% of the targets is recommended (4-fold the K_i determined in a preliminary competition binding assay). This minimizes the wash burden. If the concentration is too high, residual compound can bind the target in the tracer incubation. For example, if a 100-fold excess over K_i concentration is used, and the wash step removes 99% of the compound, the 1% that remains will be sufficient to block 50% of the targets, resulting in false appearance of a long RT compound (Figure 13).

Data Analysis to Quantify the Compound Residence Time

Measuring the dissociation rate constant of the test compound (k_4) is the goal of the analysis. A step-by-step guide is provided in the supplementary file, "Washout method analysis." The data type is specific binding, i.e. data from which nonspecific binding has been subtracted (Data Analysis and Figure 5). The analysis makes the same assumptions as the competition kinetics analysis (Competition Kinetics: Quantifying Kinetics by Competition Against a Tracer Ligand) – single-site, single-step, competitive binding mechanism with minimal ligand depletion (<20%).

There are two steps in the analysis. First, the control data are analyzed to obtain k_1 for the tracer (control being the sample without compound in the pre-incubation). The data are fit to Eq. 3 as described in Data Analysis, which can be done in Prism using the equation "Association kinetics - One conc. of hot." (47) Note the analysis requires k_2 of the tracer to be known (tracer dissociation rate constant) – this is measured in a separate experiment.

With the k_1 value in hand, the compound data can be analyzed to determine k_4, as detailed in the supplementary file, "Washout method analysis" employing Eq. 8 (Washout Kinetics Method Equation). The analysis provides fitted values of k_4; B_0 (the percentage of targets occupied by compound at the end of the pre-incubation phase); and B_{max} (the total number of ligand binding sites).

Figure 12 shows representative graphs for compounds with varying RTs (i.e. k_4 values), from 6 min to 36 hr. The shape and position of the curve makes intuitive sense. For the shortest RT (6 min), the compound curve is only slightly delayed compared with the control curve; there is minimal delay of tracer binding because the

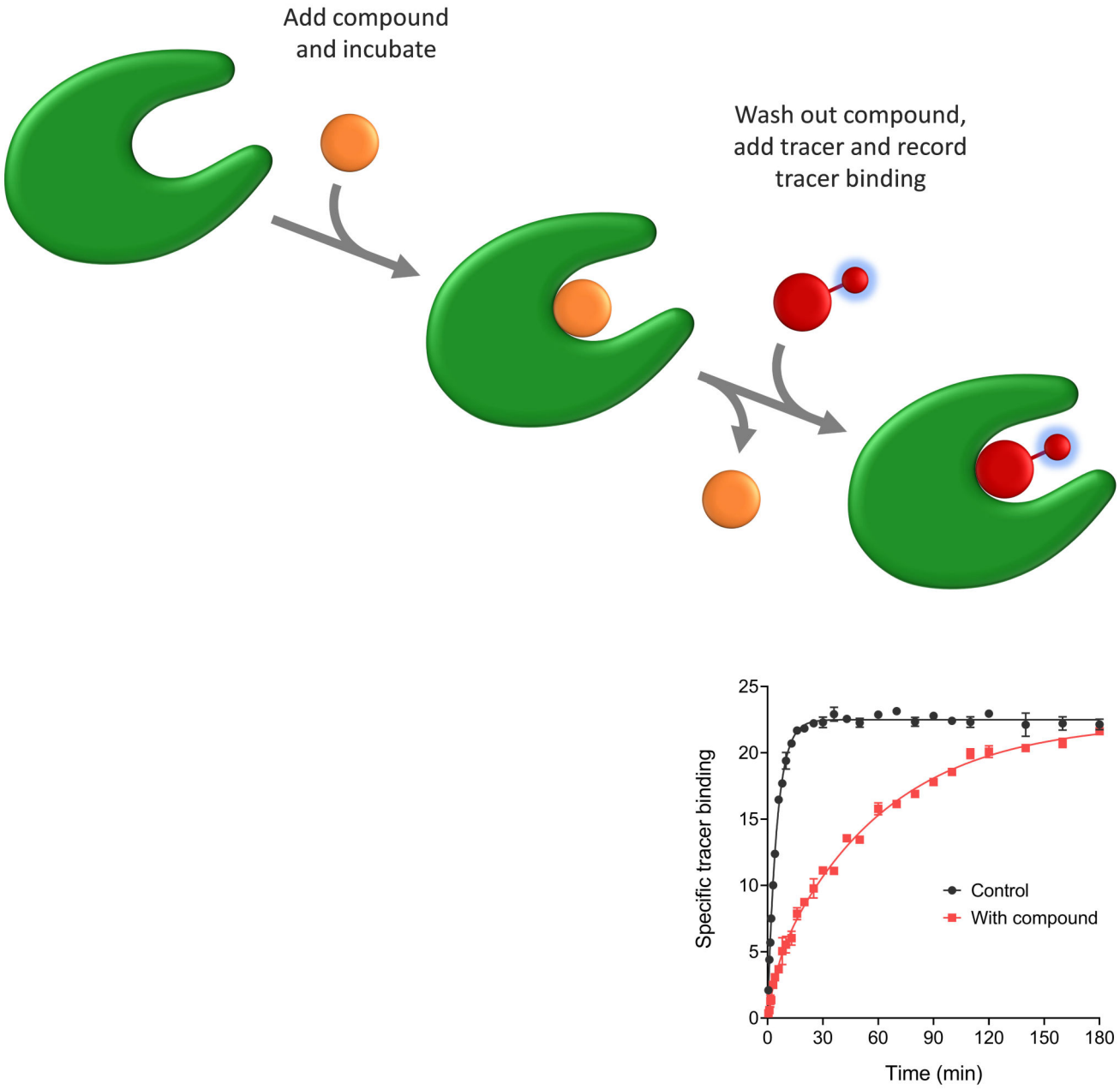

Figure 11. Washout method for quantifying unlabeled compound residence time. Target (in green) is incubated with test compound (orange) for a specified time, for the target-compound complex to form. In the next step, the unbound compound is washed out. Tracer ligand (in red) is then immediately applied and tracer binding measured using a time course binding assay (see graph). The pre-bound compound delays association of tracer with target because it first has to dissociate before the tracer can bind. The resulting data can be analyzed with an equation that quantifies the dissociation rate constant of the compound (see Figure 12), providing the unbound compound has been sufficiently well removed during the wash step. Data points are the mean ± SEM of two technical replicates.

compound dissociates so rapidly, leaving target free to bind tracer (Figure 12A). At later time points, the plateau for the compound curve reaches the same level as the control. This is because, given enough time, all of the compound-target complexes break down, leaving all of the targets free to bind tracer. Note this argument assumes the concentration of free compound in the tracer incubation is too low to significantly occupy the tracer – see below for what happens when this is not the case. For a 60 min RT compound (Fig 12B), there is a marked delay in tracer association, which is predicted because it takes time for the target to become available owing to

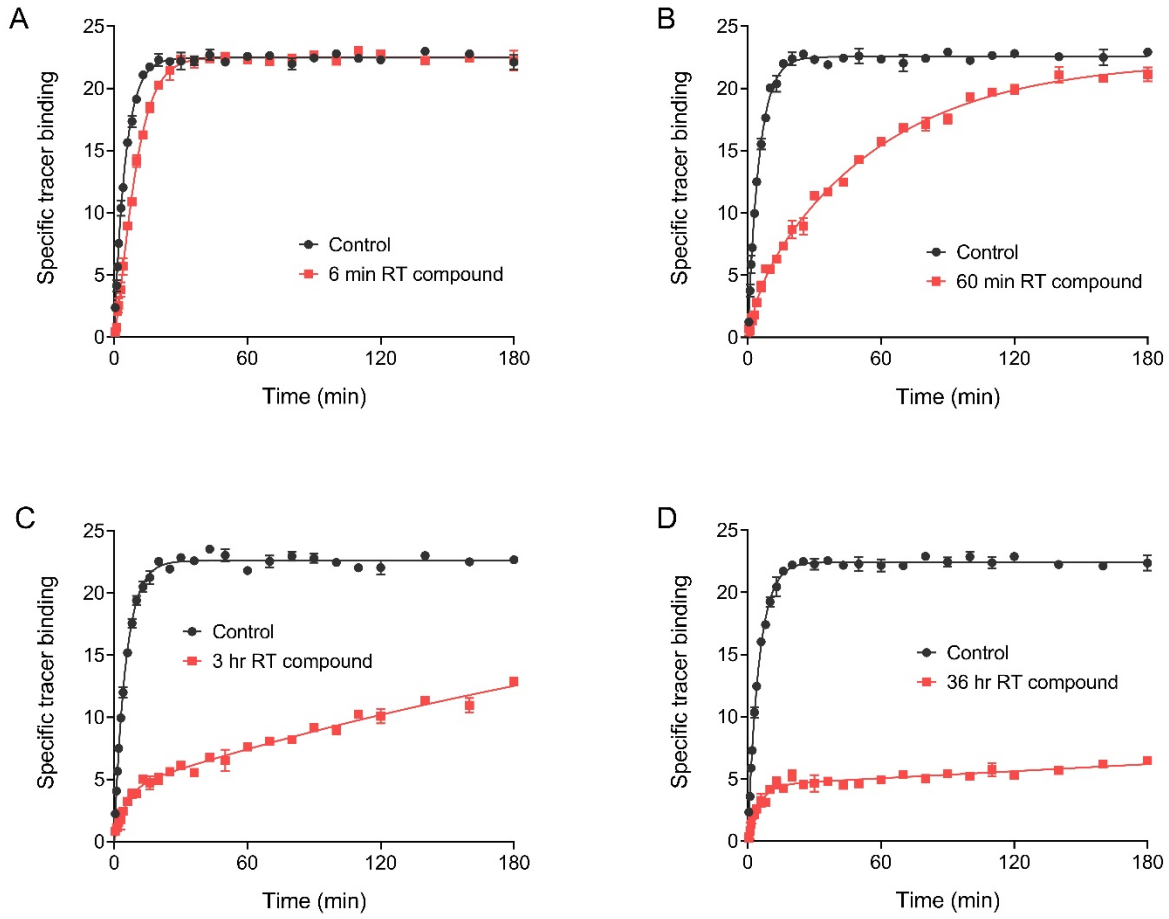

Figure 12. Washout method curve shapes for compounds with varying residence time. Data were simulated assuming 80% occupancy by compound at the end of the compound pre-incubation. When the RT is short (A, 6 min), the compound curve is only slightly delayed relative to the control curve because the compound dissociates rapidly. When the RT is longer (60 min, B), there is a clear separation between the curves owing to the slow dissociation of compound which delays association of the tracer. Note the compound curve returns to the same level of binding as the control given enough time (at the plateau) – at this point all compound has dissociated so all targets are free to bind the tracer. When the RT is long relative to the timeframe of the assay (3 hr RT, C), the curve increases slowly and the plateau is not well defined. This can be handled in the data analysis by fixing the plateau to that of the control (Box 6). When the RT is exceptionally long (36 hr, D), the curve effectively plateaus at a much lower level than the control. In this case, the only available targets are those 20% free at the end of the compound pre-incubation. Data points are the mean ± SEM of two technical replicates.

the slow dissociation of the compound. When the RT is long (3 hr), the curve is markedly biphasic (Fig 12C). There is a small rapid burst of tracer binding at the start, and a slower rise phase. The rapid phase represents tracer binding to the free targets; the experiment is set up so that 80% of targets are bound by compound, leaving 20% unoccupied and so immediately available to bind tracer. The slower rise phase represents tracer binding to targets that become available once the compound has dissociated from the target. (Note the data analysis can give ambiguous results when the top of the curve is not reached over the timeframe of the assay. This issue can be solved by fixing the B_{max} value for the compound curve to that of the control). When the RT is very long, relative to the timeframe of the assay (36 hr vs 3 hr), a near-monophasic curve results, in which binding plateaus well below the control (Fig 12D). In this case, the binding signal is effectively tracer binding only to the targets which were free at the end of the pre-incubation. Very few new targets become available because compound dissociation is so slow.

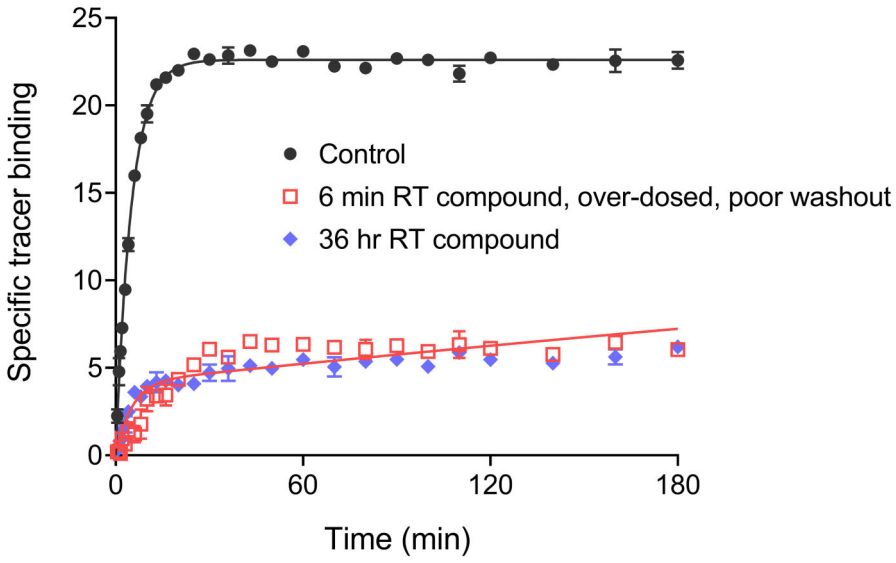

Figure 13. False positive long residence time resulting from incomplete washout in the kinetic washout assay. Kinetic washout experiments assume there is no free compound remaining after the washout step, meaning the delay of tracer association results solely from pre-bound compound-ligand complexes needing to dissociate before tracer can bind. However, if washout is inefficient, residual compound can also delay tracer binding, by simple competition binding. This can give the false impression of a long RT for the compound. Here a worse-case scenario is given. A short RT compound (6 min) is dosed at a very high concentration in the pre-incubation step (1,000 nM, 100-fold higher than the compound's K_d of 10 nM). Then an inefficient wash is performed, such that 10% of the compound remains in the well, giving a 100 nM concentration when the tracer is added. This concentration, which is 10-fold above the K_d, can easily outcompete the tracer, resulting in inhibition of tracer binding (red squares). The data closely match those for a long RT compound (36 hr) that is dosed correctly (4X K_d) and completely washed out (blue diamonds). Consequently, a short RT compound erroneously appears like a long RT compound. Analysis using the kinetic washout equation (Eq. 8) gives an RT of 10 hr, radically different from the actual RT of 6 min. See text for simulation and fit details. Data points are the mean ± SEM of two technical replicates.

The association rate constant of test compound can be determined if multiple concentrations of test compound are run. An experiment of this type will return fitted values of the percentage of target population bound, B_0, for each concentration of test compound, [I]. B_0 is plotted against [I] and the data are fit to the following equation:

$$B_0 = 100 \times \frac{B_{max}[I]k_3}{[I]k_3 + k_4}\left(1 - e^{-([I]k_3 + k_4)t_{PI}}\right)$$

Where t_{PI} is the compound pre-incubation time.

False-Positive Long Residence Time Resulting from Incomplete Washout

The kinetic washout method assumes the free compound is so well washed out that no new target-compound complexes form in the tracer incubation step. What happens when this is not the case? How do the data appear when the wash is inefficient and there is ample free compound remaining to bind the target in the tracer incubation? Compounds with short RTs can appear to possess long RTs, giving false positives in lead optimization where the goal is a long RT compound.

A worst-case scenario is presented in Figure 13, using simulated data. A compound with a short RT (6 min) is dosed at a very high concentration in the compound pre-incubation step (1,000 nM, which is 100 times the compound K_d of 10 nM). Then the free compound is washed out, but the washout is not complete – it removes only 90% of the free compound. This leaves compound in the well, at 100 nM concentration, when the tracer is

added. This concentration, at 10 times the K_d, easily competes against the tracer. This results in strong inhibition of tracer binding (red squares in Figure 13). Alarmingly, the data resemble those for a compound with a much longer RT of 36 hr, run under the proper conditions, i.e. complete washout of free compound (blue diamonds, Figure 13). Analysis of the 6 min RT compound data with the kinetic washout equation gives a fitted RT of 10 hr. These results show that incomplete washout of compound can result in a false positive long RT.

Data in Figure 13 were simulated using Eq. 5 of ref (53), with the following parameter values: [L], 6 nM; B_{max}, 30 binding units; k_1, 2.5×10^7 $M^{-1}min^{-1}$; k_2, 0.05 min-1; k_3, 1.67×10^7 $M^{-1}min^{-1}$; k_4, 0.167 min^{-1}; pre-incubation time, 30 min; pre-incubation compound concentration, 1,000 nM; tracer incubation compound concentration, 10 nM. Data were fitted to the kinetic washout equation (Eq. 8). B_{max} was constrained to that of the control curve (30 binding units).

Complex Binding Mechanisms

Often in binding kinetic studies the data do not fit well to the equations given in the preceding sections. These equations assume the binding event is of the simplest form, a single-step, single site target-ligand interaction. When the data are not fit well by the equations it can indicate a more complicated binding mechanism. Such mechanisms often include two conformational states of the target, with different binding kinetics, giving rise to multiphasic time course curves (for example, Figure 14). Thanks to the efforts of investigators, equations are available to analyze more complex binding data to obtain estimates of the kinetic parameters. While a detailed description is beyond the scope of this chapter, these mechanisms are introduced below and references are provided.

Two Conformational States Mechanism

Sometimes there is more than one conformational state of the target in the assay. GPCRs are the classic example. In binding assays, the GPCR exists in two predominant conformations, the G-protein coupled state and the uncoupled state, which bind agonist ligands with different affinity (60,61) and with different binding kinetics (44,62). This mechanism is represented by the following scheme:

$$R_A + L \underset{k_{2A}}{\overset{k_{1A}}{\rightleftharpoons}} R_AL$$

$$R_B + L \underset{k_{2B}}{\overset{k_{1B}}{\rightleftharpoons}} R_BL$$

where the subscripts A and B denote the two conformational states of the receptor. Note there is no interconversion between the states in this model. This mechanism gives rise to biphasic time course curves for ligand association and dissociation (Figure 14) – there are two components to the curves, one fast and one slow (62). Equations are available in Prism for analyzing these data ("Two phase association" and "Two phase decay"). An example of this mechanism and the data analysis is provided in refs (62,63). The mechanism has been extended to handle the competition kinetic scenario (i.e. with two ligands, an unlabeled test ligand and a labeled tracer), as described in ref (62).

Two-step "Conformational Induction" Model

This mechanism is often encountered with enzymes. The ligand first binds the target in a loose complex. The complex then undergoes a conformational change, producing a tightly-bound complex. This is a mechanism of conformational induction – the ligand induces a new conformation of the target after binding to it. This mechanism is discussed in detail in refs (42,64,65). The mechanism scheme is,

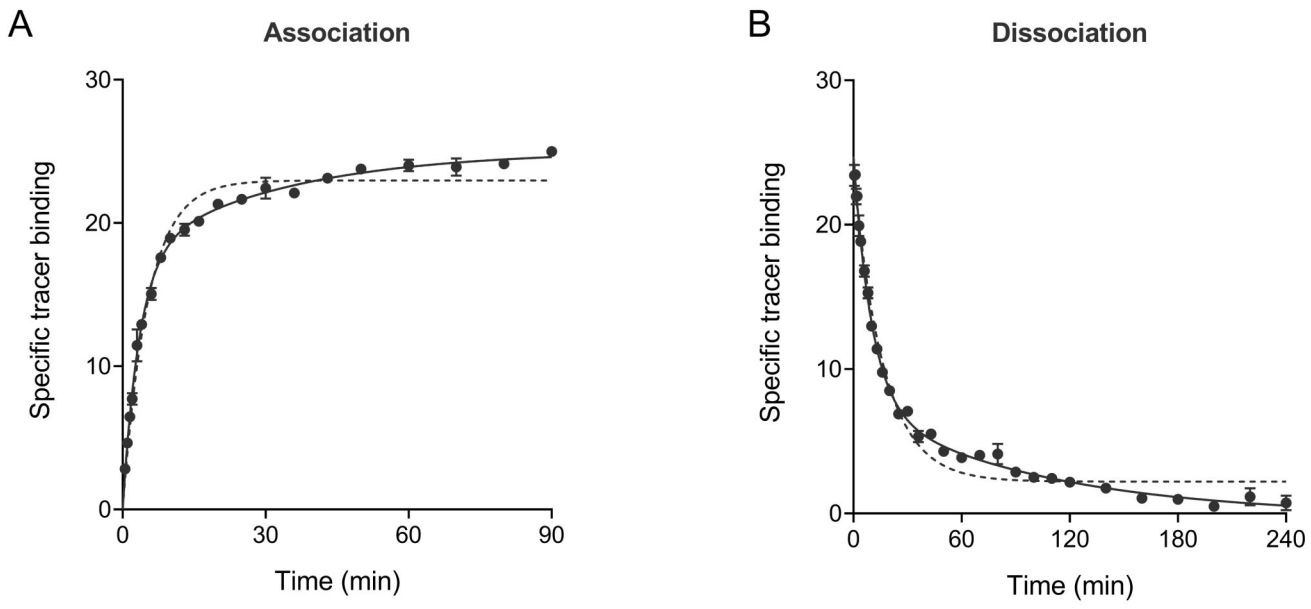

Figure 14. Two conformational states of the target – binding kinetic data. Here there are two states of the target, which bind the ligand with different kinetics. Note the biphasic curves – there is an initial burst, followed by a slower phase of binding. Solid lines are fits to biphasic association (A) or dissociation (B) equations (see ref (62)). The dashed line is the fit to the standard single-state exponential equations – note this provides a poor fit to the data. Data were simulated for a two-state mechanism (see Two Conformational States Mechanism) with following parameter values: k_{1A}, 1.0×10^8 $M^{-1}min^{-1}$; k_{2A}, 0.1 min^{-1}; K_{1B}, 1.0×10^7 $M^{-1}min^{-1}$; k_{2B}, 0.01 min^{-1}; % state A, 70; L, 2 nM; B_{max}, 37.5 target units. Data points are the mean ± SEM of two technical replicates.

$$R + L \underset{k_2}{\overset{k_1}{\rightleftharpoons}} RL \underset{k_R}{\overset{k_T}{\rightleftharpoons}} R'L$$

RL is the first, loosely-bound complex, and R'L is the second, tightly-bound state. The first step is the same as the single-site binding mechanism described in Basic Principles of Ligand Binding Kinetics. The second step is represented as an isomerization event. Transition to and from the R'L state is governed by isomerization rate constants k_T and k_R, respectively.

The shape of the curve depends on the technical properties of the assay. If the emitted binding signal for a molecule of RL and a molecule of R'L is the same (e.g. in a radioligand binding assay) then biphasic curves result, similar to the data in Figure 14 (see data in ref. (65)). Sometimes the binding signal can be dependent on the conformation of the target, for example in fluorescence assays where fluorescence intensity or resonance energy transfer can change when the conformation of the target changes. When the binding signal for R'L is lower than for R, a rise-and-fall curve shape results (unpublished results). In some cases, the initial complex RL is not detected at all, for example in filtration radioligand binding assays where the loosely-bound complex dissociates during the filtration wash step. Under this condition, a monophasic association curve results but the plot of the observed rate versus the ligand concentration is a hyperbola rather than a straight line (42,64).

The mechanism has been extended to handle competition between a labeled tracer and an unlabeled test compound, as described in ref (66).

Dimeric Target Model

In this mechanism, the target consists of a dimer of identical subunits, each subunit containing a single binding site for the ligand. Binding of ligand to one of the subunits within the dimer affects the binding kinetics of the ligand for the second subunit within the dimer.

$$R + L \underset{k_2}{\overset{k_1}{\rightleftharpoons}} RL \underset{\beta k_2}{\overset{\alpha k_1}{\rightleftharpoons}} LRL$$

α is the cooperativity effect of ligand binding to the first subunit on the association rate constant and β is the cooperativity effect on the dissociation rate constant. An equation for this model is derived in ref (67), which also includes a detailed description of the manifestation of the model in the binding data.

Binding Kinetics from Functional Assays

Introduction

In the preceding material we assume a binding assay is available for the target. Often this is not the case and instead all we have available is a functional assay, i.e. an assay of the target's biological action, e.g. product formation by an enzyme, and signaling by a receptor. This is particularly true for new targets in drug discovery. Fortunately, methods are available to quantify the binding kinetics of inhibitor compounds from functional assays. A detailed description is beyond the scope of this chapter but here the basics of the data analysis are presented together with references for further reading.

Enzymes

The binding kinetics of enzyme inhibitors and equations for analyzing the data have been extensively investigated and described (31-34). Methods are available for quantifying inhibitor binding kinetics from enzyme activity assays. The formation of product is measured over time in the absence and presence of the inhibitor. This is done under initial rate conditions, i.e. the linear portion of the time course of product formation. The data are then fit to equations to determine the RT. For enzymes, analysis can be complicated by the myriad of mechanisms by which the inhibitor inhibits the enzyme, and so consultation with an expert in enzymology is recommended.

The RT of enzyme inhibitors is often measured using the jump dilution method (32), a variant of the washout method described above. Enzyme and inhibitor are incubated together to form the enzyme inhibitor complex. Then the reaction is diluted into a much larger volume of assay buffer containing the substrate and all the necessary reaction components. The generation of product is then recorded over time. The jump dilution is designed to reduce the free inhibitor concentration sufficiently that it does not appreciably compete with substrate for the enzyme. Consequently, the inhibition that does occur in the substrate incubation is due to the pre-bound complexes from the inhibitor pre-incubation step; the complex needs to break down before the substrate can bind and product be formed. A vehicle control is included in the experiment in order to record enzyme activity without the inhibitor; the enzyme is pre-incubated with vehicle and diluted in the same way as the inhibitor sample. Data are then analyzed using an appropriate equation to determine the RT (for example, Eq. 8.14 of ref. (32)).

G-protein-coupled Receptors

The activity of GPCRs is measured by recording the signaling pathways these receptors stimulate. Signaling is initiated by binding of an activating ligand (an agonist) to the GPCR. This provides an assay of activity that can be used to quantify the kinetics of inhibitor binding to the GPCR (i.e. antagonist binding).

A straightforward qualitative method for measuring antagonist RT is available employing the washout method (Figure 15) (35,38). This procedure, called recovery of agonist responsiveness, uses the washout procedure described in Compound Washout Method. Cells bearing the receptor are pre-incubated with antagonist long enough for the receptor-antagonist complex to form, then the free antagonist is removed by washing. The cells are then incubated for various times during which the antagonist will dissociate. Following this, agonist is applied and a rapid signaling assay is conducted (e.g. Ca^{2+} mobilization). The strength of the signal provides a readout of antagonist binding – the more antagonist that is bound, the lower the signaling by the agonist. The amount of signal is plotted against the time after antagonist washout. Over time, the response increases owing to dissociation of the antagonist, freeing the receptor to bind the agonist and so generate a signal. The time it takes the response to recover can be used as an assessment of the RT of the compound for the receptor. This is usually quantified as the half-time. However, the relationship between recovery time and RT is not one-to-one, owing to the pharmacological phenomenon of receptor reserve (which dissociates the degree of receptor occupancy from the degree of functional response). The recovery time is a relative measure of RT, useful for ranking compounds. Technical considerations in this assay include the use of a short duration signaling assay (so that antagonist does not appreciably dissociate during the signaling assay), and effective washout of the antagonist to avoid false positive long RTs (as described in Compound Washout Method).

More sophisticated methods are available for quantifying binding kinetics in GPCR functional assays. These require a familiarity with receptor theory. One method utilizes the phenomenon of insurmountability, a property of slowly-dissociating antagonists in functional assays in which the antagonist reduces the maximal response to the agonist (36,37). Alternatively, if there is no receptor reserve in the functional assay the signaling time course can be directly fitted using an analogue of the competition kinetics equation (39).

Summary

The kinetics of target-ligand interaction provide an additional dimension to the understanding of drug target function and the optimization of novel therapeutics. This chapter enables the newcomer to quantify binding kinetics, specifically how to measure the rate constants for ligand association and dissociation. Analysis is straightforward for direct target-ligand binding assays. More advanced data analysis is required for indirect competition binding assays for quantifying binding kinetics of the large numbers of compounds encountered in modern drug discovery. This analysis, within the range of expertise of most investigators, is taught in easy-to-use step-by-step guides, and aided by guidance on troubleshooting and data interpretation. More complex scenarios are introduced, including complex binding mechanisms and the measurement of binding kinetics in functional assays for enzymes and GPCRs. By describing how to quantify binding kinetics, this chapter will aid investigators in applying and evaluating the role of the temporal dimension of binding activity to their targets of interest.

Appendix: Equations for Binding Kinetic Data Analysis

The equations used to analyze the data are derived from first principles applied to the binding mechanism diagrams (53). The equations define the concentration of target-ligand complex as a function of time. They are used to fit the time course data to estimate the rate constant values for the binding interaction. In this section, the techniques for deriving the basic binding equations are presented, for the direct target-ligand binding interactions (See Equations for Direct Target-Ligand Binding Kinetics Analysis). Next, the competition kinetics equation is presented, used for measuring unlabeled test compound binding kinetics in competition with a labeled tracer ligand (see Original Competition Kinetics Equation). This equation has been adapted to allow for rapid competitor dissociation (See Adaptation for Rapidly-Dissociating Compounds), and for pre-incubation of target with compound (Pre-incubating with Test Compound). Finally, an equation for analyzing data from the washout kinetics method is described.

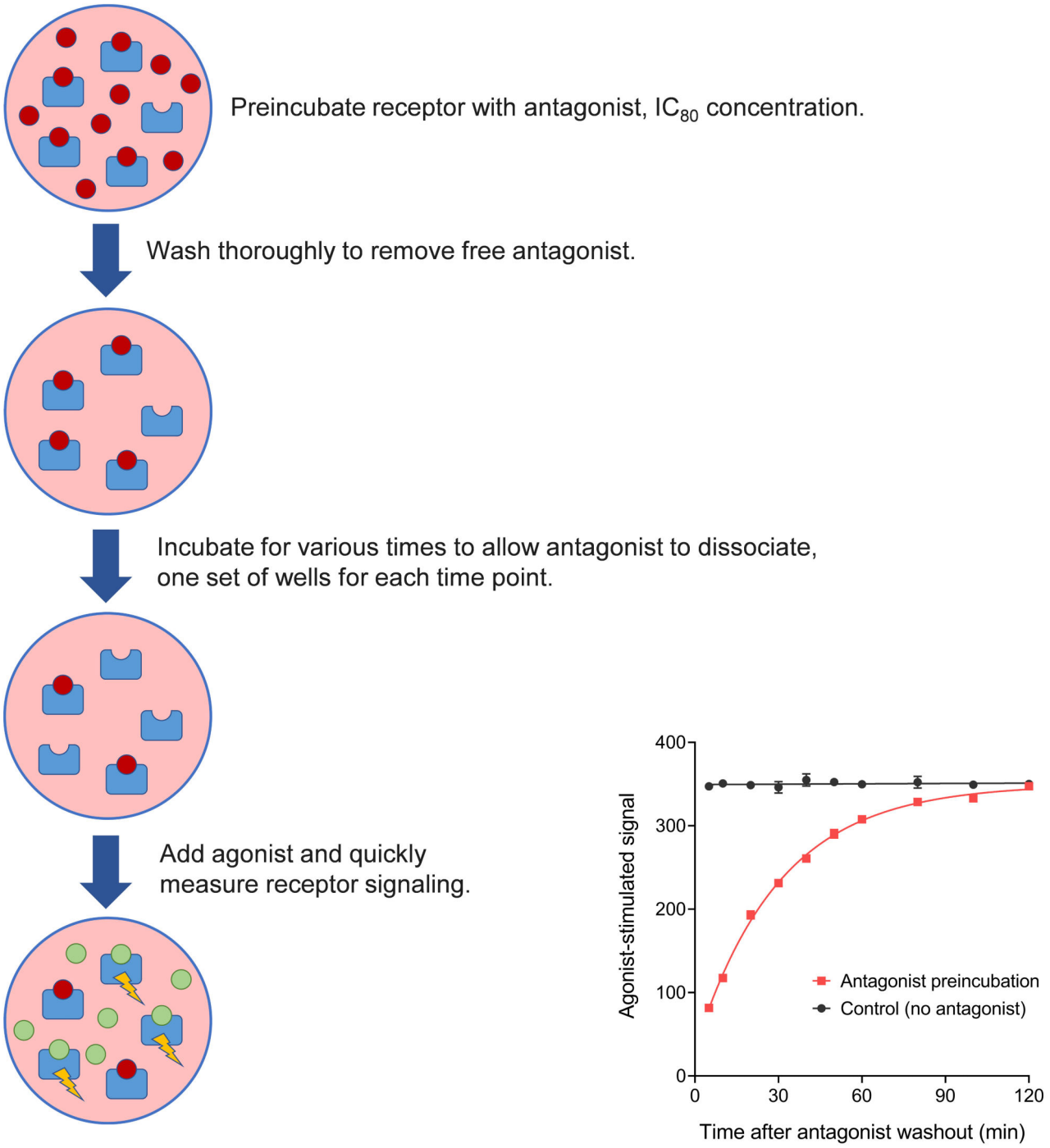

Figure 15. Recovery of agonist responsivity method for measuring antagonist residence time. In this method for signal-transducing receptors, the agonist signal is used to assess occupancy by the antagonist (35,38). Receptor-antagonist complexes are formed during a pre-incubation step. The unbound antagonist is then removed by washing. The wells are then left incubating for various times during which the antagonist will dissociate from the receptor. At the desired time points, occupancy by the antagonist is assessed indirectly by adding agonist ligand and immediately recording the signal. The more receptors are bound by the antagonist, the lower the agonist signal. Data are then plotted as shown in the graph – the response to the agonist versus the time after washout of antagonist. As time progresses, responsivity to the agonist returns (red symbols), owing to dissociation of antagonist from the receptor, freeing the receptor to respond to the agonist.

Equations for Direct Target-Ligand Binding Kinetics Analysis

Association Time Course Equation

The mechanism for the basic target-ligand interaction is:

$$R + L \underset{k_2}{\overset{k_1}{\rightleftharpoons}} RL$$

Scheme 1

This mechanism is a single-site, single-step reversible binding interaction between ligand L and target R. The binding kinetics are defined by the association rate constant k_1 and dissociation rate constant k_2. The equation derivation is for conditions of minimal ligand depletion, meaning the bound concentration is much less than the total concentration of ligand across the time course (< 20%, ideally < 10% ("Zone A")). (For ligand depletion conditions, use Eq. 11 of ref. (40).)

The goal is an equation that defines the concentration of target-ligand complex ([RL]) as a function of time (t) and the mechanism parameters of interest (k_1 and k_2). We start by writing equations that describe the rate of formation and the rate of breakdown of the target-ligand complex. From first principles, the rate of formation is the product of the free ligand concentration, free target concentration and the association rate constant:

$$\text{Rate of formation} = [R][L]k_1$$

The rate of breakdown is the product of the target-ligand complex concentration and the dissociation rate constant:

$$\text{Rate of breakdown} = [RL]k_2$$

The next step is to write the equation that defines the rate of change of the target-ligand complex concentration over time, after target and ligand are mixed together. This is a differential equation. The rate of change, $d[RL]/dt$ is equal to the rate of formation minus the rate of breakdown, giving the equation

$$\frac{d[RL]}{dt} = [R][L]k_1 - [RL]k_2$$

This equation contains two time-dependent terms, [RL] (the species we are measuring, the y axis value of the time course) and [R]. Note that [L], the free ligand concentration, is constant over time because it is not depleted by formation of [RL]. The derivation proceeds by removing the second time-dependent term [R]. This is done using a common mathematical maneuver in pharmacology and enzymology, the conservation of mass equation. This simply expresses the target species in the system as a function of a constant, the total concentration of targets, $[R]_{TOT}$. Specifically,

$$[R]_{TOT} = [R] + [RL]$$

Note that $[R]_{TOT}$ is constant over time. [R] is now expressed in terms of $[R]_{TOT}$ and [RL] by rearranging the conservation of mass equation:

$$[R] = [R]_{TOT} - [RL]k_2$$

In the context of a binding assay, it is convenient to express $[R]_{TOT}$ in terms of the total number of binding sites for the ligand, termed B_{max}. B_{max} is equal to $[R]_{TOT}$ for targets with a single binding site, so we can write,

$$[R] = B_{max} - [RL]$$

We now substitute [R] in the differential equation with B_{max} – [RL]:

$$\frac{d[RL]}{dt} = B_{max}[L]k_1 - [RL][L]k_1 - [RL]k_2$$

This equation is now simplified to the following:

$$\frac{d[RL]}{dt} = B_{max}[L]k_1 - [RL]([L]k_1 + k_2)$$

The next step is to convert the differential equation to an equation of the form [RL] = $f(t)$ where $f(t)$ is a function of time. This is called the "Analytic form" and is the format used by curve-fitting programs commonly used in ligand binding data analysis. This step requires facility with integral calculus. Fortunately, in this case the integral is well known and the integration can be done directly, giving:

$$[RL] = \frac{B_{max}[L]k_1}{[L]k_1 + k_2}\left(1 - e^{-([L]k_1 + k_2)\cdot t}\right)$$

This equation is adapted to analyze the data, as follows. First of all, it can be expressed in a general form. This general form is an equation found in curve fitting programs, and is the association exponential equation (Eq. 1):

$$[RL] = [RL]_{t(inf)} \times \left(1 - e^{-k_{obs}t}\right) \quad \text{Eq. 1}$$

where,

$$[RL]_{t(inf)} = \frac{B_{max}[L]k_1}{[L]k_1 + k_2}$$
$$k_{obs} = [L]k_1 + k_2$$

Time course data are analyzed with Eq. 1. [RL] is the y value, t the x value, and the fitted values are $[RL]_{t(inf)}$ (the binding level at the plateau) and k_{obs} (the rate constant) (see Association Rate Constant from a Direct Target-Ligand Binding Assay). In Prism, Eq. 1 is named "One-phase association" (41).

The $k_{obs} = [L]k_1 + k_2$ equation is now used to determine the k_1 value (see Association Rate Constant from a Direct Target-Ligand Binding Assay). k_{obs} is measured for a range of ligand concentrations (Figure 3A) and then k_{obs} is plotted versus the ligand concentration. This plot is a straight line with gradient of k_1 (Figure 3B) so the data are analyzed by linear regression. The fitted value of the gradient is equal to k_1.

Dissociation Time Course Equation

In the dissociation assay, the target-ligand complex is formed, and then the decay of the target-ligand complex is measured over time after an experimental intervention that blocks the association interaction (the dissociation phase). Association can be blocked by washing out the unbound ligand, or, when a labeled ligand is being used, addition of a large excess of unlabeled ligand. The mechanism in the dissociation phase of the experiment is simply breakdown of the target-ligand complex:

$$RL \xrightarrow{k_2} R + L$$

Scheme 2

The equation defining the dissociation time course is derived using the same strategy as described above for the association process. The rate of change of the target-ligand complex over time is simply the rate of decay of the complex:

$$\frac{d[RL]}{dt} = -[RL]k_2$$

Note the negative sign, indicating [RL] is declining over time. The next step is to obtain the analytic form, and this is done directly by integration, giving the equation used to analyze the data (Eq. 2):

$$[\mathrm{RL}] = [\mathrm{RL}]_{t0} \times e^{-k_2 t} \quad \text{Eq. 2}$$

This equation is used to analyze dissociation time course data (Figure 2B). [RL] is the y value, t is the x value, and k_2 and $[\mathrm{RL}]_{t0}$ are the fitted parameters. In Prism, Eq. 2 is named "One-phase decay." (43)

Competition Kinetics Equations

In the competition kinetics assay, an unlabeled compound is competed against a labeled tracer ligand for binding to the target. The analysis assumes the two ligands bind the same site on the target and that the binding events are simple single-site, single-step reversible interactions. The equations assume minimal depletion of the free ligand concentration (for both the labeled and unlabeled ligand). The mechanism is illustrated in Figure 4 and shown schematically below:

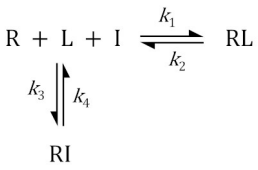

Scheme 3

By convention, k_1 and k_2 are the association and dissociation rate constants, respectively, of the labeled ligand (L), with k_3 and k_4 being the corresponding rates for the unlabeled test ligand (I).

Original Competition Kinetics Equation

In the original, commonly-used method, target is exposed simultaneously to both ligands (i.e. the target is added last to the assay). The data take the form of the time course of labeled ligand binding in the presence of the unlabeled compound (Figure 6). The equation describing these data is a bi-exponential equation and is rather complex to the uninitiated investigator, but it is a straightforward analytical equation where [RL] is a function of time and mechanism parameters. It has been loaded as a built-in equation in Prism (named "Kinetics of competitive binding" (48)) so it isn't necessary to enter it manually when using this program. The equation, Eq. 4, is:

$$[\mathrm{RL}] = \frac{\mathrm{B_{max}}[\mathrm{L}]k_1}{K_F - K_S}\left[\frac{k_4(K_F - K_S)}{K_F K_S} + \frac{k_4 - K_F}{K_F}e^{-K_F t} - \frac{k_4 - K_S}{K_S}e^{-K_S t}\right] \quad \text{Eq. 4}$$

where,

$$K_F = 0.5\left\{K_A + K_B + \sqrt{(K_A - K_B)^2 + 4[\mathrm{L}][\mathrm{I}]k_1 k_3}\right\}$$
$$K_S = 0.5\left\{K_A + K_B - \sqrt{(K_A - K_B)^2 + 4[L][I]k_1 k_3}\right\}$$
$$K_A = [\mathrm{L}]k_1 + k_2$$
$$K_B = [\mathrm{I}]k_3 + k_4$$

Note that K_F, K_S, K_A and K_B are composite parameters introduced to simplify writing of the equation into curve-fitting programs. The original papers describing the equation are refs. (18,19) and a detailed description of the mathematical methods used to derive it is in ref. (53)

Adaptation for Rapidly-Dissociating Compounds

Occasionally the unlabeled test compound dissociates too rapidly for the analysis method to quantify k_4 reliably (Limits of Sensitivity). A false fit results, where the program fits a curve to the data well, but that returns unrealistic estimates of k_3 and k_4 (see Box 5, bottom graph and data table). Effectively, the compound is immediately and constantly at equilibrium with free targets. The analysis method can be adapted to quantify the binding affinity of such a compound from the time course data. The equation for this analysis is Eq. 5 (51-52):

$$[\mathrm{RL}] = \frac{\mathrm{B_{max}}[\mathrm{L}]k_1(1-\rho_I)}{k_{obs}}\left(1-e^{-k_{obs}t}\right) \quad \text{Eq. 5}$$

where,

$$\rho_I = \frac{[\mathrm{I}]}{K_\mathrm{i}+[\mathrm{I}]}$$
$$k_{obs} = [\mathrm{L}]k_1(1-\rho_I)+k_2$$

K_i is the equilibrium binding affinity of the unlabeled test compound. Note ρ_I and k_{obs} are composite parameters introduced to simplify writing of the equation into curve-fitting programs.

This equation, named "[Pharmechanics] Kinetics of competitive binding, rapid competitor dissociation", is available in the supplementary Prism file "Custom equations for binding kinetics".

Pre-incubating with Test Compound

The original competition kinetics equation assumes target is exposed simultaneously to test compound and tracer ligand (18,19). An equation is also available that assumes the target is pre-incubated with a test compound before the tracer is added (53,54). The equation is a close analogue of the original equation – it is extended to include a term for binding of compound during the pre-incubation. The equation (Eq. 6) is:

$$[\mathrm{RL}] = \frac{\mathrm{B_{max}}[\mathrm{L}]k_1}{K_F-K_S}\left[\frac{k_4(K_F-K_S)}{K_FK_S}+\frac{k_4-K_F}{K_F}e^{-K_Ft}-\frac{k_4-K_S}{K_S}e^{-K_St}\right]-\frac{\mathrm{B_{max}}[\mathrm{L}]k_1}{K_F-K_S}\times\frac{[\mathrm{I}]k_3}{K_B}\left(1-e^{-K_Bt_{\mathrm{PI}}}\right)\left(e^{-K_S\cdot t}-e^{-K_F\cdot t}\right) \quad \text{Eq. 6}$$

The terms are defined in the section Original Competition Kinetics Equation. t_{PI} is the pre-incubation time with compound and t (the x value) is time after tracer ligand addition. This equation, named "[Pharmechanics] Kinetics of competitive binding: Competitor pre-incubation", is available in the supplementary Prism file "Custom equations for binding kinetics".

Pre-incubating with Tracer

An equation is also available that assumes the tracer is pre-incubated with the target before an unlabeled test compound is added (53). The equation (Eq. 7) is:

$$[\mathrm{RL}] = \frac{\mathrm{B_{max}}[\mathrm{L}]k_1}{K_F-K_S}\left[\frac{k_4(K_F-K_S)}{K_FK_S}+\frac{k_4-K_F}{K_F}e^{-K_Ft}-\frac{k_4-K_S}{K_S}e^{-K_St}\right]+\frac{\mathrm{B_{max}}[\mathrm{L}]k_1}{K_F-K_S}\left(1-e^{-K_At_{\mathrm{PI}}}\right)\left(\frac{K_B-K_S}{K_A}e^{-K_S\cdot t}-\frac{K_B-K_F}{K_A}e^{-K_F\cdot t}\right)$$

Here t_{PI} is the pre-incubation time with tracer and t (the x value) is time after compound addition. This equation, named "[Pharmechanics] Kinetics of competitive binding: Labeled ligand pre-incubation." is available in the supplementary Prism file "Custom equations for binding kinetics".

Washout Kinetics Method Equation

An alternative method for measuring unlabeled compound RT is the washout method, popular for certain classes of targets such as protein kinases (55). In this experiment, compound is pre-incubated with target to allow target-compound complexes to form (Figure 11). Next, the free (unbound) compound is washed out, leaving the compound-target complexes in the well. Next, a tracer ligand is added and tracer binding recorded

over time. The pre-bound compound delays association of the tracer (Figure 11 graph). This is because the compound first has to dissociate before tracer can bind. An equation, Eq. 8, has been derived for analyzing the tracer time course data (53,56):

$$[RL] = \frac{B_{max}[L]k_1}{K_A}\left[1 - \left(1 - \frac{B_0 \times 0.01 \times K_A}{K_A - k_4}\right)e^{-K_A t} - \frac{B_0 \times 0.01 \times K_A}{K_A - k_4}e^{-k_4 t}\right] \quad \text{Eq. 8}$$

where B_0 is the percentage of the target population bound by test compound at the end of the pre-incubation step.

The association rate constant of unlabeled test compound (k_3) can be determined if multiple concentrations of compound are run in the assay. Analysis using Eq. 8 will give a separate B_0 for each concentration of compound. The B_0 value can then be plotted versus the compound concentration [I], and the data analyzed using the following equation:

$$B_0 = 100 \times \frac{B_{max}[I]k_3}{[I]k_3 + k_4}\left(1 - e^{-([I]k_3 + k_4)t_{PI}}\right)$$

References

1. Copeland R. A., Pompliano D. L., Meek T. D. Drug-target residence time and its implications for lead optimization. Nat Rev Drug Discov. 2006;5:730–739. doi: 10.1038/nrd2082. doi. PubMed PMID: 16888652.
2. Swinney D. C. The role of binding kinetics in therapeutically useful drug action. Curr Opin Drug Discov Devel. 2009;12:31–39. PubMed PMID: 19152211.
3. Copeland R. A. The drug-target residence time model: a 10-year retrospective. Nat Rev Drug Discov. 2016;15:87–95. doi: 10.1038/nrd.2015.18. doi. PubMed PMID: 26678621.
4. Dahl G., Akerud T. Pharmacokinetics and the drug-target residence time concept. Drug Discov Today. 2013;18:697–707. doi: 10.1016/j.drudis.2013.02.010. doi. PubMed PMID: 23500610.
5. de Witte W. E. A., Danhof M., van der Graaf P. H., de Lange E. C. M. The implications of target saturation for the use of drug-target residence time. Nat Rev Drug Discov. 2018;18:82–84. doi: 10.1038/nrd.2018.234. doi. PubMed PMID: 30591716.
6. Folmer R. H. A. Drug target residence time: a misleading concept. Drug Discov Today. 2018;23:12–16. doi: 10.1016/j.drudis.2017.07.016. doi. PubMed PMID: 28782685.
7. Georgi V., et al. Binding Kinetics Survey of the Drugged Kinome. J Am Chem Soc. 2018;140:15774–15782. doi: 10.1021/jacs.8b08048. doi. PubMed PMID: 30362749.
8. Guo D., Hillger J. M. AP, I. J. & Heitman, L. H. Drug-target residence time--a case for G protein-coupled receptors. Med Res Rev. 2014;34:856–892. doi: 10.1002/med.21307. doi. PubMed PMID: 24549504.
9. Swinney D. C. Biochemical mechanisms of New Molecular Entities (NMEs) approved by United States FDA during 2001-2004: mechanisms leading to optimal efficacy and safety. Curr Top Med Chem. 2006;6:461–478. PubMed PMID: 16719803.
10. Tonge P. J. Drug-Target Kinetics in Drug Discovery. ACS Chem Neurosci. 2018;9:29–39. doi: 10.1021/acschemneuro.7b00185. doi. PubMed PMID: 28640596.
11. Vauquelin G. Effects of target binding kinetics on in vivo drug efficacy: koff, kon and rebinding. Br J Pharmacol. 2016;173:2319–2334. doi: 10.1111/bph.13504. doi. PubMed PMID: 27129075.
12. Vauquelin G., Charlton S. J. Long-lasting target binding and rebinding as mechanisms to prolong in vivo drug action. Br J Pharmacol. 2010;161:488–508. doi: 10.1111/j.1476-5381.2010.00936.x. doi. PubMed PMID: 20880390.
13. Zhang R., Monsma F. Binding kinetics and mechanism of action: toward the discovery and development of better and best in class drugs. Expert Opin Drug Discov. 2010;5:1023–1029. doi: 10.1517/17460441.2010.520700. doi. PubMed PMID: 22827742.

14. Hothersall J. D., Brown A. J., Dale I., Rawlins P. Can residence time offer a useful strategy to target agonist drugs for sustained GPCR responses? Drug Discov Today. 2016;21:90–96. doi: 10.1016/j.drudis.2015.07.015. doi. PubMed PMID: 26226643.
15. Sykes D. A., Stoddart L. A., Kilpatrick L. E., Hill S. J. Binding kinetics of ligands acting at GPCRs. Mol Cell Endocrinol. 2019;485:9–19. doi: 10.1016/j.mce.2019.01.018. doi. PubMed PMID: 30738950.
16. Georgi V., et al. Binding kinetics in drug discovery - A current perspective. Front Biosci (Landmark Ed). 2017;22:21–47. doi: 10.2741/4470. doi. PubMed PMID: 27814600.
17. Hoare S. R. J., Fleck B. A., Williams J. P., Grigoriadis D. E. The importance of target binding kinetics for measuring target binding affinity in drug discovery: a case study from a CRF1 receptor antagonist program. Drug Discov Today. 2020;25:7–14. doi: 10.1016/j.drudis.2019.09.011. doi. PubMed PMID: 31557449.
18. Aranyi P. Kinetics of the hormone-receptor interaction. Competition experiments with slowly equilibrating ligands. Biochim Biophys Acta. 1980;628:220–227. doi: 10.1016/0304-4165(80)90369-4. doi. PubMed PMID: 6244003.
19. Motulsky H. J., Mahan L. C. The kinetics of competitive radioligand binding predicted by the law of mass action. Mol Pharmacol. 1984;25:1–9. PubMed PMID: 6708928.
20. Bernetti M., Masetti M., Rocchia W., Cavalli A. Kinetics of Drug Binding and Residence Time. Annu Rev Phys Chem. 2019;70:143–171. doi: 10.1146/annurev-physchem-042018-052340. doi. PubMed PMID: 30786217.
21. Vauquelin, G., Huber, H. & Swinney, D. C., Experimental Methods to Determine Binding Kinetics. *Thermodynamics and Kinetics of Drug Binding* (eds G.M. Keserü & D.C. Swinney) Ch. 9, 169-189 (Wiley-VCH Verlag GmbH & Co. KGaA, 2015).
22. Auld, D. S. *et al.* Receptor Binding Assays for HTS and Drug Discovery. In *Assay Guidance Manual* (eds G. S. Sittampalam *et al.*) (2004).
23. Alberty R. A., Hammes G. G. Application of the Theory of Diffusion-controlled Reactions to Enzyme Kinetics. Journal of Physical Chemistry. 1958;62:154–159. doi: 10.1021/j150560a005. doi.
24. Hill T. L. Effect of rotation on the diffusion-controlled rate of ligand-protein association. Proc Natl Acad Sci U S A. 1975;72:4918–4922. doi: 10.1073/pnas.72.12.4918. doi. PubMed PMID: 1061081.
25. Pan A. C., Borhani D. W., Dror R. O., Shaw D. E. Molecular determinants of drug-receptor binding kinetics. Drug Discov Today. 2013;18:667–673. doi: 10.1016/j.drudis.2013.02.007. doi. PubMed PMID: 23454741.
26. Schiele, F., Ayaz, P. & Mueller-Fahrnow, A., The Use of Structural Information to Understand Binding Kinetics. *Thermodynamics and Kinetics of Drug Binding.* Vol. 65 (eds G.M. Keserü & D. C. Swinney) Ch. 12, 237-256 (Wiley-VCH Verlag GmbH & Co. KGaA, 2015).
27. Rich R. L., Myszka D. G. Survey of the 2009 commercial optical biosensor literature. J Mol Recognit. 2011;24:892–914. doi: 10.1002/jmr.1138. doi. PubMed PMID: 22038797.
28. Soave M., Briddon S. J., Hill S. J., Stoddart L. A. Fluorescent ligands: Bringing light to emerging GPCR paradigms. Br J Pharmacol. 2019. doi: 10.1111/bph.14953. doi. PubMed PMID: 31877233.
29. Zwier J. M., et al. A fluorescent ligand-binding alternative using Tag-lite(R) technology. J Biomol Screen. 2010;15:1248–1259. doi: 10.1177/1087057110384611. doi. PubMed PMID: 20974902.
30. Freyer M. W., Lewis E. A. Isothermal titration calorimetry: experimental design, data analysis, and probing macromolecule/ligand binding and kinetic interactions. Methods Cell Biol. 2008;84:79–113. doi: 10.1016/S0091-679X(07)84004-0. doi. PubMed PMID: 17964929.
31. Copeland, R. A., Slow binding inhibitors. *Evaluation of enzyme inhibitors in drug discovery* Ch. 6, 203-244 (Wiley, 2013).
32. Copeland, R. A., Drug-target residence time. *Evaluation of enzyme inhibitors in drug discovery* Ch. 8, 287-344 (Wiley, 2013).
33. Morrison J. F., Walsh C. T. The behavior and significance of slow-binding enzyme inhibitors. Adv Enzymol Relat Areas Mol Biol. 1988;61:201–301. doi: 10.1002/9780470123072.ch5. doi. PubMed PMID: 3281418.
34. Szedlacsek S. E., Duggleby R. G. Kinetics of slow and tight-binding inhibitors. Methods Enzymol. 1995;249:144–180. doi: 10.1016/0076-6879(95)49034-5. doi. PubMed PMID: 7791610.

35. Bosma R., et al. The Target Residence Time of Antihistamines Determines Their Antagonism of the G Protein-Coupled Histamine H1 Receptor. Front Pharmacol. 2017;8:667. doi: 10.3389/fphar.2017.00667. doi. PubMed PMID: 29033838.
36. Kenakin T., Jenkinson S., Watson C. Determining the potency and molecular mechanism of action of insurmountable antagonists. J Pharmacol Exp Ther. 2006;319:710–723. doi: 10.1124/jpet.106.107375. doi. PubMed PMID: 16857731.
37. Mould R., Brown J., Marshall F. H., Langmead C. J. Binding kinetics differentiates functional antagonism of orexin-2 receptor ligands. Br J Pharmacol. 2014;171:351–363. doi: 10.1111/bph.12245. doi. PubMed PMID: 23692283.
38. Sahlholm K., et al. The fast-off hypothesis revisited: A functional kinetic study of antipsychotic antagonism of the dopamine D2 receptor. Eur Neuropsychopharmacol. 2016;26:467–476. doi: 10.1016/j.euroneuro.2016.01.001. doi. PubMed PMID: 26811292.
39. Hoare S. R. J., Pierre N., Moya A. G., Larson B. Kinetic operational models of agonism for G-protein-coupled receptors. J Theor Biol. 2018;446:168–204. doi: 10.1016/j.jtbi.2018.02.014. doi. PubMed PMID: 29486201.
40. Lehnert T., Figge M. T. Dimensionality of Motion and Binding Valency Govern Receptor-Ligand Kinetics As Revealed by Agent-Based Modeling. Front Immunol. 2017;8:1692. doi: 10.3389/fimmu.2017.01692. doi. PubMed PMID: 29250071.
41. Motulsky, H. J. *Equation: One phase association.* < Available at: http://www.graphpad.com/guides/prism/latest/curve-fitting/reg_exponential_association.htm> (2019).
42. Strickland S., Palmer G., Massey V. Determination of dissociation constants and specific rate constants of enzyme-substrate (or protein-ligand) interactions from rapid reaction kinetic data. J Biol Chem. 1975;250:4048–4052. PubMed PMID: 1126943.
43. Motulsky, H. J. *Equation: One phase decay.* < Available at: http://www.graphpad.com/guides/prism/latest/curve-fitting/reg_exponential_decay_1phase.htm> (2020).
44. Hoare S. R., de Vries G., Usdin T. B. Measurement of agonist and antagonist ligand-binding parameters at the human parathyroid hormone type 1 receptor: evaluation of receptor states and modulation by guanine nucleotide. J Pharmacol Exp Ther. 1999;289:1323–1333. PubMed PMID: 10336523.
45. Sykes D. A., Jain P., Charlton S. J. Investigating the Influence of Tracer Kinetics on Competition-Kinetic Association Binding Assays: Identifying the Optimal Conditions for Assessing the Kinetics of Low-Affinity Compounds. Mol Pharmacol. 2019;96:378–392. doi: 10.1124/mol.119.116764. doi. PubMed PMID: 31436538.
46. Georgi V., Dubrovskiy A., Steigele S., Fernandez-Montalvan A. E. Considerations for improved performance of competition association assays analysed with the Motulsky-Mahan's "kinetics of competitive binding" model. Br J Pharmacol. 2019;176:4731–4744. doi: 10.1111/bph.14841. doi. PubMed PMID: 31444916.
47. Motulsky, H. J. *Equation: Association kinetics (one ligand concentration)* < Available at: http://www.graphpad.com/guides/prism/latest/curve-fitting/reg_association1.htm> (2019).
48. Motulsky, H. J. *Equation: Kinetics of competitive binding.* < Available at: http://www.graphpad.com/guides/prism/latest/curve-fitting/reg_kinetics_of_competitive_bindin.htm?q=kinetics+of+competitive+binding> (2019).
49. Sykes D. A., et al. Fevipiprant (QAW039), a Slowly Dissociating CRTh2 Antagonist with the Potential for Improved Clinical Efficacy. Mol Pharmacol. 2016;89:593–605. doi: 10.1124/mol.115.101832. doi. PubMed PMID: 26916831.
50. Sykes D. A., et al. The Influence of receptor kinetics on the onset and duration of action and the therapeutic index of NVA237 and tiotropium. J Pharmacol Exp Ther. 2012;343:520–528. doi: 10.1124/jpet.112.194456. doi. PubMed PMID: 22854200.
51. Barkan, K. *et al.* Pharmacological Characterisation of Novel Adenosine Receptor A3R Antagonists. *Sci Rep* Available at: https://pubmed.ncbi.nlm.nih.gov/33247159/ (2020).
52. Motulsky, H. J. *Extensions of the kinetics of competitive binding equation for rapid competitor kinetics or alternative order of reagant addition.* <www.graphpad.com/support/faqid/2102/> (2020).

53. Hoare S. R. J. Receptor binding kinetics equations: Derivation using the Laplace transform method. J Pharmacol Toxicol Methods. 2018;89:26–38. doi: 10.1016/j.vascn.2017.08.004. doi. PubMed PMID: 28818556.
54. Shimizu Y., Ogawa K., Nakayama M. Characterization of Kinetic Binding Properties of Unlabeled Ligands via a Preincubation Endpoint Binding Approach. J Biomol Screen. 2016;21:729–737. doi: 10.1177/1087057116652065. doi. PubMed PMID: 27270099.
55. Robers M. B., et al. Quantitative, Real-Time Measurements of Intracellular Target Engagement Using Energy Transfer. Methods Mol Biol. 2019;1888:45–71. doi: 10.1007/978-1-4939-8891-4_3. doi. PubMed PMID: 30519940.
56. Malany S., Hernandez L. M., Smith W. F., Crowe P. D., Hoare S. R. Analytical method for simultaneously measuring ex vivo drug receptor occupancy and dissociation rate: application to (R)-dimethindene occupancy of central histamine H1 receptors. J Recept Signal Transduct Res. 2009;29:84–93. doi: 10.1080/10799890902721339. doi. PubMed PMID: 19308787.
57. Packeu A., Wennerberg M., Balendran A., Vauquelin G. Estimation of the dissociation rate of unlabelled ligand-receptor complexes by a 'two-step' competition binding approach. Br J Pharmacol. 2010;161:1311–1328. doi: 10.1111/j.1476-5381.2010.00931.x. doi. PubMed PMID: 20946109.
58. Uhlen S., Schioth H. B., Jahnsen J. A. A new, simple and robust radioligand binding method used to determine kinetic off-rate constants for unlabeled ligands. Application at alpha2A- and alpha2C-adrenoceptors. Eur J Pharmacol. 2016;788:113–121. doi: 10.1016/j.ejphar.2016.06.021. doi. PubMed PMID: 27318322.
59. Packeu A., Beghin T., De Backer J. P., Vauquelin G. Antagonist-D2S-dopamine receptor interactions in intact recombinant Chinese hamster ovary cells. Fundam Clin Pharmacol. 2010;24:293–303. doi: 10.1111/j.1472-8206.2009.00777.x. [corrected]. doi. PubMed PMID: 20015228.
60. De Lean A., Stadel J. M., Lefkowitz R. J. A ternary complex model explains the agonist-specific binding properties of the adenylate cyclase-coupled beta-adrenergic receptor. J Biol Chem. 1980;255:7108–7117. PubMed PMID: 6248546.
61. Kent R. S., De Lean A., Lefkowitz R. J. A quantitative analysis of beta-adrenergic receptor interactions: resolution of high and low affinity states of the receptor by computer modeling of ligand binding data. Mol Pharmacol. 1980;17:14–23. PubMed PMID: 6104284.
62. Guo D., et al. A two-state model for the kinetics of competitive radioligand binding. Br J Pharmacol. 2018;175:1719–1730. doi: 10.1111/bph.14184. doi. PubMed PMID: 29486053.
63. Hoare S. R., Strange P. G. Regulation of D2 dopamine receptors by amiloride and amiloride analogs. Mol Pharmacol. 1996;50:1295–1308. PubMed PMID: 8913361.
64. Tummino P. J., Copeland R. A. Residence time of receptor-ligand complexes and its effect on biological function. Biochemistry. 2008;47:5481–5492. doi: 10.1021/bi8002023. doi. PubMed PMID: 18412369.
65. Schreiber G., Henis Y. I., Sokolovsky M. Analysis of ligand binding to receptors by competition kinetics. Application to muscarinic antagonists in rat brain cortex. J Biol Chem. 1985;260:8789–8794. PubMed PMID: 4019453.
66. Schreiber G., Henis Y. I., Sokolovsky M. Rate constants of agonist binding to muscarinic receptors in rat brain medulla. Evaluation by competition kinetics. J Biol Chem. 1985;260:8795–8802. PubMed PMID: 4019454.
67. White C., Bridge L. J. Ligand Binding Dynamics for Pre-dimerised G Protein-Coupled Receptor Homodimers: Linear Models and Analytical Solutions. Bull Math Biol. 2019;81:3542–3574. doi: 10.1007/s11538-017-0387-x. doi. PubMed PMID: 29349610.

Validating Identity, Mass Purity and Enzymatic Purity of Enzyme Preparations*

John E Scott, Ph.D.[1] and Kevin P Williams, Ph.D.[1]

Created: May 1, 2012; Updated: October 1, 2012.

Abstract

When developing enzyme assays for HTS, the integrity of the target enzyme is critical to the quality of the HTS and the actives, or "hits", identified through the screens. The incorrect identity or lack of enzymatic purity of the enzyme preparation will significantly affect the results of a screen. In this chapter, the authors discuss in detail the consequences of impure and mis-identified enzyme preparations, potential steps that can be taken to avoid measurement of the wrong activity and methods to validate the enzymatic purity of an enzyme preparation.

Definitions

Enzyme Identity

Enzyme identity determination is the confirmation that the protein preparation in fact contains the enzyme of interest. Enzyme identity is confirmed by demonstrating that the experimentally determined primary amino acid sequence matches the predicted primary amino acid sequence (see Identity and Mass Purity).

Mass Purity

Mass purity refers to the percentage of the protein in a preparation that is the target enzyme or protein. For instance, 90 µg of enzyme in a solution containing a total of 100 µg of protein is considered to be 90% pure (see Identity and Mass Purity).

Enzymatic Purity or Activity Purity

Enzymatic purity or activity purity refers to the fraction of activity observed in an assay that comes from a single enzyme. Typically, if 100% (or nearly so) of the observed activity in an enzyme assay is derived from a single enzyme then the enzyme preparation is considered enzymatically pure, even if it lacks mass purity. If two or more activities are detected in an enzyme assay then the enzyme preparation is enzymatically impure (see Validating Enzymatic Purity). Note that enzymatic purity is **not** the same as specific activity, which is enzymatic activity (in defined units) per unit mass of protein (typically mg of protein).

Interrelationships between Identity, Mass and Enzymatic Purity

High mass purity and high specific activity are highly desirable in an enzyme used for screening because it decreases the probability of measuring contaminating enzyme activities. However, high mass purity or high specific activity alone does not guarantee enzymatic purity. On the other hand, enzymatically pure preparations may have poor mass purity. It is also possible to have an enzymatically pure preparation with all the activity coming from the wrong enzyme! For enzyme assays, enzymatic purity is absolutely essential to establish before screening (unless intentionally screening with mixed enzymes). Arguably, enzyme identity and enzymatic purity

*Edited by Tod Holler and Andrew Napper, Ph.D.

Author Affiliation: 1 Biomanufacturing Research Institute and Technology Enterprise (BRITE) North Carolina Central University, Durham, NC; Email: jscott@nccu.edu; Email: kpwilliams@nccu.edu.

are the most critical factors. It is possible to have a valid enzyme assay with poor (or no) mass purity if it can be demonstrated that 100% of the observed activity is coming from the target enzyme.

Consequences of using Enzymatically Impure Enzyme Preparations.

The consequences of using enzymatically impure enzyme preparations for a screen are multiple and far reaching. First, if the lot of enzyme used for assay development is enzymatically impure with the chosen substrate and format then the assay conditions could be optimized for the wrong enzyme activity. In addition, the contaminating activity may not be revealed until after the screen, when abnormally shaped IC_{50} curves are obtained (see Identity and Mass Purity). Inhibitors obtained from such a screen will likely be a mixture of inhibitors for the target and/or non-target. Depending on the fraction of signal contributed by the contaminating activity, the most potent inhibitors may be ones that are non-selective and inhibit both/all enzyme activities present. In other words, the screen may produce hits that are biased towards non-selective inhibitors, compounds that interfere with the assay format (like colored compounds), "nuisance" hits such as aggregators/reactive compounds, or a combination of these undesirable results. Thus, many or most target selective compounds may not appear as hits. Furthermore, compounds in the screening database would be annotated with false and misleading data.

Signs of Enzymatic Contamination

i. Inhibitor IC_{50} values ≥10-fold different compared to literature or gold standard assay (see Inhibitor-Based Studies).
ii. Inhibitor IC_{50} slopes are shallow (Hill slope < 1) (see Inhibitor-Based Studies).
iii. Unable to reach complete inhibition of activity at high concentrations of inhibitor (see Inhibitor-Based Studies).
iv. Biphasic IC_{50} curves (see Inhibitor-Based Studies).
v. IC_{50} curves that plateau at significantly less than 100% enzyme activity at low inhibitor concentrations (see Inhibitor-Based Studies).
vi. K_m values do not match expected value (see Substrate-Based Studies).
vii. Abnormally shaped K_m plot (see Substrate-Based Studies).
viii. Unexpected substrate specificities (see Substrate-Based Studies).
ix. Lack of reproducible activity and/or IC_{50} values between two different assay formats with the same preparation of enzyme (see Comparison Studies).
x. Different sources of enzyme (e.g. from different vendors) or different batches of enzyme (produced in the same lab) produce different IC_{50} values or Hill slopes (see Comparison Studies and Importance of Batch Testing) .
xi. Post-screen: A high percentage of screen hits display Hill slopes that are very broad or do not reach complete inhibition (see Inhibitor-Based Studies) .

Solutions for Enzymatic Contamination

i. Purify enzyme further (add more steps to eliminate contaminating enzymes) or evaluate enzyme preparations from external or commercial suppliers.
ii. Use a substrate that is more specific for the target enzyme.
iii. Optimize/change buffer conditions to eliminate detection of other activities (e.g., change pH or NaCl concentration).
iv. Change assay format to one that is more specific for the target of interest.

v. Use multiple inhibitors for IC_{50} experiments, instead of just one, in case the problem lies with the reference inhibitor compound.
vi. Use inhibitors of contaminating activity in the assay buffer: The use of protease and phosphatase inhibitor cocktails may be necessary to inhibit contaminating activities. EDTA can sometimes be used to eliminate the activity of Mg^{2+}-dependent contaminating activities, assuming the target enzyme does not require a divalent metal ion like Mg^{2+} or Mn^{2+}. Control experiments should be undertaken to ensure any inhibitors do not interfere with the target protein activity.

Importance of Batch Testing

Each new batch of enzyme should be subject to some level of enzymatic purity testing since there may be contaminating enzyme present in each new preparation due to variability in expression and purification. Thus, both large and small scale purifications of enzyme need to be validated, even when the purification protocol remains the same. Batch-to-batch variability and scale-up of enzyme purifications for screening could result in subtle changes that result in, for example, differences in the percentage of target protein proteolysis or in host enzyme impurities. At minimum, new batch testing might include performing SDS-PAGE analysis for mass purity and identity along with using the most selective reference inhibitor and confirming that the IC_{50} value and Hill slope obtained using the new batch of enzyme matches the original batch. Ideally, there should only be one or two lots of enzyme – one small one for assay development and one large bulk lot for screening/follow-up. Multiple smaller batches can be pooled before assay development/validation. In theory, but not necessarily in practice, the screening lot should get the most rigorous validation (before screening).

Identity and Mass Purity

Confirming enzyme identity is important because it prevents screening with the wrong enzyme. This problem arises occasionally, particularly when the target is expressed in a heterologous host. Thus, the determination of protein identity and mass purity is essential prior to any assay development and high throughput screening (HTS). In reality, no protein is purified to absolute homogeneity. After purification, the target protein may still contain contaminants derived either from the target protein itself or from host proteins. Remaining contaminants in a protein preparation may or may not interfere with the assay format under consideration.

Methods for Confirming Identity and Mass Purity

Proteins used for HTS have typically been expressed as a recombinant form in a heterologous host. This form of expression may result in denatured, aggregated or proteolyzed forms of the target protein. Many excellent texts exist covering methods to determine protein purity including chapters in Current Protocols in Protein Sciences series (1) and Methods in Enzymology (2). A number of methods can be used to assess sample purity with the choice depending on sample availability, required accuracy and sensitivity. A simple wavelength scan also allows an assessment of non-proteinaceous contamination such as DNA/RNA.

Protein stain of SDS-PAGE

A typical first assessment for sample purity is the use of sodium dodecyl sulfate polyacrylamide gel electrophoresis (SDS-PAGE) with either Coomassie blue staining or the more sensitive silver staining. These techniques are easy, rapid and inexpensive. Gradient SDS gels (e.g., 4-20%) allow the detection of a wide range of molecular weights and are very useful for assessing sample purity. Overloading the gel with 25-50 µg of protein allows more sensitive detection of contaminating proteins. Densitometry of the stained gel allows some estimation of purity.

Western blot with specific antibody

Western blotting with antibodies specific to the target protein allows a confirmation of identity and a determination of intactness of the target protein.

Analytical gel filtration

Analytical gel filtration can be used to assess the presence of some contaminants under native conditions and also the presence and amount of target protein aggregates. A symmetrical peak eluting at the predicted molecular weight is indicative of a pure single species with no aggregation or degradation. Additional peaks eluting before the protein of interest may be aggregates, and peaks eluting after may be degradation products. To confirm, fractions can be collected and analyzed by Western blotting and mass spectrometry to assess if the additional peaks are derived from the protein of interest.

Reversed-phase HPLC

Reversed-phase HPLC (RP-HPLC) using a stationary phase, such as C4 or C8, is another rapid method for assessing target purity and the presence of contaminants in the protein sample. UV detection at 280 nm is typically used to monitor proteins, but when RP-HPLC is used in combination with a diode array detector, the simultaneous monitoring of a large number of wavelengths allows for detection of non-proteinaceous material as well.

Mass Spectrometry

Mass spectrometry (MS) is the best technique (least ambiguous) for establishing protein identity because it provides an accurate direct measurement of protein mass. Mass accuracy will depend on the size of the protein but is typically around 0.01%. Furthermore, mass spectrometry provides the best approach to measuring not only the presence of impurities, but their mass as well and hence the possibility of identification. Although many labs do not possess the requisite equipment or expertise for mass spectrometry, many mass spectrometry facilities will characterize samples as a fee-based service.

Whole mass measurement of protein

Matrix assisted laser desorption ionization (MALDI) time-of-flight (TOF) mass spectrometry is typically used for protein mass measurement because it can analyze proteins over a wide mass range, up to 200 kDa or higher. Proteins should be desalted, e.g. using a C4 ZipTip (Millipore Co.). Samples are deposited onto an α-cyano-4-hydroxycinnamic acid matrix prepared in an aqueous solvent containing 50% acetonitrile and 10 mM ammonium citrate. Protein mass is determined using a MALDI TOF mass spectrometer. A comparison of the measured mass with the predicted mass allows confirmation of identity. Masses higher than predicted may indicate protein modifications, either post-translational or experimental, e.g. oxidation. Masses lower may be degradation products. Additional peaks in the spectrum may indicate the presence of contaminants although it should be remembered that ionization efficiencies may differ. For MALDI TOF, depending on the molecular size being measured and instrument used, mass accuracy is typically approximately 10 ppm to 0.01%.

Peptide mass fingerprinting

Identity of a protein can be confirmed using peptide mass fingerprinting. In this technique, peptide fragments are generated by in-gel tryptic digestion of a Coomassie Blue stained protein band excised from a 1-D SDS-PAGE gel. The resulting peptides can be analyzed using MALDI TOF/TOF MS and observed peptide masses compared to the NCBI non-redundant database using a search algorithm such as the MASCOT MS/MS Ions search algorithm (Matrix Science: www.matrixscience.com). The observed masses of all the peptides are compared to the calculated masses of the expected peptides resulting from tryptic cleavage of the target protein.

Edman sequencing

In addition to mass spectrometry, N-terminal Edman sequencing can be used to confirm protein identity and assess the homogeneity among primary amino acid sequences in the purified target protein. To identify internal sequences from the target protein, proteins are separated by SDS-PAGE and then transferred to sequencing-grade PVDF membranes. Membranes are stained with Coomassie Blue R-250 for 3 minutes, then bands excised for tryptic peptide analysis. Peptides are separated by reversed-phase HPLC and N-terminal Edman sequencing is then performed on the peptides using a protein sequencer. A number of core facilities will perform Edman sequencing as a fee-based service.

Crude Enzyme Preparations can be used

Enzyme assays have been developed with less than pure proteins, and even cell lysates and whole serum. For example, an activity-based probe has been developed as a highly selective substrate for measuring the activity of the protease DPAP1 in *Plasmodium falciparum* cell lysates and for Cathepsin C in rat liver extracts (3). Furthermore, whole serum has been used as a source of the enzyme PON1 to develop an enzyme assay for HTS (4). The key to this enzyme assay was the use of the highly selective, unique substrate paraoxon. PON1 is the only enzyme in serum capable of hydrolyzing the chemical paraoxon. In these cases, a highly selective substrate is used such that only the target enzyme can efficiently convert it to product in the time frame of the reaction. Enzyme assays that use these crude sources of enzyme require extra rigor in validating enzymatic purity and identity. These assays can be validated with known selective inhibitors and/or multiple methods outlined below (see Validating Enzyme Purity).

Commercial Enzymes can be Impure or Misidentified

Commercial enzymes may be misidentified, have poor mass purity, and display poor enzymatic purity under a particular assay condition. Therefore, even for a commercially-obtained enzyme, it is recommended that the identity of the target protein be confirmed to ensure that not only is the correct protein being used, but that it is also from the correct species. Carrying out a high throughput screen on the incorrect target or on a target from the wrong species is an expensive control experiment! Identity of the target, including primary sequence confirmation, is critical.

Co-purification of Contaminating Enzymes

Host enzymes can co-purify with the recombinant target enzyme. These contaminating host enzymes may have size and physical-chemical properties (like isoelectric point) that are indistinguishable from those of the target enzyme, making their presence in a preparation difficult to detect. This can lead to misleading purity determinations. Multiple methods of identity and mass purity determination can reveal co-purifying contaminates that may have activity in the assay. Enzymatic purity analysis (Validating Enzyme Purity) may also reveal this contaminating activity.

Enzyme Dead Mutant or Mock Parallel Purification

One method used to aide in establishing the identity of a recombinant enzyme preparation is to use an enzymatically inactive site-directed mutant (a mutant of the target that loses all activity) to make inactive enzyme and then apply the same purification protocol to both the wild-type enzyme and the mutant. The idea is that, unlike the wild type enzyme, the mutant-derived enzyme preparation should have no activity in the assay, demonstrating that the activity originates from the recombinant protein, not from contaminating host proteins. An assumption is that the mutation does not alter the over-all structure of the enzyme. This is sometimes also done with empty vector constructs instead of mutant enzymes. While this is a useful technique, it is still

recommended that all enzyme preparations to be used for screening be tested for identity, mass and enzymatic purity as outlined in this chapter.

Reversal of Enzyme Activity by Contaminating Enzyme Activity

Contaminating enzymes can reverse the enzyme reaction by converting product back to substrate or into a different, undetected product. For instance, a contaminating phosphatase in a kinase preparation may dephosphorylate the product and alter the observed enzyme kinetics, depending on the kinase format chosen. Inhibitors of the contaminating activity, e.g. phosphatase inhibitors, can be used to prevent this. The presence of phosphatases in kinase assays may be difficult to detect. A common method is to test the kinase activity in the presence and absence of broad activity phosphatase inhibitors, such as sodium orthovanadate. Lack of an effect by these inhibitors suggests that phosphatase activity is not a problem in the assay. Increasing mass purity of the enzyme preparation can also eliminate such issues.

Assay Design Factors that Affect the Likelihood of Detecting Enzyme Impurities

How an assay is designed and configured can influence whether or not contaminating enzyme activity is detected in the assay. In practice, if a contaminating enzyme is present, but not detected in the final assay, then there is no problem. The choice of substrate, enzyme concentration, and assay format can have a profound impact on the probability of detecting any enzyme impurities, if present.

Substrate Selection

Consequences of substrate selectivity

a. **Selective substrates**: The use of a selective substrate is an excellent method of reducing the chances of detecting any contaminating enzymes that may be present in an enzyme preparation. If only the target enzyme generates a detectable signal, any contaminating enzymes that are present become irrelevant, since they do not contribute to the assay window. In fact, extremely selective substrates have been used to detect specific enzyme activity in whole cell lysates (e.g. luciferin for cell-based luciferase assays) or whole serum (e.g. hydrolysis of paraoxon by PON1 in serum).
b. **Non-selective substrates**: Using less selective substrates, those that can be converted to product by many enzymes, increases the probability that contaminating enzymes will cause a problem. Therefore, the use of non-selective substrates requires the developer to obtain more data to demonstrate that the correct activity is being measured. For a kinase assay, the presence of a contaminating kinase may impact the assay depending on the selectivity of the substrate. For instance, the polymer substrate poly-[Glu,Tyr] can be phosphorylated by most tyrosine kinases, so this substrate will also detect contaminating tyrosine kinase activity, if present. In contrast, the use of a natural protein or selective peptide substrate may reduce the chances of detecting contaminating kinase activity. Another example of a non-selective substrate is para-nitrophenol phosphate (pNPP), which can be used as a substrate for a wide variety of phosphatases.

Substrate K_m

Substrate selectivity has the largest impact on whether contaminating enzyme activity is detected in an assay. However, when choosing between equally selective substrates, the substrate with the lowest K_m is preferable (with all other considerations being equal). When substrates are used that have a high K_m value, higher amounts of substrate are needed in the reaction to obtain a good assay signal. However, with higher substrate concentration, especially for non-selective substrates, the chances are greater for detecting any contaminating enzyme activity that may be present. The use of substrates at concentrations at or below K_m value will select for

detection of the enzyme in the preparation with the greatest activity towards the substrate. Furthermore, the substrate concentration should be kept at ≤ K_m to ensure the sensitive detection of substrate competitive inhibitors, if desired.

Enzyme Concentration

The concentration of enzyme used in an assay can determine whether contaminating enzymes, if present, are detected or not. Using high concentrations of target enzyme, based on the mass purity, increases the risk of detecting contaminating activity, especially for non-selective substrates. Conversely, using a low 1 nM enzyme concentration, for example, means that picomolar levels of contaminating activity would need to be detected to interfere with the assay. Coupled enzyme assays are particularly vulnerable to the detection of impurity activities because high concentrations of the coupling enzymes, which may also be contaminated with interfering activities, are usually added so as not to be a rate-limiting factor in the assay.

Format Selection

Assay formats that are broadly applicable to a large class of enzymes are convenient, but increase the odds of detecting any contaminating activity present. For example, ADP detection methods for measuring kinase activity will detect all kinases in a preparation, and even any ATPases present. Thus, these types of assay formats should be used with care, and enzymatic purity should be verified by multiple methods (see Validating Enzymatic Purity). Highly specific formats will reduce the odds of detecting non-target activity. An example of this more selective format is a kinase assay that uses a natural substrate protein and an antibody to detect phosphorylation at a specific residue. Formats that allow very sensitive detection of the product may allow the use of low concentrations of enzyme, which may avoid the detection of very low activity/low concentration contaminating enzymes (see Enzyme Concentration).

Validating Enzymatic Purity

Enzymatic purity can be assessed using inhibitor-based studies, substrate-based studies and/or comparison studies. Inhibitor-based studies are the most commonly used and the single best way to validate enzymatic purity. Combinations of these methods can also be used to enhance confidence in the assay. Enzymatic purity can be highly substrate and format dependent; that is, the same enzyme preparation can be used with one substrate/format and have 100% of the detected activity come from the intended target enzyme, but a different substrate or format may reveal multiple enzyme activities that are present in the preparation. Note that high specific activity preparations may be obtained, but there still could be multiple enzymes present that perform the same reaction and therefore the preparation would lack enzymatic purity. This can occur, if for instance, the contaminating enzyme(s) are the same size as the target or if the contaminating enzymes are present at a small percent by mass but with higher specific activity than the target enzyme.

Inhibitor-Based Studies

Inhibitors of enzymatic activity are critical tools, and many times the only practical tool, to validate the enzymatic purity of enzyme preparations. Once an enzymatic assay has been established under kinetically valid conditions and optimized (see Basic Enzyme Assays), inhibitors described in the literature for the enzyme can be used to aide in validating that only one enzyme activity is being measured. Inhibitors are usually small organic molecules, but can also be small peptides or analogs of the natural substrate. In general, two types of inhibitors can be used for this purpose – relatively selective inhibitors and non-selective inhibitors. Selective inhibitors are preferable in verifying activity purity, but non-selective or modestly selective inhibitors are also useful when there is no practical alternative. Inhibition by selective inhibitors increases the confidence that the correct activity is being measured. However, non-selective inhibitors within a given enzyme class will frequently have a reported IC_{50} value and critical data can be ascertained concerning activity purity. For example, staurosporine is

a broad spectrum kinase inhibitor that can be used when a selective kinase inhibitor is not available. A small panel of non-selective inhibitors with a range of potencies can also be used to compare results to literature and increase confidence in the activity purity of the assay/enzyme preparation. Any known activators of enzyme activity can also be used as evidence of enzymatic identity. **There are three important values that can be derived from concentration-response inhibition curves that aide in enzymatic purity validation: IC_{50} value, Hill slope and maximal inhibition.**

For complete evaluation of IC_{50} data as outlined here, maximum and minimum signal controls must be performed along with the inhibitor titration. Maximum controls should consist of enzyme reactions with no inhibitor – just DMSO. Minimum signal controls should be performed by using DMSO only (no inhibitor) and leaving enzyme out of the reaction (adding just buffer instead) to represent 100% enzyme inhibition.

IC_{50} value

IC_{50} values for known inhibitors should match or be close to the literature values, with the caveat that different assay conditions (e.g. substrate concentration, total protein, pH, etc) may alter apparent potencies. Alternatively, inhibitors can be tested in a different validated assay format using the same enzyme preparation or a completely different source of enzyme, for example a commercially available enzyme. IC_{50} values can then be compared between the different formats. IC_{50} values are generally considered to be in close agreement if they differ by a factor of three or less.

Hill slope

The steepness or shallowness of the IC_{50} curve, referred to as the Hill slope, can provide valuable information as to whether a single enzyme is being inhibited. Inhibitors that bind to a single binding site on the enzyme should yield concentration response curves with a Hill slope of 1.0, based on the law of mass action (5, 6, and discussion of Hill slopes in Receptor Binding Assays). A negative sign in front of the Hill slope value may be ignored – the ± sign on a Hill slope signifies the direction of the curve, which changes if the data is plotted using percent activity or percent inhibition. Both selective and non-selective enzyme inhibitors should display a concentration response curve that has a Hill slope of close to 1.0. Thus, after plotting a concentration response curve for an inhibitor, there are three possible results when analyzing the slope (Figure 1):

- **Hill slope = 1.0.** This indicates a high probably that a single enzyme is generating the observed signal in the assay. An acceptable slope range under careful, manually-performed, experimental conditions is 0.8 to 1.2. The observation of this normal Hill slope using multiple inhibitors with a range of potencies greatly enhances confidence in the enzymatic purity of the assay. Multiple inhibitors are particularly useful when only non-selective inhibitors are available.
- **Hill slope < 1.0.** A shallow slope (for example <0.8) derived from the IC_{50} curve may indicate that there is more than one enzyme that is contributing to the assay signal. This occurs when two or more enzymes are generating signal, but they have different, but non-resolvable affinities for the inhibitor. The result is a blended IC_{50} curve that is broader than expected. If the two affinities are different enough to be resolved in the experiment, a biphasic curve will result. Thus, biphasic curves are also strongly suggestive of multiple activities present. However, in standard 10 point (1:3 dilutions) IC_{50} curves, a partial biphasic curve may appear as a single curve where the low concentrations of inhibitor produce a plateau at significantly less than the expected 100% enzyme activity as determined by controls (Figure 1B). This type of curve can be due to multiple enzyme activities or an artifact of the experiment caused by misleading controls due to, for example, well position or edge effects. Differentiating these two possibilities requires follow-up experiments.

- **Hill slope > 1.0.** A steep slope (Hill slope >> 1.0, for example >1.5) may indicate that the inhibitor is either forming aggregates in aqueous solution and inhibiting non-specifically (see 7 and Mechanism of Action assays for Enzymes), chemically reacting with the enzyme or chelating a required co-factor. This type of inhibitor cannot be used in enzymatic purity validation studies. One important exception to this rule is inhibitors that have IC_{50} values lower than half the active enzyme concentration in the assay – these inhibitors are sometimes referred to as tight-binding inhibitors. These inhibitors are sometimes exquisitely specific to the enzyme target and very potent, but result in steep Hill slopes due to the fact that they are titrating enzyme. If assay sensitivity allows, it may be possible to lower the concentration of enzyme in the reaction below twice the IC_{50} value (even if only for validation studies) and thus demonstrate a Hill slope of 1.0 with tight-binding inhibitors.

Tips, caveats and precautions for using Hill slope data:

- Incomplete curves may give a less accurate Hill slope – the best data is obtained when a complete top and bottom of the curve are obtained (see IC_{50} Determination). When partial curves are obtained because high concentrations of inhibitor cannot be achieved, Hill slope information can be obtained by fitting the inhibition data using a three-parameter logistic fit with the 100% inhibition value (max or min) set equal to the average value of the "no enzyme" control. Achieving high compound concentrations in an assay may be limited by compound solubility or DMSO tolerance.
- Imprecise and/or inaccurate pipetting will shift the Hill slope.
- High assay variability or too few data points can lead to unreliable Hill slope determinations.
- Method of dilution is important –for the purpose of verifying enzymatic purity, change tips between different concentrations in a serial dilution, since this prevents carry-over of compound that could result in erroneous concentrations. For HTS hit confirmation and automated follow-up assays, tip changing is often impractical because tips are expensive or because compounds are being diluted using automated equipment with fixed tips.
- For small molecules, use 100% DMSO as diluent in the initial serial dilution series. These dilutions can then be further diluted into assay buffer for assaying. This minimizes compound precipitation at high concentration when diluted into aqueous solutions, which would alter actual compound concentrations.
- An impure compound (mixture of different inhibitors) may also generate shallow Hill slopes due to different affinities for the target.
- Compound solubility problems can result in a shallow or steep slope.
- Graphing software programs capable of fitting inhibition data with a four-parameter logistic fit will return a value for the Hill slope.
- For a Hill slope of 1.0, there should be a 81-fold inhibitor concentration difference between 10% and 90% inhibition.
- Errant data points will alter the slope – suspected outlier data points should be masked (temporarily removed from the curve) and the curve fitting repeated to see if masking the data point(s) dramatically improves the fit quality (see IC_{50} Determination).
- Rarely, an enzyme may have more than one binding site and the Hill slope should be a higher integer (e.g., 2.0, 3.0, or higher).
- It is conceivable that multiple forms of the same enzyme might be present in the assay (for example due to heterogeneous post-translational modification) and that they may have different affinities for an inhibitor. It the two affinities cannot be resolved, the result will be a broadening of the IC_{50} curve.
- It is theoretically possible to have two very similar enzymes (i.e. isozymes or isoforms) present in the enzyme preparation that have identical affinities for an inhibitor resulting in ideal shaped IC_{50} curves. Isoform selective inhibitors (sometimes discovered later) may show the contamination.

A normal Hill slope is supporting evidence for enzymatic purity in the developed assay, while an unexpected Hill slope requires further investigation into the enzymatic purity of the enzyme preparation.

Maximal inhibition.

The highest concentrations in a complete IC_{50} curve should result in close to 100% inhibition of the assay signal based on controls with and without enzyme. **Lack of complete inhibition, even with a Hill slope = 1.0, is strongly suggestive that more than one enzyme activity is being measured.** This can occur if the inhibitor only inhibits one of the enzymes present, but does not inhibit the other enzymes that also contribute to assay signal. Such curves can have a "normal" shape, but at the highest concentrations of inhibitor, the curve plateaus (flattens out) at significantly less than 100% inhibition (Figure 2). Partial curves with normal Hill slopes are exempted from this criterion. Partial, or incomplete, curves show some inhibition at the highest concentrations of inhibitor, but lack data points displaying complete (100%) inhibition based on controls i.e. no clear plateau. Generally, the most accurate Hill slopes for partial curves will be obtained by using a three parameter fit where 100% inhibition is fixed to equal the average value from control wells that represent no enzyme activity (such as by leaving the enzyme out of the reaction). The most common cause of partial curves is simply low potency of the compound to inhibit the target enzyme. Poor compound solubility at higher concentrations could also explain lack of complete inhibition, but in that case, the curve is unlikely to have a normal appearance and a Hill slope of 1.0.

In summary, while inhibitor studies that result in expected IC_{50} values, display expected Hill slopes and reach complete inhibition are not infallible proof of enzymatic purity, they provide strong evidence that only one enzyme species is being measured. Conversely, inhibitor studies that result in un-expected IC_{50} values, have unexpected Hill slopes, and/or fail to achieve complete signal inhibition are not proof of contaminating enzyme activity, but are strong warning signs that should not be ignored. These results require further investigation to either rule out enzyme contamination, lay the blame elsewhere, or to prove enzyme contamination and require a change of enzyme source before proceeding. It is especially troubling when these warning signs are observed for multiple inhibitors.

Substrate-Based Studies

If no suitable inhibitors are available, or to further confirm enzymatic purity, substrate-based studies can be employed. Two approaches can be used: substrate K_m determinations and substrate selectivity studies.

Substrate K_m determination

Substrate K_m determinations are usually done during assay development (see Basics of Enzymatic Assays for HTS). The K_m value should be close to the literature value (less than 10-fold difference), though different assay conditions can alter observed K_m values. The K_m plot (initial velocity vs. substrate concentration) should follow a single-site rectangular hyperbolic curve giving a defined V_{max}. K_m values ≥10-fold different from literature values and/or abnormal shaped curves are suggestive of possible enzyme contamination or an error in enzyme identity. Hyperbolic curves may not be achievable if the Km value is very high and assay format limitations preclude testing sufficiently high concentrations of substrate.

Substrate selectivity studies

Different substrates for the same enzyme target can be tested to demonstrate selectivity. These studies can be done by performing K_m determinations and comparing k_{cat}/K_m values to the literature or expected selectivity. However, it is more easily performed by testing the different substrates at the same concentration; a concentration well below the expected K_m value. In this case, the initial velocity will be proportional to k_{cat}/K_m and therefore the measured velocities will allow a relative determination of how good a substrate is for the target.

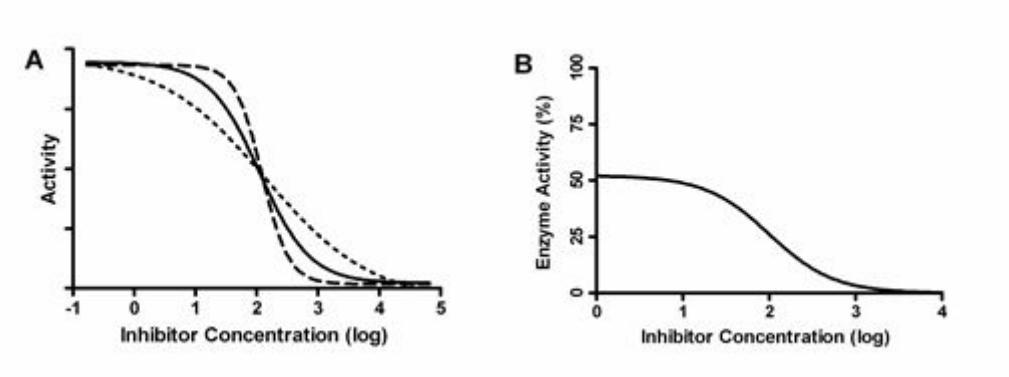

Figure 1. IC_{50} curves with a Hill slope of 1.0 (solid line), 2.0 (dashed), 0.5 (dotted) (A). Partial biphasic graph (B)

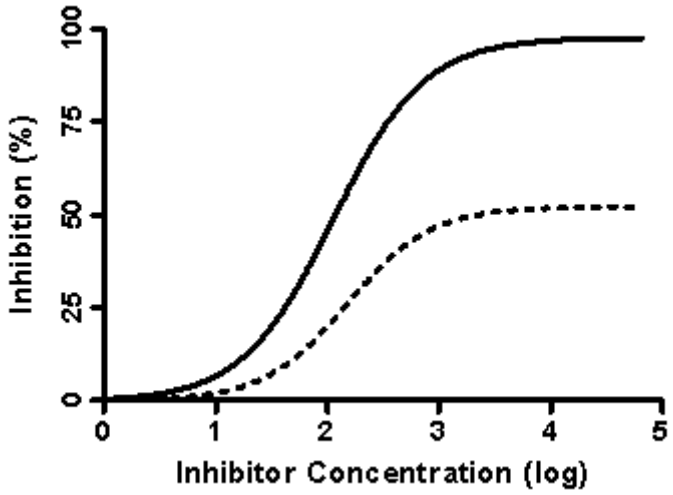

Figure 2: Complete IC_{50} curve (solid line) compared to an incomplete maximal inhibition curve (dashed line). Note that both curves have a Hill slope of 1.0.

If substrate selectivity does not match expectations, then this may be a sign of contamination or mis-identification of the enzyme preparation. Similar substrates that should not result in measurable activity using the target enzyme can also be used to exclude certain enzymes that might be contaminants in the primary assay.

Comparison Studies

For some little-studied enzymes, no or few inhibitors have been identified and substrate selectivity is unknown. For these targets, inhibitor studies and substrate studies are limited or not possible due to availability of inhibitors and substrates. In these cases, comparison studies can be done to aid in verifying purity, though the evidence for enzymatic purity that is generated is not as strong as with the inhibitor and substrate based studies.

Enzyme source comparison studies

The enzyme preparation under scrutiny may be compared to other enzyme preparations from different sources, such as commercially-generated enzyme. The basis for this comparison study is that different purification methods (and ideally different source organisms, e.g., mammalian vs. insect cells) are unlikely to generate the same contaminating enzymes at the same concentrations. An exception would be enzymes that co-purify due to physical association. Different enzyme sources can be compared by performing K_m determination studies with

each enzyme using the same substrate. The K_m values should be within 3-fold of each other if the same enzyme activity is being measured. In addition, the curve should follow a single-site rectangular hyperbolic curve giving a defined V_{max} (assuming high enough concentrations of substrate can be used). For recombinant enzymes, one can also generate enzyme inactive mutants (at least empty vector control cells) to help establish that a host enzyme is not being measured (see Enzyme Dead Mutant or Mock Parallel Purification). For a highly selective substrate, it may also be possible to demonstrate that there is no measurable target enzyme activity in host cell lysates so there is little possibility of detecting host enzyme contaminants in the assay.

Format comparison studies

In format comparison studies, the specific activities of the same enzyme preparation are determined using two different formats. If the same enzyme is measured in both formats (in the same assay buffer and substrate concentration), then such a comparison should yield similar activity in both assays (within 10-fold). Since different formats are used, standards would likely be required to convert assay signal to amount of product produced. Lack of activity in one format would be a potential warning sign that different enzymes are being measured in the two assays. This is most useful if one format is highly selective for the enzyme in question (e.g. a gold-standard assay) and this assay used to validate a less selective format. For example, for kinases, an assay where a specific antibody is used to detect phosphorylated protein product could be compared to an ADP detection format which detects all ATPase activity. Similar results would support the purity of the enzyme preparation. Furthermore, format comparison studies can be useful if even just one non-selective weak inhibitor is known for the target. In this case, an IC_{50} value comparison can be done using different formats to gain confidence in the enzymatic purity within the assay.

References

1. Begg GE, Harper SL and Speicher DW (1999) Characterizing Recombinant Proteins using HPLC Gel Filtration and Mass Spectrometry. Curr. Protoc. Protein Sci. 16:7.10.1-7.10.15.
2. Rhodes DG, Laue TM. Determination of Protein Purity. Meths Enzmol. 2009;463:680–689. PubMed PMID: 19892198.
3. Deu E, Yang Z, Wang F, Klemba M, Bogyo M. Use of Activity-Based Probes to Develop High Throughput Screening Assays That Can Be Performed in Complex Cell Extracts. PLoS One; e. 2010;11:985. PubMed PMID: 20700487.
4. Graves TL, Scott JE. A High Throughput Serum Paraoxonase Assay for Discovery of Small Molecule Modulators of PON1 Activity. Current Chemical Genomics. 2008; 2008;2:51–61. PubMed PMID: 20161844.
5. H.J. Motulsky and A. Christopoulos. (2003), Fitting Models to Biological Data using Linear and Nonlinear Regression. A practical guide to curve fitting. GraphPad Software Inc., San Diego CA
6. GraphPad Software Inc. web site: www.graphpad.com
7. Feng BY, Simeonov A, Jadhav A, Babaoglu K, Inglese J, Shoichert BK, Austin CP. A High-Throughput Screen for Aggregation-Based Inhibition in a Large Compound Library. J. Med. Chem. 2007;50:2385–2390. PubMed PMID: 17447748.

Basics of Enzymatic Assays for HTS

Harold B. Brooks,[1] Sandaruwan Geeganage, Steven D. Kahl, Chahrzad Montrose,[2] Sitta Sittampalam,[3,*] Michelle C. Smith, and Jeffrey R. Weidner[4,†]

Created: May 1, 2012; Updated: October 1, 2012.

Abstract

Enzymes are important drug targets. Many marketed drugs today function through inhibition of enzymes mediating disease phenotypes. To design, develop and validate robust enzymatic assays for HTS applications, it is critical to have a thorough understanding of the enzyme biochemistry and the kinetics of enzyme action. This chapter contains basic concepts in enzyme kinetics, selection of appropriate substrates for assay design and the estimation and significance of K_m and V_{max}, the intrinsic kinetic parameters of enzyme targets. These concepts are addressed in the context of drug discovery and HTS assay development.

Author Affiliations: 1 Eli Lilly & Company, Indianapolis, IN. 2 Eli Lilly & Company, Indianapolis, IN. 3 National Institutes of Health, Rockville, MD. 4 AbbVie, Chicago, IL.

* Editor

† Editor

Enzyme Assay Development Flow Chart

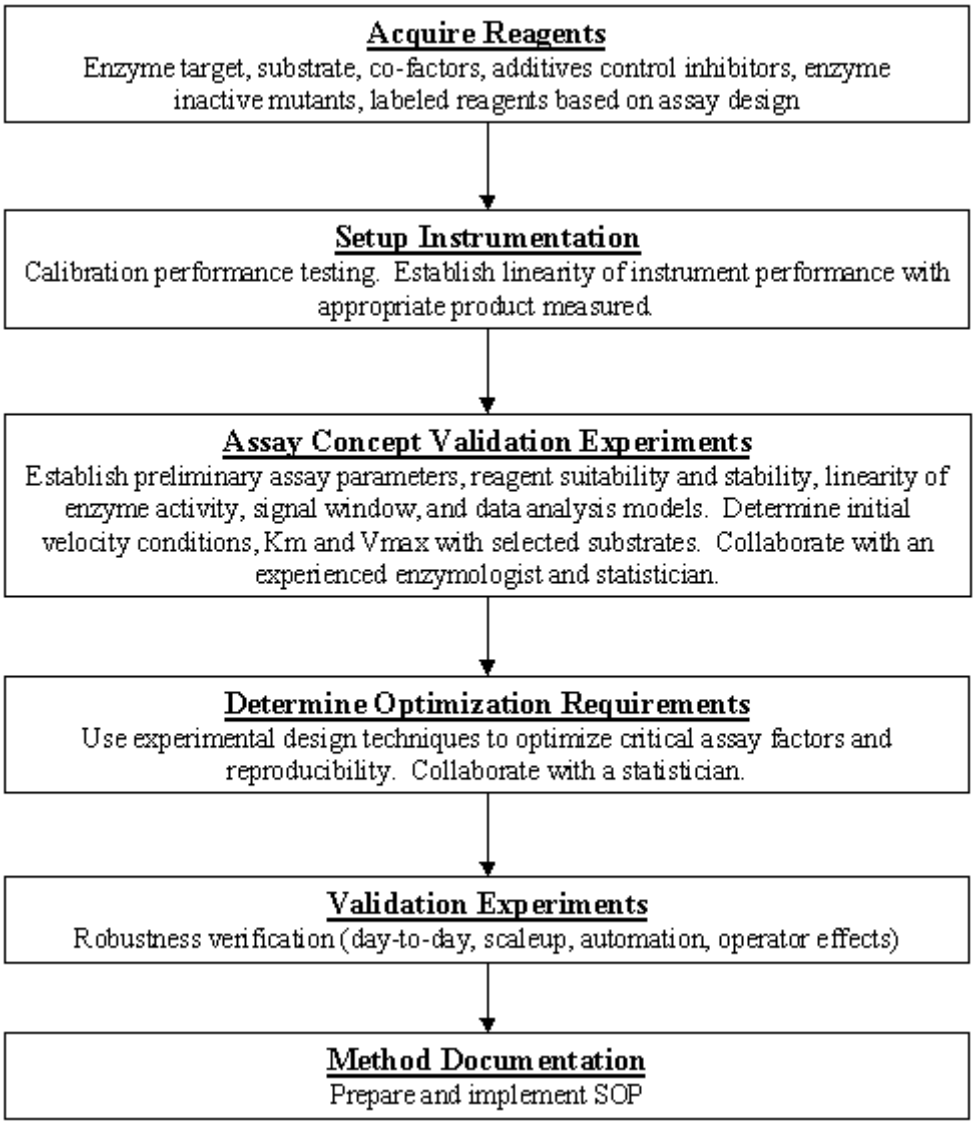

Introduction

Enzyme inhibitors are an important class of pharmacological agents. Often these molecules are competitive, reversible inhibitors of substrate binding. This section describes the development and validation of assays for identification of competitive, reversible inhibitors. In some cases other mechanisms of action may be desirable which would require a different assay design. A separate approach should be used if seeking a non-competitive mechanism that is beyond the scope of this document and should be discussed with an enzymologist and chemist (1).

Concept

Enzymes are biological catalysts involved in important pathways that allow chemical reactions to occur at higher rates (velocities) than would be possible without the enzyme. Enzymes are generally globular proteins that have one or more substrate binding sites. The kinetic behavior for many enzymes can be explained with a simple model proposed during the 1900's:

$$E + S \underset{k_{-1}}{\overset{k_1}{\rightleftharpoons}} ES \xrightarrow{k_2} E + P$$

where E is an enzyme, S is a substrate and P is a product (or products). ES is an enzyme-substrate complex that is formed prior to the catalytic reaction. Term k_1 is the rate constant for enzyme-substrate complex (ES) formation and k_{-1} is the dissociation rate of the ES complex. In this model, the overall rate-limiting step in the reaction is the breakdown of the ES complex to yield product, which can proceed with rate constant k_2. The reverse reaction (E + P → ES) is generally assumed to be negligible.

Assuming rapid equilibrium between reactants (enzyme and substrate) and the enzyme-substrate complex resulted in mathematical descriptions for the kinetic behavior of enzymes based on the substrate concentration (2). The most widely accepted equation, derived independently by Henri and subsequently by Michaelis and Menten, relates the velocity of the reaction to the substrate concentration as shown in the equation below, which is typically referred to as the Michaelis-Menten equation:

$$v = \frac{[S]\ V_{max}}{[S] + K_m}$$

where

v = rate if reaction

V_{max} = maximal reaction rate

S = substrate concentration

K_m = Michaelis-Menten constant

For an enzymatic assay to identify competitive inhibitors, it is essential to run the reaction under ***initial velocity conditions*** with substrate concentrations at or below the K_m value for the given substrate. The substrate should either be the natural substrate or a surrogate substrate, like a peptide, that mimics the natural substrate. The optimal pH and buffer component concentrations should be determined before measuring the K_m (see Optimization Experiments).

What is initial velocity?

- Initial velocity is the initial linear portion of the enzyme reaction when less than 10% of the substrate has been depleted or less than 10% of the product has formed. Under these conditions, it is assumed that the substrate concentration does not significantly change and the reverse reaction does not contribute to the rate.
- Initial velocity depends on enzyme and substrate concentration and is the region of the curve in which the velocity does not change with time. This is not a predetermined time and can vary depending on the reaction conditions.

What are the consequences of not measuring the initial velocity of an enzyme reaction?

- The reaction is non-linear with respect to enzyme concentration.
- There is an unknown concentration of substrate.
- There is a greater possibility of saturation of the detection system
- The steady state or rapid equilibrium kinetic treatment is invalid

Measuring the rate of an enzyme reaction when 10% or less of the substrate has been depleted is the first requirement for steady state conditions. At low substrate depletion, i.e. initial velocity conditions, the factors listed below contribute to non-linear progression curves for enzyme reactions do not have a chance to influence the reaction.

- Product inhibition
- Saturation of the enzyme with substrate decreases as reaction proceeds due to a decrease in concentration of substrate (substrate limitation)
- Reverse reaction contributes as concentration of product increases over time
- Enzyme may be inactivated due to instability at given pH or temperature

Reagents and Method Development

For any enzyme target, it is critical to ensure that the appropriate enzyme, substrate, necessary co-factors and control inhibitors are available before beginning assay development. The following requirements should be addressed during the method design phase:

1. Identity of the enzyme target including amino acid sequence, purity, and the amount and source of enzyme available for development, validation and support of screening/SAR activities. One should also ensure that contaminating enzyme activities have been eliminated. Specific activities should be determined for all enzyme lots.
2. Identify source and acquire native or surrogate substrates with appropriate sequence, chemical purity, and adequate available supply.
3. Identify and acquire buffer components, co-factors and other necessary additives for enzyme activity measurements according to published procedures and/or exploratory research.
4. Determine stability of enzyme activity under long-term storage conditions and during on bench experiments. Establish lot-to-lot consistency for long-term assays.
5. Identify and acquire enzyme inactive mutants purified under identical conditions (if available) for comparison with wild type enzyme.

Detection System Linearity

Instrument capacity needs to be determined by detecting signal from product and plotting it versus product concentration. Figure 1 below demonstrates what can happen if a detection system has a limited linear range. In the Capacity 20 trace, the system becomes non-linear at concentrations of product that are greater than 10% of the total product generated. This limited linear range would severely compromise measurements, since it is essential that the enzyme reaction condition be within the linear portion of the instrument capacity. Subsequent assay analysis would be affected if the enzyme reaction were performed outside of this linear portion. The Capacity 100 trace represents a more ideal capability of an instrument that allows a broad range of product to be detected.

The linear range of detection for an instrument can be determined using various concentrations of product and measuring the signal. Plotting the signal obtained (Y-axis) versus the amount of product (X-axis) yields a curve that can be used to identify the linear portion of detection for the instrument.

Enzyme Reaction Progress Curve

A *reaction progress curve* can be obtained by mixing an enzyme and its substrate together and measuring the subsequent product that is generated over a period of time. The initial velocity region of the enzymatic reaction needs to be determined and subsequent experiments should be conducted in this linear range, where less than 10% of the substrate has been converted to product. If the reaction is not in the linear portion, the enzyme

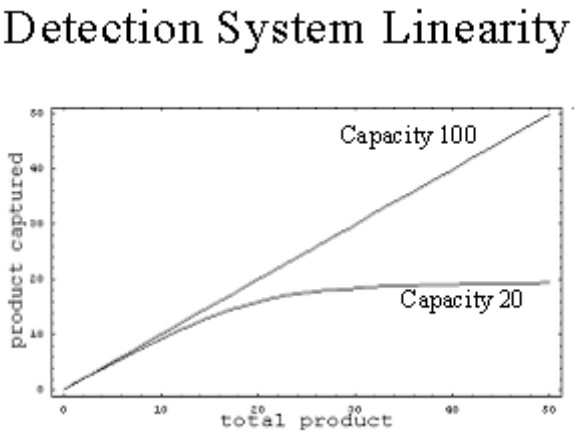

Figure 1: Signal saturation can lead to false measurements of assay parameters, such as K_m

concentration can be modified to retain linearity during the course of the experiments. Both of these steps (modifying the enzyme and analyzing the reaction linearity) can be conducted in the same experiment. An example is shown below in Figure 2.

In this set of data, product is measured at various times for three different concentrations of enzyme and one substrate concentration. The curves for the 1x and 2x relative levels of enzyme reach a plateau early, due to substrate depletion. To extend the time that the enzyme-catalyzed reaction exhibits linear kinetics, the level of enzyme can be reduced, as shown for the 0.5x curve. These curves are used to define the amount of enzyme, which can be used to maintain initial velocity conditions over a given period of time. These time points should be used for subsequent experiments.

Note that all three of the reaction progress curves shown in the example above approach a similar maximum plateau value of product formation. This is an indication that the enzyme remains stable under the conditions tested. A similar experiment performed when enzyme activity decreases during the reaction is shown in Figure 3. In this case, the maximum plateau value of product formed does not reach the same for all levels of tested enzyme, likely due to enzyme instability over time.

Measuring initial velocity of an enzyme reaction

- Keep temperature constant in the reaction by having all reagents equilibrated at the same temperature.
- Design an experiment so pH, ionic strength and composition of final buffer are constant. Initially use a buffer known for the enzyme of interest either by consulting the literature or by using the buffer recommended for the enzyme. This buffer could be further optimized in later stages of development.
- Perform the time course of reaction at three or four enzyme concentrations.
- Need to be able to measure the signal generated when 10% product is formed or to detect 10% loss of substrate.
- Need to measure signal at t=0 to correct for background (leave out enzyme or substrate).

For kinase assays, the background can be determined by leaving out the enzyme or the substrate. The condition resulting in the highest background level should be used. EDTA is **not** recommended for use as the background control during validation of a kinase assay. Once the assay has been validated, if the background measured with EDTA is the same than both the no enzyme and no substrate control, then EDTA could be used.

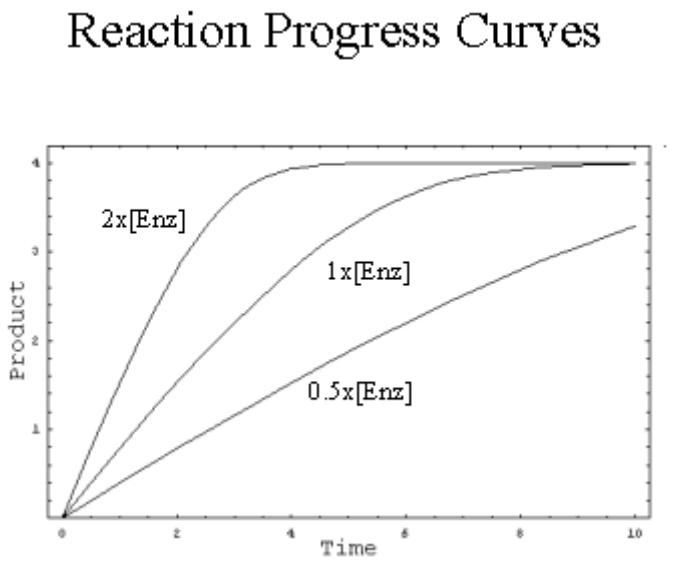

Figure 2: Plateau is due to substrate depletion

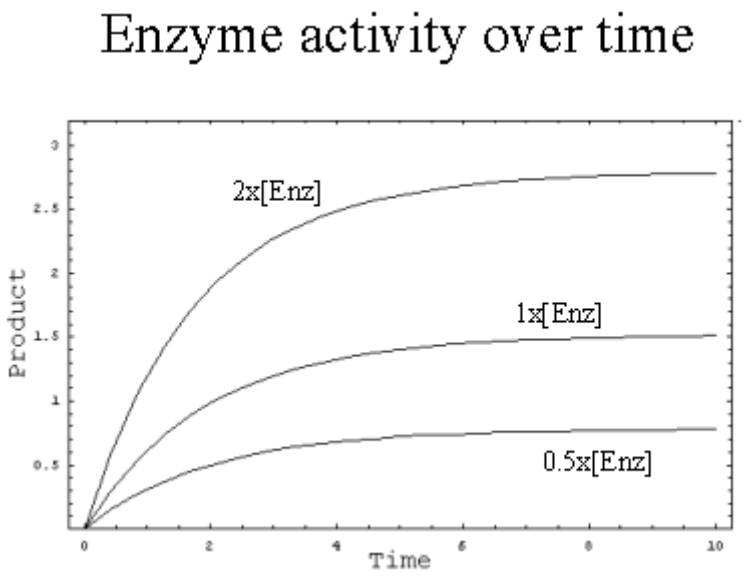

Figure 3: Plateau is due to loss of enzyme activity (note: plateaus do not converge)

Measurement of K_m and V_{max}

Once the initial velocity conditions have been established, the substrate concentration should be varied to generate a saturation curve for the determination of K_m and V_{max} values. **Initial velocity conditions must be used**. The Michaelis-Menten kinetic model shows that the K_m = [S] at $V_{max}/2$. In order for competitive inhibitors to be identified in a competition experiment that measures IC_{50} values, a substrate concentration around or below the K_m must be used. Using substrate concentrations higher than the K_m will make the identification of competitive inhibitors (a common goal of SAR) more difficult.

For kinase assays, the K_m for ATP should be determined using saturating concentrations of the substrate undergoing phosphorylation. Subsequent reactions need to be conducted with optimum ATP concentration, around or below the K_m value using initial velocity conditions. However, it would be best to determine K_m for

ATP and specific substrate simultaneously. This would allow maximum information to be gathered during the experiment as well as address any potential cooperativity between substrate and ATP.

A requirement for steady state conditions to be met means that a large excess of substrate over enzyme is used in the experiment. Typical ratios of substrate to enzyme are greater than 100 but can approach one million.

What does the K_m mean

- If K_m >>> [S], then the velocity is very sensitive to changes in substrate concentrations. If [S] >>> K_m, then the velocity is insensitive to changes in substrate concentration. A substrate concentration around or below the K_m is ideal for determination of competitive inhibitor activity.
- K_m is constant for a given enzyme and substrate, and can be used to compare enzymes from different sources.
- If K_m seems "unphysiologically" high then there may be activators missing from the reaction that would normally lower the K_m *in vivo*, or that the enzyme conditions are not optimum.

How to measure K_m

- Measure the initial velocity of the reaction at substrate concentrations between 0.2-5.0 K_m. If available, use the K_m reported in the literature as a determinant of the range of concentration to be used in this experiment. Use 8 or more substrate concentrations.
- Measuring K_m is an iterative process. For the first iteration, use six substrate concentrations that cover a wide range of substrate concentrations, to get an initial estimate. For subsequent iterations, use eight or more substrate concentrations between 0.2-5.0 K_m. Make sure there are multiple points above and below the K_m.
- For enzymes with more than one substrate, measure the K_m of the substrate of interest with the other substrate at saturating concentrations. This is also an iterative process. Once the second K_m is measured, it is necessary to check that the first K_m was measured under saturating second substrate concentrations.
- Fit the data to a rectangular hyperbola function using non-linear regression analysis. Traditional linearized methods to measure K_m's should not be used.

Figures 4 and 5 demonstrate a typical procedure to determine the K_m for a substrate. In Figure 4, reaction product is measured at various times for 8 different levels of substrate. The product generated (Y-axis) is plotted against the reaction time (X-axis). Each curve represents a different concentration of substrate. Note that all the curves are linear, indicating that initial velocity conditions (<10% of substrate conversion) have been met.

The initial velocity (v_o) for each reaction progress curve is equivalent to the slope of the line, which is defined as the change in the product formed divided by the change in time. This is expressed by the equation below and can be calculated using linear regression or other standard linear method:

$$\frac{\Delta Y}{\Delta X} = \text{Slope} = v_o$$

The resulting slopes (initial velocity, v_o) for each of the reaction progress curves are plotted on the Y-axis versus the concentration of substrate (X-axis) and a nonlinear regression analysis using a rectangular hyperbola model is performed as shown in Figure 5.

The V_{max} and K_m for the system is calculated from the nonlinear regression analysis. The meaning of each term is shown in Figure 5. The K_m is the substrate concentration which results in an initial reaction velocity that is one-half the maximum velocity determined under saturating substrate concentrations.

Linear transformations, such as a double reciprocal Lineweaver-Burke plot of the initial velocity/substrate concentration data (i.e. $1/v_o$ vs. 1/[S], should not be used for calculating the K_m and V_{max} from saturation type experiments such as those described above. These linear transformations tend to distort the error involved with the measurement and were used before programs that can perform nonlinear regression analysis were widely available.

An additional parameter, often seen in the literature, which can sometimes be useful to describe the efficiency of an enzyme, is the catalytic constant (or turnover number) that is termed k_{cat}. The k_{cat} value can be determined from saturation data (Figure 5) from the following equation:

$$k_{cat} = \frac{V_{max}}{[E]_i}$$

Where $[E]_i$ is the initial enzyme concentration and V_{max} is the maximum velocity determined from the saturation hyperbola.

For kinase reactions where the K_m for ATP and substrate need to be determined, it is best if a multi-dimensional analysis is used to measure both K_m's simultaneously. An example is shown in Figure 6.

If this method is used, it is important to demonstrate that in the extreme conditions (particularly low substrate, high ATP concentrations) the linearity of the instrument is maintained. In addition, it is important that linearity of the reaction is maintained at all conditions. Proper background controls must be used. The best condition would be a combination of the best signal to noise ratio while maintaining the substrate and ATP concentration as low as possible. Consult with a biochemist and statistician experienced in these techniques to ensure appropriate data analysis methods are utilized.

Determination of IC_{50} for Inhibitors

Concentration-response plots are used to determine the effects of an inhibitor on an enzymatic reaction. These experiments are performed at constant enzyme and substrate concentrations and are the primary type of analysis performed for structure-activity relationship (SAR) measurements for compounds of interest.

A typical concentration-response plot is shown in Figure 7. Fractional activity (Y-axis) is plotted as a function of inhibitor concentration (X-axis). The data are fit using a standard four-parameter logistic nonlinear regression analysis.

The concentration of compound that results in 50% inhibition of maximal activity is termed the IC_{50} (inhibitor concentration yielding 50% inhibition). It is important to use enough inhibitor concentrations to provide well-defined top and bottom plateau values. These parameters are critical for the mathematical models used to fit the data. Other criteria for successful concentration-response curves are listed in the discussion below.

IC_{50} Determination for SAR

- Use a minimum of 10 inhibitor concentrations for an accurate IC_{50} determination. Equally spaced concentration ranges (i.e. 3-fold or half-log dilutions) provide the best data sets for analysis.
- Ideally, half the data points on the IC_{50} curve are above the IC_{50} value and half are below the IC_{50} value, including a minimum and maximum signal.
- The lower limit for determining an IC_{50} is ½ the enzyme concentration (tight binding inhibitors, 3).
- Screening strategies for defining an initial SAR include: determination of the % inhibition at a single concentration; determination of the % inhibition at a high and a low concentration of inhibitor; and finally, determination of an apparent IC_{50} using fewer concentrations.

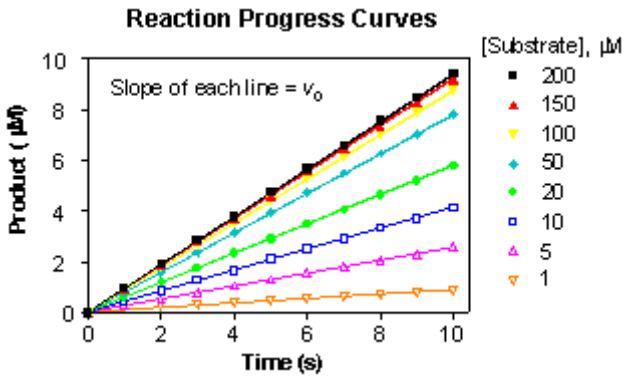

Figure 4. Reaction progress curves at 8 substrate concentrations

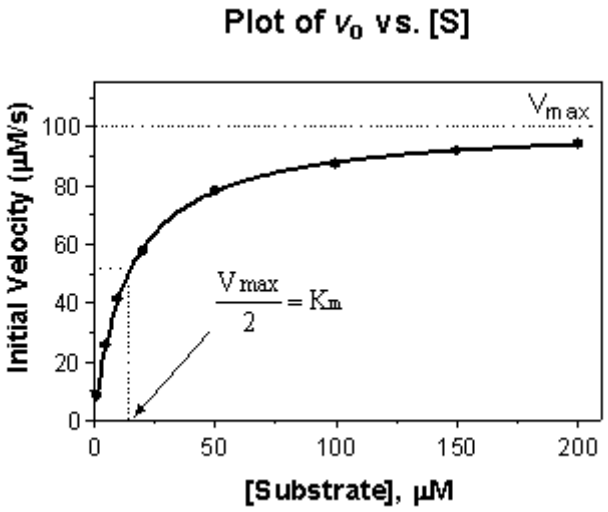

Figure 5. Initial velocity versus substrate concentration

Criteria for reporting IC_{50}'s

- The maximum % inhibition should be greater than 50%.
- Top and bottom values should be within 15% of theory.
- The 95% confidence limits for the IC_{50} should be within a 2-5 fold range.

Since the IC_{50} value is the most common result reported for enzymatic assays, it is important to understand how experimental conditions affect IC_{50} determinations. Generally the concentrations of substrate relative to the K_m and the amount of product produced have the greatest effect on the measured IC_{50}. Figure 8 demonstrates the effect of both substrate concentration and percent conversion on measured IC_{50} values for a competitive inhibitor.

Figure 8 shows the effect of both substrate concentration and % conversion on measured IC_{50} values. Increased substrate conversion as well as increased substrate concentrations will increase the resulting IC_{50} value for a given inhibitor. The data were modeled assuming $K_i = 1.0$ for a competitive inhibitor with no product inhibition.

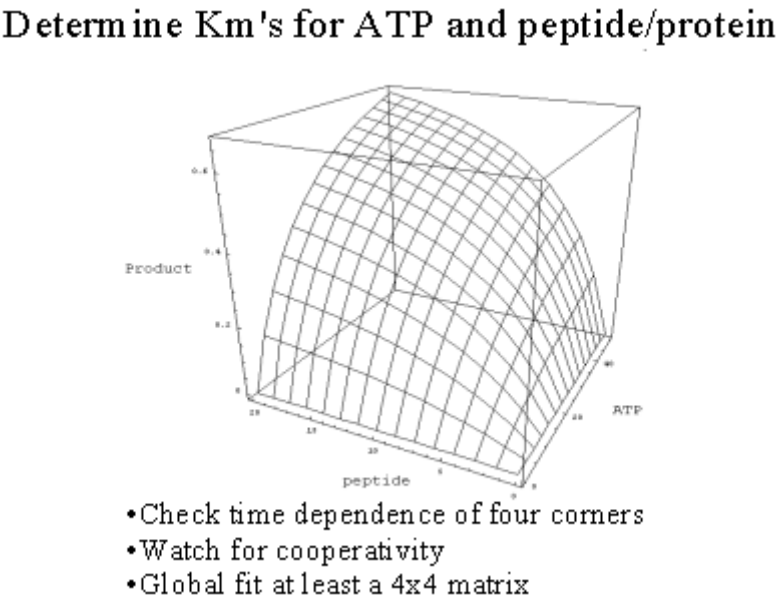

Figure 6. Simultaneous determination of K_m for ATP and specific substrate

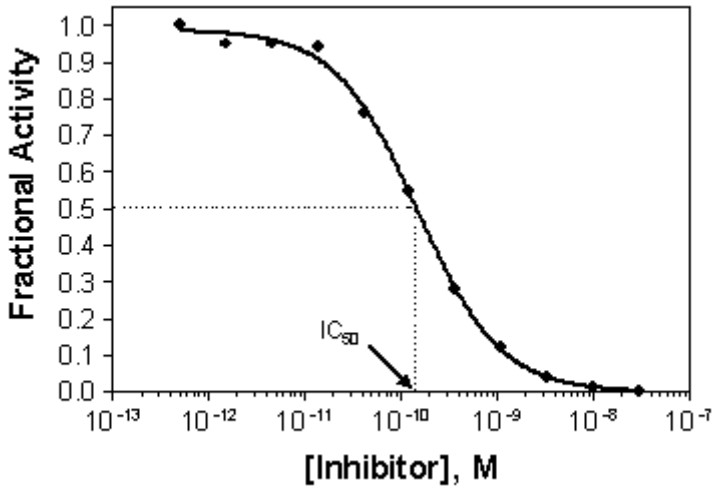

Figure 7. Concentration-Response plot for an enzyme inhibitor

Optimization Experiments

Published literature information should be used in selecting these factors. For example a factorial design experiment could be conducted while varying:

- Divalent cations, for example Ca^{2+}, Mg^{2+}, Mn^{2+}
- Salts, for example NaCl, KCl
- EDTA
- Reducing agents such as βME, DTT, glutathione
- Bovine serum albumin
- Detergents such as Triton, CHAPS

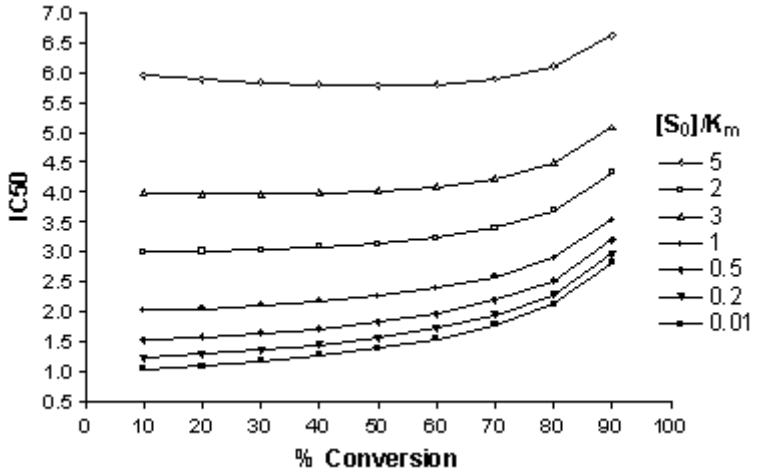

Figure 8. Effect of substrate concentration and % conversion on the IC_{50} for an inhibitor

- DMSO
- Buffer source, for example HEPES *vs.* acetate
- pH

In addition to assay conditions, enzyme stability may be affected if appropriate measures are not taken during long-term storage. Many enzymes need to be stored at -70°C to maintain activity, but freeze-thaw cycles are not recommended. Other enzymes can be stored for long periods of time at -20°C using an additive in the storage buffer such as 50% glycerol.

The presence of carrier proteins in the buffer (bovine serum albumin, ovalbumin, others…) as well as use of polypropylene plates (or non-binding polystyrene plates) may be essential to retain proper enzyme activity.

Enzyme instability can also occur during an assay, as demonstrated previously in Figure 3. This type of instability can occur if the active conformation of the enzyme is not stable in the chosen assay conditions of pH, temperature, ionic strength, etc. In addition, for enzymes that are dimerized, a large dilution into assay buffer may result in inactivation.

Assay Validation

Parameters such as substrate K_m and control inhibitor IC_{50}'s need to be determined in three separate experiments to assess variability. Refer to HTS Assay Validation to assess variability of the assay.

References

General Enzyme Kinetics references on the Internet:

http://themedicalbiochemistrypage.org/enzyme-kinetics.php

http://www.ultranet.com/~jkimball/BiologyPages/E/EnzymeKinetics.html

Enzyme kinetics simulations:

http://www.rpi.edu/dept/chem-eng/Biotech-Environ/Canada/enzkin.html

http://interactive-mathvision.com/PaisPortfolio/Ckm/EnzymeKinetics/EKJava.html

Software examples for fitting enzyme kinetics data:

Graphpad Prism (http://www.graphpad.com/prism/Prism.htm)

Sigma Plot (http://www.sigmaplot.com/products/sigmaplot/sigmaplot-details.php)

GraFit (http://www.erithacus.com/grafit/)

Literature References:

1. Fersht, Alan. Enzyme Structure and Mechanism. WH Freeman and Co., NY, 1985, pp327-330.
2. Segel, Irwin H. Enzyme Kinetics: Behavior and analysis of rapid equilibrium and steady state enzyme systems. John Wiley and Sons, NY 1975.
3. Copeland, Robert A. Enzymes: A practical introduction to structure, mechanism and data analysis. Wiley-VCH, NY, 2nd Edition, 2000.
4. Dixon, M. and Webb, E.C. Enzymes, 3rd Edition. Academic Press, NY 1979.
5. Lai C-J. -,Wu JC A Simple Kinetic Method for Rapid Mechanistic Analysis of Reversible Enzyme Inhibitors. Assays and Drug Dev. Technologies. 2003;1(4):527–535. PubMed PMID: 15090249.

Mechanism of Action Assays for Enzymes*

John Strelow, Walthere Dewe, Phillip W Iversen,[1] Harold B Brooks, Jeffrey A Radding, James McGee,[2] and Jeffrey Weidner[3]

Created: May 1, 2012; Updated: October 1, 2012.

Abstract

Many drugs are inhibitors of enzymes involved in mediating the disease processes. Understanding the mechanism of action (MOA) of the target enzyme is critical in early discovery and development of drug candidates through extensive Structure-Activity Relationship (SAR) studies. This chapter contains a primer on the MOA of enzymes and its significance in drug discovery, types of inhibition, development and validation of MOA assays, data analysis and guidelines for performing these assays. New and experienced investigators will find this chapter useful when starting new projects involving enzyme targets.

Overview of MOA in Drug Discovery

The purpose of a mechanism of action (MOA) study is to characterize the interaction of a compound with its target to understand how the compound interacts with the target and how natural substrates at physiologic concentrations will modulate this activity. These compounds are often inhibitors of enzymes but only rarely become drugs due to the requirements for a drug to not only inhibit the target but to have acceptable solubility, permeability, protein binding, and selectivity, metabolism and toxicity profiles. This potential for the compound to become a drug is slowly revealed through the analysis and tracking of these characteristics, as chemistry elaborates the structure-activity relationship (SAR). As described in the body of this document, certain types of biochemical behavior are associated with good drug-like properties both *in vitro* and *in vivo*.

Most biochemical screens are designed to provide a chemical starting point based upon the most robust, simple and inexpensive modality for screening. This is due to the required reproducibility in the screening process and the potentially large number of molecules to be run through the screen. Most enzymatic screens are designed to identify inhibitors regardless of their mode of action. Thus, screens are usually run at or below the K_m for the substrate(s). In the case of an enzyme with two substrates, the screen is often designed to run under pseudo-first order kinetics by running the assay under conditions where one substrate is at saturation, well above its K_m, and the second is at or below its K_m for the enzyme. One can therefore identify inhibitors that have competitive, noncompetitive and uncompetitive behavior with regard to the substrate at or below K_m and noncompetitive or uncompetitive behavior with regard to the other substrate at well above its K_m for the enzyme.

In the drug discovery process, the screening phase casts a wide net and the ability to further analyze compounds in more detail is limited, therefore the number of actives isolated from a screen for follow-up are determined by the overall hit rate, the repeat rate upon retesting and determination of the IC_{50} in a concentration response curve (CRC) test. In general, activities range from mid-micromolar to sub-micromolar for enzyme inhibitors right out of the screen. It is this piece of information (the IC_{50}), along with an analysis of the structural classes of active molecules by a medicinal chemist, which defines the initial SAR, if there is one in the data. It is after this initial analysis that MOA studies can prove valuable by further defining the nature of the inhibitor from a biochemical point of view. MOA studies at this point in the drug discovery process define the nature of the SAR by elucidating the type of inhibition by which the discovered molecules operate. Thus, one can define if the

* Edited by James McGee and Jeffrey Weidner

Author Affiliations: 1 Eli Lilly and Company. 2 Eli Lilly and Company. 3 AbbVie, Chicago, IL.

discovered inhibitor is competitive with substrate, for example, and as described below, potentially suffers from certain liabilities associated with this mechanism.

Cell based assays of biochemical actives are usually utilized to identify promising molecules in a second round of low to medium throughput screening. If a molecule shows significant activity in a cell based assay, then it continues through the flow scheme. The lack of cell based activity of biochemically potent actives is usually attributed to lack of cellular permeability, with a wave of the hand; however, an understanding the MOA of a compound at this stage can add depth to the interpretation of cellular activity or its absence. Knowing a compound is competitive with a substrate helps establish the binding pocket and, in combination with structural and SAR information, provides an immediate direction for further chemical synthesis. However, these competitive compounds with promising structure and potent biochemical activity might compete with a cellular substrate present at high intracellular concentration thus show no significant cell based activity. Alternatively, more potent cell based activity than is biochemically predicted from IC_{50} curves might correlate with unusual kinetic behaviors such as slow binding behavior and/or slow off rates (tight binding). As there is no single, unique answer, biochemical MOA studies help in interpretation of cell based activities and provides further support for molecules with desirable characteristics to move forward in the flow scheme. Traditionally, as MOA studies were slow, laborious efforts, only a few selected molecules could be readily analyzed. With the advent of laboratory automation and enhanced data processing, it is now possible to assess a larger number of compounds rapidly. Therefore, it is feasible (and desirable) to examine the results of a screening campaign, in addition to standard cell based assays in the second tier, by an analysis of MOA.

Types of Inhibition

There are three main types of inhibition (competitive, noncompetitive, and uncompetitive) that are most commonly used to describe the binding of an inhibitor to a target enzyme (Figure 1). However, a complete analysis of the mechanism of action requires the scientist to also evaluate other potential inhibition events, including allosteric, partial, tight-binding, and time-dependent inhibition. A review of these types of inhibition is provided in the sections that follow.

Competitive Inhibition

A competitive inhibitor binds only to free enzyme. Often this binding event occurs on the active site of the target, precisely where substrate also binds. Although this is the case for a majority of competitive inhibitors, it is a misleading oversimplification. It is more appropriate to state that the binding of a competitive inhibitor and the binding of substrate are mutually exclusive events. Figure 2 provides illustrations of some possible mutually exclusive binding events.

Despite the differences in binding to the free enzyme illustrated in Figure 2, all competitive inhibitors have the same effects on substrate binding and catalysis. A competitive inhibitor will raise the apparent K_m value for its substrate with no change in the apparent V_{max} value. As a result, it is often stated that competitive inhibition can be overcome, observed by an increase in the apparent K_i value, at higher concentrations of substrate. This characteristic will have physiological consequences on the observed efficacy of drugs. As an enzyme's reaction is inhibited by a competitive inhibitor, there is an increase in the local concentration of substrate. Without a mechanism to clear the substrate, a competitive inhibitor will lose potency. This is not the case for a noncompetitive inhibitor.

Noncompetitive Inhibition

A noncompetitive inhibitor binds equally well to both free enzyme and the enzyme-substrate complex. These binding events occur exclusively at a site distinct from the precise active site occupied by substrate. Figure 3 provides some illustrations of the more common noncompetitive binding events.

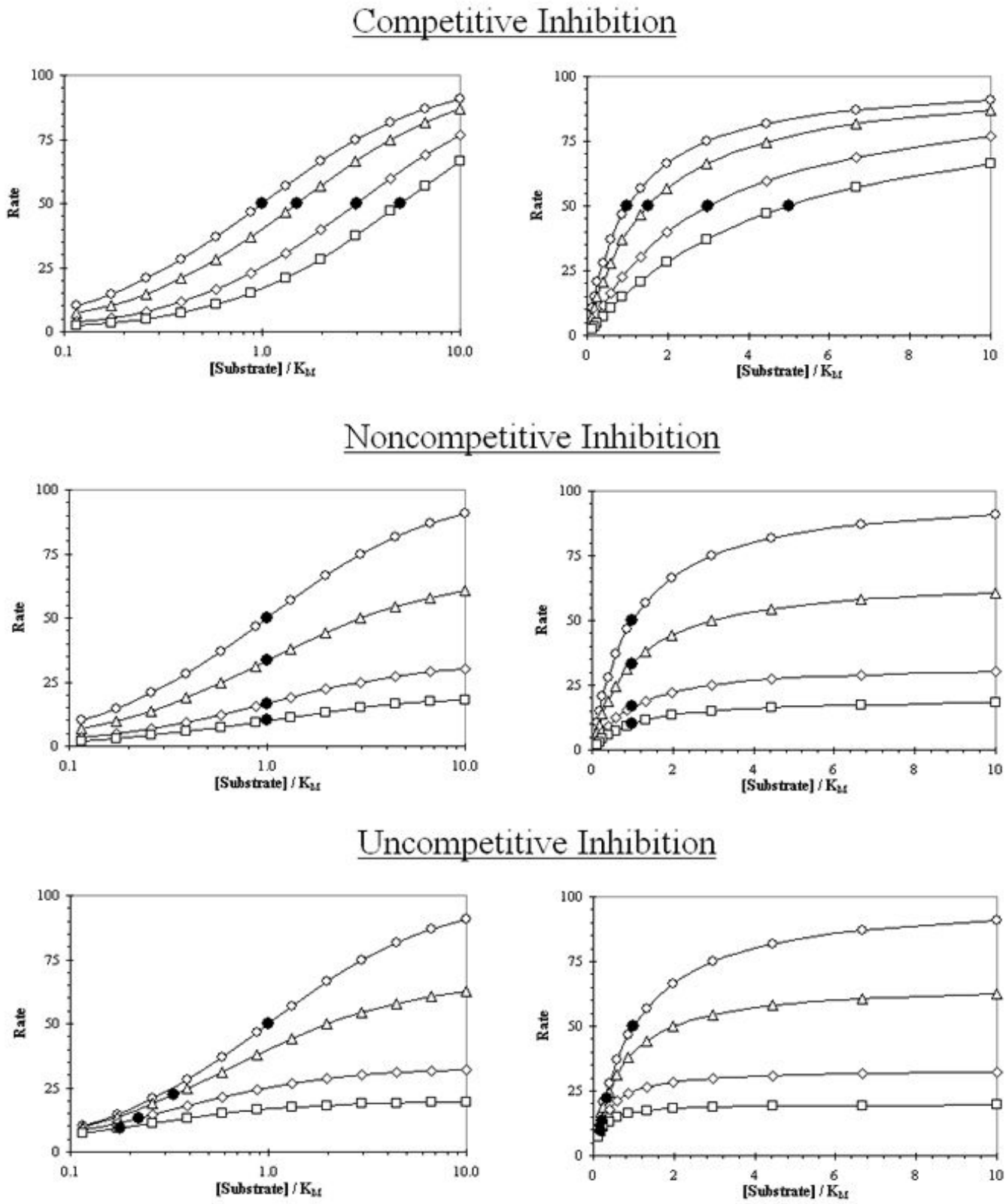

Figure 1 – Illustrations of data demonstrating Competitive, Noncompetitive, and Uncompetitive Inhibition. The circles represent those rates obtained without the addition of inhibitor. The triangles contained $0.5\times K_i$ of inhibitor, the diamonds contained $2.0\times K_i$ of inhibitor, and the squares contained $4.0\times K_i$ of inhibitor. The black circles depict the shifts in the apparent K_m for each binding modality.

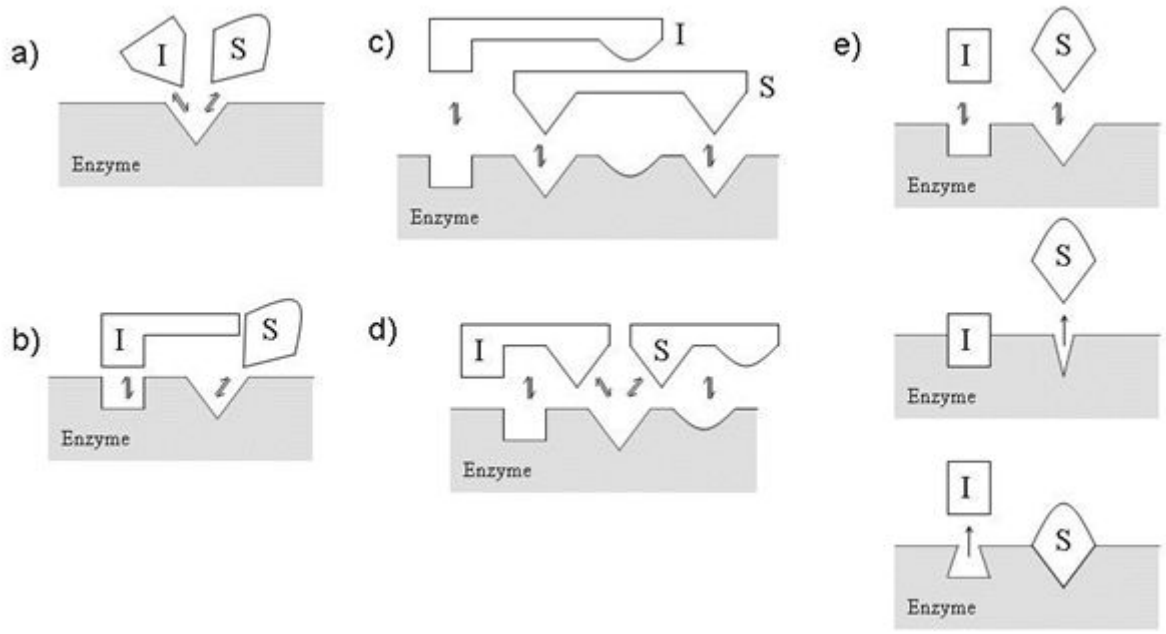

Figure 2 – Examples of Competitive Inhibition where Substrate (S) and Inhibitor (I) binding events are mutually exclusive. (a) Classical model for competitive inhibition where S and I compete for the same precise region of the active site. (b) I does not bind to the active site, but sterically hinders S binding. (c) S and I binding sites are overlapping. (d) S and I share a common binding pocket on the enzyme. (e) I binding can result in a conformational change that prevents S binding (and vice versa). This was adapted from Segal, Enzyme Kinetics.

In contrast to a competitive inhibitor, a noncompetitive inhibitor will lower the apparent V_{max} value, yet there is no effect on the apparent K_m value for its substrate. Essentially, the K_i of the inhibitor does not change as a function of the substrate concentration.

In some circumstances, a compound may have unequal affinity for both free enzyme and the enzyme-substrate complex. This mixture of competitive and noncompetitive phenotypes is called mixed inhibition.

Uncompetitive Inhibition

An uncompetitive inhibitor binds exclusively to the enzyme-substrate complex yielding an inactive enzyme-substrate-inhibitor complex (Figure 4). When encountered, the apparent V_{max} value and the apparent K_m value should both decrease. Despite their rarity in drug discovery programs, uncompetitive inhibitors could have dramatic physiological consequences. As the inhibitor decreases the enzyme activity, there is an increase in the local concentration of substrate. Without a mechanism to clear the buildup of substrate, the potency of the uncompetitive inhibitor will increase.

Allosteric Inhibition

An allosteric inhibitor decreases activity by binding to an allosteric site other than or in addition to the active site on the target. This interaction is characterized by a conformational change in the target enzyme that is required for inhibition. These conformational changes can affect the formation of the usual enzyme-substrate active site complex, stabilization of the transition state, or reduce the ability to lower the activation energy of catalysis. Figure 2e and Figure 3a are classical examples of allosteric inhibition. As such, an allosteric inhibitor may display a competitive, noncompetitive, or uncompetitive phenotype with respect to substrate binding.

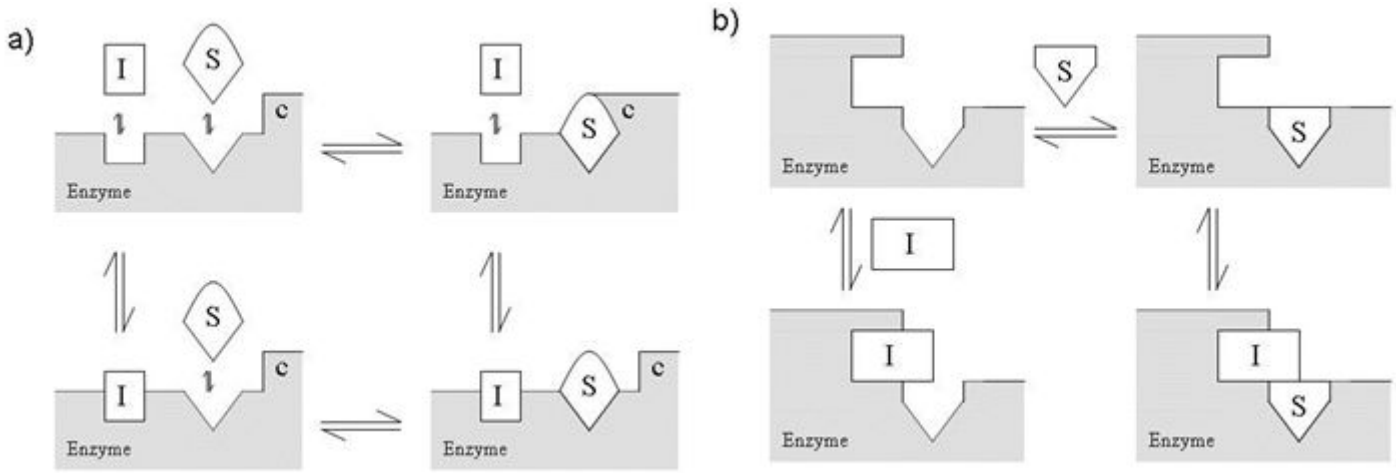

Figure 3 – Examples of Noncompetitive Inhibition where Inhibitor (I) binding occurs at a site distinct from the Substrate (S) binding site and the Catalytic center (c) of the active site. (a) In this model, the binding of S induces a conformational change to align the catalytic center near S for catalysis. However, when I binds at a separate site, the conformational change does not occur and enzyme activity is inhibited. (b) In this model, I can sterically hinder S binding and release. However, unlike Figure 1-B, I and S can occupy the enzyme at the same time. This was adapted from Segal, Enzyme Kinetics.

Figure 4 – An example of Uncompetitive Inhibition where Inhibitor (I) only binds in the presence of Substrate (S).

Partial Inhibition

Partial inhibition results from the formation of an enzyme-substrate-inhibitor complex that can generate product with less facility than the enzyme-substrate complex. This can be illustrated in Figure 3a. When "I" is a partial inhibitor bound in the enzyme-substrate-inhibitor complex, the catalytic center may retain some ability to align near the substrate and facilitate catalysis. As a consequence of these structural changes, partial inhibitors can also be allosteric inhibitors of enzyme activity. In direct contrast, full inhibition results in an enzyme-substrate-inhibitor complex where the catalytic center is not capable of aligning near the substrate for catalysis.

Tight-Binding Inhibition

In this type of inhibition, the population of free, soluble inhibitor is significantly depleted by the formation of the enzyme-inhibitor or enzyme-substrate-inhibitor complex. While tight-binding inhibitors can bind to the target enzyme in a competitive, noncompetitive, or uncompetitive manner with respect to substrate binding, they can display noncompetitive phenotypes. However, a tight-binding inhibitor typically binds with an apparent affinity (K_i) near the concentration of enzyme (active sites) present in the biochemical assay.

Time-Dependent Inhibition

Time-dependent inhibitors bind slowly to the enzyme on the time scale of enzymatic turnover, thus displaying a change in initial velocity with time. This has the effect of slowing the observed onset of inhibition. Time-dependent inhibitors also impede the observed recovery of enzyme activity following inhibition, resulting in

slow k_{off} values. As illustrated in Figure 5, these inhibitors typically yield nonlinear initial velocities and nonlinear recoveries of enzyme activity.

Interestingly, many successful therapeutic drugs are time-dependent inhibitors. For these inhibitors with slow k_{off} values, the rate of release of inhibitor from the enzyme-inhibitor complex (recovery of enzyme activity) proceeds independent of the substrate concentration and the physiological mechanism to remove inhibitor. This makes time-dependent inhibition a very attractive and proven strategy for the discovery and development of drugs.

Some time-dependent inhibitors covalently attach to the target enzyme. For those inhibitors, the k_{off} value is zero and the inhibition is said to be irreversible. These are typically less attractive molecules, unless the formation of the covalent species is specific to the reaction mechanism of the enzyme. Some inhibitors are for all practical purposes irreversible, with very low k_{off} values, despite their inability to covalently attach to the enzyme. This stands in direct contrast to rapid equilibrium, reversible inhibitors that bind to and release from the enzyme at rates that are rapid in comparison to the rate of enzyme turnover.

Performing MOA Studies

When performing classical steady-state mechanism of action studies, the scientist should carefully consider and incorporate the proper biochemical and statistical guidelines provided in this section. These guidelines should assist in the initial characterization of the enzyme-inhibitor complex. However, in some cases the classical steady-state experiment is not sufficient and additional characterizations are required. Examples include compounds that display tight-binding inhibition, time-dependent inhibition, covalent modification, or nonspecific inhibition of the enzyme. Therefore, we also provide guidelines to identify these additional types of inhibitors and plan the appropriate follow-up analysis.

Classical Steady-State Experiments

These types of studies involve measurements of the V_{max} and K_M of a substrate at a range of inhibitor concentrations. The scientist should refer to Basic Enzyme Assays chapter of this manual, for a description of how to perform measurements of the V_{max} and K_m for a substrate. As mentioned previously, changes in the apparent V_{max} and K_m give the scientist a view of the binding modality (competitive, noncompetitive, or uncompetitive) and the potency (K_i and K_i'). Figure 6 illustrates the classical steady-state experiment used to determine the binding modality and potency.

The methodology proposed here to determine the binding potency and modality of an inhibitor is derived from a steady-state model of enzyme kinetics. The term steady-state refers to a constant concentration of the enzyme-substrate complex present during the reaction. As summarized by Copeland (1) and Segal (2), there are several assumptions that simplify the mathematical treatment of the kinetics. When these assumptions fail, the steady-state MOA model proposed here is not valid.

1. The enzyme is acting catalytically and the concentration of substrate is much greater than the concentration of enzyme.
2. During the initial phase of the reaction (initial velocity), there is no buildup of any intermediate other than the enzyme-substrate complex.
3. There is very little product formed over the course of the reaction so that the depletion of substrate is minimal and the reverse reaction is insignificant.
4. The concentration of inhibitor is much greater than the concentration of enzyme so that the depletion of free inhibitor resulting from the formation of the enzyme-inhibitor complex is minimal.

The scientist should utilize the following guidelines in the design, execution, and analysis of a classical MOA experiment.

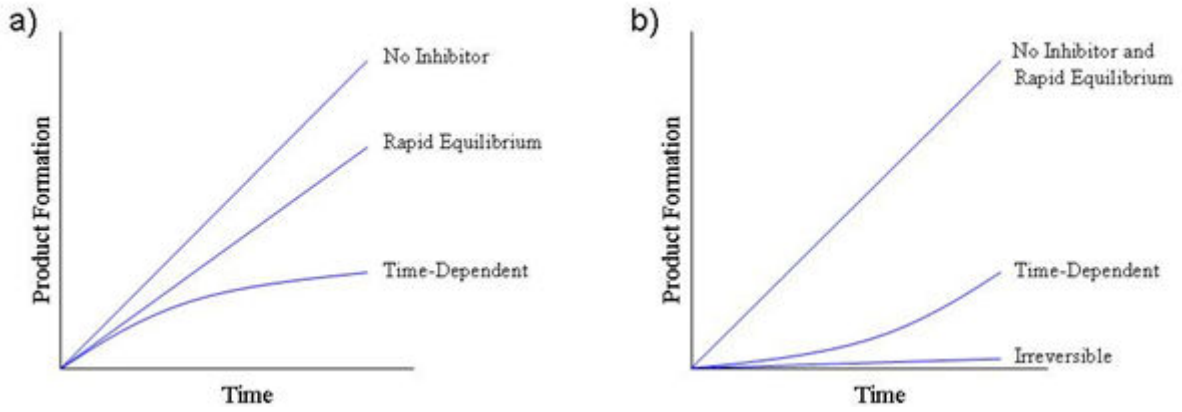

Figure 5 – Illustrations of time-dependent inhibition. (a) This graph depicts the decrease in the initial velocity (product formed vs time) observed for classical, rapid equilibrium inhibitor and a time-dependent inhibitor. The latter yields a nonlinear progress curve consistent with a slow kon value. (b) This graph depicts the recovery of enzyme activity (product formed vs time) following dilution of the enzyme-inhibitor complex with substrate. Dilutions of classical, rapid equilibrium inhibitor complexes recover full activity immediately after dilution. Dilutions of time-dependent inhibitor complexes recover enzyme activity more slowly, indicative of a compound with a slow koff value. Dilutions of irreversible inhibitor complexes maintain the enzyme-inhibitor complex after dilution.

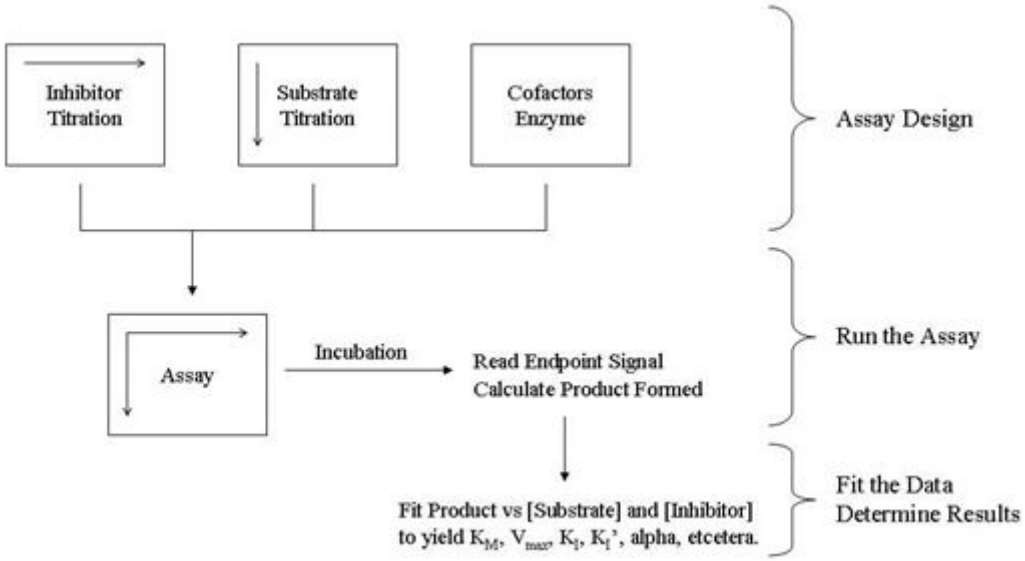

Figure 6 – Classical Steady-State analysis of the mechanism of action. The inhibitor and substrates are serially diluted to achieve concentrations in the assay that span their respective binding constants (K_i and K_m). The addition of enzyme and cofactors will initiate the enzymatic reaction. The order of addition typically depends on the assay in question and may be altered for time-dependent inhibitors (discussed later). The assay incubates for some period of time, the signal is read, the data is fit, and the results are analyzed.

Guidelines for Assay Design

- It is essential to ensure that the enzyme, substrate, co-factors, and buffer conditions have been fully evaluated and characterized. Wherever possible, the scientist should strive to achieve *in vitro* conditions that will best represent the physiological conditions in a robust, reproducible manner. The selection of these factors can have a large impact on the binding modality and potency observed.
- An enzyme titration should be performed to determine the concentration of active sites in the assay. Consult Copeland, Enzyme 2ed, pg313 or an experienced enzymologist for more information (1).

- There should be at least 5 concentrations of substrate tested, spanning a range of at least ½×K_m to 5×K_m, for each concentration of inhibitor tested. As illustrated in Figure 7, the ability to distinguish a competitive inhibitor from a noncompetitive or uncompetitive inhibitor is increasingly enhanced at concentrations of substrate above its K_m value. The ability to distinguish noncompetitive inhibition from uncompetitive inhibition is more challenging and can be improved with very accurate determinations of the apparent K_m. Therefore, the scientist should strive to judiciously increase the range and number of concentrations of substrate tested.
- The plot of the [substrate] vs initial velocity should not display sigmoidal kinetics, unless it is a mechanistic feature of substrate binding and catalysis for that enzyme. The impact of sigmoidal kinetics on the K_m curve is illustrated in Figure 8. Sigmoidal kinetics may be a sign of an impure enzyme or the presence of multiple isoforms of the enzyme (ex. multiple phosphorylation states of the same kinase). Refer to Copeland, Enzyme 2ed, pg382 or an enzymologist experienced with sigmoidal kinetics (1).
- The initial velocity should be measured. In order for the steady-state assumptions to hold, it is recommended that less than 10% of the substrate be converted to product. The chapter on Basic Enzyme Assays describes this in more detail. However, initial velocity conditions do not infer linearity and the user should refer to the guideline directly below.
- The formation of product should be linear with respect to time. This is best achieved by measuring the rate of product formation at the chosen concentrations of substrate using the assay conditions, detection system, and instruments that will be used for the final assay. Linearity should be assessed visually from plots of the raw data.
- There should be at least 8 concentrations of inhibitor tested at each concentration of substrate. The range of inhibitor concentrations tested should span the K_i or K_i', depending on the binding modality. Reporting of binding constants outside of the range of concentrations tested should be avoided. It is also recommended to include inhibitor concentrations at or above ~10×K_i to ensure maximum inhibition and the identification of any potential partial inhibitors. It should be noted that any observation of partial inhibition could instead be a consequence of a compound's poor solubility.
- Where available, a control inhibitor should be evaluated under the exact conditions that will be used for the final assay.
- In addition to the experimental wells containing a matrix of substrate and inhibitor dilutions, the final assay should include both high and low controls. The high control should contain the substrate titration without inhibitor to reflect the maximum enzyme activity at each substrate concentration. The low control should contain the substrate titration without enzyme or substrate and without inhibitor. The low controls should reflect the signal expected for no enzyme activity at each substrate concentration. Depending on the composition of the inhibitor stocks, DMSO might be needed in the control wells to assure consistency across all the experiments.
- The concentration of DMSO should be kept constant in MOA experiments for a particular target. DMSO can have a significant impact on enzyme activity and the concentration of DMSO in the wells containing compound should be identical to the concentration of DMSO in the control wells (described directly above). DMSO can also impact the solubility of a compound and its observed potency. Therefore, the concentration of DMSO should be consistent in replicate MOA experiments (or in comparison to IC_{50} experiments).
- It is recommended to evaluate, in the standard assay conditions, dependence of [enzyme] on the IC_{50} of the compounds to be tested. Shifts in the IC_{50} as a function of the [enzyme] is an indication of tight-binding inhibition and/or solubility issues. When this is encountered, the scientist should consult with an enzymologist experienced with tight-binding inhibition.
- If detergents are required for enzyme activity or automation, the scientist should strive to maintain their concentrations well below the critical micelle concentration (CMC). The formation of micelles, at high concentrations of detergents, can interfere with the determinations of the binding modality and potency. An exception to this rule would include assays requiring detergents as part of the mechanistic evaluation.

If the assay can only be run above the CMC, the scientist should consult with an enzymologist experienced with lipids, micelles, and surface dilution kinetics.
- The reaction should be measured under steady-state conditions that includes the following: 1) there should not be any appreciable buildup of any enzyme intermediates other than the ES complex, 2) the [substrate] should be >> [enzyme], and 3) the initial phase of the reaction is measured so that the [product] ~ 0, the depletion of substrate is minimal, and the reverse reaction is insignificant (1).
- The concentration of a required cofactor should be >> [enzyme].

Statistical Validation of the Designed Assay

The requirements for statistical validation of a MOA assay can be divided into two situations: 1) high-throughput assays using automation that can test many compounds, and 2) low-throughput assays in which only one or a few compounds are tested. In the first case, a replicate-experiment study should be performed as described in the Assay Validation chapter of this manual. Briefly, 20 to 30 compounds should be tested in two independent runs. Then the MSD or MSR and limits of agreement are determined for each of the key results, including V_{max}, K_m, K_i, K_i', and α or α_{inv}. Specific acceptance criteria have not been determined. The reproducibility should be judged as suitable or not for each situation. For low-throughput assays, a replicate-experiment study is not required. At a minimum, key results from the MOA experiment, such as V_{max}, K_m, and K_i, should be compared to previous/preliminary experiments to ensure consistency. The data from the MOA experiment should be examined graphically for outliers, goodness of fit of the model to the data, and consistency with the assumptions and guidelines for designing and running the assay (see Guidelines for Assay Design above and Guidelines for Running the Assay below).

Guidelines for Running the Assay

- The assay should be run under the exact same conditions as developed using the guidelines above. In addition, the assay should be run within the timeframe where the reagents are known to be stable.
- When a control inhibitor is included, then the K_i (and/or K_i') value should be compared with legacy data to ensure robust, quality results. It is also recommended to include additional inhibitors with alternative binding modalities, if available.
- The K_m and V_{max} values from the high controls and the signal from the low controls should be compared with the legacy values determined in identical conditions, as described above.
- A standard curve should be included for detection systems yielding signals that are nonlinear with respect to the amount of product formed. This nonlinearity is a common feature in fluorescent-based assays. The standard curve should be used to covert the signal produced to the amount of product formed. The resulting amount of product formed over the course of the assay time should be used in the data fitting methodologies. Please refer to the Immunoassay Methods chapter.

Guidelines for Data Fitting and Interpretation

- The multivariate dataset (v, [I],[S]) should be fit using a non-linear regression analysis with the appropriate models described below. Linear transformations of the data should be avoided as they will distort the error of the experiment and were historically used only before the introduction of computer algorithms.
- The scientist should perform any necessary background corrections, before the multivariate fitting, so that a signal or rate of 0 represents that expected for conditions lacking enzyme activity. Depending on the assay design, this may include a single background correction applied to the entire experiment or several different corrections. The latter should be used when the background signal varies with the [substrate] tested. Here there should be a background correction for each [substrate] tested.

The traditional model of general mixed inhibition is:

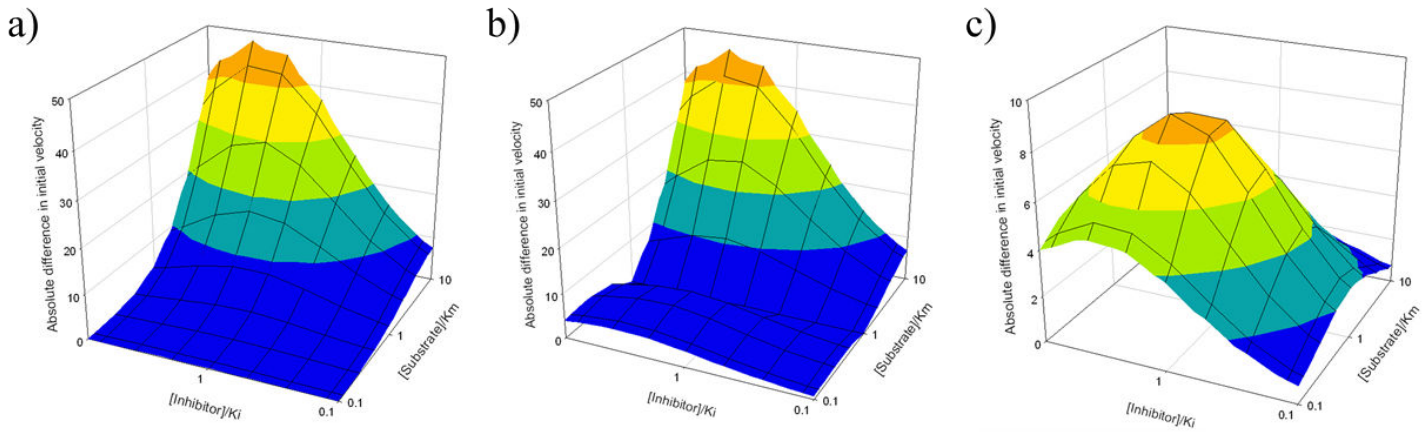

Figure 7 – Residual plots demonstrating the difference in observed rate of enzyme activity (z–axis) at each concentration of substrate (y-axis) and inhibitor (x-axis) for 2 binding modalities. (a) Competitive Inhibition vs Noncompetitive inhibition. (b) Competitive inhibition vs Uncompetitive inhibition. (c) Noncompetitive vs Uncompetitive inhibition. Taken together, competitive inhibitors are best distinguished from noncompetitive and uncompetitive inhibitors at both high [substrate] and high [inhibitor]. Noncompetitive and uncompetitive inhibitors are best distinguished from each other at [substrate] and [inhibitor] near their binding constants (K_m and K_i). Therefore, the range and density of concentrations tested are both important.

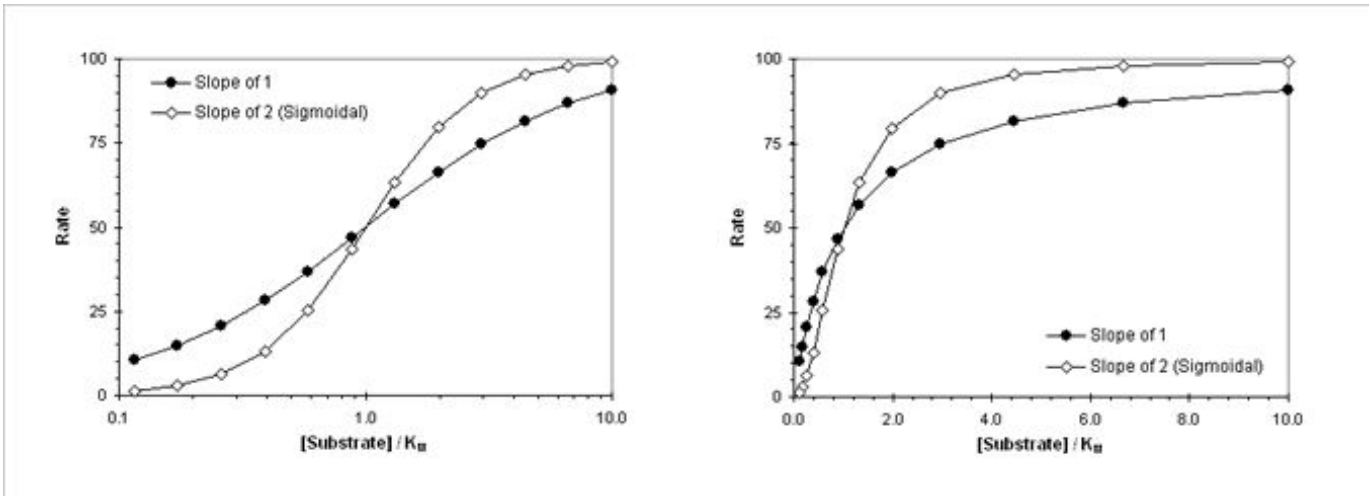

Figure 8 – Comparison on enzyme data for a system with a proper slope of 1 and another displaying a sigmoidal relationship (ex. slope of 2) between the substrate concentration tested and the rate observed.

$$v = \frac{V_{max}[S]}{K_m\left(1+\frac{[I]}{K_i}\right)+[S]\left(1+\frac{[I]}{K_i'}\right)} \qquad \text{(P1)}$$

Where v is the speed of the reaction (slope of product formed vs. time), V_{max} is the upper asymptote, [S] is the substrate concentration, and [I] is the inhibitor concentration. See the glossary for definitions of K_m, K_i, and K_i'. This model can also be written as:

$$v = \frac{V_{max}[S]}{K_m\left(1+\frac{[I]}{K_i}\right)+[S]\left(1+\frac{[I]}{\alpha K_i}\right)} \quad \text{(P2)}$$

$$v = \frac{V_{max}[S]}{K_m\left(1+\frac{[I]}{K_i}\right)+[S]\left(1+\frac{\alpha_{inv}[I]}{K_i}\right)} \quad \text{(P3)}$$

where $\alpha = 1/\alpha_{inv} = K_i'/K_i$. This model reduces to specific models for competitive, non-competitive, and un-competitive inhibition as described in Table 1.

Another form of this model that has better statistical properties, in terms of parameter estimation and error determination, is:

$$v = \frac{[S]}{\theta_1+\theta_2[I]+\theta_3[S]+\theta_4[I][S]} \quad \text{(P4)}$$

where,

$$V_{max} = \frac{1}{\theta_3} \qquad K_I = \frac{\theta_1}{\theta_2}$$

$$K_M = \frac{\theta_1}{\theta_3} \qquad K_I' = \frac{\theta_3}{\theta_4}$$

$$\alpha = \frac{\theta_2\theta_3}{\theta_1\theta_4} = \frac{1}{\alpha_{inv}} = \frac{K_I'}{K_I}$$

More details on these models can be found in a manuscript in preparation by the primary authors of this chapter.

1. Fit a robust multiple linear regression of 1/v vs. 1/[S], [I]/[S], and [I]. This provides starting values of the θ parameters for the non-linear regression in the next step.
2. Fit model P4 to the data (v, [I], [S]).
3. Calculate the parameters of interest from the θ values.
4. Calculate confidence limits for each key parameter value using Monte Carlo simulation.
5. Make decisions of mechanism based on the value of α or α_{inv} and the associated confidence limits.
    - α or α_{inv} should be used to assign the binding modality. If α is less than 1, the mechanism is:
        a. Uncompetitive if the upper confidence limit of $\alpha < 0.25$
        b. Noncompetitive if the lower confidence limit of $\alpha > 0.25$
        c. Not competitive, otherwise

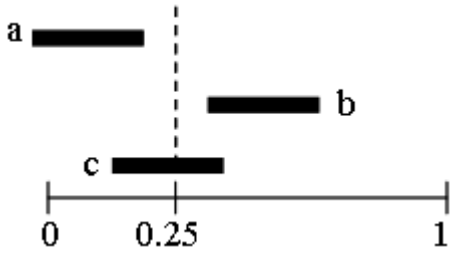

- If $\alpha_{inv} < 1$, then the mechanism is:
  a. Competitive if the upper confidence limit of $\alpha < 0.1$
  b. Noncompetitive if the lower confidence limit of $\alpha > 0.1$
  c. Mixed, if both confident limits are within [0.1, 0.5]
  d. Not declarable, otherwise

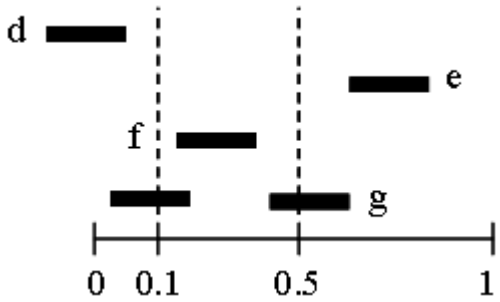

The details of how these cutoffs were chosen are in a manuscript in preparation.

- When the signal measured at $10\times K_i$ (representing full enzyme inhibition by the compound) is >>0 (baseline corrected), the compound is displaying partial (and/or allosteric) Inhibition. This difference might also be observed when the incorrect conditions were chosen for the low control to represent no enzyme activity, if there was not enough inhibitor (relative to the K_i or K_i') to achieve maximum inhibition, and/or if the compound tested is poorly soluble.
- When the K_i or K_i' resulting from the fit is within 10-fold of the concentration of active sites in the assay, the compound will start to display tight-binding inhibition. Inaccuracies in the binding modality and potency will result. In some cases where the inhibitor is not soluble, tight binding inhibition may exist at much higher K_i or K_i' values. As recommended previously, the dependency of the enzyme concentration on the inhibitor's potency is the best method to identify tight-binding inhibition. The scientist should consult with an expert in tight-binding inhibition to further characterize the inhibitor.
- Data suggesting that a compound is noncompetitive (and in some cases mixed) should be handled with caution. Compounds that are time-dependent, irreversible, poorly soluble, nonspecific, and/or tight-binding will display a noncompetitive/mixed phenotype in this type of classical steady-state experiment. As such, it is critical to evaluate these additional potential mechanisms of action, described herein.
- Additional recommendations for data analysis can be found in the next section.

Table 1: Summary of competitive, non-competitive and uncompetitive inhibition models.

Inhibition	Description	K_i	K_i'	K_i'/K_i
Competitive	The inhibitor binds only to free enzyme. This binding most often occurs in the active site at the precise location where substrate or cofactor (being evaluated in the MOA study) also binds.	finite	Infinite	infinite
Mixed	These inhibitors display properties of both competitive and noncompetitive inhibition.	finite	Finite	> 1
Noncompetitive	The inhibitor binds equally well to both free enzyme and the enzyme-substrate complex. Consequently, these binding events occur outside the active site.	finite	Finite	= 1

Table 1 continued from previous page.

Inhibition	Description	K_i	K_i'	K_i'/K_i
Uncompetitive	The inhibitor binds only to the enzyme-substrate complex at a location outside the active site.	infinite	Finite	= 0

When the Steady-State Assumptions Fail

The steady-state MOA model proposed for here for data fitting requires several important assumptions hold true. While a majority of these assumptions are covered in the previous sections, the invalidation of a few key assumptions should prompt the scientist to perform additional mechanistic characterizations. These key assumptions, a mechanism to flag their breakdown in the steady-state MOA model, and a recommended plan of action are presented.

Tight Binding Inhibition

The [inhibitor] in solution should be much greater than the [enzyme] in the assay. This assumption fails most frequently in 2 circumstances. First, some compounds bind to their target with such high affinity ($_{app}K_i$ values within 10 fold of the [enzyme]) that the population of free inhibitor molecules is significantly depleted by formation of the EI complex. Second, some compounds are both very potent and poorly soluble. The poor solubility of the inhibitor will increase the observed $_{app}K_i$ value (relative to the [enzyme]). In both cases, the compounds are called tight binding inhibitors.

- How can tight binding inhibitors be flagged in the steady-state MOA model?
  - Regardless of their true binding modality, they display a noncompetitive phenotype.
  - They have observed $_{app}K_i$ values between ½ and 10-fold of the [enzyme] in the assay.
  - Poorly soluble compounds may also display tight binding inhibition. This is often masked by an inflated observed $_{app}K_i$ value.
- What is the recommended plan for an appropriate characterization?
  - Calculate the dependence of the IC_{50} values on the [enzyme]. Using a fixed concentration of substrate at K_m, the IC_{50} of the inhibitor should be measured at ≥5 concentrations of enzyme. If the IC_{50} changes significantly as a function of the [enzyme], the inhibitor is displaying tight binding properties and requires further characterization. If the IC_{50} does not change significantly, the compound is not tight binding, this key assumption ([Inhibitor]>>[Enzyme]) is true, and the steady-state MOA model is valid. These two phenotypes are illustrated in Figure 9.
  - Calculate the dependence of the IC_{50} values on the [substrate]. Using a fixed concentration of enzyme, the IC_{50} of the inhibitor should be measured at >5 concentrations of substrate. The range of concentrations of substrate should span the K_m (as recommended previously). As illustrated in Figure 10, the change in the IC_{50} vs [substrate] is described by the equation listed below and yields the true binding potency (K_i and K_i'). The ratio of K_i'/K_i (termed alpha, α) reflects the binding modality. Inhibitors with alpha values statistically equal to 1.0 are noncompetitive, values statistically less than 1.0 are uncompetitive, and values statistically greater than 1.0 are competitive.

Model to Determine Tight Binding MOA:

$$IC_{50} = \frac{[S] + K_M}{\frac{K_M}{K_I} + \frac{[S]}{K_I'}} + \frac{[E]}{2}$$

- These methodologies are described in more detail in Chapter 9 of Enzymes 2nded by Copeland (1). We also recommend consulting with a statistician and an enzymologist experienced with tight binding inhibition.

Time-Dependent Inhibition

When the reaction is started with enzyme, there should be a linear relationship between the enzyme reaction time and the amount of the product formed from that reaction. This linearity should be preserved for all enzyme reactions lacking inhibitor or having rapid equilibrium binding events outside of the time window measured. However, the addition of inhibitor may result in a nonlinear progress curve (Figure 11) with an initial burst of enzyme activity (v_i) followed by a final, slower steady-state rate (v_s). Although the steady-state MOA model may still apply under some circumstances, additional characterizations are required.

- How can time dependent inhibitors be flagged in the steady-state MOA model?
  - For kinetic enzyme assays, the progress curve showing product formation over time is nonlinear (Figure 11).
  - For endpoint enzyme assays, time dependent inhibitors can display a noncompetitive phenotype regardless of their true binding modality. Otherwise, they can be identified by observing a shift in inhibitor potency with either a change in the enzyme reaction time and/or a change in the enzyme/inhibitor pre-incubation time.
- What is the recommended plan for an appropriate characterization?
  - More appropriately characterize and model the nonlinear progress curves (product formed vs time) observed. Illustrations of these progress curves and the appropriate models to use are found below in Figure 11. The resulting fit of the data to the nonlinear model should produce the v_i, v_s, and k_{obs} for all the [substrate] and [inhibitor] tested.
- During this evaluation, k_{obs} values reflecting timepoints (t) outside of the window tested should be avoided. For example, valid k_{obs} values from a kinetic run starting at 2 min and ending at 60 min should range between 0.5 min^{-1} to 0.08 min^{-1}. As a general rule, the total time of the reaction should be 5 times greater than $1/k_{obs}$. As a result, the scientist may need to choose a smaller range of [substrate] spanning K_m and [inhibitor] spanning $_{app}K_i$.
- In most cases, the initial (v_i) and steady-state (v_s) velocities can be fit separately to the steady-state MOA model (presented in the previous section) to yield the binding potency ($K_i$and/or K_i' value) and modality for each phase of inhibition.
- A more traditional approach to determine the apparent potency of the inhibitor requires the scientist to plot the k_{obs} values as a function of the [inhibitor] at a fixed [substrate]. This can yield 2 main types of plots illustrated in Figure 12 below: 1) If there is a linear relationship between the k_{obs} and the [inhibitor] tested, the one-step model shown should be used to determine the $_{app}K_i$ (potency at the steady-state velocity, v_s). 2) If there is a hyperbolic relationship between the k_{obs} and the [inhibitor] tested, the two-step model shown should be used to determine the $_{app}K_i$ (potency at the initial velocity, v_i) and the $_{app}K_i^*$ (potency at the steady-state velocity, v_s).
- A more traditional approach to determine the binding modality of a time dependent inhibitor requires a determination of the $_{app}K_i$, from the previous k_{obs} vs [inhibitor] plot, at each [substrate] spanning the K_m. The $_{app}K_i$ (and $_{app}K_i$*) can then be graphed as a function of [substrate] and fit to the model shown below (Figure 13). The ratio of K_i'/K_i (termed alpha, α) determined from the model below will reflect the binding modality. Inhibitors with alpha values statistically equal to 1.0 are noncompetitive, values statistically less than 1.0 are uncompetitive, and values statistically greater than 1.0 are competitive.

Model to Determine Time Dependent MOA

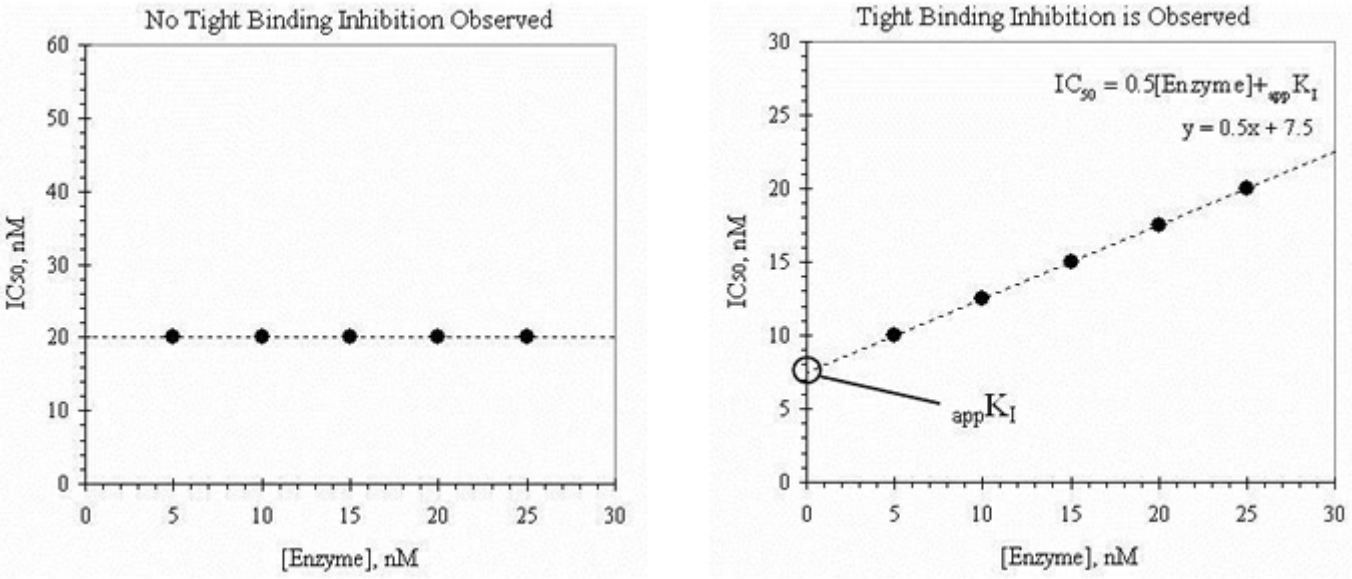

Figure 9 – Plotting the IC_{50} vs [Enzyme] will reveal whether a compound is tight binding. As depicted on the left, no change in the IC_{50} suggests that the compound is not tight binding and the assumption ([I] >> [E]) holds true. As depicted on the right, a change in the IC_{50} (with a slope of 0.5) suggests that the compound is tight binding and requires additional characterization.

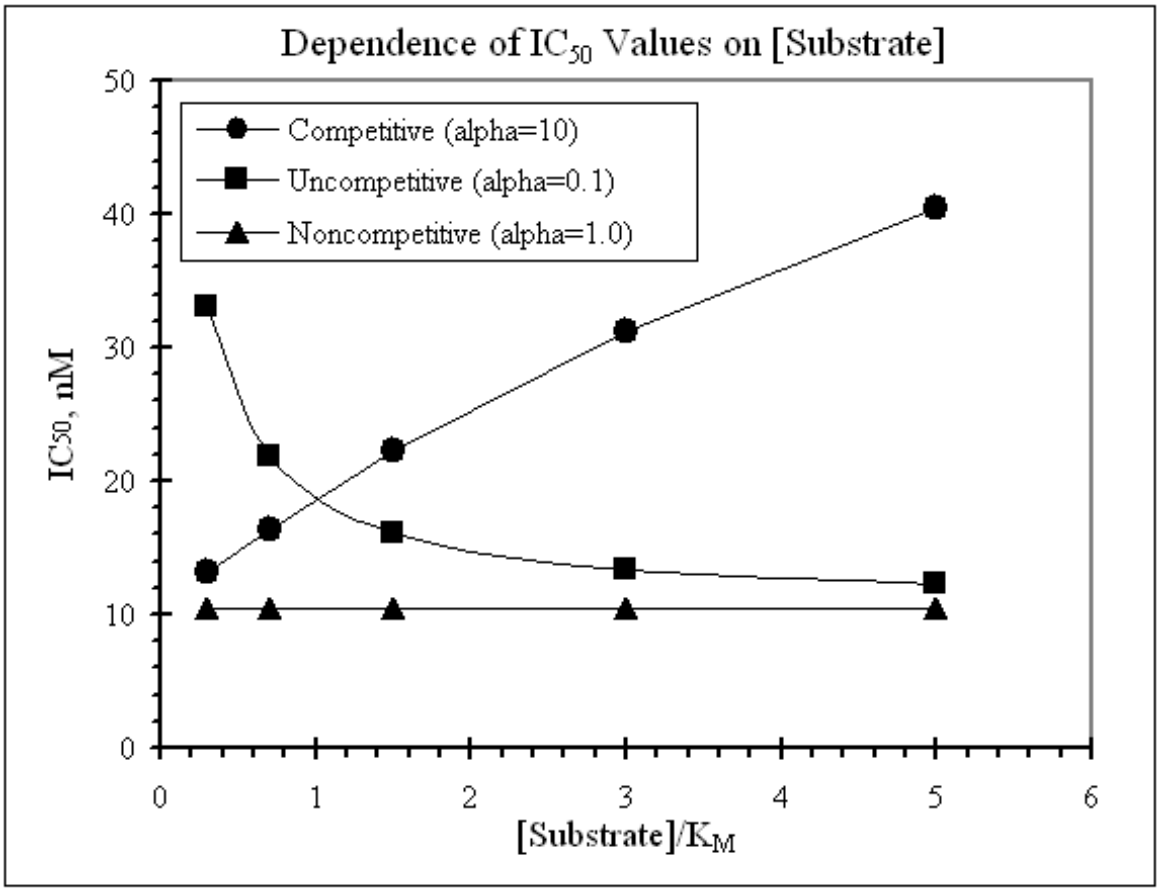

Figure 10 – A plot of the IC_{50} vs [substrate] will reveal the binding modality for a tight binding inhibitor. The quality of this assessment is predicated on the choice of a range of substrate concentrations that span the K_m. The graph illustrates that competitive inhibition is best identified at substrate concentrations above K_m. In contrast, uncompetitive inhibition is best identified at substrate concentrations below K_m. The true K_i and/or K_i' values can be obtained from a fit using the model below.

$$_{app}K_I = \frac{[S] + K_M}{\frac{K_M}{K_I} + \frac{[S]}{K_I'}}$$

Where possible, we recommend avoiding the iterative fitting into the one-step or two-step models and the model directly above. The scientist should consult with a statistician and enzymologist to perform a global fit of the data to an equation where the one-step or two-step models are solved for the $_{app}K_i$ shown directly above.

- A parallel approach to determine the binding modality requires the scientist evaluate the k_{obs} values as a function of the [substrate] at a fixed [inhibitor]. The k_{obs} of a competitive inhibitor will decrease with increasing [substrate] relative to K_m. The k_{obs} of an uncompetitive inhibitor will increase with increasing [substrate] relative to K_m. The k_{obs} of a noncompetitive inhibitor will not change with increasing [substrate] relative to K_m). These trends are illustrated in Figure 14.
- These methodologies are described in more detail in Chapter 10 of Enzymes 2nded by Copeland (1). Also be aware that a compound can display both time dependent and tight binding properties. This would require a combination of experiments described above that may require the assistance of a statistician or an experienced enzymologist.

Covalent Modification

During the initial phase of the reaction (initial velocity), there is no buildup of any intermediate other than the enzyme-substrate complex. This assumption most often fails when a compound is an irreversible inhibitor of the enzyme. This type of inhibition can be the result of an immeasurably slow k_{off} value and/or covalent modification of the enzyme.

- How can irreversible inhibitors be flagged in the steady-state MOA model?
  - Regardless of their true binding modality, they display a noncompetitive phenotype.
  - Irreversible inhibitors are time dependent with v_s values that approach zero. In contrast, reversible time dependent inhibitors have finite, non-zero v_s values. The quality of this observation can be limited by the timepoints measured and the [inhibitor] evaluated.
  - The observed k_{off} value is zero. This can be observed in a plot of the kobs as a function of the [inhibitor], shown in Figure 12. Irreversible inhibitors will yield a y–int (k_{off}) of zero.
- What is the recommended plan for an appropriate characterization?
  - In addition to the characterizations described in the sections above, the scientist can measure the release of inhibitor from the enzyme-inhibitor complex. This is often performed by pre-incubating the enzyme with inhibitor at $10\times K_i$ to achieve 100% inhibition (all enzyme is in the EI complex reflecting v_s), then diluting the assay 30 fold with substrate, and continuously (kinetically) measuring product formation. As illustrated in Figure 15, reversible inhibitors will regain enzyme activity while irreversible inhibitors remain inactive. This experiment can be properly interpreted when 3 controls are included containing 1) no inhibitor throughout to reflect full enzyme activity at the amount of DMSO tested, 2) $10\times K_i$ throughout to achieve 100% inhibition, and 3) $0.3\times K_i$ throughout to reflect the expected amount of inhibition remaining after substrate dilution. Assuming the $10\times K_i$ control is inactive, the final rate (v_s) for the experiment can be divided by the final rate of the $0.3\times K_i$ control to yield the fraction of recovered activity.

It is important to remember the there is no clear distinction between reversible and irreversible time dependent inhibition. The quality of the determination can often reflect the range and density of timepoints measured, [inhibitor] chosen, and other limitations specific to the assay. Therefore, it would be wise for the scientist to consult an analytical chemist to perform a MS-based strategy to confirm irreversible inhibition resulting from covalent modification of the enzyme.

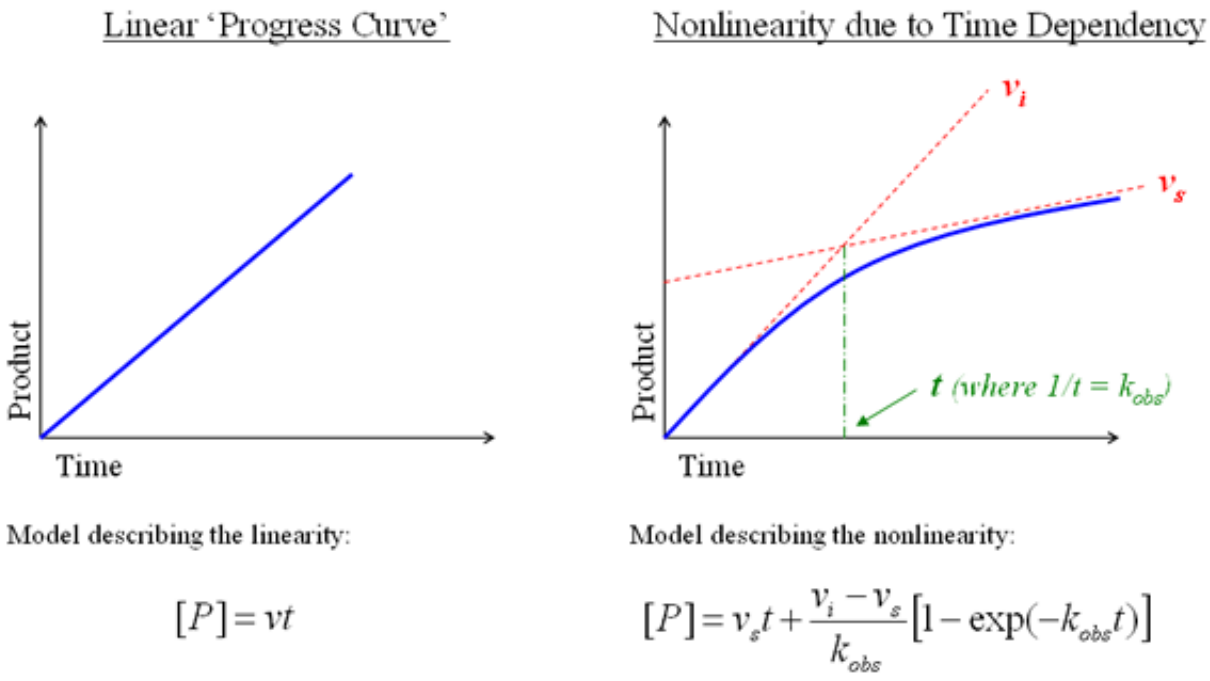

Figure 11 – Progress curves for linear, rapid equilibrium inhibition (left) and nonlinear, time dependent inhibition (right). Nonlinear progress curves resulting from time dependent inhibition can be fit to the model shown above. The resulting fit will yield the initial velocity (v_i), steady-state velocity (v_s), and the rate constant for the interconversion between v_i and v_s (k_{obs}), under the conditions tested. These values can be used to assess the true binding potency and modality.

Nonspecific Inhibition

Some compounds may form large colloid-like aggregates that inhibit activity by sequestering the enzyme. These types of compounds can display enzyme dependency, time-dependent inhibition, poor selectivity against unrelated enzymes, and binding modalities that are not competitive. This can be especially problematic when an enzyme is screened against a large diversity of compounds in a screening campaign. Although these compounds do not formally violate the steady-state assumptions, they can generate misleading results which produce inaccurate characterizations of the inhibitor-enzyme complex. The scientist is encouraged to read the Shoichet review published in Drug Discovery Today (3). The chart below was taken from that reference and provides an introduction to the considerations that should be made for evaluating these types of inhibitors.

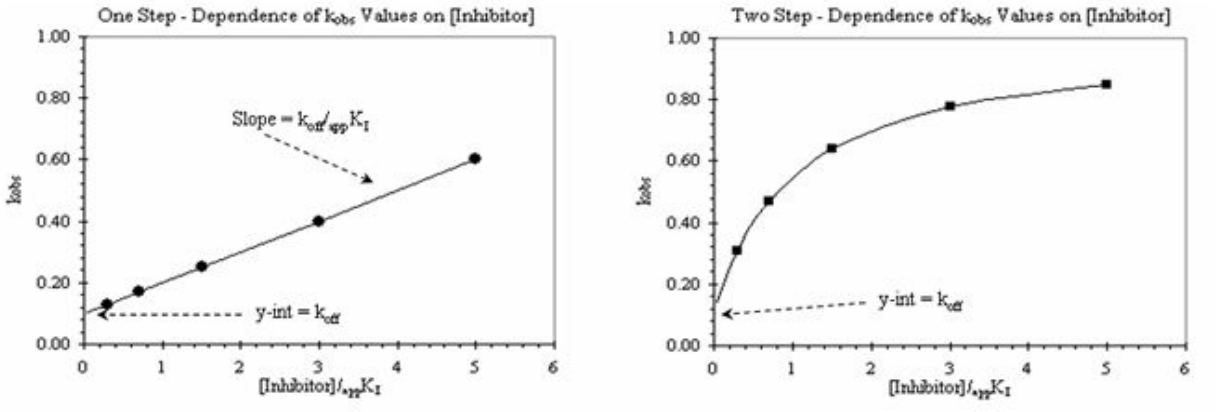

One Step Model:

$$k_{obs} = k_{off}\left(1 + \frac{[I]}{{}_{app}K_I}\right)$$

Two Step Model:

$$k_{obs} = k_{off}\left(\frac{1 + \frac{[I]}{{}_{app}K_I^*}}{1 + \frac{[I]}{{}_{app}K_I}}\right)$$

Figure 12 – A plot of the k_{obs} vs [inhibitor] will allow for the determination of the $_{app}K_i$ value for a time dependent inhibitor. If the relationship between k_{obs} and the [inhibitor] is linear, the one-step model shown above should be used. If the relationship is nonlinear, the two-step model should be used.

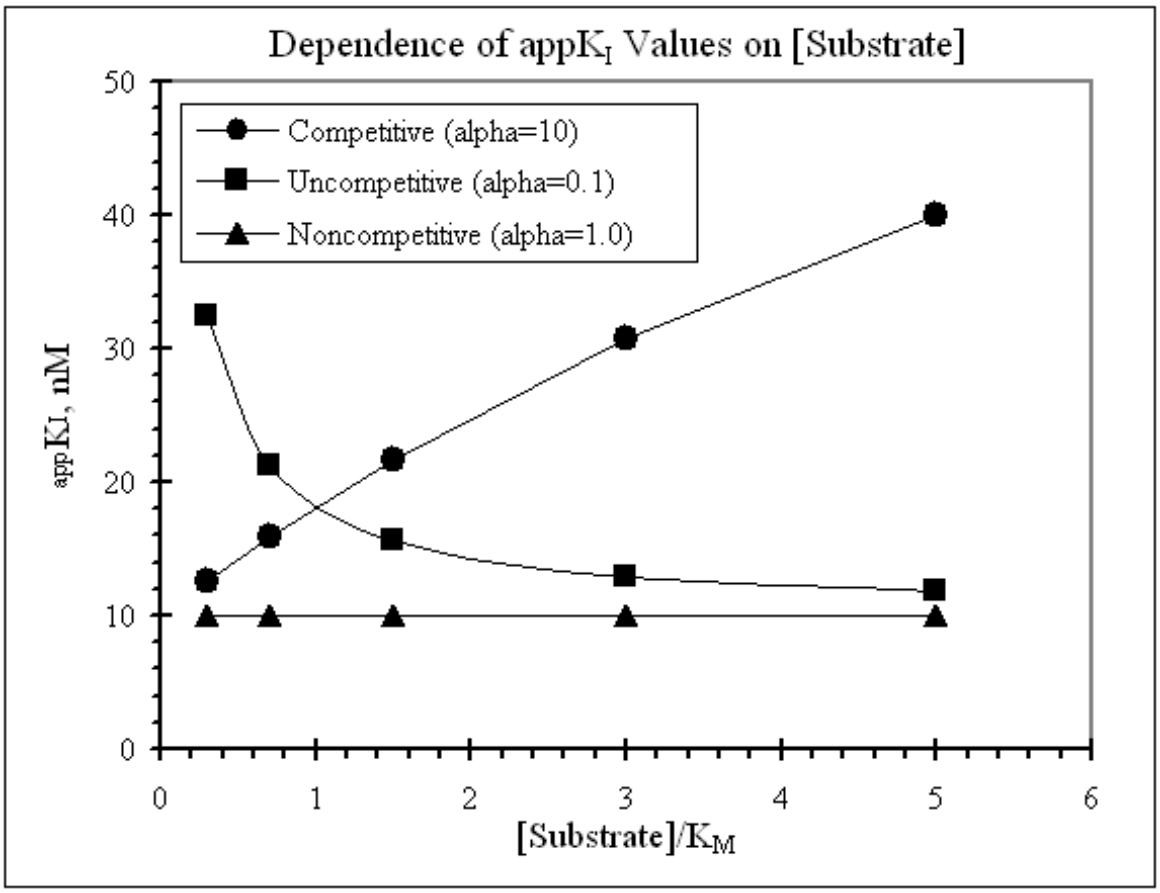

Figure 13 – A plot of the $_{app}K_i$ (and $_{app}K_i$*) vs [substrate] will allow for the determination of the true binding potency and modality. The modeled lines above are generated using the equation shown directly below where alpha = K_i'/K_i.

BOX 1

Evaluating candidate hits for aggregation-based inhibition:

1. Is inhibition significantly attenuated by small amounts of nonionic detergent?
   (i) If so, the compound is very likely acting through aggregation.
   (ii) In cases where you cannot use detergent, e.g. cell-based assays, it may be possible to use high (1 mg/ml) concentrations of serum albumin instead.
2. Is inhibition significantly attenuated by increasing enzyme concentration?
   (i) If so, the compound is very likely an aggregator. Except when the enzyme concentration to K_i ratio is high, increasing enzyme concentration should not affect percent inhibition.
3. Is inhibition competitive? If so, the compound is unlikely to be an aggregator.
4. Does the inhibitor retain activity after spinning for several minutes in a microfuge? If not, particle formation is likely (see point 5).
5. Can you directly observe particles in the 50 to 1000 nm size range? We have typically used dynamic light scattering for this. Formation of particles does not guarantee promiscuous inhibition, but it is a worrying sign.
6. Is the dose–response curve unusually steep? There are classical reasons for curves, but they too are a worrying sign.

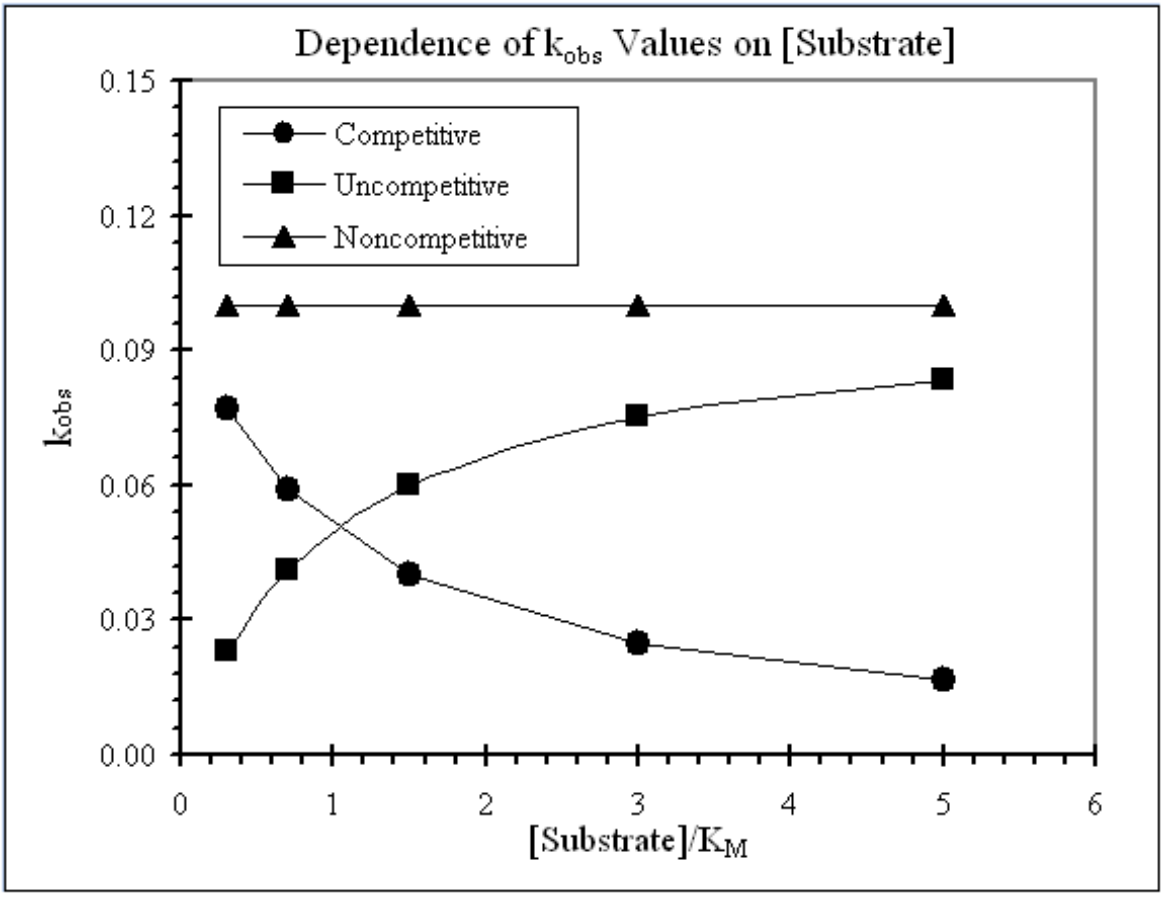

Figure 14 – A plot of the k_{obs} vs [substrate] will reveal the binding modality for a time dependent inhibitor. It is important to choose [substrate] well above and below the K_m to improve the ability to best distinguish the true binding modality.

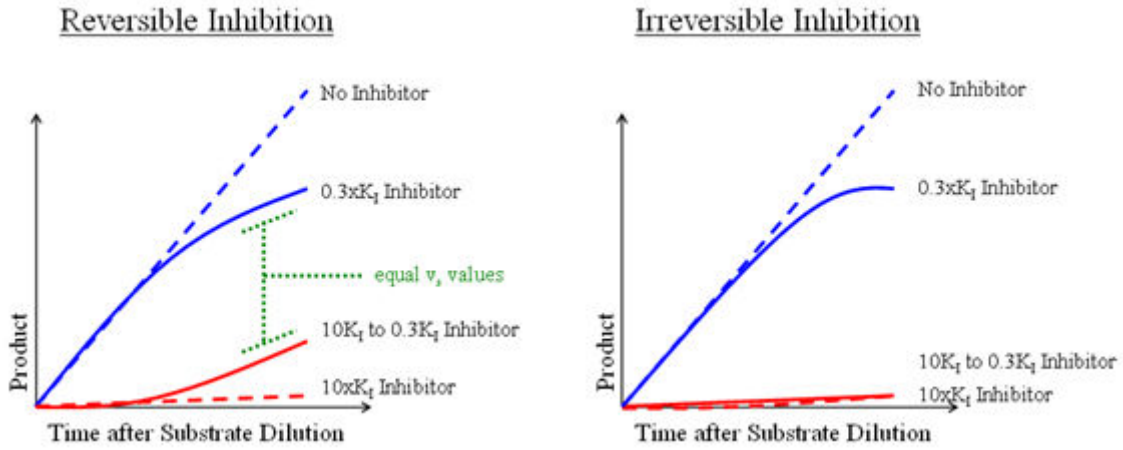

Figure 15 – The recovery of enzyme activity following dilution of the EI complex can be an indication of the reversibility of the inhibitor. Irreversible inhibitors (right) will not recover any enzyme activity following dilution of the EI complex with substrate. In contrast, a reversible inhibitor (left) will recover enzyme activity equivalent to the 0.3×K_i control.

References

Literature Cited

1. Copeland RA. Enzymes: A Practical Introduction to Structure, Mechanism, and Data Analysis, second edition. 2000, Wiley, New York.
2. Segal IH. Enzyme Kinetics: Behavior and Analysis of Rapid Equilibrium and Steady-State Enzyme Systems. 1975, Wiley, New York.
3. Shoichet BK. Screening in a Spirit Haunted World. *Drug Discovery Today* 2006, v11, pgs 607-615.

Additional References

Copeland RA. Mechanistic Considerations in High-Throughput Screening. *Analytical Biochemistry* 2003, v320, pgs 1-12.

Copeland RA. Evaluation of Enzyme Inhibitors in Drug Discovery: A Guide for Medicinal Chemists and Pharmacologists. 2005, Wiley, New York,

Copeland RA, Pompliano DL, Meek TD. Drug-Target Residence Time and Its Implications for Lead Optimization. *Nature Reviews Drug Discovery* 2006, v5, pgs 730-739.

Fehrst A. Structure and Mechanism in Protein Science: A Guide to Enzyme Catalysis and Protein Folding. 1999, W.H. Freeman, New York.

Kenakin TP. A Pharmacology Primer: Theory, Application, and Methods. 2004, Elsevier, San Diego.

Robertson JG. Mechanistic Basis of Enzyme-Targeted Drugs. *Biochemistry* 2006, v44, pgs 5561-5571.

Swinney DC. Biochemical Mechanisms of Drug Action: What Does It Take For Success? *Nature Reviews Drug Discovery* 2004, v3, pgs 801-808.

Swinney DC. Biochemical Mechanisms of New Molecular Entities (NMEs) Approved by United States FDA During 2001-2004: Mechanisms Leading to Optimal Efficacy and Safety. Current Topics in Medicinal Chemistry 2006, v6, pgs 461-478.

Glossary of MOA Terms

The definitions for these terms were gathered from references

Active site — the specific and precise location on the target responsible for substrate binding and catalysis.

Allosteric activators — an allosteric effector that operates to enhance active site substrate affinity and/or catalysis. (Copeland, Enzymes, pg368)

Allosteric effector — small molecule that can bind to sites other than the enzyme active site and, as a result of binding, induce a conformational change in the enzyme that regulates the affinity and/or catalysis of the active site for its substrate (or other ligands). (Copeland, Enzymes, pg368)

Allosteric repressors — an allosteric effector that operates to diminish active site substrate affinity and/or catalysis. (Copeland, Enzymes, pg368)

Allosteric site — a site on the target, distinct from the active site, where binding events produce an effect on activity through a protein conformational change. (Kenakin, A Pharmacology Primer, p195).

Alpha — typically noted as the ratio, K_I'/K_I. It reflects the effect of an inhibitor on the affinity of the enzyme for its substrate, and likewise the effect of the substrate on the affinity of the enzyme for the inhibitor. (Copeland, Enzyme, pg268)

Biochemical assay — the in vitro based mechanism used to measure the activity of a biological macromolecule (enzyme).

Cofactor — nonprotein chemical groups required for an enzyme reaction.

Enzyme — protein that acts as a catalyst for specific biochemical reaction, converting specific substrates into chemically distinct products.

Multivariate fitting — Fitting a more than 2 variable model (Example: Response, [Inhibitor], [Substrate]) to all of the data from a MoA experiment using nonlinear regression.

Inhibitor — any compound that reduces the velocity of an enzyme-catalyzed reaction measured in a biochemical assay, as represented by percent inhibition or IC_{50}.

Initial velocity — the initial linear portion of the enzyme reaction when less than 10% of the substrate has been depleted or 10% of the product has formed. (QB Manual, Section IV, pg5)

In vitro — (to be defined later)

Ligand — a molecule that binds to the target. (Kenakin, A Pharmacology Primer, pg 198)

Linearity — A relationship between two variables that is best described by a straight line. In MoA experiments, the amount of product formed should be linear with respect to time.

Substrate — a molecule that binds to the active site of an enzyme target and is chemically modified by the enzyme target to produce a new chemical molecule (product).

Target — a macromolecule or macromolecular complex in a biochemical pathway that is responsible for the disease pathology. (QB manual, Section XII, pg3)

$\mathbf{k_{cat}}$ — turnover number representing the maximum number of substrate molecules converted to products per active site per unit time. (Fehrst, Str Mech Prot Sci, pg109)

$\mathbf{K_I}$ — the affinity of the inhibitor for free enzyme.

$\mathbf{K_I'}$ — the affinity of the inhibitor for the enzyme-substrate complex.

$\mathbf{K_M}$ — the concentration of substrate at ½ Vmax, according to the Henri-Michaelis-Menten kinetic model (QB manual, Section IV, pg9)

$\mathbf{k_{off}}$ — the off-rate associated with the release of inhibitor from an enzyme-inhibitor complex.

$\mathbf{k_{on}}$ — the on-rate associated with the formation of an enzyme-inhibitor complex.

Assay Development for Protein Kinase Enzymes

J. Fraser Glickman, M.S.P.H., Ph.D.[1]

Created: May 1, 2012; Updated: October 1, 2012.

Abstract

Kinases are important drug targets that control cell growth, proliferation, differentiation and metabolism. This process involves phosphorylation of multiple substrates in cellular signal transduction pathways. Here, the authors provide a synopsis on assay technologies, mechanistic considerations for assay design and development pertaining to kinase enzymes. This chapter, along with some of the earlier chapters in this manual on basics of enzyme assays, mechanism of action and purity and identity considerations, serves as an excellent resource for beginners in HTS applications.

Introduction

Enzymatic phosphate transfers are one of the predominant mechanisms for regulating the growth, differentiation and metabolism of cells. The post-translational modification of proteins with phosphate leads to dramatic changes in conformation resulting in the modulation of binding, catalysis and recruitment of effector molecules that regulate cellular signaling pathways. Examples include the recruitment of SH2 domain containing proteins, the activation of gene transcription pathways and the activation or deactivation of specific cell surface receptors. The practical design and implementation of these assays for drug discovery and development applications will be the focus of this section.

The keys to protein kinase assay development lie in the ability to 1) choose an appropriate "readout" technology, 2) have ample quantities of enzymes, cell lines, antibodies and reference compounds, and 3) optimize the assay for buffer conditions, reagent concentrations, timing, stopping, order of addition, plate type and assay volume. The readout technologies present many options for assay development and often depend on the laboratory infrastructure, the cost of reagents, the desired substrate and the secondary assays needed to validate the compounds and determine the structure activity relationships (Table 1). In the end, they all require the measurement of photons emitted from the assay well in a microtiter plate. They differ in how the photons are generated, and what property (ie. wavelength or polarity) of the photons are measured.

Protein kinase enzyme assays require the co-factors ATP, magnesium (and sometimes manganese) and a peptide or protein substrate (Table 2). One must have a method to detect the conversion of substrate by detecting either the formation of phosphopeptide, phosphoprotein, the disappearance of ATP, or the formation of ADP. There are many commercially available kits and many published references describing these methodologies (Table 1). The subject of the choice of assay technologies is vast, changing and interestingly controversial (1-3) since many technologies are marketed as kits which come with strong pressure to establish "market share." Also, in the past 15 years there has been a steady development and refinement of new kinase technologies. Examples of highlighted features in assay kits can include higher dynamic range with respect to ATP, greater sensitivity to known inhibitors, flexibility of substrate choice, statistical robustness, lowered susceptibility to artifacts and simpler assay protocol. Cost is often a consideration when choosing a technology or kit as well as the availability of instrumentation. This chapter will attempt to concisely review some of the key technologies below, highlighting the theory behind the assay, some of the underlying principles with strengths and weaknesses, in hope that the reader can make more informed decisions when reviewing the options.

Author Affiliation: 1 The Rockefeller University, New York, NY, 10065; Email: fglickman@rockefeller.edu.

Table 2. Kinases F. Glickman

Assay Optimization Cycle and Typical Test Parameters

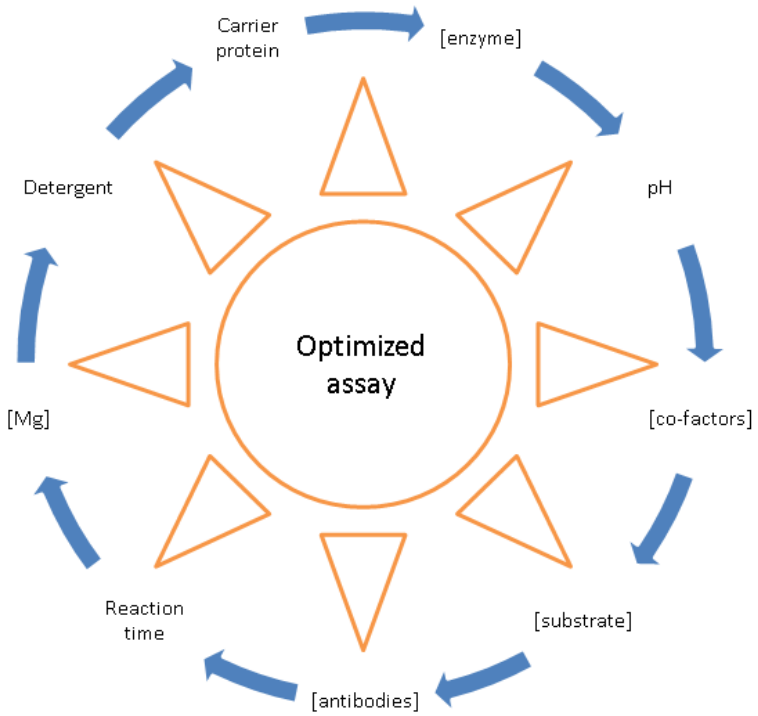

Assay Component	Example Range
Enzyme conc.	1-50 nM
pH value	5-9
Co-factors	0.1-10 uM
Substrate conc.	0.1-10 uM
time	0.25-3 hours
divalents	Mg, Mn (mM)
buffer	20 mM HEPES, TRIS,MES
detergent	0.05% NP-40, Tween-20, CHAPS, pluronic
carriers	BSA, gelatin,casein, 0.1 %
Antibodies	5-20 nM

Table 2. Assay Optimization Cycle and Typical Test Parameters

Table 1.

Assay Technology (Commercial names and aliases)	Technology Principles	Advantages	Disadvantages	References
Fluorescence Polarization (anisotropy) version 1 (InVitroGen Polar Screen)	A fluorescently-labeled substrate peptide binds to an anti-phospho antibody after phosphorylation. A change in the Brownian motion of the peptide-antibody complex results in a change in anisotrophy measured by polarization of incoming light.	high throughput, only one labeled substrate required	susceptible to compound interference, peptide must be relatively small, precludes use of protein substrates	Parker (2000), Sills (2002), Newman (2004), Turek-Etienne (2003b)
Fluorescence Polarization (anisotropy) version 2 (IMAP)	fluorophore-labeled peptides bind to special detection beads coated with trivalent metal. Binding results in change in Brownian motion measured as with FP1.	Versatile without need for antibody	susceptible to compound interference, peptide must be relatively small, precludes use of protein substrates	Turek-Etienne (2003a)

Table 1 continued from previous page.

Assay Technology (Commercial names and aliases)	Technology Principles	Advantages	Disadvantages	References
Scintillation Proximity (FlashPlate, SPA)	product of reaction is a 33P labeled peptide-biotin which can be captured on a detection bead which scintillates from proximity to 33P. Dephosphorylation by phosphatases can be detected in a signal decrease assay	high throughput, relatively artifact free in imaging based systems, universal readout for kinases, versatile	radioactive waste disposal, can be less sensitive than TR-FRET	Park (1999), Sills (2002), von Ahsen (2006)
Fluorescence Resonance energy Transfer (Quenched Fluorescence, InVitroGen Z'-LYTE))	Peptide labeled with fluorescein and coumarin is quenched until cleaved by a protease, modification by phosphorylation or dephosphorylation by a kinase or phosphatase results in a resistance to proteolytic cleavage	miniaturizeable, ratiometric readout normalizes for pipetting errors, can be applied to kinases and phosphatases	Coupled assay can be susceptible to protease inhibitor compounds.	Rodems (2002)
Immunosorbant Assays (enzyme-linked or fluorescent linked, cell signaling PathScan))	antibodies coated onto MTP wells capture kinase or phosphatase substrate and the phosphorylation state is detected by anti-phosphopeptide antibody coupled to detector dye. Can be read by time-resolved fluorescence (DELFIA) technique	Can be used as a sensitive probe for cell lysates in cell-based assays	lower throughput and wash steps are required. Must have suitable cell line and antibody pair	Waddleton (2002), Minor (2003), Zhang (2007)
luciferase-based ATP detection (Promega kinase Glo, Perkin-Elmer Easylite Kinase)	ATP-dependent luminescent signal from luciferase conversion of luminol. The kinase dependent depletion of ATP is measured.	Versatile and non-radioactive	Signal Decrease assay, susceptible to luciferase inhibitors	Koresawa (2004)
Luminsescent Oxygen Channeling (Perkin-Elmer AlphaScreen, Surefire)	Antiphosphotyrosine or phosphopeptide antibodies bind only to the phosphorylated substrate. The complex is detected by streptavidin and protein A functionalized beads which when bound together results in a channeling of singlet oxygen when stimulated by light. The singlet oxygen reacts with the acceptor beads to give off photons of lowered wavelength than their excitation frequency.	Sensitive, high throughput, can be applied to cell lysates as a substitute for an ELISA type assay. Proximity distances can be very large relative to Energy transfer. Emission frequency is lower than excitation frequency, thus eliminating potential artifacts by fluorescent compounds. Can be applied to whole cell assays	Can be susceptible to interference by compounds which trap singlet oxygen. Must work under subdued or specialized lighting arrangements	Von Leoprechting (2004), Warner (2004)

Table 1 continued from previous page.

Assay Technology (Commercial names and aliases)	Technology Principles	Advantages	Disadvantages	References
Time Resolved Forster Resonance Energy Transfer (version 1: InVitroGen LanthaScreen, Perkin-Elmer LANCE, CysBio KinEase)	phosphopeptide formation is detected by a "Europium chelate and Ulight acceptor dye PKA substrates Dephosphorylation by phosphatases can be detected in a signal decrease assay	Very Sensitive and miniaturizeable, ratiometric readout normalizes for pipetting errors	Required two specialized antibodies, susceptible to interference, low dynamic range for substrate turnover.Binding interaction should be within restricted proximity for optimal efficiency	Moshinsky (2003), Vogel (2006), Von Ahsen (2006), Schroeter (2008)
Time Resolved Forster Resonance Energy Transfer (version 2:BellBrook Labs Transcreener,Adapta)	ADP formation by the kinase is detected by displacement of a red shifted TR-FRET system between Alexafluor647-ADP analog and a Europium-chelated- anti ADP antibody.	High Throughput, miniaturizeable, versatile, ratiometric readout	signal decrease assay.Binding interaction should be in close proximity (7-9 nM)	Huss (2007)
Enzyme Fragment complementation (DiscoveRx ED-NSIP HitHunter	Two fragments of a reporter protein fusion are brought together through a biomolecular interaction, thus reconstituting the activity of the reporter protein. Kinases can be assayed in a displacement mode using a staurospaurine conjugate to one fragment and a kinase fused to the second fragment of b-galactosidase (ED-NSIP). Test compound displaces kinase-staurospaurine interaction, and decreases B-gal activity.	High Throughput, sensitive, amplified enzymatic, chemiluminescent signal less susceptible to interference	coupled assay can have interference with b-galactosidase binding compounds. Compound must be competitive with probe	Eglen (2002), Vainshtein (2002)

Radioactive Assay Technologies

Traditional kinase assays measure the transfer of the ^{32}P from the γ position of ATP to a peptide or protein substrate results in a ^{32}P labeled peptide or protein that may be separated away from the ATP by capture on a filter and subsequent washing. The quantity of phosphoprotein is quantified by scintillation counting (4).

The availability of [^{33}P]ATP as an alternative to ^{32}P provides benefits of safety and longer half-life. The lowered energy is also better suited for scintillation proximity assays (SPAs, www.perkinelmer.com; 5). SPA was a major step forward because it eliminated the need for wash steps by capturing the [^{33}P]-labeled peptide on a functionalized scintillating crystal, usually via a biotin-streptavidin interaction.

The specific signal in the SPA is a consequence of a radiolabeled peptide or protein substrate becoming closely bound to the scintillation material. As a result, photons are given off due to a transfer of energy from the decaying ^{33}P particle to the scintillation material. Non-specific signals (non-proximity affects) can result from decay particles emitted from free [^{33}P]ATP molecules interacting with the scintillation material at greater distances(Figure 1).

All SPAs are based upon the phenomenon of scintillation. Scintillation is an energy-transfer that results from the interaction between particles of ionizing radiation and the de-localized electrons found in conjugated aromatic

hydrocarbons or in inorganic crystals. When the decay particle collides with the scintillation material, electrons are transiently elevated to higher energy levels. Because of the return to the ground state, photons are emitted. Frequently, scintillation materials are doped with fluorophores, which capture these photons (usually in the ultraviolet spectrum) and fluoresce at a "red-shifted" wavelength more "tuned" to the peak sensitivity of the detector.

Conventionally, the scintillation materials used in bioassays were liquids composed of aromatic hydrocarbons. These bioassays required a wash step before the addition of the scintillation liquid and counting in a liquid scintillation counter. With SPA technology crystals of polyvinyltoluene (PVT), Yttrium silicate (YS), polystyrene (PS) and Yttrium oxide (YOx) are used as the scintillant. These materials are functionalized with affinity tags to detect the decay particles directly in the bioassay without wash steps. The newer generation of "red-shifted" FlashPlates and SPA beads yields emission frequencies of around 615 nM, and thus, can be detected by CCD (charge-coupled device) imagers rather than photomultiplier tube (PMT) readers. The advantages of these "imaging" beads and plates lie in both the ability to simultaneously read all wells in a microtiter plate (MTP) and in the reduction of interference from colored compounds (www.perkinelmer.com).

Because of the cost of disposing of radioactive reagents and the requirement for special safety infrastructure, the use of this approach is becoming less frequent, although it presents some distinct advantages (5). First, one needs no phosphopeptide or phosphotyrosine-specific antibodies (an advantage shared with "coupled assays", mentioned below), as the ATPγ^{33}P is the only co-factor required. Second, because analyte detection is performed at only one emission wavelength, there are less potential sources of interference by light-absorbing compounds versus fluorescent assays. SPA techniques are well suited toward utilizing a variety of biologically relevant substrate proteins. Universal substrates that are biotinylated, such as poly-GlutamineTyrosine (polyEY), can be used for the tyrosine kinases. Generalized substrates such as myosin basic protein or casein, or specialized peptide substrates must be used for the serine-threonine kinases. A discussion of the choice of substrates in kinase assays is presented in the assay development section below.

Fluorescence Assays

Although fluorescent assays are very useful in HTS, the classic issue with these assays is that they are susceptible to interference from compounds that either absorb light in the excitation or emission range of the assay, known as an inner filter effects (6), or that are themselves fluorescent resulting in false negatives. At typical compound screening concentrations of greater than 1 μM, these types of artifacts can become significant.

There are several approaches to minimizing this interference. One approach is to use longer wavelength fluorophores (red-shifted). This reduces compound interference since most organic medicinal compounds tend to absorb at shorter wavelengths (7). The percentage of compounds that fluoresce in the blue emission (4-methyl umbelliferone) has been estimated to be as high as 5% in typical LMW compound libraries. However, this drops to <0.1% at emission wavelengths >500 nm (8). Another approach is to use as "bright" a fluorescent label as possible. Bright fluorophores have a high efficiency of energy capture and release. This means that an absorbant or fluorescent compound will have a lowered impact on the total signal of the assay. Assays with higher photon counts will tend to be less sensitive to fluorescent artifacts from compounds as compared with assays having lower photon counts. Minimizing the test compound concentration can also minimize these artifacts and one must balance the potential of compound artifacts versus the need to find weaker inhibitors by screening at higher concentrations.

The availability of anti-phosphotyrosine antibodies, anti-phosphopeptide antibodies and antibodies to fluorescent ADP analogs enabled the performance of several homogeneous methods using fluorophores, among these time-resolved Förster resonance energy transfer (TR-FRET) and fluorescence polarization (FP).

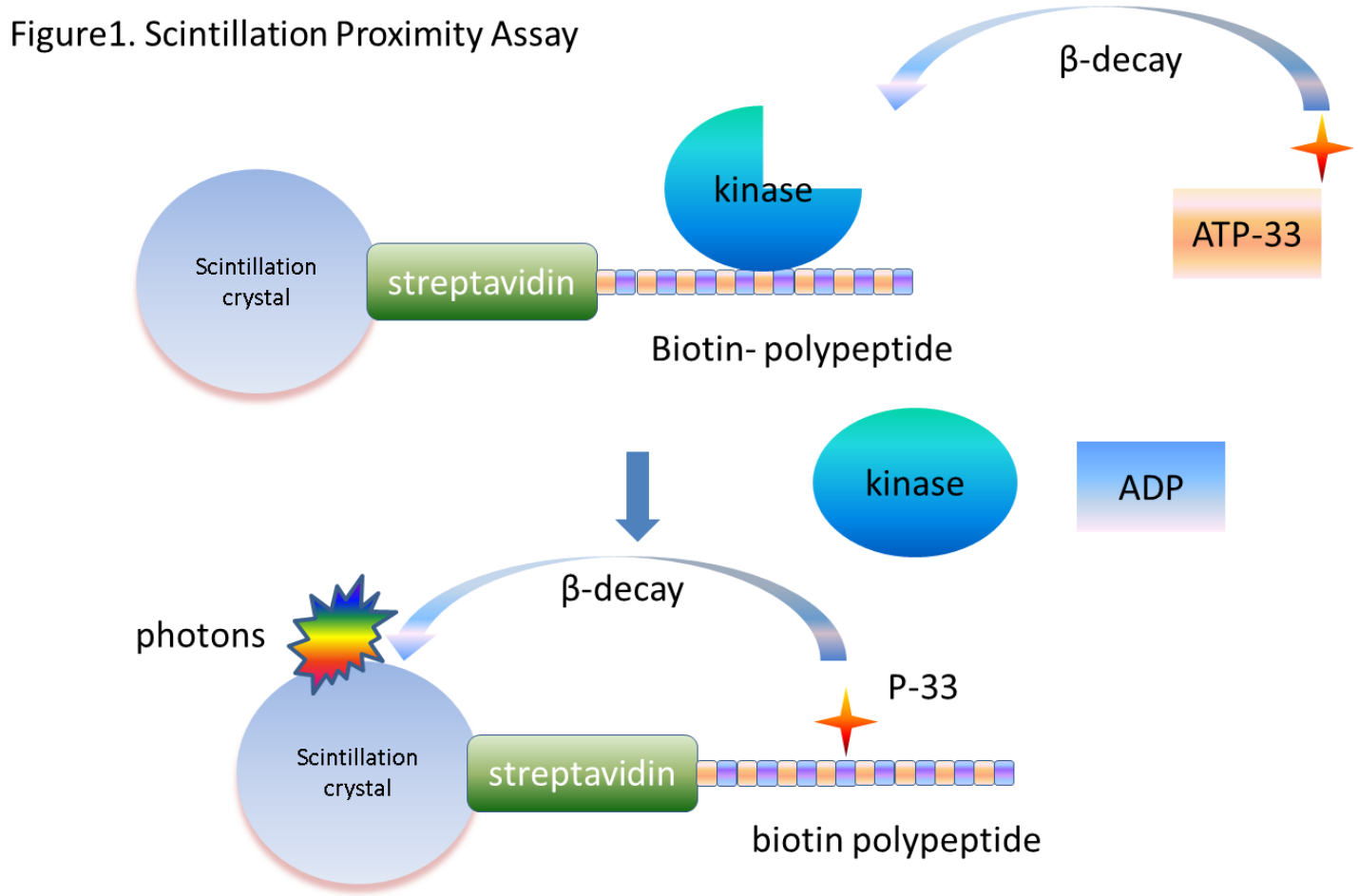

Figure 1. Scintillation Proximity Assay

Fluorescence Anisotropy (Polarization)

Anisotropy can be measured when a fluorescent molecule is excited with polarized light. The ratio of emission intensity in each polarization plane, parallel and perpendicular relative to the excitation polarization plane, gives a measure of anisotropy, more commonly referred to in HTS as "fluorescence polarization" or FP. This anisotropy is proportional to the Brownian rotational motion of the fluorophore. Changes in anisotropy occur when the fluorescent small molecule binds to a much larger molecule affecting its rotational velocity. Kinase assays are set up using anti-phosphopeptide antibodies and labeled phosphopeptides (Figure 2, 9) or by using a metal ion affinity material to capture labeled phosphopeptides (10). The formation of the phosphopeptide in an enzymatic reaction causes an increase in binding to an antibody or affinity resin and consequently a change in anisotropy. The advantage of FP is that it requires only one small polypeptide labeled (instead of two labeled moieties as with TR-FRET or AlphaScreen).

FP assays are known to be susceptible to artifacts (11). In principle, the assays are ratiometric and should normalize for variations in total excitation energy applied as would occur with inner filter effects (see Assay Guidance Manural chapter on Spectrophotometry), and newer generations of red-shifted fluorophores should help to eliminate interference (7). However, introducing a test compound with fluorescent or absorbent properties at greater than 5 μM with the typically nanomolar concentrations of fluorescently-labeled peptide in an FP assay can significantly skew the measurements. One way to reduce this potential issue is to simultaneously collect total fluorescence data and exclude those compounds which significantly affect the total fluorescence of the assay well.

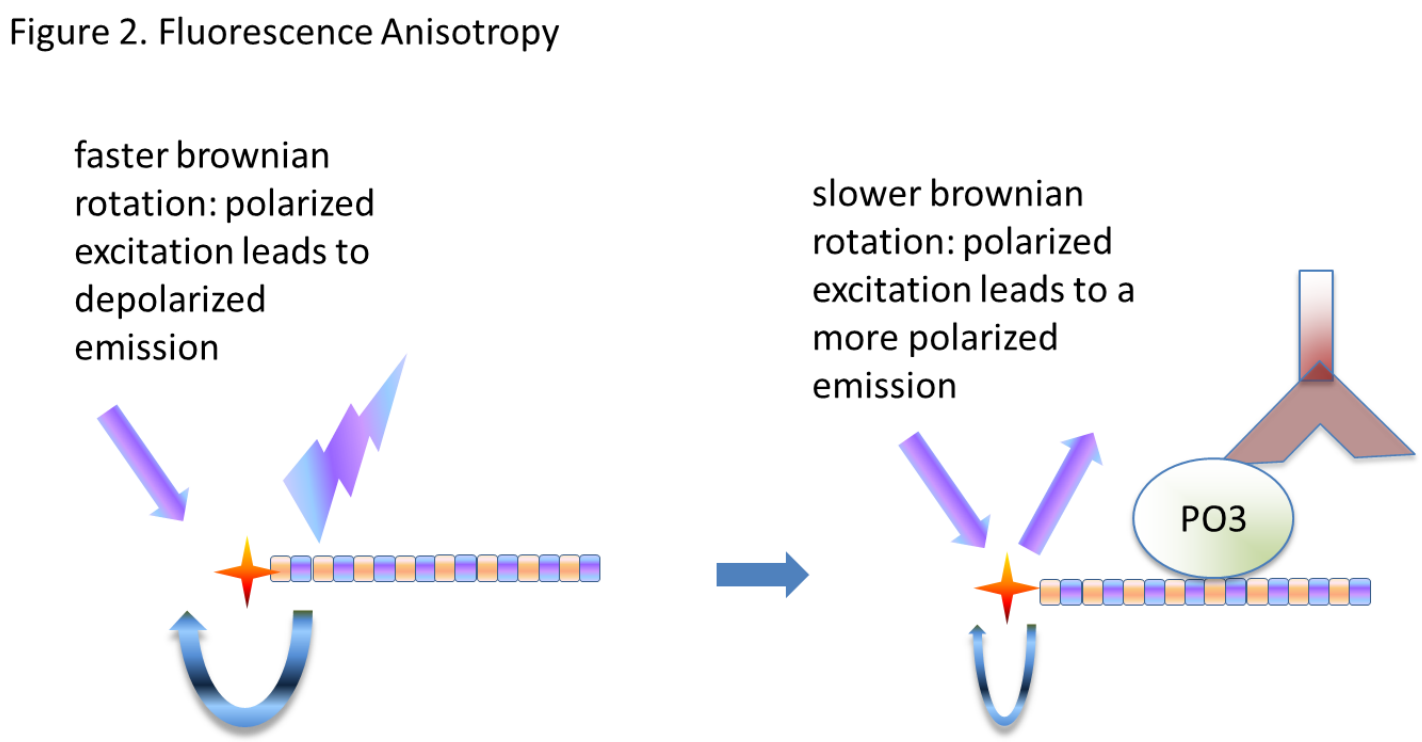

Figure 2. Fluorescence Anisotropy

Time-Resolved (Gated) Förster Resonance Energy Transfer (TR-FRET)

These assays are based upon the use of a Europium or Terbium chelate (a transition metal-ligand complexes displaying long-lived fluorescent properties), and labeled anti-phosphopeptide or anti-phosphotyrosine antibodies that bind to phosphorylated peptides. The antibodies are usually labeled with aromatic fluorescent tags such as Cy5, Rhodamine, or fluorescent proteins such as allophycocyanin. Allophycocyanin is a light-harvesting protein which absorbs at 650 nM and emits at 660 nm (9, 12, 13). When the anti-phosphotyrosine or anti-phosphopeptide antibodies bind to a labeled phosphorylated peptide the proximity of the antibody to the labeled peptide results in a transfer of energy (Figure 3). The energy transfer is a consequence of the emission spectrum of the metal-ligand-complex overlapping with the absorption of the labeled peptide. If the donor fluor is within 7-9 nM of the acceptor fluor then Förster resonance energy transfer can occur although the optimal distance between fluorophores is also influenced by effects of proximal fluorophores on the emission lifetime in the time-gated system (14). The action of a kinase enzyme increases the concentration of phosphopeptide over time and results in an increased signal in such an assay.

TR-FRET assays have two main advantages. The first advantage is in the "time-gated" (the term "resolved" is commonly misused from a biophysical perspective) signal detection, which means that the emission is measured 100-900 μs after the initial excitation frequency is applied, resulting in a reduction in fluorescence background from the microtiter plate, buffers, and compounds. Data is acquired by multiple flashes per read, to improve the sensitivity and reproducibility of the signal. The second advantage is that the one can measure the ratio of the emission from the acceptor molecule to the emission from the donor molecule. Because of this ratiometric calculation, variations in signal due to variations in pipetting volume can be reduced. Therefore, one generally observes less inter-well variation in TR-FRET assays versus other enzyme or biomolecular assay systems (15).

Figure 3. Time-gated forster resonance energy transfer

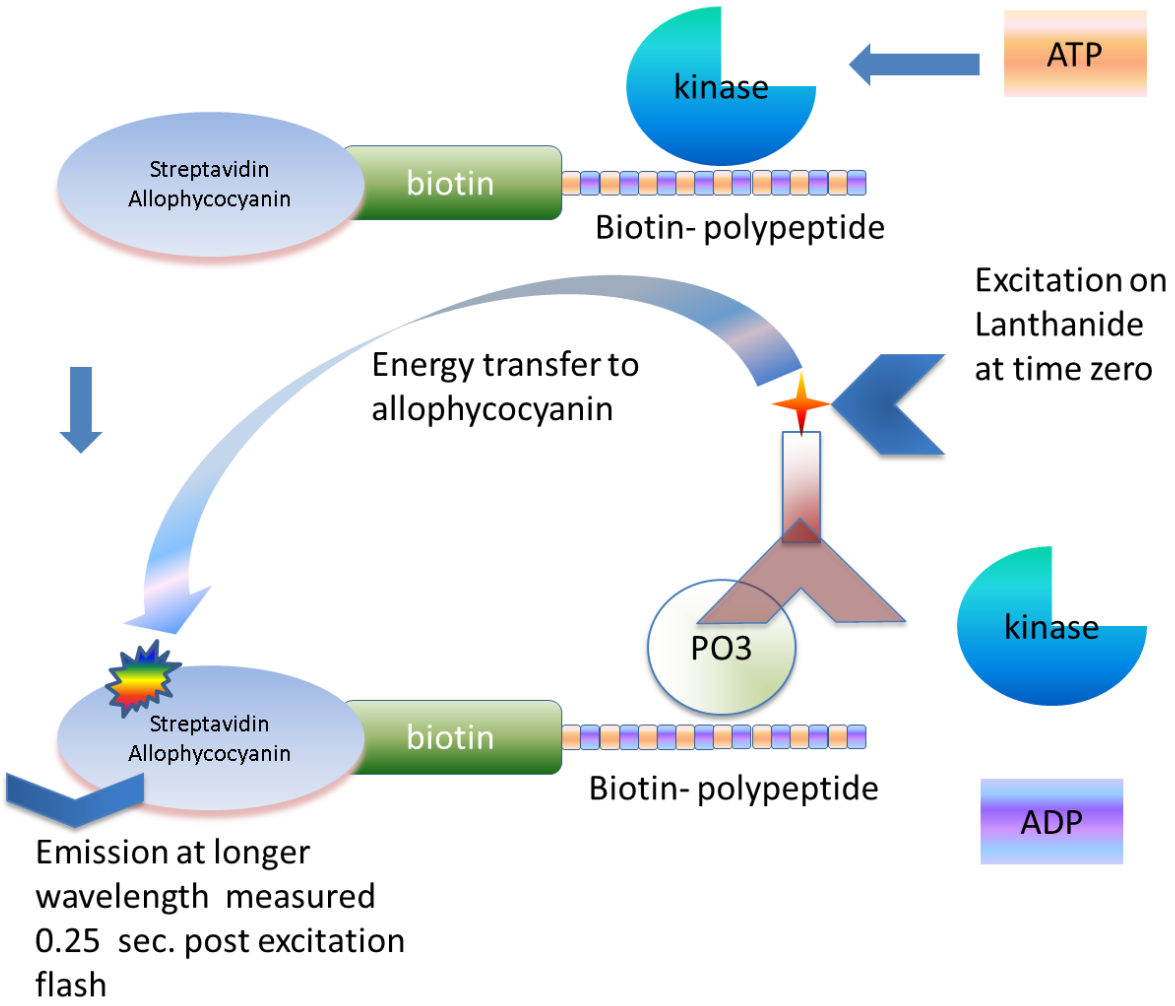

Figure 3. Time-gated Forster resonance energy transfer

Luminescent Oxygen Channeling (AlphaScreen™, AlphaLISA™)

AlphaScreen technology, first described in 1994 by Ullman and based on the principle of luminescent oxygen channeling, has become a useful technology for kinase assays (16). AlphaScreen is a bead-based, non-radioactive, Amplified Luminescent Proximity Homogenous Assay. In this assay, a donor and an acceptor pair of 250 nm diameter reagent-coated polystyrene microbeads are brought into proximity by a biomolecular interaction of anti-phosphotyrosine and anti-peptide antibodies immobilized to these beads (www.perkinelmer.com). Irradiation of the assay mixture with a high intensity laser at 680 nm induces the conversion of ambient oxygen to a more excited singlet state by a photosensitizer present in the donor bead. The singlet oxygen molecules can diffuse up to 200 nm and, if an acceptor bead is in proximity, can react with a thioxene derivative present in this bead generating chemiluminescence at 370 nm that further activates the fluorophores contained in the same bead. The fluorophores subsequently emit light at 520-620 nm. The donor bead generates about 60,000 singlet oxygen molecules resulting in an amplified signal. Since the signal is very long-lived, with a half-life in the one second range, the detection system can be time-gated, thus eliminating short-lived background (the AlphaScreen signal is measured with a delay between illumination and detection of 20 msec). Furthermore, the detection wavelength is of a shorter wavelength than the excitation wavelength, thus

further reducing the spotential for fluorescence interference. The sensitivity of the assay derives from the very low background fluorescence. The larger diffusion distance of the singlet oxygen enables the detection of binding distance up to 200 nm, whereas TR-FRET is limited to 9 nm (15), allowing the use of much larger protein substrates. A newer version of the same principle is called AlphaLISA^{TM} (Perkin-Elmer) . While AlphaScreen uses acceptor beads with an emission from rubrene, AlphaLISA acceptor beads use Europium. Thus the emission wavelength is different between AlphaScreen beads (520-620 nm) and AlphaLISA beads (615 nm). The narrow emission spectrum of AlphaLISA should, in principle, lessen interference.

Kinase assays based on the AlphaScreen principle are similar to TR-FRET assays in that they usually require a biotinylated substrate peptide and an anti-phosphoserine or tyrosine antibody. These two reagents are "sandwiched" between biotin and protein-A functionalized acceptor and donor beads. A kinase assay shows an enzyme dependent increase in antibody binding (and thus signal) over time. In some cases, the phosphorylation of an epitope will block the antibody binding which can be used as the basis of for product detection (17, 18). Like other optical assays, AlphaScreen assays are susceptible to inner filter effects (6). Additionally, compounds which react with singlet oxygen can cause false positives. One can easily re-test AlphaScreen hits in an independent AlphaScreen assay, for example measuring the effect of the compound on biotin-streptavidin bead interactions optimized to the same level of photon counts as the primary assay. Artifact compounds would be expected to inhibit this signal and can thus be eliminated as false positives.

"Coupled" Assays

"Coupled" assays are those that require the addition to the assay of more enzymes to convert a product or substrate into a detectable signal. All coupled enzyme assays share potential artifacts from "off-target" inhibition of the enzymes used to couple the reaction to a detectable product. Thus, with all coupled assays, one must be careful that inhibitors or activator compounds are not inhibiting the coupling systems. It is usually easy to design a secondary assay system to establish that this is not the case, simply by "feeding" the coupling system with suitable substrates (in the absence of kinase enzyme) and measuring the effect of putative inhibitors on the coupling system. For protein kinases, the most common manifestation of a coupled assay uses luciferase to detect ATP formation, and yet others use proteases, ATPases and other non-disclosed commercial enzymes to produce a kinase assay kit. These are briefly described below.

Protease Sensitivity Assays

Kinase substrates can become resistant to the actions of proteases due to phosphorylation. Thus, fluorescence quench assays for proteases can be used to measure kinase activity. With kinase assays, the formation of phosphopeptide inhibits the protease action on the peptide and the signal remains quenched and, therefore, lower when the kinase is active (19). Inhibiting the kinase results in an increase in protease sensitivity and an increase in signal.

Luciferase-based Kinase Assays

Because kinases convert ATP into ADP, the activity of purified kinase enzymes can be measured in a "coupled" assay, which detects the ATP depletion over time by using the phosphorescence of luciferase and luciferin (commercially sold as "Kinase-Glo^{TM}", www.promega.com; 13, 20). Luciferases are enzymes that produce light by utilizing the high energy bonds of ATP to convert luciferin to oxyluciferin. Oxygen is consumed in the process, as follows:

- luciferin + ATP → luciferyl adenylate + PPi
- luciferyl adenylate + O_2 → oxyluciferin + AMP + light

The reaction is very energy efficient: nearly all of the energy input into the reaction is transformed into light. A reduction in ATP results in a reduction in the production of photons. This type of assay has the advantage of not

needing any specialized antibodies and is applicable to all kinases. It is also easy to run the assays with high ATP concentrations as a way of selecting against ATP-competitive inhibitors (21).

A potential limitation of this assay is that it is a "signal decrease assay." In signal decrease assays, the enzyme-mediated reaction proceeds with a decrease in signal over time. As the kinase depletes the ATP over time, less light is produced by the luciferase reaction. An inhibitor compound prevents this decrease. A 50% consumption of ATP is required to obtain a two-fold signal-to-background using the 100% inhibited reaction as a control. Therefore, these assays must be run under conditions of relatively high turnover, which has the effect of slightly weakening the apparent potency of compounds (22). Another consequence of a signal decrease assay is that it can have low sensitivity for particularly low turnover enzymes (i.e., having a small k_{cat}). For slower enzymes, one may require a long incubation time (several hours) to reach a suitable signal. With other assay formats that measure phosphopeptide formation, (especially TR-FRET, AlphaScreen), only a 2-10% conversion is required before the assay can be read, since the detecting reagents are product-specific.

Kinase assays that are coupled to luciferase have the disadvantage of being sensitive to luciferase inhibitors, which bind to the ATP-binding site of luciferase, resulting in false negatives. A kinase inhibitor which also inhibits the luciferase would result in an artificially low light signal. However, one can overcome this by additionally using a luciferase-based assay that measures ADP formation (commercially available from Promega as "ADP-Glo™". By running Kinase-Glo™ and ADP-Glo® as orthogonal assay one can identify luciferase inhibitors as these will make the signal go down in both assays while with a true kinase inhibitor the signal would go up in an Kinase-Glo assay and down in an ADP-Glo® assay (23).

The ADP-Glo system detects the ADP formed in a kinase reaction by first adding an undisclosed commercial reagent (presumably an enzyme) to deplete the ATP in the kinase reaction and then adding another undisclosed reagent to convert the ADP back into the ATP (presumably another enzyme). Coupled systems that detect ADP gain the advantage of being able to detect product formation, rather than substrate depletion, which means that small catalytic turnover percentages can be detected.

Fluorescent Coupling

Another manifestation of coupled ADP detection is the ADP-Quest™ kit (DiscoverRx, 24). In this kit, ADP is measured by a coupled enzyme reaction with pyruvate kinase and pyruvate oxidase to convert ADP to hydrogen peroxide, which is detected using a fluorogenic substrate and horseradish peroxidase. The detection wavelength is around 590 nM, which tends to be less susceptible to inner filter effects (6).

Assay Development

Much of the cited literature in this chapter offers good protocols as a basis for kinase assay development. A general strategy for assay development should include the following steps:

1. Choose an appropriate readout technology.
2. Synthesize, purify and characterize enzymes, substrates. Generally, highly pure preparations of kinase (greater than 98% by silver-stained SDS-PAGE or by Mass-Spectrometry) are required. It is a possibility that small amounts of contaminating kinases can result in a false detection of activity from the kinase of interest. Well-characterized preparations of enzyme are critical.
3. Design a starting protocol based on prior literature or experimental information on substrate specificity. Test the protocol for enzymatic activity and use reference inhibitors when possible.
4. Gain knowledge of kinetic and thermodynamic parameters as guidelines for assay optimization (25).
5. Set-up "matrix" experiments varying pH, ionic strength, buffers and various other parameters mentioned below to optimize signal to background ratios (Table 2.)
6. Choose volumes appropriate for HTS workstations or automated systems.

7. Test a screening protocol in a pilot study and determine assay quality based on the coefficient of variations across the assay wells, the Z' measurements (26) and dynamic range towards various control or reference compounds.

Considerations of Mechanism

Mechanism of Action of Kinase Inhibitors

When designing protein kinase assays it is important first to consider the desired mechanism of action (MOA) of the inhibitor MOA is quite a complex topic which is nevertheless well described in terms of drug discovery strategies by David Swinney (27); examples are given of drugs that work by a variety of mechanisms and fall into three basic categories: 1) competition with the substrate or ligand in an equilibrium or steady-state, 2) inhibiting at a site distinct from substrate binding or 3) inhibiting in a non-mass action equilibrium. (See Assay Guidance Manual section on mechanism of action).

A good overview of the mechanism of action of protein kinase inhibitors has been presented by Vogel and Zhong (28). Protein tyrosine kinase inhibitors can act by binding directly in the ATP binding site competitively, (type I inhibitors), but these tend to be less specific because of the shared characteristics of the ATP binding pocket among various kinases. More specificity can be attained with the type II inhibitors, which can extend into an allosteric site next to the ATP pocket and which is only available in the inactive (non-phosphorylated form) of the enzymes. Imatinib is an example of this, with a 200-fold increased potency to the inactive form of the enzyme, observed in cell based assays versus enzyme assays. Often, these inhibitors bind with a slower off-rate and on-rate due to a requirement for conformational changes.

Type III inhibitors bind to sites distal to the ATP binding site and are often inactive in simple kinase enzyme assays. This apparent inactivity is because these compounds can bind to the kinase and render it a poor substrate for an activating upstream kinase, thus disabling its activation. As a consequence, a "cascade assay" or a cell-based assay might be required.

Applying Mechanistic Principles to Assay Design

Important questions related to the desired inhibitor or agonist mechanism such as whether, in the HTS, one desires to find allosteric, competitive, slow-binding inhibitors, or inhibitors of an active or inactive form of the enzyme should be considered when designing HTS assays. These mechanisms might suggest the appropriate incubation times, substrate design and concentrations, order of addition and the appropriate recombinant construct to use. Unfortunately, the decisions of assay set up are not always straightforward. There are advantages to each type of inhibitor and it also depends largely upon the biology of the disease that is going to be treated. For example, purely ATP site competitive inhibitors might have advantages with respect to drug resistance, but disadvantages with respect to selectivity, potency and cellular activity. Small molecule inhibitors that compete with the peptide binding site are generally difficult to find since the peptide-enzyme interaction presents a large surface area. Allosteric site inhibitors might have an advantage in potency and selectivity, but also may be resistance-prone. Layered on top of this complexity is the difficulty in expressing a well-defined form of the enzyme target that is physiologically relevant.

One important consideration for assay design is that a pre-incubation step of compound with the target enzyme can be included before starting the reaction. This pre-incubation can help to favor the identification of slow, tight binding inhibitors (29), depending on the stage of the enzyme progress reaction at which the assay is stopped. The longer the reaction progress time the lower the effect of the pre-incubation step on the detection of slow-binding inhibitors. This step may add significant time to a screening protocol (pre-incubation of 15-30 minutes) and also may be difficult if the enzyme preparation is unstable. It is sometimes necessary to pre-incubate the kinase enzyme with ATP to activate it through autophosphorylation. This can be accomplished in the "stock"

solution of enzyme, at stoichiometric amounts of ATP, before diluting the enzyme (and thus the ATP) into the assay. With protein kinase hit lists, it is possible to distinguish the ATP-competitive from the non-competitive inhibitors by re-screening under high and low ATP concentrations, and looking for shifts in the IC_{50} or percent inhibition. An ATP-dependent shift in compound potency suggests competition with ATP site according to the equation, (30)

$$IC50 = \left(1 + \frac{S}{Km}\right)(Ki)$$

When working with purified enzymes, it can be useful to perform a close examination of their phosphorylation state and molecular masses. Mass spectrometry is often useful for this purpose. Post-translational modifications or sequence truncations can potentially alter the compound binding sites available and can also change the structure of potential inhibitory sites. For example, with protein kinases, phosphorylations distal from the ATP binding site can inactivate the kinase whereas phosphorylations near the ATP binding site can activate the catalytic activity. Often, practice does not permit control of such situations because the purified systems are often mixtures and cannot be controlled in the commonly used recombinant expression technologies.

To favor the identification of uncompetitive or non-competitive inhibitors, one should run the assays with concentrations of substrates at least 10-fold higher than K_m. To favor competitive inhibitors, one should run the assay at or below the K_m values for the substrates. A balanced condition which provides for detection of all mechanisms is to keep the [S] = K_m (31). Thus, for making suitable conclusions for assay design, knowledge of the kinetic and binding constants of receptors and enzymes, such as K_d, k_{cat} ,K_m, B_{max} , is useful. Stoichiometric information, such as the number of enzyme molecules per assay, is also very useful since these can be used as guidelines to ensure that the assays are maximally sensitive to compounds with the desired mechanism of action. Problems in assay development often occur when the conditions required for sensitivity to the desired mechanism of action do not yield the best conditions for statistical reproducibility; therefore, compromises and balances between these two opposing factors must be often made.

The percent substrate consumption at which time the data is collected is also of importance in enzyme assay design. Typically, enzymologists like to ensure the steady-state conditions are maintained in the study of inhibitor constants such as K_i or IC_{50}. However, many assay technologies, combined with the requirements for a robust signal to background giving a good Z′ factor (26), necessitate assay set-up where more turnover is required. This typically causes a trend toward the reduction of compound potency depending on the mechanism of action. Therefore, one must balance the need to have the most sensitive assay toward inhibition by low MW compounds with the need for sufficient signal-to-noise and signal-to-background to have statistically relevant results, for example with a coefficient of variation less than 10% around the positive and negative controls, a 5-fold difference between the positive control signal and negative control signal and/or Z' greater than 0.5. These types of effects have been modeled by Wu and Yuan (22) and additionally confirmed by empirical determination. These investigators have found that 50% inhibition at low conversion (near zero) can translate into 31% inhibition if the assay is run at 80% conversion. IC_{50} values can shift as much as three fold.

Assay Optimization

It is very difficult to give specific guidelines for assay optimization in HTS due to the complexity of variables involved and because one often must balance cost, speed, sensitivity, statistical robustness, automation requirements and desired mechanism. The assay development and optimization process can be thought of as a cycle in which several variables can be tested and the parameters that give a better "reading window" can be fixed, after which further parameters can be tested under the prior fixed conditions (see Table 2). Often, one observes interactions between the various parameters. For example, the optimal detergent concentration to use may not be the same for every pH and that is why the same fixed parameters must sometimes be retested under any newly-identified optimal parameters. Furthermore, the type of optimization experiments depends upon the

particular technology being used. A very important aspect of optimization is to improve the reproducibility and statistical performance of the assay, by finding conditions that increase the signal-to-noise ratio with respect to positive and negative controls, and to decrease the inter-well variations that occur due to such factors as pipetting errors and temperature gradients across the microtiter plate. In general, coefficient of variations of less than 10% and Z values greater than 0.5 are desirable.

In its simplest form, building an assay is a matter of adding several reagent solutions to a microtiter plate (MTP) with a multi-channel pipette, with various incubation times, stopping the reaction if required, and reading the MTP in a plate reader. A typical procedure might involve the following steps: 1) adding the enzyme solution to a compound-containing microtiter plate and incubating for 15 minutes; 2) adding substrates and incubating for 15 minutes to 1 hour; 3) adding a stopping reagent such as EDTA; 4) adding sensor or detector reagents, such as labeled antibodies or coupling enzymes; 5) measuring in a plate reader. The particular detector reagents to use, the assay reagent volumes, the concentrations of reagents, the incubation times, the buffer conditions (Table 2), the MTP types and the assay stopping reagents are all important parameters which need to be tested in order to obtain the very high level of reproducibility yet maintain the physiological and thermodynamic conditions to find a lead compound with the desired mechanism of action.

A very important aspect of assay development is making an appropriate choice of substrates. When possible, one should consider using a relatively physiological substrate. This means for example, using the substrate protein involved in the pathway of interest for serine-threonine kinases, rather than commonly used general substrates like maltose binding protein or, for example using a true-substrate-derived peptide sequence representing the phosphotyrosine site within the amino acid context that is found in the native substrate primary sequence, rather than an artificial substrate such as poly-Glu-Tyr. Once again this is not always practical because the natural substrates are either not well-characterized, and the artificial substrates often give a much higher turnover (k_{cat}) and thus can yield a much more robust assay signal. If natural substrates are not readily available or robust, secondary assays can be designed using the natural substrates, to ensure the screening hits work equivalently under physiologic conditions. Additionally, it is often possible to perform a substrate screen where many random peptide sequences are tested to identify good substrates.

The danger of using solely statistical parameters (such as Z') in assay optimization is that these do not take into account the desired physiological or biochemical mechanism of action in determining the optimal reagent concentration. For example, the optimal substrate concentration to use in an enzyme assay may not necessarily be the one that gives the best statistics with respect to reproducibility. The optimal salt concentration required for reproducibility may be far different from physiological conditions. Therefore, one must be careful to use statistical performance in a way that is consistent with the desired mechanism of action of the lead compound.

Enzyme Preparations

One cannot over-emphasize the importance of the enzyme preparation in the ability to develop a kinase assay. First, purity is important because even the slightest contamination with another enzyme can lead one to screen with a measurement of the wrong activity. Specific reference inhibitors can be used to establish that the observed catalytic activity is the correct one. Of course, when working with novel targets, such reference inhibitors may not exist. With recombinant expression systems one can generate catalytically inactive mutations to establish that the host cell is not the source of a contaminating phosphatase or kinase. In the end, however, the key requirement is to have an extremely pure and highly active enzyme preparation. If most of the enzyme molecules are inactive or if the enzyme molecules have a very low catalytic efficiency (k_{cat}/K_m), then one will need to have a high concentration of enzyme in the assay to obtain a good signal; this can limit the ability to distinguish between weaker and stronger inhibitors. If one needs to have a 100 nM enzyme concentration in the reaction, then inhibitors with a K_i of 10 nM cannot be distinguished from those with a K_i of 50 nM in a steady-state IC_{50} experiment.

Assay Volumes

Assay volumes usually range from 3 µL (for 1536-well MTPs) to 50 µL (384-well MTPs). Within a given total assay volume, smaller volumes of reagents are added. Frequently it is convenient to add reagents into the assay in equivalent volumes of assay buffer. As an example, for a 15 µL assay, one might add 5 µL of compound solution, 5 µL of enzyme solution, and 5 µL of substrate mix, followed by 10 µL of quench solution in a "stop" buffer. For kinase assays, this can be EDTA, which works by chelating magnesium, an essential cofactor for protein kinase catalysis. The advantages of using equal volumes are that it keeps the volumes at a level that is best for the particular pipette during automation; it minimizes the requirement for various specialized instruments and helps in the mixing of the reagents. The disadvantage of this method is that it introduces transient changes in the final concentration of reagents during the times between the various additions. In addition, enzymes are not always stable in large batches of dilute buffer required for HTS. Therefore, it can be preferred to add a low volume of a more concentrated stock solution (10X - 50X) into a higher volume of assay buffer in the well. This step often requires a liquid dispenser able to handle very low volumes of sub-microliter liquid.

Assay miniaturization helps to reduce the consumption of assay reagents, which can be very expensive. The problems encountered as one attempts to miniaturize an assay are in the change in surface to volume ratio, the lowered sensitivity and in the low volume dispensing of materials. For instance, as one moves to smaller volumes, the surfaces available for nonspecific binding increase relative to the volume. Furthermore, the smaller the volume, the less the amount of product-sensing material can be added; thus the sensitivity of the assay is reduced.

Plate Types

Generally, white plates are preferred for phosphorescent assays, such as those employing luciferase because they reflect emitted photons. Black plates are preferred for fluorescent assays because they reduce reflection. Transparent plates are generally used for imaging assays. Polystyrene is the material of choice because it can be molded reproducibly such that the plates are consistently-sized to fit into automated systems. Polystyrene tends to have some level of non-specific affinity for biomolecular reagents and, therefore, some manufacturers produce proprietary low binding plates. Polypropylene plates have low non-specific binding levels, but are more difficult to shape consistently. However, these plates are often useful as "source plates" for reagents due to their tolerance to freezing and their low level of "stickiness." The use of 96-, low volume 96-, 384-, low volume 384-, or 1536-well depends on the assay volume and throughput that one needs. For 96-well plates, volumes range from 80-100 µl; for 384-well plates, volumes range from 15 to 100 µl; for 384-well, small-volume plates, volumes range from 4 to 10 µl; and for 1536-well MTPs, volumes range from 3 to 8 µl.

Incubation Times

Incubation times at different steps depend upon the binding kinetics or enzyme kinetics and can range anywhere from 10 minutes to 15 hours. It is generally preferred to read the reaction at a point before the reactants are depleted and the enzyme progress curve is slowing. Adding a short pre-incubation step of compound with enzyme before the initiation of the reaction allows for detection of slow-binding inhibitors, which require a conformational change of the enzyme to form a tight complex. Longer incubation steps can add significant amounts of plate processing time in HTS automation because incubation time often represents the rate-limiting step in the HTS process. Reaction rates can be increased by increasing the enzyme concentration or temperature and, in this fashion, incubation times can be reduced.

Buffers and Solvents

The concentrations of detergents, buffers, carrier proteins, reducing agents, and divalent cations can affect the specific signal and the apparent potency of compounds in concentration response curves (32). In principle, it is

good to stay as close to physiological conditions as possible, but for practical reasons, there are many exceptions. For example, full-length fully regulated kinases are often impossible to express, and thus, for practical purposes non-regulated kinase domains are used in screening. Furthermore, the true physiological conditions in the microcellular environment are not always known. Sometimes carrier proteins are required for enzyme stability and to reduce nonspecific binding to reaction vessels. It is often necessary to provide additives such as protease inhibitors to prevent digestion of the assay components or phosphatase inhibitors such as vanadate to keep the product of a kinase assay intact and protected from contaminating phosphatases. Also, it is often necessary to quench assays or to add a stop reagent such as EDTA at the end of the reaction and before reading in a plate reader. A quench step or stop step is especially important when the automated HTS system does not allow for precise timing or scheduling of the assay protocol. A very good summary of solvent and buffer conditions used in kinase assay optimization is described by von Ahsen and Bomer (33).

The presence of "promiscuous" inhibitors or "aggregating" compounds in a chemical library has become a recent area of research. These compounds can cause false positives that can be reduced with certain detergents and can frequently be recognized by steep concentration response curves or by enzyme concentration-dependent shifts in the IC_{50} (34, 35). The exact mechanism of these false positives is not known but it is possible that these compounds induce the formation of compound-enzyme clusters, which reduce enzyme activity. Thus, it is important to have some non-denaturing detergent present in enzyme assays and to re-test hits in orthogonal assays to reduce the possibility of identifying promiscuous inhibitors in the HTS.

DMSO Concentration

In most cases, the test compounds are dissolved in DMSO and are added from a source plate into the assay. Thus, the tolerance of the assay for DMSO should be tested, by looking at the activity at various increasing concentrations of DMSO. Generally, enzymatic or biomolecular binding assays are more tolerant of high DMSO concentrations (often up to 5 - 10% DMSO). Cell based assays usually can tolerate up to 0.5% DMSO.

Detector Reagent Concentrations

Given the very large variety of assay detection methods, it is difficult to cover all the parameters needed to optimize for each detection system; however, it is important to mention that these various systems discussed in the assays readout technology section above all need to be optimized. For example, when using an antibody pair in a TR-FRET assay, it is important to find a concentration of antibodies that can trap the product efficiently at the desired time point in the reaction. In SPA, for example, an optimal SPA bead concentration should be determined empirically. In principle, the detector reagents should be present in high enough concentration to capture the analyte stoichiometrically. Having too high a concentration of detectors can be wasteful and expensive and can create higher background signals and having too low concentrations of detector reagents can compromise the dynamic range and sensitivity of the assay. A control product can sometimes be useful as a calibration standard for these types of optimization experiments. Often times, the commercial assay kit providers provide excellent protocols in optimizing the use of the detector reagents.

Pilot Screens

The final step in the assay development process is to run a "pilot" screen, where a small subset of libraries are screened to observe the hit rate, the distribution of the high signal and the low signal, typically employing the Z and Z-prime principle of Zhang and Chung (26) to assess quality. The Z factors combine the principle of signal to background ratio, coefficient of variation of the background and the coefficient of variation of the high signal into a single parameter, which gives one a general idea of the screening quality. One should be careful to closely examine the raw data and data trends from screening rather than to rely only on the Z-factor for quality control.

For pilot studies, the microtiter plates should be arrayed with reference compounds at various concentrations, to control that the screening procedure gives adequate dynamic range and sensitivity to inhibitors or activators. In general, coefficient of variations of less than 10% and Z values greater than 0.5 are desirable. The pilot studies may be used to adjust the compound concentration to obtain a reasonable hit rate; for example, one hit for every two thousand compounds tested. The hit rate will depend on the particular library screened; biased libraries may have higher hit rates than random libraries.

Acknowledgements

The author would like to acknowledge Dr. Douglas Auld for his valuable insights and comments on the draft, and Dr's Andrew Napper, Jeff Weidner and Sittampalam Gurusingham for critical review and editing.

References

1. Lowery RG, Vogel K, Till J. ADP detection technologies. Assay Drug Dev Technol. 2010 2010 Aug;8(4):1–2author reply 1. PubMed PMID: 20804418.
2. Goueli S., Zegzouti H., Vidugiriene J. Response to the Letter of Lowery et al. ADP Detection Technologies. Assay Drug Dev.Technol. 2010;8(4):1.
3. Inglese J, Napper A, Auld D. Improving success by balanced critical evaluations of assay methods. Assay Drug Dev Technol. 2010 Aug;8(4):1. PubMed PMID: 20804419.
4. Gopalakrishna R, Chen ZH, Gundimeda U, Wilson JC, Anderson WB. Rapid filtration assays for protein kinase C activity and phorbol ester binding using multiwell plates with fitted filtration discs. Anal BiochemOct. 1992;206(1):24–35. PubMed PMID: 1456438.
5. Glickman J. F., Ferrand S. Scintillation Proximity Assays In High Throughput Screening. Assay Drug Dev.Technol. 2008.:6. PubMed PMID: 18593378.
6. Palmier MO, Van Doren SR. Rapid determination of enzyme kinetics from fluorescence: overcoming the inner filter effect. (2007). Anal Biochem. 2007 Dec 1;371(1):43–51. Epub 2007 Jul 18. PubMed PMID: 17706587.
7. Vedvik K. L., Eliason H. C., Hoffman R. L., Gibson J. R., Kupcho K. R., Somberg R. L., Vogel K. W. Overcoming compound interference in fluorescence polarization-based kinase assays using far-red tracers. Assay.Drug Dev.Technol. 2004;2(no. 2):193–203. PubMed PMID: 15165515.
8. Simeonov A, Jadhav A, Thomas CJ, et al. Fluorescence spectroscopic profiling of compound libraries. J Med Chem. 2008;51:2363–2371. PubMed PMID: 18363325.
9. Newman M., Josiah S. Utilization of fluorescence polarization and time resolved fluorescence resonance energy transfer assay formats for SAR studies: Src kinase as a model system. J.Biomol.Screen. 2004;9(no. 6):525–532. PubMed PMID: 15452339.
10. Turek-Etienne T. C., Kober T. P., Stafford J. M., Bryant R. W. Development of a fluorescence polarization AKT serine/threonine kinase assay using an immobilized metal ion affinity-based technology. Assay.Drug Dev.Technol. 2003;1(no. 4):545–553. PubMed PMID: 15090251.
11. Turek-Etienne Tammy C., Small Eliza C., Soh Sharon C., Xin Tianpei A., Gaitonde Priti V., Barrabee Ellen B., Hart Richard F., Bryant Robert W. Evaluation of fluorescent compound interference in 4 fluorescence polarization assays: 2 kinases, 1 protease, and 1 phosphatase. J.Biomol.Screening. 2003;8(no. 2):176–184. PubMed PMID: 12844438.
12. Moshinsky D. J., Ruslim L., Blake R. A., Tang F. A widely applicable, high-throughput TR-FRET assay for the measurement of kinase autophosphorylation: VEGFR-2 as a prototype. J.Biomol.Screen. 2003;8(no. 4):447–452. PubMed PMID: 14567797.
13. Schroter T., Minond D., Weiser A., Dao C., Habel J., Spicer T., Chase P., Baillargeon P., Scampavia L., Schurer S., Chung C., Mader C., Southern M., Tsinoremas N., LoGrasso P., Hodder P. Comparison of miniaturized time-resolved fluorescence resonance energy transfer and enzyme-coupled luciferase high-

throughput screening assays to discover inhibitors of Rho-kinase II (ROCK-II). J.Biomol.Screen. 2008;13(no. 1):17–28. PubMed PMID: 18227223.
14. Vogel K. W., Vedvik K. L. Improving lanthanide-based resonance energy transfer detection by increasing donor-acceptor distances. J.Biomol.Screen. 2006;11(no. 4):439–443. PubMed PMID: 16751339.
15. Glickman J. F., Wu X., Mercuri R., Illy C., Bowen B. R., He Y., Sills M. A comparison of ALPHAScreen, TR-FRET, and TRF as assay methods for FXR nuclear receptors. J.Biomol.Screen. 2002;7(no. 1):3–10. PubMed PMID: 11897050.
16. Ullman E. F., Kirakossian H., Singh S., Wu Z. P., Irvin B. R., Pease J. S., Switchenko A. C., Irvine J. D., Dafforn A., Skold C. N. Luminescent oxygen channeling immunoassay: measurement of particle binding kinetics by chemiluminescence. Proc.Natl.Acad.Sci.U.S.A. 1994;91(no. 12):5426–5430. and. PubMed PMID: 8202502.
17. Von Leoprechting A., Kumpf R., Menzel S., Reulle D., Griebel R., Valler M. J., Buttner F. H. Miniaturization and validation of a high-throughput serine kinase assay using the AlphaScreen platform. J.Biomol.Screen. 2004;9(no. 8):719–725. PubMed PMID: 15634799.
18. Warner G., Illy C., Pedro L., Roby P., Bosse R. AlphaScreen kinase HTS platforms. Curr.Med.Chem. 2004;11(no. 6):721–730. PubMed PMID: 15032726.
19. Rodems, S. M., B. D. Hamman, C. Lin, J. Zhao, S. Shah, D. Heidary, L. Makings, J. H. Stack, and B. A. Pollok. 2002. A FRET-based assay platform for ultra-high density drug screening of protein kinases and phosphatases. *Assay.Drug Dev.Technol.* 1, no. 1 Pt 1:9-19.
20. Koresawa M., Okabe T. High-throughput screening with quantitation of ATP consumption: a universal non-radioisotope, homogeneous assay for protein kinase. Assay.Drug Dev.Technol. 2004;2(no. 2):153–160. PubMed PMID: 15165511.
21. Kashem M. A., Nelson R. M., Yingling J. D., Pullen S. S., Prokopowicz A. S. III, Jones J. W., Wolak J. P., Rogers G. R., Morelock M. M., Snow R. J., Homon C. A., Jakes S. Three mechanistically distinct kinase assays compared: Measurement of intrinsic ATPase activity identified the most comprehensive set of ITK inhibitors. J.Biomol.Screen. 2007;12(no. 1):70–83. PubMed PMID: 17166826.
22. Wu Ge, Yuan Yue, Nicholas Hodge C. Determining appropriate substrate conversion for enzymatic assays in high-throughput screening. J.Biomol.Screening. 2003;8(no. 6):694–700. PubMed PMID: 14711395.
23. Tanega C, Shen M, Mott BT, et al. Comparison of bioluminescent kinase assays using substrate depletion and product formation. Assay Drug Dev Technol. 2009;7:606–614. PubMed PMID: 20059377.
24. Charter NW, Kauffman L, Singh R, Eglen RM. A Generic, Homogenous Method for Measuring Kinase and Inhibitor Activity via Adenosine 5'-Diphosphate Accumulation. J. Biomol Screen. 2006;11(4):390–399. PubMed PMID: 16751335.
25. Pedro L, Padrós J, Beaudet L, Schubert HD, Gillardon F, Dahan S. Development of a high-throughput AlphaScreen assay measuring full-length LRRK2(G2019S) kinase activity using moesin protein substrate. Anal Biochem. 2010 Sep 1;404(1):45–51. Epub 2010 Apr 29. PubMed PMID: 20434426.
26. Zhang J. H., Chung T. D., Oldenburg K. R. A Simple Statistical Parameter for Use in Evaluation and Validation of High Throughput Screening Assays. J.Biomol.Screen. 1999;4(no. 2):67–73. PubMed PMID: 10838414.
27. Swinney D. C. Biochemical mechanisms of drug action: what does it take for success? Nat.Rev.Drug Discov. 2004;3(no. 9):801–808. PubMed PMID: 15340390.
28. Vogel Kurt W., Zhong Zhong, Bi Kun, Pollok Brian A. Developing assays for kinase drug discovery - where have the advances come from? Expert Opin.Drug Discovery. 2008;3(no. 1):115–129. PubMed PMID: 23480143.
29. Glickman J. F., Schmid A. Farnesyl pyrophosphate synthase: real-time kinetics and inhibition by nitrogen-containing bisphosphonates in a scintillation assay. Assay.Drug Dev.Technol. 2007;5(no. 2):205–214. PubMed PMID: 17477829.
30. Segal, I, 1975. Enzyme Kinetics: Behavior and analysis of rapid equilibrium and steady-state Enzyme systems. New York, Wiley and Sons, p106.

31. Yang J, Copeland RA, Lai Z. Defining balanced conditions for inhibitor screening assays that target bisubstrate enzymes. J Biomol Screen. 2009;14:111–120. PubMed PMID: 19196704.
32. Schröter A, Tränkle C, Mohr K. Modes of allosteric interactions with free and [^{3}H]N-methylscopolamine-occupied muscarinic M2 receptors as deduced from buffer-dependent potency shifts. Naunyn Schmiedebergs Arch Pharmacol. 2000 Dec;362(6):512–9. PubMed PMID: 11138843.
33. Von Ahsen Oliver, Boemer Ulf. High-throughput screening for kinase inhibitors. ChemBioChem. 2005;6(no. 3):481–490. PubMed PMID: 15742384.
34. Feng B. Y., Shoichet B. K. A detergent-based assay for the detection of promiscuous inhibitors. Nat.Protoc. 2006;1(no. 2):550–553. PubMed PMID: 17191086.
35. Shoichet B. K. Interpreting steep dose-response curves in early inhibitor discovery. J.Med.Chem. 2006;49(no. 25):7274–7277. PubMed PMID: 17149857.

Additional References:

Daub H., Specht K., Ullrich A. Strategies to overcome resistance to targeted protein kinase inhibitors. Nat.Rev.Drug Discov. 2004;3(no. 12):1001–1010. PubMed PMID: 15573099.

Johnston P. A., Foster C. A., Shun T. Y., Skoko J. J., Shinde S., Wipf P., Lazo J. S. Development and implementation of a 384-well homogeneous fluorescence intensity high-throughput screening assay to identify mitogen-activated protein kinase phosphatase-1 dual-specificity protein phosphatase inhibitors. Assay.Drug Dev.Technol. 2007;5(no. 3):319–332. PubMed PMID: 17638532.

Lakowicz, J. R. 2006. *Principles of Fluorescence Spectroscopy*. 3rd ed. Berlin: Springer.

Lawrence David S., Wang Qunzhao. Seeing is believing: peptide-based fluorescent sensors of protein tyrosine kinase activity. ChemBioChem. 2007;8(no. 4):373–378. PubMed PMID: 17243187.

Olive D. M. Quantitative methods for the analysis of protein phosphorylation in drug development. Expert.Rev.Proteomics. 2004;1(no. 3):327–341. PubMed PMID: 15966829.

Parker Gregory J., Law Tong Lin, Lenoch Francis J., Bolger Randall E. Development of high throughput screening assays using fluorescence polarization: nuclear receptor-ligand-binding and kinase/phosphatase assays. J.Biomol.Screening. 2000;5(no. 2):77–88. PubMed PMID: 10803607.

Zegzouti H, Zdanovskaia M, Hsiao K, Goueli SA.2009. ADP-Glo: A Bioluminescent and homogeneous ADP monitoring assay for kinases. *Assay Drug Dev Technol.* Dec;7(6):560-72. PubMed PMID: 20105026.

Receptor Binding Assays for HTS and Drug Discovery

Douglas S Auld,[1] Mark W. Farmen,[2] Steven D. Kahl,[3,*] Aidas Kriauciunas,[2] Kevin L. McKnight,[4] Chahrzad Montrose,[3] and Jeffrey R. Weidner[†]

Created: May 1, 2012; Updated: July 1, 2018.

Abstract

Receptor binding assay formats for HTS and lead optimization applications are discussed in detail in this chapter. Critical considerations that are discussed include appropriate selection of detection technologies, instrumentation, assay reagents, reaction conditions, and basic concepts in receptor binding analysis as applied to assay development. Sections on special circumstances that address high affinity binders and Hill slope variations are also included and may be useful for data analysis and trouble shooting. A discussion on Scintillation Proximity (SPA), filtration binding and Fluorescence Polarization (FP) assays for receptor binding analysis are also included with detailed accounts on assay development using these technologies.

Introduction

There are two typical assay formats used for analysis of receptor-ligand interactions in screening applications, filtration and scintillation proximity assay (SPA). Both formats utilize a radiolabeled ligand and a source of receptor (membranes, soluble/purified). Receptor binding assays using non-radioactive formats (fluorescence polarization, time-resolved fluorescence, etc.) which are continually being investigated for feasibility, would have similar assay development schemes to those presented in this document.

Selection of the detection method to be used (SPA, filtration, non-radioactive) is the first step to receptor binding assay development. In some cases, investigation into more than one format may be required to meet the following desired receptor binding criteria:

- Low nonspecific binding (NSB)
- > 80% specific binding at the K_d concentration of radioligand
- Less than 10% of the added radioligand should be bound (Zone A)
- Steady-state obtained and stability of signal maintained
- For competition assays, the radioligand concentration should be at or below the K_d
- No dose response in the absence of added receptor
- Reproducible
- Appropriate signal window (i.e. Z-factor > 0.4, SD window > 2 SD units)

While developing receptor binding assays, some of the experiments may need to be performed in an iterative manner to achieve full optimization. In addition preliminary experiments may be required to assess the system.

In many instances, a multi-variable experimental design can be set up to investigate the impact of several parameters simultaneously, or to determine the optimum level of a factor. It is strongly recommended that full assay optimization be performed in collaboration with an individual trained in experimental design.

Experimental design and assay variability is addressed in detail in other sections of this handbook.

Author Affiliations: 1 Novartis Institutes for Biomedical Research, Boston, MA. 2 Eli Lilly & Company, Indianapolis, IN (Deceased). 3 Eli Lilly & Company, Indianapolis, IN. 4 University of North Carolina, Chapel Hill, NC.

* Editor

† Editor

The following pages should be used as a general developmental guide to receptor binding assays using SPA or filtration formats.

Flow Chart of Steps to Assay Development for SPA Format

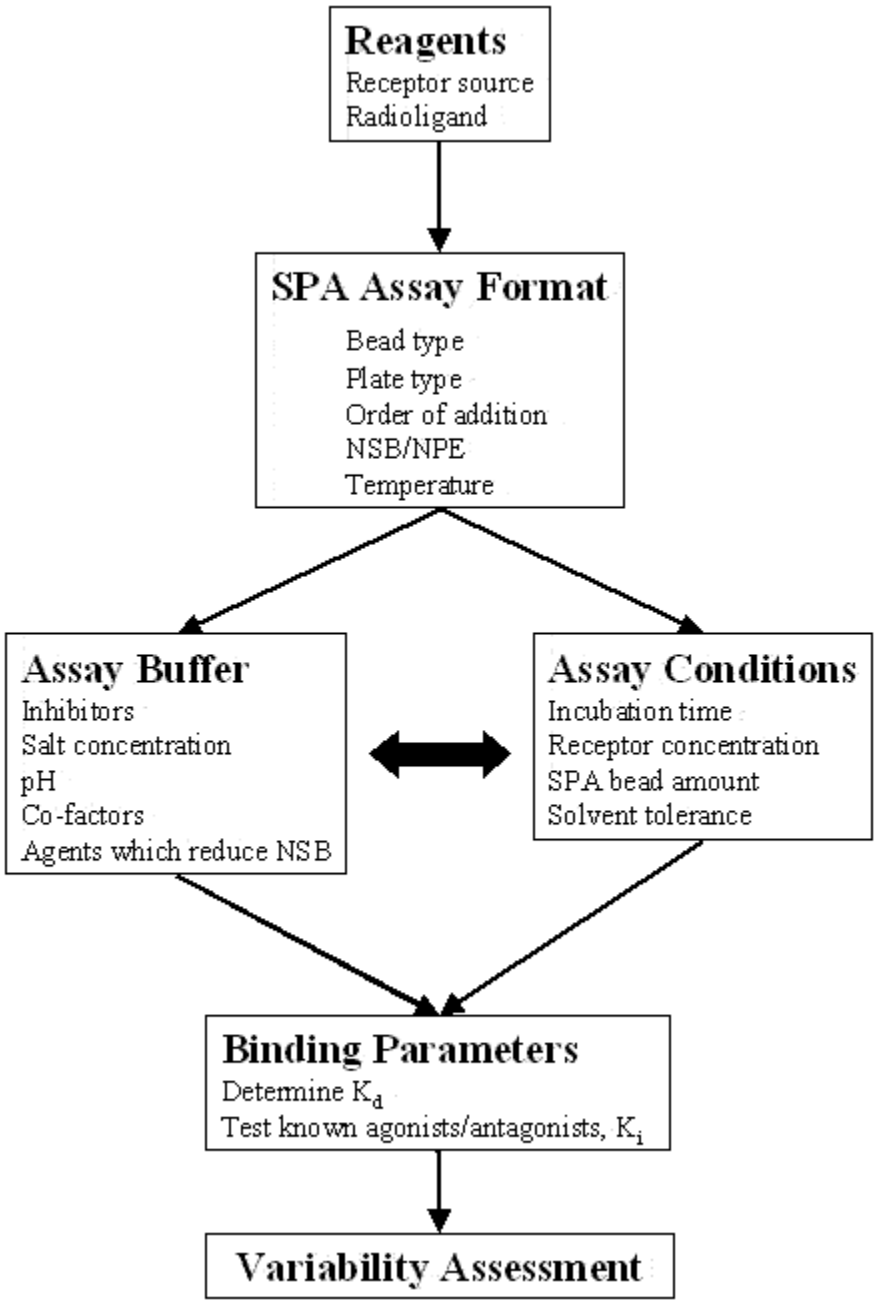

Flow Chart of Steps to Assay Development for Filter Format

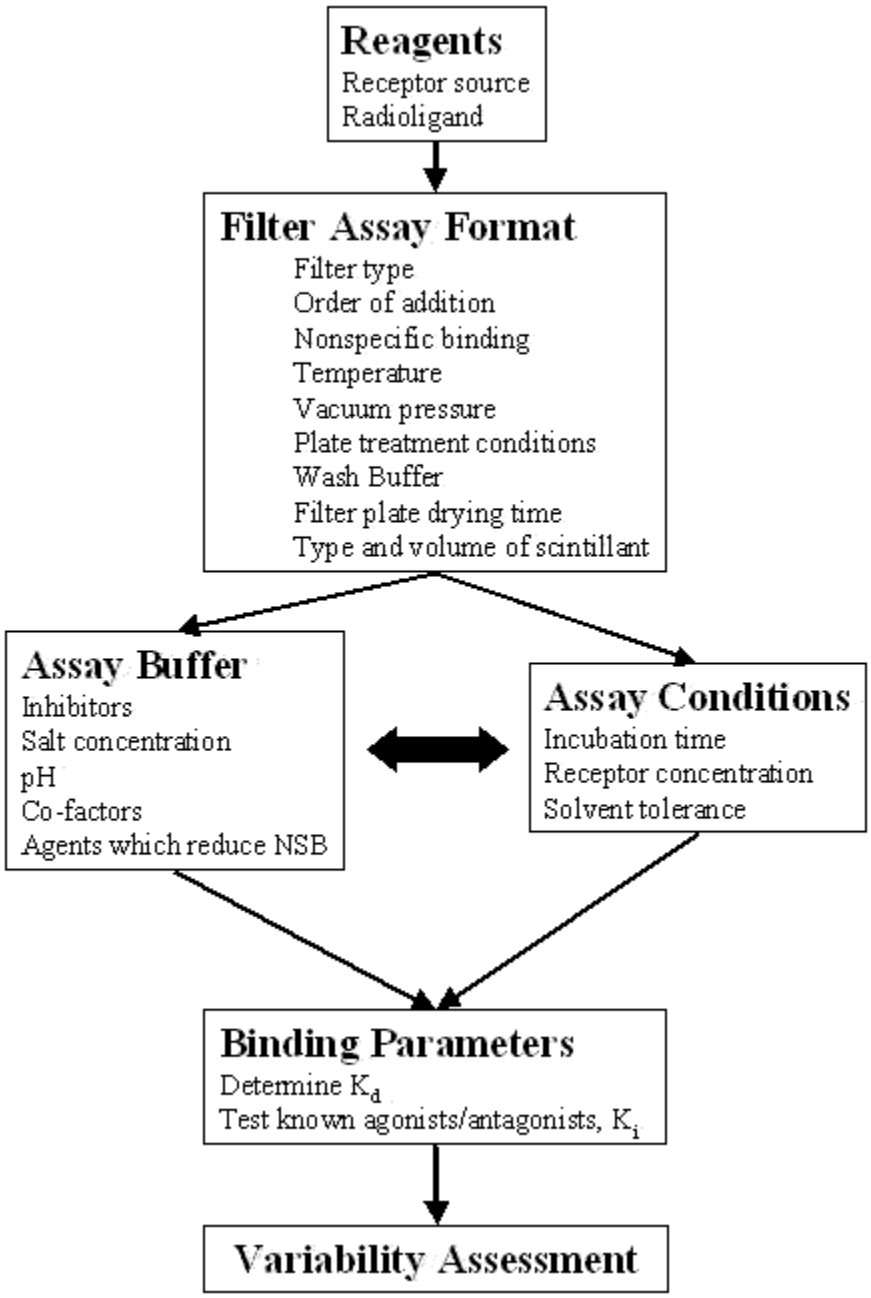

Reagents

Quality reagents are one of the most important factors involved in assay development. Validated reagents of sufficient quantity are critical for successful screen efforts over a long period of time. The primary reagents required for a radioactive receptor binding assay which are discussed on the following pages are receptors (membranes or purified) and radioligands.

Scintillation Proximity Assays (SPA)

Concept

SPA assays do not require a separation of free and bound radioligand and therefore are amenable to screening applications. A diagram for a standard receptor binding SPA is shown below for a ^{125}I radioligand (Figure 1).

General Steps for an SPA Assay:

1. Add and incubate test compound, radioligand, receptor and SPA beads in a plate (in some cases, the SPA beads are added at a later time point).
2. Count plates in microplate scintillation counter. The appropriate settling time needs to be determined experimentally.

Advantages	Disadvantages
Non-separation method No scintillation cocktail required Reduced liquid radioactive waste Reduced handling steps (add, incubate, read) Multiple bead types (WGA, PEI-coated, etc.)	More expensive - requires license Lower counting efficiency Primarily for ^{3}H and ^{125}I (^{33}P, ^{35}S possible) Non-proximity effects Quenching by colored compounds Difficult to perform kinetic experiments Bead settling effects

Many of the advantages and disadvantages are addressed in the following sections.

SPA Assay Format

The main components of an SPA receptor binding assay format include bead type, plate type, order of addition, non-specific binding (NSB)/non-proximity effects, and temperature. Each of these items are described in detail in the sections below.

Bead Type

The SPA bead surface-coupling molecule selected for use in a receptor binding assay must be able to capture the receptor of interest with minimal interaction to the radioligand itself. Table 1 lists the available SPA bead capture mechanisms that can be used with various receptor sources.

In addition to the capture mechanism, two types of SPA beads are available:

- Plastic SPA beads, made of polyvinyltoluene (PVT), act as a solid solvent for diphenylanthracine (DPA) scintillant incorporated into the bead
- A Glass SPA bead, or Yttrium silicate (YSi), uses cerium ions within a crystal lattice for the scintillation process. In general, YSi is a more efficient scintillator than PVT is, but YSi SPA beads require continuous mixing even during dispensing.

Typical experiments to investigate nonspecific binding of radioligand to SPA beads include varying the amount of radioligand (above and below the predicated K_d value) and the amount of SPA beads (0.1 mg to 1 mg) in the absence of added membrane protein. Results from this experiment can identify the proper type of SPA beads to use in future experiments, as well as the baseline background due to non-proximity effects. An example experiment using a kit from Perkin Elmer that contains several different SPA bead types (Select-a-Bead kit, #RPNQ0250) is provided in Figure 2. For this example, which was performed in the absence of added membrane receptor, the PVT-PEI WGA Type A SPA beads yields the lowest interaction with the radioligand and was used for further assay development. An increase in signal with an increasing amount of added SPA beads is normal.

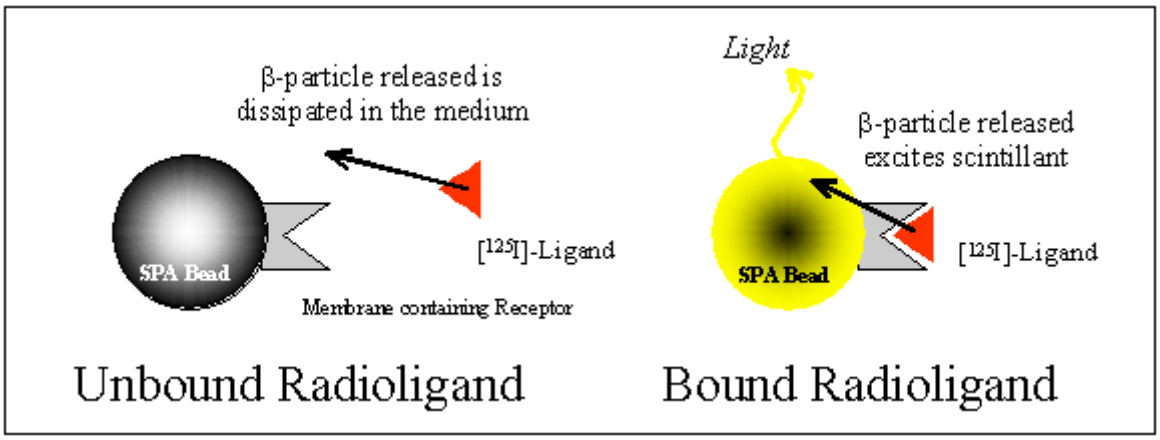

Figure 1: Diagram for standard receptor-binding SPA for ^{125}I radioligand.

Additives may be useful in decreasing high levels of nonspecific binding of radioligand to the SPA beads (see Table 2).

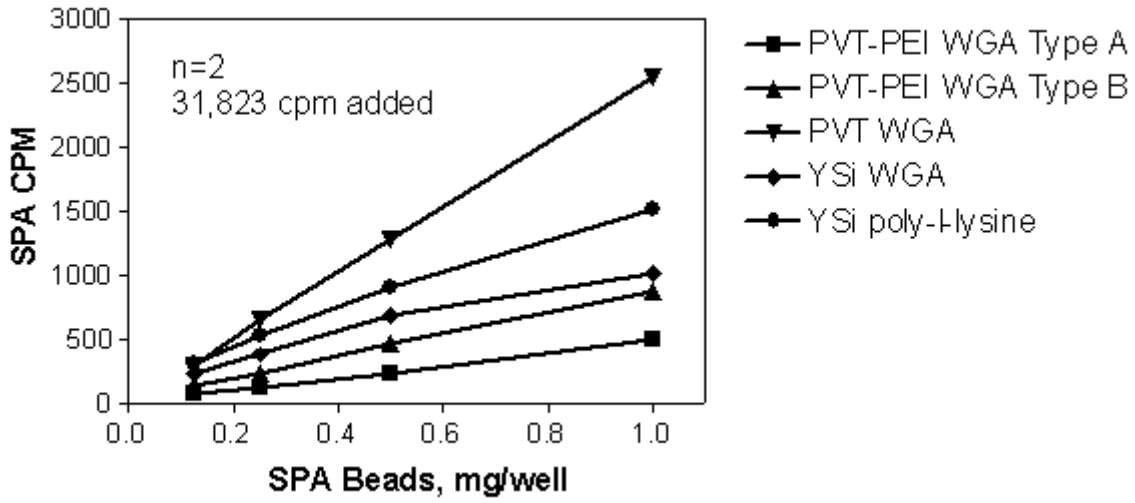

Figure 2: Example experiment using kit from Perkin Elmer containing several different SPA bead types (performed in absense of added membrane receptor).

Table 1: Available SPA bead capture mechanisms

Receptor	SPA Bead	Capture Mechanism
Membranes	WGA [1]	Glycosylation sites
	Poly-L-lysine	Negative charges
Soluble/Purified	WGA	Glycosylation sites
	Streptavidin	Biotinylated site
	Antibody [2]	Specific antibody
	Copper	His-Tag
	Glutathione	GST-fusion

[1] Wheat germ agglutinin (WGA) SPA beads are available in standard untreated format and two different versions that have been treated with polyethyleneimine (PEI).
[2] Secondary antibody SPA beads are available to capture specific antibodies from the following species: Rabbit, Sheep, mouse. Protein A SPA beads are also available for antibody capture.

Table 2: Agents which reduce NSB

BSA	0.05% - 0.3%
Ovalbumin	0.05% - 0.3%
NP-40	0.05% - 0.3%
Triton X-100	0.05% - 0.1%
Gelatin	0.05% - 0.3%
Polyethylenimine	0.01% - 0.1%
CHAPS	0.5%
Tween-20	0.05% - 0.1%
Fetal bovine serum (FBS)	up to 10%

Plate Type

The type of plate that is used for SPA receptor binding assays may be influenced by the following factors:

- Counting instrument used (Trilux, TopCount, , LeadSeeker)
- Miniaturization (96-well, 384-well)
- Binding of radioligand to plastics
- Liquid dispensing/automation equipment

Table 3 lists typical plate choices for SPA assays:

The data shown in Figure 3 demonstrates an advantage of the NBS plates when using a radioligand, which binds nonspecifically to plate plastic.

69,000 CPM of 125I-labeled ligand added to the well, incubated for 60 min. Radioactivity removed and wells washed. SPA beads then added. Data demonstrates that a radioligand sticking to the plate surface can elicit an SPA signal. NBS plate yields significantly less nonspecific binding of radioligand.

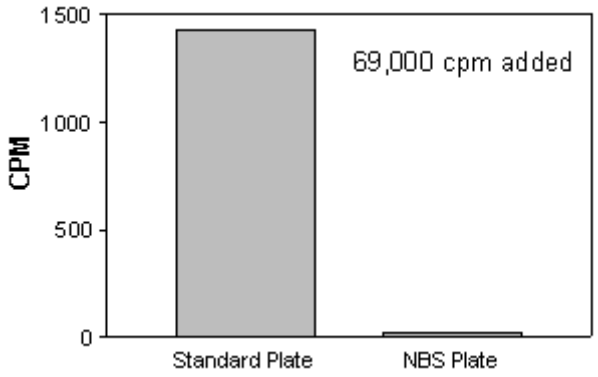

Figure 3: Advantage of NBS plate over standard plate when using radioligands that may bind nonspecifically to plastic plates.

Table 3: Typical plate choices for SPA assays

Plate Type	Instrument	of Wells	Comments
Costar #3632	Trilux	96	White/Clear-bottom, 96-well
Costar #3604	Trilux	96	White/Clear-bottom, 96-well, non-binding surface (NBS), may be useful when ligands are sticky
Perkin Elmer 401	Trilux	96	Clear/flexible, not easily amenable to automation or liquid dispensing instrumentation
Costar #3706	Trilux	384	White/Clear-bottom, 384-well
Perkin Elmer Optiplate	TopCount	96	White/solid bottom, 96-well
Perkin Elmer IsoPlate	Trilux	96	White/Clear-bottom, 96-well

Order of Addition

The order of addition for reagents may affect assay performance as well as ease of automation. Three basic formats are listed in Table 4.

Time zero or delayed additions are the most commonly used formats in HTS, with time zero addition requiring fewer manipulation steps. Experiments may be required to determine the optimum method to be used for a particular receptor to maximize signal to background levels.

In addition, the effect of DMSO on intermediate reactants should be investigated. If compounds in DMSO are added into the wells first (most common method for screening efforts), other reagents added (i.e. radioligand, membranes, beads, etc.) may be affected by the concentration of DMSO, or if the time before reaching the final reaction mixture becomes significant.

Table 4: Basic formats for order of addition for reagents.

Method	Advantage
Membrane precoupled to SPA bead Time zero (T=0) addition of SPA beads Delayed addition of SPA beads	May aid in lowering NSB Easily automated Optimum ligand/receptor interaction possible

Non-Specific Binding (NSB)/Non-proximity Effects (NPE)

In order to obtain the maximum signal to noise ratio possible for SPA receptor binding assays, it is important to understand the two different types of signals associated with the radioligand and SPA beads, which may contribute to the total assay background levels.

Non-Specific Binding (NSB) to SPA Beads

The NSB signal is attributed to the radiolabel which may adhere to the SPA beads themselves and not through a specific interaction with the receptor attached to the SPA bead (Figure 4, left). This component of background signal can be determined in the presence of an excess concentration of competitor in the absence of the membrane receptor. Reduction of this factor can be accomplished through the careful use of buffering systems and the appropriate bead type. Determination of NSB to the SPA beads is separate from the NSB associated with membrane receptor preparations.

A competition experiment using an unlabeled compound in the absence or presence of added receptor may assist in identifying nonspecific binding problems.

Non-Proximity Effects (NPE)

NPE occurs when either the concentration of the radioligand or the concentration of SPA beads is sufficiently high enough to elicit a signal from the emitted β-particles. This can occur even though the labeled ligand is not attached directly to the SPA bead through the interaction with the receptor or the nonspecific interaction with the bead (Figure 4, right). In general, this signal is a linear function, directly proportional to the concentrations of each of these reagents. Therefore, a careful balance between radiolabel and SPA beads is crucial to maximize signal and sensitivity while minimizing NPE and ultimately cost. The only technique available to minimize NPE is adjustment of the SPA bead or radiolabel concentrations.

For routine SPA binding assays, nonspecific binding may be a combination of nonspecific binding to SPA beads as well as nonspecific binding to the receptor, and are expressed as one. Total nonspecific binding is measured in the presence of an excess concentration of unlabeled competitor.

Temperature

Typically, receptor binding assays used in screening efforts are performed at room temperature. Comparison experiments may be required if other temperatures are considered. A kinetic analysis may be necessary as well (Figure 5).

Note: Since in nearly all cases, the microplate scintillation counter is at room temperature, and a 96-well plate requires approximately 12 minutes to read on a 12-detector instrument, it is difficult to perform SPA assays at temperatures other than room temperature. The information is useful in areas where there are significant variations in day-to-day laboratory temperatures.

Assay Buffer

Identify appropriate starting buffer from literature sources or based on experience with similar receptors. Binding assays may require $CaCl_2$, $MgCl_2$, NaCl or other agents added to fully activate the receptor. pH is generally between 7.0 to 7.5. Commonly used buffers include TRIS or HEPES at 25 mM to 100 mM. Protease inhibitors may be required to prevent membrane degradation

The tables below provides possible factors that can be investigated in a statistically designed experiment to improve radioligand binding to membrane receptors, or reduce radioligand binding to SPA beads (Agents which Reduce NSB – Table 2; Antioxidants/Reducing Agents – Table 5; SPA Bead Settling Effects - Table 6; Divalent

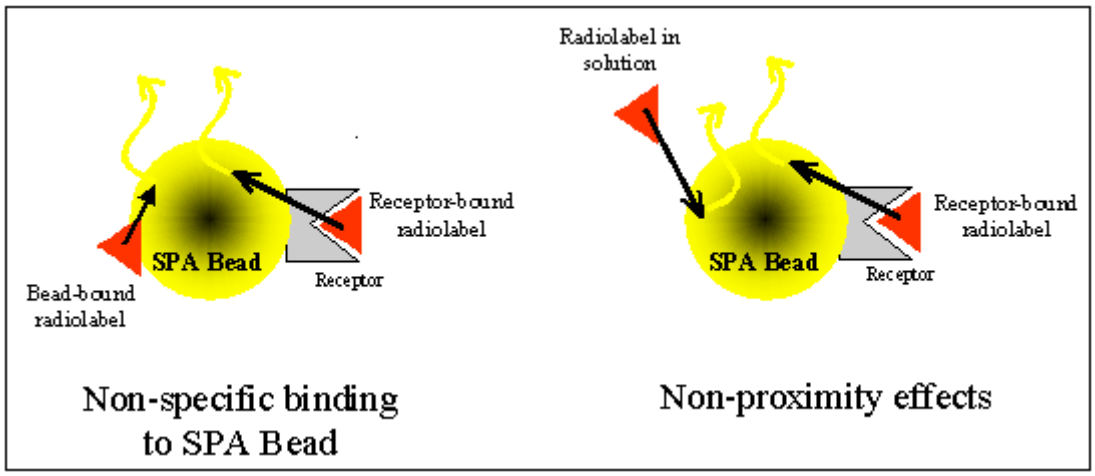

Figure 4: Non-specific binding (left), and non-proximity effects (right) associated with SPA beads.

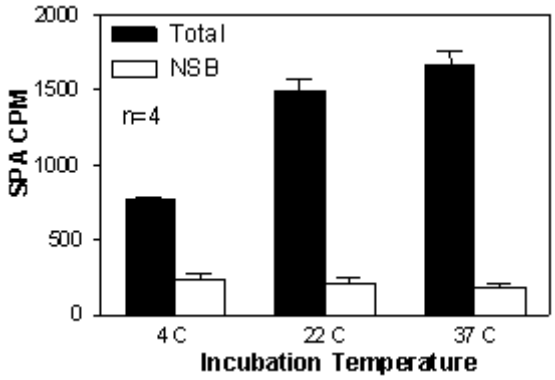

Figure 5: SPA receptor binding assay performed at three temperatures. Data shown at the left was generated by incubation of a limited number of wells (n=4, different plates) at the indicated temperatures and counting them rapidly in the instrument.

Cations – Table 7; Other Buffer Additives – Table 8). The optimization of the assay buffer may be an iterative process in conjunction with the optimization of the assay conditions to achieve acceptable assay performance. Typical concentrations or concentration ranges for some reagents are listed in the tables below. Other reagents may be required depending on the individual receptor/ligand system.

Note that for most instances, the highest purity reagents should be tested. In some cases, such as with BSA, several forms (fatty acid free, fatty acid containing) may need to be investigated.

In addition to Aprotinin and EDTA, other protease inhibitors may be required for receptor stability. As a starting point, Complete™ tablets from Roche Molecular Biochemicals are commonly used.

Table 5: Antioxidants/Reducing agents

Agent	Concentration Range
Ascorbic Acid	0.1%
Pargyline	10 µM
DTT	1 mM

Table 6: **Reduce SPA bead settling effects**

Agent	Concentration Range
Glycerol	10 - 20%
Glucose	10 mM
Polyethylene glycol (PEG)	5 - 10%

Table 7: **Divalent cations**

Cation	Concentration Range
Magnesium (Mg2+)	1 mM - 10 mM
Sodium Acetate	10 mM - 50 mM
Calcium (Ca2+)	1 mM - 10 mM
Zinc (Zn2+)	10 µM - 50 µM

Table 8: **Other buffer additives**

Additive	Concentration Range
NaCl	100 mM - 150 mM
KCl	5 mM - 80 mM
TRIS	10 mM - 50 mM
HEPES	5 mM - 100 mM
Phosphate Buffer	20 mM
pH	7.0 - 8.0
Aprotinin	500 units/ml
EDTA	0.51 mM - 5 mM

Table 9: **Pharmacological profile with representative IC_{50}, K_i and rank affinity data.**

Drug	IC_{50}, nM	Ki, nM	Relative Affinity
4	103	53	1.00
5	190	95	0.56
1	0.25	0.13	424
2	8.9	4.5	11.9
3	30.9	15.5	3.4

Solvent Interference Conditions

Incubation Time - Signal Stability

Setup: Measure total binding (receptor + radioligand + SPA beads) and nonspecific binding (receptor + radioligand + excess unlabeled competitor + SPA beads) at various times using repetitive counting on the microplate scintillation counter.

Results Analysis: Plot total, NSB and specific binding (total binding - NSB) versus time

Since steady state will require a longer time to reach at lower concentrations of radioligand, these experiments are usually performed at radioligand concentrations below the K_d (i.e. 1/10 K_d) if signal strength permits. In addition, the total concentration of radioligand bound should be equal to less than 10% of the concentration added to avoid ligand depletion. The receptor concentration added must be lowered, or the volume of radioligand increased, if this condition is not met.

This experiment is used to determine when a stable signal is achieved and how long a stable signal can be maintained. The signal is a combination of receptor/ligand reaching steady state and bead settling conditions. As SPA beads become packed at the bottom of the well, the efficiency of counting (particularly with ^{125}I) increases. Therefore, it is important to determine when a uniform signal is obtained and adopt this time window as standard practice. In many assays. 8-16 hours are required for stable signal counting. Use approximately 0.1-0.5 mg SPA beads depending on results from preliminary experiments.

An example of an incubation time course is provided in Figure 6. A minimum incubation time of 10 hours was chosen in this example and the interaction was stable for at least 24 hours. Failure to operate a receptor/ligand binding assay at steady state conditions may result in erroneous calculations for binding constants (K_d or K_i).

Receptor Concentration - Zone A

Setup: Measure total binding (receptor + radioligand + SPA beads) and nonspecific binding (receptor + radioligand + excess unlabeled competitor + SPA beads) at various levels of added receptor (typical µg amounts vary depending on the source and purity of receptor).

Results Analysis: Plot total and NSBversus receptor amount. Plot total bound/total added expressed as a percent versus receptor concentration. Determine the level of receptor that yields <10% total binding/total added (Zone A).

It is ideal to keep the total amount of radioligand bound at less than 10% of the total amount added to avoid ligand depletion. This is considered the acceptable limit and is commonly referred to as "Zone A". Saturation experiments should be performed at <10% total ligand binding at all concentrations tested (0.1 x K_d to 10 x K_d), so an initial protein variation experiment at a radioligand concentration that is 0.1 x K_d is typically performed.

The example shown in Figure 7 uses radioligand at < 0.1 K_d and an increasing amount of membrane receptor protein. Two plots are shown: Figure 7, left, raw SPA data for total, NSB and specific; Figure 7, right total bound/total added expressed as a percent. In this example, receptor levels less than ~2 µg/well would meet Zone A requirements.

Total counts added (using liquid scintillation counting) are determined differently than the bound counts (SPA), therefore, in order to plot the % Total Bound/Added, the efficiency for each method must be taken into account, and any CPM data converted to DPM (described in Calculations and Instrumentation Used for Radioligand Binding Assays). You cannot compare the CPM data from one instrument/scintillation method to that of another. The Section entitled "DPM Mode for SPA" demonstrates a representative method for determining efficiency for SPA bead counting. DPM for liquid scintillation counting can be obtained from the instrument directly. The stable signal count time must be determined prior to these experiments. If the signal dips after a high concentration of receptor, then the SPA beads may be in limited amounts.

SPA Bead Amount

Setup: Measure total binding (receptor + radioligand + SPA beads) nonspecific binding (receptor + radioligand + excess unlabeled competitor + SPA beads) and non-proximity effects (radioligand + SPA beads) at various SPA bead levels (typically 0.125 mg to 1.5 mg) using the determined optimum incubation time and optimum receptor concentration.

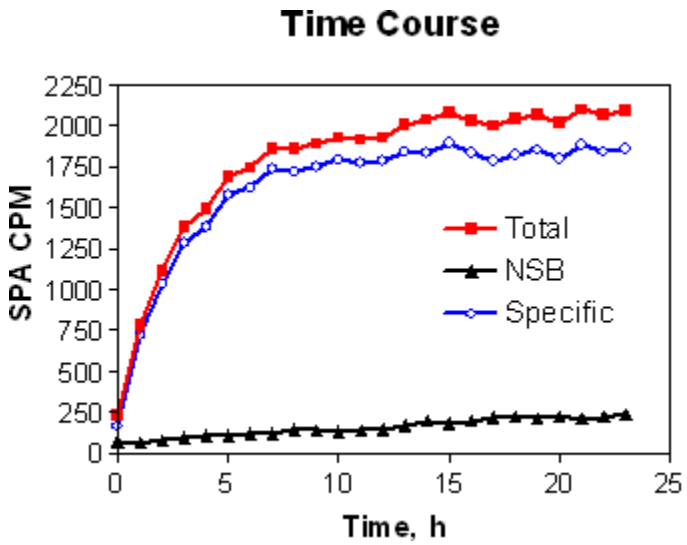

Figure 6: Example of incubation time course

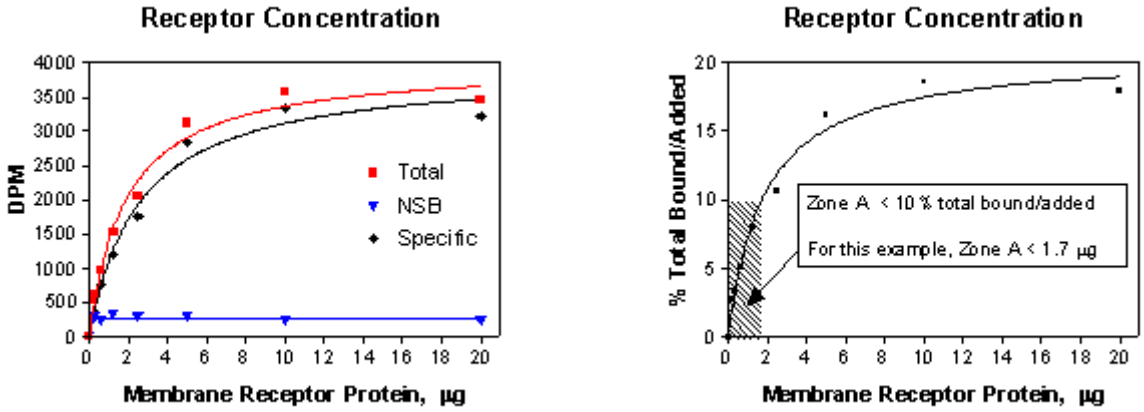

Figure 7: Example of radioligand at < 0.1 K_d and an increasing amount of membrane protein. Left: raw SPA data for total and NSB; right: total bound / total added expressed as a percent.

Results Analysis: Plot total, NSB, NPE, and specific binding (total - NSB) versus SPA bead amount. Choose a bead concentration beyond the linear range, at or near the initial saturation level on the specific binding curve (Figure 8).

Non-proximity effects (NPE) can be determined in the absence of added receptor. Ideally, the NPE signal would be identical to the nonspecific signal in the presence of unlabeled competitor. A level of SPA beads below 0.4 mg would provide the best economical signal for this example.

Solvent Interference

Setup: Measure total binding (receptor + radioligand + SPA beads) and nonspecific binding (receptor + radioligand + excess unlabeled competitor + SPA beads) at various concentrations of DMSO (or other solvent) using the determined optimum incubation time, optimum receptor concentration and optimum SPA bead amount.

Results Analysis: Plot total and NSB versus final assay concentration of DMSO.

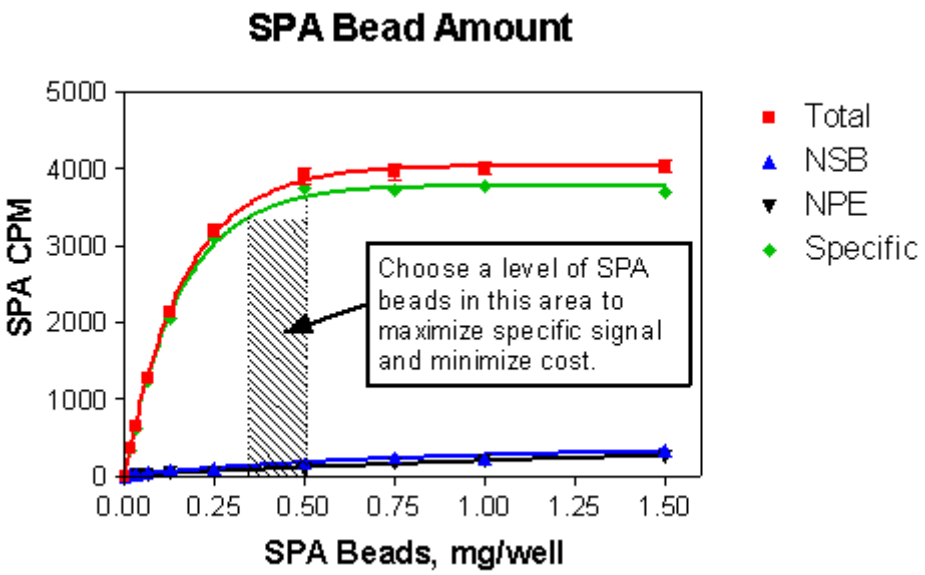

Figure 8: Plot demonstrating how to choose an appropriate bead concentration.

If the developed SPA receptor binding assay will be used to test organic compounds, interference with DMSO will need to be determined. As shown in Figure 9, there can be significant signal reduction if the DMSO concentration becomes too high.

The level of DMSO in a SPA binding assay is determined by data in experiments such as the one in the example above and by the requirement set to maintain compound solubility.

Additional solvents (methanol, ethanol, etc.) or other agents (i.e. β-cyclohexadextrin) may need to be tested if compounds will be received in these other diluents.

Once determined, the solvent should be included in any further assay development or compound testing, including controls.

As an additional verification of minimal solvent interference, test competitive binding with a known competitor in the absence or presence of solvent at the determined level to be used in assays. Ideally, the test compound will have high affinity for the receptor and be freely soluble in aqueous buffer. The IC_{50} should not change in the absence or presence of the solvent.

Binding Parameter

The determination of the equilibrium dissociation constant for the radioligand (K_d) or equilibrium dissociation constants for unlabeled compounds (K_i) should be performed after the SPA receptor binding assay has been fully optimized for the conditions outlined in the prior sections.

Three methods are described for the determination of the receptor affinity for the radioligand, K_d:

- Saturation analysis
- Homologous competition
- Association rate at various radioligand concentrations

A heterologous competition binding assay is used to determine the affinity of the receptor for an unlabeled compound, K_i.

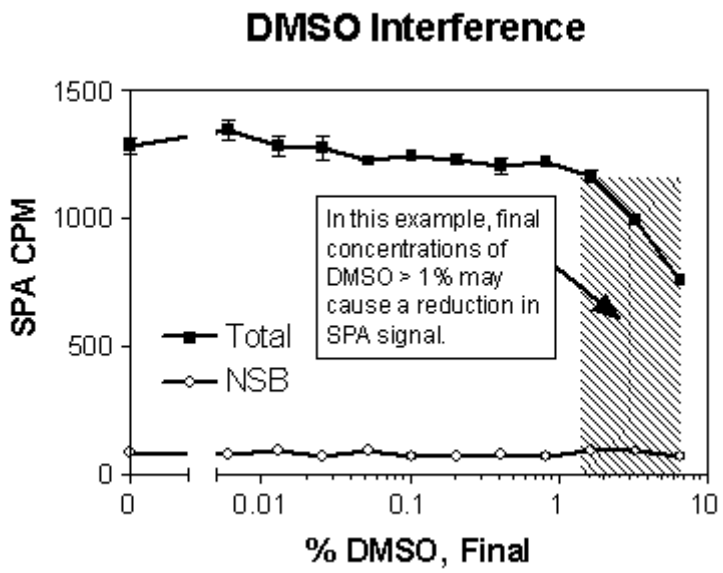

Figure 9: Example of DMSO interference determination and potential for signal reduction.

Saturation Binding

An equilibrium saturation binding experiment measures total and nonspecific binding at various radioligand concentrations. The equilibrium dissociation constant or affinity for the radioligand, K_d, and the maximal number of receptor binding sites, B_{max}, can be calculated from specific binding (total - NSB) using non-linear regression analysis.

Requirements:

- Steady state for low concentrations of radioligand (i.e. 1/10 estimated K_d) has been determined
- Ensure that <10% of the added radioligand is bound (at all radioligand concentrations tested) to prevent ligand depletion - if this is not met, lower the receptor concentration.

The range of radioligand concentrations tested in a saturation binding experiment is typically from 1/10 K_d to >10 × K_d to yield an appropriate curve for nonlinear regression analysis methods. Radioligand specific activity, concentration or expense may prevent a wide range of concentrations from being used.

A high concentration of unlabeled compound (1000 × K_i or K_d value) is used to determine nonspecific binding. Ideally, the unlabeled compound should be structurally different than the radioligand. Nonspecific binding should be less than 50% of the total binding at the highest concentration of [L] tested.

Calculate K_d for specific binding using a one-site binding hyperbola nonlinear regression analysis (i.e. GraphPad Prism) as shown in the equation below:

$$Bound = \frac{B_{max} \times [L]}{[L] + K_d}$$

Bmax is the maximal number of binding sites (pmol/mg), and K_d (nM, pM, etc.) is the concentration of radioligand required to reach half-maximal binding.

Setup: Measure total binding (receptor + radioligand + SPA beads) and nonspecific binding (receptor + radioligand + excess unlabeled competitor + SPA beads) at various concentrations of radioligand using the determined optimum incubation time, optimum receptor concentration and optimum SPA bead amount.

Include the expected concentration of DMSO or other solvent for compound testing. To assess non-proximity effects (NPE), a condition without receptor can be included (radioligand + SPA beads).

Results Analysis: Plot total, NSB and specific binding (total - NSB) versus free concentration of radioligand. Plot NPE if no receptor condition was performed (Figure 10).

A listing of the calculations required for analysis of saturation binding data is shown below. Details for each of these calculations are shown in Calculations and Instrumentation Used for Radioligand Binding Assays

1. Determine total radioactivity added per well by counting an aliquot of each radioligand mix in a gamma counter or a liquid scintillation counter. Convert to DPM if necessary using the equation: DPM = CPM/ Efficiency
2. Convert binding data (total bound, NSB) from CPM to DPM data using above equation.
3. Calculate specific binding in DPM: Specific bound = Total Bound - NSB
4. Calculate unbound (free) DPM: Free = Total Added - Total Bound
5. Convert free DPM to concentration units (i.e. nM) using the radioligand specific activity (expressed as DPM/fmol) and the volume of sample used.
6. Convert Total bound, NSB and Specific bound DPM to pmol/mg units using specific activity expressed as DPM/fmol and the amount of receptor added per assay well in mg units.
7. Plot Bound (in pmol/mg) on Y-axis versus Free concentration of radioligand (in nM) on X-axis.
8. Determine K_d and B_{max} using a non-linear regression analysis for a single site binding (hyperbola).

Considerations/Assumptions for Saturation Binding Experiments

The binding reaction must be at equilibrium for all concentrations of radioligand. Lower concentrations of radioligand require longer times to reach equilibrium.

Less than 10% of the total added radioligand should be bound at all concentrations of radioligand tested. At lower concentrations of radioligand, it is more likely that greater than 10% of the added radioligand will be bound (if this is the case, receptor concentration should be lowered).

If reagents and the assay system allow, radioactive concentrations of at least 10 times the K_d should be tested to provide suitable data for a nonlinear regression analysis and accurate determination of the binding parameters. The K_d and B_{max} values can be calculated from less than complete data sets, but the statistical reliability of the returned values may be lower.

Ideally, nonspecific binding should be less than 50% of the total binding. No positive or negative binding cooperativity. Binding is reversible and obeys the Law of Mass Action.

Scatchard Plots

In the past, nonlinear saturation binding data was transformed into linear data followed by analysis using linear regression, resulting in a Scatchard (or Rosenthal) plot. Although useful for the display of data, the Scatchard plot is not used anymore for the determination of K_d or B_{max} values. These values are determined using nonlinear regression analysis as described in Saturation Binding above. Scatchard plots distort the experimental error (X-value is used to calculate Y), hence the assumptions of linear regression are violated and the resulting values are not accurate.

It is inappropriate to analyze transformed data for the determination of K_d and B_{max}.

Homologous Competition

A homologous competition is a concentration response curve with an unlabeled compound that is identical to the radioligand being used. Radioligand concentration is constant in the experiment. Homologous competition

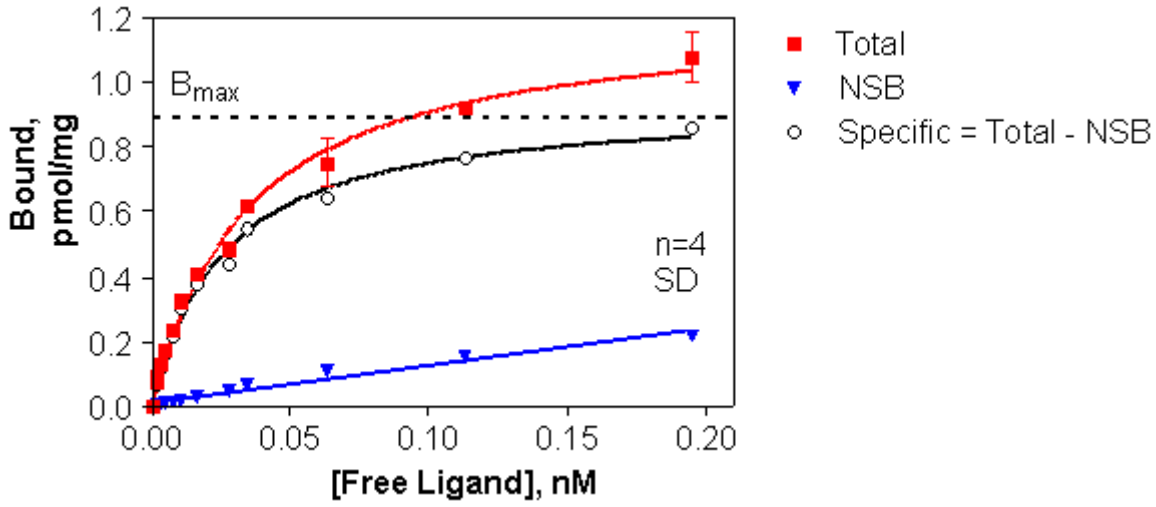

Figure 10: A representative saturation binding experiment. Y-axis data has been expressed in pmol/mg.

experiments can be used as an alternative to saturation experiments to determine receptor affinity (K_d) and density (B_{max}), provided the criteria shown below are met. When using [^{125}I]-ligands, a non-radioactive iodo-ligand should be used if possible.

Assumptions:

1. The receptor has identical affinity for the radioligand and unlabeled ligand.
2. There is no cooperativity.
3. No ligand depletion (<10% of the total added radioligand is bound)
4. Nonspecific binding is proportional to the concentration of labeled ligand.

The concentration-response curve should ideally descend from 90% specific binding to 10% specific binding over an 81-fold (or approximately 2 log scales) increase in concentration of the unlabeled ligand.

A homologous competition experiment has been designed correctly if the IC_{50} is between 2 and 10 times the concentration of radioligand.

Two methods can be used to analyze data from a homologous competition experiment and determine the K_d and B_{max}. They are described below as Results Analysis 1 and Results Analysis 2. The experimental setup is identical for both types of analysis.

Setup: Measure binding (receptor + radioligand + SPA beads) at various concentrations of unlabeled competitor using a single concentration of radioligand (≤K_d) and the determined optimum incubation time, optimum receptor concentration and optimum SPA bead amount. In some cases (^{3}H-label with low specific activity), concentrations above the K_d may be required. Total binding is determined in the absence of any added competitor. Nonspecific binding (receptor + radioligand + excess unlabeled competitor + SPA beads) is included for calculation of specific binding.

Results Analysis 1

Plot specific bound (Bound - NSB) at each concentration of unlabeled competitor. Conversion to percent specific bound is performed using the following equation:

$$\%\ Specific\ Bound = \frac{Bound - NSB}{Total\ Bound - NSB}$$

Step 1. Determine the IC_{50} using a sigmoidal dose-response (variable slope), which is also known as a four-parameter logistic nonlinear regression analysis (i.e. using GraphPad Prism) as shown in the equation below (use log concentration values for proper analysis) and in Figure 11.

$$Y = Bottom + \frac{(Top - Bottom)}{\left(1 + 10^{(LogEC_{50} - X) + HillSlope}\right)}$$

Step 2. Determine the K_d and B_{max} using nonlinear regression analysis (i.e. GraphPad Prism) for the following equation:

$$Y = \frac{B_{max} \times [Hot]}{([Hot] + [Cold] + K_d)} + NSB$$

[Hot] is the concentration of radioligand used in the assay (in nM) [Cold] is the concentration of competitor, which varies, (in nM)

In GraphPad Prism, enter Y in CPM or DPM and X in log concentration of competitor.

Calculate K_d and B_{max} with above curve fit analysis. Use instrument counting efficiency and specific activity of radioligand to convert the calculated maximum signal units (CPM or DPM) to pmol/mg units.

The calculated IC_{50} for this homologous competition experiment is 1.5×10^{-10} M. The concentration of [L] used in this homologous competition is 3.8×10^{-11} M.

The calculated IC_{50} is between 2 and 10 times the concentration of added [L].

The concentration-response curve descends from 90% specific binding to 10% specific binding over an 86-fold increase in concentration of the unlabeled ligand.

Inputting X (log concentration) and Y (Total DPM) into the homologous binding analysis equation above yields (in parentheses are the values obtained from saturation binding analysis): Log K_d = -9.962 → Antilog of -9.962 = 1.09×10^{-10} M = 109 pM (79 pM) B_{max} = 27773 DPM → Convert using specific activity, B_{max} = 12.5 pmol/mg (5 pmol/mg)

Results Analysis 2:

Alternatively, convert specific DPM bound to molar units (i.e. nM) bound.

1. The molar concentration of labeled ligand ([L]) is calculated using the DPM added per well, the specific activity and the conversion factor, 1 μCi = 2.2 × 106 DPM.

   The formula is [L] nM = (specific counts) × (1/2200000) × (1 / Specific Activity) × 10000
2. This concentration is added to all concentrations of unlabeled ligand to determine the final added ligand concentration.
3. As the added ligand concentration increases (due to increase added unlabeled ligand), the specific activity of the labeled ligand is decreased.
4. For each specific DPM bound determine the specific molar units bound by using the corresponding specific activity in that condition.
   The formula is [RL] = (added ligand) × (specific DPM) / (DPM added per well).
5. Use a one-site binding (hyperbola) similar to the saturation binding data to calculate K_d and B_{max}.

Example: Labeled ligand specific activity is 90 Ci/mmol and 66398 dpm are added per well (100 μl final volume). The concentration of labeled ligand in all wells is 3.3 nM. At unlabeled ligand concentration of 125 nM, the final added ligand (unlabeled + labeled) is 128.3 nM.

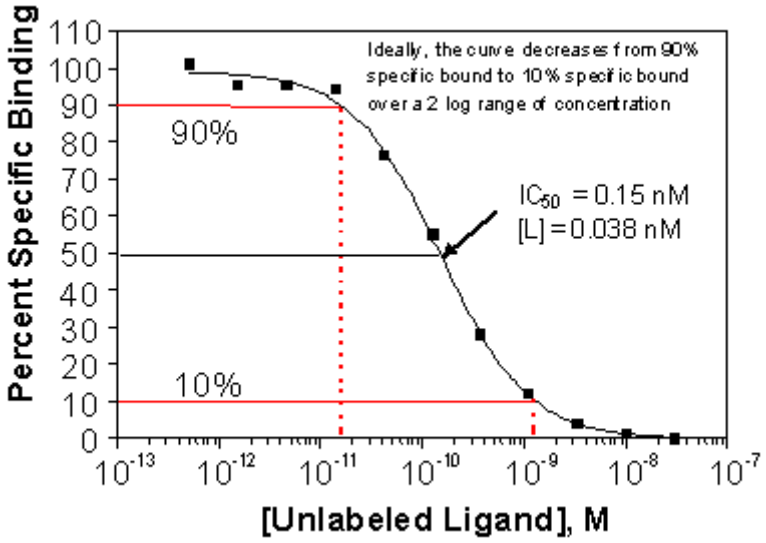

Figure 11: Representative data for a homologous competition.

If the specific binding at 125 nM unlabeled ligand condition is 3283 DPM, then the specific molar unit bound would be:

(3283 × 128.3)/66398 = 6.34 nM.

Representative results for homologous competition analyzed using the Results Analysis 2 method is shown in Figure 12. The Kd determined from this example was 12.6 nM.

Association Rate at Various Radioligand Concentrations (Optional)

An optional method, which can be used early in development for both determination of optimum incubation time and provide an estimate for the K_d, is to perform an association rate experiment at various radioligand concentrations.

Setup: Measure total binding (receptor + radioligand + SPA beads) and nonspecific binding (receptor + radioligand + excess unlabeled competitor + SPA beads) at various times and at various concentrations of added radioligand.

Results Analysis: Plot specific binding (total binding - NSB) versus time at each radioligand concentration tested.

Calculate the observed association rate constant (k_{obs}) by fitting the signal versus time data to a one-phase exponential association nonlinear regression analysis for each concentration of radioligand tested. The k_{obs} value is returned as one of the resulting curve fit parameters. There will be different k_{obs} for each radioligand concentration.

Plot the observed association rate constant (k_{obs}) versus concentration of [L].

This should result in a linear function with a slope equal to the association rate constant (k_{on}) and the Y-intercept equal to the dissociation rate constant (k_{off}). An estimate for the equilibrium dissociation constant (K_d) can be calculated using the equation below with the kinetically determined rate constants (see Figure 13):

$K_d = k_{off}/k_{on}$

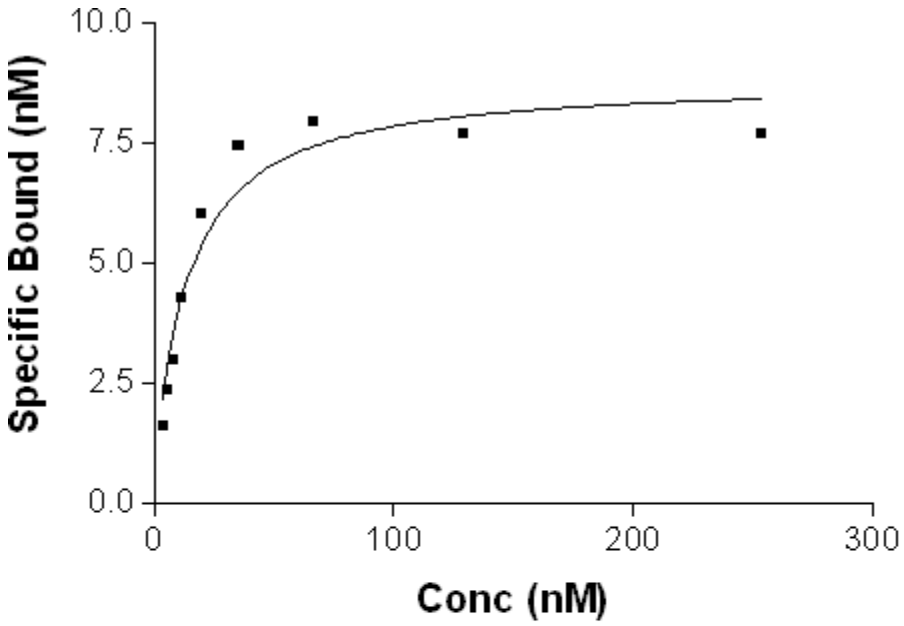

	Specific Bound (nM)
BMAX	8.830
KD	12.59
Std. Error	
BMAX	0.5050
KD	2.509
95% Confidence Intervals	
BMAX	7.636 to 10.02
KD	6.654 to 18.52
Goodness of Fit	
Degrees of Freedom	7
R^2	0.9426

Figure 12: Homologous Competition for Determination of K_d. In this example data, the K_d determined from a homologous competition experiment is 12.6 nM.

Heterologous Competition

Experimentally, a heterologous competition is identical to a homologous competition. Heterologous competition assays measure concentration-response binding with unlabeled ligands that are ***structurally different*** than the radioligand. The IC_{50} for the unlabeled compound is determined from the experimental data and the equilibrium dissociation constant, K_i, can be calculated using a mathematical formula (Cheng-Prusoff equation).

Setup: Measure binding (receptor + radioligand + SPA beads) at various concentrations of unlabeled competitor using a single concentration of radioligand (≤ K_d) and the determined optimum incubation time, optimum receptor concentration and optimum SPA bead amount. Total binding is determined in the absence of any added competitor. Nonspecific binding (receptor + radioligand + excess unlabeled competitor + SPA beads) is included for calculation of specific binding.

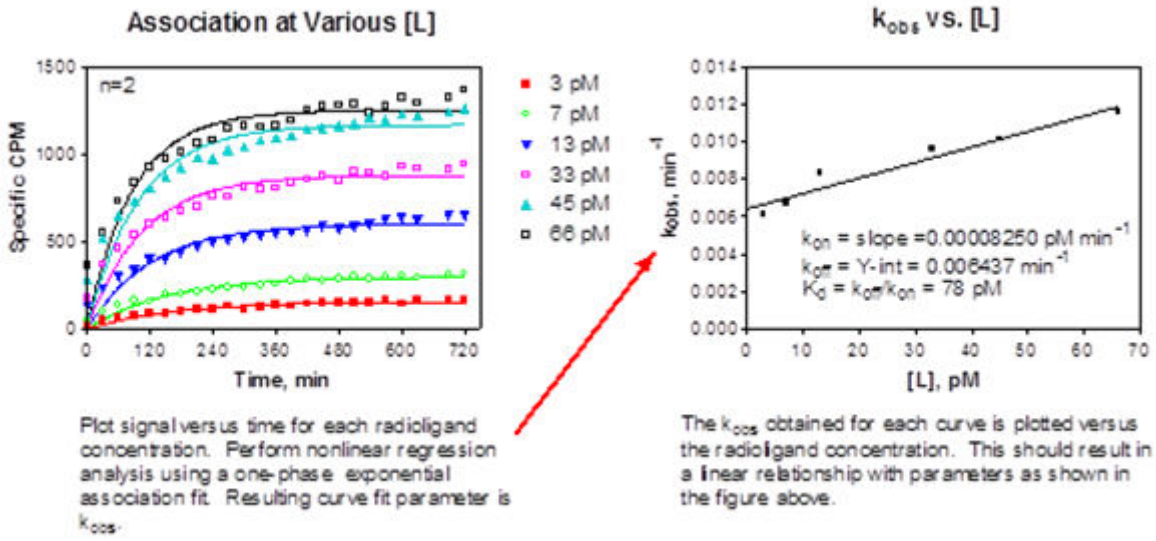

Figure 13: SPA Method: Reaction mix was read at different time points. The K_d calculated from saturation binding for this receptor was 35 pM.

Results Analysis: Plot specific bound (Bound - NSB) at each concentration of unlabeled competitor. Conversion to percent specific bound is performed using the following equation:

$$\%\ Specific\ Bound = \frac{Bound - NSB}{Total\ Bound - NSB} \times 100$$

Determine IC_{50} using a sigmoidal dose-response (variable slope), which is also known as a four-parameter logistic nonlinear regression analysis (i.e. using GraphPad Prism) as shown in the equation below:

$$Y = Bottom + \frac{(Top - Bottom)}{\left(1 + 10^{(LogEC50 - X) + HillSlope}\right)}$$

where Y is the specific binding and X is the log concentration of competitor.

Calculate the equilibrium dissociation constant for the unlabeled compound (K_i) using the Cheng-Prusoff equation (valid when Hill Slope is near unity):

$K_i = IC_{50}/[1 + ([L]/K_d)]$

where

- K_i is the equilibrium dissociation constant for the unlabeled compound
- IC_{50} is the concentration causing 50% inhibition of binding
- [L] is the concentration of radioligand
- K_d is the equilibrium dissociation constant for the radioligand
- Further calculation details on the Cheng-Prusoff equation can be found in Data Standardization for Results Management.

A representative heterologous competition curve is similar to the one shown in the homologous competition section.

Several assumptions, based on specific criteria, are made to allow calculations using the Cheng-Prusoff equation to be reliable:

1. Law of Mass Action applied (10-90% of displacement occurs over 81-fold concentration range)
2. A single class of receptor binding sites
3. No ligand depletion
4. Receptor concentration < K_d
5. Assay is at equilibrium or steady state
6. The concentration of the added inhibitor is equal to the free concentration of the inhibitor

For special cases associated with high affinity compounds, where ligand depletion must be accounted for; see the section on High Affinity Competitors.

Pharmacological Profile

A pharmacological profile is a heterologous competition testing several unlabeled compounds simultaneously. The K_i for each compound can be computed and compared to each other. A rank affinity can also be calculated. The data below demonstrates a typical pharmacological profile with representative IC_{50}, K_i and rank affinity data shown in Table 9.

Notice that different concentration ranges may be required for each drug to fully define top and bottom portions of the curves (Figure 14).

The IC_{50} is determined from experimental data, the K_i is calculated using the Cheng-Prusoff equation and the Relative Affinity is relative to a particular compound of interest (Drug 1 in this example).

L = 0.025

K_d = 0.025

Relative Affinity = IC_{50} for Drug 1/IC_{50} for Drug

A control compound is tested on each plate and can be used for determination of the relative affinity. This process aids in analyzing the statistical significance of differences between the individual compounds.

Filtration Assays

Concept

Filter assays differ from SPA because a separation of free radioligand and radioligand bound to the receptor is required for measurement. However, many of the assay development and optimization steps are the same. Specific information to the filter assay format is included in this section, and reference back to the text under the SPA section is made when there is no significant difference between the two formats (Figure 15).

General Steps for a filtration assay:

1. Add and incubate test compound, radioligand and receptor in a plate (this can be a separate plate or if validated, the filtration plate directly)
2. Apply vacuum to "trap" receptor and bound radioligand onto filter and remove unbound radioligand. Wash several times with an appropriate buffer to minimize nonspecific binding.
3. Allow filters to dry. Add liquid scintillation cocktail or other scintillant (i.e. solid Meltilex).
4. Count filters in microplate scintillation counter. Some time between adding the scintillant and counting may be required.

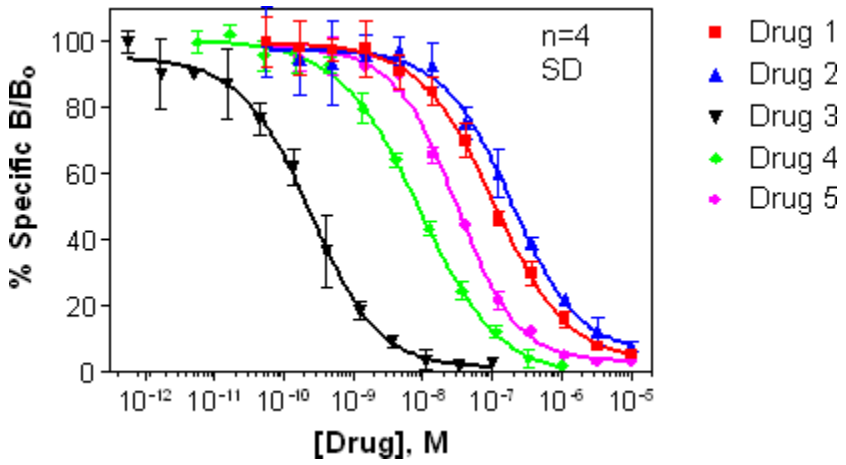

Figure 14: Example concentration curves for 5 drugs, calculated using the data in Table 9.

Advantages	Disadvantages
Less color quenching Traditional, trusted method Higher efficiency than SPA Kinetic experiments easier Association/Dissociation	Separation method (dissociation of ligand) Generated large volumes of liquid waste Variable vacuum across plate Nonspecific binding to filters Accumulation of radioactivity on unit Requires more handling steps

Filter Assay Format

Exposure Time to Scintillant

Filter Type

The most commonly used filters for receptor binding are listed below:

- GF/B - glass fiber filters with 1.0 µM pore size
- GF/C - glass fiber filters with 1.2 µM pore size
- Durapore - PVDF filters with various pore sizes such as 0.22, 0.65, 1.0 µM.

Depending on the radioligand, receptor and other assay factors, it may be necessary to perform experiments with more than one type of filter to determine the best one for the system under investigation (Table 10).

The speed of separation is important, particularly for lower affinity interactions (<1 nM), and can be influenced by the filter plate type. Dissociation of bound radioligand from a receptor interaction with an affinity of 1 nM can occur in under 2 min. Lower affinity interactions can dissociate even quicker, when the separation process disrupts equilibrium.

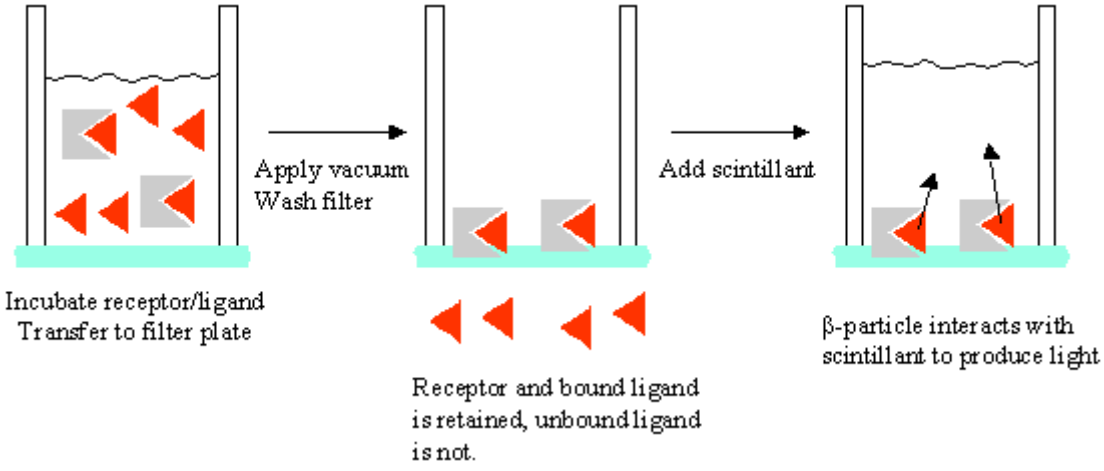

Figure 15: Diagram for a standard filtration assay

Table 10: Summary of plate types that can be used for filter assays.

Plate Type	Harvester Instrument	Counting Instrument	Comments
Unifilter GF/C or GF/B	Packard or Brandel	Trilux or TopCount	Filter from an assay plate to the filter plate with washing of the assay plate possible
Multiscreen-FC or Multiscreen-FB	MAP or individual manifold	Trilux or TopCount	Removable bottom plastic piece. Requires solid white adapter for TopCount or clear plastic liner and cassette for Trilux
Multiscreen-GV	MAP or individual manifold	Trilux or TopCount	0.22 mM Durapore membrane. Removable bottom plastic piece. Requires solid white adapter for TopCount or clear plastic liner and cassette for Trilux

Order of Addition

The order of addition for reagents may affect assay performance as well as ease of automation. A standard format for order of reagent addition in a filtration method is as follows:

1. Test compound
2. Radioligand
3. Receptor

Experiments may be required to determine the optimum order of addition and if there is any effect by locally high concentrations of DMSO present during the initial additions into the wells.

Non-Specific Binding

Radioligands may bind nonspecifically to components of the assay system such as tubes, pipette tips, assay plates or filters. This may lead to ligand depletion and certain binding assumptions may not be met. To test for nonspecific binding, perform an experiment in the absence of membranes. The amount of activity added can be tracked at each step of the assay to determine where any losses or nonspecific binding is occurring.

Some potential solutions to minimize nonspecific binding include the following:

- Pretreatment of tubes (siliconization)
- Additions to assay buffers (see Table 2)
- Different filter plate manufacturers (Perkin Elmer, Millipore, Brandel, Polyfiltronics, etc.)

- Different filter plate types (GF/C, GF/B, Durapore, etc.)

Since there may be non-receptor binding (to system components as described above), the use of an unlabeled ligand at a 100-fold excess may not be adequate to fully define all of the nonspecific binding.

Temperature

See SPA section on Temperature.

The filtration format can accommodate temperatures other than room temperature easier than the SPA format. The receptor, ligand and/or compound can be incubated at the desired temperature and then filtered to capture bound radioactivity. Since the filtration process is rapid, there is not a significant temperature drop during the separation time. Once the scintillant is added, the filter plates can be counted in the microplate scintillation counter at room temperature.

Plate Treatment Conditions

Filter plates are usually pre-wetted to ensure even distribution of the receptor/ligand reagents. If there is no ligand sticking problems, the pre-wet can be accomplished with wash buffer.

Pretreatment of filters with polyethylinimine (PEI) is a common practice to minimize ligand binding to filters:

1. Presoak 30 to 60 min in 0.1% to 0.5% PEI (in water)
2. Treat at 4°C to minimize filter degradation
3. Filter away PEI, then wash with ice-cold buffer prior to filtration of receptor sample

Pretreatment with carrier proteins, serum, or detergents has also been used to minimize binding of ligands to filter plates.

Note of Caution: Millipore Multiscreen glass fiber filter plates have a 0.65 mm Durapore support membrane under the GF filter. Some treatments (including PEI) may change or compromise the stability of this support membrane. Appropriate experiments should be designed to test for stability when using these types of plates.

Vacuum Pressure

The vacuum pressure used for filtration binding assays is a balance between having enough pressure to filter the samples rapidly and prevent ligand dissociation and having too much pressure which can affect filter integrity or the level of membranes retained on the filter. The pressure to be used should be determined experimentally, with a starting guideline of 5 to 10 mm Hg. If necessary, install an appropriate regulator to control consistent vacuum pressure.

Wash Buffer

Several washes of the filters are required to remove as much unbound radioligand as possible and to maximize specific binding. Generally, an ice-cold buffer is used to prevent or reduce dissociation of bound radioligand from the receptor.

Filter Plate Drying Time

If filters are not completely dry prior to the addition of liquid scintillant, the residual water present in the filters can interact with the scintillant to reduce counting efficiency. Dry filters require less liquid scintillant to achieve maximum signal than wetted filters. Drying filters completely may not be practical for medium or high throughput screening applications.

Type and Volume of Scintillant

The type of microplate scintillation counter being used may dictate the type of scintillant required for proper counting conditions.

TopCount - must use a "slow" scintillator such as Microscint-20 or Microscint-40

Trilux - can use virtually any scintillant designed for microplate scintillation counting (Microscint-20/ Microscint-40, Optiphase Supermix, Meltilex)

Regular liquid scintillation cocktail such as Ready Pro should not be used, as a rule, for microplate scintillation counting as their load capacities may not be adequate and they may not be compatible with microplate plastics.

General volumes of liquid scintillant used are in the range of 40 to 150 µl. As mentioned above, the volume of scintillant used may depend on the dryness of the filters.

Exposure Time to Scintillant

With filter plates, some of the radioligand may be embedded within the filter and require some time to become accessible to the liquid scintillant for photon generation and signal detection. Therefore, an incubation time may be required following the addition of liquid scintillant and prior to counting. In addition to increasing the maximum signal, the variability of the signal may be reduced following an incubation time as demonstrated in the figure on the following page.

When processing large numbers of plates, it is important that a stable counting signal has been reached, so that all plates from the first counted to the last counted, are comparable.

Over time, more radioactive particles will be removed from the filter and make contact with the liquid scintillant in the well. As the data in Figure 16 shows, this can improve signal strength and decrease variability.

Assay Buffer (Filter)

See the Assay Buffer section in the SPA part of this chapter. Many of the buffer additives and reagents described for the SPA format are relevant for receptor binding assays in a filtration format.

Assay Conditions (Filter)

Incubation Time - Signal Stability

Setup: Measure total binding (receptor + radioligand) and nonspecific binding (receptor + radioligand + excess unlabeled competitor) at various times.

At least two methods could be used to obtain the association/dissociation data. Both methods should yield the same result. If not, there may be a problem with receptor stability.

Method 1: Add and mix together enough receptor and radioligand for all time points in the experiment. At various times, filter an aliquot of the receptor/radioligand mixture and wash the filters with Wash Buffer. The last aliquots to be filtered will be the longest incubation time points.

Method 2: Prepare receptor and radioligand separately. At various time points, combine the two in the microplate. After all points have been added, filter the reactions at the same time. The last wells to be mixed will be the shortest incubation times.

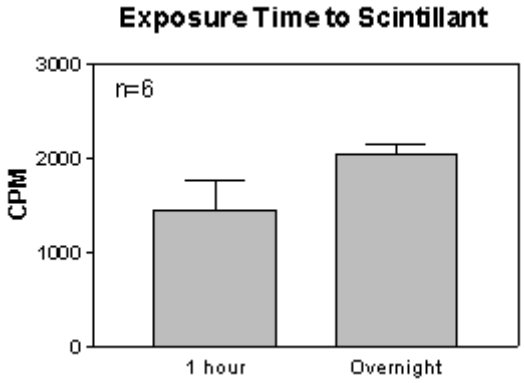

Figure 16: Exposure time to scintillant.

Dissociation, which can be measured more conveniently using the filtration format than SPA, is performed by adding an excess amount of unlabeled competitor after a receptor/radioligand mixture has reached steady state (plateau on the association curve, Figure 17)

Results Analysis: Plot specific binding (total binding - nonspecific binding) versus time. Fit the association data to a one-phase exponential association curve and the dissociation data to a one-phase exponential decay curve. In the example above, a minimum reaction time of 2.5 hours would be adequate.

In addition to determination of the appropriate primary incubation time for steady state, a kinetic estimate for the equilibrium dissociation constant, K_d, can be made from the results of an association/dissociation experiment.

Association Experiment:

- Obtain k_{obs}, expressed in min^{-1}, from the nonlinear regression analysis of data

Dissociation Experiment:

- Obtain k_{off} , expressed in min^{-1}, from the nonlinear regression analysis of data

Calculate association rate constant, k_{on} (in $Molar^{-1}$ min^{-1})

$$kon = \frac{kobs - koff}{[radioligand]}$$

Calculate equilibrium dissociation constant, K_d (in Molar):

$K_d = k_{off}/k_{on}$

Receptor Concentration - Zone A

Setup: Measure total binding (receptor + radioligand) and nonspecific binding (receptor + radioligand + excess unlabeled competitor) at various levels of added receptor.

Results Analysis: Plot total, NSB and specific binding (total - NSB) versus receptor amount. Plot total bound/total added expressed as a percent versus receptor concentration. Determine the level of receptor that yields <10% total binding/total added (Zone A).

See the Receptor Concentration - Zone A section in the SPA part of this document for further details and an example.

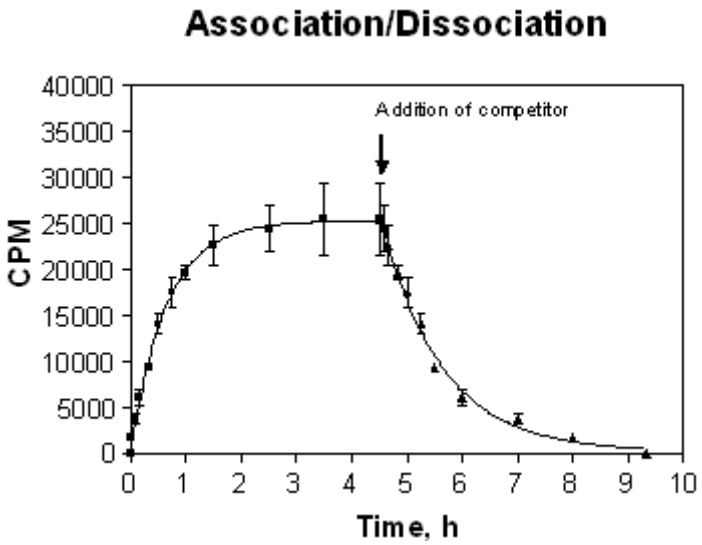

Figure 17: Association/dissociation experiment (total binding only shown).

Solvent Tolerance

Setup: Measure total binding (receptor + radioligand) and nonspecific binding (receptor + radioligand + excess unlabeled competitor) at various concentrations of DMSO (or other solvent) using the determined optimum incubation time and optimum receptor concentration.

Results Analysis: Plot total and NSB versus final concentration of solvent

See the **Solvent Tolerance** section in the SPA part of this document for further details and an example.

Binding Parameters (Filter)

Saturation Binding: See the Saturation Binding section in the SPA part of this document for further details and an example.

Homologous Competition: See the Homologous Competition section in the SPA part of this document for further details and an example.

Association Rate at Various Radioligand Concentrations (Optional): See the Association Rate at Various Radioligand Concentrations (Optional) section in the SPA part of this chapter for further details and an example.

Heterologous Competition: See the Heterologous Competition section in the SPA part of this chapter for further details and an example.

Pharmacological Profile: See the Pharmacological Profile section in the SPA part of this chapter for further details and an example.

High Affinity Competitors

For high affinity competitors, the assumption related to inhibitor depletion may not be met and an alternative analysis method can be used.

When the assay is designed properly, ligand depletion should not be a problem. However, once competitors reach an activity 2 to 3 fold lower than the ligand, inhibitor depletion can be an issue. Assuming that the hill

slope for these compounds is near 1, the K_i computed using the Cheng-Prusoff equation could be compared to the K_i found by fitting the tightly bound inhibitor model below.

$$a = K_d\left(1 + \frac{K_d}{[L]}\right)$$
$$b = \left([I]_t K_d + K_i[L]\left(1 + \frac{K_d}{[L]}\right) - K_d[R]_t\right)$$
$$c = -[R]_t[L]K_i$$
$$[RL] = \frac{-b + \sqrt{b^2 - 4ac}}{2a}$$

The ligand concentration [L] and the K_d are exactly those that would be used in the Cheng-Prusoff equation. The inhibitor concentration, $[I]_t$, is the concentration tested. The K_i and receptor concentration $[R]_t$ are obtained by fitting the model. In order to use this model, the response determined by the plate reader, which measures the amount of receptor ligand complex [RL], must be converted to the same concentration units that are used for the ligand [L] and inhibitor $[I]_t$. This requires the specific activity of the label and a plate reader that is calibrated well.

Even though the Tight Binding (T-B) model looks much more complex than the sigmoid curve model or the one site competition model in GraphPad Prism, both the fitted curve and the K_i are virtually identical unless a substantial portion of the inhibitor is bound (Figure 18). The ratio of the K_i determined by Cheng-Prusoff to the K_i determined using the T-B model is plotted against the K_i determined by the T-B model. Inhibitor depletion will always result in understating the true potency of the molecule. Hence, the ratios are always greater than one. Also, the K_i values are virtually identical unless the K_i is much lower than the K_d.

Hill Slope Deviations

A standard competitive binding curve that follows the law of mass action will descend from 90% specific binding to 10% specific binding over an 81-fold range of unlabeled drug concentrations. The steepness of the competition curve is given by a slope factor, called the Hill slope. This parameter is determined from a nonlinear regression analysis of the competition data when using a four-parameter logistic equation. A standard competition curve (plotted with percent bound) that meets all assumptions would have a Hill slope of -1.0. If the slope factor deviates from -1.0 significantly, then the binding may not follow the law of mass action and you may be dealing with a receptor that has more than a single class of binding sites, solubility issues or an assay artifact.

There is no adequate way to interpret the absolute value of the Hill Slope. However, there are several possible explanations when a competition curve has a calculated Hill Slope that is significantly less than 1 (shallow curve):

1. Experimental problems such as improper serial dilution of the compound
2. Curve fitting problems due to undefined top and bottom plateaus or too few data points
3. Negative cooperativity - binding on one ligand molecule reduces affinity of other binding sites
4. Heterogeneous receptors - different populations of receptors with different affinities
5. Assay variability

Although the Hill slope for a compound may not be -1.0, repetitive determinations for the same compound should yield similar Hill slopes each time. If this is not the case, further optimization of the receptor binding assay may be required.

Some compounds being tested may not be soluble in the standard solvent, DMSO. In addition, compounds at high concentrations may not be soluble. Both of these cases can affect the shape of competition curves (i.e. Hill slope, top or bottom plateau, etc.) and the calculated parameters. Therefore, it is important to review each competition curve for the following features:

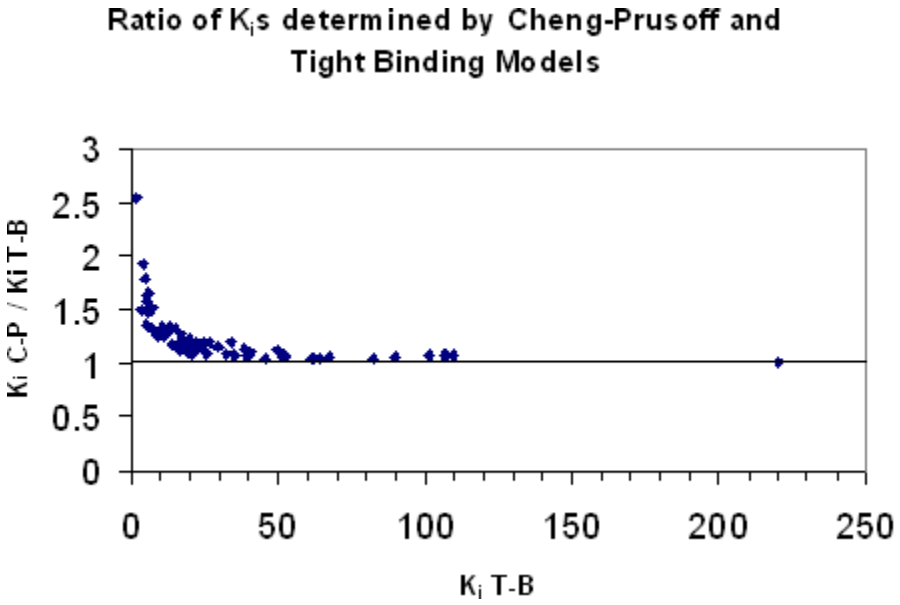

Figure 18: Radioligang binding results from an assay with $K_d \approx 100$ and ligand concentration of 4 nM.

- Specific binding descends from 90% to 10% over an 81-fold concentration range
- The Hill slope is at or near -1.00
- Top and bottom plateaus have been appropriately defined
- Data points are evenly spaced along the entire range of concentrations tested

Figure 19 demonstrates a compound tested in Diluent 1 and Diluent 2. In Diluent 2, the compound appears to have limited solubility and exhibits a very shallow Hill slope and poorly defined top and bottom plateaus. In Diluent 1, the compound competes with the radioligand in the expected manner.

Practical Use of Fluorescence Polarization in Competitive Receptor Binding Assays

Principles of Fluorescence Polarization

Fluorescence polarization (FP) measurements have become a popular assay format for receptor binding assays. The principle of this assay is illustrated in Figure 20 and its design and implementation are also covered in Inhibition of Protein-Protein Interactions: Non-Cellular Assay Formats.

A fluorophore whose absorption vector is aligned with polarized excitation light is selectively excited. If the fluorophore tumbles rapidly relative to its fluorescent lifetime then it will be randomly orientated prior to light emission and therefore will show a low polarization value (situation A above). However, if this fluorophore's rotation is slowed down so that it tumbles slowly with respect to the fluorescent lifetime (e.g. by binding to a large receptor as shown in B above) it will not rotate much before light emission and will show a high polarization value (Figure 21).

Typical fluorophores include fluorescein- or BODIPY-labels that have fluorescence lifetimes allowing FP measurements to be made between a small labeled-ligand (<1500 Da) and a large receptor (e.g. > 10,000 Da).

The increase in polarization can be measured with several microplate readers where the fluorescence is measured using polarized excitation and emission filters. Two measurements are performed on every well. Data is obtained for the fluorescence perpendicular to the excitation plane (the "P-channel") and fluorescence that is

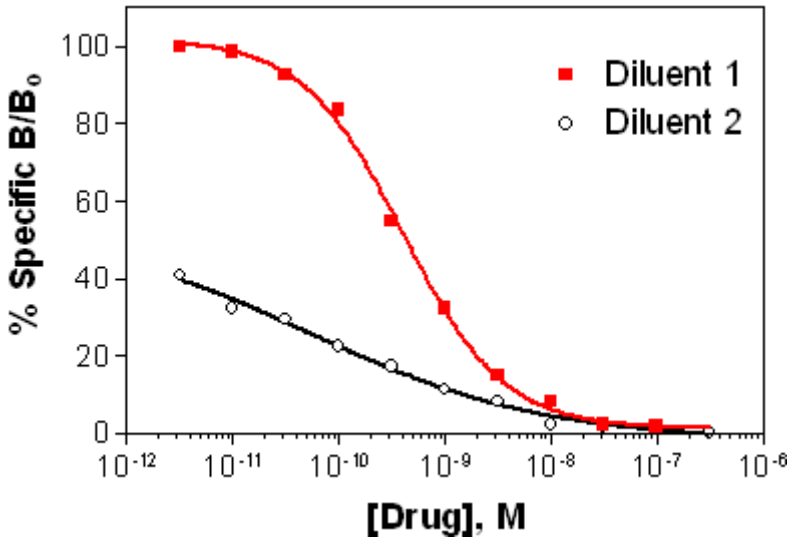

Figure 19: Example of a Hill slope plot for the same compound tested in two diluents.

parallel to the excitation plane (the "S-channel"). For screening applications, the millipolarization units (mP) are often calculated using:

$$mP = \left[\frac{(S - P \times G)}{S + P \times G}\right] \times 1000$$

The proper use of S and P channel data requires two corrections. First, accurate calculation of polarization using fluorescent readers requires calculation of the instrument "G-factor". This factor corrects for any bias toward the P channel. For microplate readers, a 1 nM fluorescein solution is typically used and the G-factor that yields a value of 27 mP is entered (27 mP is the known value for a 1 nM fluorescein solution at RT). Secondly, the S and P values should have the background fluorescence subtracted (determined using assay buffer without labeled-ligand in the well).

Fluorescence Polarization and Receptor Binding

Receptor-binding FP assays use a small molecule labeled ligand (so called tracer) and a large unlabeled receptor. An example is a fluorescently labeled-steroidal ligand binding to a nuclear receptor-ligand binding domain (kits of this type are sold by Invitrogen/PanVera). This type of assay typically yields a minimum signal of approximately 50 mP for the unbound tracer and a maximum signal of approximately 300 mP when the tracer is fully bound to the receptor.

Validate Activity of Fluorescent Tracer

The receptor binding activity of a fluorescent-labeled tracer can be determined in a competition assay using a radiolabeled ligand and traditional methods of receptor binding (filtration, SPA, charcoal precipitation, etc.). As shown in Figure 22, some loss of receptor binding activity may occur following fluorescent tagging. It is important to identify lower binding activity prior to further experiments with the fluorescent tracer. Functional receptor assays, such as cAMP measurement, calcium mobilization or GTPγS binding, can also be performed to determine if there has been a loss in biological activity as a result of the labeling process.

Choosing Tracer and Receptor Concentrations

The K_d of the tracer and the amount of tracer bound under the chosen assay conditions will be required for analysis of competitive binding parameters. Typically, the K_d can be estimated using radioligand-binding techniques (SPA, filtration) discussed in previous sections, provided there is not significant deviation in the

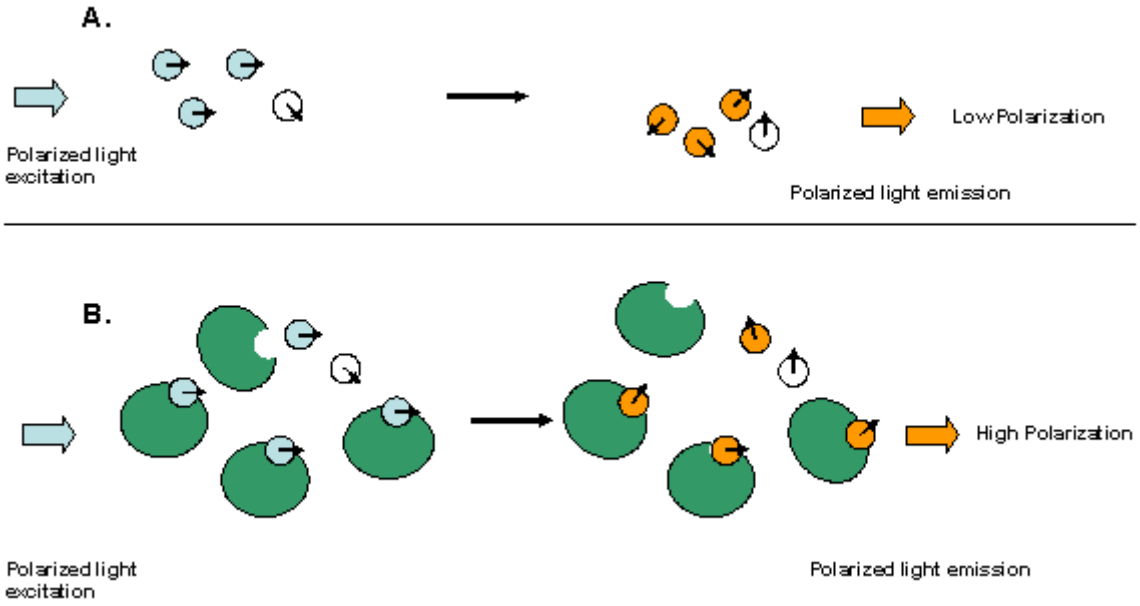

Figure 20: Principle of fluorescence polarization assay.

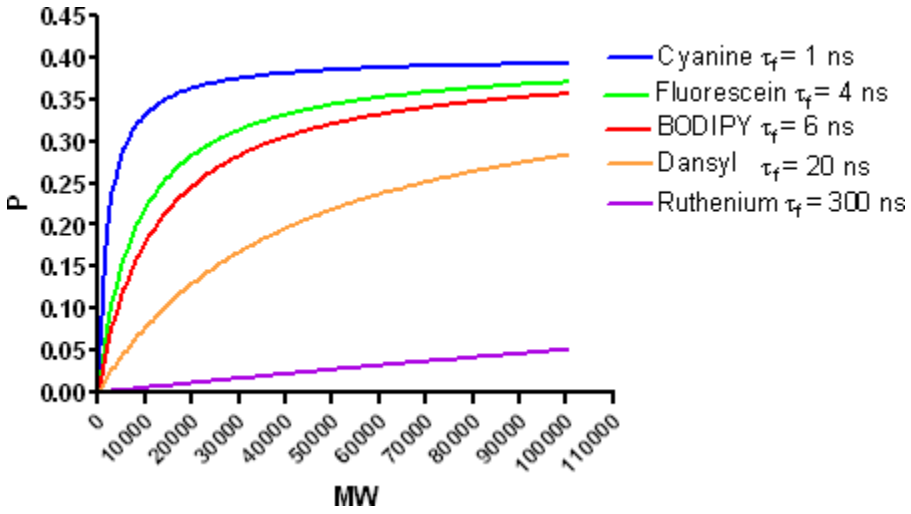

Figure 21: The dependence of polarization on fluorescent life-time is shown below. The graph contains simulated data using the Perrin equation (1) and taking the limiting polarization as 0.5 using T = 293 K and assuming a spherical protein in water with the fluorescence probe rigidly attached.

potency of the tracer and the unlabeled molecule (see figure above). It may be useful to perform a tracer calibration curve by varying the amount of tracer and ensuring that the polarization signal is constant over a reasonable concentration range, inclusive of the estimated K_d. By definition, the polarization signal is independent of the intensity of the tracer. This also identifies the variability at the tracer concentration to be used (Figure 23).

The amount of bound tracer can be measured in an experiment where the tracer is held at a constant concentration near its K_d and the receptor concentration is then varied. An example of this type of experiment using the glucocorticoid receptor (GR) included in the FP kit available from Invitrogen/PanVera is shown in Figure 24.

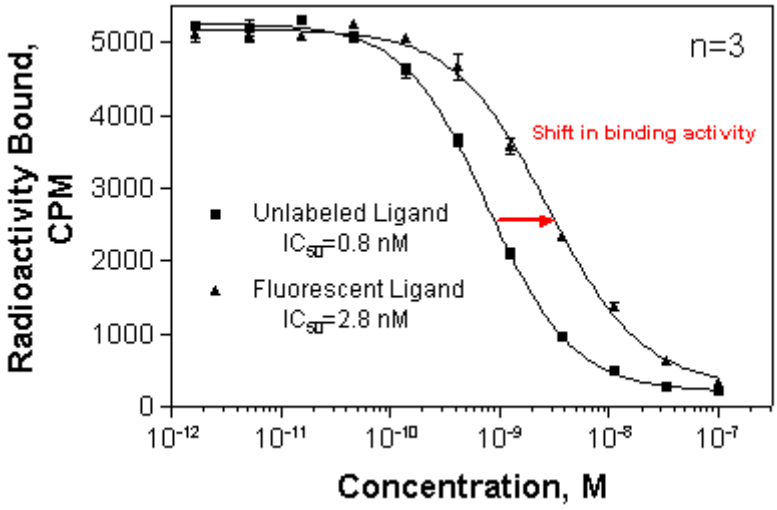

Figure 22: Example of the loss of receptor binding activity following fluorescent tagging.

In these types of FP experiments no correction for nonspecific binding (NSB) is performed as was shown in earlier sections for radioligand-binding experiments. This is because the tracer (what is the radioactive ligand concentration in traditional assays) is held constant at a concentration usually near the K_d and the protein receptor concentration is then varied over several orders of magnitude. However, this assumption should be checked by observing the polarization of the ligand in the absence of receptor. (Caution: it is possible to observe increasing FP signals when membrane receptors are used due to light scattering. In those cases, a correction may need to be made by measuring the signal in the presence and absence of the fluorescent tracer). If binding to non-specific buffer components or microtiter plates surfaces is observed then this tracer should be avoided. An analytical treatment of FP competitive-binding data has recently been presented by Roehrl et al. (2) that allows one to quantify the effect of non-specific binding on FP titration curves.

Examination of the curve above allows one to choose a receptor concentration that yields an acceptable assay window (typically a ΔmP of between 150 mP and 300 mP).

Pharmacological Profile

Sensitivity to known competitors should be checked at this stage to ensure that the developed FP assay is adequate for the intended purpose (Figure 25).

Ligand Depletion

The FP assay format is homogenous in nature and therefore lends itself to simple "mix and read" protocols. However, to obtain an acceptable signal, the assay must be set-up with a large fraction of the tracer bound to the receptor (typically >80%). The high amount of bound tracer requires a specific set of equations to be used when interpreting FP derived competition binding results.

In these cases, where a large amount of bound tracer exists, the Cheng-Prusoff equation as mentioned in the discussion of heterologous competition-receptor binding will always lead to an overestimation of the K_i from the IC_{50}. This is because the Cheng-Prusoff equation is strictly given as:

$$K_i = \frac{IC_{50}}{1 + L_f/K_d}$$

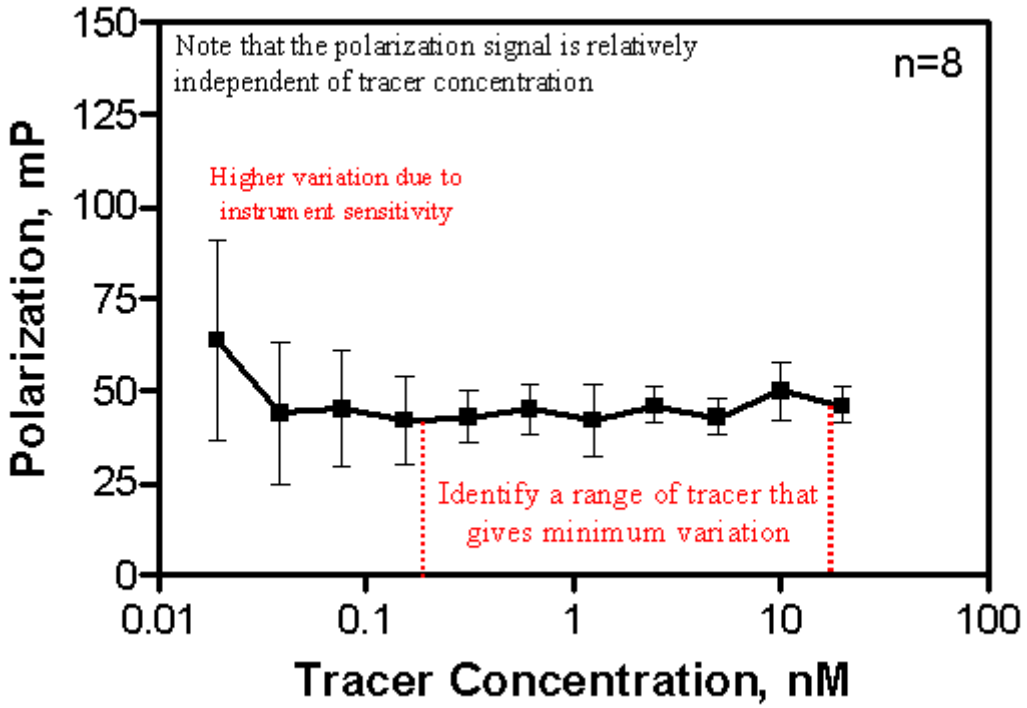

Figure 23: The polarization signal as a function of tracer concentration is shown for a representative tracer. Note that as the signal nears the limits of sensitivity for the detector, the variation increases.

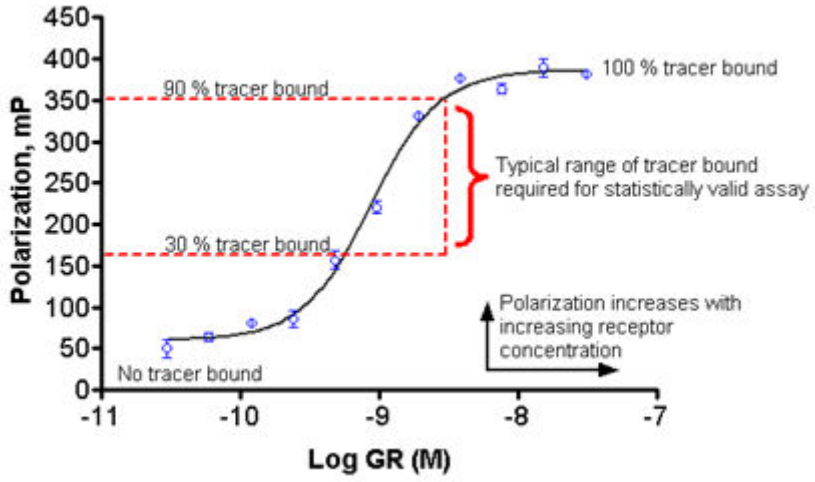

Figure 24: Measuring amount of bound tracer by varying receptor concentration and keeping tracer concentration constant. Here the ligand-binding domain of GR is varied using a constant Kd concentration of a labeled-steroidal ligand (Fluormone™, Invitrogen/ Panvera kits; Data provided by Pharmacopeia).

In the case of FP displacement-binding, the free ligand term [L_f] cannot be substituted for the total ligand concentration [L] because there is little free ligand available. This differs from the typical saturation-binding experiments mentioned in previous sections.

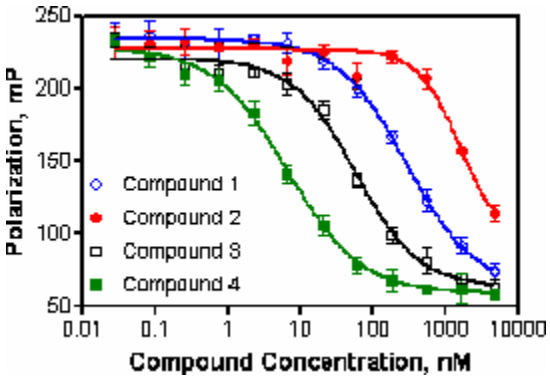

Figure 25: Example pharmacological profile using fluorescence polarization.

Three equations have been presented in the literature to provide a solution to this situation for simple competitive-binding. Munson and Rodbard (3) provide a correction that takes into account the amount of bound tracer. This takes the form of:

$$K_i = \frac{IC_{50}}{1 + \frac{L_0(y_0+2)}{[2K_d(y_0+1)]} + y_0} - K_d[y_0/(y_0+2)]$$

Where y_o is the bound/free ratio of tracer and L_o is the total tracer concentration.

Huang provides an alternative form of this correction in terms of the fraction of bound tracer (4). Rearrangement of Equation 15 given in Huang to solve for K_i yields:

$$K_i = \frac{IC_{50}}{\frac{1}{(1-F_0)} + L_0(2-F_0)/2K_d} - K_d[F_0/(2-F_0)]$$

Where F_o is the fraction of tracer bound and L_o is the total tracer concentration. Huang's result is redundant with the earlier Munson and Rodbard equation except for expressing the equation in terms of the fraction of tracer bound (3,4). Therefore, Eq. 2 and Eq 3 yield the same correction (see below).

These equations should be used instead of Cheng-Prusoff when > 10% of the tracer is bound to the receptor in the assay. A web-based tool to convert IC_{50} values to K_i values in fluorescence-based competitive assays is also available here.

Application of ligand depletion equations once a suitable choice of receptor and tracer concentrations have been made and the resulting assay has been shown to be useful for competitive binding analysis, one can calculate the amount of bound tracer under the assay conditions taking the lower and upper asymptotes as values for free and bound tracer respectively.

Some example competition-binding data (Fluormone™ kit, Invitrogen/Panvera) are shown in Table 11 to illustrate the differences between using the Cheng-Prusoff equation without correction for the amount of bound tracer or each of the above equations which correct for tracer depletion. For these competition-binding experimental results the conditions were:

- Equilibrium dissociation constant, K_d = 0.6 nM (Fluormone™ ligand), determined using
- Bound Tracer Concentration, L_b = 0.9 nM, determined from receptor concentration experiment at constant tracer (L_o), by reading the mP signal and determining the % of maximum
- Total Tracer Concentration, L_o = 1 nM, concentration set near the Kd value
- Total Receptor Concentration, R_o = 4 nM (GR ligand-binding domain), determined from receptor concentration experiment at constant tracer – yields statistically valid assay with robust signal

These concentrations yield the following terms required for Equations 2-4:

- Bound/Free ratio of Tracer, $y_o = L_b/(L_o - L_b) = 0.9/(1\text{-}0.9) = 9$
- Fraction of Tracer Bound, $F_o = L_b/L_o = 0.9/1 = 0.9$

A graphical representation of the data is shown in Figure 26.

Application of Cheng-Prusoff under these conditions can lead to more than 10-fold overestimations of K_i. In many cases all three equations yield similar corrections and as mentioned above Munson & Rodbard and Huang yield identical values (3,4). However, one issue with the Munson & Rodbard and Huang type corrections is that certain combinations of IC_{50}, K_d and bound tracer yield impractical negative values of K_i. This has been discussed in the literature as a breakdown in additional assumptions buried within these equations such as competitive inhibition with a single binding site. For this reason, the Kenakin equation is commonly chosen for performing this correction. Additionally, curve fitting to the equations given in Roehrl et al. (5) can be used to examine if complete inhibition is achieved as well as the K_d of the competitor compound.

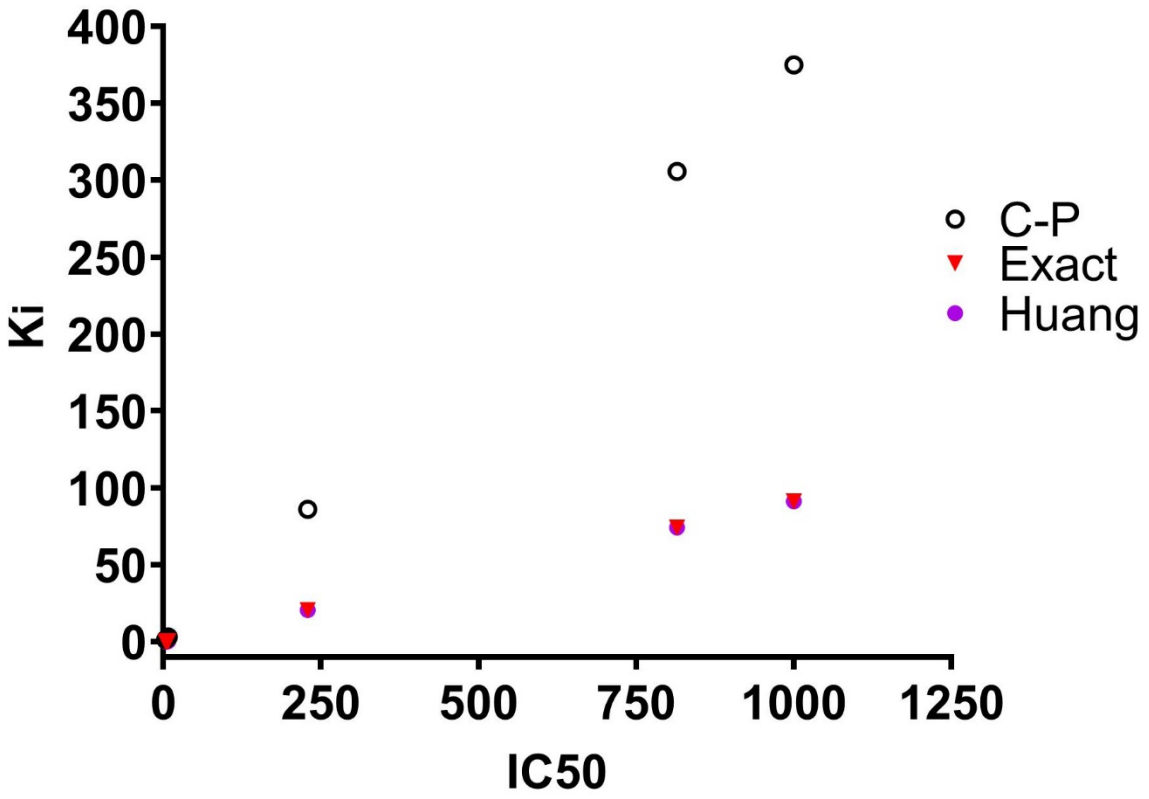

Figure 26: Graphical representation of data in Table 11.

Table 11: Comparison of K_i values determined from ligand depletion correction formulas. Values are in nM. IC_{50} shown is the measured IC_{50} under the assay conditions described in the text. All other values are calculated values. Data provided by Pharmacopeia.

		(1)	Ki, nM	
Ligand	IC_{50}	Cheng-Prusoff	Munson-Rodbard	Huang
Cortisone	8.0	3.0	0.24	0.24
Dexamethasone	3.6	1.3	-0.16	-0.16
Estradiol	815	306	74	74
Testosterone	229	86	20	20
Compound 1	6.4	2.4	0.09	0.09
Compound 2	1000	375	91	91

Detection of Fluorescence Interference from Compounds in FP Screens

All FP experiments start with measuring polarized prompt fluorescence from the assay well. This makes these experiments susceptible to fluorescence interference by compounds present in the well. However, a helpful method to address this issue has been presented by Turconi et al. (6). This paper calculates the total fluorescence intensity from a well (given by S + 2P; see references in above paper) and the observed anisotropy [1] from the each well to flag false positive wells due to fluorescence interference. Figure 27 illustrates the use of this method.

Three cases are illustrated in Figure 27. In case A, the compounds in the wells are not active or fluorescent. Therefore the measured Fluormone tracer is bound to GR ligand-binding domain (GR-LBD) and the anisotropy

values are clustered around the 0% inhibition value. Furthermore, there is no change in fluorescence intensity in the compound-containing wells relative to the control wells. In case B, the compounds in the well are active in the assay but not fluorescent. Therefore, the tracer is being displaced from the GR-LBD and the anisotropy values distribute from high to low inhibition values. Again, there is no change in the total fluorescence intensity. In case C, the compounds appear active as they show a decrease in anisotropy values suggesting that the tracer has been displaced from the GR-LBD. However there is a correlation between decreasing anisotropy and increasing fluorescence intensity in the wells with the lowest anisotropy values showing more than a 35-fold increase in the fluorescent intensity relative to control values. This suggests that the measured FP is due to the compounds themselves rather than the tracer.

In typical FP-receptor binding experiments the tracer is kept at a low nM concentration while the compounds that are being screened are typically in the μM range. If these compounds are fluorescent at the detection wavelengths then their fluorescence can easily overcome that of the tracer. As compounds in screening campaigns are typically of low molecular weight (<500 Da) they will exhibit low anisotropy values. Compounds in case C was of this type and subsequent secondary assays showed them to be inactive. A final case not shown above is where the compounds are both fluorescent and active. Turconi et al. present an equation that can be used to fit the fluorescent intensity data to the case where anisotropy changes without displacement of the ligand (6). The solid line in case C above shows an example of this fit. One can then evaluate outliers from this curve fit in terms of potential active but fluorescent compounds.

It is also possible to observe changes in polarization that are due to fluorescent compounds present as aggregates. In this case, the fluorescence intensity will increase along with the polarization as long as the aggregation does not quench the fluorescence. Additionally, light scattering from particulates or compound participates can lead to apparently high polarization values. For receptor binding experiments as described above this superfluous increase in polarization may mask any decrease in polarization due to an active compound and thus result in a false negative. Careful examination of the fluorescence intensity versus polarization plots should identify these artifacts.

1 Anistropy is derived by measuring the S and P channels as described above, however the fluorescence is expressed with the denominator representing the total fluorescence intensity from the sample. The equation for calculating anisotropy is given by:
$$a = \frac{(P - S)}{(S + 2P)}$$

Anisotropy and polarization are related by the equations given below where P is the polarization and a is the anisotropy:

$$P = \frac{(3a)}{(2 + a)} \; AND \; a = \frac{2P}{(3 - P)}$$

In general, anisotropy is more useful analyzing complex systems or mixtures as the equations are simpler to express in terms of anisotropy (1). Arguably, screening data should be presented in terms of anisotropy rather than polarization but this convention has not been adopted as yet.

- [L] - Radioligand Concentration
- [R] - Receptor Concentration
- [RL] - Concentration of Receptor-Ligand complex
- K_d - equilibrium dissociation constant for radioligand ([RL] yielding Bmax/2)
- K_i - equilibrium dissociation constant for an unlabeled compound
- IC_{50} - concentration of unlabeled drug which results in 50% inhibition of binding activity
- k_{on} - association rate constant
- k_{off} - dissociation rate constant
- k_{obs} - observed association rate constant

- B_{max} - maximum number of binding sites
- NPE - Non-proximity Effects
- NSB - Nonspecific binding
- K_i C-P = K_i Cheng-Prusoff
- K_i T-B = K_i Tight-Binding

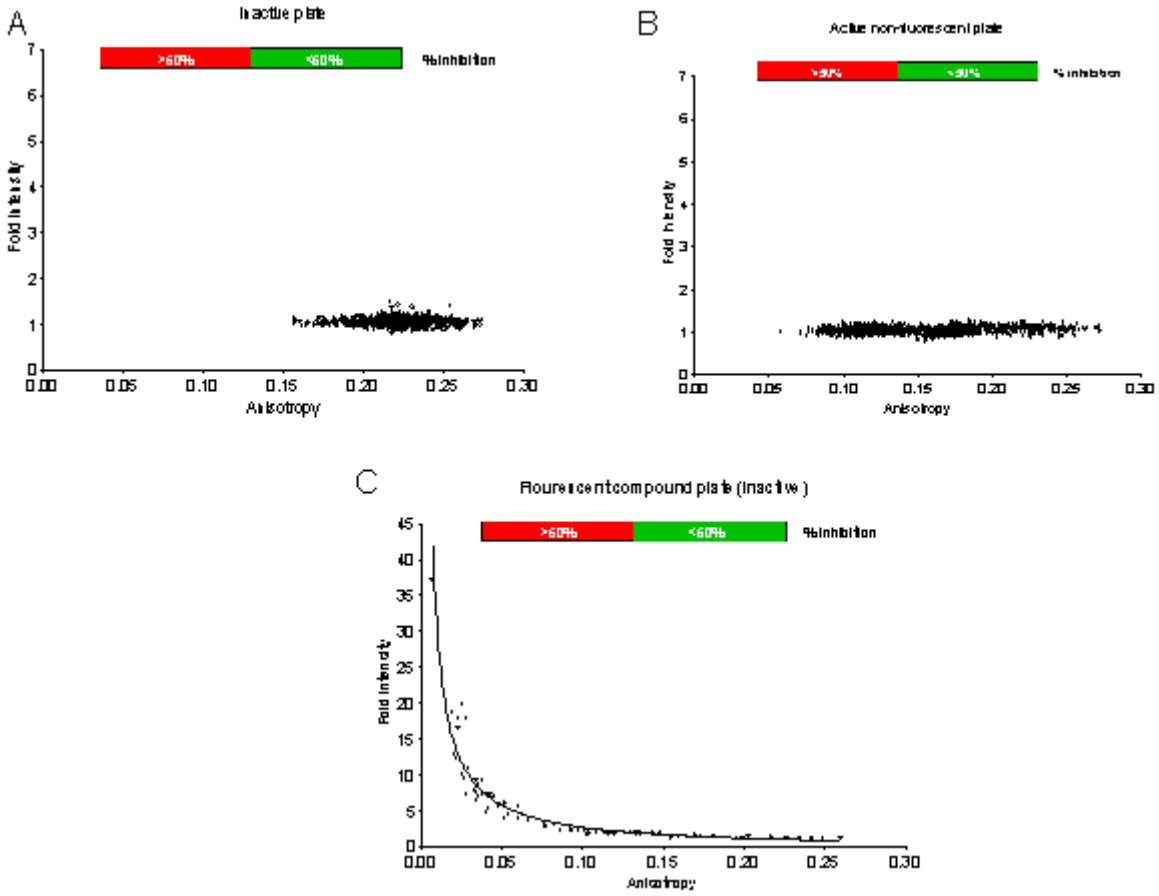

Figure 27: Plots of the total fluorescence intensity (normalized to the control well values, e.g. the total fluorescence intensity of the assay in the absence of compounds) versus the anisotropy. A) the compounds in the wells are not active or fluorescent. B) the compounds in the well are active in the assay but not fluorescent. C) the compounds appear active as they show a decrease in anisotropy values.

References

Primary References

1. Cantor and Schimmel in Biophysical Chemistry Part II: Techniques for the study of biological structure and function. pp. 454-465. (1980).
2. Roehrl MHA, Wang JY, Wagner G. A General Framework for Development and Data Analysis of Competitive High-Throughput Screens for Small-Molecule Inhibitors of Protein-Protein Interactions by Fluorescence. 2004. Biochemistry. 2004;43(51):16056–16066. PubMed PMID: 15610000.
3. Munson PJ, Rodbard D. An exact correction to the "Cheng-Prusoff" correction. J. Receptor. Res. 1988.:533–546. PubMed PMID: 3385692.
4. Huang X. Fluorescence polarization competition assay: The range of resolvable inhibitor potency is limited by the affinity of the fluorescent ligand. J. Biomol. Screening. 2003;8:34–38. PubMed PMID: 12854996.
5. Roehrl MHA, Wang JY, Wagner G. Discovery of Small-Molecule Inhibitors of the NFAT-Calcineurin Interaction by Competitive High-Throughput Fluorescence Polarization Screening. 2004. Biochemistry. 2004;43(51):16067–16075. PubMed PMID: 15610001.
6. Turconi S, Shea K, Ashman S, Fantom K, Earnshaw DL, Bingham RP, Haupts UM, Brown MJB, Pope A. Real experiences of uHTS: A prototypic 1536-well fluorescence anisotropy-based uHTS screen and application of well-level quality control procedures. J. Biolmol. Screening. 2001;6:275–290. PubMed PMID: 11689128.

Websites

1. GraphPad Prism (https://www.graphpad.com/scientific-software/prism/)
2. Receptor Binding Key Concepts on GraphPad Prism site (https://www.graphpad.com/guides/prism/7/curve-fitting/index.htm?reg_principles_of_radioligand_bind.htm)
3. Perkin Elmer SPA Information (http://www.perkinelmer.com/category/scintillation-proximity-assay-spa)

General Receptor Binding: Suggested Reading

Textbook of Receptor Pharmacology. (2003). Second Edition. Foreman, J.C. and Johansen, T., Editors. CRC Press, New York.

Kenakin, T. (1997): Pharmacologic Analysis of Drug-Receptor Interaction. Lippincott-Raven Publishers, Philadelphia.

Receptor Binding Techniques. (1999). Methods in Molecular Biology Series, Volume 106, Keen, M., Editor. Humana Press, New Jersey.

The Pharmacology of Functional, Biochemical, and Recombinant Receptor Systems. (2000). Handbook of Experimental Biology, Volume 148, Kenakin, T and Angus, J.A., Editors. Springer-Verlag, New York.

Receptor-Ligand Interactions: A Practical Approach. (1992). The Practical Approach Series. E.C. Hulme, Editor. Oxford University Press, New York.

Receptor Biochemistry: A Practical Approach. (1990). The Practical Approach Series. E.C. Hulme, Editor. Oxford University Press, New York.

Motulsky, H.J. Analyzing Data with GraphPad Prism. (1999). GraphPad Software, San Diego, CA. Available at: http://www.graphpad.com/manuals/analyzingdata.pdf

Limbird, L.E. Cell Surface Receptors: A Short Course on Theory and Methods. (1996). Kluwer Academic Publishers, Boston.

Winzor, D.J. and Sawyer, W.H. Quantitative Characterization of Ligand Binding. (1995). Wiley-Liss, Inc., New York.

Lutz M. W., Menius J. A., Choi T. D., Gooding-Laskody R., Domanico P. L., Goetz A. S., Saussy D. L. Experimental design for high-throughput screening. Drug Discovery Today. 1996;1(7):277–286.

Kahl S. D., Hubbard F. R., Sittampalam G. S., Zock J. M. Validation of a High Throughput Scintillation Proximity Assay for 5-Hydroxytryptamine1E Receptor Binding Activity. J. Biomol. Screen. 1997;2(1):33–39.

Sun S., Almaden J., Carlson T.J., Barker J., Gehring M.R. Assay development and data analysis of receptor-ligand binding based on scintillation proximity assay. Metab Eng. 2005;7:38–44. PubMed PMID: 15721809.

Fluorescence Polarization: Suggested Reading

Lin S, Bock CL, Gardner DB, Webster JC, Favata MF, Trzaskos JM, Oldenburg KR. Anal Biochem. 2002;300:15–21. A high-throughput fluorescent polarization assay for nuclear receptor binding utilizing crude receptor extract. PubMed PMID: 11743686.

Lee PH, Bevis DJ. Development of a homogeneous high throughput fluorescence polarization assay for G protein-coupled receptor binding. J. Biomol. Screening. 2000;5:415–419. PubMed PMID: 11598459.

Banks P, Harvey M. Considerations for using fluorescence polarization in the screening of g protein-coupled receptors. J Biomol Screen. 2002;7:111–7. PubMed PMID: 12006109.

Do EU, Choi G, Shin J, Jung W-S. Anal. Biochem. 2004;330:156–163. and Kim, S-I Fluorescence polarization assays for high-throughput screening of neuropeptide FF receptors. PubMed PMID: 15183774.

Allen M, Reeves J, Mellor G. High throughput fluorescence polarization: A homogeneous alternative to radioligand binding for cell surface receptors. J. Biomol. Screen. 2000;5:63–69. PubMed PMID: 10803605.

Burke TJ, Loniello KR, Beebe JA, Ervin KM. Development and application of fluorescence polarization assays in drug discovery. Combinatorial Chemistry & High Throughput Screening. 2003;6:183–194. PubMed PMID: 12678697.

Beasely J.R., Dunn DA, Walker TL, Parlato SM, Lehrach JM, Auld DS. Evaluation of compound interference in immobilized metal ion affinity-based fluorescence polarization detection with a four million member compound collection. Assays and Drug Development Technologies. 2003;1:455–459. PubMed PMID: 15090182.

Protease Assays

Guofeng Zhang, Ph.D.[1]

Created: May 1, 2012; Updated: October 1, 2012.

Abstract

Proteases are important drug targets; the first drugs to reach the market were antihypertensives and antivirals. Designing HTS assays for these targets requires thorough understanding of the biochemistry and biology of these enzymes as well as various assay formats. In this chapter, the authors present basic properties of protease enzymes, sensitive fluorescent assay formats compatible with HTS, both in homogeneous and separation-based approaches. Sections on hit selection and data analysis concepts for identifying inhibitors are also included with an extensive set of literature references.

Introduction

The study of proteases has a long history, and the scientific community has accumulated a wealth of knowledge, which makes the proteases one of the few well studied enzyme families. A simple search using the NIH PubMed server will find hundreds of thousands of protease related articles. In fact, the accumulated knowledge of some protease family members is comprehensive enough to make them classical teaching materials in college Biochemistry textbooks.

Proteases play critical roles in multiple biological pathways - the human genome sequencing project revealed that ~2% of our genes encode proteases - and are implicated in many diseases, including infectious diseases, inflammation, cancer, degenerative diseases, and many others (1). The search for small molecule drugs that target proteases has been an area of intensive research in both academia and industry for decades. These efforts have been noticeably productive, leading to more than two dozen FDA-approved drugs for diverse indications (http://www.ddw-online.com/s/2003/p142685/winter-2003-edition.html) and many more currently in clinical trials and development. A simple search for protease inhibitors in the Drugbank database (http://www.drugbank.ca/) returns several hundred hits, (although the majority of hits are different names for the same drug). The first protease inhibitors that became approved drugs were antihypertensives and antivirals. Since the approval of the angiotensin-converting enzyme (ACE) inhibitor Captopril from Bristol-Myers Squibb for the treatment of hypertension in 1981, there have been eight ACE inhibitors developed by various companies and approved for the same indication. Similarly, there are now more than ten approved drugs targeting HIV proteases or HCV proteases. HIV protease inhibitors were instrumental in proving the viral etiology of AIDS; they have turned this once deadly infection into a manageable condition. The HCV protease inhibitors are revolutionizing the treatment of this disease, enabling faster, more reliable treatment (http://www.fda.gov/ForConsumers/ByAudience/ForPatientAdvocates/HIVandAIDSActivities/ucm118915.htm). Since these early protease inhibitors became available, protease inhibitors have proved useful in other therapeutic areas. Key examples include Argatroban from GlaxoSmithKline, the thrombin inhibitor that the FDA approved for the treatment of coagulation disorders in 2000; the DPP4 inhibitor JANUVIA® (Sitagliptin) from Merck, approved for the treatment of diabetes in 2006; and VELCADE® (Bortezomib), a proteasome inhibitor from Millennium, approved for the treatment of multiple myeloma in 2003 (2). These examples are a fraction of the total, but they

Author Affiliation: 1 Platform Technology and Science, GlaxoSmithKline, 1250 S. Collegeville Road, Collegeville, PA 19426; Email: Guofeng.2.zhang@gsk.com.

Corresponding author.

*Edited by Tod Holler and Andrew Napper, Ph.D.

represent both the large number of companies that have conducted research targeting proteases, and the diversity of disease states in which proteases are important. In this section, we will define the term "protease" broadly. The definition will include endopeptidases, which cleave peptide bonds between non-terminal amino acids, and exopeptidases, which remove an amino acid from the end of a polypeptide chain. The exopeptidases include both aminopeptidases, which cleave from the amino end of a peptide and carboxypeptidases, which cleave from the carboxylic end of a peptide. We will also include protease-like enzymes that cleave isopeptide bonds, such as the deubiquitinases and de-Neddylase, in our definition. Finally, we will extend our definition to include an enzyme complex that contains multiple components, such as the 26S proteasome and the COP9 signalosome (CSN).

To clarify the terms used in this section, Figure 1 shows a general protease reaction in which the protease cleaves a scissile amide bond from the substrate, which can be either a protein or a synthetic peptide. Substrate amino acids that are on the amino (N) side of the scissile bond are numbered P1, P2, and P3 … (called P sites) with the one closest to the scissile bond numbered P1. The same scheme applies to the residues that are on the carboxyl (C) side of the scissile bond. In this case, the residues are numbered P1', P2', P3' … (called P' sites). Depending on the nature of the protease, the number of amino acids on either side of the scissile bond of the substrate (shown in Figure 1) can vary. There will be only one or two amino acids on the N-terminal side of the scissile bond of aminopeptidase substrates and one or two amino acids on the C-terminal side of the scissile bond of carboxypeptidase substrates, but there will be more amino acids on both sides of the scissile bond of endopeptidase substrates.

The search for small molecules that modulate protease activity continues to be a hot area of research, with multiple targets in play. As a result, the demand for robust biochemical assays that can efficiently assess structure-and-activity relationships still exists. In addition, the discovery of new protease-like drug targets, such as the cysteine protease-like deubiquitinases and zinc-dependent COP9 signalosome (CSN), demands innovation in protease assay methodology. Like many enzyme target classes, both binding assays, which assess the interaction between a small molecule and the target protein, and functional assays, which measure a small molecule's effect on enzyme activity, are useful in the search for protease inhibitors. This section will mainly focus on biochemical assays that are amendable for high throughput screening. Binding assays in general have been recently reviewed (3, 4) and will be mentioned only briefly, when needed. Many biochemical assays exist for proteases, and they can be grouped according to the basic principles they share. To simplify the discussion, we will categorize the assays into two groups: homogenous assays and separation-based assays. In a homogenous assay, substrate turnover can be detected as a signal change directly from the reaction mixture without further sample processing. In a separation based assay, the product and/or remaining substrate are separated from the reaction mixture for detection after the enzymatic reaction is stopped.

Homogenous Assays

A homogenous assay does not require separation of product and/or substrate from the reaction mixture. Instead, it relies on a physical change accompanying substrate turnover. This change is usually a readily-detected colorimetric or fluorescent signal from a synthetic peptide substrate. A native peptide substrate does not usually offer such convenience. Fortunately, most proteases can tolerate some degree of substrate modification. This makes it feasible to add reporter groups, for example fluorogenic or chromogenic moieties, to the substrate to assist the detection of turnover. Fluorescence-based approaches have been widely used in assays for proteases and other drug targets mainly because of their high sensitivity. This characteristic makes fluorescence-based assays particularly suitable for the dense, low volume formats employed in high throughput screening.

A number of fluorescence-based approaches have been used to measure protease activity. Those most widely used, shown in Figure 2, include (a) measuring the change in fluorescence intensity of a fluorophore chemically quenched by amide linkage to the peptide, (b) measuring the change in fluorescent signal from a pair of

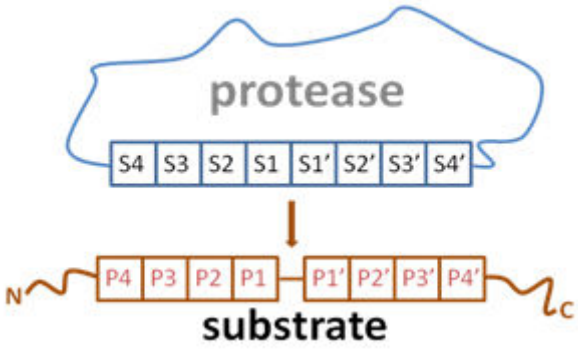

Figure 1. Conventional nomenclature for protease reactions. The amino acids on amino side of the scissile bond are labeled with the letter P and the ones on the carboxyl side are labeled with P'. Their corresponding binding sites on the protease are labeled with S and S', respectively.

fluorescent dyes that interact via a resonance energy transfer (FRET) system, (c) measuring the change in fluorescent intensity from a fluorescent dye that is quenched by a near-by nonfluorescent dye, and (d) measuring a change in fluorescence polarization. These four formats will be discussed in detail in the next sections.

Fluorescence intensity assays monitoring change from chemically quenched dyes

In this approach, a fluorescent dye that contains a reactive amine group can be covalently attached to the carboxyl end of a peptide substrate *via* an amide bond. The sequence of the peptide moiety provides protease specificity, and the dye moiety functions as a reporter for enzymatic activity. The target protease will cleave the amide bond when the peptide binds and forms a productive complex. The fluorescence of the attached dye, which is quenched when covalently attached to the peptide, increases dramatically when released by a protease cleavage, as shown in Figure 2a. When the assay is configured properly, the fluorescence intensity of the released dye is linearly proportional to the enzyme activity. The most commonly used fluorophores are coumarin derivatives (5, 6), such as 7-amino-4-methylcoumarin (AMC) and 7-amino-4-(trifluoromethyl) coumarin (AFC). The fluorescent dye rhodamine has also been used in this approach. A bisamide of rhodamine is non-fluorescent, while a monoamide derivative is highly fluorescent. Rhodamine-based substrates for serine proteases (7) and a ubiquitin-linked rhodamine 110-glycine deubiquitinase substrate (8, 9) have been reported. This chemically quenched approach has been widely used in protease assays, particularly in high throughput assays designed to find inhibitors of proteases implicated in human diseases, such as cathepsins, caspases and deubiquitinases.

The chemically quenched approach applies only to proteases that can tolerate major modifications on the P1' site of the substrate (see Figure 1); it does not work for proteases that have strict specificity requirement for P1' site, such as carboxypeptidases. However, a similar approach based on colorimetric difference between substrate and product was developed for carboxypeptidases. As an example, furylacryloyl-Ala-Lys and furylacryloyl-Ala-Arg were developed as substrates for carboxypeptidase N; enzyme activity could be followed by measuring absorption decrease at 340 nm (10). Unfortunately, its application in drug discovery screening is limited by the low sensitivity of measurement and its vulnerability to interference from compounds that absorb at 340 nm.

Fluorescence resonance energy transfer (FRET) assays

In order to use the fluorescence intensity format described above, the amino acids on the C-terminal side of the cleavage site (P' sites, Figure 1) must be replaced with a fluorogenic group, and therefore the integrity of the peptide sequence surrounding the scissile bond is sacrificed. In some cases, particularly for endopeptidases, deubiquitinase and deubiquitinase-like enzymes, maintaining the sequence integrity surrounding the cleavage

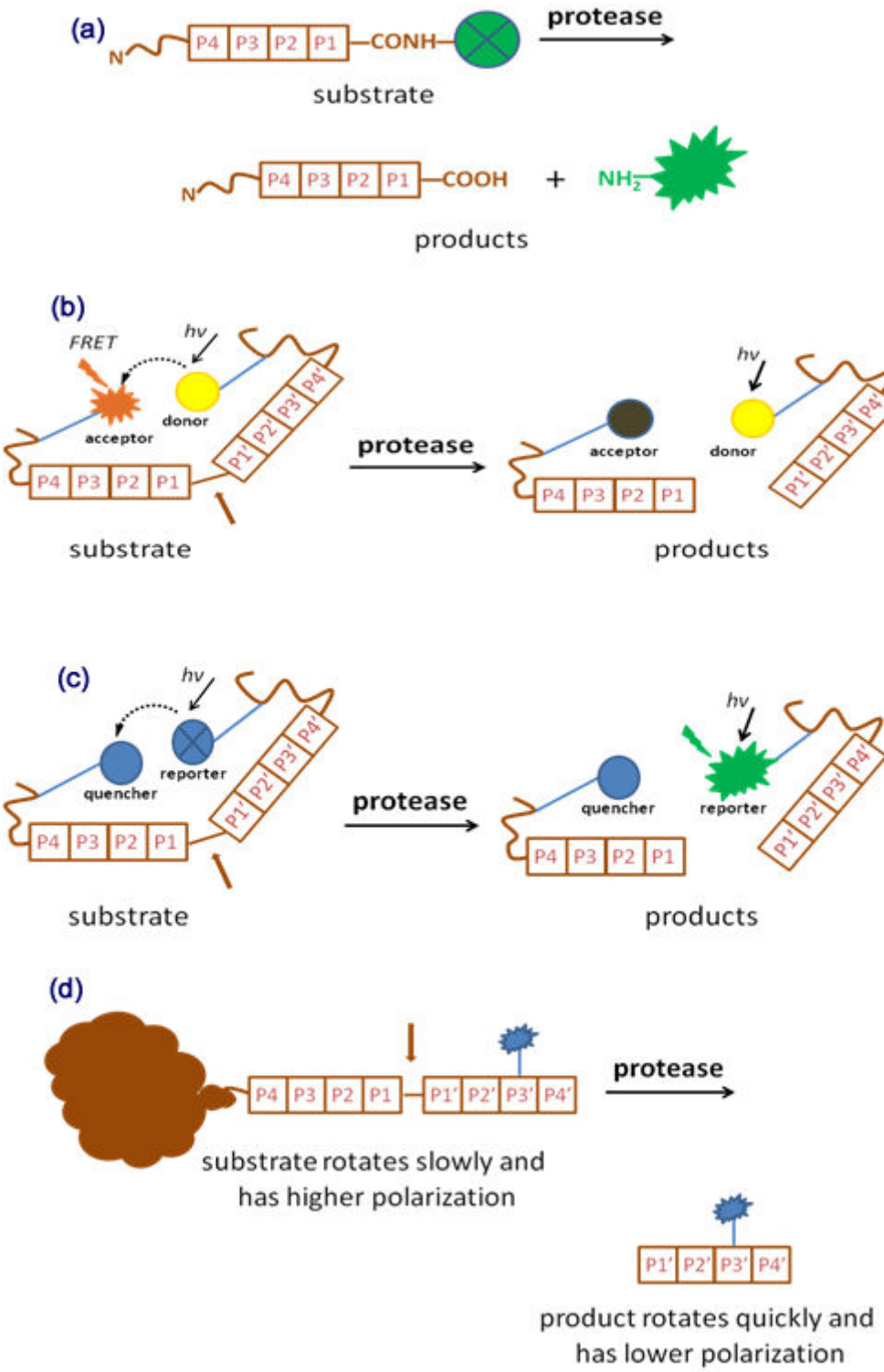

Figure 2. Basic principles of fluorescence-based homogenous assays for measuring protease activity. (a) Fluorescence intensity assay in which a fluorogenic group is linked to the carboxyl end of a peptide *via* an amide bond, and its fluorescence increases upon release by the action of a protease; (b) Resonance-energy-transfer-based assay in which a FRET signal can be detected when the donor and acceptor are in close proximity. The pair separates upon peptide cleavage and the FRET signal decreases; (c) Dual-label quenched-pair fluorescent assay in which the fluorescence intensity of the reporter is suppressed by the quencher because of its close proximity. The pair separates upon peptide cleavage and the fluorescence intensity from the reporter group is significantly increased; (d) Fluorescence

polarization assay in which the substrate and the product give different emission polarization signals because of their different sizes ("digestive" fluorescence polarization assay) .

site is critical, so modification of the P' sites close to the scissile bond should be avoided. For these targets, a FRET-based approach can be employed. In this approach (Figure 2b), two fluorescent groups are placed on each side of the scissile bond, one called "donor" and the other "receptor". The donor and the receptor are chosen such that the emission wavelength of the donor overlaps with the excitation wavelength of the receptor. The locations of the donor and receptor groups are chosen such that they will not compromise the sequence integrity near the scissile bond, but are close enough to each other that FRET can efficiently take place. Upon cleavage of the scissile bond, the fluorescent pair disassembles and the FRET signal decreases.

This particular format is limited in that it is a signal decrease assay and a relatively large percentage of substrate-turnover is required for a statistically meaningful readout in endpoint format. In addition, it can be subject to a low signal–to-noise , from time to time, due to overlap between donor and receptor fluorescence spectra. Fortunately, a practical solution had been achieved thanks to the efforts from various laboratories (11-14), which are discussed separately below.

Fluorescence intensity assays monitoring change from dual-label quenched pairs

To convert a signal-decrease FRET assay into a signal-increase assay, one can choose a donor and receptor pair to allow a maximal overlap between the donor's fluorescence and the receptor's absorption, and then monitor the donor emission as readout. With the receptor in close proximity, the donor's emission is re-absorbed upon excitation and cannot reach the detector, which results in a low level of fluorescent signal. Upon cleavage by a protease, the pair separates and the donor no longer transfers its emission to the receptor, which leads to an increase in the fluorescence intensity observed from the donor. In these cases, the donor alone takes the role as the "reporter" for enzymatic activity and the receptor functions solely as a "quencher" for the reporter's fluorescence when they are in close proximity, as shown in Figure 2c.

Two types of quenchers exist. The early quenchers were generally a second fluorescent dye; examples include fluorescein and rhodamine (reporter and quencher) and their derivatives. The readout can be either the reporter fluorescence alone or the ratio between fluorescence of the reporter and the fluorescence of the quencher. Assays using fluorescent quenchers are usually limited by high background signal caused by incomplete separation of the reporter and quencher spectra. In the last decade a new generation of "dark quenchers" have been developed to address this issue. These quenchers do not have native fluorescence and therefore do not contribute significantly to background noise. This type of quencher offers excellent signal increase upon the separations of the energy transfer pair. Examples include Dabcyl (4,(4'-dimethylaminophenylazo)benzyl) (12, 15), and the "black hole quenchers" built on a polyaramatic-azo backbone (13). Recently, this approach has been extended to construct internally quenched fluorescent diubiquitin substrates for deubiquitinases (commercialized as IQF-DiUb™ by Lifesensors Inc.). This substrate maintains the isopeptide nature of the scissile bond and provides full occupancy of both the S and S' pockets from the deubiquitinases. It is hypothesized that using this substrate might increase the chance of finding inhibitors with various modes of action. A similar approach can be designed for deneddylases and desumolyases, which catalyze the deneddylation and desumoylation in some protein modification processes by cleaving the isopeptide bonds between NEDD8 or SUMO and the protein being modified (16, 17).

Fluorescence polarization (FP) assays

Proteases can also be assayed using an FP-based format. In this assay format, a protein or a long peptide substrate is labeled with one or more fluorescent dyes. These substrates give a high polarization signal due to

their large size. Upon cleavage by a protease, the large substrate is converted into smaller fragments that give a lower polarization signal due to an increased rotation rate. This approach, which relies on the protease enzymatic activity and is sometimes referred to as a digestive fluorescence polarization assay is illustrated in Figure 2d.

In some cases, a competition binding assay can be configured using FP as the readout. In this format, the FP signal from a fluorescently labeled non-cleavable peptide substrate analog is monitored, as shown in Figure 3. Its FP signal is higher when the peptide is bound to a larger protein due to the slower rotation rate of a large complex; if the binding of a fluorescently silent small molecule prevents the binding of the peptide to the larger protein, the peptide will remain unbound in solution and tumble faster, which gives a lower FP signal. Therefore a FP signal decrease indicates the presence of a small molecule that competes with the labeled peptide analog for the protease's substrate binding site. The length of the peptide used in this approach is limited to 15 – 20 amino acids, since the difference between the FP signals of the bound and the unbound peptide decreases when its length increases, reducing the assay signal window. The affinity of the labeled peptide must be strong enough, such that the fraction of protein-bound peptide to total peptide can be set between ~0.3 - 0.7, typically at enzyme concentration well under 1 μM (preferably at nM level). This usually gives a reasonable polarization signal window and a decent sensitivity to small molecule competition.

It is worth noting that FP measures a ratio of polarized to non-polarized fluorescence and, in general, is concentration-dependent only in a moderate range. Outside that range the signal change will not be sensitive to changes in product concentration, which limits the general application of this approach.

Separation-Based Assays

Assays based on labeled peptides offer great advantages. Not only are they suitable for large library screening (cost and throughput), in many cases they also enable a kinetic reading of the enzymatic reaction. Kinetic reads are valuable when characterizing a compound's interaction with the target in detail, such as investigating the time-dependence of inhibition, or the on- and off-rate constants for binding to target. However, there are cases where a substrate cannot be labeled, or where a labeled substrate cannot meet the requirements for specific studies. A separation-based assay will be needed in these cases. In separation-based assays the product and/or the substrate can be isolated from the reaction mixture and measured independently. Typically, the reaction is stopped when its progress is within a pre-determined linear range, but enough substrate has to be turned over to give a robust signal. This approach is illustrated in Figure 4.

The substrate and the product can often be separated by liquid chromatography and then monitored either by their retention times on a column, or by their molecular weights in a mass spectrometer. The principles of liquid chromatography and mass spectrometry are well documented, and high throughput assay platforms have been developed for both. For example, a multichannel microscale HPLC systems has been developed that can run several micro-columns simultaneously (18), making it suitable for screening fairly large compound sets. Additionally, the RapidFire™ high-throughput mass spectrometry system developed by BIOCIUS Life Sciences (now part of Agilent) can run at a speed of seconds per sample (in most case, this is not total separation of product and substrate, rather it is separation from the reaction buffer) (19, 20). These technologies can be used for primary screening when labeled assays are not suitable and can also be used to confirm hits from label-based assays.

Triaging Assay Hits

The major application of the methods described above is to find and characterize small molecule protease inhibitors, usually through screening large compound collections. It is prudent to note that all of these assays are subject to false hits. False hits can be categorized into two groups based on the origin of the interference: those that interfere with the detection of the assay signal (assay format dependent), and those that interact

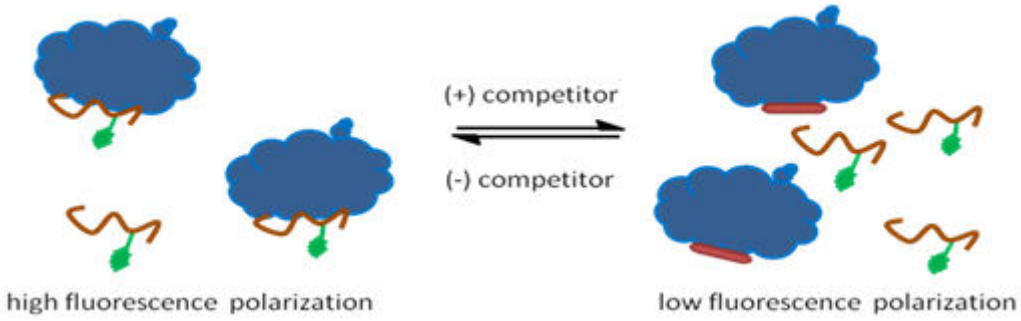

Figure 3. Fluorescence polarization based competition assay. Binding of a small molecule (represented by the brown bars) to the same site on target displaces the fluorescence labeled peptide analog and results in signal decrease.

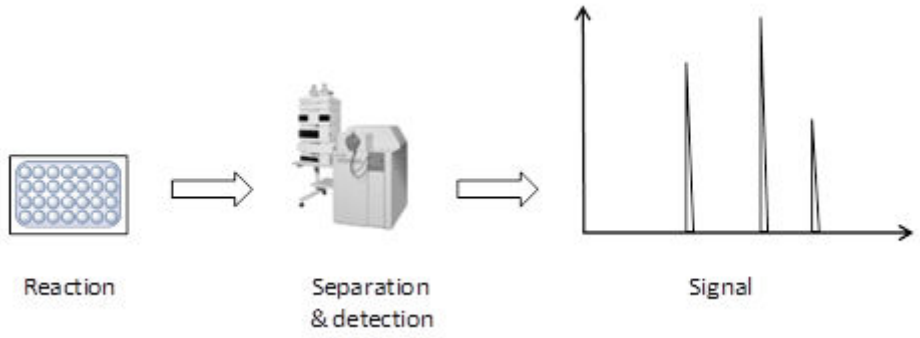

Figure 4. Schematic illustration of a separation-based protease assay in which the product and substrate are separated before being analyzed.

nonspecifically with the target enzyme (assay format independent). False hits can be misleading and should be eliminated from consideration as early as possible using a triage process. False hits that interfere with signal detection in fluorescence-based assays are either auto-fluorescent at the detection wavelength, or quench the fluorescence signal used as the enzyme activity readout. These types of interference can be detected by measuring the fluorescence signal of a stopped enzyme reaction in the presence of compounds that are added post-reaction (this way only the compound interference with detection is measured), preferably at varying compound concentrations. A signal increase will be observed if a compound is auto-fluorescent and a signal decrease will be observed if a compound is a fluorescence quencher.

Interference with signal detection can also be observed in chromatography-based assays if a compound co-elutes with substrate or product. For example, a compound will be a false inhibitor if it co-elutes with a substrate and only the substrate decrease is monitored, because there will be less "apparent" substrate decrease in the presence of this compound. Similarly, a compound will appear to be an activator if it co-elutes with product and only the product peak is monitored. This kind of interference can be addressed by changing the chromatography protocols, for example by changing the mobile phase or gradient, which may resolve the overlapping peaks, or by monitoring both substrate and product, which will allow aberrant results to be detected more easily.

The occurrence of nuisance hits that interact non-specifically with the target enzyme is usually assay format independent. A number of mechanisms of nuisance inhibition have been proposed and investigated (21), including inhibition *via* compound aggregation, *via* enzyme degradation and precipitation, *via* chemical reactivity and/or oxidation (22), and *via* trace amount of impurity, for example a metal catalyst leftover from synthesis. Cysteine proteases are generally more susceptible to nuisance inhibition *via* chemical reactivity, oxidation and trace metal contamination (23) because of the high reactivity of the thiol (or thiolate) group at the

enzyme active site. Several diagnostic assays for nuisance inhibitors can be found in the literature. The kinetics of inhibition exhibited by nuisance inhibitors, for example, are usually time-dependent and non-stoichiometric, which is often manifested by a high Hill slope for the dose-response curve. Nuisance inhibitors commonly inhibit a number of unrelated enzymes, and their IC_{50} values usually show a significant shift when assay conditions are changed. Increasing the concentration of the target enzyme and including a detergent in the buffer are changes typically employed. It is not trivial, and frequently impractical, to test HTS hits in all these assays. The most reliable and efficient first filter to eliminate nuisance hits is to change the concentration of the enzyme target (24).

Data Analysis for Time Dependent Inhibitors and Covalent Inhibitors

Data analysis for protease inhibition is not very different from other enzyme targets, in that a compound's potency is calculated based on percentage inhibition of enzymatic activity at different compound concentrations. However, this simple approach only works well when a rapid equilibrium between the free inhibitor and the enzyme-inhibitor complex is established during the assay. Time-dependent inhibitors have been developed for most proteases. Important examples include the boronic acids that inhibit serine proteases (25, 26), the ketones and aldehydes that inhibit thiol proteases (27-29), and the metal chelators that inhibit metalloproteases (30, 31). For those inhibitors, an accurate assessment of compound potency requires careful data analysis that takes into account the shift in equilibrium over time. Scheme 1, in which the rapid initial formation of an enzyme inhibitor complex (E•I) is followed by a slow isomerization step that leads to a tighter complex (E•I)*(32).

Scheme 1

$$E + I \underset{k_4}{\overset{k_3}{\rightleftharpoons}} E\bullet I \underset{k_6}{\overset{k_5}{\rightleftharpoons}} E\bullet I^*$$

The presence of a time-dependent inhibitor makes the transition from free enzyme to the final stable E•I* complex more pronounced over time, and the rate of product formation (P) follows time (t) in an inverse exponential manner, as illustrated in Figure 5.

Equation 1

$$P = v_s t + (v_0 - v_s)(1 - e^{-kt})/k$$

where v_0 is the initial reaction velocity, v_s is the steady state velocity and k is the first order rate constant for conversion of E•I to E•I*.

Because many approved drugs are covalent modifiers (33, 34), it is worth mentioning that this relationship is also valid for covalent inhibitors that inactivate the enzyme irreversibly. For covalent inhibitors the final steady state velocity is zero, which reduces Equation 1 to Equation 2, as shown below.

Equation 2

$$P = v_0(1 - e^{-kt})/k$$

where, k is the enzyme inactivation rate constant.

Good review articles addressing data analysis of time-dependent inhibition and covalent modification of enzymes have appeared in the literature. For a discussion of this topic and examples, please refer to those articles (32, 35, 36). It is worth noting that the equations describing this phenomenon, especially equation 1 mentioned

above, must be modified to account for the diminished populations of free enzyme and free inhibitor upon the formation of enzyme-inhibitor complex when dealing with time-dependent inhibitors that are also tight-binding (K_i ~ [E]). Morrison and Walsh address the mathematical solutions explicitly (32).

Conclusion

Proteases are important drug targets and they are among the best studied enzymes. Most assays discussed here are amenable to HTS and cost-efficient, which enables protease drug discovery in a variety of research organizations. Challenges do exist. Among them, the challenge of designing assays that are less susceptible to nuisance hits, especially for cysteine proteases, persists.

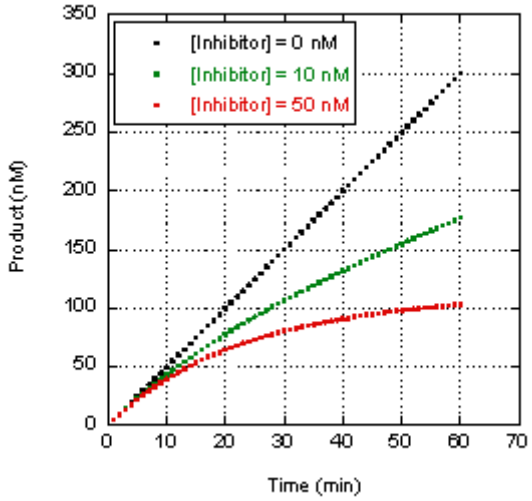

Figure 5. Illustration of time courses of product formation in the presence of a time-dependent inhibitor. The overall decrease in product formation rate depends on the concentration of the inhibitor added into the assay.

References

1. Turk B. Targeting proteases: successes, failures and future prospects. Nat Rev Drug Discov. 2006;5(9):785–99. PubMed PMID: 16955069.
2. Chen D., et al. Bortezomib as the first proteasome inhibitor anticancer drug: current status and future perspectives. Curr Cancer Drug Targets. 2011;11(3):239–53. PubMed PMID: 21247388.
3. Zhu Z., Cuozzo J. Review article: high-throughput affinity-based technologies for small-molecule drug discovery. J Biomol Screen. 2009;14(10):1157–64. PubMed PMID: 19822881.
4. Mayr L.M., Bojanic D. Novel trends in high-throughput screening. Curr Opin Pharmacol. 2009;9(5):580–8. PubMed PMID: 19775937.
5. Zimmerman M., Yurewicz E., Patel G. A new fluorogenic substrate for chymotrypsin. Anal Biochem. 1976;70(1):258–62. PubMed PMID: 1259147.
6. Zimmerman M., et al. Sensitive assays for trypsin, elastase, and chymotrypsin using new fluorogenic substrates. Anal Biochem. 1977;78(1):47–51. PubMed PMID: 848756.
7. Leytus S.P., Melhado L.L., Mangel W.F. Rhodamine-based compounds as fluorogenic substrates for serine proteinases. Biochem J. 1983;209(2):299–307. PubMed PMID: 6342611.
8. Tirat A., et al. Synthesis and characterization of fluorescent ubiquitin derivatives as highly sensitive substrates for the deubiquitinating enzymes UCH-L3 and USP-2. Anal Biochem. 2005;343(2):244–55. PubMed PMID: 15963938.
9. Hassiepen U., et al. A sensitive fluorescence intensity assay for deubiquitinating proteases using ubiquitin-rhodamine110-glycine as substrate. Anal Biochem. 2007;371(2):201–7. PubMed PMID: 17869210.
10. Plummer T.H. Jr, Kimmel M.T. An improved spectrophotometric assay for human plasma carboxypeptidase N1. Anal Biochem. 1980;108(2):348–53. PubMed PMID: 7457880.
11. Packard B.Z., et al. Intramolecular Excitonic Dimers in Protease Substrates: Modification of the Backbone Moiety To Probe the H-Dimer Structure. J. Phys. Chem. B. 1998;102(10):1820–1827.
12. Grahn S., Ullmann D., Jakubke H. Design and synthesis of fluorogenic trypsin peptide substrates based on resonance energy transfer. Anal Biochem. 1998;265(2):225–31. PubMed PMID: 9882396.
13. Johansson M.K., Cook R.M. Intramolecular dimers: a new design strategy for fluorescence-quenched probes. Chemistry. 2003;9(15):3466–71. PubMed PMID: 12898673.

14. Feng B.Y., et al. High-throughput assays for promiscuous inhibitors. Nat Chem Biol. 2005;1(3):146–8. PubMed PMID: 16408018.
15. Tyagi S., Bratu D.P., Kramer F.R. Multicolor molecular beacons for allele discrimination. Nat Biotechnol. 1998;16(1):49–53. PubMed PMID: 9447593.
16. Nalepa G., Rolfe M., Harper J.W. Drug discovery in the ubiquitin-proteasome system. Nat Rev Drug Discov. 2006;5(7):596–613. PubMed PMID: 16816840.
17. Bedford L., et al. Ubiquitin-like protein conjugation and the ubiquitin-proteasome system as drug targets. Nat Rev Drug Discov. 2011;10(1):29–46. PubMed PMID: 21151032.
18. Sajonz P., et al. Multiparallel microfluidic high-performance liquid chromatography for high-throughput normal-phase chiral analysis. J Chromatogr A. 2007;1145(1-2):149–54. PubMed PMID: 17300788.
19. Holt T.G., et al. Label-free high-throughput screening via mass spectrometry: a single cystathionine quantitative method for multiple applications. Assay Drug Dev Technol. 2009;7(5):495–506. PubMed PMID: 19715455.
20. Jonas M., LaMarr W.A., Ozbal C. Mass spectrometry in high-throughput screening: a case study on acetyl-coenzyme a carboxylase using RapidFire--mass spectrometry (RF-MS). Comb Chem High Throughput Screen. 2009;12(8):752–9. PubMed PMID: 19531010.
21. Shoichet B.K. Screening in a spirit haunted world. Drug Discov Today. 2006;11(13-14):607–15. PubMed PMID: 16793529.
22. Lor L.A., et al. A simple assay for detection of small-molecule redox activity. J Biomol Screen. 2007;12(6):881–90. PubMed PMID: 17579124.
23. Jadhav A., et al. Quantitative analyses of aggregation, autofluorescence, and reactivity artifacts in a screen for inhibitors of a thiol protease. J Med Chem. 2010;53(1):37–51. PubMed PMID: 19908840.
24. Habig M., et al. Efficient elimination of nonstoichiometric enzyme inhibitors from HTS hit lists. J Biomol Screen. 2009;14(6):679–89. PubMed PMID: 19470716.
25. Kettner C.A., et al. Kinetic properties of the binding of alpha-lytic protease to peptide boronic acids. Biochemistry. 1988;27(20):7682–8. PubMed PMID: 3207699.
26. Bachovchin W.W., et al. Nitrogen-15 NMR spectroscopy of the catalytic-triad histidine of a serine protease in peptide boronic acid inhibitor complexes. Biochemistry. 1988;27(20):7689–97. PubMed PMID: 3207700.
27. Tavares F.X., et al. Design of potent, selective, and orally bioavailable inhibitors of cysteine protease cathepsin k. J Med Chem. 2004;47(3):588–99. PubMed PMID: 14736240.
28. Tavares F.X., et al. Ketoamide-based inhibitors of cysteine protease, cathepsin K: P3 modifications. J Med Chem. 2004;47(21):5057–68. PubMed PMID: 15456249.
29. Deaton D.N., et al. Novel and potent cyclic cyanamide-based cathepsin K inhibitors. Bioorg Med Chem Lett. 2005;15(7):1815–9. PubMed PMID: 15780613.
30. Agrawal A., et al. Zinc-binding groups modulate selective inhibition of MMPs. ChemMedChem. 2008;3(5):812–20. PubMed PMID: 18181119.
31. Jacobsen J.A., et al. To bind zinc or not to bind zinc: an examination of innovative approaches to improved metalloproteinase inhibition. Biochim Biophys Acta. 2010;1803(1):72–94. PubMed PMID: 19712708.
32. Morrison J.F., Walsh C.T. The behavior and significance of slow-binding enzyme inhibitors. Adv Enzymol Relat Areas Mol Biol. 1988;61:201–301. PubMed PMID: 3281418.
33. Robertson J.G. Mechanistic basis of enzyme-targeted drugs. Biochemistry. 2005;44(15):5561–71. PubMed PMID: 15823014.
34. Singh J., et al. The resurgence of covalent drugs. Nat Rev Drug Discov. 2011;10(4):307–17. PubMed PMID: 21455239.
35. Szedlacsek S.E., Duggleby R.G. Kinetics of slow and tight-binding inhibitors. Methods Enzymol. 1995;249:144–80. PubMed PMID: 7791610.
36. Duggleby R.G. Analysis of enzyme progress curves by nonlinear regression. Methods Enzymol. 1995;249:61–90. PubMed PMID: 7791628.

Inhibition of Protein-Protein Interactions: Non-Cellular Assay Formats

Michelle R. Arkin, PhD,[1,*] Marcie A. Glicksman, PhD,[2,*] Haian Fu, PhD,[3] Jonathan J. Havel,[3] and Yuhong Du[3]

Created: March 18, 2012; Updated: October 1, 2012.

Abstract

Protein-protein interactions (PPI) are critical in cellular signal transductions that play a key role in both normal and abnormal functions in cells. Therefore, modulating the activity of these interactions is a major focus in drug discovery research. In this chapter, the authors address the development, optimization and validation of HTS assays to identify small molecule modulators of PPI. They also discuss the sources of artifacts, detailed accounts of assay technologies compatible with HTS for PPI and validating the inhibition of PPI. An extensive set of references is provided, and is a must read for beginners and a review for experienced investigators.

Overview and Introduction

Introduction

Protein-protein interactions (PPI) are central to most cellular processes and, as such, are the focus of many probe- and drug-discovery programs. However, it has been difficult to identify small molecule or peptide inhibitors of PPI that bind stoichiometrically to a single site on the protein surface. Often sited reasons for this challenge include a) the flat nature of PPI interfaces, which sometimes lack deep grooves where small molecules can stick, b) the large contact area at the interface, which often exceeds the surface area of a drug-sized molecule, and c) bias in the screening libraries, which are selected by adherence to criteria – like the Rule of 5 (1, 2) – that might not suit PPI inhibitors. Furthermore, early screening approaches to PPI were prone to artifacts and tended to select hydrophobic compounds with non-drug-like mechanisms of action, such as aggregation-based inhibition or protein denaturation (3, 4, 5). Despite these challenges, there are now a number of drug-like inhibitors of PPI in the literature (5, 6, 7, 8). From these examples, we are beginning to develop "best practices" for selecting tractable targets, applying appropriate screening assays, and evaluating mechanisms of action. This chapter focuses on the selection and development of screening assays for identifying small molecules that can modulate PPI, and will touch on secondary assays used to remove artifacts and demonstrate binding. General introductions to assay development for HTS and to common assay equipment and instrumentation can be found in Basics of Assay Equipment and Instrumentation for High Throughput Screening.

The screening assays described here monitor the binding of the two proteins, and can be used to measure inhibition or augmentation of the PPI by small molecules or other modulators (e.g. antibodies, peptides). Table 1 provides a brief summary of the assays. All assays can be used for primary high-throughput screening (HTS) at single concentrations of test compounds and for dose-response assays to obtain IC_{50} values. These formats are regularly used in 96- and 384-well plates and can often be adapted to 1536-well plates. Traditional high-throughput assays involve binding one of the protein partners to the plate; here, we provide an overview of these ELISA-like assays, including DELFIA. Increasingly, screening scientists utilize mix-and-read assay formats such as fluorescence polarization/anisotropy (FP), fluorescent/Foerster resonance energy transfer (FRET, TR-FRET, HTRF), and bead-based assays like AlphaScreen (Perkin Elmer). These solution-phase assays are often easier to

Author Affiliations: 1 University of California San Francisco, San Francisco, CA. 2 Harvard NeuroDiscovery Center, Boston, MA. 3 Emory University School of Medicine, Atlanta, GA.

*Editor

develop than ELISAs because they have fewer components, and are simpler and faster to run because they avoid multiple incubation/wash cycles. On the other hand, ELISA and DELFIA can be very sensitive and are still used for diagnostics and some high throughput screens.

Table 1: Overview of Assay Formats

Method	FP	ELISA/DELFIA	FRET	AlphaScreen
Size of protein and/or complex	Labeled ligand needs to be <1500 Da and protein needs to be >10,000 Da.	No real limit	Distance between donor and acceptor needs to be <9 nm	Distance between donor and acceptor needs to be <200 nm
Pure protein?	Label needs to be pure protein or small molecule	Can use purified protein or complex sample	Can use purified protein or complex sample	Can use purified protein or complex sample
Sensitivity	[FP probe] ~ nM; [protein] determined by K_d of PPI	Can be as low as femtograms/well	Depends on K_d of PPI; typically 1 – 100 nM	Can be as low as femtograms/well
Dye(s)	Most organic, fluorescent dyes; red-shifted preferred (e.g. Bodipy, Alexa Fluors)	Lanthanide (DELFIA) or enzyme (Horse Radish Peroxidase, Alkaline Phosphatase)	FRET: see Table 2, below	Donor bead generates singlet oxygen that excites acceptor bead with organic or lanthanide fluorophore
Need washing steps?	no	yes	no	no
Signal range (high/low)	~3 – 5 fold	4-5 log	< 10 fold	2-3 log
Cost	Low - moderate	Low - moderate	Moderate - high	High
Other advantages	Standard deviations tend to be low; is a direct PPI measurement	Low spectroscopic interference from compound	Ratiometric, readily controlled for spectral artifacts	Can monitor the widest range of complex size
Principal disadvantages	Dye "propeller" rotations must be considered; fluorescence of compounds can interfere	Sensitive to off-rates, laborious, often without clear benefit	Signal window dependent on distance and dye orientation	Sensitive to ambient light

General Considerations

Screening in general, and for PPI inhibitors in particular, identifies compounds with many mechanisms of inhibition. Some of these mechanisms are undesired, such as direct assay interference, nonspecific binding, and covalent modification. To reduce the likelihood of finding such compounds, we recommend the following practices for in vitro assays:

1. **Use of detergents in biochemical assays.** Low concentrations of detergents tend to stabilize proteins, reduce nonspecific binding of proteins to assay plates, and break up compound aggregates. We favor using one detergent in a screen, then following up with alternate detergents, since no one detergent removes all aggregates. Commonly used detergents include Triton X-100 (0.01%), Tween 20 (0.005%), and Chaps (0.1%); in general, detergents should be used at concentrations below their critical micelle concentration (CMC).
2. **Use of carrier proteins.** As with detergents, non-interfering proteins such as gamma globulin, casein, or Prionex (Centerchem) can be used to reduce nonspecific binding of compounds and assay proteins. Bovine serum albumin (BSA), used in most cell-based assays, binds many compounds that are viable drug leads and may not be the best choice for primary biochemical screens. Using carrier proteins is less common than detergents, but should be considered for primary or secondary testing.

3. **Diluting compounds in DMSO.** Most HTS libraries are dissolved in DMSO, and small concentrations of DMSO (typically <0.1%) are thus carried into assays. The sensitivity of an assay to DMSO must be determined during assay development. In addition, since compounds vary in their solubility, it is best practice to limit intermediate dilutions into buffer. In particular, when running dose-response titrations, the compounds should be serially diluted in DMSO, then transferred into the assay buffer as close to the final concentration as possible. The use of nanoliter volume dispensers has made this approach practical for 384-well and higher format plates.
4. **Use of orthogonal assays.** Compounds will interfere with assays in multiple ways, some of which are difficult to predict. It is therefore important to follow up any primary assay with an orthogonal secondary assay that uses a different modality (e.g. colorimetric vs luminometric) or format (plate-bound, vs mix-and-read, vs label-free). Finally, unless the goal is to discover covalent modifiers of a PPI, reversibility of inhibition should be demonstrated. This can be accomplished by mixing the reagents at high concentration, then diluting to a condition well below the affinity of the inhibitor. Additionally, the PPI partners can be incubated with inhibitor, then analyzed by mass spectroscopy.

ELISA-type assays

Concept

Enzyme-Linked Immunosorbant Assays (ELISAs) follow the basic design shown in Figure 1. These formats can be used to measure PPI and thus to measure competition between a PPI and a small-molecule inhibitor. To measure a PPI, one of the proteins is attached to a plate surface and the second protein is then allowed to bind to the first protein. The second protein is detected by binding of an antibody that is linked to an enzyme. When substrate is added, the enzyme produces a measurable readout that is quantitatively linked to the amount of the second protein. ELISAs can be very sensitive, because the readout is amplified by using an enzyme. Further amplification can be achieved by using multiple layers, such as secondary antibodies.

ELISA technically means that the detection event uses an antibody and enzyme-based detection; however, this term is commonly used to describe plate-bound detection of a reagent, even if the affinity reagent is not an antibody or if the detection reagent is not an enzyme. One commonly used, non-enzymatic format is called Dissociation-Enhanced Lanthanide Fluorescent Immunoassay (DELFIA, Perkin Elmer). In DELFIA, the detection signal is time-resolved fluorescence of a lanthanide ion (such as europium). The lanthanide ion is bound to the affinity reagent through a chemical linkage; upon adding a proprietary detergent mixture, the europium fluoresces, providing a highly sensitive measurement of the concentration of bound protein. Three features of lanthanide fluorescence lead to highly sensitive and selective assays: a) a long emission lifetime (milliseconds) allows the measurement to start after the fluorescence of organic material (proteins, test compounds) has decayed, b) the emission occurs at around 600 nm, where few biological materials absorb or emit light, and c) the narrow emission spectrum of lanthanides allow them to be multiplexed.

ELISA-style assays can be designed in many ways. Attachment of the surface-bound protein can occur by passive adsorption to a plastic plate, by capture with an adsorbed antibody, or by biotinylation and avidin capture. Detection of the second protein can occur by direct labeling the protein with a signal-generating enzyme, by binding of an enzyme-labeled antibody, by binding of an unlabeled primary antibody followed by a labeled secondary antibody, or by biotinylation followed by enzyme-linked avidin. Detection enzymes can include colorimetric, fluorogenic, or luminogenic reactions. Selection criteria for of each of these steps are described below.

General Considerations

Consider the affinity of the PPI when designing a plate-based assay. Such assays involve multiple wash steps, which will remove unbound protein. If binding kinetics are rapid, as with most weak interactions (ca. > 1 μM),

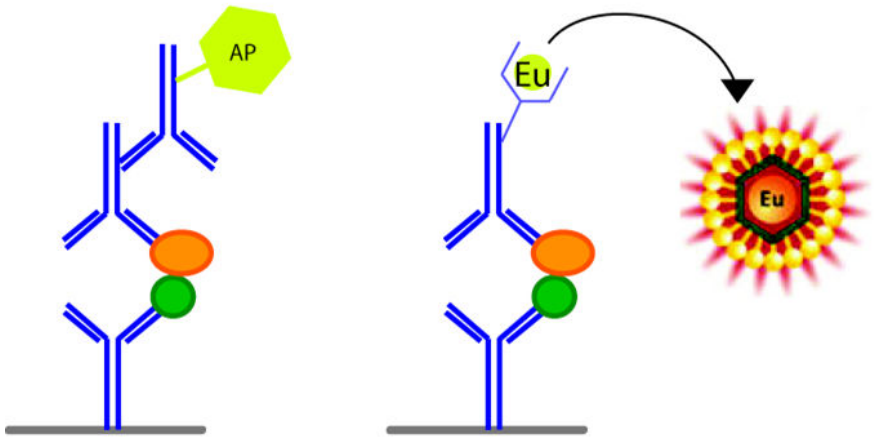

Figure 1: Format for ELISA and DELFIA assays. **Left:** An ELISA is built up in several steps, starting with antibody to protein 1, protein 1 (green), protein 2 (orange), anti-protein 2, and an anti-species antibody conjugated with an enzyme (AP = alkaline phosphatase). The signal produced by enzyme activity is proportional to the amount of PPI. **Right:** If protein 2 (orange) has an epitope tag, the anti-epitope antibody is often labeled with the detection reagent. In DELFIA, the detection reagent is a rare earth element such as europium.

signals will be lower. The fewer amplification steps (e.g. direct conjugation of the enzyme to the solution-phase protein), the less signal is lost to washing. Assay format is therefore a compromise between assay complexity and signal amplification.

In principle, either member of the PPI could be immobilized, but several issues should be considered:

1. Is there a potential for avidity in the interaction? Avidity occurs when multiple contacts are made simultaneously, as with a trimeric protein binding to a trimeric ligand, or when a trimeric protein binds to a plate with a high density of ligand. This Velcro-like effect results in slowed unbinding kinetics (off-rates) and thus an apparent affinity that is tighter than the 1:1 binding affinity. For weak interactions, such avidity allows the PPI to survive washing, but it also complicates quantitative analysis. If one member of the PPI is monomeric, it is generally recommended to use this protein as the solution-phase protein, while a multimeric partner is immobilized on the plate.
2. Is one protein more likely to bind to the small molecule? Compounds are more likely to bind to the side of the PPI that is concave, such as when a bit of secondary structure from the other protein binds into a groove (examples include MDM2/p53, PDZ domains). If the grooved protein is kept in solution, then the ELISA will monitor a solution-phase binding event.
3. Is one protein more apt to precipitate or aggregate? If one protein is known to precipitate, it might be more stable as the captured, plate-bound partner.
4. Is one PPI partner limiting? Generally, more of the immobilized protein is used, so if one protein is easier to obtain and purify, it should be considered for immobilization.
5. Another option is if one of the proteins is expressed with a tag such as his or GST or FLAG, a plate coated with antibodies to the tag would serve to immobilize the protein to the plate. A protein can be biotinylated and streptavidin-coated plate can be used.

If there is no compelling reason to use one protein for surface-immobilization, then both orientations of the assay should be evaluated. In the ideal case, the same IC_{50} values should be obtained from both formats.

Assay design and development

1. **Instrumentation**: The assays described here can be performed with most multimodal plate readers, and the readout can be selected based on available instrumentation. Typical readouts are absorbance,

fluorescence, luminescence, or time-resolved fluorescence (TRF). Time-resolved fluorescence, used by DELFIA, is the least-standard modality, but most HTS facilities will have TRF-compatible instruments.

2. **Plates:** ELISA-type assays are generally performed in polystyrene microwell plates with high-binding surfaces to adsorb proteins. The color of the plate is selected based on the readout: clear (absorbance), black (fluorescence), and white (luminescence). DELFIA can be performed in clear, white or yellow plates.
3. **Binding of first protein (protein 1)**: The first immobilized protein can be bound to the plate by passive adsorption or by capture. Passive adsorption is simple – the protein is added to a bare plate; however, some proteins will denature upon adsorption and the orientation of proteins on the surface will be random. After the protein is adsorbed, the rest of the well surface is blocked with a nonspecific protein, such as casein (1%), nonfat milk (5%), or bovine serum albumin (1%). Critical steps for passive adsorption include a) selecting a concentration of protein to maximize ELISA signal and b) selecting a blocking protein that reduces nonspecific binding of the second protein partner and detection reagents. At any step in the ELISA process, a blocking protein or detergent can be used to reduce nonspecific binding.

   If assay sensitivity is low when the protein is adsorbed, a capture step can be added. In this format, an antibody or avidin is adsorbed to the plate first. Generally, the capture protein is plated at a saturating condition. The plate is then blocked with nonspecific proteins and protein 1 is added. If an antibody is used for capture, it should not block the PPI and should be available in sufficient supply for the scale of the assay. If avidin is used, there are different versions (e.g. streptavidin and neutravidin) that could alter the degree of nonspecific binding. The protein to be captured must be biotinylated, which can be accomplished during expression (via AviTag; Avidity) or chemically (via reaction with amines, acids, or cysteine residues). Biotinylation using AviTag sequences will provide homogeneous labeling near the N- or C-terminus of the protein.
4. **Binding of the second protein (protein 2):** Protein 2 in the PPI can also be added to the ELISA plate in several formats. The protein can be unmodified, it can be biotinylated (if the first protein was not immobilized by biotin/avidin binding), or it can be labeled directly with the detector (e.g. enzyme or DELFIA probe). As mentioned above, the decision to label or use secondary detection is a balance between the number of washing steps and signal amplification. Directly labeled proteins, such as horseradish peroxidase (HRP)-protein conjugates, can be less soluble and more prone to artifacts; compounds can also interfere with detection, such as by inhibiting the detection enzyme itself. Therefore, ELISAs usually use a secondary detection step. In either case, protein 2 should be titrated to achieve a robust but non-saturating signal. Incubation times should allow equilibrium to be reached. After incubation, the unbound protein 2 should be thoroughly washed from the plate, usually using 3 cycles of phosphate-buffered saline with 0.01% Tween 20 (or other detergent).
5. **Affinity reagents (e.g. antibodies or streptavidin):** When protein 2 is not directly labeled with a detection reagent, one or two binding steps are required to add the detector. When protein 2 is biotinylated, avidin is conjugated with the detection reagent. When the protein is unmodified, an antibody to protein 2 is usually used. This primary antibody can be labeled with detection reagent or a secondary antibody (e.g. rabbit anti-murine IgG) can be labeled and bound. The affinity reagents should be titrated to reach a maximal signal-to-background; the binding can be saturated, but care should be taken to ensure that the reagent is not binding non-specifically to wells without protein 2. Incubation time is another optimize-able parameter, and can vary from 1 hour to overnight. After incubation, the plate should be thoroughly washed to remove unbound reagents.
6. **Detection methodology:** The final step of the ELISA involves adding a substrate; when the linked enzyme turns over the substrate, a measurable change (e.g. color) occurs. Two commonly used enzymes are horseradish peroxidase (HRP) and alkaline phosphatase (AP); avidin and antibody conjugates of these enzymes are widely available, as are chromogenic and luminogenic substrates. Generally speaking,

luminescent substrates are more sensitive, requiring smaller amounts of material and/or less incubation time than chromogenic substrates and have a wider dynamic range than chromogenic substrates. On the other hand, chromogenic products tend to be more stable over time. ELISAs can be read kinetically (monitoring the color change over time) or at a fixed endpoint. Endpoint readings can include a quenching step, such as the addition of acid (e.g. equal volume of 1 M HCl or H3PO4) or base (e.g. 1 M ammonium chloride) to stop enzyme turnover and stabilize the ELISA signal.

DELFIA assays are processed similarly to ELISAs. Some europium-labeled reagents are commercially available, including anti-IgGs, anti-tag antibodies (such as anti-Histag antibodies), and streptavidin, and others can be prepared in the lab or by custom synthesis (for example, see Perkin Elmer and Cisbio). Detection requires the addition of a commercial "dissociation-enhancement solution."

Benefits and limitations

ELISA and DELFIA have some important benefits. They are very flexible and sensitive, and can be inexpensive to run. They are also less likely to have compound interference since the compound is not present in the processing step. They also have significant limitations that have led to their reduced use in HTS. Most ELISAs have multiple incubation and washing steps, which are time-consuming for automated and bench-top assays. Washing can also disrupt weak interactions (e.g. $K_d > 1$ μM). Finally, it is important to demonstrate that potential PPI inhibitors are not interfering with the detection system or acting nonspecifically with the proteins and detection reagents. Changing formats and using complementary detection methods (such as those described below) will help to validate potential inhibitors.

Related technologies

PPI assays have also been performed with bead-based separation, e.g. using flow cytometry (9).

Mix-and-read assays

Three main formats are available with both similarities and differences with regard to label, secondary detection, and maximum distance allowable between the protein partners. FRET and AlphaScreen are proximity measurements, meaning that they rely on the protein partners being within 10 – 100 angstroms. Fluorescent Polarization measures the tumbling time, related to the molecular mass, experienced by a fluorophore. A principal advantage of these mix-and-read assay formats is that they requiring no washing steps, leading to a wider dynamic range and higher plate throughput.

Fluorescence polarization/anisotropy

Concept

Fluorescence polarization (FP) is a sensitive nonradioactive method for the study of molecular interactions in solution (10). This method can be used to measure association and dissociation between two molecules if one of the molecules is relatively small and fluorescent. When a fluorescently labeled molecule is excited by polarized light, it emits light with a degree of polarization that is inversely proportional to the rate of molecular rotation. Molecular rotation is largely dependent on molecular mass, with larger masses showing slower rotation. Thus, when small, fluorescent biomolecule, such as a small peptide or ligand (typically < 1500 Da), is free in solution, it will emit depolarized light. When this fluorescent ligand is bound to a bigger (e.g. > 10, 000 Da) molecule, such as a protein, the rotational movement of the fluorophore becomes slower and thus the emitted light will remain polarized. Thus, the binding of a fluorescently labeled small molecule or peptide to a protein can be monitored by the change in polarization (Figure 2).

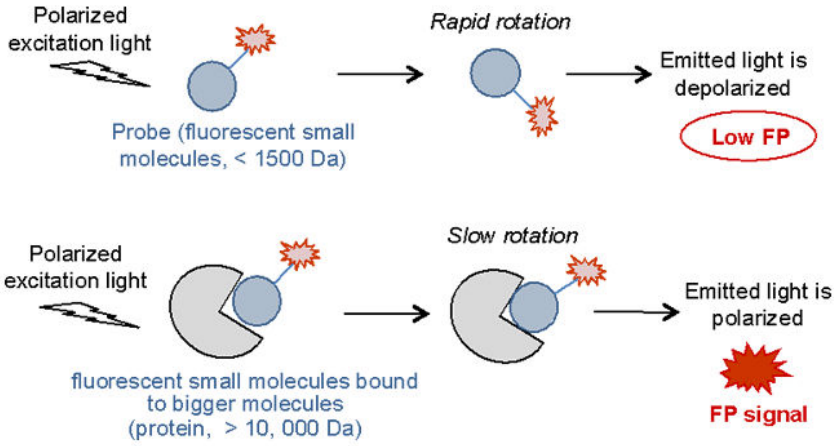

Figure 2: Diagram of a fluorescence polarization assay. Rapidly rotating small molecule fluorophore gives low FP signal (low mP). The association of a relatively large molecule, such as a protein, with the small molecule fluorophore slows down the motion of the fluorophore, leading to increased FP signal.

Assay design

1. **Selection of FP probe:** Protein-protein interactions can be monitored by FP if one of the components of the PPI is small. Typically, the molecular weight of the ligand/probe is less than 1500 Da, although up to 5000 Da can be acceptable if the binding partner is very large. For most PPI, FP will be practical only a) if one side of the PPI can be minimized to a peptide, b) if there is a synthetic peptide known to bind at the interface (e.g. via phage display), or c) if an organic compound binds at the interface (or to a mutually exclusive binding site). Fortunately, there are several examples of peptides that mimic the epitope of a protein in a PPI, including PDZ domains, IAPs, Bcl2-family proteins, and others.
2. **Selection of fluorescent dye:** Once a probe molecule has been selected, it must be labeled with a fluorescent dye. Dyes are typically available in amine-reactive, cysteine-reactive, and acid-reactive forms and are chemically attached to the probe peptide/molecule using simple chemistry. Typical fluorophores used in FP are fluorescein, rhodamine, and BODIPY dyes. The BODIPY dyes have longer excited- state lifetimes than fluorescein and rhodamine, making their fluorescence polarization sensitive to binding interactions over a larger molecular weight range (11). Red-shifted dyes are preferable to reduce the number of compounds that will cause interference with the 405nm (e.g. fluorescein) range.
3. **Selection of buffer:** the buffer must have low fluorescence background. Frequently used buffers have neutral pH such as PBS, HEPES.
4. **Instrumentation for FP measurement with microtiter plate:** Many commercially available instruments are capable of measuring the FP signal from solution in 96/384/1536-well microtiter plate format for high throughput screening (HTS). The fluorescence is measured using polarized excitation and emission filters. Two measurements are performed on every well and fluorescence polarization is defined and calculated as:

   $$\text{Polarization} = P = (I_{vertical} - I_{horizontal})/(I_{vertical} + I_{horizontal})$$

   Where $I_{vertical}$ is the intensity of the emission light parallel to the excitation light plane and $I_{horizontal}$ is the intensity of the emission light perpendicular to the excitation light plane (10). All polarization values are expressed as the milli-polarization units (mP).

   All commercial microplate readers have built-in software for mP calculation. Depending on the instrument used, three sets of data are generally reported, including calculated mP values, raw

fluorescence intensity counts of vertical (or Parallel/S-channel) and horizontal (or perpendicular/P-channel) measurements for each well.

mP calculation for different instruments requires the proper use of measured fluorescence intensity of parallel/S-channel and perpendicular/P-channel. As optical parts of fluorometers possess unequal transmission or varying sensitivities for vertically or horizontally polarization light, such instrument artifacts should be corrected for accurate calculation of the absolute polarization state of the molecule using fluorescent readers. This correction factor is known as the "G Factor" which is instrument-dependent. G-factor corrects for any bias toward the horizontal (or perpendicular/P-channel) measurement. Most commercially available instruments have an option for correcting the single-point polarization measurement with G factor. For example, the mP values for FP measurement with Envision Multilabel plate reader are calculated as:

$$mP = 1000 * (S - G * P) / (S + G * P)$$

In practice for HTS applications, however, it is unnecessary to measure absolute polarization states; the assay window is what is important. The assay window is insignificantly changed by G Factor variation.

5. **Determining the concentrations of fluorescent probes for the FP binding assay:** In order to select the proper concentrations of fluorescent probe for the binding assay, increasing concentrations of fluorescent probe is prepared in assay buffer without the binding protein. The fluorescence intensity (FI) in the parallel channel is then measured with defined settings in a plate reader with FP mode. A concentration of the fluorescent probe with at least 10-fold or higher FI signal compared to that of buffer only should be selected for the subsequent binding assay. Notice that the FP signal is expressed as a ratio of fluorescence intensities. Thus, the signal is not influenced by changes in intensity brought about by changes in the tracer concentration.
6. **FP Binding assay development:** To determine the binding of the fluorescent probe with the protein of interest, increasing concentrations of protein are mixed with a fixed concentration of the probe. The FP signal as expressed in mP is then measured with a plate reader. mP vs [protein] is then plotted to generate a binding isotherm for the calculation of association parameters such as Kd and maximal binding. For the FP inhibition assay, select a concentration of protein that provides ca. 80% of the maximum change in polarization for the probe (e.g. 80% bound).
7. **Data analysis:** The dynamic range of the FP assay, i.e. assay window, is defined as mPb – mPf, where mPb is recorded mP value for the specific binding in the presence of a particular protein concentration and mPf is the recorded mP value for free tracer from specific binding proteins (12). Typically, the assay window is 3-5 fold (e.g. 50 mP – 150 mP).
8. **Selectivity:** once the concentrations of probe and protein are determined, the specificity of the interaction should be assessed. First, an unlabeled version of the probe is titrated into a mixture of the FP-probe and protein. As the concentration of unlabeled probe competes with bound fluor-probe, the FP should decrease. The IC_{50} for this interaction should be similar to the Kd measured above. Similarly, other known inhibitors should yield the expected IC_{50} values.
9. **Fluorescence of the bound probe**: often the fluorescence of the probe changes when it binds to the protein. In this case, anisotropy measurements should be used in place of polarization, since unlike FP, anisotropy is directly proportional to fluorescence intensity. Anisotropy is calculated with the following expression:

$$\text{Anisotropy: } r = (I_{vertical} - I_{horizontal})/(I_{vertical} + 2\, I_{horizontal})$$

where $I_{vertical}$ is the intensity of the emission light parallel to the excitation light plane and $I_{horizontal}$ is the intensity of the emission light perpendicular to the excitation light plane.

Case study: Monitoring 14-3-3 protein interactions with a homogeneous FP assay

The 14-3-3 proteins mediate phosphorylation-dependent protein-protein interactions. Through binding to numerous client proteins, 14-3-3 controls a wide range of physiological processes and has been implicated in a variety of diseases, including cancer and neurodegenerative disorders (13). We have designed a highly sensitive fluorescence polarization (FP)-based 14-3-3 assay (Figure 3), using the interaction of 14-3-3 with a fluorescently labeled phosphopeptide from Raf-1. The specificity of the assay has been validated with known 14-3-3 protein antagonists, e.g., R18 peptide, in a competitive FP assay format. The signal-to-background ratio is greater than 10 and a Z' factor is greater than 0.7 (12). Because of its simplicity and high sensitivity, this assay is generally applicable to studying 14-3-3/client protein interactions and for HTS.

Materials:

1. Protein (14-3-3γ): the recombinant GST-14-3-3 protein was expressed in *Escherichia coli* strain BL21 (*DE3*) as a GST-tagged product and purified
2. Probe (TMR-pS259-Raf): a phosphopeptide derived from Raf-1 was synthesized and labeled with 5/6 carboxytetramethylrhodamine (TMR)
3. Buffer: HEPES buffer containing 10 mM HEPES, 150 mM NaCl, 0.05% Tween 20 DTT 0.5 mM DTT, pH 7.4
4. 384-well black plate (Corning Costar Cat#: 3573)
5. Instrument for FP measurements: FP measurements were performed on Analyst HT plate reader (Molecular Devices, Sunnyvale, CA) using FP protocol. For Tetramethylrhodamine (TMR)-labeled probe (Excitation: 545 nm; Emission: 610 nM), a dichroic mirror of 565 nm was used.

Protocol:

1. **Selection of probe concentration:** 1 nM of the TMR-pS259-Raf peptide was chosen for the binding assay based on the observation that 1 nM of the TMR-labeled peptide exhibited about 10 times more fluorescence intensity in the parallel channel than the "buffer-only" control samples.
2. **Prepare probe and protein solutions:** 2 basic solutions were prepared. Solution A contained TMR-pS259-Raf peptide in the HEPES buffer (2× solution with 2 nM of the peptide probe or as specified). Solution B contained 14-3-3 proteins in HEPES buffer (2× solution with increasing concentrations of 14-3-3 protein; a serial dilution approach is generally used for the protein titration).
3. **Binding FP assay:** The 14-3-3 FP binding assay was carried out in black 384-well microplates in a total volume of 50 μl in each well. For each assay, a 25 μl of Solution A (probe) is mixed with 25 μl of solution B (protein) in 384-well plate. Probe only without protein is always included as blank control.
4. **FP measurement:** the polarization value in mP was measured at room temperature (RT) with an AnalystHT reader immediately, or after incubating at RT as desired time period for the equilibration of the interaction.
5. **Competitive FP assays:** the specificity of the FP binding assay is generally evaluated with known antagonists, e.g, unlabeled probe, peptide or small molecule antagonists, in competitive FP assay. To achieve the desired sensitivity, the concentrations of fluorescent Raf peptide probe and 14-3-3 protein are carefully chosen to maximize the difference between the highest and lowest polarization values. Serial dilutions of competitive peptide (R18) are added to a reaction buffer containing TMR-pS259-Raf (1 nM) and GST-14-3-3γ (0.5 μM) and incubated at RT for 1 hr. The mP values were measured and the competitive effect was expressed as percentage of control mP (TMR-pS259-Raf and GST-14-3-3γ) after subtracting the background mP (TMR-pS259-Raf alone).

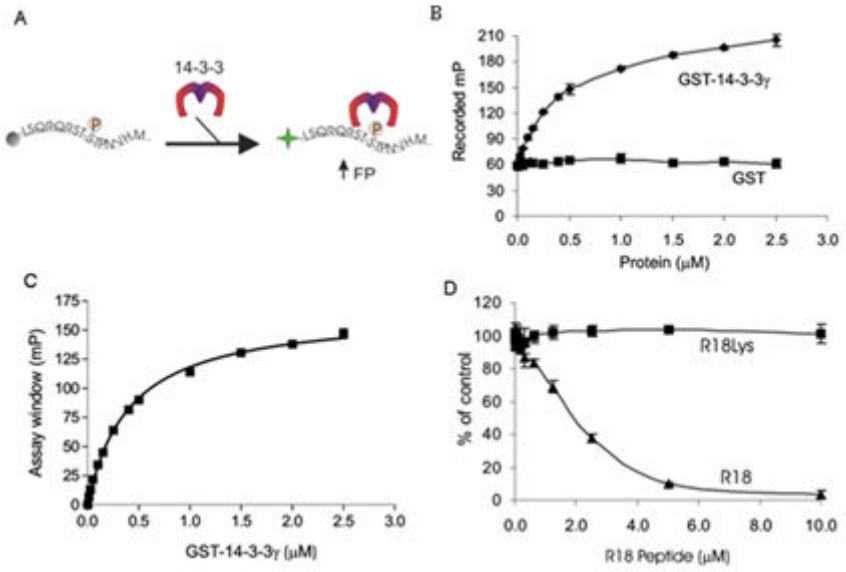

Figure 3: Development of FP assay for TMF-pS259-Raf/14-3-3. **A:** The interaction of 14-3-3 with TMR-pS259-Raf gave rise to a significant FP signal with a minimal background polarization with the peptide probe alone or with increasing concentrations of a nonbinding protein (GST). With increasing amounts of GST-14-3-3γ protein, polarization values progressively increased to reach saturation, suggesting that a greater fraction of fluorescent peptide was bound to the 14-3-3 protein. **B:** The maximum assay window (ΔmP = mP of bound peptide – mP of free peptide) reached approximately 150 mP with an estimated dissociation constant, Kd, of 0.412 + 0.01 μM for the Raf peptide. **C:** A well-known 14-3-3 antagonist peptide, R18, can compete the 14-3-3 binding as measured by a dose-dependent decrease of FP signal; however, a mutant R18 peptide cannot compete the binding (Adapted from Du, 2006).

Benefits and limitations:

FP-based technology has a number of key advantages for monitoring bimolecular interactions, especially for HTS applications. It is nonradioactive and is in homogenous "mix-and-read" format without wash steps, multiple incubations, or separations. FP measurement is directly carried out in solution; no perturbation of the sample is required, making the measurement faster and perhaps more native-like than immobilization-based methods like ELISA. It is readily adaptable to low volume (30 μl for a 384-well plate or 5 μl for a 1536-well plate). In addition to measuring PPI, FP assays have been used to study a wide variety of targets including protein-nucleic acid interactions, kinases, phosphatases, proteases, G-protein-coupled receptors (GPCRs), and nuclear receptors (14, 15).

As a fluorescence-based technology, FP is subject to optical interference from compounds that absorb at the excitation or emission wavelengths of the fluorescent probe. Being a ratiometric technique makes FP somewhat resistant, though enough light must be available to obtain an emission signal. FP is also sensitive to the presence of fluorescence from test compounds. The use of red-shifted probes will minimize background fluorescence interference.

Fluorescent/Förster resonance energy transfer and time-resolved (TR) FRET

Concept

Fluorescence/Förster Resonance Energy Transfer (FRET) is the phenomenon of non-radiative energy transfer between two fluorophores with specific spectral properties. In order for FRET to occur, the emission spectrum of one fluorophore, i.e. the "donor," must overlap the excitation spectrum of the second fluorophore, i.e. the "acceptor." When the donor is excited by incident light, energy can be transferred to the acceptor via long-range

dipole-dipole interactions, resulting in acceptor emission; however, this FRET event will only occur if the donor and acceptor are in sufficient proximity to one another. FRET efficiency E is defined by the equation

$$E = \frac{1}{1 + (r/R_0)^6}$$

where r is the distance between the fluorophores and R_o is the Förster distance and which FRET efficiency is 50% for the specific donor/acceptor pair. Two key factors arise from this equation. First, the amount of energy transfer decays with the sixth power of the distance between the fluorophores. Second, the term R_o depends on the spectral overlap of the donor emission spectrum and the acceptor absorbance spectrum; FRET can be observed over longer distances when the spectral overlap is large. Fortunately, the proximity limit for several donor/acceptor pairs is approximately 10 nm, which happens to be the distance over which many biomolecular interactions occur. Therefore, FRET can be used to monitor biomolecular interactions in a homogeneous mix-and-read assay format by tagging or labeling interacting biomolecules "A" and "B" with acceptor and donor fluorophores, respectively. In such a scenario, the ratio of acceptor to donor emission following donor excitation is used to quantify and monitor "AB" binding. Table 2 lists some common donor/acceptor pairs.

Due to the spectral properties of biological media and traditional FRET donor/acceptor pairs, the FRET signal can be significantly contaminated by 1) autofluorescence of biological media and test compounds; 2) a wide acceptor excitation spectrum that allows the acceptor to be directly excited by incident light; and 3) a wide donor emission spectrum that bleeds through into the acceptor emission detection window. These signal contaminants must be corrected for and can significantly diminish the sensitivity of traditional FRET assays.

One elegant solution to the problem of FRET signal contamination is the use of donor fluorophores with exceptionally long emission half-lives (up to 1500 μs), such as the rare earth metals Europium or Terbium, in a modification of FRET known as Time Resolved (TR) FRET (also called HTRF). In TR-FRET, Europium or Terbium cryptates (ligands that coordinate the metal ion and provide an "antenna" dye) serve as donors that have a very long luminescence half-life. This long emission decay allows for a time delay (50-150 μs) between donor excitation and the recording of acceptor emission. During this time delay, both media autofluorescence and acceptor excitation due to incident light will rapidly decay (ns scale) and be extinguished by the time acceptor emission is measured. This essentially eliminates signal contaminants 1 and 2 above. Signal contaminant 3 – donor emission bleedthrough into acceptor detection – is attenuated by the use of acceptors with red-shifted emission (Table 2) such as allophycocyanin, Alexa 680 (Invitrogen), Cy5, or d2 (Cisbio Bioassays). Another advantage of TR-FRET is that the rare earth metals have a modestly larger proximity limit for FRET (up to 20 nm), allowing for the detection of larger biomolecular complexes. TR-FRET assays are well suited for certain HTS applications due to their homogenous mix-and-read design, high signal-to-background ratios, and enhanced proximity detection range (Figure 4).

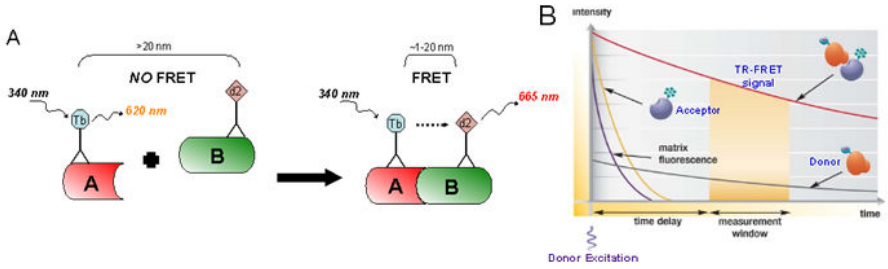

Figure 4: Principles of TR-FRET. **A:** Schematic of a typical FRET bioassay. Protein 1 is bound to an antibody fused to a donor fluorophore, e.g. Terbium (Tb), and Protein 2 is bound to an antibody fused to an acceptor fluorophore, e.g. d2 or XL665. If A and B interact, the donor and acceptor are brought into sufficient proximity for FRET to occur. In the case of a positive FRET event, acceptor emission is detected upon donor excitation. **B:** The primary sources of FRET signal contamination (matrix fluorescence, direct excitation of the acceptor) are avoided in TR-FRET by inserting a time delay between donor excitation and detection of acceptor emission ("measurement window") (adapted from Degorc, 2009).

Table 2: Common donor/acceptor pairs for FRET and TR-FRET/HTRF[1]

Donor	Acceptor	R_0 (Å)[2]
Fluorescein	Tetramethylrhodamine	55
IAEDANS	Fluorescein	46
EDANS	Dabcyl	33
BODIPY FL	BODIPY FL	57
Fluorescein	QSY 7 and QSY 9 dyes	61
Alexa Fluor 488	Alexa Fluor 555	70
Alexa Fluor 594	Alexa Fluor 647	85
Europium (III) cryptate	XL665 (allophycocyanine) or d2	90
Terbium (III)	Fluorescein	70

[1] Adapted from Invtrogen.com (FRET; Alexa dyes) and Cysbio (TR-FRET); [2]Ro is the distance at which FRET efficiency is 50%.

Assay Design

Instrumentation: A plate reader capable of allowing a time delay between excitation and fluorescence detection is required. The multimodal readers Envision (PerkinElmer) and Analyst HT (Molecular Devices) and PheraStar (BMG) are well suited for this application.

2. **Plates**: TR-FRET assays are performed in black opaque plates. Assays may be performed in 96- 384-, 1536-well formats.

3. **Buffers**: The following buffer is used routinely at the Emory Chemical Biology Discovery Center for all TR-FRET assays: 20 mM Tris, pH 7.5, 0.01% Nonidet P40, and 50 mM NaCl. However, multiple buffers can be used. As noted in the general considerations above, the use of detergents (e.g. Nonidet P40, Triton X-100, Tween 20) and carrier proteins (e.g. - Prionex) should be optimized during assay development to reduce nonspecific effects. Similarly, salt conditions can affect PPI.

4. **Labeling Reagents**: Proteins can be directly labeled with FRET donor and acceptor, using amine-, acid-, or cysteine-reactive dyes. Because random chemical coupling can disrupt the PPI, it is more common to use anti-epitope tag antibodies or streptavidin labeled with FRET and TR-FRET dyes. These general protein-dye conjugates are commercially available for proteins containing GST, HA, Flag, 6xHis, myc, or biotin tags. If it is necessary to measure binding of untagged or endogenous biomolecules, kits for labeling primary (anti-protein)

antibodies with FRET and TR-FRET fluorophores are also available for purchase. FRET and TR-FRET reagents are available from Cisbio Bioassays, PerkinElmer, and Invitrogen, among others.

5. **Assay Conditions**: FRET and TR-FRET assays are performed at room temperature. Assay performance has been shown to be stable for up to 24 hours at room temperature. In some formats, the quality of the signal improves with time and can be much better after overnight incubation. The timing for signal development and decay should be confirmed for each assay.

Steps for developing a TR-FRET Assay

1. **Select binding partners to be used**. Typically, the greatest TR-FRET sensitivity is obtained when the purified, recombinant protein-binding domains of interacting proteins are used. However, if the binding domains are not known, full-length recombinant proteins can also be used. Additionally, if purified proteins cannot be generated, or if it is critical to evaluate the PPI in a complex milieu, TR-FRET can also be performed using cell lysates containing over expressed, epitope-tagged versions of the interacting proteins. If using cell lysates, it may be best to develop stable cell lines expressing one of each binding pair to ensure consistent protein expression.
2. **Select protein concentrations.** When proteins are directly labeled with fluorophores, simply titrate each binding partner in a matrix to determine concentrations that yield optimal assay window, signal-to-background ratio, and Z' values. When proteins are not directly labeled, the concentrations of the PPI and the dye-conjugated antibodies/avidin must also be optimized. It is typical to start with constant concentrations of the dye-conjugated antibody/avidin, and titrate the PPI partners. Most commercial reagents suggest starting conditions; in general, the concentrations of FRET-conjugate antibodies should be higher than the concentrations of the proteins they detect (e.g. 20 nM anti-HA antibody and 10 nM HA-tagged protein).
3. **Select concentrations of (TR-)FRET reagents.** Once the PPI concentrations have been selected, the FRET-tagged antibodies/avidin should be titrated to optimize the assay window, signal-to-background, and Z' values. When concentrations of antibodies are too high, the efficiency of FRET can decrease. This effect, called "hooking," is described in the General Consideration: Hooking Effect section below.
4. **Test effect of DMSO.** Assay performance should be measured over a range of DMSO concentrations to ensure that screening results are not skewed by vehicle effects. For HTS, DMSO generally ranges from 0.1 – 1%, but higher levels are sometimes acceptable.
5. **Assess assay performance.** Positive controls are then titrated in a competition format to ensure that IC_{50} values match expectation. Either known interaction inhibitors or non-labeled binding partners can be used as positive controls for binding competition/disruption.

Example: Performing a TR-FRET Assay

1. All assay components are combined with assay buffer (e.g. 20 mM Tris, pH 7.5, 0.01% Nonidet P40, and 50 mM NaCl) to their optimized concentrations and 19 µL are transferred to each well of a 384-well plate.
2. Test compounds are added. In this case, test compound stocks are at 1 mM, and 0.5 µL is added to each well to give a final compound concentration of 25 µM.
3. All assay plates must contain at least one column of minimal FRET/background control (e.g., all assay components minus one binding partner, usually the one that binds the acceptor fluorophore) and at least one column of maximal FRET vehicle control (i.e., all assay components plus DMSO).
4. The plate is incubated at room temperature for one hour or overnight and then the FRET signal is recorded.
5. Background is subtracted from all FRET values and test compounds are compared to the maximal FRET control to determine percent inhibition of binding for each compound.

Benefits and Limitations

Several factors make FRET and TR-FRET attractive techniques to measure PPIs. As with the other mix-and-read formats, FRET methods are relatively easy to automate and to miniaturize. The approach is also flexible, since many dyes and dye-antibody conjugates are available. In contrast to FP, FRET can be used with a wide range of protein sizes, with the proviso that the FRET pairs must come within a few nanometers of each other. Thus, TR-FRET assays can be performed with peptides, full-length recombinant proteins, transfected cell lysates, and, in some cases, with endogenous proteins in cell lysates. This potentially allows for the development of robust HTS screening assays using binding pairs in a less artificial environment. FRET and TR-FRET are usually performed as ratiometric assays, which reduce the effects of autofluorescence and spectral interference of media and test compounds. TR-FRET further reduces the effect of autofluorescence by allowing organic fluorescence to decay before TR-FRET is measured. Finally, TR-FRET formats allow multiplexing. For instance, FRET acceptors can be multiplexes with a single lanthanide donor, allowing two or three pairs of PPI to be monitored in a single well (16, 17). TR-FRET has been multiplexed with FP, providing increased information in the primary HTS screen (18).

There are limitations to the FRET and TR-FRET formats, however. The signal window for FRET experiments depends on several factors implicit in the Forster equation, including the orientation of the dyes and the size of the complex – including the size of the FRET-labeled antibodies. For very large complexes, AlphaScreen (see AlphaScreen Format) could yield a stronger signal. Furthermore, while TR-FRET's ratiometric format does reduce interference from test compounds, those compounds that absorb a lot of UV light can inhibit excitation of the FRET donor, which absorbs in the far-UV (ca. 350 nm). Finally, if a test compound interferes with the binding of the fluorophore-tagged antibodies to their epitopes it will be detected as a hit in a TR-FRET screen, even though it has no effect on the binding of the target molecules themselves. Following up with controls and secondary assays will remove such compounds from consideration.

AlphaScreen Format

Concept

AlphaScreen™ is bead-based format commercialized by PerkinElmer (http://www.perkinelmer.com) and used to study biomolecular interactions in a microplate format. A newer, more sensitive version of the technology is called AlphaLISA. The acronym ALPHA stands for Amplified Luminescent Proximity Homogeneous Assay. The technology of AlphaScreen was originally developed under the name LOCI® (Luminescent Oxygen Channeling Immunoassay) by Dade Behring, Inc. of Germany (19). Like FRET, AlphaScreen is a non-radioactive, homogeneous proximity assay. Binding of two molecules captured on the beads leads to an energy transfer from one bead to the other, ultimately producing a fluorescent signal. Excitation of the donor bead leads to the formation of singlet oxygen, which diffuses to the acceptor and stimulates emission. Unlike FRET, acceptor emission occurs at a higher energy (lower wavelength) than donor excitation.

The AlphaScreen assay beads are latex-based and approximately 250 nm in diameter. Both bead types (Donor and Acceptor) are coated with a hydrogel that minimizes non-specific binding and self-aggregation and provides reactive aldehyde groups for conjugating biomolecules to the bead surface. The beads are small enough that they do not sediment in biological buffers and bead suspensions do not clog the tips used commonly in liquid handling devices. The beads are typically used at ug/mL concentration and are very stable, even if heated to 95°C for example, for PCR, or lyophilized.

Donor beads contain a photosensitizer, phthalocyanine, which converts ambient oxygen to an excited form of O_2, singlet oxygen, upon illumination at 680 nm. Like other excited molecules, singlet oxygen has a limited lifetime prior to returning to ground state. Within its 4 µsec half-life, singlet oxygen can diffuse approximately 200 nm in solution. If an Acceptor bead is within that distance, energy is transferred from the singlet oxygen to

thioxene derivatives within the acceptor bead, resulting in light production. Without the interaction between donor and acceptor bead, singlet oxygen falls to ground state and no signal is produced. AlphaScreen Acceptor beads use rubrene as the final fluorophore, emitting light between 520 and 620 nm. AlphaLISA acceptor beads use a Europium chelate as the final fluorophore, emitting light in a narrower peak at 615 nm (Figure 5). The AlphaLisa light is less likely to be affected by particles and other substances commonly found in biological samples (for example, plasma and serum), thereby reducing background noise and optimizing precision.

AlphaScreen assays have been developed to quantify enzymes, molecular (protein, peptide, small molecule) interactions, as well as DNA and RNA hybridizations. Due to the large diffusion distance of singlet oxygen, the binding interactions of even very large proteins and phage particles can be quantified by AlphaScreen and AlphaLISA. The high sensitivity and large distance range have led to increasing use of these technologies in HTS settings.

General Consideration: Hooking Effect

The hook effect is a common phenomenon found when using any sandwich-type assay, including AlphaScreen, ELISA, and some of the FRET-based formats described above. When the PPI components are titrated (e.g. during assay development), both donor and acceptor beads become progressively saturated by their target molecules, and the signal increases with increasing protein concentration. At the "hook" point, either the Donor or the Acceptor component is saturated with the target molecule and a maximum signal is detected. Above the hook point, there is an excess of target molecules for the donor or the acceptor beads, which inhibits their association and causes a progressive signal decrease (Figure 6). When the affinity of the PPI is higher (weaker) than the concentrations used in the assay, the hooking effect can be masked, resulting in what looks like a traditional saturation curve that reaches a plateau, rather than hooking. In this case, two competing equilibria are occurring: the signal is decreasing because of the hooking effect on the bead, but the protein-protein interaction is still being increasing because higher concentrations of protein drive the equilibrium toward more protein-protein complex. In either event, choose a protein concentration below the hook point (or saturation point) for your assay.

Assay Design and Development

1. **Instrumentation:** Specialized instrumentation is required to read AlphaScreens since a high-energy laser is needed to excite the donor. However, most major companies who manufacture plate readers now provide models with AlphaScreen capability. Multimode readers suitable for AlphaScreen/AlphaLisa include PerkinElmer's Envision and Enspire, Biotek's Synergy, BMG's PheraStar, FluoStar, and PolarStar, and Berthold Technologies Mithras LB 940. Specialized Alpha readers include PerkinElmer's AlphaQuest and FusionAlpha.
2. **Plates**: AlphaScreen assays are performed in white opaque plates. Assays may be performed in 96-, 384- or 1536-well formats. Some plates, such as the ProxiPlate (PerkinElmer), have been optimized for AlphaScreen to place the sample closer to the detector and therefore give an increased signal. Excitation and signal measurement are both accomplished from the top of the plate. The measured signal is in part dependent upon reflected light, therefore the reflective properties of the plate influence signal. Higher density plates (e.g. 384- vs 96-well, 1536- vs 384-well) generally provide more sensitive AlphaScreen assays. First, the higher density wells are narrower and more efficiently reflect the emitted light back to the detector. Second, higher density plates allow a higher proportion of the sample to be excited by the 1 mm laser beam, leading to proportionately greater signal generation. Higher density plates also allow less reagent use, lowering the overall cost of the screen.
3. **Buffers**: Choose pH buffering capacity and salt concentration that will facilitate the desired interactions between the components of the assay. The following buffers have been used without problems: Acetate, HEPES, Bis-Tris, MES, Bis-TRIS propane, MOPS, CAPS, Phosphate, Carbonate, PIPES, Citrate, Formate, and Tris. pH values between pH 2.5 to 9 are well tolerated. Higher pH is also tolerated but there may be

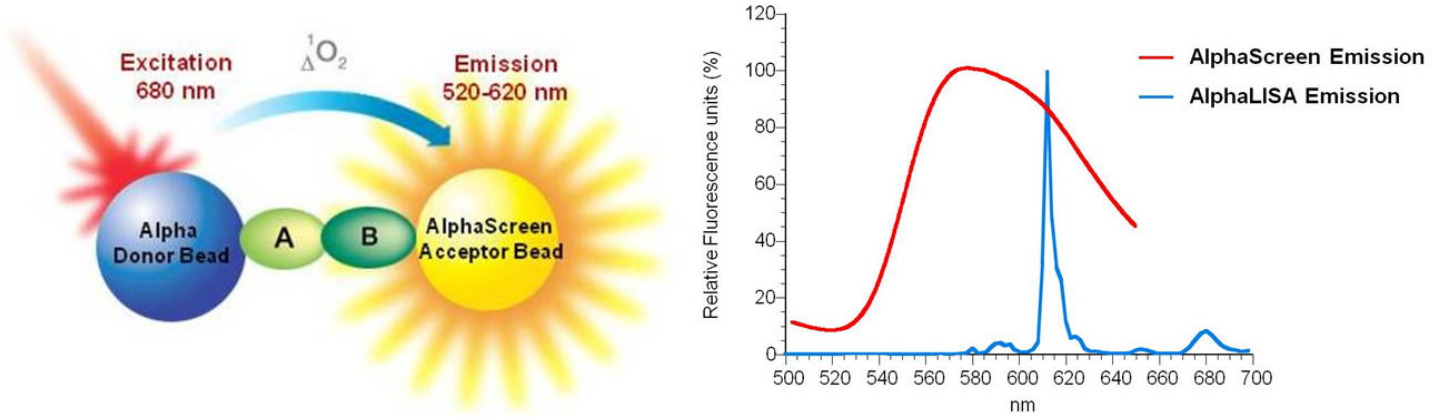

Figure 5: AlphaScreen and AlphaLisa. **Left**: Binding of biological partners (represented by small ovals A and B) brings Donor and Acceptor beads (represented by the large blue and yellow circles) into close proximity (≤200 nm) and thus a fluorescent signal between 520–620 nm is produced in the case of AlphaScreen and 615 nm in the case of the AlphaLisa. When there is no binding between biological partners, Donor and Acceptor beads are not in close proximity. Singlet oxygen decays and no signal are produced. **Right**: comparison of emission spectra for AlphaScreen (red) and AlphaLISA (blue).

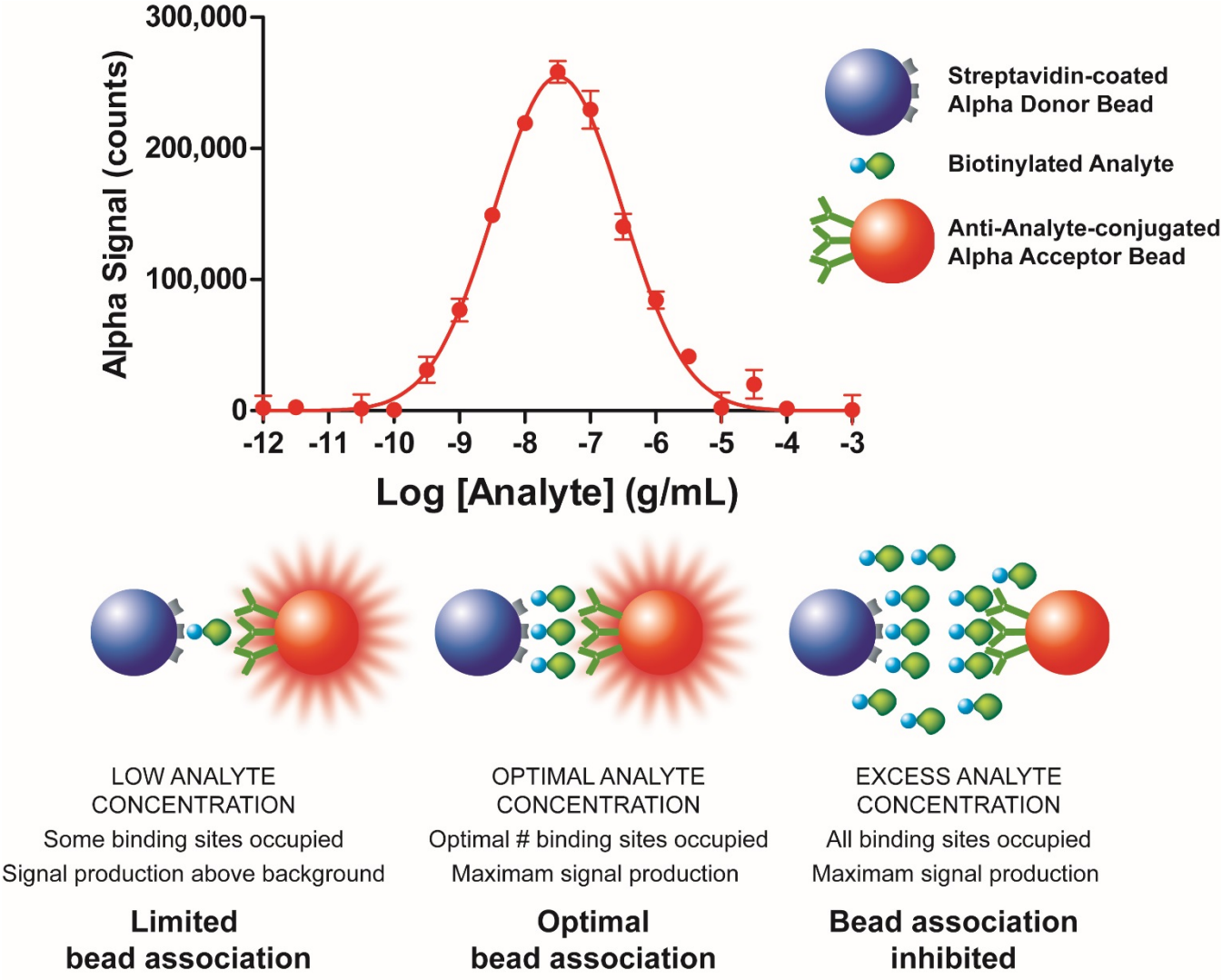

Figure 6: Hooking Effect **in** AlphaScreen. These principles hold for all sandwich-based assay formats (adapted from PerkinElmer).

some loss of signal. If metal co-factors are needed for the PPI, it is best to titrate these components appropriately, but note that high concentrations will quench the signal; in particular, Al^{2+}, Fe^{2+}, Fe^{3+}, Cu^{2+}, Ni^{2+} and Zn^{2+} have been shown to quench singlet oxygen in the mM and sub-mM ranges (100 μM for Fe2+).

Detergents and/or blocking proteins should be used to reduce non-specific binding (see General Considerations). For most AlphaScreen applications, a BSA concentration of 0.1% (w/v) is sufficient to minimize non-specific interactions; alternate blocking reagents such casein, gelatin, heparin, poly-lysine, salmon sperm DNA, or Dextran T500 can be used (see Assay Design). The preservative azide can act as a potent scavenger of singlet oxygen and will inhibit the AlphaScreen signal, so Proclin 300 (Sigma-Aldrich) is recommended as a preservative and anti-microbial agent.

4. **Kits**: Generic detection kits from PerkinElmer include pre-coated beads that capture biotinylated, FITC-labeled, DIG-labeled, GST-tagged, 6X His-tagged, Protein A, Protein G, Protein L and anti-species beads. Unconjugated Donor and Acceptor beads are also available for direct conjugation of an antibody or other reagent of choice. Note that if you have purified your GST-tagged proteins or His-tagged proteins using an affinity column and will be using a GSH or Ni^{2+} bead in your Alpha assay, you will need to dialyze away any glutathione or imidazole in your purified protein preparation. These components will interfere with the interaction between the tagged protein and the bead. PerkinElmer also sells specific kits for various applications.
5. **Titration of reagents**: It is important to optimize the concentrations of each protein conjugated to the Donor and Acceptor beads. On the one hand, the amount of PPI formed is dependent on the concentrations of each protein and the affinity of the interaction. Until saturation is achieved, increasing the concentration of either protein will push the equilibrium towards higher complex formation. On the other hand, each type of Alpha bead has a specific binding capacity; once the beads are saturated with associated protein, additional protein may lead to a hooking effect (see above).

   Binding capacities are influenced by a number of factors, including the size of the protein and the affinity of the bead for the protein. First, there is usually a higher binding capacity for smaller proteins. For instance, streptavidin-coated beads at 20 μg/mL usually saturate at around 30 nM of biotinylated peptide (ca 1.5 KDa), but saturate at around 2-3 nM of biotinylated antibody (ca 150 KDa). Second, the saturation point of a bead varies depending on its affinity reagent. For instance, anti-GST antibody beads bind more tightly to GST-labeled proteins than do glutathione beads. Hence, the saturation point is usually 20 nM of GST tagged protein binding to anti-GST beads, but 200 nM of GST-protein binding to glutathione-conjugated beads. More information on capacity can be found at the Perkin Elmer website (www.perkinelmer.com).
6. **Assay Conditions:** The beads are sensitive to light and temperature. It is important to store the beads in the dark and conduct the parts of the assay that include the beads in low light conditions (less than 100 Lux) or to use green filters. Affected areas of the lab include the bench, plate reader and liquid handler. Finally, the chemistry is designed to give best results at room temperature (e.g.: 20–25°C); do not chill plates or incubate on ice before reading. Typically the AlphaScreen signal variation is 8% per °C so consistent temperature is important.

Steps for developing the assay:

1. Choose a suitable buffer system, noting the boundaries described above.
2. Titrate each binding partner to ascertain the optimal concentrations. For initial experiments, a final bead concentration of 20 μg/ml is recommended for both Donor and Acceptor beads. Subsequent dilution of the beads may be assessed once it is known that a sufficiently high signal/background can be achieved. Typically, most AlphaScreen assays will utilize a final concentration of biotinylated binding partner in the

nanomolar range (e.g.: 0.5 nM–30 nM with 20 µg/mL of beads). Concentration ranges for each binding partner that interact directly with a capture molecule on the AlphaScreen beads vary considerably (ex.: 0.1 nM–300 nM) depending on the affinity of the binding partners, the efficiency of labeling, and/or stoichiometry of the capture tag/epitope.

3. It may also be necessary to vary the order of addition of the components to permit the most efficient interactions.
4. Incubation times need also to be optimized.

Benefits and limitations

Alpha technologies have become popular in recent years, likely because they are adaptable to many assay types, are very sensitive, and are active over long distances (200 nm vs 10-20 nm for TR-FRET). The central limitations to AlphScreen and AlphaLisa are the increased expense vs other mix-and-read formats and the sensitivity of the materials to ambient light.

Glickman, et al (20), compared FRET, TR-FRET and AlphaScreen formats (20), and concluded that the ALPHAScreen format had the best sensitivity and dynamic range. Of the three formats, TR-FRET assay had the least inter-well variation, most likely because it is a ratiometric type of measurement. Both FRET-type and AlphaScreen formats can measure a wide range of affinities (K_d's ranging from low pM to low mM) because there are no wash steps. It is noteworthy that AlphaScreen beads have 300-3000 proteins/bead, and the protein density can be varied. This multi-valency can significantly increase sensitivity, because one PPI per bead pair leads to the maximal signal. Furthermore, high concentrations can cause avidity. On the one hand, avidity augments the apparent binding affinity of the PPI, so less material is required. On the other hand, avidity might not be desired (e.g. for high affinity PPI or high affinity inhibitors), and the apparent IC_{50} values for inhibitors could be significantly weaker than the actual affinity of the inhibitor/protein interaction. With FRET methods, each binding partner carries a single label so that if some beads are unbound, a lower signal will be generated. However, monovalency also implies that the signal will be proportional to the number of binding interactions.

Validating drug-like binding of PPI inhibitors

The goal of primary screening is to select a set of compounds that *might be active*. Among "actives," however, are many compounds that act by mechanisms that will not be optimizable into a qualified drug lead or biological probe. Some of the artifactual mechanisms that lead to activity in a primary assay are specific to the assay format; as described above, compounds could autofluoresce or quench the fluorescence signal used to detect the PPI. Thus, it is very valuable to develop at least one orthogonal assay formats, or an *in vitro* assay and a cell-based assay, plus an independent way to measure binding directly.

Other artifacts are less selective to the assay methodology, though they may be somewhat selective for the proteins or assay conditions. A well-described and very common example is compound aggregation (3). Aggregates can be quite large (30-200 nM) and can interfere with protein structure in a number of pathological ways. Aggregation can also be very dependent on the assay condition; rather than thinking of compounds as "aggregators," it is more accurate to think of aggregation as a form of molecular interaction, dependent on salt, pH, detergents, carrier proteins, and concentration of the compound. Thus, it is not sufficient to demonstrate that a compound is selective for a particular screen over other screens; to be a bona fide PPI inhibitor, the compound must bind at a distinct site(s) on one of the proteins in the complex. Binding stoichiometry is therefore a key metric for selecting useful and optimizable probes/leads.

There are a number of biophysical assays that measure binding of the small molecule to the protein. It is very beneficial to use at least two assays, since no assay is infallible, and different types of information can be gleaned from each format. Depending on the size of the protein(s), the binding affinity of the molecule, and other details, the following methods can be used:

Optical Biosensors: There are several related technologies for measuring the binding of a surface-immobilized "ligand" to a soluble "analyte." In general, optical biosensors detect changes in the angle, color, or phase of light reflected off of a solid/liquid interface. Many instruments are sensitive enough to monitor the binding of a small-molecule analyte to a surface-bound protein. These systems can also be used in competition experiments, in which a PPI is monitored in the presence of increasing concentrations of inhibitor. Because the signals are proportional to the change in mass of the analyte, PPI are usually easier to monitor than protein/small-molecule interactions.

The first popular optical biosensor was the surface plasmon resonance (SPR) instrument developed by Biacore (GE Healthcare). The technology is now widely used, and numerous companies market SPR instruments (e.g. Bio-Rad, ICX, and others). Most SPR instruments use microfluidics to introduce the analyte, and monitor the binding in real time. The concentration of analyte can be varied to develop a dose-response. Through kinetic and/or steady-state experiments, SPR provides a measure of binding stoichiometry, reversibility, and affinity to a protein bound to a surface. For recent descriptions of how to analyze and evaluate small-molecule SPR data, see Rich et al, 2011 and Gianetti et al, 2008 (21, 22).

Other technologies include optical gradients (SRU BIND, Corning Epic) and interferometry (Forte Bio Octet Red). The optical gradient systems are plate-based, allowing high throughput, but more limited kinetic resolution. In interferometry, the ligand is coated onto fiber optic sensors that are then dipped into solutions of analyte. This technology is developing rapidly, and could soon have the throughput, cost/assay, and sensitivity to rival SPR for measuring small-molecule/protein interactions.

Nuclear Magnetic Resonance (NMR): NMR measures the response of nuclei in a magnetic field, and is very sensitive to the chemical environment of the nucleus. Due to the flexibility of the method, NMR has many uses in small-molecule characterization and protein structure determination. Small-molecule/protein NMR experiments come in two general formats – ligand-detected and protein-detected. Ligand-detected experiments measure the change in the compound's NMR signals ("resonances") as a function of binding to protein. Energy can be transferred from the solvent and/or protein to the compounds (Saturation Transfer Difference, WaterLOGSY) or the apparent mass of the compound can be increased due to binding a large protein (translation, diffusion). Ligand-detected measurements are often used qualitatively, to assess the presence of binding to the target. Saturation Transfer Difference is particularly popular for moderate-throughput applications, because the protein concentration is low (micromolar) and it is particularly effective for compounds in fast exchange (weaker than micromolar). There is no limit on the protein size for ligand-detected experiments.

Protein-detected NMR provides a measurement of the effect of the compound on the protein. The most popular moderate-throughput methods are ^{15}N-1H HSQC and ^{13}C-1H HSQC and the related ^{15}N- and ^{13}C-TROSY. N-H HSQC measures the environment of the amide N-H bond, and thus provides a single peak for each amino acid in a protein sequence (except for proline; asparagine and glutamine also have primary NH signals). ^{13}C-1H HSQC uses labeled methyl groups to detect changes to valine, methionine, isoleucine, and leucine. If the NMR spectrum has been assigned, changes to the resonances in the presence of compound will suggest the binding site. Even without assigning the protein resonances, however, compounds can be binned by binding site, and non-binders or multi-site binders can be identified. Protein-detected NMR used to be reserved for relatively small proteins; however, technical improvements in NMR hardware and pulse sequences, deuteration of the protein, and selective labeling have made many more proteins amenable to these experiments.

Isothermal calorimetry (ITC): ITC measures the heat generated or absorbed by a binding interaction. For weakly binding PPI inhibitors (in the mid micromolar range), ITC can be challenging because protein usage is high, compound solubility can be limited, and the heats of binding are small. It is important to match the protein and compound buffers and to control for the heat-of-dilution as the compound sample is added to the protein (or vice versa). Despite these challenges, ITC can be very valuable due to the fact that unlike some other

methods, ITC is truly label-free, and all components are in solution. By directly measuring the energy of binding, ITC provides information on the entropy and enthalpy of the interaction, the binding affinity (by titrating one of the partners) and the binding stoichiometry. More detail on how to conduct these studies can be found at the MicroCal website.

Thermal stabilization - differential scanning calorimetry (DSC) and differential scanning fluorimetry (DSF, Thermafluor, Protein Thermal Shift): One way to define protein stability is by the temperature at which the protein unfolds. Unfolding is usually a highly cooperative process, and gives a defined melting temperature (T_m) under a given condition of concentration, buffer, etc. When a compound binds to the protein, the complex is more stable than the protein alone, and the protein's T_m increases. To measure the binding affinity of a compound for a protein, one monitors the increase in T_m (ΔT_m) as the concentration of compound is increased. T_m measurements are generally done with micromolar concentrations of protein, and are therefore most sensitive to determining binding affinities in this range. This method also has the advantage that all components are in solution.

There are several methods for measuring the change in T_m. Differential scanning calorimetry (DSC) monitors the heat absorbed by the protein as the temperature is increased; the energy/degree increases at the T_m. Differential scanning fluorimetry (DSF) monitors the binding of a hydrophobic dye to the protein as the temperature is increased. The dye binds preferentially to hydrophobic portions of a protein that are exposed when a protein melts; this binding is accompanied by a change in fluorescence as a function of temperature. Typical DSF dyes include SYPRO orange and 1,8-ANS; DSF measurements are read in specialized instruments or in real-time PCR machines. The magnitude of DSC and DSF signals, and the ΔT_ms obtained from small-molecule binding studies, is dependent on both the protein and the assay conditions. Thermodynamic statements are only valid in the cases that thermal denaturation is reversible. Nevertheless, ΔT_m measurements can provide a rapid assessment of binding affinity, and are increasingly being used in primary screening assays as single-concentration measurements. Sample assay development guidelines can be found in Niesen, et al (23).

Sedimentation Analysis (SA; Analytical ultracentrifugation): Sedimentation analysis measures the sedimentation of proteins in response to a centrifugal force. The protein concentration is measured along the length a centrifugation cell using the proteins absorbance, refractive index, or fluorescence. Two general types of SA experiments are Velocity Sedimentation and Equilibrium Sedimentation. Equilibrium sedimentation gives a first-principle measurement of molecular mass, and is often used to measure self-association (e.g. dimerization) constants. It can also be used, however, to assess the binding of a small molecule to the protein, particularly if the molecule has absorbance at wavelengths distinct from the protein (e.g. > 300 nm). The compound's aggregation state and the compound's affect on the apparent molecular mass of the protein provide a quick readout of aggregation-based artifacts. Direct binding of the compound to protein can also be assessed (24). Analytical centrifuges are sold by Beckman Coulter, and add-on fluorescence detection is available from Aviv Biomedical.

X-ray crystallography: X-ray crystallography continues to be the gold standard for characterizing protein/small molecule interactions. The high-resolution (ca. 1.5 – 3 angstrom) structure fit from x-ray diffraction data provides information on the binding site and the specific contacts between compound and protein. The presence of a single molecule bound to a single binding site suggests – but does not prove – that the compound's inhibition of a PPI arises from binding at that site. Co-structures of compounds and proteins are generally prepared by soaking the compound into a crystal of the protein or by co-crystallization of the protein and compound together. In many cases, it is difficult to obtain co-crystal structures, either because the protein does not crystallize well, the compound induces changes to the protein structure that inhibit crystallization (e.g. binding at a crystal contact, changing the protein conformation), or the compound is not soluble enough.

Useful websites

General

Microplates: http://www.perkinelmer.com/Catalog/Category/ID/Microplates

Avitag, for in vitro biotinylation: http://www.avidity.com/t-technology.aspx

In vitro assays:

ELISA: http://www.piercenet.com/browse.cfm?fldID=F88ADEC9-1B43-4585-922E-836FE09D8403#detectionmethods

http://www.biotek.com/resources/articles/kinetic-elisa-advantage.html

http://www.biocompare.com/Articles/ApplicationNote/1727/Optimisation-Of-Assays-Interference-In-Immunoassays-Recognize-And-Avoid.html

FP: http://www.invitrogen.com/..../Fluorescence-Polarization-FP.html

FRET, TR-FRET: http://www.htrf.com/technology/assaytips

http://www.invitrogen.com/.../Fluorescence-Resonance-Energy-Transfer-FRET.html

http://www.perkinelmer.com/Catalog/Category/ID/lance%20Protein%20Binding

AlphaScreen, AlphaLISA: http://www.perkinelmer.co.jp/tech/tech_ls/protocol_collection/AlphaScreen_guidebook.pdf

http://www.TGR-Biosciences.com

Biophysical Assays

SPR: http://www.sprpages.nl/Index.php

Isothermal Calorimetry: http://www.microcal.com/technology/itc.asp

Differential Scanning Calorimetry: http://www.microcal.com/technology/dsc.asp

Differential Scanning Fluorimetry: http://thermofluor.org/

http://www3.appliedbiosystems.com/cms/groups/mcb_marketing/documents/generaldocuments/cms_095306.pdf

References

1. Lipinski CA, Lombardo F, Dominy BW, Feeney PJ. Experimental and computational approaches to estimate solubility and permeability in drug discovery and development settings. Adv. Drug Deliv. Rev. 2001;46:3–26. PubMed PMID: 11259830.
2. Lipinski CA. Lead- and drug-like compounds: the rule-of-five revolution. Drug Discovery Today: Technologies. 2004;1:337–341. PubMed PMID: 24981612.
3. McGovern SL, Helfand BT, Feng B, Shoichet BK. A specific mechanism of nonspecific inhibition. J. Med. Chem. 2003;46:4365–4272. PubMed PMID: 13678405.
4. Boehm H-J, Boehringer M, Bur D, et al. Novel inhibitors of DNA gyrase: 3D structure based biased needle screening, hit validation by biophysical methods, and 3D guided optimization. A promising alternative to random screening. J. Med. Chem. 2000;43:2664–2674. PubMed PMID: 10893304.

5. Arkin MR, Wells JA. Small-molecule inhibitors of protein-protein interactions: progressing towards the dream. Nature Reviews Drug Discovery. 2004a;3:301–317. PubMed PMID: 15060526.
6. Fry D. Protein-Protein interactions as targets for small molecule drug discovery. Biopolymers. 2006;84:535–553. PubMed PMID: 17009316.
7. Khoury K, Dömling A. P53 Mdm2 Inhibitors. Curr Pharm Des. 2012;(May):29. [Epub ahead of print]. PubMed PMID: 22650254.
8. Saupe J, Roske Y, Schillinger C, et al. Discovery, structure-activity relationship studies, and crystal structure of the nonpeptide inhibitors bound to the Shank3 PDZ domain. Chem Med Chem. 2011;6:1411–22. PubMed PMID: 21626699.
9. Simons PC, Young SM, Carter MB, Waller A, Zhai D, Reed JC, Edwards BS, Sklar LA. Simultaneous in vitro molecular screening of protein-peptide interactions by flow cytometry, using six Bcl-2 family proteins as examples. Nature Protocols. 2011;6:943–952. PubMed PMID: 21720309.
10. Jameson DM, Croney JC. Fluorescence polarization: past, present and future. Comb Chem High Throughput Screen. 2003;6:167–73. PubMed PMID: 12678695.
11. Schade SZ, Jolley ME, Sarauer BJ, Simonson LG. BODIPY-alpha-casein, a pH-independent protein substrate for protease assays using fluorescence polarization. Anal Biochem. 1996;243:1–7. PubMed PMID: 8954519.
12. Du Y, Masters SC, Khuri FR, Fu H. Monitoring 14-3-3 protein interactions with a homogeneous fluorescence polarization assay. J Biomol Screen. 2006;11:269–76. PubMed PMID: 16699128.
13. Fu H, Subramanian RR, Masters SC. 14-3-3 proteins: structure, function, and regulation. Ann Rev Pharmacol Toxicol. 2000;40:617–47. PubMed PMID: 10836149.
14. Burke TJ, Loniello KR, Beebe JA, Ervin KM. Development and application of fluorescence polarization assays in drug discovery. Comb Chem High Throughput Screen. 2003;6:183–94. PubMed PMID: 12678697.
15. Owicki JC. Fluorescence polarization and anisotropy in high throughput screening: perspectives and primer. J Biomol Screen. 2000;5:297–306. PubMed PMID: 11080688.
16. Hilal T, Puetter V, Otto C, Parczyk K, Bader B. A dual estrogen receptor TR-FRET assay for simultaneous measurement of steroid site binding and coactivator recruitment. J Biomol Screen. 2010;3:28–78. PubMed PMID: 20150592.
17. Jeyakumar M, Katzenellenbogen JA. A dual-acceptor time-resolved Föster resonance energy transfer assay for simultaneous determination of thyroid hormone regulation of corepressor and coactivator binding to the thyroid hormone receptor: Mimicking the cellular context of thyroid hormone action. Anal Biochem. 2009;1:73–8. PubMed PMID: 19111515.
18. Du Y, Nikolovska-Coleska Z, Qui M, Li L, Lewis I, Dingledine R, Stuckey JA, Krajewski K, Roller PP, Wang S, Fu H. A dual-readout F2 assay that combines fluorescence resonance energy transfer and fluorescence polarization for monitoring bimolecular interactions. ASSAY and Drug DevTechnol. 2011;9:382–393. PubMed PMID: 21395401.
19. Ullman EF, et al. Luminescent oxygen channeling immunoassay: Measurement of particle binding kinetics by chemiluminescence. Proc. Natl. Acad. Sci. USA. 1994;91:5426–5430. PubMed PMID: 8202502.
20. Glickman JF, Wu X, Mercuri R, Illy C, Bowen BR, He Y, Sills M. Comparison of ALPHAScreen, TR-FRET, and TRF as Assay Methods for FXR Nuclear Receptors. J Biomol Screen. 2002;7:3. PubMed PMID: 11897050.
21. Rich RL, Myszka DG. Survey of the 2009 commercial optical biosensor literature. J. Molecular Recognition. 2011;24:892–914. PubMed PMID: 22038797.
22. Giannetti AM, Koch BD, Browner MF. Surface plasmon resonance based assay for the detection and characterization of promiscuous inhibitors. J. Med. Chem. 2008;51:574–580. PubMed PMID: 18181566.
23. Niesen FH, Berglund H, Vedadi M. The use of differential scanning fluorimetry to detect ligand interactions that promote protein stability. Nature Protocols. 2007;2:2212–2221. PubMed PMID: 17853878.
24. Arkin, MR (2004b). Sedimentation for success. Modern Drug Discovery Nov: 45-47. (pdf)

Additional References

Degorce F, Card A, Soh S, Trinquet E, Knapik GP, Xie B. HTRF: A technology tailored for drug discovery – a review of theoretical aspects and recent applications. Curr Chem Genomics. 2009;3:22–32. PubMed PMID: 20161833.

Karimova G, Pidoux J, Ullmann A, Ladant D. A bacterial two-hybrid system based on a reconstituted signal transduction pathway. Proc Natl Acad Sci U S A. 1998;95:5752–5756. PubMed PMID: 9576956.

Immunoassay Methods

Karen L. Cox, BS,[1] Viswanath Devanarayan, PhD,[2] Aidas Kriauciunas,[1] Joseph Manetta, BS,[1] Chahrzad Montrose, PhD,[1] and Sitta Sittampalam, PhD[3]

Created: May 1, 2012; Updated: July 8, 2019.

Abstract

Immunoassays are used to quantify molecules of biological interest based on the specificity and selectivity of antibody reagents generated. In HTS and lead optimization projects, assays are designed to detect molecules that are produced intracellularly or secreted in response to compounds screened. This chapter describes the basics of designing and implementing robust, automation friendly immunoassays for HTS, modes of immunoassay formats (competitive and sandwich), instrumentation, reagent selection, experimental design and detailed data analysis concepts. The importance of an appropriate curve-fitting model for calibration curves used for quantification is also addressed in detail. This is an excellent primer for beginners as well as for experienced investigators.

Author Affiliations: 1 Eli Lilly & Company, Indianapolis, IN; Email: cox_karen_l@lilly.com; Email: manetta_joseph@lilly.com; Email: montrose-rafizadeh_chahrzad@lilly.com. 2 AbbVie, Chicago, IL; Email: viswanath.devanarayan@abbvie.com. 3 National Institutes of Health, Rockville, MD; Email: gurusingham.sittampalam@nih.gov.

Immunoassay Development, Optimization and Validation Flow Chart

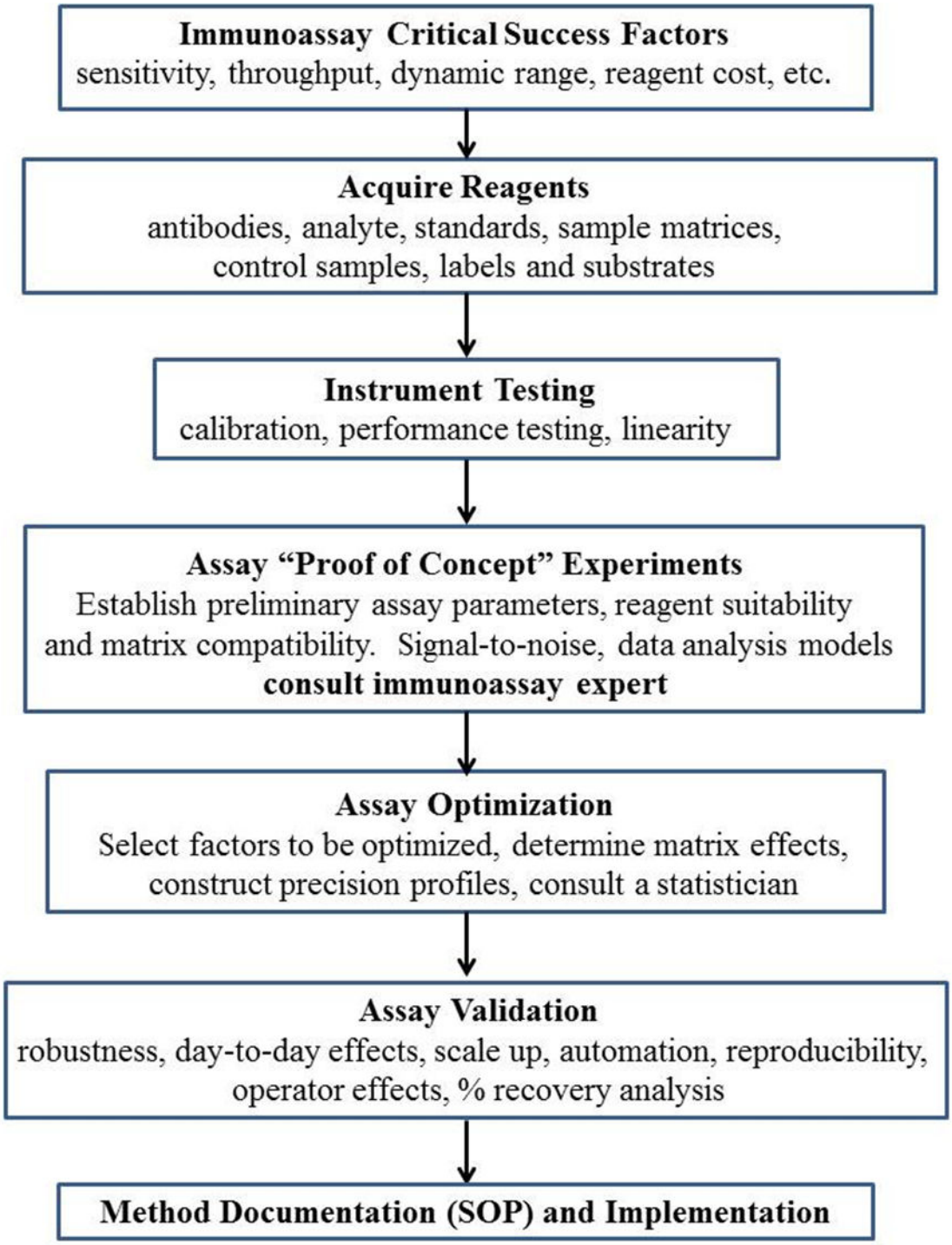

Introduction

The intent of this document is to provide general guidelines to aid in the development, optimization and validation of an immunoassay. Following these guidelines will increase the likelihood of success in developing a robust immunoassay that will measure consistent values for unknown samples.

Immunoassays are used when an unknown concentration of an analyte within a sample needs to be quantified. To obtain the most accurate determination of the unknown concentration, an immunoassay must be developed based not only on the usual assay development criteria (standard deviation or optimal signal window) but also on how well the immunoassay can predict the value of an unknown sample. First, one needs to establish the assay critical success factors. Then the immunoassay needs to be developed, which establishes proof of concept. During the optimization phase, the quantifiable range of the immunoassay method is determined by calculating a precision profile in the matrix in which the experimental samples will be measured. A spiked recovery is then performed by spiking the analyte into the matrix and determining the percent recovery of the analyte in the matrix. If the precision profile is within the desired working range, then assaying spiked recovery samples over several days completes the validation of the immunoassay. If the precision profile limits are not within the desired working range, further optimization of the immunoassay is required prior to validation.

Basic Steps for Developing and Running an Immunoassay

1. Establish assay critical success factors (i.e. sensitivity required).
2. Ensure appropriate antibody and antigen reagents are available.
3. Adsorb antigen or capture antibody to a solid surface.
4. Wash off unbound reagents.
5. Block nonspecific binding sites to reduce background.
6. Incubate the secondary antibody with the sample.
7. Wash off unbound reagents.
8. Incubate secondary antibody-conjugate with sample.
9. Wash off unbound reagents.
10. Incubate substrate to generate signal.
11. Calibration curve fitting, data analysis and quantitation by non-linear regression.

Basic Steps in Using Immunoassays for High Throughput Screening (HTS)

Immunoassays are used in screening to quantify the production or inhibition of antigens/haptens related to a disease target. These antigens or haptens are characteristic of the disease process and mediated by the target, such as cytokines or growth factors. Hence the screening procedure will involve incubating compounds with the specified target, usually expressed in cells, and collecting the cell medium or lysates to quantify the activity of the compounds. Several examples of this approach for using immunoassay procedures have been described in the literature (1-5). The critical steps in setting up a screen are as follows:

1. Develop a validated immunoassay as described above.
2. Acquire antibody, antigen/calibrator, label and buffer reagents in quantities needed for HTS.
3. Establish liquid handling and automation procedures for screening and immunoassay methods.
4. Establish stability of the capture antibody or antigen bound to a plate. Determine compound collections to be tested.
5. Develop and validate a method for incubation of compounds with a relevant target in the screening mode.
6. Develop a sample collection procedure from screening experiments.
7. Develop data analysis procedures to use immunoassay data to derive compound potency such as IC_{50} or EC_{50}.

Immunoassay Parameters

It is important to define the relevant immunoassay parameters before one begins the development, optimization and validation of an immunoassay:

1. Analyte (hapten or antigen) to be measured.
2. Sample matrices in which measurements will be made (serum, plasma, cell lysates, culture media, etc.).
3. Source of antibody, analyte standards and detection reagents (labeled antibody, enzyme substrates, etc.). Availability of these reagents is a critical requirement.
4. Detection mode (colorimetric, fluorescence or chemiluminescence) and appropriate plate readers.
5. Type of immunoassay to develop: Sandwich, competitive or antigen-down formats.
6. Expected analyte concentration ranges to be measured: pg/ml, ng/ml or µg/ml in the sample matrix of choice. This would determine the detection limits and the measurable range that should be achieved in a validated assay.
7. Data analysis models and format for reporting results.
8. Validation and optimization criteria using statistical experimental design tools.
9. Recovery, accuracy and precision expected at the limits of quantification and the measurable range.
10. Sample throughput, frequency of use, automation and the number of laboratories that would run the assay.
11. Control samples that would be used for optimization, validation and quality control runs.

Reagents

Reagents are a critical piece of any assay development process. This refers to all of the reagents that will be used in the assay. There are certain items that need to be considered when obtaining reagents:

1. Quality of standards and antibodies.
2. Quantity of standards and antibodies.
3. Purity of standards and antibodies (when possible antibodies are affinity purified).
4. Selectivity and specificity of antibodies.

Example Plate Types

Greiner high binding plates, Costar EIA/RIA high-low binding plates, Immunotech, Falcon, Nunc

Note: Other plate types can also be used based on the experience of the investigator and appropriate quality control to demonstrate acceptability.

Coating Buffers

50 mM sodium bicarbonate, pH 9.6

0.2 M sodium bicarbonate, pH 9.4

PBS - 50 mM Phosphate, pH 8.0, 0.15 M NaCl

Carbonate-bicarbonate

Phosphate Buffer: 1.7 mM NaH_2PO_4, 98 mM $Na_2HPO_4 \cdot 7H_2O$, 0.1% NaN_3, pH 8.5

TBS - 50 mM TRIS, pH 8.0, 0.15 M NaCl

Blocking Buffers

1% BSA or 10% host serum in TBS, or TBS with 0.05% Tween-20

Phosphate Buffer: 73 mM Sucrose, 1.7 mM NaH_2PO_4, 98 mM $Na_2HPO_4 \cdot 7H_2O$, 0.1% NaN_3, pH 8.5

1% HSA in PBS

Casein Buffer: Pierce Blocker cat# 37528

Protein Free Block: Pierce cat# 37573

Pierce has many blocking buffers that are available in their catalog.

Heterophilic Blocking Reagent (HBR): Scantibodies Laboratory, Inc., cat# 3KC533

Scantibodies has many other blocking reagents that are available in their catalog.

Wash Buffers

PBST, 0.05% Tween-20

TBST, 0.05% Tween-20

Antibody Diluents Buffers

1% BSA or 10% host serum in TBS, or TBS with 0.05% Tween-20

1% BSA or 10% host serum in PBS, or PBS with 0.05% Tween-20

50 mM HEPES, 0.1 M NaCl, 1% BSA, pH 7.4

Blocking buffer

Matrix Diluent

1. Serum or plasma from the sample species (this might contain the analyte to be measured which will interfere with the assay)
2. Serum or plasma from a species different from the sample (the analyte, if present, might not cross react with the antibody)
3. 0.1 M HEPES, 0.1 M NaCl, 1% BSA, 0.1% Tween-20
4. Tissue culture medium for samples
5. Cell lysates (these might contain SDS or other denaturing reagents that might interfere with the assay)

Enzymes and Substrates

1. Horseradish peroxidase (HRP) substrates:
    a. TMB: 3, 3', 5,5'-tetramethyl benzidine (colorimetric)
    b. OPD: o-phenylene diamine (colorimetric)
    c. ABTS: 2, 2'-azino-bis (3-ethylbenzthiazoline-6-sulfonic acid) (colorimetric)
    d. Pierce Supersignal (chemiluminescent)
    e. Pierce QuantaBlu (chemifluorescent)
    f. Pierce QuantaRed (chemifluorescent)
    g. Pierce has other substrates that provide strong signal and sensitivity with HRP enzyme conjugates that are available in their catalog.
2. Alkaline phosphatase substrate:

a pNpp (p-Nitrophenyl Phosphate)

Stop Solutions

1. HRP/TMB: 2M H_2SO_4 solution (at a 1:1 volume with the HRP/TMB substrate/enzyme solution)
2. OPD: 3M H_2SO_4 solution, (at a 1:1 volume with the OPD substrate/enzyme solution)
3. ABTS: 1% SDS

Absorbance Readout

1. HRP TMB: 450 nm
2. OPD: 490 nm
3. ABTS: 405 nm

Fluorescent Readout (Emax/Amax)

1. QuantaBlu 420/325
2. QuantaRed 585/570
3. FITC 518/494

Luminescent Readout

1 An immunoassay technique where the antibody or the antigen is labeled with a molecule capable of emitting light during a chemical reaction. For detection, a luminescent plate reader is required (available from PerkinElmer).

Specific Antibodies

1. Sandwich Immunoassay: matched pair of antibodies, one for analyte capture on a solid surface and one for detection that binds to the antigen/hapten/analyte. Antibodies need to be affinity purified for optimal results.
2. Competitive Immunoassay: a single antibody specific for the hapten/analyte. For optimal results affinity purified reagents are preferred.

Standards or Antigen (Analyte)

1. The analyte to be measured is typically a recombinant form of the natural analyte or peptide.
2. Enough standard should be obtained for use in the development phase, validation phase and the continued support of the method to avoid changing lots and/or running out of standard.
3. Standard quality: Can vary from vendor to vendor and from lot to lot from a vendor.
4. Standard stability: Information on the stability of a standard can be obtained from the vendor and their recommendations should be followed in storing the standards.

Control Samples

1. Control samples are real samples where the antigen analyte level has been determined by another validated method. Samples are aliquoted, frozen and used as control samples in each experiment to track assay performance.
2. Spiked controls are created by adding a known concentration of the standard analyte into the matrix (for example: tissue culture, serum, plasma, or cell lysates). Spiked controls can be used to determine assay performance based on calculating the percent recovery.

Instrumentation

Instrument Linearity and Performance

The instrument used to read the output of the immunoassay should be tested initially for both linearity and performance. Instrument performance should be regularly calibrated according to manufacturer's specifications. The majority of plate readers employ UV-Vis Absorbance, fluorescence or chemiluminescence signals as the measured response, because the products of enzyme labels are chromophores, fluorophores or emit luminescent signals. Linearity in response to the specific enzyme product of an enzyme-linked immunoassay (ELISA) should be checked at the appropriate wavelengths and instrument settings.

Spectrophotometric/Colorimetric Plate Readers

Lamp sources and Photomultiplier Tubes (PMT) vary in quality and performance in many plate readers. The linear range of many plate readers is generally between 0-3 Absorbance Units (AU), but other instruments have a linear range up to 4.0 AU. A malfunctioning lamp source or photomultiplier tube can significantly affect the linear response range.

Fluorescence Plate Readers

These readers employ excitation and emission filter sets in addition to excitation lamp sources and PMTs. In addition to the lamps and PMTs, the filter sets also vary in quality, light throughput and bandwidth. Fluorescence signals are generally in Relative Fluorescence Units (RFU) and linearity should be verified with appropriate filter sets for the fluorophore employed according to instrument specifications.

Chemiluminescence Readers

These instruments have sensitive photomultipliers to detect light emitted from a chemical reaction. No Lamp sources are necessary. These readers usually have a much larger dynamic range, thus allowing for the increase in sensitivity. Signals or responses are measured in Relative Light Units (RLU) and can be significantly different depending on the instrument design.

Immunoassay Formats

An ELISA is one of several methods used in the laboratory to detect and quantify specific molecules. ELISAs rely on the inherent ability of an antibody to bind to the specific structure of a molecule. In order to optimize an ELISA and obtain the sensitivity and dynamic range required for the particular assay being developed, all the various components of the assay must be evaluated. The components will vary depending on the immunoassay format selected. The following is a description of the various types of ELISA formats as well as reagents that need to be optimized in order to obtain a robust assay.

Types of ELISA Formats

Three frequently used types of ELISA are: sandwich assays, competitive assays and antigen down assays. The format selected depends on the reagents that are available and the dynamic range required for the particular assay. Sandwich assays tend to be more sensitive and robust and therefore tend to be the most commonly used.

Sandwich Immunoassay (ELISA)

A sandwich immunoassay is a method using two antibodies, which bind to different sites on the antigen or ligand (Figure 1). The capture antibody, which is highly specific for the antigen, is attached to a solid surface. The antigen is then added, followed by addition of a second antibody referred to as the detection antibody. The

detection antibody binds the antigen at a different epitope than the capture antibody. As a result, the antigen is 'sandwiched' between the two antibodies. The antibody binding affinity for the antigen is usually the main determinant of immunoassay sensitivity. As the antigen concentration increases, the amount of detection antibody increases, leading to a higher measured response. The standard curve of a sandwich-binding assay has a positive slope. To quantify the extent of binding, different reporters can be used. These reporters (i.e. enzyme, fluorophore, or biotin) can be directly attached to the detection antibody or to a secondary antibody which binds the detection antibody (i.e. goat, anti-mouse IgG – HRP). In this latter case, the capture antibody and the detection antibody must be from different species (i.e. if the capture antibody is a rabbit antibody, the detection antibody would be from goat, chicken, etc., but not rabbit). If the detection antibody is directly labeled, then the capture and detection antibodies can be from the same species. Polyclonal antibodies often contain multiple epitopes and the same affinity purified polyclonal can be used as the capture and labeled detection antibody. The substrate for the enzyme is added to the reaction that forms a colorimetric readout as the detection signal. The signal generated is proportional to the amount of target antigen present in the sample.

The antibody linked reporter used to measure the binding event determines the detection mode. For an ELISA, where the detection is colorimetric, a spectrophotometric plate reader is used. Several types of reporters have been developed in order to increase sensitivity in an immunoassay. For example, chemiluminescent substrates have been developed which further amplify the signal and can be read on a luminescent plate reader. Also, a fluorescent readout where the enzyme step of the assay is replaced with a fluorophore tagged antibody is becoming quite popular. This readout is then measured using a fluorescent plate reader. When the detection antibody is labeled with biotin, you have the flexibility to use a number of different types of streptavidin conjugated reporters.

Competitive Binding Assay

A competitive binding assay is based upon the competition of labeled and unlabeled ligand for a limited number of antibody binding sites (Figure 2). Only one antibody is used in a competitive binding ELISA. Competitive binding assays are often used to measure small analytes. These assays are also used when a matched pair of antibodies to the analyte does not exist. A fixed amount of labeled ligand (tracer) and a variable amount of unlabeled ligand are incubated with the antibody. According to the law of mass action, the amount of bound labeled ligand is a function of the total concentration of labeled and unlabeled ligand. As the concentration of unlabeled ligand is increased, less labeled ligand can bind to the antibody and the measured response decreases. Thus the lower the signal, the more unlabeled analyte there is in the sample. The standard curve of a competitive binding assay has a negative slope. Alternatively, the antigen can be coated on the plate with the antibody and the sample in solution. Fewer antibodies will be available to bind the coated antigen as the amount of antigen in the sample increases. The antibody and labeled antigen concentrations are the important parameters that need to be optimized.

Antigen-Down Immunoassay or Immunometric Assay

An antigen-down immunoassay or immunometric assay involves binding the antigen to a solid surface instead of an antibody (Figure 3). This is done by coating the solid surface with the antigen, allowing for passive absorbance to the solid surface. Antigen-down immunoassays are used to bind antibodies found in a sample or in a competitive ELISA format (discussed above). When the sample is added (such as human serum), the antibodies (IgE for example) from the sample bind to the antigen coated on the plate. A species-specific antibody (anti-human IgE for example) labeled with HRP is added next. The signal is directly proportional to the amount of antibody present in the sample; the more antibodies there are in the sample, the higher the signal.

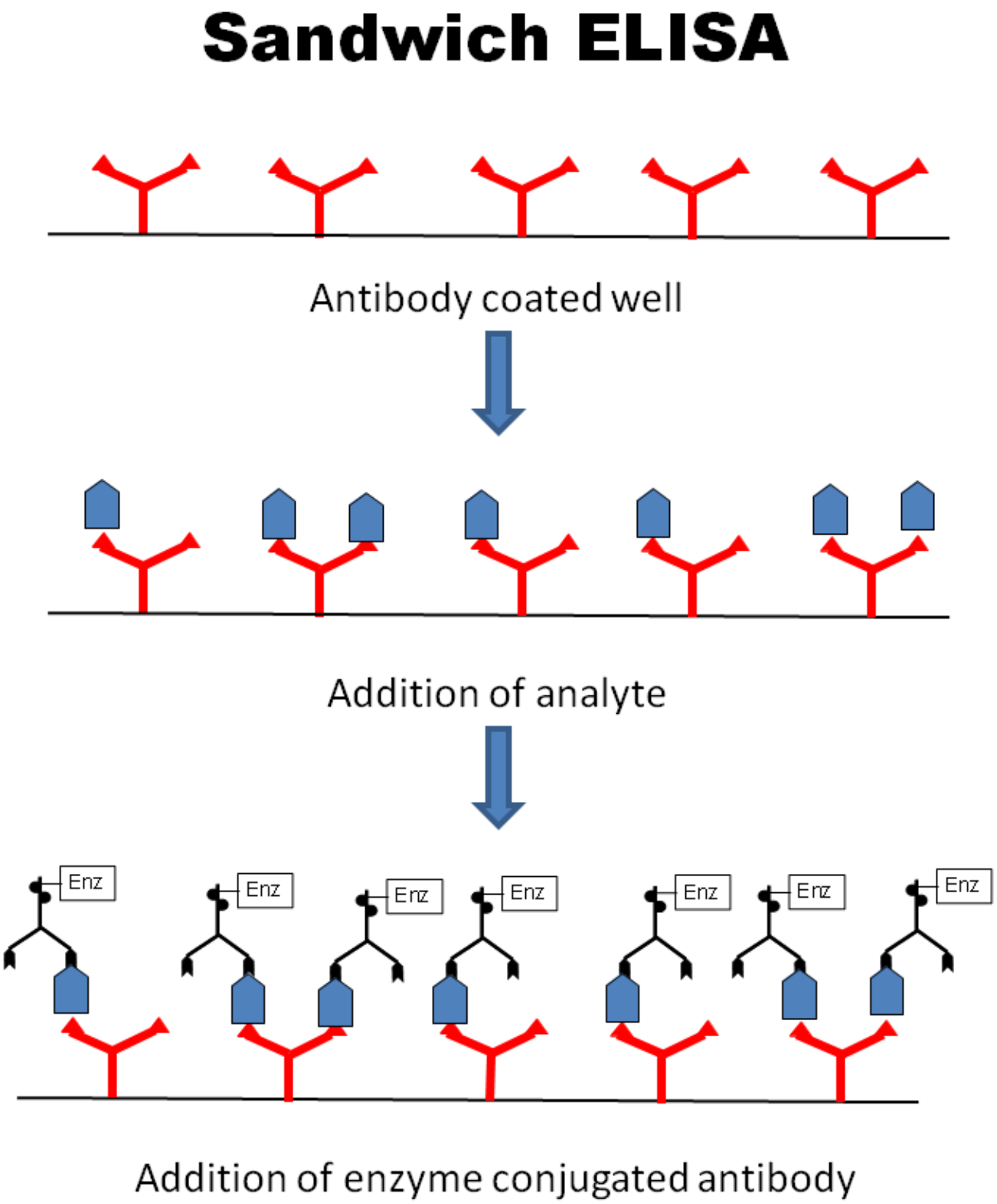

Figure 1: Diagram of a sandwich ELISA. The addition of the enzyme's substrate leads to color development. The amount of color (absorbance) is directly proportional to the analyte concentration.

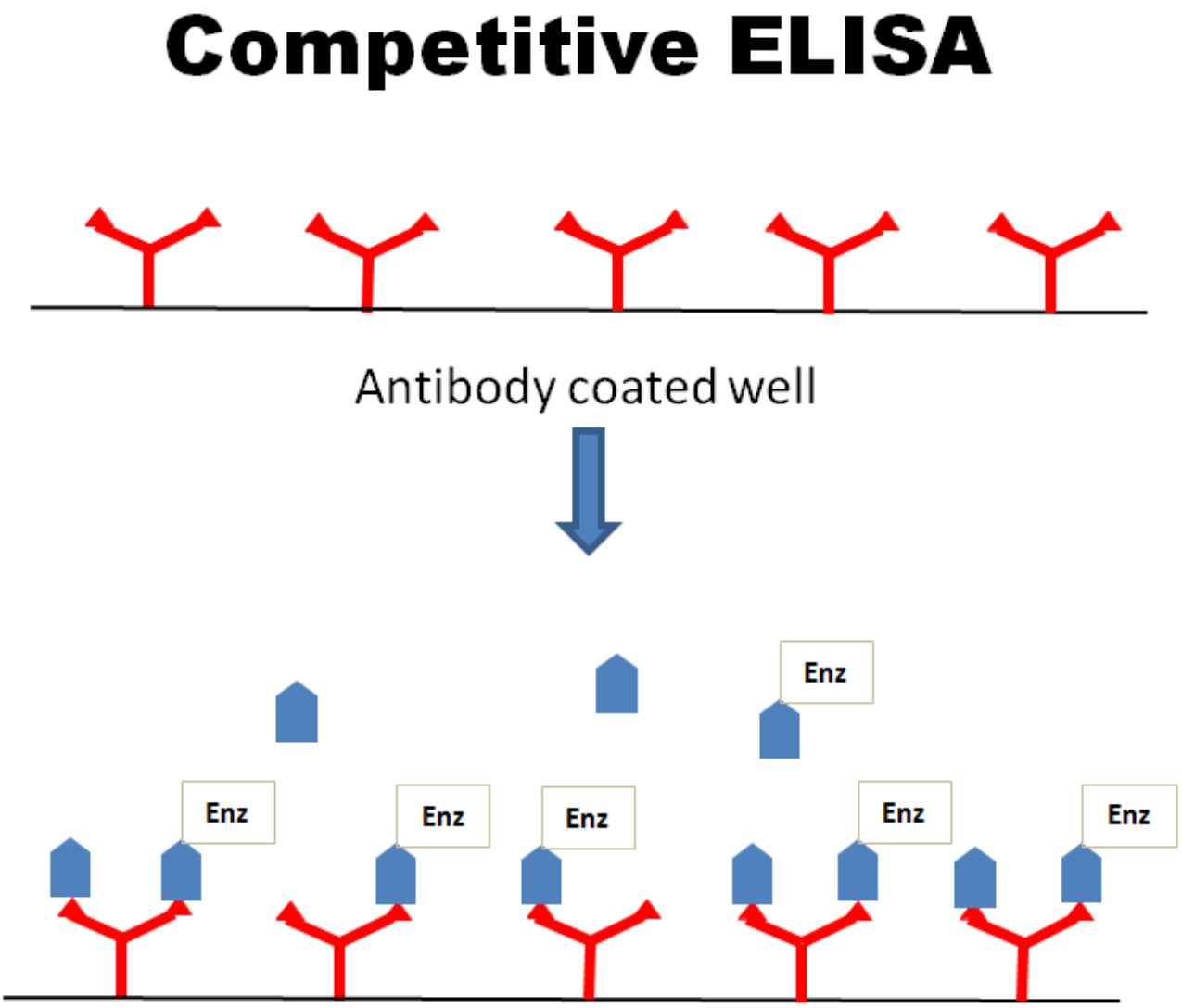

Figure 2: Diagram of a competitive binding assay. After addition of both the analyte and the enzyme-conjugated analyte, competition occurs between the two for binding to the antibody. The addition of the enzyme's substrate leads to color development. The amount of color (absorbance) is indirectly proportional to the analyte concentration

Single Antibody Two Plate ELISA Format

A single antibody ELISA format is considered when there is only one antibody available that recognizes the analyte (Figure 4). The assay is configured using the same antibody as both capture and detection. The antibody is biotinylated for use as the detection antibody. The method also utilizes two plates. The basic concept is to capture the antibody to an ELISA plate and allow the analyte of interest to bind to the capture antibody. Unbound material is removed by washing the plate and then adding an acid solution to elute the analyte from the capture antibody. The eluted analyte is then transferred to another ELISA plate containing the neutralization solution. The eluted analyte is then allowed to bind to the second ELISA plate. The unbound material is removed and the plate is blocked followed by a wash step. The detection antibody, which is biotinylated, is then added to the plate, followed by an incubation period. Another wash step is performed to remove excess detection antibody, followed by addition of a streptavidin reporter. The last wash step is performed to remove the excess

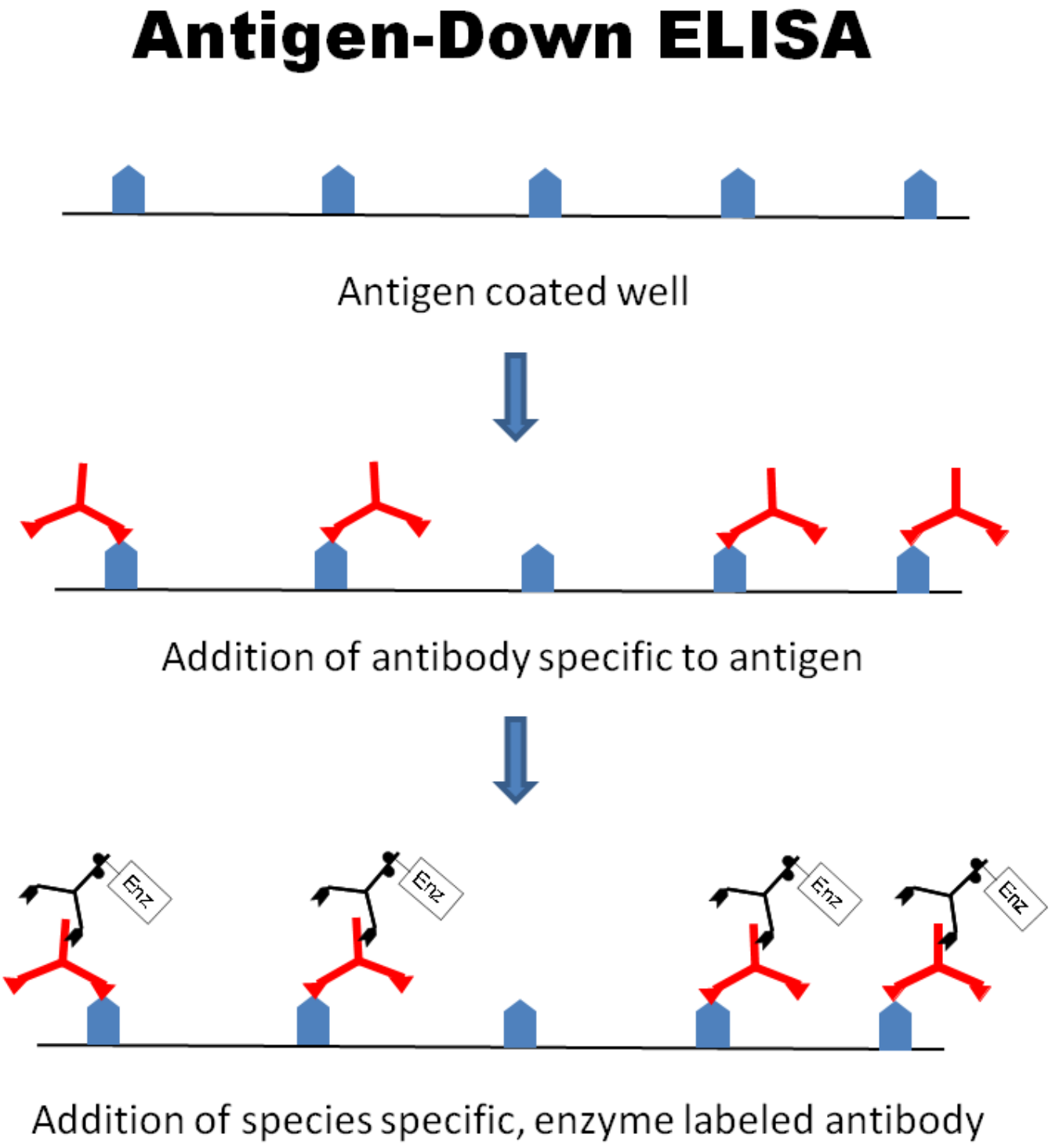

Figure 3: Diagram of an antigen-down ELISA. The addition of the enzyme's substrate leads to color development. The amount of color (absorbance) is directly proportional to the antigen specific antibody concentration.

reporter, followed by addition of the substrate. Below is a generic protocol that can be used to set up a Single Antibody Two Plate ELISA Method.

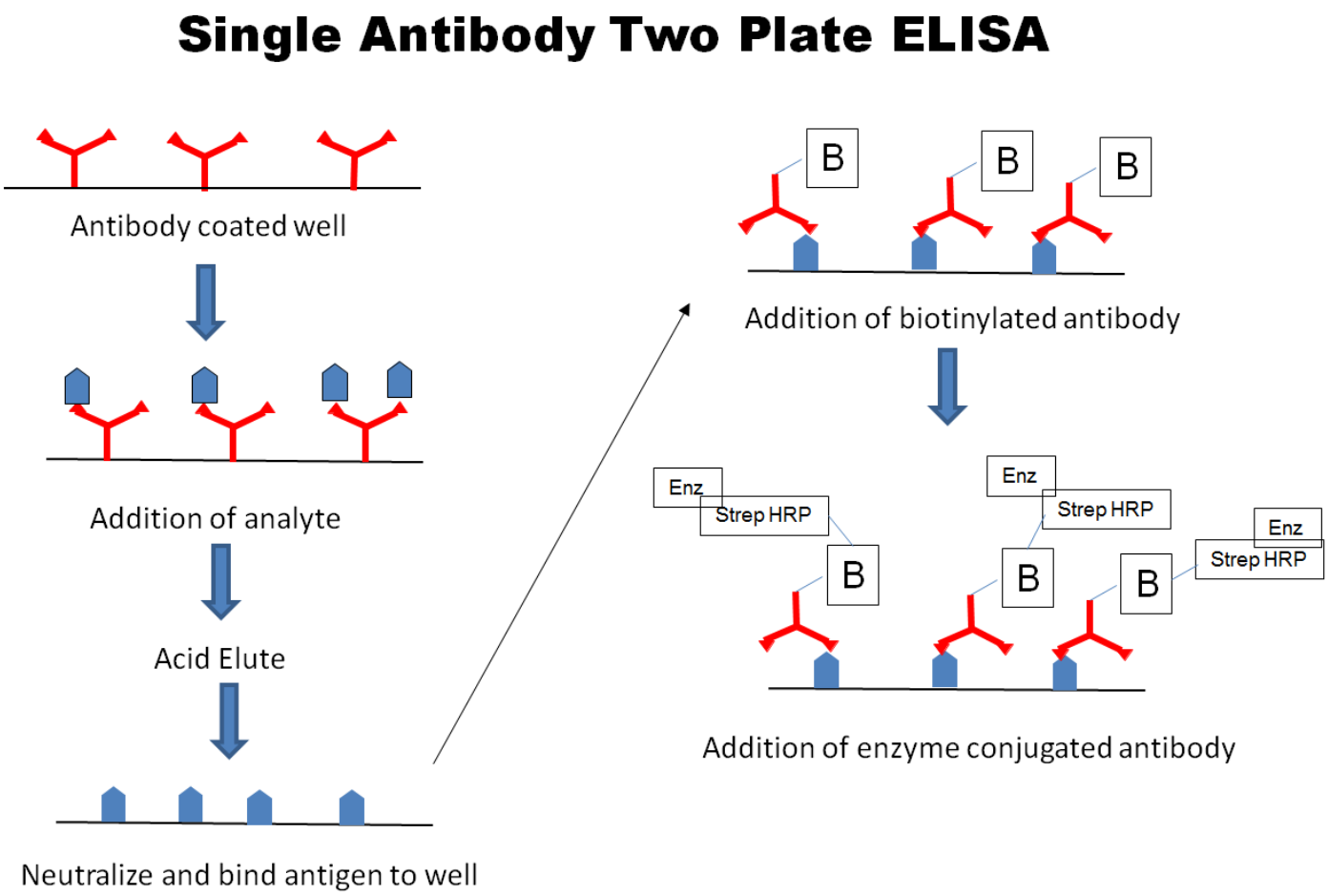

Figure 4: Diagram of a Single Antibody Two Plate ELISA. The addition of the enzyme's substrate leads to color development. The amount of color (absorbance) is directly proportional to the analyte concentration.

Reagents and basic concepts

Included in the list below are the plate type and buffers that are a good starting point for single antibody ELISA assays.

1. One antibody that recognizes the analyte.
2. The optimal capture and detection antibody concentrations need to be determined experimentally.
3. Nunc immunoassay plate
4. Coating buffer: TBS
5. Blocking buffer: 1% BSA, TBS, 0.1% Tween-20
6. Antibody diluent buffer: 1% BSA, PBS or TBS, or 0.1% Tween-20
7. Acid elution buffer: 200 mM Acetic Acid
8. Neutralizing buffer: 1M Tris pH 9.5
9. Wash buffer: TBS 0.1% Tween-20
10. TMB and HRP are used for enzyme/substrate readout.
11. Acid stop buffer
12. The conditions for the following need to be tested and optimized for optimal assay performance: pH, buffers, incubation times, concentrations of antibodies, volumes used, etc.

Basic Protocol for Single Antibody Two Plate ELISA Method Day1

1. Prepare the capture antibody in coating buffer

2. Add 100 µl of the capture antibody in coating buffer to Plate 1- Nunc 96-well microtiter plate
3. Incubate plate with gentle shaking for 1 hour at room temperature
4. Remove the unbound capture antibody from the microtiter plate by dumping the plate
5. Wash the plate 3 times with wash buffer
6. Prepare serial dilutions of the analyte in dilution buffer
7. Add 100 µl of the analyte to the plate
8. Incubate plate with gentle shaking for 1 hour at room temperature
9. Wash the plate 3 times with wash buffer
10. Add 65 µl of 200 mM Acetic Acid for 5 minutes at room temperature with gentle shaking
11. Prepare Plate 2 by adding 100 µl of 1 M Tris pH 9.5 to the microtiter plate
12. After 5 minutes of incubation transfer the 65 µl of acidified analyte from Plate 1 to Plate 2
13. Incubate overnight at 4°C with gentle shaking

Day2: Plate 2

1. Wash Plate 2, 3 times with wash buffer
2. Add 200 µl of blocking buffer to the plate
3. Incubate for one hour at room temperature with gentle shaking
4. Wash the plate 3 times with wash buffer
5. Add 100 µl of the biotinylated detection antibody (this is the same antibody that was used as the capture antibody)
6. Incubate for one hour at room temperature with gentle shaking
7. Wash the plate 3 times with wash buffer
8. Add Streptavidin HRP
9. Incubate for 20-30 minutes at room temperature with gentle shaking
10. Wash the plate 3 times with wash buffer
11. Add TMB substrate to the plate
12. Incubate according to manufacturer's suggestions with gentle shaking
13. Add Stop Solution, mix thoroughly
14. Read optical density at 450 nm

Multiplex Immunoassay Technologies

Biomarker research has expanded over the years, producing a need to quantitatively measure multiple analytes simultaneously from one sample. In the pre-clinical research area there is a need to measure endpoints from rodents and non-human primates to determine safety and efficacy of drug candidates. Typically the samples from these animal models are limited in volume and expensive to obtain, which produces a challenge in obtaining data if more than one analyte needs to be quantified. The same issues apply to clinical samples being assayed for Biomarker, Pharmacokinetic, and Pharmacodynamic studies. A single endpoint ELISA tends to use a larger volume of sample than a multiplexed assay.

Two of the widely used multiplex technologies that have been developed are the Luminex xMAP technology (LMX) and the Meso Scale Discovery (MSD). Both technologies have well validated immunoassays that cover a wide range of secreted and intracellular proteins. In most cases, numerous analytes can be measured with sample volumes of less than 50 µl.

Meso Scale Discovery is a multiplexed technology based on MULTI-ARRAY® technology. The technology utilizes a proprietary electrochemiluminescence detection system and an array of spots in a standard 96-well format. The electrochemiluminescence technology allows for an increase in dynamic range of the standard curve as well as an increase in sensitivity over normal ELISA readouts, such as HRP/TMB. The MSD technology utilizes a 96- or 384-well microtiter plate, allowing an immunoassay to be developed and optimized using the

same variables of antibody concentrations, buffers, and incubation times that are used in a standard ELISA. The plates are read using a Sector 6000 instrument yielding Relative Light Units that can be back calibrated off the standard curve to the analyte concentration that is being analyzed. Additional information on the MSD platform can be found at: http://www.mesoscale.com/.

Luminex xMAP is a bead based technology that allows capture antibodies to be coupled to color coded beads or microspheres that contain different emission spectra. A sandwich assay format is performed with the analyte added to the capture antibody bound beads, followed by the addition of a biotinylated antibody. The detection occurs by adding a streptavidin-conjugated flourochrome to the complex containing the sandwiched immunoassay. The fluorescent readout is detected using a Luminex xMAP which is a flow cytometry based instrument. The microspheres are classified based on their emission spectra and the amount of analyte detected is directly proportional to the fluorescent signal. Additional details on the LMP technology can be found at: http://www.luminexcorp.com/TechnologiesScience/xMAPTechnology/.

Studies have been performed by numerous laboratories directly comparing the MSD technology to the Luminex xMAP as well as to commercially available enzyme-linked immunosorbent assays (6-12). Validation data has been generated for spiked recovery in various matrixes, including other validation parameters for both the MSD and Luminex technologies. Overall the results from numerous studies show that while there usually is a quantitative difference between the technologies (most likely due to the use of different antibodies), the relative differences are comparable. Data from these numerous studies demonstrate that multiplexed technologies are suitable for screening for trends in cytokine profiles and other secreted proteins to support pre-clinical and clinical studies.

Important Parameters for Development of an Immunoassay

1. Capture antibody
2. Detection antibody
3. Plate type
4. Coating buffer
5. Blocking buffer/diluent buffer
6. Wash buffer
7. Coating antibody concentration
8. Coated antibody stability
9. Timing of each step in the immunoassay
10. Detection and/or secondary antibody concentration
11. Reporter concentration
12. Readout
13. Instrument linearity

Initial Concept and Method Development for a Sandwich Immunoassay

Initial Development Experiment

The goal is to develop a basic working method by determining the antibody which should be the capture antibody and which antibody should be the detection antibody. Determine the optimum antibody concentrations for both the capture and detection antibody. The optimal antibody for capture vs. detection can only be determined empirically. If multiple antibodies to the analyte exist, it is best to examine all possible pairs of the antibodies.

Experiment

Coat the ELISA plate with several dilutions of each antibody that will be used as part of the sandwich assay. Add the analyte to be measured at a high, low and zero concentration. Use each of the antibodies, at several concentrations, as a detection antibody. The results of this experiment will determine which antibody is best for the capture antibody and which is best for the detection antibody. Furthermore, the dilution needed for both antibodies will also be determined.

Reagents

Included in the list below are the plate type and buffers that will work for the majority of immunoassays. Use these conditions as a starting point.

1. Two antibodies that recognize different epitopes on the analyte.
2. The optimal antibody pair for the sandwich assay was determined empirically in the experiment above.
3. Greiner immunoassay plate
4. Coating buffer: PBS
5. Blocking buffer: 1% BSA, TBS, 0.1% Tween-20
6. Antibody diluent buffer: 1% BSA, PBS or TBS, or 0.1% Tween-20
7. Wash buffer: PBS or TBS 0.1% Tween-20
8. TMB and HRP are used for enzyme/substrate readout
9. Acid stop buffer

Protocol (see plate layouts in Table 1 and Table 2):

1. Dilute both antibodies in coating buffer at 0.5, 1, 2 and 5 µg/ml and add 100 µl of each concentration to 24 wells of the 96-well microtiter plate.
2. Incubate the plate containing the capture antibody overnight at 4°C and continue the experiment the next day. (Stability of the capture antibody bound to the plate can be determined in later experiments.)
3. Remove the unbound capture antibody solution from the microtiter plates by aspirating or dumping the plate.
4. Add 200 µl of blocking buffer to each well of the 96-well microtiter plate. Incubate the plate for one hour at room temperature.
5. Remove the blocking buffer from the plate by aspirating or dumping the plate.
6. Determine the desired working range of the analyte. This will give you the high and low concentrations to incubate with each capture antibody dilution. The zero analyte wells will give you the non-specific binding (NSB).
7. Add 100 µl of the analyte to each well in the microtiter plate and incubate for 2.5 hours at room temperature.
8. Wash the plates 3 times with wash buffer.
9. Dilute the detection antibody serially at 1:200, 1:1000, 1:5000 and 1:25000 in diluent.
10. Add 100 µl of detection antibody to each well of the microtiter plate and incubate for 1.5 hours at room temperature.
11. Wash the plates 3 times with wash buffer.
12. Dilute streptavidin-HRP (if detection antibodies are biotinylated) or appropriate secondary antibody (if capture and detection antibodies are from different species) according to manufacture instructions in antibody diluent and add 100 µl to each well in the microtiter plate and incubate for 1 hour at room temperature.
13. For HRP readout add TMB as a substrate to allow color development and incubate for 10-20 minutes at room temperature.
14. Add acid stop reagent to stop the enzyme reaction.

15. Read at 450 nm for TMB/HRP.

Table 1: Plate 1 layout for initial experiment. H=High, L=Low and 0=Zero. High analyte or ligand concentration in combination with the low ligand concentration will give an indication of the dynamic range. Low analyte or ligand concentration will give an indication of sensitivity. Zero ligand will give the non-specific binding and indicate if there are background issues.

Detection Antibody	Capture Antibody A											
	5 µg/ml			2 µg/ml			1 µg/ml			0.5 µg/ml		
1:200	H	L	0	H	L	0	H	L	0	H	L	0
	H	L	0	H	L	0	H	L	0	H	L	0
1:1000	H	L	0	H	L	0	H	L	0	H	L	0
	H	L	0	H	L	0	H	L	0	H	L	0
1:5000	H	L	0	H	L	0	H	L	0	H	L	0
	H	L	0	H	L	0	H	L	0	H	L	0
1:25000	H	L	0	H	L	0	H	L	0	H	L	0
	H	L	0	H	L	0	H	L	0	H	L	0

Table 2: Plate 2 layout for the initial experiment. H=High, L=Low and 0=Zero. High analyte or ligand concentration in combination with the low ligand concentration will give an indication of the dynamic range. Low analyte or ligand concentration will give an indication of sensitivity. Zero ligand will give the non-specific binding and indicate if there are background issues.

Detection Antibody	Capture Antibody B											
	5 µg/ml			2 µg/ml			1 µg/ml			0.5 µg/ml		
1:200	H	L	0	H	L	0	H	L	0	H	L	0
	H	L	0	H	L	0	H	L	0	H	L	0
1:1000	H	L	0	H	L	0	H	L	0	H	L	0
	H	L	0	H	L	0	H	L	0	H	L	0
1:5000	H	L	0	H	L	0	H	L	0	H	L	0
	H	L	0	H	L	0	H	L	0	H	L	0
1:25000	H	L	0	H	L	0	H	L	0	H	L	0
	H	L	0	H	L	0	H	L	0	H	L	0

Results

Determine the absorbance units that yield the maximum signal to noise ratio or the greatest difference between the high and low analyte concentrations with the lowest variability. These are the conditions that will be selected for the antibody to be used as the capture antibody and the dilution of the antibodies to be used in the next experiment.

- If the background signal is unacceptably high (greater than 0.2 A.U.) then run additional experiments varying the plate type, blocking buffers, blocking buffers with a diluent agent like species specific IgG, antibody diluent buffers, wash buffers, and the reporter type.
- If the above general conditions have an acceptable NSB then it can be determined if the dynamic range and sensitivity are in the appropriate range. To improve the sensitivity of the assay, the buffers, timing of incubations and matrix conditions can be varied in the next experiment.

- Antibodies are the reagents that play a major role in the sensitivity and dynamic range of an immunoassay. This is due to the actual antibody affinity for the analyte. If after attempting to develop the assay the sensitivity is still not in the desired range, different antibody pairs will need to be evaluated.

Example 2

An ELISA was set up to measure the amounts of a protein where there is only one polyclonal antibody available. The polyclonal antibody was used as both the capture antibody and the detection antibody. In this example the detection antibody is biotinylated.

Reagents:

1. Affinity pure polyclonal antibody
2. Analyte protein
3. Biotinylated affinity pure polyclonal antibody

Protocol:

Follow the same basic protocol above using these parameters (see plate layout in Table 3).

1. Coat the affinity purified antibody at 3 levels: 2, 1 and 0.5 µg/ml.
2. Dilute the biotinylated antibody at 3 levels: 1:1000, 1:5000, and 1:25000.
3. Dilute the analyte protein in buffer to 50 ng/ml, 1 ng/ml, and zero.

Conclusions:

As seen in Table 4, the lowest NSB and best signal to noise ratio from low to high analyte concentration are the 0.5 µg/ml concentration for the capture antibody and the 1:25000 dilution of the biotinylated detection antibody.

Detection Antibody	Capture Antibody											
	2 µg/ml			1 µg/ml			0.5 µg/ml					
1:1000	H	L	0	H	L	0	H	L	0			
	H	L	0	H	L	0	H	L	0			
1:5000	H	L	0	H	L	0	H	L	0			
	H	L	0	H	L	0	H	L	0			
1:25000	H	L	0	H	L	0	H	L	0			
	H	L	0	H	L	0	H	L	0			

Table 3: Plate layout to determine the capture and detection antibody concentrations.

Table 4: Results from Example 2: to determine the capture and detection antibody concentrations. Values are averages of absorbance measurements at A450.

Capture Antibody		2 µg/ml			1 µg/ml			0.5 µg/ml		
Analyte protein ng/ml		50	1	0	50	1	0	50	1	0
Detection Antibody	1:1000	3.69	1.81	1.37	3.63	1.89	1.33	3.3	1.79	0.99
	1:5000	3.22	0.7	0.49	3.24	0.81	0.47	3.1	0.83	0.36
	1:25000	1.61	0.21	0.15	1.75	0.25	0.16	1.72	0.26	0.12

Second Development Experiment-Matrix Compatibility

The goal is to determine the matrix effect or sample type on the immunoassay method. The matrix is based on what the sample is found in, for instance tissue culture media, serum, plasma, cell lysate, buffers, etc. Serum matrix, due to its complexity, can have a significant effect on the method. In this example the samples are in rat serum so the matrix effect of rat serum needs to be determined.

Experiment

The samples that need to be measured in this assay will be in either mouse or rat serum. Use the conditions established in the first experiment for the concentration of the capture antibody and the detection antibody. Serially dilute the standard (analyte) to obtain a full standard curve in 3 different matrices (10% rat serum, 30% rat serum and the original buffer diluent used in the first experiment). This will determine the effect of the matrix used for the experimental samples.

Reagents:

1. Use all of the reagents and buffers listed in the first experiment (Example 2).
2. Matrix diluent: 10% rat serum in antibody diluent or 30% rat serum in antibody diluent.

Protocol:

Follow the standard protocol, changing only the matrix diluent to include rat serum.

1. Dilute the coating antibody in coating buffer at 0.5 µg/ml and add 100 µl to each well of the 96-well microtiter plate.
2. Incubate the plate containing the capture antibody overnight at 4°C and use the next day.
3. Stability of the capture antibody bound to the plate can be determined in later experiments.
4. Remove the capture antibody solution from the microtiter plates by aspirating or dumping the plate.
5. Add 200 µl of blocking buffer to each well of the 96-well microtiter plate.

6. Incubate the plate for one hour at room temperature.
7. Remove the blocking buffer from the plate by aspirating or dumping the plate.
8. Serially dilute the standard in antibody dilution buffer containing either 10% or 30% rat serum, or diluent alone.
9. Add 100 µl of the standard to each well in the microtiter plate and incubate for 2.5 hours at room temperature.
10. Wash the plates 3 times with wash buffer.
11. Dilute the detection antibody to 1:25000 in antibody diluent.
12. Add 100 µl of detection antibody diluent to each well of the microtiter plate and incubate for 1.5 hours at room temperature.
13. Wash the plates 3 times with wash buffer.
14. Dilute streptavidin-HRP according to manufacturer's instructions in antibody diluent and add 100 µl to each well in the microtiter plate and incubate for 1 hour at room temperature.
15. For HRP readout add TMB as substrate to allow color development and incubate for 10-20 minutes at room temperature.
16. Add acid stop reagent to stop the enzyme reaction.
17. Read at 450 nm for TMB/HRP.

Results:

Use the standard curve data and construct a precision profile. Check the background levels. See the next section for standard or calibration curve model fitting. Note that the standard curves under all three matrix diluent conditions give the dynamic range and sensitivity necessary for the intended use (Figure 5). For this particular assay, no further development is needed (based on the standard curve, low background and precision profile).

Precision Profile:

Generate the precision profile for the standard curve of the appropriate matrix for the experiment. The precision profile is a plot of coefficient of variation (CV) for the calibrated concentration levels of the replicates of each calibrator versus the nominal analyte concentration in the calibrator samples. The dynamic range of the calibration curve (quantification limits) are then defined by the concentrations where the precision profile intersects the 20% CV. The calculation of this CV has to take into consideration both the sampling variability and the lack of fit to the calibration curve, and is therefore not straightforward. A statistician should be consulted for this evaluation. An SAS program for this evaluation has been published (13).

Calibration Curve and Precision Profile for the Three Different Matrix Conditions

Calibration Curve Model Selection:

A significant source of variability in the calibration curves can come from the choice of the statistical model used for the calibration curve. It is therefore extremely important to choose an appropriate calibration curve model. For most immunoassays, the following models are commonly available from most instrument software.

Linear Model:

$$\text{Response} = a + b^{*}(\text{Concentration}) + \text{error}$$

where parameters, a and b are the intercept and slope respectively, and "response" refers to signal readout, such as optical density or fluorescence from an immunoassay. Often this linear model is fitted after log transformation of the response and concentration. This is sometimes referred as the "log-log linear model".

Quadratic Model:

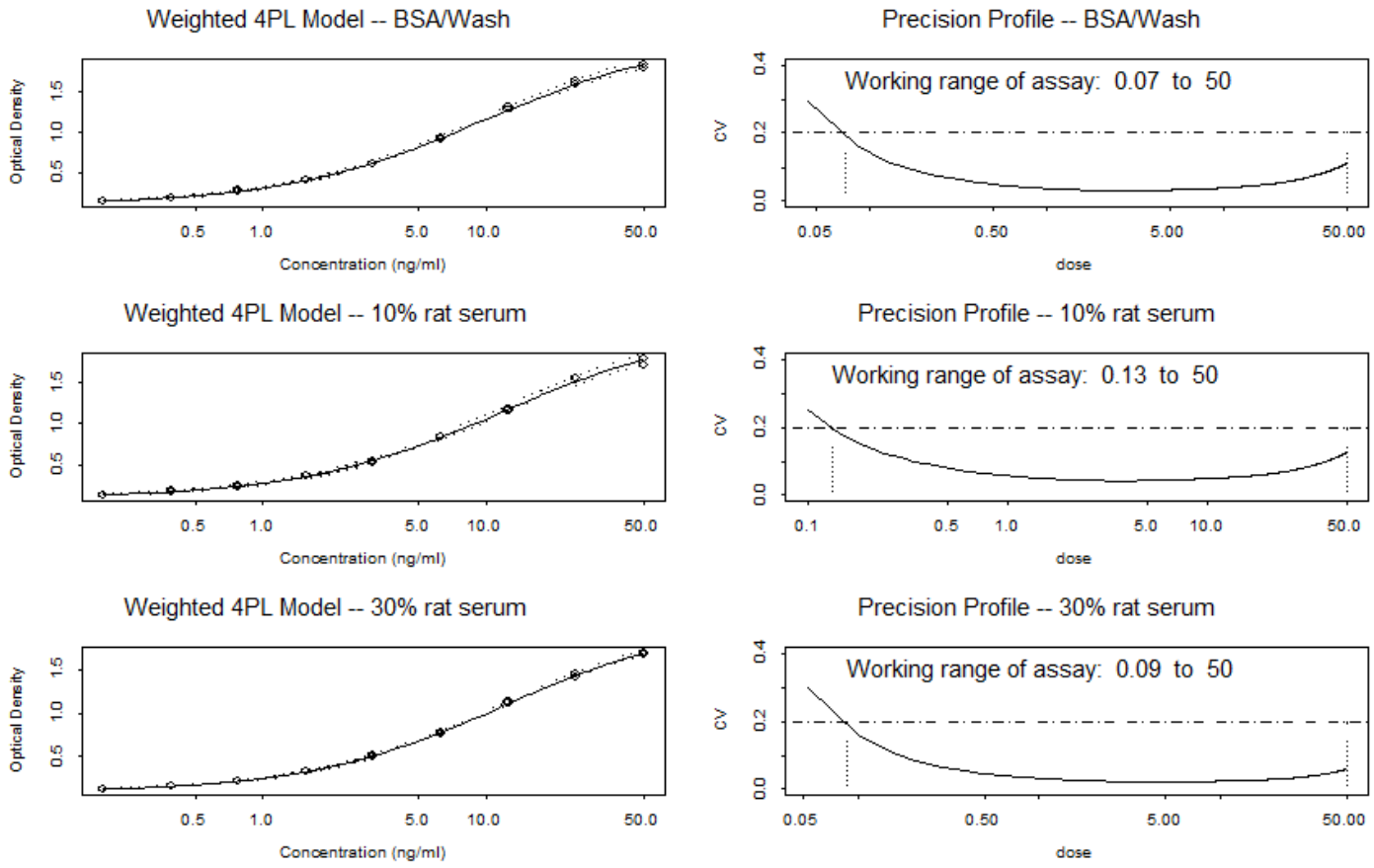

Figure 5: Calibration curve and precision profile for the three different matrix conditions using a Four Parameter Logistic (4PL) Model.

$$\text{Response} = a + b^{*}(\text{Concentration}) + c^{*}(\text{Concentration})^{2} + \text{error}$$

where a, b and c are the intercept, linear and quadratic term coefficients, respectively, of this quadratic model.

Four Parameter Logistic Model:

$$\text{Response} = \text{Top} + \frac{(\text{Bottom} - \text{Top})}{1 + \left(\frac{\text{concentration}}{EC_{50}}\right)^{\text{Slope}}}$$

The four parameters to be estimated are Top, Bottom, EC_{50} and Slope. Top refers to the top asymptote, Bottom refers to the bottom asymptote, and EC_{50} refers to the concentration at which the response is halfway between Top and Bottom.

Five Parameter Logistic Model:

$$\text{Response} = \text{Top} + \frac{(\text{Bottom} - \text{Top})}{\left[1 + \left(\frac{\text{concentration}}{EC_{50}}\right)^{\text{Slope}}\right]^{\text{Asymmetry}}}$$

Asymmetry is the fifth parameter in this model. It denotes the degree of asymmetry in the shape of the sigmoidal curve with respect to "EC_{50}". A value of 1 indicates perfect symmetry, which would then correspond to the four-parameter logistic model. However, note that the term referred to as "EC_{50}" in this model is not truly the EC_{50}. It is the EC_{50} when the asymmetry parameter equals 1. It will correspond to something very different such as EC_{20}, EC_{30}, EC_{80}, etc., depending on the value of the asymmetry parameter for a particular data set.

For most immunoassays, the four or five parameter logistic model is far better than the linear, quadratic or log-log linear models. These models are available in several software packages, and are easy to implement even in an Excel-based program. As illustrated in the plots shown in Figure 6, the quality of the model should be judged based on the dose-recovery scale instead of the lack-of-fit of the calibration curve (R^2). In this illustration, even though the R^2 of the log-log linear model is 0.99, when assessed in terms of the dose-recovery plot, this model turns out to be significantly inferior to the four parameter logistic model. Before the assay is ready for production, the best model for the calibration curve should be chosen based on the validation samples using dose-recovery plots.

Importance of Weighting in Calibration Curves

The default curve-fitting method available in most software packages assigns equal weight to all of the response values, which is appropriate only if the variability among the replicates is equal across the entire range of the response. However, for most immunoassays, the variability of assay signal among replicates of each calibrator increases proportionately with the response (signal) mean. Giving equal weight can lead to highly incorrect conclusions about the assay performance and will significantly affect the accuracy of results from the unknown samples. More specifically, lack of weighting leads to higher variability of results in the lower end of the assay range, thus greatly compromising the sensitivity of the assay. It is therefore extremely important to use a curve-fitting method/software that has appropriate weighting methods/options. This is illustrated in Figure 7 where we compare the total error results from the validation controls after fitting the calibration curves using log-log linear, four-parameter logistic and five-parameter logistic models. For this example, the performance of the validation samples is better overall when the five-parameter logistic model is used.

Third Development Experiment

The two-step experiment detailed above is a very simple example of how to develop a sandwich ELISA method. If the dynamic range and sensitivity of the assay does not meet the experimental needs then further experimental parameters should be tested using experimental design. With experimental design all of the factors involved in the ELISA including buffers, incubation time and plate type can be analyzed.

In a sandwich ELISA method the antibodies chosen are the major drivers of the assay parameters. If at this point in the method development, the precision profile of the standard curve does not encompass the desired dynamic range and sensitivity, instead of continuing with the development experiment, antibodies should be further characterized. Changing some of the variables such as the antibody concentrations can significantly improve the calibration curve and hence its precision profile.

The goal is to determine the optimal conditions for the variables in the immunoassay, including incubation steps, buffers, substrate, etc. Also, determine the optimal antibody concentrations and the stability of the capture antibody bound to the plate.

Experiment:

Dilute the standard in the matrix compatible to the sample (as determined in the second experiment). Vary the incubation times, dilution buffers and other variables in order to optimize the immunoassay. Analyze by using experimental design software and precision profiles.

Reagents:

1. Antibodies
2. Coating buffers
3. Blocking buffers
4. Wash buffers

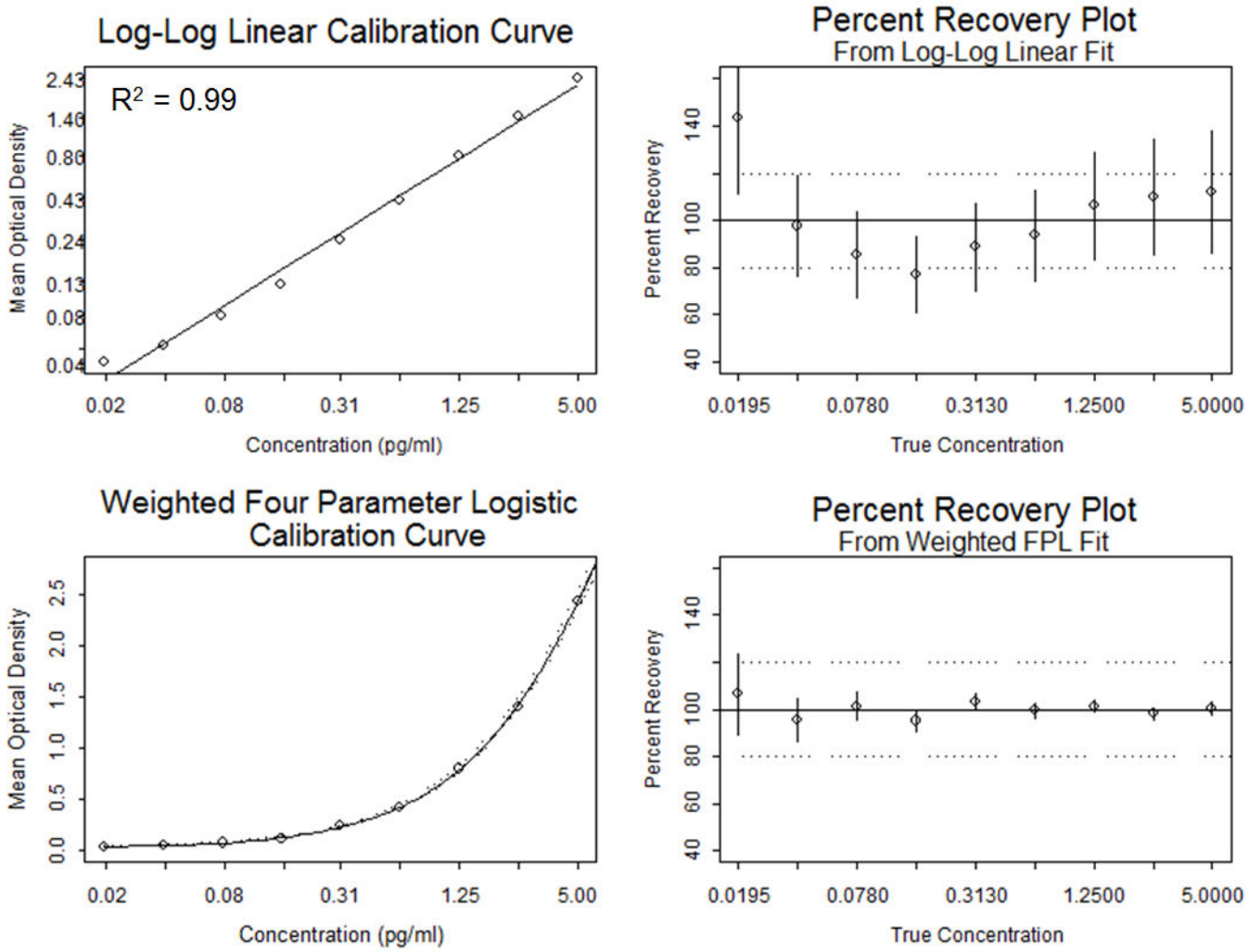

Figure 6: Example of log-log linear and weighted four parameter logistic calibration curves.

5. Antibody diluents
6. Substrate

Protocol:

1. Coat the microtiter plate with the capture antibody at the concentration determined in the initial experiment. Incubate overnight at 4°C.
2. Discard the capture antibody solution from the microtiter plate.
3. Block the plate for 1 hour at room temperature using various blocking reagents.
4. Store plates at 4°C, desiccated, for several periods of time 0-5 days.
5. Repeat steps 1-3 the day of the actual experiment.
6. Serially dilute, using an 8-point standard curve, the known standard in the appropriate matrix for the experiment. For the control also dilute the standard in the same buffer as was used in the initial experiment. Add 100 µl of standard to each well in the 96-well microtiter plate.
7. Incubate the diluted standard with the capture antibody for 1 hour and 3 hours at room temperature and overnight at 4°C. Each time point will have to be run in a separate plate.
8. Wash plates 3 times (if background or NSB is high, try different wash buffers).
9. Add 100 µl of diluted detection antibody. If background is high again different diluents can be tested.

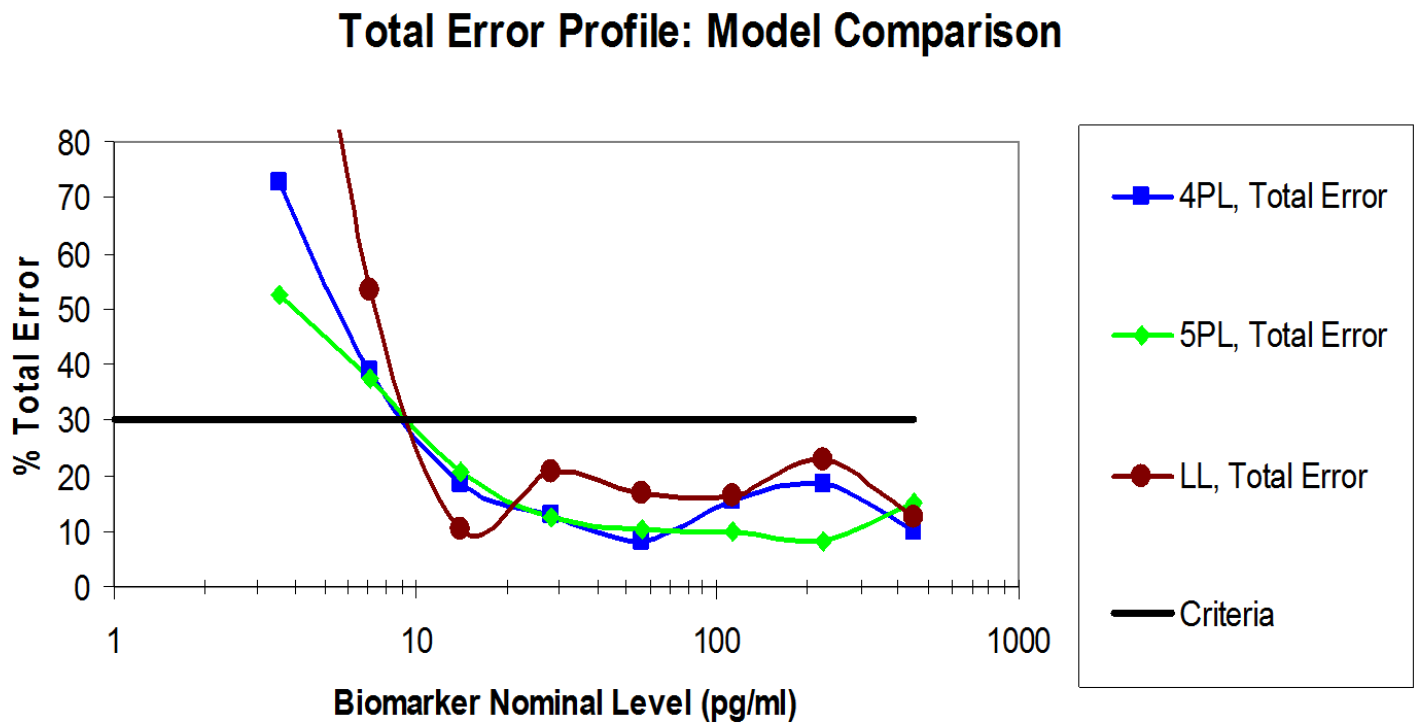

Figure 7: Validation samples are plotted with different calibration curve models. It is clear from the plot that the five-parameter logistic (5PL) model is better than the four-parameter logistic (4PL) and log-log linear (LL) models. For this particular assay, 5PL is the optimal choice for the in-study (production) phase.

10. Incubate the detection antibody for different time periods and again different plates will have to be used for each time condition.
11. Wash plates 3 times.
12. Add 100 µl of substrate to the wells containing the detection antibody conjugated to the enzyme and allow incubation according to the manufacturer's conditions.
13. Add 100 µl of stop buffer.
14. Read at 450 nm.

Data Analysis:

Compute the standard curves and their precision profiles for all the experimental design conditions. Derive the optimization endpoints using the precision profiles. Then analyze the optimization endpoints using software such as JMP (http://www.jmp.com) to determine the optimum levels of the assay factors. See next section for the details and illustration.

Experimental Designs for Increasing Calibration Precision

Step 1:

Identify all the factors/variables that potentially contribute to assay sensitivity and variability. Choose appropriate levels for all the factors (high and low values for quantitative factors, different categories for qualitative factors). Then use fractional-factorial experimental design in software such as JMP to derive appropriate experimental "trials" (combinations of levels of all the assay factors). Run 8-point calibration curves in duplicate for each trial. With each trial taking up two columns in a 96-well plate, 6 trials per plate can be tested. All trials should be randomly assigned to different pairs of columns in the 96-well plates. However,

certain factors such as incubation time and temperature are inter-plate factors. Therefore, levels of such factors will have to be tested in separate plates (see Table 5).

After the above experiment is run, the calibration curves should be fit for each trial using an appropriately weighted-nonlinear regression model. Then the precision profile for the calibration curve of each trial should be obtained along with the important optimization end-points such as working-range, lower quantitation limit and precision area (area of the region intersected by the precision profile with 20% CV). Now analyze these data to determine the optimal level of all qualitative factors and determine which subset of quantitative factors should be further investigated.

Table 5: Example plate layout to increase calibration precision.

	Trial 1		Trial 2		Trial 3		Trial 4		Trial 5		Trial 6	
	1	2	3	4	5	6	7	8	9	10	11	12
A	8pt calibration curve; duplicate		8pt calibration curve; duplicate		8pt calibration curve; duplicate		8pt calibration curve; duplicate		8pt calibration curve; duplicate		8pt calibration curve; duplicate	
B	8pt calibration curve; duplicate		8pt calibration curve; duplicate		8pt calibration curve; duplicate		8pt calibration curve; duplicate		8pt calibration curve; duplicate		8pt calibration curve; duplicate	
C	8pt calibration curve; duplicate		8pt calibration curve; duplicate		8pt calibration curve; duplicate		8pt calibration curve; duplicate		8pt calibration curve; duplicate		8pt calibration curve; duplicate	
D	8pt calibration curve; duplicate		8pt calibration curve; duplicate		8pt calibration curve; duplicate		8pt calibration curve; duplicate		8pt calibration curve; duplicate		8pt calibration curve; duplicate	
E	8pt calibration curve; duplicate		8pt calibration curve; duplicate		8pt calibration curve; duplicate		8pt calibration curve; duplicate		8pt calibration curve; duplicate		8pt calibration curve; duplicate	
F	8pt calibration curve; duplicate		8pt calibration curve; duplicate		8pt calibration curve; duplicate		8pt calibration curve; duplicate		8pt calibration curve; duplicate		8pt calibration curve; duplicate	
G	8pt calibration curve; duplicate		8pt calibration curve; duplicate		8pt calibration curve; duplicate		8pt calibration curve; duplicate		8pt calibration curve; duplicate		8pt calibration curve; duplicate	
H	8pt calibration curve; duplicate		8pt calibration curve; duplicate		8pt calibration curve; duplicate		8pt calibration curve; duplicate		8pt calibration curve; duplicate		8pt calibration curve; duplicate	

Step 2:

We now need to determine the optimum levels for the key factors determined in the previous step. Choose appropriate low, middle and high levels for each of these factors based on the data analysis results from step 1. Now use software such as JMP to generate appropriate trials (combinations of low, middle and high levels of all the factors) from a central-composite design. Then run duplicate 8-point calibration curves for each trial using a similar plate format as in step 1.

Now obtain the precision profile and the relevant optimization end-points of the calibration curve of each trial. Perform the response-surface analysis of these data to determine the optimal setting of each of the quantitative factors run in this experiment.

Illustration of Experimental Design and Analysis for Sandwich ELISA Optimization

In Table 6, we have the experiment plan from the second step of the optimization process using experimental design for a sandwich ELISA. These four factors (capture antibody, detection antibody, enzyme and volume) were picked out of the six factors considered in the first step of this optimization process (screening phase) for further optimization. We use a statistical experimental design method called central composite design to

generate the appropriate combinations of the high, mid and low levels of the four factors in this second step. For example, trial #6 in this table refers to the middle level of the first, third and the fourth factors, and the low level of the second factor.

Eight-point standard curves in duplicate were generated for each of these trials, in adjacent columns of a 96-well plate. This resulted in six trials per plate, and with 36 trials in 6 plates. We computed the precision profiles of the calibration curves for each of these 36 trials. From these precision profiles, we computed the working range (lower and upper quantification limits), CV and related variability and sensitivity measures. We then used a statistical data analysis method called "response surface analysis" on these optimization endpoints. This resulted in polynomial type models for all the factors. Using the shape of the curve and other features from this model, the optimum levels for these factors were determined. This gave us the most sensitive dynamic working range possible for this assay.

An experiment was then performed for this ELISA to compare these optimized levels to the pre-optimum levels and the assay kit manufacturer's recommendation. The results from this comparison are summarized in Figure 8.

The optimized levels derived from statistical experimental design for this ELISA resulted in the following improvements over the pre-optimum and assay kit manufacturer's recommendation.

- Lower quantification limit decreased more than two-fold to 13.6 nM.
- Upper quantification limit by up to 10-fold to 1662.3 nM.
- Precision area increased by 2-fold and the working range increased by 2-fold to two log cycles.

This improvement is evident from the precision profiles shown in Figure 8.

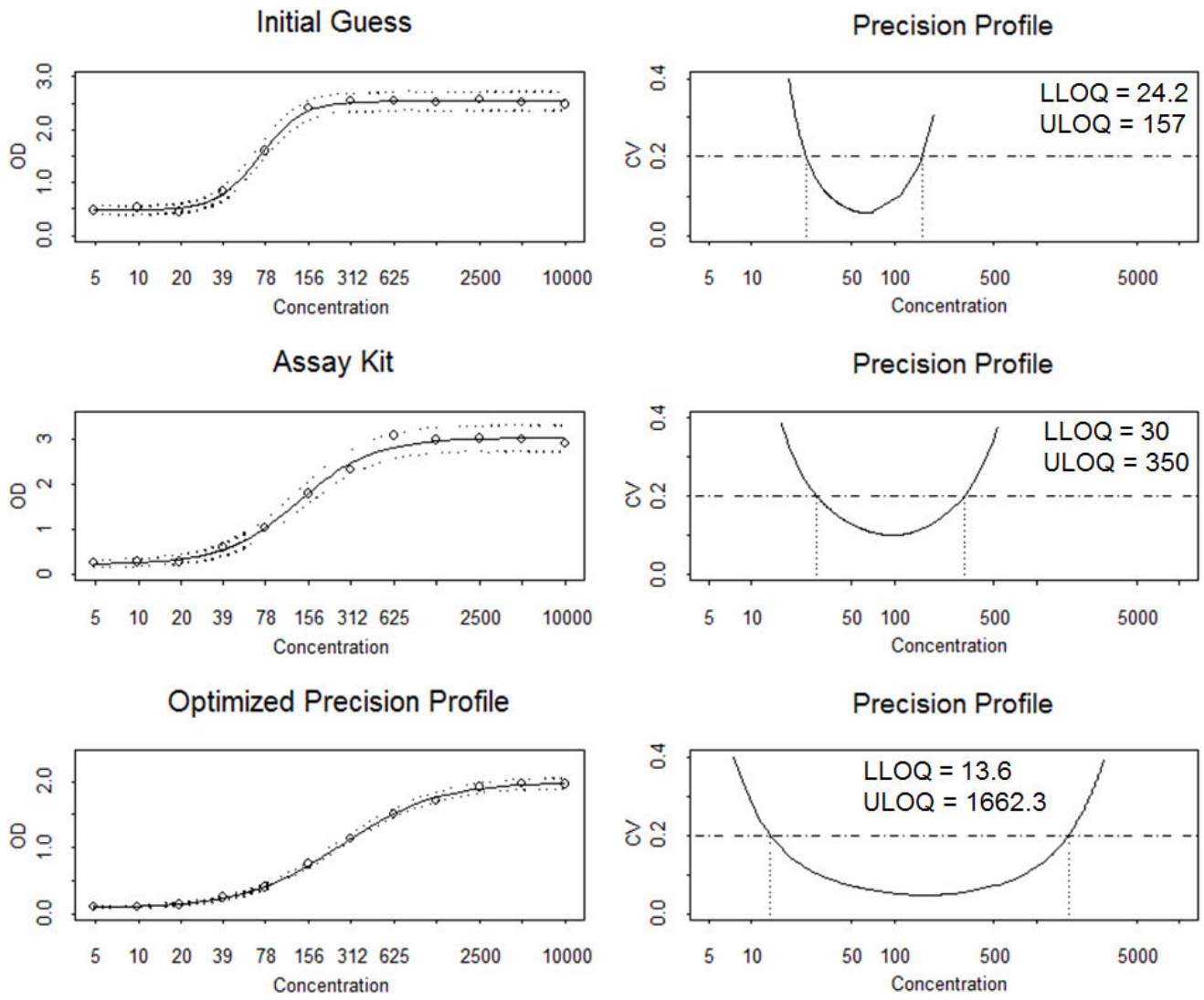

Figure 8: Comparison of optimized levels to pre-optimum levels and those recommended by the manufacturer.

Table 6: Experimental plan from the second step of the optimization process using the experimental design for a sandwich ELISA.

Trial #	Pattern	Capture A	Biotin A	EnzCult	Volume
1	– – – +	250	250	300	100
2	0 0 0 0	500	425	525	75
3	– + + +	250	600	750	100
4	– + + –	250	600	750	50

Table 6 continued from previous page.

Trial #	Pattern	Capture A	Biotin A	EnzCult	Volume
5	– – – –	250	250	300	50
6	0 – 0 0	500	250	525	75
7	0 0 0 0	500	425	525	75
8	0 0 0 0	500	425	525	75
9	0 0 + 0	500	425	750	75
10	– – + +	250	250	750	100
11	+ – – +	750	250	300	100
12	0 0 0 0	500	425	525	75
13	0 0 0 0	500	425	525	75
14	+ + + –	750	600	750	50
15	0 0 0 0	500	425	525	75
16	0 0 0 0	500	425	525	75
17	0 0 0 0	500	425	525	75
18	– + – –	250	600	300	50

Table 6 continued from previous page.

Trial #	Pattern	Capture A	Biotin A	EnzCult	Volume
19	+ 0 0 0	750	425	525	75
20	0 0 0 0	500	425	525	75
21	0 + 0 0	500	600	525	75
22	– + – +	250	600	300	100
23	+ + – –	750	600	300	50
24	0 0 0 –	500	425	525	50
25	0 0 – 0	500	425	300	75
26	0 0 0 +	500	425	525	100
27	0 0 0 0	500	425	525	75
28	0 0 0 0	500	425	525	75
29	0 0 0 0	500	425	525	75
30	+ – + +	750	250	750	100
31	+ + – +	750	600	300	100
32	– – + –	250	250	750	50

Table 6 continued from previous page.

Trial #	Pattern	Capture A	Biotin A	EnzCult	Volume
33	– 0 0 0	250	425	525	75
34	+ – + –	750	250	750	50
35	+ – – –	750	250	300	50
36	+ + + +	750	600	750	100

Initial Concept and Method Development of a Competitive Assay

Competitive Binding Immunoassay

Development and validation of a competition immunoassay requires considerable expertise in reagent characterization and method development. Sandwich and antigen-down immunoassays formats should be explored before attempting the competitive immunoassay format.

Drawbacks Using a Competitive Immunoassay

1. A competitive immunoassay is not as sensitive as a sandwich ELISA.
2. A competitive immunoassay is more sensitive to matrix issues, especially serum matrix, which can affect assay performance.
3. Timing of the various incubation steps is less robust in a competitive assay. That is the IC_{50} of the standard curve will shift with minor changes in incubation of the various steps of the immunoassay.
4. The labeling of the hapten or analyte can change the analyte binding affinity for the antibody. Experiments need to determine the effect of the label on the binding affinity of the antibody to the analyte.

Development of a Competitive Immunoassay

Initial Development Experiment

The goal of the initial development experiment is to determine the optimal coating concentration of the antibody used for capture and the labeled ligand.

Reagents

1. Antibody- mono or polyclonal, specific to the analyte.
2. Buffers- same as for a competitive assay.
3. Labeled ligand- the enzyme or biotin is labeled directly to the analyte or ligand.

Experiment

Coat the ELISA plate with various antibody concentrations to determine the optimal concentration of antibody and labeled ligand.

Protocol

1. Determine the desired analyte working range.
2. The capture antibody is titrated using high, low and zero analyte concentration levels.
3. Dilute the capture antibody in coating buffer at 0.1, 0.5, 1 and 2 µg/ml and add 100 µl to each well of the 96-well microtiter plate. The capture antibody might need to be titrated down further. The amount of antibody coated on the plate will be proportional to the sensitivity of the assay.
4. Incubate the plate containing the capture antibody overnight at 4°C and use the next day.
5. Stability of the capture antibody bound to the plate can be determined in later experiments.
6. Remove the coating antibody solution from the microtiter plates by aspirating or dumping the plate.
7. Add 200 µl of blocking buffer to each well of the 96-well microtiter plate.
8. Incubate the plate for one hour at room temperature.
9. Remove the blocking buffer from the plate by aspirating or dumping the plate.
10. Dilute the labeled standard in antibody dilution buffer over a wide range. The desired result is the condition that gives a readable signal with the least amount of antibody coated, in combination with the least amount of labeled standard.
11. Zero concentration will give you the NSB.
12. Add 100 µl of the labeled standard to each well in the microtiter plate and incubate for 2.5 hours at room temperature. (The standard can either be directly labeled with the enzyme or biotinylated).
13. Wash the plates 3 times with wash buffer.
14. If a biotinylated standard is used, dilute streptavidin-HRP according to the manufacturer's instructions in antibody diluent and add 100 µl to each well in the microtiter plate and incubate for 1 hour at room temperature.
15. For HRP readout, add either OPD or TMB as a substrate to allow color development and incubate for 10-20 minutes at room temperature.
16. Add acid stop reagent to stop the enzyme reaction.
17. Read at 405 nm for TMB/HRP.
18. Determine the linearity of the instrument being used for the readout.

Second Development Experiment

The goal of the second development experiment is to determine the potential dynamic range and sensitivity. Take the conditions established in the initial experiment for the concentration of the antibody and labeled ligand and incubate with a wide range of unlabeled analyte. The resulting standard curve and precision profile calculation will give an estimate of the sensitivity and dynamic range of the assay.

Reagents

Reagents are the same as in the initial experiment.

Protocol

1. Dilute the capture antibody in coating buffer at the concentration determined in the initial experiment. Add 100 µl to each well of the 96-well microtiter plate.
2. Incubate the plate containing the capture antibody overnight at 4°C and use the next day.
3. Remove the capture antibody solution from the microtiter plates by aspirating or dumping the plate.
4. Add 200 µl of blocking buffer to each well of the 96-well microtiter plate.

5. Incubate the plate for one hour at room temperature.
6. Remove the blocking buffer from the plate by aspirating or dumping the plate.
7. Dilute the labeled standard in antibody dilution buffer at the concentration determined in the initial experiment.
8. Dilute the unlabeled ligand in antibody dilution buffer over a wide range of concentrations.
9. Add 100 µl of the labeled standard to each well in the microtiter plate and 100 µl of the various dilution of the unlabeled ligand. Incubate for 2.5 hours at room temperature. This is the competitive part of the assay and will allow for the competition between the labeled and unlabeled ligand for the sites on the antibody.
10. Wash the plates 3 times with wash buffer.
11. If a biotinylated standard is used, dilute streptavidin-HRP according to the manufacturer's instructions in antibody diluent and add 100 µl to each well in the microtiter plate and incubate for 1 hour at room temperature.
12. For HRP readout, add either OPD or TMB as a substrate to allow color development and incubate for 10-20 minutes at room temperature.
13. Add acid stop reagent to stop the enzyme reaction.
14. Read at 405 nm for TMB/HRP.

Third Development Experiment

The goal of the third development experiment is to determine the optimal buffers, incubation periods, temperatures, matrix effects, and other variables that might affect the assay.

Reagents

Reagents are the same as in the initial experiment.

Protocol

Same as in the second development experiment except for the following changes at steps 8 and 9:

8. Dilute the unlabeled ligand in antibody dilution buffer, and the matrix appropriate for the experiment, over a wide range of concentrations. Again the dilution buffer can be varied according to the experimental design.

9. Add 100 µl of the labeled standard to each well in the microtiter plate and 100 µl of the various dilutions of the unlabeled ligand. Incubate for 2.5 hours at room temperature. This incubation time can be varied for longer and shorter periods of time to potentially increase the sensitivity and dynamic range of the assay.

RESULTS

Analysis of the results is by the stasticial software JMP or any other appropriate statistical software can be used to determine the optimal conditions for incubation timing, buffers for dilution, and matrix effects.

Method Validation (Pre-Study)

It is important to note that the precision profile evaluation described earlier in this chapter is based on just the calibration curve. Consequently, only the calibration curve factors (quality and stability of reference standards, quality and stability of reagents, statistical validity of the calibration curve model) are taken into account for deriving these quantitation limits. Sample factors such as analyte (similar physicochemical substances), matrix (other substances that can affect analytical results) and operational factors can affect the performance of the assay/method as well. Thus the quantitation limits derived from the precision profile of a calibration curve is an optimistic assessment of the method performance. If these limits are not satisfactory the assay needs further optimization.

If the quantitation limits from the precision profile are close to the limits desired for the method's intended use, proceed to a full validation experiment as outlined below. This validation experiment is used to establish the method quantitation limits using the analysis of recovery data from validation samples (spiked standards). This experiment will take into account the three major sources of variation described above (calibration curve factors, sample factors and operational factors).

For the full validation experiment, generate the following data in at least three independent runs.

- Calibration curve in each run, preferably in triplicate.
- Validation/Quality Control (QC) samples (independent set of samples spiked with a known amount of standards) in each run at seven or more concentrations with at least two replicates; two concentrations near the precision profile estimates of the lower quantification limit and similarly two more near the upper quantification limit, and three or four that are equally spaced between lower and upper quantification limits.
- Estimate the concentrations of the validation samples of each run using the respective calibration curves. Then compute the % recovery of these validation samples using the following formula:

% Recovery = 100 × (Calibrated Concentration/Nominal Concentration)

- Now compute the average and standard deviation of the % recovery data of the validation samples from all runs for each concentration. The evaluation of standard deviation should be based on a separate variance component analysis of the multiple runs of validation data, and it should include the sources of variability relevant during the use of the assay in production. At the minimum, it will include inter-run and intra-run variability. Some of the other sources to consider might be analyst, plate, equipment, etc. As evident from the above formula for evaluating the percent recovery, note that the standard deviation of percent recovery can be considered as the coefficient of variation (%CV) of the calibrated results. This is essentially the intermediate precision (inter-run %CV) of the assay. We will hereafter refer to this as Intermediate Precision (IP).
- Plot the average % recovery values along with the IP (as calculated above) versus the nominal concentrations. Note that the % recovery along with the intermediate precision as determined above reflects the total error of the assay.
- The % recovery and the IP limits must be within +/- X% of the nominal value. If X is 30%, the percent recovery +/- IP must be within 70 to 130% of the nominal value. This means that the Total Error of the assay must be within 30%. The value of X should be set based on the intended use of the assay. Recommendations on the acceptance criteria are discussed later in this chapter.
- If X is set at 30%, the lower quantification limit is the lowest concentration at which the % recovery +/- IP is within 70% to 130%. The upper quantification limit is the highest concentration at which the % recovery +/- IP is within 70% to 130%.

Method Validation (In-Study)

The in-study validation phase is about making sure that the assay continues to perform according to pre-defined specifications in each study run. During production phase, when the assays are being used for screening the unknowns, it is important to run validation/QC samples in every run, with at least 2 replicates at high, middle and low concentrations (just one or two columns of a 96-well plate). Compute the average % recovery of these samples to make sure that the average recovery is within a reasonable range of accuracy (say, 80% to 120%). This might be adequate for quality control and is a reasonable compromise for any loss in assay throughput. Various methods might be considered for setting criteria for accepting or rejecting an actual assay where samples are being tested during a study (in-study validation). This is addressed in a subsequent section in this chapter.

Example of an Immunoassay Validation Experiment

Set up numerous aliquots of the standard and store frozen at -70°C. If the standard concentration is much higher than the first point on your curve, pre-dilute it so that a single, simple dilution can be made in order to set up the standard curve.

Dilute the standards serially to obtain an 8-point standard curve in the matrix appropriate for the samples that need to be measured. For example, if measuring tissue culture samples then the standards should be diluted in the same tissue culture medium that the samples are in. For serum samples, the standards should be diluted in serum diluted with an optimized buffer to the same dilution that the samples will be diluted.

Set up a series of spiked samples, again in the matrix appropriate for the samples that will be measured. The spiked control samples should not be the same concentration as in the standard curve and should cover the detectable range that the samples are thought to cover.

Follow the immunoassay protocol established during the optimization experiments. Set up the plate with 3-4 replicates of the standard curve and 4 or more replicates of the spiked control samples (See Table 7).

Assay at least 3 plates over 3 different days for a complete validation.

Validation Results from an IL-10 Immunoassay

The percent recovery and the standard error that takes into account the relevant sources of variation are plotted in Figure 9. If X is 30%, then the quantification limits are the lowest and highest concentrations where the % recovery +/- IP is within 70% to 130%. So for this assay, the lower quantification limit is the lowest concentration tested in this validation study (6.2 pg/ml), and the upper quantification limit is 3265 pg/ml (see Table 8)

St1	St1	St1	St1	SP1	SP1	SP1	SP1				
St2	St2	St2	St2	SP2	SP2	SP2	SP2				
St3	St3	St3	St3	SP3	SP3	SP3	SP3				
St4	St4	St4	St4	SP4	SP4	SP4	SP4				
St5	St5	St5	St5	SP5	SP5	SP5	SP5				
St6	St6	St6	St6	SP6	SP6	SP6	SP6				
St7	St7	St7	St7	SP7	SP7	SP7	SP7				
St8	St8	St8	St8	SP8	SP8	SP8	SP8				

Table 7: Validation Plate Layout.

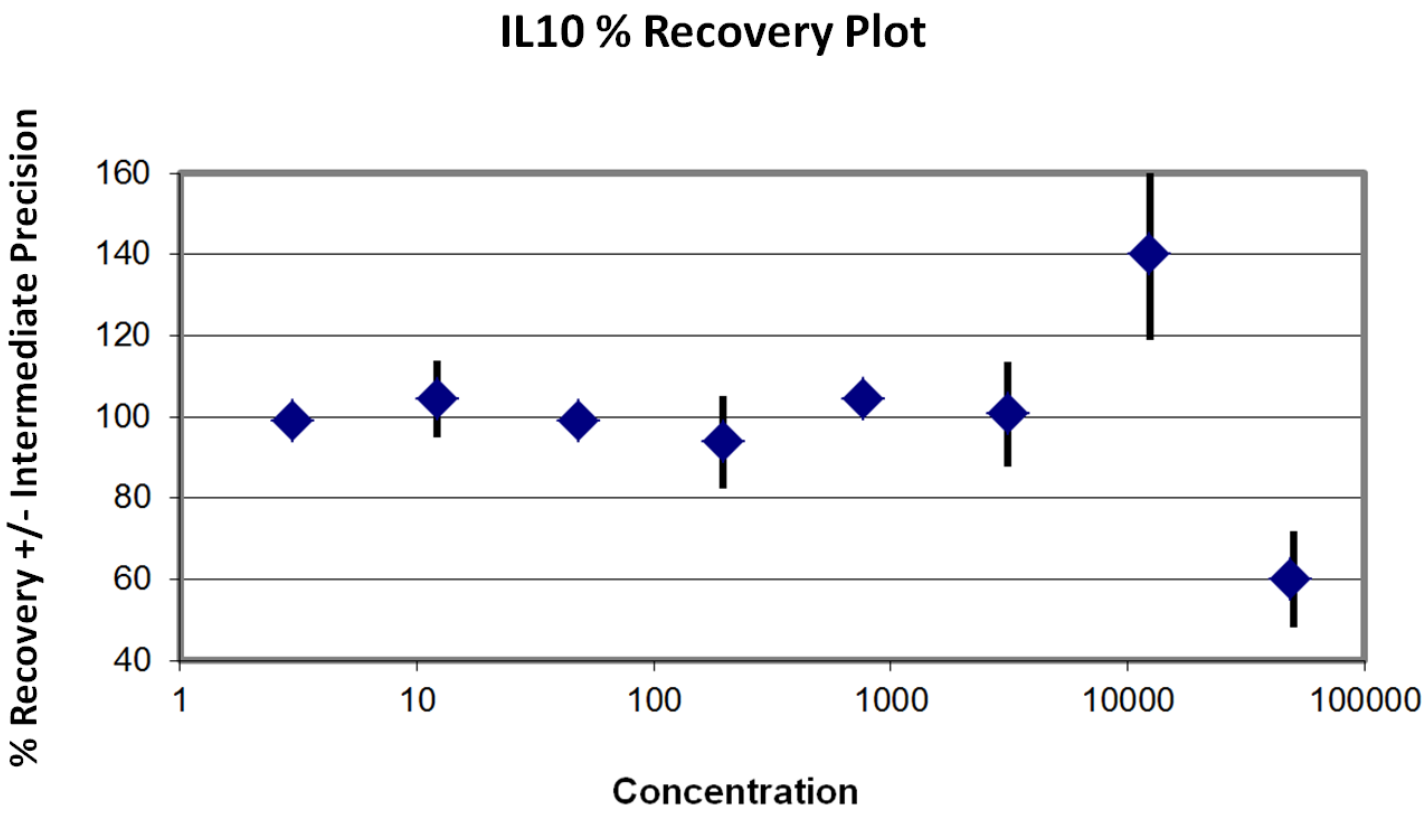

Figure 9: Validation results from IL-10 immunoassay.

Table 8: Validation results from IL-10 immunoassay

IL-10		
Expected Value	Average 4,5,6	% Recovery
40000	36924.96	92.31
11428.57	13846.57	121.16
3265.306	2966.42	90.85
932.9446	892.76	95.69
266.5556	242.70	91.05
76.15874	71.65	94.08

Table 8 continued from previous page.

IL-10		
Expected Value	Average 4,5,6	% Recovery
21.75964	22.32	102.60
6.21704	6.06	97.50

Plate Uniformity and Variability Experiment

It is important to check whether there is any systematic data trend across rows or columns of the 96-well plate and whether there is any significant variability between plates. An experiment with three plates and four concentrations of the standard can be done using the plate-layout in Figure 10. In this layout, C1, C2, C3 and C4 denote the standard concentrations from lowest to highest. For the purpose of illustration, data from one of the plates and a plot of the data from this experiment are given below for a sandwich ELISA. A systematic trend across columns is evident from this plot. For determining the statistical significance of this trend and the plate to plate variability, further statistical analysis of the data can be done with the help of a statistician.

Pre-Study & In-Study Acceptance Criteria

Different methods of quality control are available and routinely used in analytical methods. It is important that the methods used for assessment of method performance are suitable for the intended purpose. Shah et al. (14) proposed the 4-6-X rule for in-study validation phase that has become popular and widely used. This rule states that 4 out of the total 6 samples should be within X% of the nominal/reference value, and at least one out of the two samples at each level must be within X% of the reference value. The choice of X is specified a priori based on the intended use and purpose of the assay, and it was set at 20% by Shah and colleagues. DeSilva et al. (15) proposed a criteria (see Table 9) for pre-study and in-study validation phase of ligand-binding assays for assessing pharmacokinetics of macromolecules.

It should be noted that the acceptance criteria for biomarker assays will depend heavily on the intended use of the assay and should ideally be based on physiological variability as well. According to the criteria listed in Table 9, X is set at 30% for in-study validation, and the total error is set to be within 30% for the pre-study validation, along with the 20% limits for each component of total error (bias and precision). The pre-study criteria (Total Error < X %) and the in-study criteria (4-6-X rule) are not entirely consistent because the variability of the total error estimate and the consequent decision error rates are not taken into account. Thus the uncertainty in these estimates will depend on the magnitude of the errors and the number of measurements, and will in turn impact the level of decision error rates (16). The appropriate value of X in 4-6-X can be determined based on the variability of the total error estimates in pre-study validation. When it is feasible to use more QC samples in each run, 8-12-X or 10-15-X will have much better statistical outcomes than the 4-6-X criteria. In addition, the use of control charts as described by Westgard or tolerance limits based on pre-study validation data might be considered when possible.

The concept of total error as the primary parameter, and with bias and precision as additional constraints, is very useful. This is because total error has a more practical and intuitive appeal as it relates specifically to our primary question of interest about the assay; How far are my observed test results from the reference/nominal value? Because this is the primary practical question in the minds of most laboratory scientists, the criteria on the assay performance for the in-study phase is defined with respect to this question.

If the plate-format is not the same as indicated below, type in the necessary changes below:

	1	2	3	4	5	6	7	8	9	10	11	12
A	C1	C2	C3	C4	C1	C2	C3	C4	C1	C2	C3	C4
B	C2	C3	C4	C1	C2	C3	C4	C1	C2	C3	C4	C1
C	C3	C4	C1	C2	C3	C4	C1	C2	C3	C4	C1	C2
D	C4	C1	C2	C3	C4	C1	C2	C3	C4	C1	C2	C3
E	C1	C2	C3	C4	C1	C2	C3	C4	C1	C2	C3	C4
F	C2	C3	C4	C1	C2	C3	C4	C1	C2	C3	C4	C1
G	C3	C4	C1	C2	C3	C4	C1	C2	C3	C4	C1	C2
H	C4	C1	C2	C3	C4	C1	C2	C3	C4	C1	C2	C3

Paste the plate-data below:

	1	2	3	4	5	6	7	8	9	10	11	12
A	1.24	2.53	1.23	0.81	2.16	2.61	1.41	1.02	1.99	3.27	1.60	1.10
B	2.31	1.29	0.73	2.12	3.24	1.75	1.00	2.12	3.32	1.81	1.14	2.27
C	1.11	0.91	1.89	3.08	1.74	1.03	1.99	3.61	1.88	1.30	2.43	3.36
D	0.63	1.95	2.92	1.64	1.09	2.30	3.46	1.92	1.21	2.51	3.63	1.90
E	1.84	2.63	1.53	1.06	2.35	3.41	1.70	1.15	2.47	3.45	1.83	1.27
F	2.41	1.90	1.05	2.09	3.29	1.79	1.11	2.35	3.58	1.90	1.24	2.38
G	1.28	0.86	2.02	3.50	1.79	1.13	2.33	3.56	1.91	1.24	2.45	3.50
H	0.65	1.82	2.88	1.72	1.04	2.22	3.05	1.85	1.23	2.33	3.41	1.99

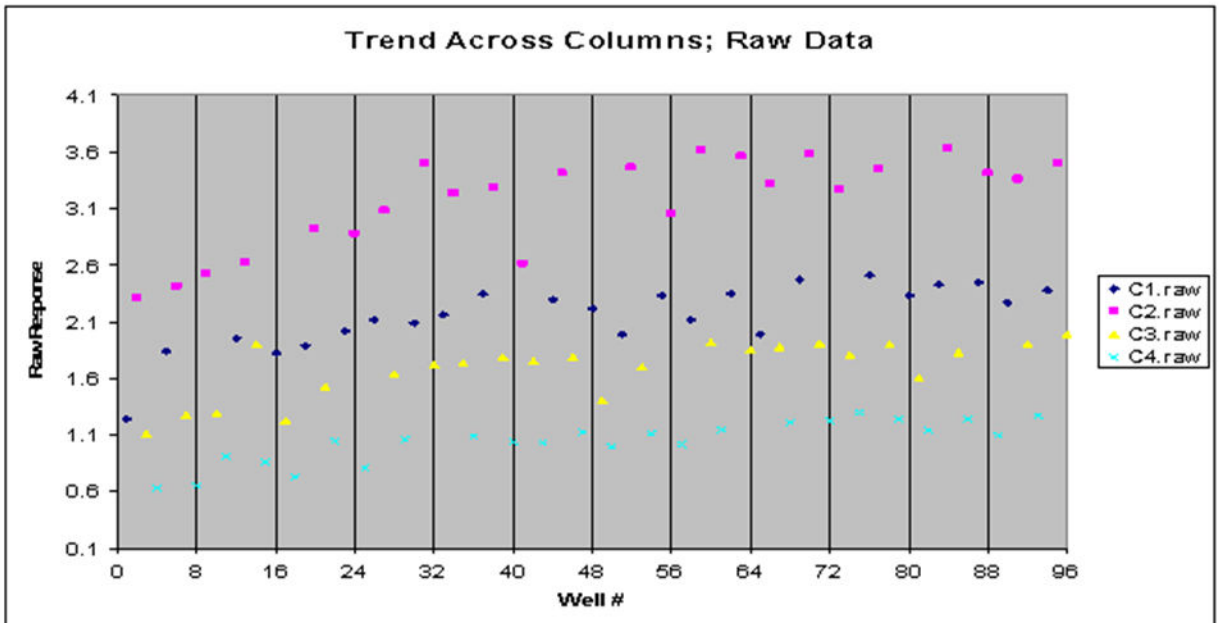

Figure 10: Data from one plate and a data plot from a plate uniformity and variability experiment where C1, C2, C3 and C4 denote the standard concentrations from lowest to highest.

Table 9: Criteria for pre-study and in-study validation phase of ligand-binding assays for assessing pharmacokinetics of macromolecules.

Characteristic	Pre-Study Validation	In-Study Validation
Trueness (%Relative Bias)	≤ ± 20 (± 25 at LQL)	-
Intermediate Precision (%CV)	≤ 20 (25 at LQL)	-
Total Error	≤ 30%	"4-6-30" rule

Consideration of Physiological Variation for Acceptance Criteria

One of the most important considerations for defining the performance criteria of most biomarker methods is the physiological variability in the study population of interest. That is, in order to determine whether a biomarker method is 'fit-for-purpose', we should determine whether it is capable of distinguishing changes that are statistically significant based on the intra-subject and inter-subject variability. The term "subject" here might

refer to animal or human. For example, an assay with 50% total error during pre-study validation might still be adequate for detecting a 2-fold treatment in a clinical trial for a certain acceptable sample size. Thus whenever possible, the acceptance criteria for pre-study validation should be based on physiological variation in the study. An example of the use of intra-subject and inter-subject variation for defining the pre-study acceptance criteria can be found in http://www.westgard.com/guest17.htm (17).

When the relevant physiological data (say, treated patients of interest) are not available during the assay validation phase, then healthy donor samples should be used to estimate the intra-subject and inter-subject variation, and hence the desired specifications on the pre-study assay validation. This can be updated at a later time when there is access to the relevant patient data. If access to healthy donor samples is also not feasible, then other flexible biological rationale should be considered and updated periodically as more information becomes available over time. In the absence of physiological data or other biological rationale, the acceptance criteria for pre-study validation should not be strictly defined. Instead, only the performance characteristics from pre-study validation such as the bias, precision and total error should be reported. Any decision regarding the acceptance of the assay (pre-study acceptance criteria) and consequently the determination of the dynamic range such as the Lower Quantification Limit (LQL) and Upper Quantification Limit (UQL) should be put on hold until adequate information related to the physiological data become available.

As the high, mid and low QC samples are used in the acceptance criteria, it is important to choose their concentrations such that they span the expected range of the study samples. For example, it is of no value to reject batches when large numbers of high concentration quality controls fail, but where the low and medium quality controls are good and when all the study sample results are in the low to medium range. Here the positioning of the high quality control based on expectation before the analysis of incurred samples is flawed – but it does not necessarily make the study sample results invalid.

Precision Profile Tool for Estimating Assay Performance Characteristics

Download the Precision Profile tool here.

Download the Precision Profile data example here.

Download the Precision Profile ReadMe instructions here.

This tool is for the calculation of accuracy, imprecision, sensitivity, dynamic range, etc., for a relative quantitative assay such as Immunoassays or Chromatography assays where the analyte levels are reported in concentration units via calibration from a sample from a reference standard/calibration curve. Data from pre-study validation with the spiked validation/QC samples of different concentrations from multiple assay runs can be pasted in this tool for the calculation of assay performance characteristics listed above. This version can handle any number of runs, replicates, concentrations, etc.

Please see the attached ReadMe for detailed instructions.

Immunogenicity Cut Point Analysis Tool (I-CAT)

Download the I-CAT tool here.

Download the I-CAT data example here.

Download the I-CAT ReadMe instructions here.

We are pleased to provide this Excel-based immunogenicity cut point analysis tool (I-CAT) for the calculation of cut points needed in the assays used for the immunogenicity (anti-drug antibody) assessment of biotherapeutics

in pre-clinical and clinical studies. The different formulae recommended and widely used in practice [Shankar et al. (2008), Shen et al. (2015), Devanarayan et al. (2017), FDA final guidance (2019)] and a simplified version of the analysis method provided in the last paragraph of page 1490 of Devanarayan et al (2017) that is amenable for direct implementation in a program such as Microsoft Excel have been implemented in this tool. This tool also includes the evaluation of distributions, identification of analytical and biological outliers, and several visual aids (graphs) to better understand the assay characteristics related to the analytical and biological factors. A detailed explanation of the criteria to be used for selecting the appropriate cut points is also provided.

Please see the attached ReadMe for detailed instructions.

References

1. Swartzman, et al. A Homogeneous Multiplexed Immunoassay for High-Throughput Screening Using Fluorometric Microvolume Assay Technology. Anal. Biochem. 1999;271(2):143–151. PubMed PMID: 10419629.
2. Stockwell, et al. High-throughput screening of small molecules in miniaturized mammalian cell-based assays involving post-translational modifications. Chem. Biol. 1999;6(2):71–83. PubMed PMID: 10021420.
3. Martens, et al. A generic particle-based nonradioactive homogeneous multiplex method for high-throughput screening using microvolume fluorimetry. Anal. Biochem. 1999;273(1):20–31. PubMed PMID: 10452795.
4. Zuck, et al. Ligand-receptor binding measured by laser-scanning imaging. Proc. Natl. Acad. Sci. 1999;96(20):11122–11127. PubMed PMID: 10500140.
5. Kitamura, et al. A fluorescence sandwich ELISA for detecting soluble and cell-associated human interleukin-2. J. Immunol. Methods. 1989;121(2):281–288. PubMed PMID: 2788194.
6. Findlay, et al. Validation of immunoassays for bioanalysis: a pharmaceutical industry perspective. J. Pharm. Biomed. Anal. 2000;21(6):1249–1273. PubMed PMID: 10708409.
7. Pavkovic, et al. Comparison of the MesoScale Discovery and Luminex multiplex platforms for measurement of urinary biomarkers in a cisplatin rat kidney injury model. J. Pharmacol. Toxicol. Methods. 2014;69(2):196–204. PubMed PMID: 24333954.
8. Ray, et al. Development, validation, and implementation of a multiplex immunoassay for the simultaneous determination of five cytokines in human serum. J. Pharm. Biomed. Anal. 2005;36(5):1037–1044. PubMed PMID: 15620530.
9. Smolec, et al. Bioanalytical method validation for macromolecules in support of pharmacokinetic studies. Pharm. Res. 2005;22(9):1425–1431. PubMed PMID: 16132353.
10. Kellar, et al. Multiplexed fluorescent bead-based immunoassays for quantitation of human cytokines in serum and culture supernatants. Cytometry. 2001;45(1):27–36. PubMed PMID: 11598944.
11. Chowdhury, et al. Validation and comparison of two multiplex technologies, Luminex and Mesoscale Discovery, for human cytokine profiling. J. Immunol. Methods. 2009;340(1):55–64. PubMed PMID: 18983846.
12. Elshal, et al. Multiplex bead array assays: performance evaluation and comparison of sensitivity to ELISA. Methods. 2006;38(4):317–323. PubMed PMID: 16481199.
13. Boulanger et al. (2007). Statistical Considerations in Analytical Method Validation. Pharmaceutical Statistics Using SAS: A Practical Guide, 69.
14. Shah, et al. Pharm. Res. 1992;9(4):588–592.
15. DeSilva, et al. Recommendations for the Bioanalytical Method Validation of Ligand-binding Assays to Support Pharmacokinetic Assessments of Macromolecules. Pharm. Res. 2003;20(11):1885–1900. PubMed PMID: 14661937.
16. Kringle, et al. Pharm. Res. 2007;24(6):1157–1164. PubMed PMID: 17373576.
17. Glasziou et al. (2007). Evidence-based medical monitoring: From principles to practice, Blackwell Publishing.

Additional References

Weblinks

Available at: http://www.brendan.com/

Available at: http://www.waichung.demon.co.uk/webanim/Menu1.htm

Available at: http://www.piercenet.com/method/elisa-development-optimization

Available at: http://www.piercenet.com/method/overview-elisa#elisaprobes

Available at: http://www.piercenet.com/method/overview-detection-probes

GTPγS Binding Assays

Neil W. DeLapp,[1,*] Wendy H. Gough, Steven D. Kahl,[†] Amy C. Porter, and Todd R. Wiernicki[2]

Created: May 1, 2012; Updated: October 1, 2012.

Abstract

Signal transduction via G-protein coupled receptors (GPCRs) is mediated through binding of GTP to GTP–binding proteins. Evaluation of GPCR agonists in drug discovery requires GTP binding assays to confirm agonist activity. This chapter addresses the development and optimization of robust GTPγS binding assays with discussions on basic protocols, assay buffers, effect of required additives (Mg^{2+}, NaCl, Saponin) and data analysis. An extensive set of recent references is included for beginners and experienced investigators.

Author Affiliations: 1 Eli Lilly & Company, IN, USA. 2 Eli Lilly & Company, IN, USA.

Corresponding author.

* Retired

† Editor

Flow Chart for Assay Development

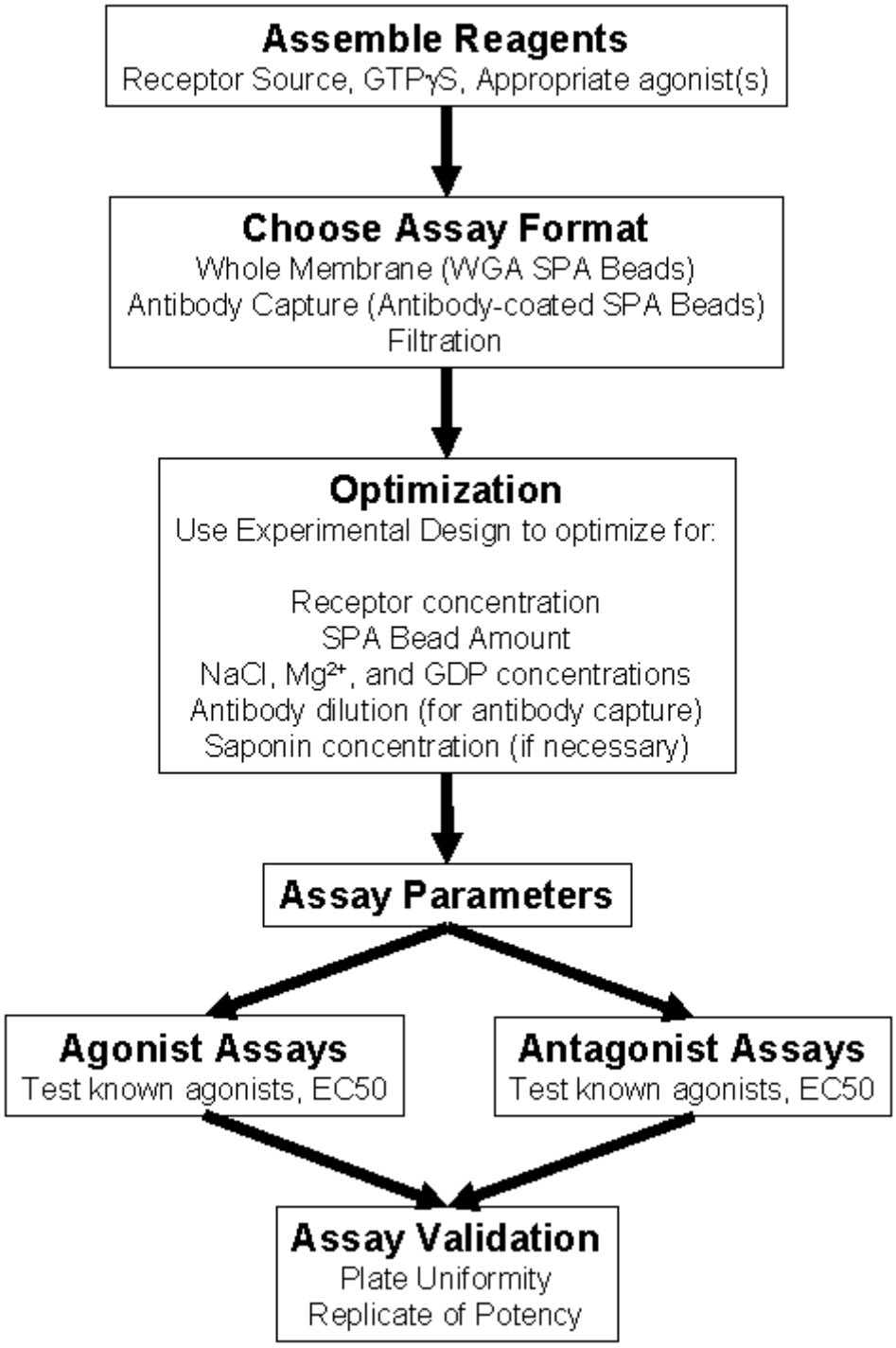

Introduction

Binding of GTP to the alpha (α) subunit of heterotrimeric GTP binding proteins is an early event in agonist-induced activation of G-protein coupled receptors (GPCRs). Although GTPγS binding assays are carried out using membrane preparations in much the same way as radioligand binding assays, these are functional assays and can thus be used to differentiate agonist, antagonist, and inverse agonist activities. Such assays are carried out using [^{35}S]guanosine-5'-O-(3-thio) triphosphate which provides a radioactive ligand with high affinity for G-protein α subunits that is highly resistant to the inherent GTPase activity of α subunits such that it remains bound for sufficient periods of time to allow counting of radioactivity.

Although the classical method used for GTPγS binding has been filtration of radiolabeled membranes, scintillation proximity assays (SPA) are much more convenient and allow the use of an antibody capture technique which permits determination of receptor-mediated activation of specific G-protein families. There are two basic methods for running homogeneous SPA GTPγS binding assays in 96-well plate format: 1) whole membrane binding in which labeled membranes are bound to wheat germ agglutinin (WGA)-coated SPA beads in the same way as these beads are used for radioligand binding assays, and 2) antibody capture binding assays in which membranes are solubilized with detergent followed by isolation of the desired G-protein using a specific antibody along with capture of antibody-G-protein complexes onto anti-IgG coated SPA beads.

Advantages of GTPγS functional assays in comparison to determinations of second messengers produced as a result of receptor activation are:

1. The assays are very simple to run and utilize membrane preparations which can be frozen at -80°C for periods of months.
2. Because GTP exchange is an event proximal to receptor activation these assays typically have lower degrees of receptor reserve than other functional assays and are thus useful for differentiating full from partial agonists.
3. The assays are useful for determination of antagonist inhibition constants since agonists and antagonists can be equilibrated prior to starting the incubation by addition of GTPγ^{35}S.
4. One can often measure specific coupling of receptor subtypes to different G-protein families, even in native tissues, under very similar assay conditions.

The major disadvantage is the relatively low signal to background which limits GTPγS binding to medium throughput evaluations. The power of the antibody capture technique is its ability to easily generate multiple concentration response curves thus allowing true pharmacological evaluation of receptor-mediated coupling to individual G-proteins, an accomplishment that is prohibitive by older immunoprecipitation techniques.

Materials and Reagents

The list below includes materials and reagents, which have been used successfully to enable GTPγS binding assays for a variety of GPCRs (1-3):

96-well plates: Costar 3632, white clear bottom

WGA SPA beads: Amersham SPQ0031

Anti-rabbit SPA beads: Amersham RPNQ 0016

Anti-mouse SPA beads: Amersham RPNQ 0017

GTPγ^{35}S: Perkin Elmer Life Sciences NEG030H

NP40 detergent 10%: Roche 1 332 473

Anti-G_s/olf: Santa Cruz SC-383, rabbit polyclonal

Anti-G_{i-3}: Santa Cruz SC-262, rabbit polyclonal (recognizes G_{i-1}, G_{i-2}, and G_{i-3})

Anti-G_q/11: Santa Cruz SC-392, rabbit polyclonal

Anti-G_o: Chemicon MAB3073, mouse monoclonal

Although the commercially available antibodies listed above have been used successfully in the antibody capture assay, certain lots of these antibodies have been found to be unsatisfactory. For this reason and because of cost

considerations it may be preferable to obtain antibodies to G-proteins through in-house resources or by contracting out peptide synthesis and antibody production for specific G-proteins of interest (4–6).

Membrane Preparations and Assay Buffers

Types of membrane preparations used

1. Crude homogenates (7)
2. Plasma membrane preparations (P2 fraction, 1)
3. Sucrose density gradient enriched receptors (8)
4. Commercially available membranes, which include
    i. Receptors cloned into mammalian cells (Perkin Elmer, Euroscreen, Cerep)
    ii. Receptors cloned into *Sf*9 insect cells co-expressing mammalian G-proteins (9)

Types of Assay buffers

1. Lazareno and Birdsall buffer (7) 20 mM HEPES, 100 mM NaCl, 5 mM $MgCl_2$, pH 7.4
2. Buffers with HEPES replaced by 50 mM Tris HCl (8,10)

Basic Assay Protocol

Whole membrane assay using WGA SPA beads

1. Incubate membranes, GTPγ^{35}S, and compounds tested in 200 µl/well at room temperature for 30 – 60 minutes.
2. Add 50 µl per well of suspended WGA beads (1 mg/well).
3. Seal plates and incubate for one hour or more at room temperature.
4. Centrifuge at 200 x g and count plates in a Wallac microbeta.

Antibody Capture assay

1. Incubate membranes as for whole membrane assay.
2. Add 20 µl per well of 3% NP40 and incubate for 15 minutes.
3. Add 20 µl per well of primary antibody and incubate for 15 minutes.
4. Add 50 µl per well of anti-rabbit or anti-mouse SPA beads (1 mg).
5. Seal and incubate for three hours, centrifuge as above and count.

Assay Optimization

Membrane protein/well and [GDP]

Using a starting buffer such as listed under assay buffer above, determine the optimal amount of membrane protein per well from 5 to 50 µg in the presence of varying concentrations of GDP (guanosine diphosphate) from 0 – 10 µM for transfected cell membranes and from 0 up to 300 µM for native tissue membranes using a concentration of 200 –500 pM GTPγ^{35}S. Note that $G_{i/o}$ coupled receptors will require higher concentrations of GDP than G_s or G_q-coupled receptors which may give optimal signals in the absence of added GDP. Figure 1 illustrates the marked difference in GDP requirement for determination of muscarinic agonist-stimulated GTPγS binding in rat brain striatal membranes measured by anti-G_q/11 (M1 receptor) versus anti-G_o (M4 receptor).

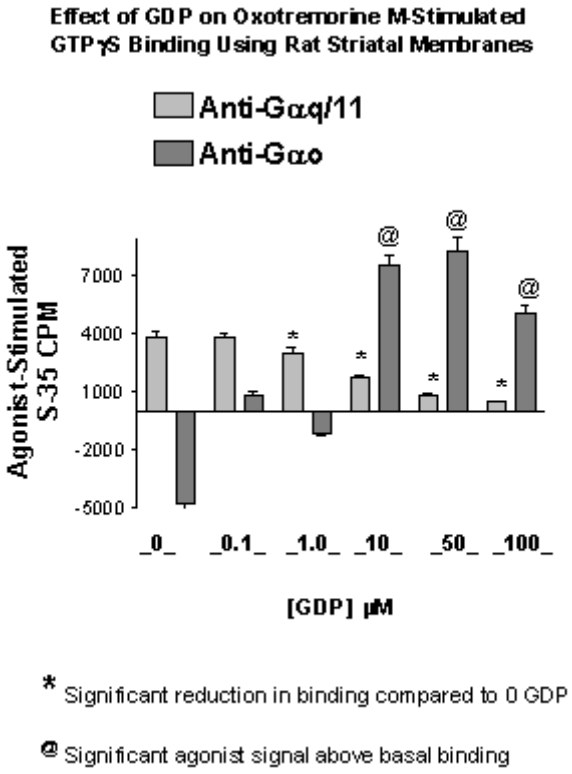

Figure 1. Difference in [GDP] required for G_q versus G_o-coupled GPCRs

Effect of Mg^{2+}

Determine the optimal Mg^{2+} concentration for the best signal to noise over the range of 1 mM to 10 mM. Figure 2 shows the variation of Mg^{2+} on dopamine-stimulated GTPγS binding mediated by D2 receptors in rat striatal membranes

Effect of NaCl

Determine the optimal amount of NaCl for best signal to noise over the range of 0 – 200 mM. Although 100 mM NaCl is commonly used in these assays note that at times better agonist stimulation may be achieved at lower Na^{2+} and if higher constitutive activity is desired (for evaluating inverse agonists) lowering Na^{2+}will likely provide the best opportunity. Figure 3 demonstrates the effect of NaCl on the constitutive activity of orphan receptor 19BG.

Effect of saponin

The effect of adding saponin at 3 – 100 μg/ml can be explored, but recognize that while saponin may increase signal to background, it may also compromise the quality of concentration response curves. Figure 4 demonstrates the optimization of saponin to achieve the highest signal to background for an orphan receptor where constitutive activity was measured to allow evaluation of inverse agonists. Figure 5 shows how saponin may compromise the quality of some concentration response curves.

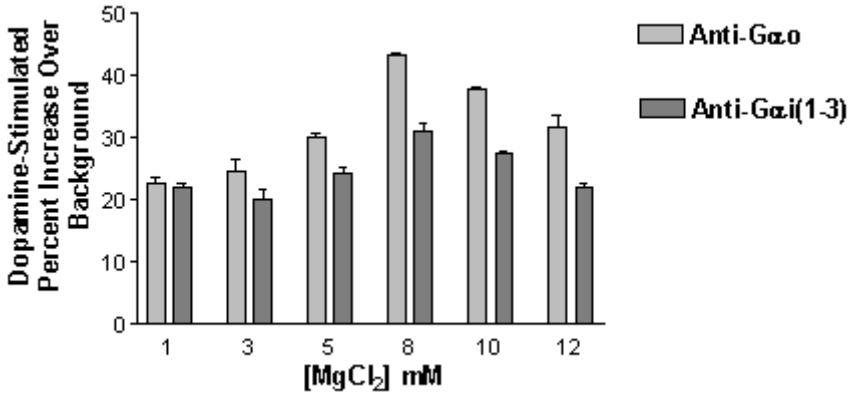

Figure 2. Dopamine stimulated GTPγS binding in brain membranes

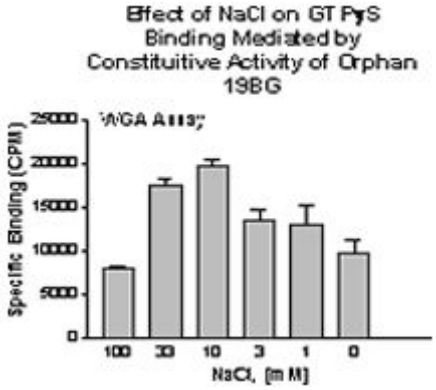

Figure 3. Optimization of NaCl to measure constitutive activity of an orphan GPCR

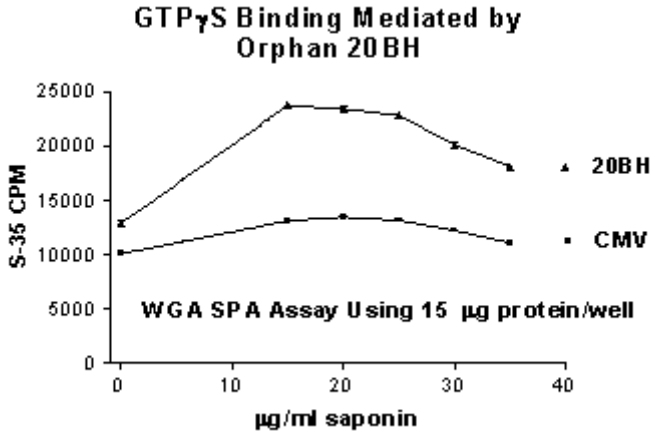

Figure 4. Optimization of saponin to measure constitutive activity of an orphan GPCR

Incubation Time

The optimal incubation time for the best signal to background may be determined, but thirty minutes is usually satisfactory for cell membranes and one hour for native tissue membranes.

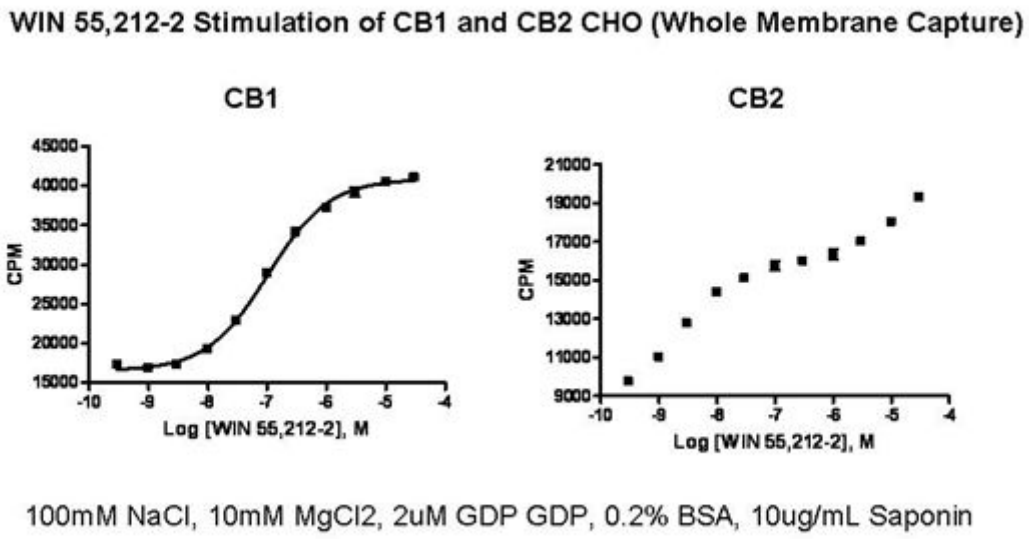

Figure 5: Effect of saponin on agonist concentration response curves for some receptor subtypes

Antibody dilution for antibody capture assays

If using the antibody capture method the optimal dilution will have to be determined for each lot of antibody. Figure 6 below illustrates the effect of various dilutions of anti-$G_{s/olf}$ on GTPγS binding mediated by the rat 5-HT_6 receptor.

The use of experimental design and JMP analysis for assay optimization

Experimental design and JMP analysis are convenient tools for optimizing a variety of conditions in a small number of experiments and determining if there are any interactions among the factors. Figure 7A shows an example in which four factors were optimized in a single experiment. Figure 7B shows the two factor interaction profiles from JMP analysis. Parallel lines indicate no interaction and intersecting lines indicate interactions. For instance in this experiment there is virtually no interaction between NaCl and saponin, but there is a significant interaction between the amount of protein and GDP concentration.

Signal window and Z' factor

Determine the signal window for the assay under the optimal conditions by running background and maximal stimulation multiple times across assay plates on separate days. Calculate the Z' factor for the assay using the formula:

$$Z' = 1 - (3(SD_{max}) + 3(SD_{min})/Max\text{-}Min)$$

A Z' factor of > 0.5 indicates a useful assay. GTPγS binding assays can be quite reproducible and will give reliable results when signals are greater than 40-50% over background. Even with smaller signals, one can generate reliable concentration response curves by using 4 to 8 replicates per data point.

Evaluation of standard compound concentration response curves

After determining optimal conditions for the assay concentration response curves should be run for standard agonists and antagonists to determine variability and comparability to literature values if available. Most assays will require duplicate determinations per concentration but with exceptional signals one may be able to use single data points for each.

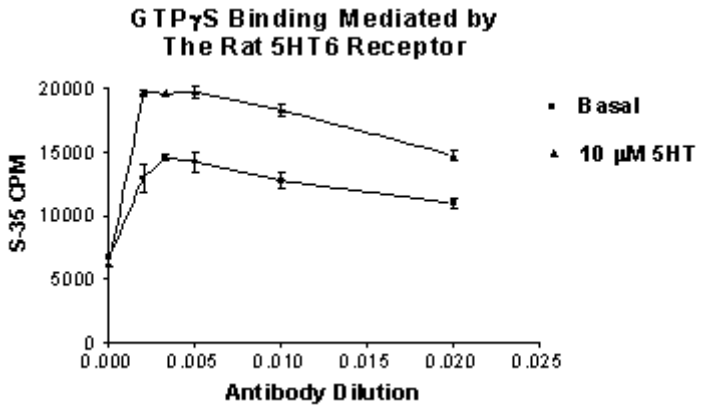

Figure 6. Effect of antibody dilution on basal and agonist-stimulated binding

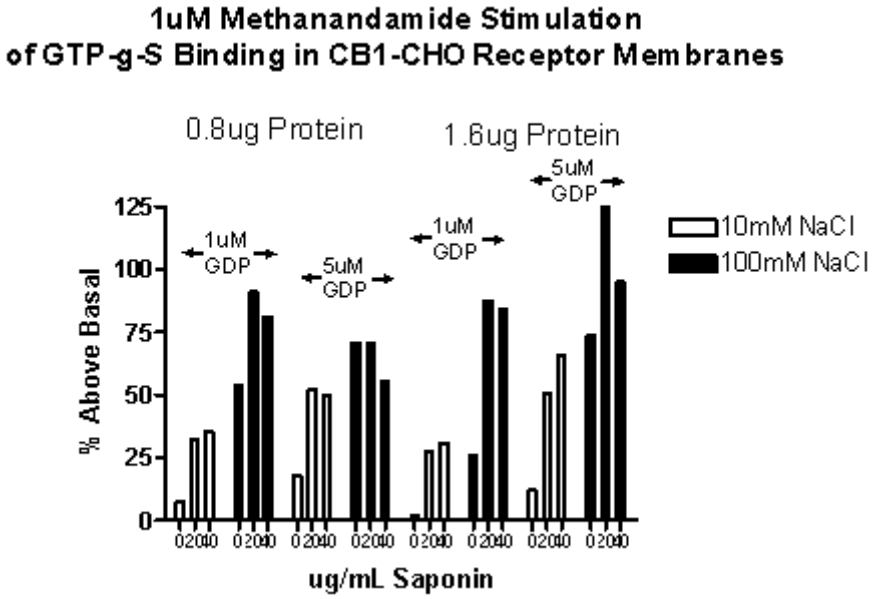

Figure 7A: Experimental design with 4 factors (GDP, Saponin, NaCl and Membrane protein)

Choice of whole membrane versus antibody capture

Good assays for $G_{i/o}$ may be developed using whole membranes and WGA beads. Use of antibody capture for $G_{i/o}$-coupled receptors, however, may reduce assay variability. For G_q- and G_s-coupled GPCRs, the antibody capture assay will most likely be superior since most cells and tissues are dominated by inhibitory G-proteins and it is often not possible to develop reliable signals without the antibody technique unless receptors are fused to G_s or G_q (1, 9, 11). Challiss and coworkers have found, using *post mortem* human brain tissue, that the M1 receptor signal generated using antibody capture via an anti-$G_{q/11}$ antibody was markedly improved by treatment of the membranes with N-ethylmaleimide (6). High throughput assays for G_i-linked receptors have been reported using the WGA whole membrane technique (12,13).

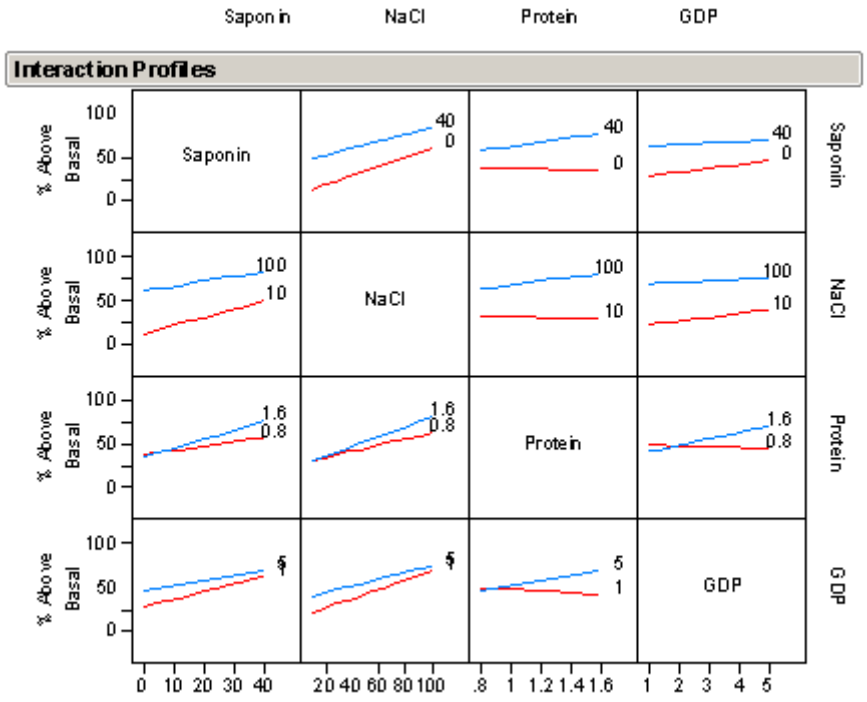

Figure 7B: Interaction Plots for Experimental Design (using JMP)

Data Analysis

As with other functional assays, concentration response data may be fitted using a four-parameter logistic equation with variable slope to determine half maximal responses. Keep in mind that GTPγS assays will often show some degree of receptor reserve even though typically less than a cAMP or Ca^{2+} mobilization assay and for this reason agonist EC_{50}'s may not agree with K_i values for agonists determined in radioligand binding assays. For antagonists, K_b values may be determined from rightward curve shifts in the presence of a fixed antagonist concentration or from antagonist concentration response curves run at a fixed agonist concentration (at or somewhat below the concentration that produces a maximal response). For curve shift at a single antagonist concentration the following equation may be used to determine the K_b:

$$EC_{50}b = EC_{50}a\ (1 + [\text{antagonist}]/\text{antagonist } K_b)$$

where $EC_{50}a$ is the agonist EC_{50} in the absence of antagonist and $EC_{50}b$ is the agonist EC_{50} in the presence of antagonist.

For antagonist concentration responses the following equation is used (14):

$$K_b = IC_{50}/\ (2 + ([\text{agonist}]/\text{agonist } EC_{50})^n)^{1/n} - 1$$

where n is the slope of the agonist curve.

In antagonist concentration response experiments it is desirable to determine the agonist EC_{50} in each experiment along with the IC_{50} for the antagonist. Figure 8 below illustrates the use of both methods for measuring antagonist K_b values. By measuring multiple shifts in agonist concentration response curves at increasing concentrations of antagonist it is possible to calculate via Schild analysis the PA2 of the antagonist and to ascertain whether the antagonist is competitive (15,16).

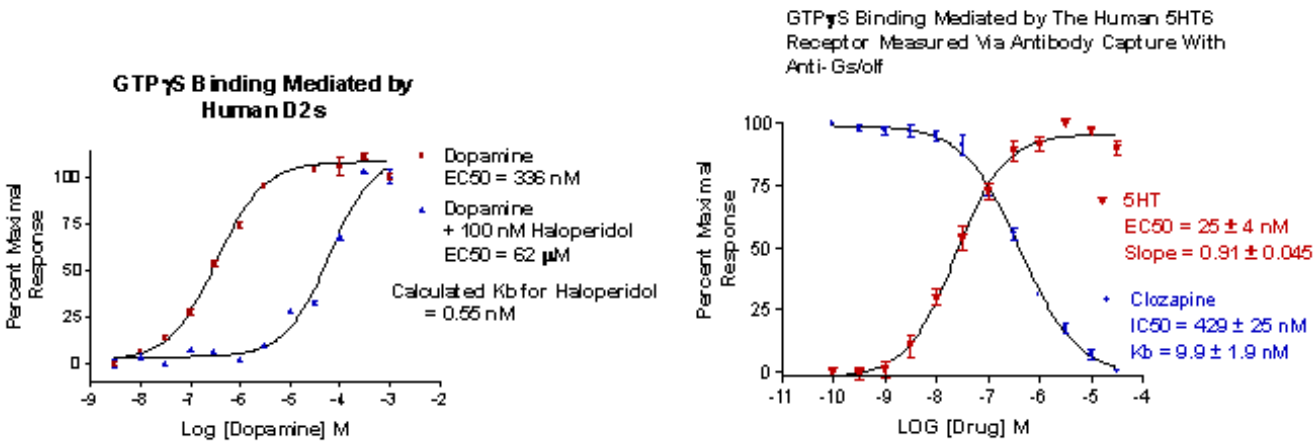

Figure 8. Examples of determining antagonist K_b values in GTPγS assays with a single antagonist concentration

Filtration Assays

Filtration whole membrane assays may be used for GTPγS binding using the same methods employed for radioligand binding. The potential advantages of filtration assays are the lack of non-proximity effects which are present in SPA assays and the ability to use higher concentrations of GTPγ^{35}S. Such advantages are not usually worth sacrificing the convenience of homogeneous SPA assays. There are many examples of the use of filtration for GTPγS binding in the literature (7,8,10,17). As for WGA whole membrane binding, filtration assays are mostly limited to Gi/o coupled receptors since they cannot employ antibody capture.

Non-Radiometric GTPγS Assays

Perkin Elmer Life Sciences has developed an assay based on the use of a europium-GTP complex (11). This is a fluorescent whole membrane assay which does not require radioactivity, exhibits no non-proximity effect, and produces reliable data (Figure 9). Although the Eu-GTPγS assay has traditionally employed a filtration step using 96 well filter plates (11), a single tube assay has been reported employing quenching resonance energy transfer (18). Eu-GTPγS assays have not been configured to provide measurement of binding to specific G-proteins. The Eu-GTPγS assay has been formatted to provide high throughput (19).

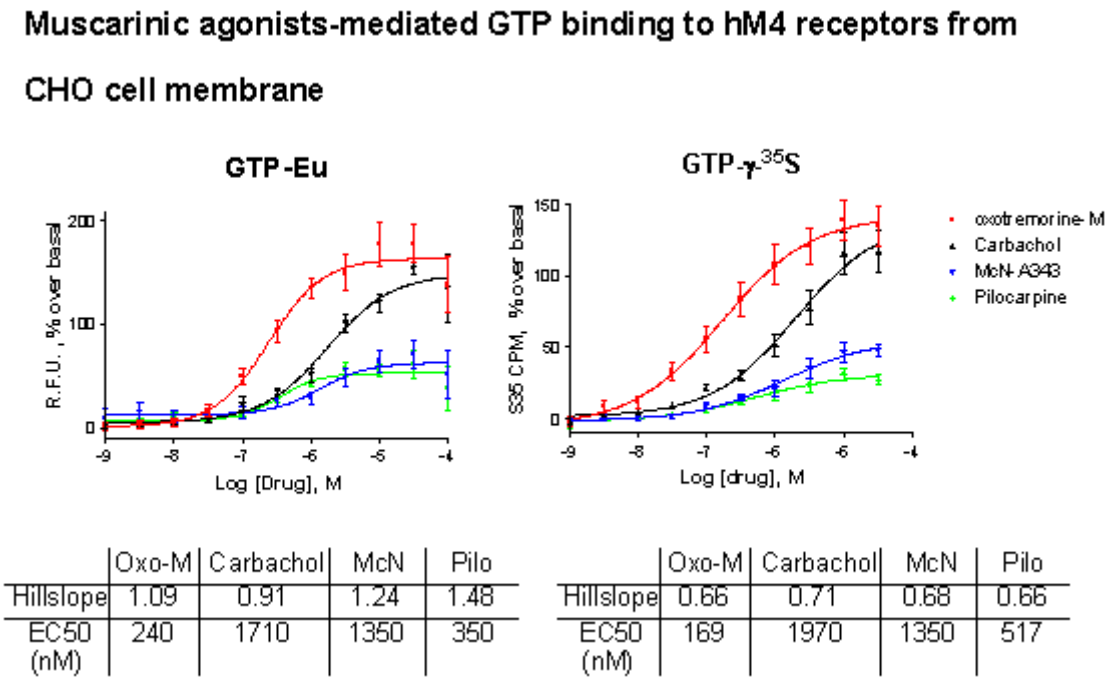

	Oxo-M	Carbachol	McN	Pilo
Hillslope	1.09	0.91	1.24	1.48
EC50 (nM)	240	1710	1350	350

	Oxo-M	Carbachol	McN	Pilo
Hillslope	0.66	0.71	0.68	0.66
EC50 (nM)	169	1970	1350	517

Figure 9: Side by side comparison of GTP-Eu vs. GTPγ^{35}S assay methods.

References

1. DeLapp N, McKinzie J, Sawyer BD, Vandergriff A, Falcone J, McClure D, Felder CC. Determination of [^{35}S] guanosine-5'-O-(3-thio)triphosphate binding mediated by cholinergic muscarinic receptors in membranes from Chinese hamster ovary cells and rat striatum using an anti-G-protein scintillation proximity assay. J. Pharmacol. Exp. Ther. 1999;289:946–955. PubMed PMID: 10215674.
2. Bymaster FP, Falcone J, Bauzon D, Kennedy JS, Schenk K, DeLapp NW, Cohen ML. Potent antagonism of 5HT$_3$ and 5HT$_6$ receptors by olanzapine. Eur. J. Pharmacol. 2001;430:341–349. PubMed PMID: 11711053.
3. Cussac D, Pasteau V, Millan MJ. Characterization of Gs activation by dopamine D$_1$ receptors using an antibody capture assay: antagonist properties of clozapine. Eur. J. Pharmacol. 2004;485:111–117. PubMed PMID: 14757130.
4. DeLapp NW. The antibody capture [^{35}S] GTPγS scintillation proximity assay: a powerful emerging technique for analysis of GPCR pharmacology. Trends Pharmacol. Sci. 2004;25:400–401. PubMed PMID: 15276707.
5. Porter AC, Bymaster FP, DeLapp NW, Yamada M, Wess J, Hamilton SE, Nathanson N, Felder CC. M1 muscarinic receptor signaling in mouse hippocampus and cortex. Brain Res. 2002;944:82–89. PubMed PMID: 12106668.
6. Salah-Uddin H, Thomas DR, Davies CH, Hagan JJ, Wood MD, Watson JM, Challiss RAJ. Pharmacological Assessment of M1 Muscarinic Acetylcholine Receptor-Gq/11 Protein Coupling in Membranes Prepared from *Post Mortem* Human Brain Tissue. J. Pharmacol. Exp. Ther. 2008;325:869–874. PubMed PMID: 18322150.
7. Lazareno S, Birdsall NJM. Pharmacological characterization of acetylcholine-stimulated [^{35}S]-GTPγS binding mediated by human muscarinic m1-m4 receptors: antagonist studies. Br. J. Pharmacol. 1993;109:1120–1127. PubMed PMID: 8401923.
8. Hilf G, Gierschik P, Jakobs KH. Muscarinic acetylcholine receptor-stimulated binding of guanosine 5'-O-(3-thiotriphosphate) to guanine-nucleotide-binding proteins in cardiac membranes. Eur. J. Biochem. 1989;186:725–731. PubMed PMID: 2514098.

9. Milligan G. Principles: Extending the utility of [^{35}S]GTPγS binding assays. Trends Pharmacol. Sci. 2003;24:87–90. PubMed PMID: 12559773.
10. Gupta SK, Pillarisetti K, Thomas RA, Aiyar N. Pharmacological evidence for complex and multiple site interaction of CXCR4 with SDF-1α: Implications for development of selective CXCR4 antagonists. Immunology Letters. 2001;78:29–34. PubMed PMID: 11470148.
11. Strange PG. Use of the GTPγS ([^{35}S] GTPγS and Eu-GTPγS) binding assay for analysis of ligand potency and efficacy at G protein-coupled receptors. Br. J. Pharmacol. 2010;161:1238–1249. PubMed PMID: 20662841.
12. Ferrer M, Kolodin G, Zuck P, Peltier R, Berry K, Mandala SM, Rosen H, Ota H, Ozaki S, Inglese J, Strulovici B. A Fully Automated [^{35}S]GTPγS Scintillation Proximity Assay for the High-Throughput Screening of Gi-Linked G Protein-Coupled Receptors. Assay Drug Dev. Technol. 2003;1:261–273. PubMed PMID: 15090191.
13. Johnson EN, Shi X, Cassaday J, Ferrer M, Strulovici B, Kunapuli P. A. 1536-well [^{35}S]GTPγS scintillation proximity binding assay for ultra-high-throughput screening of an orphan Gαi-coupled GPCR. Assay Drug Dev. Technol. 2008;6:327–337. PubMed PMID: 18537464.
14. Leff P, Dougall IG. Further concerns over Cheng-Prusoff analysis. Trends Pharmacol. Sci. 1993;14:110–112. PubMed PMID: 8516953.
15. Christopoulos A, Kenakin T. G. Protein-Coupled Receptor Allosterism and Complexing. Pharmacol. Rev. 2002;54:323–374. PubMed PMID: 12037145.
16. Olianas MC, Onali P. Stimulation of Guanosine 5'-O-(3-[^{35}S] Thiotriphosphate) Binding by Cholinergic Muscarinic Receptors in Membranes of Rat Olfactory Bulb. J. Neurochem. 1996;67:2549–2556. PubMed PMID: 8931489.
17. Alper RH, Nelson DL. Characterization of 5-HT1A receptor-mediated [^{35}S]GTPγS binding in rat hippocampal membranes. Eur. J. Pharmacol. 1998;343:303–312. PubMed PMID: 9570480.
18. Rozwandowicz-Jansen A, Laurila J, Martikkala E, Frang H, Hemmila I, Scheinin M, Pekka H, Harma H. Homogeneous GTP Binding Assay Employing QRET Technology. J. Biomol. Screen. 2010;15:261–267. PubMed PMID: 20103692.
19. Labrecque J, Wong RS, Fricker SP. A time-resolved fluorescent lanthanide (Eu)-GTP binding assay for chemokine receptors as targets in drug discovery. Methods Mol. Biol. 2009;552:153–169. PubMed PMID: 19513648.

Additional References

1. Cussac D, Newman-Tancredi A, Duqueyroix D, Pasteau V, Millan MJ. Differential activation of Gq/11 and Gi3 proteins at 5-HT_{2C} receptors revealed by antibody capture assays: influence of receptor reserve and relationship to agonist-directed trafficking. Mol. Pharmacol. 2002;62:578–58. PubMed PMID: 12181434.
2. Newman-Tancredi A, Cussac D, Marini L, Tousard M, Millan MJ. h5-$HT1_B$ receptor-mediated constitutive Gαi3-protein activation in stably transfected Chinese hamster ovary cells: an antibody capture assay reveals protean efficacy of 5HT. Br. J. Pharmacol. 2003;138:1077–1084. PubMed PMID: 12684263.
3. Mannoury la Cour C, Vidal S, Pasteau V, Cussac D, Millan MJ. Dopamine D1 receptor coupling to Gs/olf and Gq in rat striatum and cortex: A scintillation Proximity assay (SPA)/antibody-capture characterization of benzazepine agonists. Neuropharmacology. 2007;52:1003–1014. PubMed PMID: 17178132.
4. Dupuis DS, Mannoury la Cour C, Chaput C, Verriele L, Lavielle G, Millan MJ. Actions of novel agonists, antagonists and antipsychotic agents at recombinant rat 5-HT_6 receptors: A comparative study of coupling to GαS. Eur. J. Pharmacol. 2008;588:170–177. PubMed PMID: 18511034.
5. Eglen RM, Reisine T. New Insights into GPCR Function: Implications for HTS. In: G-Protein Coupled Receptors in Drug Discovery, series. Methods in Molecular Biology. 2009;551:1–13. PubMed PMID: 19521862.

Histone Acetyltransferase Assays in Drug and Chemical Probe Discovery

Sanket Gadhia, Ph.D.,[1] Jonathan H. Shrimp, Ph.D.,[2] Jordan L. Meier, Ph.D.,[2] James E. McGee, Ph.D.,[3] and Jayme L. Dahlin, M.D., Ph.D.[4]

Created: July 26, 2017; Updated: July 1, 2018.

Abstract

Histone acetyltransferases (HATs) are a class of epigenetic enzymes involved in critical cellular processes like nucleosome assembly, DNA damage repair, and transcriptional regulation. HATs are implicated in many human pathologies including cancers. This chapter describes essential experimental considerations for performing high-throughput screening and follow-up assays, and offers practical strategies for assay optimization and validation. Illustrative walkthroughs for several HAT assay formats are provided. This content should be useful for those performing HTS assays, orthogonal assays, and counter-screens involving HATs in the context of drug discovery, chemical biology, and molecular pharmacology.

Flowchart

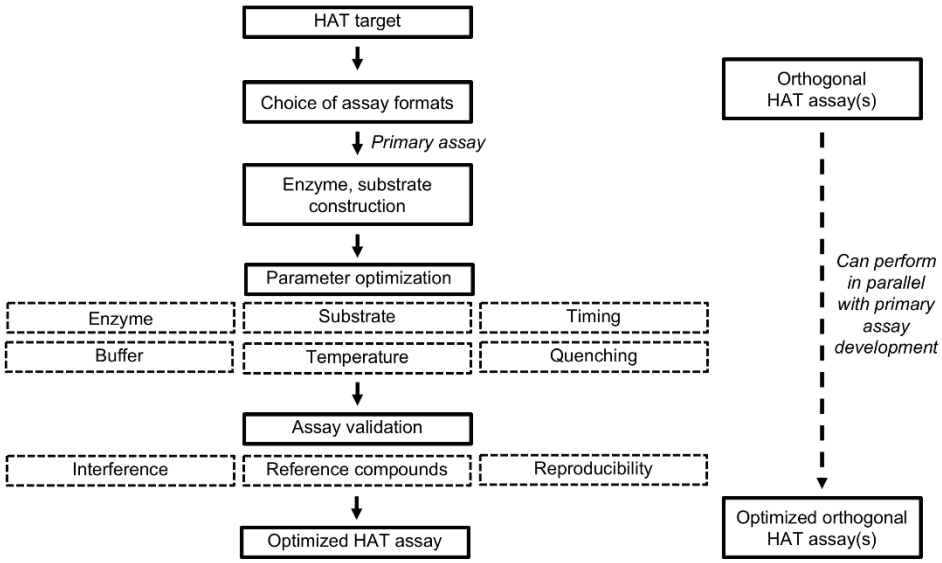

Abbreviations

Acetyl-CoA	acetyl coenzyme A
BSA	bovine serum albumin
CoA	coenzyme A
CPM	*N*-[4-(7-diethylamino-4-methylcoumarin-3-yl)phenyl]maleimide

Author Affiliations: 1 Division of Pre-Clinical Innovation, National Center for Advancing Translational Sciences, National Institutes of Health, Rockville, MD, USA. 2 Chemical Biology Laboratory, Center for Cancer Research, National Cancer Institute, National Institutes of Health, Frederick, MD, USA. 3 Quantitative Biology, Eli Lilly and Company, Indianapolis, IN, USA. 4 Department of Pathology, Brigham and Women's Hospital, Boston, MA, USA; Email: jdahlin@bwh.harvard.edu.

Corresponding author.

Table continued from previous page.

DMSO	dimethyl sulfoxide
DTT	dithiothreitol
EDTA	ethylenediaminetetraacetic acid
ELISA	enzyme-linked immunosorbent assay
FRET	fluorescent/Förster resonance energy transfer
HAT	histone acetyltransferase
HDAC	histone deacetylase
HEPES	hydroxyethyl piperazineethanesulfonic acid
HTS	high-throughput screening
IS	internal standard
KAT	lysine acetyltransferase
LoD	limits of detection
LoQ	limits of quantitation
MS	mass spectrometry
MSR	minimum significant ratio
NEM	N-ethylmaleimide
PAINS	pan assay interference compounds
PTM	post-translational modification
SIRT	sirtuin
SPE	solid-phase extraction
TCEP	*tris*(2-carboxyethyl)phosphine

Introduction and Background

Introduction

HATs are a class of epigenetic enzymes involved in many critical cellular processes. Aberrancies in HAT function have been implicated in human disease. Modulators of HAT activity may therefore be highly useful for chemical probes of epigenetic systems, or potential therapeutics in HAT-related pathologies.

This chapter describes essential experimental factors needed to develop, optimize, and validate assays for the purpose of assessing compound modulation of HAT activity. Several example protocols of representative HAT assays are provided. This information should be useful for novices as well as more seasoned researchers. While this chapter specifically focuses on HAT assays, the general methodologies should also be informative to a variety of epigenetic systems (e.g., methyltransferases, deacetylases) as well as non-epigenetic bi-substrate enzymatic systems.

Note: This chapter emphasizes biochemical HAT assays. Cell-based HAT assays are briefly discussed. However, many of the same principles discussed with respect to biochemical HAT assays should apply to cell-based HAT assays.

Background

Epigenetics is defined as heritable changes in gene expression that occur without altering the underlying genetic sequence. This process is regulated in part by a series of epigenetic enzymes acting *via* post-translational modifications (PTM) such as histone acetylation, methylation, phosphorylation, and ubiquitylation. Histone PTMs are regulated by histone reader, writer, and eraser enzymes.

Histone acetylation is critical for regulation of gene transcription, nucleosome assembly, and DNA repair (1,2). HATs have been implicated in a variety of human pathologies, including cancers (3). Consequently, there is great interest in developing potent and specific small-molecule modulators of HAT activity, either as chemical probes or potential therapeutics (4,5).

Human HATs can be divided into several large families: MYST (TIP60, MOZ/MYST3, MORF/MYST4, HBO1/MYST2, MOF/MYST1), p300/CBP (P300, CBP), and GNAT (GCN5, PCAF, ELP3). In addition, there are also transcription factors with HAT activity and nuclear receptor co-activators. HATs are also present in other eukaryotic species, including *Drosophila* and fungi, the latter of which includes opportunistic human pathogens such as *Aspergillus*, *Candida*, and *Pneumocystis*.

HATs catalyze the transfer of an acetyl moiety from acetyl-CoA to lysine side chains present on histone proteins (**Figure 1**). Catalysis can occur through a random-order ternary complex mechanism, a compulsory-order ternary complex, or a ping-pong mechanism. The final product neutralizes the positively-charged lysine ε-amino group and reduces steric bulk, which effectively "loosens" the interaction between histone proteins and negatively-charged DNA, leading to less compacted chromatin and increased transcription. Acetylated histone residues can be specifically recognized by histone reader domains called bromodomains. The biological counterpart to HATs are histone deacetylases (HDACs) and sirtuins (SIRTs), epigenetic enzymes which catalyze the removal of the acetyl moiety from acetylated histone lysines. HATs are complex bi-substrate systems, utilizing both an acetyl donor (acetyl-CoA) and an acetyl acceptor (histone protein).

HATs acetylate many histone lysine residues. (6) These occur on H2A (K5), H2B (K12, K15), H3 (K9, K14, K18, K36, K56), and H4 (K5, K8, K12, K16). Often a specific HAT can acetylate multiple histone lysine residues. HAT activity and substrate specificity can be regulated by multiple factors, including autoacetylation and chaperone proteins (7-9). Note that certain HATs can also acetylate non-histone substrates, and can also be referred more broadly as lysine acetyltransferases (KATs).

Introduction to Common HAT Assays

Multiple biochemical HAT assays have been described (**Table 1**). These assays measure HAT activity by detecting either the acetylated histone-based product ("direct") or the free CoA product ("indirect").

So-called indirect methods utilize fluorescent thiol-scavenging probes or enzyme-coupling reactions. In general, these assays are inexpensive and straightforward to establish, but are highly susceptible to compound-mediated assay interference. This can necessitate multiple counter-screens and orthogonal assays to rule-out interference and confirm true compound activity. While they are usually highly amenable to HTS, the time and resources required to perform interference counter-screens and orthogonal studies to triage assay artifacts and poorly tractable chemical matter has the potential to offset the initial up-front benefits of indirect assays.

Direct HAT assays can measure the acetylated histone-based product by one of multiple technologies. These include radiolabels (e.g., filter-binding, scintillation proximity), mass spectrometry (MS), microfluidic mobility, and antibody-based techniques such as traditional enzyme-linked immunosorbent assay (ELISA), Alpha-based technologies (e.g., AlphaScreen, AlphaLISA), and FRET (including time-resolved FRET). The advantage of direct assays is that they measure the actual protein product from the HAT reaction. Direct assays can require more technical expertise, specific instrumentation, and more customized and expensive reagents compared to

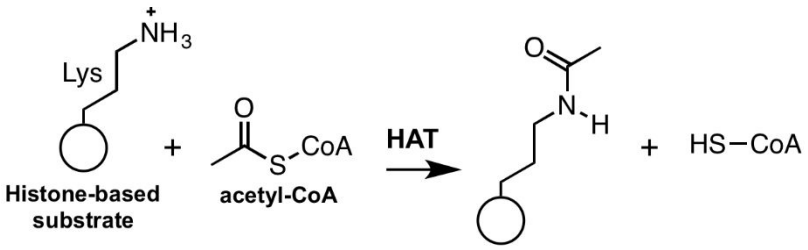

Figure 1. Schematic of HAT reaction. HATs catalyze the transfer of an acetyl moiety from acetyl-CoA to a histone substrate. The resulting products are free coenzyme A ("CoA-SH" or "CoA") and an acetylated histone lysine residue.

the most common indirect methods. Furthermore, even direct HAT assays are susceptible to compound-mediated assay interference, and should be accompanied with appropriate readout interference counter-screens and orthogonal assays.

Each HAT assay technology has characteristic advantages and disadvantages (**Table 1**). When selecting an assay type for either a primary or orthogonal assay, one should consider multiple (and often competing) factors, including but not limited to: available instrumentation, resources, expertise, project timelines, the nature of the HAT system being assayed, possible technology-related interferences, and the number and type of test compounds.

The indirect assays and most of the direct assays can be suitable for HTS (**Table 1**), while the direct and indirect assays can all be adapted for orthogonal assays. Suggestions for specific primary assay-orthogonal assay pairings are discussed in the subsequent section "Use of Orthogonal Assays/Common Interferences".

Table 1. Common HAT assay formats. Each HAT assay format has advantages and disadvantages, including susceptibilities to technology-related compound-mediated assay interferences.

Assay technology	Assay principle	Advantages	Disadvantages	Compound-mediated readout interferences	General suitability for HTS	Example references
Fluorometric (thiol-scavenging probe)	Free CoA forms fluorescent adduct with probe (indirect)	-Inexpensive -Easy to set-up -High-throughput -Label-free	-Significant potential for compound-mediated interference -Enrichment of thiol-reactive compounds -Can require large concentrations of product formation for detection	-Light-based interferences (absorbance, auto-fluorescence, quenching, light scattering) -Thiol-scavenging	+	(10-14)
Enzyme-coupling	Second enzyme requires CoA, secondary product measured (indirect)	-Inexpensive -Easy to set-up -High-throughput -Adaptable to continuous readout -Label-free	-Significant potential for compound-mediated interference -Enrichment of thiol-reactive compounds -Can require large concentrations of product formation for adequate signal	-Secondary enzyme system modulation -Light-based interferences (absorbance, auto-fluorescence, quenching, light scattering) -Thiol-scavenging	+	(15)

Table 1. continued from previous page.

Assay technology	Assay principle	Advantages	Disadvantages	Compound-mediated readout interferences	General suitability for HTS	Example references
Radiolabeled substrate (filter-binding)	Radiolabeled acetate (*via* acetyl-CoA) incorporated onto histone product (direct)	-High S:N -Few compound-mediated interferences -Label-free	-Cost -Radiation -Lower-throughput in most settings	-Scintillation quenching	–	(10,16-18)
Alpha technology (AlphaScreen, AlphaLISA)	Amplified luminescent proximity (direct)	-High S:N -Customizable -No radiation -Amenable to miniaturization -Homogenous format	-Cost -Specialized instrumentation -Dependent on antibody quality -Light sensitivity	-Singlet oxygen quenching -Light-based interferences (absorbance, quenching, auto-fluorescence, light-scattering) -Capture reagent disruption (e.g., disruption of antibody/tag interaction)	+	(19)
FRET	Fluorescent/ Förster resonance energy transfer (direct)	-Customizable -No radiation -Usually cheaper than Alpha -Can enhance with time-resolved FRET (TR-FRET) -Homogenous format	Dependent on antibody quality	-Light-based interferences (absorbance, quenching, auto-fluorescence, light-scattering) -Capture reagent disruption (e.g., disruption of antibody/tag interaction)	+	(20)
Fluidic mobility	Electrophoretic separation of histone-based products (direct)	-Monitor multiply-acetylated substrates -No radiation -Adaptable to continuous readouts	-Highly specialized instrumentation -Highly-charged substrates challenging -Large substrates challenging		+	(21,22)
Mass spectrometry	Histone-based products ionized and *m/z* measured (direct)	-Highly sensitive (less product formation required) -Label-free -Monitor multiply-acetylated products -No radiation	-Highly specialized instrumentation -Throughput	-Ion suppression -Compound-analyte adducts	+	(23)
Traditional antibody (ELISA, Western)	Antibody binds to acetylated histone product (direct)	-Straightforward to establish -Highly sensitive -No radiation	-Dependent on antibody quality -Lower-throughput (heterogeneous format)	-Antibody interference -Quenching of antibody reporter -Lower dynamic ranges	–	(10,11,17)

Table 1. continued from previous page.

Assay technology	Assay principle	Advantages	Disadvantages	Compound-mediated readout interferences	General suitability for HTS	Example references
Scintillation	Radiolabeled product scintillates in proximity to capture matrix (direct)	-High S:N -Homogenous format	-Radiation -Specialized instrumentation	Scintillation quenching (24,25)	+	(20,26-28)

Section Summary

HATs are epigenetic enzymes involved in critical cellular processes, and have been linked to human disease. There are multiple robust, orthogonal assay platforms assessing modulation of HAT activity by test compounds.

General Considerations for HAT Assays

Introduction

Regardless of technology choice, HAT assays require optimization of many experimental parameters. This section describes essential experimental considerations for performing HAT assays, including optimization of enzyme and substrates, other reaction components, reaction timing, and reaction quenching.

Enzyme/Substrate Source

HATs and histone-based substrates can be purchased commercially or produced in-house. Commercially-sourced HATs and histones have the advantage of being readily available, but often they are prohibitively expensive in amounts needed for an HTS. Proteins produced in-house can allow for greater customization and control over the purification process, but production can be time-consuming, and can be difficult to achieve at large scales and acceptable purities.

Commercially-sourced enzymes and substrates are often "one size fits all" entities, and may not have the specific features optimal for a particular HAT assay. Users may need to customize: (a) a specific affinity or purification tag, (b) the construct of the HAT enzyme or histone (e.g., truncations), (c) the introduction of PTMs such as fluorophores, and (d) expression and purification conditions to optimize protein folding and stability. For some applications, full-length HAT or histone substrate may be necessary to capture the essential features of the native system being probed by the HTS. In other cases, users may only need the catalytic HAT domain or specific histone peptides. In some cases, supposed non-catalytic domains may have profound effects on catalysis, system stability, and substrate specificity.

Depending on the research question and HTS method, users may need to produce their own HAT or histone substrate (29). While the details of producing recombinant enzymes are beyond the scope of this chapter, we recommend first consulting any original literature on the specific HAT or histone substrate to be assayed for details about potential production and purification strategies.

The identity and purity of HAT enzymes and protein substrates should be rigorously validated, especially when performing experiments on the HTS scale. For details, refer to Validating Identity, Mass Purity and Enzymatic Purity of Enzyme Preparations.

Acetyl-CoA

There are several important considerations with respect to the acetyl-CoA substrate:

- Acetyl-CoA is often sold in salt/hydrate preparations with variable stoichiometry. Most commercial forms are sold as a sodium or lithium salt.
- To ensure accurate K_M determination and to enhance assay precision, the concentration of acetyl-CoA should be determined spectrophotometrically. For example, acetyl-CoA (tri-lithium salt) can be measured by monitoring light absorbance at 260 nm (ε = 16000 M^{-1} cm^{-1} in H_2O) or at 232 nm (ε = 8700 M^{-1} cm^{-1} in H_2O) (30).
- In solid form, acetyl-CoA should be stored in desiccated conditions and in -20°C.
- In solution, acetyl-CoA stocks should be stored at -20°C. Acetyl-CoA is unstable in alkaline conditions and in highly acidic conditions. A recommended storage buffer is 50 mM sodium acetate, pH 5.0. Minimize freeze-thaw cycles.
- Commercial acetyl-CoA can contain minor amounts of free CoA. This may interfere with some types of HAT assay readouts or inhibit certain HATs by product inhibition (22). Free CoA can be treated with acetic anhydride to mitigate this effect (13).

Histone-Based Substrates

Many choices of substrates are available for HAT assays (**Table 2**). These include (in order of complexity): histone peptides, full-length histones, histone dimers, core histones, histone-chaperone complexes, and nucleosomes.

For any given HAT assay, the optimal histone-based substrate is multifactorial. One factor is the nature of the specific HAT system being assayed, as HAT specificity and catalytic efficiency can depend on whether the histone is presented in monomeric or multimeric form(s), or whether histone chaperones are present. Users should also consider the physiologic context of the HAT target. As with the choice of enzyme constructs, using full-length substrates and/or include chaperone proteins can potentially better approximate physiological catalysis, HAT stability, and substrate specificity. Generally speaking, it is best to approximate physiologic conditions in any given assay, but such considerations must be weighed against practical and competing factors such as compatibility with assay technology, overall system complexity, and reagent costs.

In general, histone peptides are practical and relatively easy to customize (with respect to length, sequence, labels, affinity tags), and can reduce system complexity. Depending on the particular epigenetic system, histone peptides can have a higher K_M than their full-length counterparts (31). Furthermore, a potential downside to peptide substrates is that they may not sufficiently model the physiologic context of a given HAT system.

Full-length histone products may therefore be required in this regard. Potential downsides to full-length protein use are their more challenging production procedures and the increased assay complexity due to many HATs that can acetylate multiple lysine residues. Fortunately, full-length histone monomers and multimers can be produced using recombinant technology in large scales with sufficient technique. For additional details regarding histone product production, we refer the reader to several published protocols (32-35). For full-length histone products, users should pay particular attention to protein precipitation at higher concentrations. This potential problem can often be mitigated by carefully optimizing pH and salt conditions.

Users should also consider the species of the histone-based substrate. While histones are highly conserved species in eukaryotes, subtle inter-species sequence variations may have dramatic consequences. For some applications, it may be acceptable to use histones derived from *Drosophila*, yeast, chicken, or calf thymus. In other cases, human-based histones may be required.

Table 2. Common histone-based substrates in HAT assays. Each substrate type has advantages and disadvantages. The optimal substrate will depend on the nature of a given HAT system, the choice of assay, and other factors.

Substrate type	Potential advantages	Potential disadvantages
Histone peptide	-Soluble -Customizable -Can simplify complex multi-substrate histones	-Non-native substrate -Potentially higher K_M
Full-length histone protein	Potential physiologic substrate	-Precipitation risk -PTM heterogeneity (e.g., non-recombinant source)
Histone dimer/multimer/core	Potential physiologic substrate	-Precipitation risk -Increased assay complexity -PTM heterogeneity (e.g., non-recombinant source)
Histone-chaperone complex	Potential physiologic substrate	-More laborious to prepare in bulk quantities -Precipitation risk -Increased assay complexity -PTM heterogeneity (e.g., non-recombinant source)
Nucleosome	Potential physiologic substrate	-More laborious to prepare in bulk quantities -Precipitation risk -Increased assay complexity -PTM heterogeneity

Reaction Buffer and Additives

The essential components of a biochemical HAT reaction include buffer, salts, chelating agents, reducing agents, detergents, and carrier proteins.

- Buffer
  - Buffers are used to maintain the reaction solution within a fixed pH range optimal for HAT activity.
  - Common buffering agents include Tris HCl and HEPES, typically at 50-100 mM final concentrations.
  - Most HAT reactions are performed in slightly alkaline conditions (usually pH 7.5-8.0).
  - A common buffering agent is 50 mM Tris, pH 8.0.
- Salts
  - Most biochemical HAT assays utilize NaCl, though KCl can often be used in its place.
  - The most common ionic strength is 50-100 mM NaCl.
  - Full-length histone substrates (± chaperones) can be highly sensitive to salt concentrations, especially at higher concentrations.
- Chelating agents
  - Chelating agents can be added to prevent metal-catalyzed proteolysis and oxidation.
  - The most common chelating agent used in HAT reactions is ethylenediaminetetraacetic acid (EDTA), often at 0.1 mM final concentrations.
  - Be aware that certain HAT systems may show metal-dependent activity. Therefore, it is reasonable to assess the performance of a HAT assay in the presence and absence of chelating agents like EDTA, as well as using similar methods to investigate compounds for chelation-related bioactivity. (36)
- Reducing agents
  - Reducing agents are added to prevent oxidation of protein side chains, most notably cysteine thiols. Reducing agents can also mitigate the effect of thiol-reactive screening compounds by acting as scavenging reagents (17).

    - Strong reducing agents have the potential to fuel redox-cycling, a phenomenon in which compounds produce H_2O_2 *in situ* (37,38).
    - Examples of commonly used reducing agents include dithiothreitol (DTT), β-mercaptoethanol (BME), and *tris*(2-carboxyethyl)phosphine (TCEP).
    - The most common reducing agent is DTT, often at 1-5 mM final concentrations.
    - Note that DTT is unstable in aqueous conditions. Freshly prepare solutions containing DTT, and keep on ice.
- Detergents
    - Detergents are added for two reasons: (a) to prevent nonspecific protein adsorption to container walls, and (b) to mitigate aggregation formation by test compounds, which can nonspecifically modulate HAT activity.
    - Examples detergents include Triton X-100, Tween 20, Pleuronic F-68, and Brij 35.
    - The authors have had good experience with 0.01% Triton X-100 (v/v). Triton X-100 can produce H_2O_2 *in situ*, which should be considered in systems highly sensitive to oxidation. This effect can be mitigated by preparing fresh detergent-containing buffers.
    - Many detergents are highly viscous. Handling can be enhanced by preparing as 10% (v/v) solutions and pipetting slowly. Allow time (often several hours with gentle mixing) for detergents to fully dissolve in water.
- Carrier proteins
    - Carrier proteins are included in many biochemical reactions to enhance enzymatic stability, as many enzymes are unstable in dilute concentrations. Carrier proteins can prevent nonspecific adsorption of assay proteins to container walls.
    - Carrier proteins (also known as "decoy proteins" in the context of preventing aggregation) can also mitigate compound aggregation (39), and can also serve as low-level thiol-scavenging reagents to mitigate the effect of thiol-reactive screening compounds.
    - The most common carrier protein used in biochemical HAT assays is bovine serum albumin (BSA). Common concentrations of BSA range from 5 to 100 μg/mL.
- Protease, HDAC inhibitors
    - Protease inhibitors are typically added to certain biochemical solutions to prevent proteolysis. Examples include phenylmethylsulfonyl fluoride (“PMSF”) and 4-(2-aminoethyl)benzenesulfonyl fluoride (“Pefabloc”). Commercial cocktails are also widely available.
    - While useful in protein purification, protease inhibitors are generally not required for most biochemical HAT assay applications.
    - Inhibitors are often used at relatively high concentrations (high micromolar/low millimolar) and have the potential to cause assay interference.
    - Consider adding protease inhibitors if there is evidence of significant protein degradation. Extended incubation or reaction times may also warrant trials of protease inhibitors.
    - Nonspecific HDAC inhibitors such as sodium butyrate are occasionally added to prevent deacylatation. They are typically used at low millimolar concentrations. In purified systems, such inhibitors are probably unnecessary. When analyzing reactions containing cellular extracts, appropriate control experiments should be performed to determine whether HDAC inhibitors are necessary and whether they interfere with HAT activity or assay readout.
- Example reaction buffer
    - The following is a useful initial reaction buffer: 50 mM Tris, pH 8.0, 50 mM NaCl, 0.1 mM EDTA, 1 mM DTT, 0.01% Triton X-100 (v/v), 50 μg/mL BSA.
    - It is often useful to prepare reaction buffers in concentrated form. Consider making a 5X solution (250 mM Tris, pH 8.0, 250 mM NaCl, 0.5 mM EDTA, 5 mM DTT, 0.05% Triton X-100 (v/v), 250 μg/mL BSA).

- Consider performing simple titration experiments with each reagent to determine optimal reaction conditions and components.

Timing/Enzyme Concentration

Assay timing and enzyme concentration can usually be optimized in one experiment. Monitor HAT reactions over time at multiple enzyme concentrations at multiple time points (**Figure 2**). Optimal timing in HAT assays is during the linear reaction phase, at times feasible for the desired throughput, instrumentation, and system stability, among other factors. Sampling too soon after reaction initiation (e.g., seconds to minutes) may be impractical in many HTS settings, and may lead to imprecise results if the reaction proceeds quickly. Later sampling times are more susceptible to system stability effects (e.g., enzyme instability). For most compounds, enzyme modulation is best apparent at earlier reaction times. For inhibitors, the continued product accumulation by uninhibited enzyme can eventually confound the final readout (40). Reaction times can range from approximately five minutes to several hours, depending on the nature of the HAT system and assay specifics. Linearity can change with subtle perturbations in reaction conditions, so it is advised to periodically reassess linearity when changing assay conditions.

Optimal enzyme concentration should produce a readout intensity sufficient for robust sampling above background. Too much enzyme, and the reaction can be completed too quickly to practically measure in the linear range. Too little enzyme, and the readout is not strong enough to reliably measure relative to background signal. For reference, high picomolar to lower nanomolar concentrations of HAT enzyme are most often reported in the literature.

For additional details, refer to Basics of Enzymatic Assays for HTS.

Substrate Concentrations

The choice of substrate concentrations is an important consideration when screening for compound modulators of enzymatic activity. The choice of substrate concentrations can favor the selection of various modes of compound modulation. For instance, screening at high substrate concentrations relative to K_M will disfavor substrate-competitive inhibition, as competitive inhibitors will have more competition by the natural substrate for target binding to the substrate site. Sometimes, screening conditions are chosen to enrich certain mechanisms of target modulation. Most often, screens are performed around the K_M (so-called "balanced screening conditions") so as not to favor any particular mechanism. In either case, the K_M for each HAT substrate must be experimentally determined under the final assay conditions.

The bi-substrate nature of HATs requires determining the K_M of each substrate: acetyl-CoA and the histone-based substrate (**Figure 3**). While holding the concentration of acetyl-CoA constant and in excess, the reaction rates can be determined with titrations of histone-based substrate, and plotted to determine the K_M of the histone-based substrate. Next, while holding the concentration of histone-based substrate constant and in excess, the reaction rates can be determined with titrations of acetyl-CoA, and plotted to determine the K_M of acetyl-CoA.

A few technical reminders on K_M determination:

- Reaction rates should be based on initial reaction velocity (linear range).
- A general guideline for excess substrate is > 100:1 substrate:enzyme.
- A guideline for substrate titrations is between 0.2-5.0 K_M. Use at least eight substrate concentrations to determine K_M.
- Examine literature for reports on K_M to help guide initial conditions.

For additional details on optimizing substrate concentrations, refer to Basics of Enzymatic Assays for HTS.

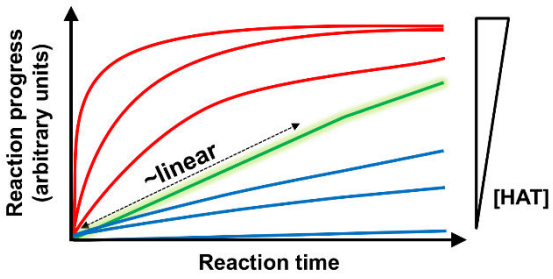

Figure 2. Optimization of enzyme concentration and timing in HAT assays. Optimal enzyme concentration and assay timing can be determined by a straightforward time-course experiment combined with enzyme titrations. In an ideal assay, HAT activity should be measured during the linear phase of the reaction. In this cartoon, the reaction progress curves in blue, performed with lower enzyme concentrations, are sufficiently linear but signal strength would be insufficient. The red progress curves, performed with higher enzyme concentrations, produce sufficient amounts of product but linearity is relatively transient. In this example, the green curve denotes an optimal enzyme concentration, as it is linear for sufficient duration to be assayed, and has a sufficient amount of product to measure. Assay timing should also consider other factors, including system stability, instrumentation, and workflow.

Determining balanced screening conditions for bi-substrate reactions can be complex, especially in cases with significant substrate cooperativity (i.e., the concentration of one substrate significantly alters the binding behavior of another substrate). Cooperativity can be assessed by determining the K_M for each substrate at several different fixed concentrations of its partner substrate. In cases where significant cooperativity is suspected, additional mechanistic details about the HAT system should be characterized. For this undertaking, and for subsequently selecting optimal screening conditions, we recommend collaborating with an experienced enzymologist (40).

Quenching

For end-point assays, the HAT reaction should be quenched. This prevents additional substrate consumption and guards against time-dependent enzyme modulation. This is especially important in HTS applications, as there can be a significant time lag between reading the initial and subsequent microplates. Quenching can also have the effect of increasing assay precision by ensuring reproducible reaction and sampling times.

There are several strategies for efficiently quenching biochemical HAT assays:

- Chaotropic agents: ethanol, isopropanol, urea, guanidine HCl (often comparable in volume to reaction sample).
- Detergents such as SDS.
- Strongly basic or acidic solutions.
- Rapid freezing or heating.
- Directly spotting of the reaction solution onto filter paper.
- High concentrations of a HAT inhibitor at compound concentrations sufficient to ensure complete quenching (>> IC_{50}) (20,41).
- Hydroxylamine (21).

Consider several factors when picking quenching conditions.

- Depending on the specifics of the assay, quenching can be accomplished by adding the quencher to the reaction, or transferring the reaction mixture to a known quantity of quencher.
- With any of these approaches, verify that the HAT reaction is in fact quenched. This can be done by attempting to quench the reaction, and taking serial measurements to ensure a stable signal. Changing readouts usually indicate a non-quenched reaction.

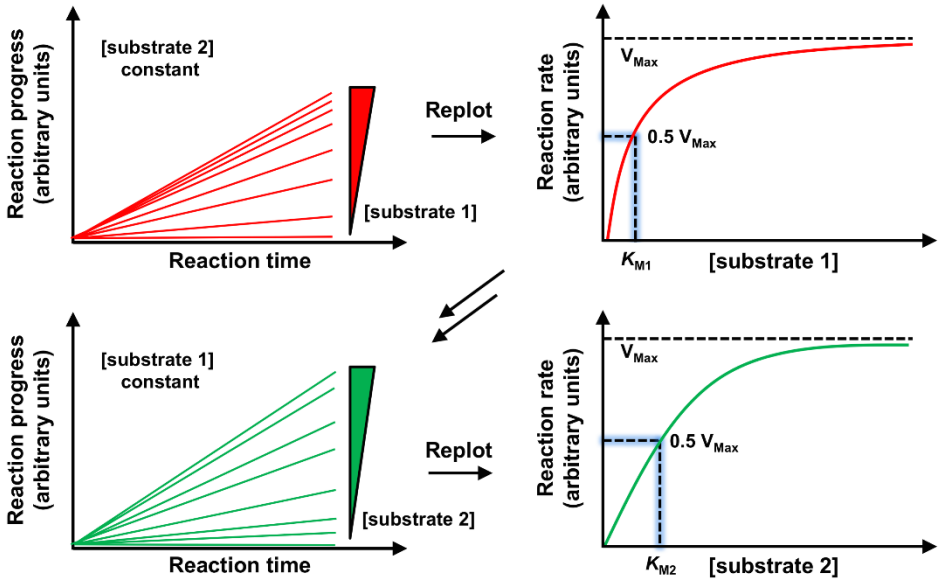

Figure 3. Optimization of substrate concentrations in HAT assays. Optimal substrate concentrations should be guided by the K_M for both HAT substrates. These can be determined experimentally. (Top) While keeping the concentration of substrate **2** constant (in excess), measure the enzymatic rates while titrating substrate **1**, and calculate K_{M1}. (Bottom) Next, while keeping concentration of substrate **1** constant (in excess), measure the enzymatic rates while titrating substrate **2**, and calculate K_{M2}.

- The type of quenching should be compatible with the assay readout. For example, certain quenching reagents may interfere with a given fluorescence readout, while general protein denaturants may prevent protein capture.

Compound Solvent

Determine the optimal percentage of DMSO (or other compound solvent) in the assay. This can be done by straightforward titration of the particular compound solvent (which is usually neat DMSO in most compound libraries). This percentage is often less than 2.5% total volume, though some assays may tolerate less organic solvent. The amount of compound solvent should be kept constant regardless of compound concentration.

Temperature

During the assay optimization process, determine the effect of temperature on the reaction system. Most biochemical HAT assays perform reactions at 30°C. This is a reasonable starting temperature point for most HAT assays. Users should experimentally determine the optimal reaction temperature that balances between convenience, reaction rate, and system stability for their particular assay application.

For HTS and even smaller scale follow-up experiments, it may be possible to conduct assays at room temperature. This convenience can circumvent the need to perform reactions in a heating oven and can reduce temperature gradient effects.

Higher temperatures can accelerate the reaction rate, which may be desirable depending on the assay timetable (this is true to a point, as too high of a temperature will eventually result in reagent or protein denaturation). Lower assay temperatures can slow the reaction rate and better stabilize the assay system, which again may be desirable for some applications.

Regardless of temperature, one should ensure assay temperature equilibration, especially if certain assay components are being kept on ice. Strategies include short pre-incubation steps and concentrated stock solutions.

Controls/Reference Compounds

It is often useful to test the effect of positive controls or reference compounds when validating an assay. Their use can help in proof-of-concept, can monitor assay performance over time, and can help compare results from different experiments.

There are many small-molecule HAT inhibitors reported in the scientific literature, many of which are sold commercially (**Table 3**) (5). Unfortunately, to-date most are insufficiently validated with respect to target selectivity in biochemical assays, and most have not been demonstrated to show specific target engagement in cells (42,43). Many of these reported compounds contain thiol-reactive moieties, while others form aggregates in common assay conditions. Both of these properties are associated with assay interference and poor target selectivity (39,44,45). Many of these compounds have the potential to interfere with certain light-based readouts, and several appear to be chemically unstable in biological buffer (36).

Using most of these small-molecules in HAT assay development should be done with full knowledge of their considerable off-target liabilities. For example, many of their reported activities may become significantly attenuated if detergents and/or reducing agents are included in the reaction buffer. Furthermore, their reactive or aggregating tendencies may interfere with some assay readouts. Until more promising HAT inhibitors are developed (especially for HATs other than p300/CBP) that demonstrate better potency and target selectivity in biochemical and cell-based assays (among other criteria), we recommend that most currently reported small-molecule HAT inhibitors be restricted to monitoring assay performance (such as intra- and inter-run precision). Their use in more complex cell-based HAT assays should be used with extreme caution or in many cases avoided, as evidence of direct, selective target engagement in cells have not been demonstrated. While many of the reported HAT inhibitors produce decreases in histone acetylation in cells at low-to-mid micromolar compound concentrations, such readouts could also be produced by well-characterized promiscuous compounds, suggesting some observed decreases in histone acetylation may be due to a variety of nonspecific target engagements at these relatively high compound concentrations (36).

Recently, the discovery of A-485, a potent, selective indane spirooxazolidinedione inhibitor of p300 was reported by Lasko and colleagues (43). While external validation of this compound is pending, it appears promising as a useful chemical probe given strong supporting evidence for potent and selective target engagement, including: (a) low nanomolar IC_{50} values versus human p300/CBP, (b) approximately 1000-fold biochemical selectivity versus other HATs and greater than 100 unrelated biological targets, (c) biophysical evidence of target engagement (SPR, x-ray crystallography), (d) robust chemical characterization and SAR including the description of an inactive analog A-486, (e) nanomolar potencies in multiple cellular assays for histone acetylation, and (f) multiple lines of evidence consistent with target engagement in cells and *in vivo*. If using A-485 in HAT assays, we strongly encourage inclusion of its inactive analog A-486 as a negative control.

It is also worth mentioning Lys-CoA, a bi-substrate inhibitor (46). This compound, not a small-molecule *per se*, may be useful as a control compound in biochemical HAT assays involving p300. As it is cell-impermeable, this specific compound is not recommended in cell-based HAT assays, though cell-permeable analogs such as Tat-CoA have been reported (47).

Table 3. Reported HAT inhibitors. Most of the reported HAT inhibitors have structural alerts or poor physicochemical properties, and most inhibit HATs by nonspecific reactivity or aggregation. Most should be used in validating HAT assays with caution and with knowledge of their potential liabilities (36).

Compound	Chemical structure	Reported target, *in vitro* IC_{50} (μM)	Comments	Reference
A-485	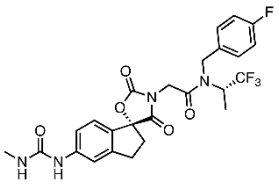	p300-BHC, 0.010 CBP-BHC, 0.003	-External validation on-going, though promising potential chemical probe -Nanomolar cellular activities -Paired with A-486 inactive analog control	(43)
A-486	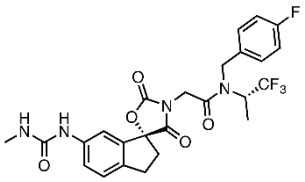	p300, > 50	External characterization on-going; use with active analog A-485	(43)
Anacardic acid	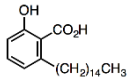	p300, 8.5	Aggregator	(41)
C646	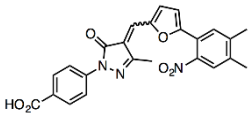	p300, 1.6	Thiol-reactive	(48)
Curcumin	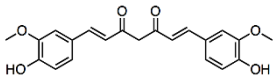	p300, 25	Thiol-reactive, aggregator, unstable	(49)
Garcinol	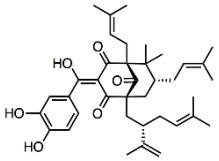	p300, 5	Aggregator	(50)
L002	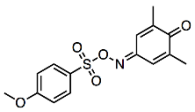	p300, 1.98	Thiol-reactive	(51)
Lys-CoA	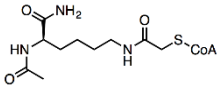	p300, 0.5	Cell-impermeable	(46)
MB-3	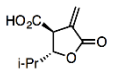	Gcn5, 100	Thiol-reactive	(52)
NU-9056	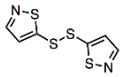	Tip60, 2	Thiol-reactive	(53)

Use of Orthogonal Assays/Common Interferences

Assay technologies are subject to various modes of compound-mediated interference (**Table 1**). Specific modes of interference for several assay technologies are also described in further detail in the subsequent section "BIOCHEMICAL HAT ASSAYS". It is best practice to perform at least one orthogonal assay method to help confirm actual modulation of HAT activity (11,17,54). Depending on project and test compound specifics, a

second orthogonal assay may also be useful to provide additional mechanistic confidence and further de-risk interference.

In the authors' opinion, the gold standard of confirmatory biochemical HAT assays is some variation of the radiolabeled acetyl-CoA filter-binding method because: (a) it offers excellent signal:noise ratio, (b) it is a direct measurement of substrate acetylation, (c) it does not require much specialized instrumentation aside from a scintillation counter, (d) and is not prone to many of the common interference modalities seen in other assay types because test compounds are removed by filtration. While it requires specialized instrumentation, chromatographic separation coupled to mass spectrometry (i.e., LC-MS) is another high-quality HAT assay format.

There are numerous combinations of primary assays and orthogonal assays. The choice of primary and orthogonal assays will depend on a variety of factors (discussed in prior sections). In general, indirect primary assays should be paired with direct orthogonal assays, while direct primary assays can be paired with direct and/or indirect orthogonal assays (**Table 4**). Note that compound activity in both a primary and an orthogonal assay does not completely rule out compound-mediated interference. For example, many of the assays discussed in this chapter are (in principal) susceptible to light-based interferences across multiple assay formats, which can be analyzed with appropriate interference counter-screens.

HAT systems will almost inevitably show some degree of susceptibility to generalized compound-mediated assay interferences (so-called because they will often modulate biological targets regardless of technology), such as nonspecific reactivity or aggregators. Additional studies should also confirm tractable mechanisms of target modulation by test compounds, as HATs sensitive to nonspecific modes of target modulation by thiol reactivity, redox activity, chelation, or aggregation may still show activity, albeit poorly tractable, in orthogonal assays.

Table 4. Potential primary assay-orthogonal assay pairings.

Primary assay	Potential orthogonal assays	Comments
Fluorometric, enzyme-coupling (indirect)	-Filter-binding radiolabel -Antibody-based (Western, ELISA, Alpha) -Scintillation proximity -MS* -Fluidic mobility*	-Pair indirect primary assay with direct orthogonal assay -Caution when pairing with light-based orthogonal assay readouts without separation steps
Alpha technology (AlphaScreen, AlphaLISA)	-Filter-binding radiolabel -MS* -Fluidic mobility* -Scintillation proximity -Fluorometric, -Enzyme-coupling	-Pair direct primary assay with direct and/or indirect orthogonal assays -Prioritize a non-antibody-based orthogonal assay -Caution when pairing with light-based orthogonal assay readouts without separation steps
TR-FRET	-Filter-binding radiolabel -MS* -Scintillation proximity -Fluidic mobility* -Enzyme-coupling	-Pair direct primary assay with direct and/or indirect orthogonal assays -Prioritize a non-antibody-based orthogonal assay -Caution when pairing with light-based orthogonal assay readouts without separation steps
Fluidic mobility	-Filter-binding radiolabel -Scintillation proximity -MS* -Fluorometric -Enzyme-coupling	Pair direct primary assay with direct and/or indirect orthogonal assays

Table 4. continued from previous page.

Primary assay	Potential orthogonal assays	Comments
MS	-Filter-binding radiolabel -Scintillation proximity -Fluidic mobility*	-Pair direct primary assay with direct and/or indirect orthogonal assays -Can also monitor Ac-CoA depletion, CoA production by MS; non-MS-based orthogonal assay still recommended
Scintillation proximity	-Antibody-based (Western, ELISA, Alpha) -MS* -Fluidic mobility* -Fluorometric -Enzyme-coupling -Filter-binding radiolabel	-Pair direct primary assay with direct and/or indirect orthogonal assays -Caution when pairing with light-based orthogonal assay readouts without separation steps

* MS and fluidic mobility orthogonal assays useful to minimize light-based compound interferences, but their implementation may be limited by available instrumentation and resources.

Assay Validation

Assay validation represents a critical last step in assay development and optimization, but often overlooked or rushed. Best practices for HTS assay validation should include:

- Characterization of reagent stability.
- Characterization and correction of plate effects.
- Characterization and optimization of signal variability (e.g., intra-plate, inter-plate, day-to-day).
- Characterization of assay performance using reference compounds (e.g., intra-plate, inter-plate, day-to-day).
- Characterization of HTS performance using mini-compound libraries such as LOPAC (e.g., inter-plate, day-to-day).

Assay performance can be assessed with several statistical methods during both the validation and production phases:

- *Z*' factor (55). This calculation can monitor assay signal dynamic range and data variation on each microplate, as well as assay performance over time when examining multiple microplates.
- Minimum significant ratio (MSR) (56). In a robust assay, a given compound should have similar bioactivity across independent experiments. This calculation utilizes reference compound activity to monitor assay performance and variability. For an excellent discussion, the reader is referred to Minimum Significant Ratio – A Statistic to Assess Assay Variability.

For more detailed discussion on assay validation, the reader is referred to HTS Assay Validation and *In Vivo* Assay Guidelines.

Section Summary

Constructing and validating a robust assay capable of identifying modulators of HAT activity requires careful thought and experimental optimization of multiple, often competing parameters.

Biochemical HAT Assays

Introduction

This section describes special considerations for multiple types of biochemical HAT assays. For several assay platforms, generic HAT assay protocols are provided.

Filter-Binding Radiolabeled HAT Assays

Radiolabeled substrate HAT assays were some of the first HAT assays to be reported. Benefits include directly measuring acetylated histones, intrinsic high signal:noise ratios which can facilitate lower amounts of enzyme and substrate, absence of required protein labels, and resistance to certain forms of compound-mediated assay interference such as compound fluorescence. The main drawback is the use of radioisotopes, which necessitates additional safety disposal protocols and regulatory compliance.

The assay principle is relatively simple: acetyl-CoA substrate is labeled with radioactive tritium ([^{3}H]) or carbon ([^{14}C]) on the acetyl moiety. HATs catalyze the transfer of the labeled acetate to histone-based substrates, and the amount of radiation can be quantified by capturing the radiolabeled histone-based product and quantifying radioactivity, usually though a scintillation counter. HAT activity is therefore proportional to radioactivity (**Figure 4**).

Even though filter-based radiolabeled HAT assays are generally less susceptible to light-based forms of compound-mediated interference relative to homogenous light-based assay formats (because in filter-based assays most test compounds are removed by filtration prior to scintillation counting), orthogonal assay(s) should still be performed to rule out compound-mediated interference. For example, scintillation quenchers can still interfere with the assay readout if they are not separated from the radiolabeled analyte by filtration. Another source of potential interference are compounds that prevent the binding of acetylated product onto capture matrix.

In parallel with liquid scintillation counting, reaction aliquots can be separated by SDS-PAGE and analyzed by autoradiography to verify radiolabeled acetate incorporation onto the desired substrate.

The following is a sample protocol for a generic radioisotope-based HAT assay. Specific parameters may vary for a particular assay. Specific reagents, concentrations, volumes, dispensing procedures, and time intervals would need to be optimized for a particular application.

Consumable specifications

- Microplates: standard-volume polystyrene 384-well microplates (final reaction volume = 15 µL).
- For lower-throughput applications, reactions can be performed in Eppendorf-style tubes instead of microplates.

Instrumentation specifications

- Compound dispenser: capable of dispensing in nL increments; usually acoustic droplet or pintool transfer.
  - Alternatively, serial dilutions can be made and subsequently transferred by manual pipetting. In such cases, accurate and precise compound dispensation may require higher reaction volumes.
- Fluid dispenser: capable of dispensing in 0.5 µL increments.
  - Alternatively, solution can be dispensed by serial pipetter or multichannel pipette.
- Liquid scintillation counter.

Solutions (for total reaction volume, 15 µL)

- 5X reaction buffer: 250 mM Tris, pH 8.0, 250 mM NaCl, 0.5 mM EDTA, 0.05% Triton X-100 (v/v), 250 µg/mL BSA, 5 mM DTT.
- 1X reaction buffer: 50 mM Tris, pH 8.0, 50 mM NaCl, 0.1 mM EDTA, 0.01% Triton X-100 (v/v), 50 µg/mL BSA, 1 mM DTT.
- Reaction solution: 375 nM histones (H3H4 tetramers), 15 nM HAT enzyme in 1X reaction buffer (dilute concentrated histones and HAT enzyme with appropriate volumes of H_2O and 5X reaction buffer).

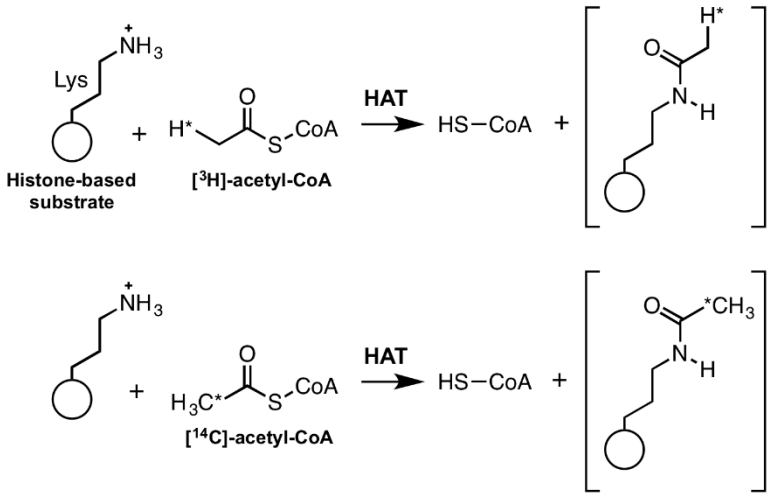

Figure 4. General schematic of cell-free radioisotope HAT assays. Radiolabeled acetyl-CoA is used to directly quantify HAT activity, either in the form of (top) [^{3}H]-acetyl-CoA or (bottom) [^{14}C]-acetyl-CoA. After the HAT reaction, histones are bound to a capture matrix (e.g., filter), and unreacted radiolabeled acetyl-CoA is removed by washing steps. The amount of radiolabeled (*) acetate incorporated onto histone-based substrates (brackets) is proportional to HAT activity.

- Control solution: 375 nM histones (H3H4 tetramers), 0 nM HAT enzyme in 1X reaction buffer (dilute concentrated histones with appropriate volumes of H_2O and 5X reaction buffer).
- Acetyl-CoA solution: 7.5 µM [^{3}H]-acetyl-CoA in 1X concentration (dilute concentrated enzyme stock solution with appropriate volumes of H_2O and 5X reaction buffer).
- Compounds: 10 mM DMSO stocks.

Safety and disposal considerations

- Radioactive waste should be disposed of in concordance with institutional radioactive safety protocols.
- Always wear personal protective equipment when handling radioactive material, including lab coat, gloves, and eye protection.

Sample protocol

1. Dispense compounds and vehicle controls in microplates.
    - Ensure equal organic solvent in each reaction.
    - Add 15 nL DMSO in control wells with fluid dispenser; 15 nL test compound in test wells (to assay at 10 µM final compound concentration) with compound dispenser.
2. Dispense reaction buffer into appropriate wells.
    - Add 10 µL reaction solution into test wells and positive control wells with fluid dispenser.
    - Add 10 µL control buffer into negative control wells with fluid dispenser.
3. Allow compounds to pre-incubate for 10 min at 30°C.
    - Perform incubation in temperature-controlled microplate oven.
4. Initiate HAT reaction by adding acetyl-CoA solution.
    - Add 5 µL acetyl-CoA solution into all wells with fluid dispenser.
    - Seal microplates.
5. Allow system to equilibrate.
    - Mix reaction contents with microplate shaker for 1 min.
    - Centrifuge microplates for 1 min.
6. Allow HAT reaction to proceed for 10 min at 30°C.
    - Perform incubation in temperature-controlled microplate oven.

7. Quench reaction.
    - Transfer 12.5 µL aliquot of reaction mixture into 12.5 µL neat isopropanol with pipette. Gently mix.
8. Transfer reaction aliquots onto filter paper.
    - Transfer 20 µL aliquot of quenched reaction solution from Step 7 to Whatman P-81 phosphocellulose paper. Allow to air dry completely (approximately 30 min).
9. Wash filter paper.
    - Wash filter paper disks with 50 mM $NaHCO_3$, pH 9.0 for 5 min with gentle agitation. Repeat 3 times.
    - Wash filter paper disks with acetone for 5 min with gentle agitation. Allow to air dry completely.
10. Read samples.
    - Transfer washed filter paper disks from Step 9 to 20 mL liquid scintillation vials containing 5 mL liquid scintillation cocktail and briefly vortex.
    - Read radioactivity of samples using liquid scintillation counter.
11. Analyze data.
    - Calculate the average readout for the negative controls. This value constitutes the background signal.
    - Subtract the background signal from the remaining reactions.
    - Calculate the average readout for the positive (vehicle) controls. This value constitutes the uninhibited reaction.
    - Calculate the percent HAT modulation for each reaction. Percent HAT inhibition (%) = (1 - (test solution/positive control)) x 100.

Miscellaneous notes

- Phosphocellulose filter disks are often used as a capture matrix (57).
- DTT and other reducing agents can be used in this assay.
- Labelled acetyl-CoA can often be mixed with unlabeled acetyl-CoA. This reduces the amount of total assay radioactivity, and expensive radiolabeled substrate. The exact ratio labelled:unlabelled acetyl-CoA will depend on the specific radioactivity of labelled acetyl-CoA, instrument settings, assay parameters, and amount of radioisotope transferred to capture matrix.
- Ensure scintillation counter is properly calibrated.
- Filter-binding assays are end point assays, but they can be adapted for continuous reaction monitoring by sampling reaction aliquots.
- Always keep solutions containing proteins and peptides on ice when not in use.

Additional examples/protocols: For additional examples of radioisotope-based HAT assays, we refer the reader to several studies (11,16,17,30,57).

Other Radiolabeled HAT Assay Methods

Several other radiolabeled methods have been reported for assaying HAT activity:

Scintillation proximity assays (SPA) have been applied to HATs (26,43,58). SPA is a solid-phase homogenous technique that couples a scintillation matrix (beads; coated plate, “FlashPlate”) to a capture system (e.g., anti-histone antibody, or biotin-tagged histones and streptavidin-coated beads/plates). Histone-based products can be captured in close proximity to the matrix surface. In certain cases, histone-based products can also be immobilized to the matrix (i.e., microplate) without special tags through nonspecific adsorption. When a radiolabeled product is in close proximity to the scintillator, the signal from radioactive decay of the radioisotope is amplified. Unbound radiolabeled acetyl-CoA in solution is not in close enough proximity to the scintillation matrix, and therefore does not generate signal. An advantage of SPA is that it does not require a

separation event such as filter-binding. Consequently, SPA is an attractive assay technique when the detection sensitivity of radiolabels is needed in a high-throughput setting. Development and optimization of SPA-based HAT assays utilizes the same general assay development principles described in this chapter. For additional information on SPA assay development, several reviews may be useful (24,59).

Some SPA-specific comments include:

- Reducing agents such as DTT should not interfere with SPA-based technologies.
- A potential source of compound-mediated interference in SPA are compounds that disrupt scintillation (24). For example, such inner-filter effects can be quite significant in certain scintillation proximity assays where photon emission occurs in the blue region (which can by quenched by yellow-colored compounds) (25). Orthogonal assays, including filter-binding assays that remove interfering compounds, can help identify this type of assay interference.
- Excessive radiolabels can lead to high background signals, causing nonproximity effects. This can be countered by reducing the concentration of radiolabels, or aspirating reaction solution before measuring.
- Nonspecific protein binding to either beads or surfaces can also cause high background. This effect can often be mitigated with blocking agents, change of matrix, or detergent.
- Interactions between anionic acetyl-CoA and cationic histone interactions can also lead to nonspecific background signal, though these can be disrupted with appropriate selection of quenching agent to disrupt this interaction (e.g., guanidine HCl) (58). This effect can be identified by high background signal in the presence of acetyl-CoA and histone-based substrates and the absence of HAT enzyme.
- High-throughput plate-based SPA requires specialized instrumentation, such as PMT-based microplate-compatible scintillation counters or CCD-based readers (25).

Autoradiography of HAT reactions is well-described in the literature (60). Autoradiography methods are typically employed for lower-throughput confirmatory applications. If reaction aliquots are separated by gel chromatography, they can be useful for confirming acetylation of specific substrates in multi-protein reaction mixtures (61). Reactions can also simply be applied to a capture matrix (e.g., filter paper, nitrocellulose membrane) and assayed for total radioactivity (60,62). Radiation can be quantified by radiodensitometry. The main drawback is lower-throughput. For example, gel separation requires a separate gel lane for each reaction. Furthermore, signal acquisition depends on the specific radioisotope and the amount of radioisotope per reaction. Development can require hours to days of product exposure to film.

Antibody-Based HAT Assays

Another common class of HAT assays probes for histone acetylation using antibodies targeting either specific acetylated histone residues (e.g., H3K27ac) or nonspecific histone acetylation (e.g., H3ac). These assays directly probe for the acetylated histone-based product. Antibody-based assays are versatile and come in several varieties, including Western blot, slot blot (a modified Western blot), and ELISA. For examples of immunoassays, we refer the reader to several studies (10,11,17).

For details on developing immunoassays, we refer readers to Immunoassay Methods. Some considerations for antibody-based HAT assays include:

- Certain chemotypes, such as acetimides, have been reported to interfere with acetylated histone antibodies (19). Useful counter-screens include a second, independent antibody, as well as orthogonal assays.
- Immunoassays are limited by the quality and specificity characteristics of the antibody. Verify antibody performance. Antibodies designed for specific acetylated histones have potential for significant cross-reactivity (63,64).

Fluorometric HAT Assays

Cell-free fluorometric HAT assays are relatively inexpensive, are straightforward to establish, and require only standard HTS instrumentation. The assay principle is relatively simple: free CoA produced by the HAT reaction reacts with a sulfhydryl-scavenging probe such as *N*-[4-(7-diethylamino-4-methylcoumarin-3-yl)phenyl]maleimide (CPM), to form a highly fluorescent CoA-CPM adduct quantified by fluorescence intensity (**Figure 5**).

The actual acetylated histone product is not directly measured in this assay platform. Therefore, a significant drawback to this method is the significant burden of compound-mediated assay interference (17). The method also has a lower signal:noise ratio compared to radioisotopic methods. In principle, the detection of the CoA reaction product can serve as a convenient orthogonal assay to direct HAT assays. The decision to utilize this assay format, and whether to implement as a primary screen or orthogonal assay, will depend on multiple factors including: available resources, the availabilities of other orthogonal assays, the desired throughput and timelines at each project stage, and the expected test compound chemotypes. For instance, if many of the test compounds are colored or contain potential reactive groups, this assay format may not be an ideal choice due to the high likelihood of readout interference.

If choosing this method for assaying HAT activity, assay-specific counter-screens should be included to characterize any compound-mediated fluorescence interference (both quenching and auto-fluorescence) and CoA-scavenging reactions by test compounds. For details on performing these counter-screens, we refer the reader to several worked-out examples (14,16,17).

Furthermore, at least one orthogonal assay that directly quantifies the protein product (acetylated histone) is all but required when utilizing this assay method.

The following is a sample protocol for a generic CPM-based HAT assay. Specific parameters may vary for a particular assay. Specific reagents, concentrations, volumes, dispensing procedures, and time intervals would need to be optimized for a particular application.

Consumable specifications

- Microplates: low-volume black polystyrene 384-well microplates (final reaction volume = 20 µL)
- Note: this assay can be miniaturized to 1536-well format with reaction volumes less than 5 µL (11).

Instrumentation specifications

- Compound dispenser: capable of dispensing in nL increments; usually acoustic droplet or pintool transfer.
  - Alternatively, serial dilutions can be made and subsequently transferred by manual pipetting. In such cases, accurate and precise compound dispensation may require higher reaction volumes.
- Fluid dispenser: capable of dispensing in 0.5 µL increments.
  - Alternatively, solution can be dispensed by serial pipetter or multichannel pipette.
- Microplate reader: capable of reading fluorescence intensity.

Solutions (for total reaction volume, 15 µL)

- 5X reaction buffer: 250 mM Tris, pH 8.0, 250 mM NaCl, 0.5 mM EDTA, 0.05% Triton X-100 (v/v), 250 µg/mL thiol-deactivated BSA.
- 1X reaction buffer: 50 mM Tris, pH 8.0, 50 mM NaCl, 0.1 mM EDTA, 0.01% Triton X-100 (v/v), 50 µg/mL thiol-deactivated BSA.
- Substrate solution: 150 µM histone peptide, 30 µM acetyl-CoA in 1X reaction buffer (dilute concentrated peptide and acetyl-CoA stock solutions with appropriate volumes of H_2O and 5X reaction buffer).

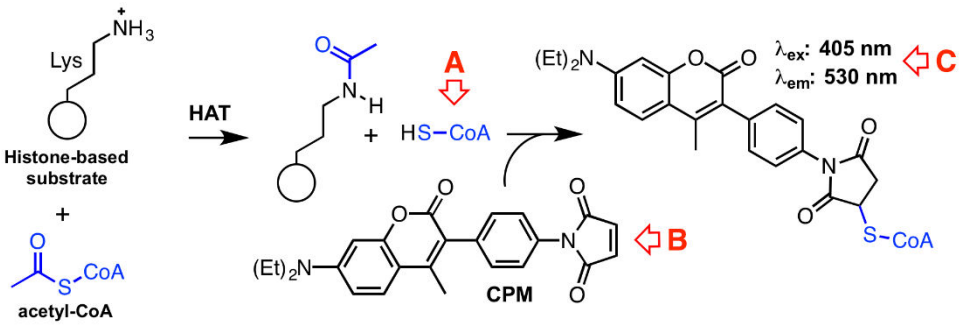

Figure 5. General schematic of cell-free fluorometric HAT assays. HATs produce acetylated histone-based products and free CoA (CoA-SH). After quenching the reaction, HAT activity is assayed by adding a sulfhydryl-scavenging probe, CPM, which reacts with CoA to produce highly fluorescent adducts. In absence of interference, the amount of fluorescence is proportional to HAT activity. There are three main sources of compound-mediated readout interference: (A), thiol-scavenging of CoA-SH by electrophilic test compounds; (B), formation of compound-CPM adduct by nucleophilic test compounds; and (C), fluorescence interference by test compounds (auto-fluorescence, quenching, inner-filter effects, light scattering).

- Enzyme solution: 60 nM HAT enzyme; add appropriate amounts of 5X reaction buffer in 1X concentration (dilute concentrated enzyme stock solution with appropriate volumes of H_2O and 5X reaction buffer)
- Quenching/probe solution (concentrated): 80 µM CPM in 1:1 H_2O:EtOH, 1% DMSO solution.
- Test compounds: 10 mM DMSO stocks.

Sample protocol

1. Dispense compounds and vehicle controls in microplates.
   - Ensure equal organic solvent in each reaction.
   - Add 15 nL DMSO in control wells with fluid dispenser; 15 nL test compound in test wells (to assay at 10 µM final compound concentration) with compound dispenser.
2. Dispense reaction buffer into appropriate wells.
   - Add 5 µL reaction buffer (1X) into control wells, 2.5 µL reaction buffer into test wells with fluid dispenser.
3. Dispense concentrated enzyme solution into appropriate wells.
   - Add 2.5 µL enzyme in reaction buffer into test wells with fluid dispenser.
4. Allow compounds to pre-incubate for 5-10 min at 30°C.
   - Perform incubation in temperature-controlled microplate oven.
5. Initiate HAT reaction by adding concentrated acetyl-CoA solution.
   - 10 µL substrate solution in reaction buffer into all wells with fluid dispenser.
   - Seal microplates.
6. Allow system to equilibrate.
   - Mix reaction contents with microplate shaker for 1 min.
   - Centrifuge microplates for 1 min.
7. Allow HAT reaction to proceed for 1 h at 30°C.
   - Perform incubation in temperature-controlled microplate oven.
8. Quench reaction and initiate CoA-CPM adduct formation by adding quenching/probe solution.
   - Add 5 µL quenching/probe solution into all wells with fluid dispenser.
9. Allow thiol-probe reaction to proceed for 15 min at room temperature
   - Mix reaction contents with microplate shaker for 1 min.
   - Centrifuge microplates for 1 min.
10. Read fluorescence intensity of microplate wells.

    - Settings: excitation 405 nm; emission 535 nm.
11. Analyze data.
    - Calculate the average readout for the negative controls. This value constitutes the background signal.
    - Subtract the background signal from the remaining reactions.
    - Calculate the average readout for the positive (vehicle) controls. This value constitutes the uninhibited reaction.
    - Calculate the percent HAT modulation for each reaction. Percent HAT inhibition (%) = (1 - (test solution/positive control)) x 100.

Miscellaneous notes

- DTT and other reducing agents are omitted from this assay, as they will react with the thiol-scavenging probe. This includes TCEP, whose phosphine lone pair of electrons can also react with maleimides (65).
- Besides CPM, there are several other maleimide-based fluorogenic probes available. We refer the reader to an excellent comparative study of such probes (12).
- Note some HAT enzymes may also contain free cysteine residues that may contribute to background.
- BSA can be highly useful for stabilizing HAT reactions, especially in the prolonged reaction times often necessitated in large-scale HTS settings. As BSA contains multiple cysteine residues (greater than 30 in mature BSA), free thiols on BSA must be deactivated ("capped") to prevent interference with sulfhydryl-scavenging probes. A facile workaround involves treating BSA with excess N-ethylmaleimide (NEM) (taking into account BSA contains multiple cysteine residues), and multiple rounds of dialysis to remove excess, unreacted NEM (11,13). Ensure thiol inactivation by performing a test reaction with CPM and measuring the fluorescence intensity under assay-like conditions.
- Substrates may contain free cysteine residues. To reduce background from probe-peptide/protein adducts, it may be necessary to replace cysteine residues with alternative residues (e.g., peptide synthesis or site-directed mutagenesis for recombinant proteins), or alternatively treated with NEM or similar reagent.
- CPM and other probes can usually be prepared as 10 or 50 mM stock solutions in DMSO. Store in -20°C, protect from light.
- Protect probe solutions from light. Prepare working probe solutions fresh to prevent degradation/non-specific hydrolysis in alkaline, aqueous conditions (66).
- The reaction between free CoA and maleimide probes is relatively fast, usually on the order of minutes (12). However, during assay optimization verify the reaction is complete by monitoring fluorescence intensity over time. Look for a signal plateau to signify reaction completion. Continued increases in fluorescence intensity may indicate inadequate mixing, insufficient reaction quenching, or CPM-protein adduct formation.
- Ensure microplate reader is properly calibrated.
- Fluorometric assays are end point assays given the ability of thiol-scavenging probes to modulate HAT activity. Like filter-binding assays, they can be adapted for continuous reaction monitoring by sampling reaction aliquots.
- Always prepare solutions containing proteins and peptides on ice. Keep on ice when not in use.
- An advantage of this assay is that the protein product may also be assayed by an orthogonal method such as Western blot which may be useful for examining compound-mediated assay interference (10,17).

Additional examples/protocols: For additional examples of fluorometric HAT assays, we refer the reader to several studies (10-14).

Microfluidic-Based HAT Assays

The development of a microfluidic mobility shift platform for cell-free, fluorescence-based HAT assays provides a useful approach for both HTS and mechanistic analysis of HAT modulators (21,22,67). The assay principle is

straightforward: fluorescent HAT substrates (peptides of histones H3 and H4 tails) are acetylated by a given HAT system, altering the charge-to-mass ratio on the peptide. Subsequently, acetylated peptides are separated from non-acetylated peptides *via* electrophoretic separation, enabling distinguishable fluorescent detection of each peptide. The ratiometric measurement of substrate/product fluorescence peak heights gives the percent conversion that can be directly related to HAT enzyme activity once correcting for non-enzymatic acetylation (**Figure 6)**.

An advantage of this assay platform is its versatility in facilitating compound discovery by HTS and also compound mechanism of action studies. A hydroxylamine-based reaction quench allows for uniform HAT assay conditions amenable to HTS of large compound libraries in 384-well plates. Small sample aliquots and relatively fast electrophoretic separations allow for multiple end-point measurements of a single reaction. Therefore, when the hydroxylamine-based quench is not used, consecutive measurements of HAT activity can be obtained to determine time-dependent HAT modulation. An additional advantage of this assay platform is the direct measurement of the acetylated product. Therefore, this method can be an effective counter screen to triage hits from high-throughput primary screens, such as the CPM assay, that may yield several compound-mediated assay interference molecules. Lastly, the microfluidic aspect of this assay allows for following enzymatic reactions in small reaction volumes with a minimum amount of sample, increasing its feasible applications from an economic perspective.

As this assay technique directly measures fluorescently-labeled, electrophoretic-separated acetylated histone products, the assay readout is not subject to certain types of compound-mediated interference. For instance, light-based interference compounds are usually separated by the electrophoresis. However, like the other methods described in this chapter, the enzymatic system itself will be susceptible to nonspecific sources of bioassay interference, such as redox cycling compounds, aggregators, and nonspecific reactivity. The magnitude is dependent on the experimental conditions (target, concentrations, detergent, scavenging reagents, etc.).

A critical factor in experimental design is substrate choice. Users should verify that the acetylated and non-acetylated histone products can be adequately resolved. This is often achievable for peptide-based histone substrates, but may be considerably more difficult for larger (> 30-mer), multiply-charged histone-based substrates, as electrophoretic separation is based upon mass/charge ratios. The net charge ideal for commercial microfluidic capillary electrophoresis instruments is from +3 to -3, and the substrate histone peptides used for HAT assays typically have net charges ranging from +3 (for the H4 peptide) and +4 (for the H3 peptide). Therefore, this system presents challenges for HAT assays requiring larger histone-based substrates (e.g., full-length histones, chaperones). The choice of fluorophore for microfluidic assays will depend on the light source and detector, as well as the spectral properties and other behaviors of the labelled analyte in the assay. Common fluorophores for the EZ-Reader include FITC, 5-FAM, and Alexa 488.

The following is a sample protocol for a generic microfluidic mobility shift HAT assay. Specific reagents, concentrations, volumes, dispensing procedures, and time intervals should be optimized for a particular application.

Consumable specifications

- 384-well microplates from E&K Scientific (EK2253): 58 µL well capacity volume with a U-bottom, clear, natural polypropylene (final reaction volume = 30 µL).
- PerkinElmer ProfilerPro^{TM} Separation Buffer (Cat# 760367): Prior to the first use of the separation buffer, add 2 mL of coating reagent 8 (CR8) that comes with the purchase of the separation buffer. CR8 is a positively-charged additive for coating the Lab-Chip sipper channels. Store separation buffer at 4°C but warm to room temperature before use.

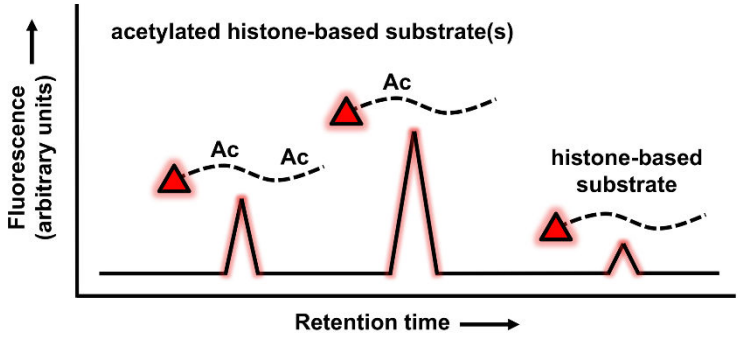

Figure 6. General schematic of the microfluidic mobility shift HAT assay. Acetyl-CoA and fluorescent-labeled histone peptides are the HAT substrates. Reaction aliquots are analyzed by microfluidic electrophoresis. Lysine acetylation alters the retention time of the histone peptide *via* decreasing product net charge and increasing product mass. HAT activity is proportional to the amount of acetylated product produced.

Instrumentation specifications

- PerkinElmer Lab-Chip EZ-Reader instrument (obtains fluorescence measurements following microfluidic electrophoresis).
    - Suggested initial electrophoresis separation conditions: downstream voltage of -500 V, upstream voltage of -2500 V, and a pressure of -1.5 psi for both FITC H3/H4 peptides
- Lab-Chip EZ Reader 12-sipper chip: capable of sipping as little as 10 nL reaction mixture while simultaneously monitoring 12 reactions (proper treatment and troubleshooting points are listed under *Miscellaneous notes*).

Substrate peptide sequences

- FITC-H4 (3-14, FITC-Ahx-RGKGGKGLGKGG [Ahx = 6-amino-hexanoic acid])
- FITC-H3 (5-20, FITC-Ahx-TARKSTGGKAPRKQL)
- These peptides were synthesized by automated peptide synthesis on Rink amide resin, using Fmoc-based chemistry. Peptides can be synthesized in-house with appropriate instrumentation. Alternatively, custom peptides can be synthesized by commercial vendors.

Solutions (for total reaction volume, 30 µL)

- 10X reaction buffer: 500 mM HEPES, pH 7.5, 500 mM NaCl, 20 mM EDTA.
- Miscellaneous assay components (prepare new each experiment): 0.5% Triton X-100 (v/v) in PBS (10X), 20 mM DTT in PBS (10X), 0.5 M hydroxylamine in PBS (for reaction quench).
- Master mix solution: 1X reaction buffer, 0.05% Triton X-100 (v/v), 2 mM DTT, 2 µM FITC-H3/H4 peptide, 150 nM p300.
- Quenching solution: 0.5 M hydroxylamine in PBS, pH 7.5.
- Test compounds: 10 mM DMSO stocks.

Sample protocol

1. Dispense 0.5 µL of compounds (dissolved in DMSO) and vehicle controls in screening microplates.
    a. When screening large compound libraries for inhibitor discovery, include samples having no enzyme as this will represent the percentage of non-enzymatic acetylation.
    b. DMSO percentage for the assay is 1.7%. Higher DMSO amounts will decrease enzyme activity.
2. Dispense 26.5 µL master mix into appropriate wells.
3. Allow compounds to pre-incubate with master mix solution for 10 min at room temperature.

4. Initiate HAT reaction by adding 3.0 µL of 10 µM acetyl-CoA (total reaction volume – 30 µL).
5. Allow HAT reaction to proceed for 10-15 min at room temperature.
    a. When performing an end-point analysis, keep product accumulation between 10-15%.
    b. For kinetic measurements, transfer the microplate to the PerkinElmer Lab-Chip EZ-Reader immediately following the addition of acetyl-CoA to begin obtaining fluorescence measurements.
6. If quenching the reaction, add 5 µL of 0.5 M hydroxylamine to each well.
7. Read fluorescence intensity of microplate wells.
    a Light source: LED.
8. Analyze data.
    a. Calculate averages and standard deviations of percent conversion for negative (no inhibitor) controls and positive (vehicle) controls.
    b. Calculate averages and standard deviations of percent conversion for inhibitor samples.
    c. Calculate the HAT percent activity: normalize the percent conversions by setting the negative controls to 0% and the positive control to 100% conversion.

Miscellaneous notes

- The separation resolution (SR) is calculated using the formula $SR = \Delta L/2(\sigma 1 + \sigma 2)$, where ΔL, $\sigma 1$, and $\sigma 2$ are the distance between peaks, standard deviation of the first peak, and standard deviation of the second peak, respectively.
- Protect fluorescent peptide solutions from light to prevent photo-catalyzed degradation.
- Always prepare solutions containing proteins and peptides on ice. Keep on ice when not in use.
- Prior to use in an experiment, proper treatment for the Lab-Chip EZ Reader 12-sipper chip includes:
    - Washing entire chip with distilled water thoroughly, followed by a complete drying *via* aspiration.
    - Washing the chip wells using separation buffer (2 x 250 µL), followed by filling the smaller wells with 250 µL and the two larger wells with 500 µL of separation buffer.
- Following completion of an experiment, proper treatment for the Lab-Chip EZ Reader 12-sipper chip and EZ Reader instrument includes:
    - Filling 12 wells within a screening microplate with 5% DMSO in water and running the Lab-Chip EZ reader instrument at 15 cycles with a final delay time of 300 s. while running at a pressure of -4.0 psi. This will rinse the chip sipper channels with the 5% DMSO followed by a 300 s rinse with separation buffer.
    - For the EZ Reader instrument, switch out separation buffer for distilled water and wash the lines for 10 min prior to either starting a new experiment or shutting the instrument down. Carryover may occur from one experiment to another if lines are not washed.
- Due to evaporation of reaction solution, the maximum kinetic runtime of a single experiment is 40 h when screening microplates utilizing 500 µL reactions. When less than 500 µL is used, wells will dry out quicker and runtimes should be reduced. Additionally, chip wells should be refreshed by removing old separation buffer and adding fresh separation buffer every 12 h.
- It is important to be vigilant for declining chip performance, which can occur due to blockage of a sipper, presence of air bubbles, or standard wear and tear. Signs a chip may need to be refreshed or retired include a lack of reproducibility among replicate samples, broadening of peak shape, or delayed elution of peptide when compared to a properly functioning chip.
- In cases when a chip shows signs of failing (potentially due to sipper blockage or heavy usage), we have found the following protocol can be useful to refresh and restore chip performance:
    - Run the Lab-Chip EZ-Reader instrument at a positive pressure of 4.0 psi for 1 h with no microplate loaded. This can aid the clearance of any blockages from the channel. Follow this with an additional wash step, by filling 12 wells within a microplate with 5% DMSO in water and running the EZ-

Reader instrument at 50 cycles with a final delay time of 300 s and pressure of -4.0 psi. This wash should be performed for approximately 1 h.

- Purchase a fresh bottle of separation buffer. Since reaction solutions are circulated through a bottle of separation buffer, poorly performing chip sipper channels can often be resolved by simply using a fresh bottle of separation buffer.

MS-Based HAT Assays

Mass spectrometry (MS) is an analytical technique that ionizes analytes and separates them based on their mass-to-charge ratios (m/z). Components of HAT reactions can be ionized through one of several technologies (e.g., electrospray, MALDI), then passed through an electric field where the ionized analytes are measured based on their m/z ratios. Prior to ionization, HAT reaction components can be separated by liquid chromatography and/or subjected to various extraction/enrichment strategies such as solid-phase extraction (SPE).

MS-based detection allows for the monitoring of multiple analytes in a single injection, which facilitates the detection of substrate, product, an internal standard (IS), and/or an orthogonal reaction. For instance, the net loss of histone lysine methylation catalyzed by an α-ketoglutarate-dependent recombinant demethylase can be simultaneously quantified by monitoring the production of modified histone and also succinate, with the conversion of α-ketoglutarate to succinate being an orthogonal reaction **(Figure 7)**. Similarly, in addition to monitoring histone-based substrates and products themselves, the production of histone acetylation states can also be validated by monitoring the deacetylation of acetyl-CoA and the production of free CoA (23). Measuring orthogonal reaction products can enable real-time identification of signal enhancement or suppression.

As a representative example of available HTS-compatible MS technology, the Agilent RapidFire (RF) MS system is a micro-SPE system enabling rapid sample analysis (7-10 s/sample) from 96- and 384-well assay plates. Aspirated sample is loaded onto a micro-SPE cartridge, washed (to remove MS-incompatible components such as salts), and immediately reverse-eluted to the mass spectrometer. The RF-MS system is amenable to wide range of SPE packing materials (e.g., C4, C18, HILIC). The SPE packing method is chosen based on the desired levels of chromatographic separation and sample clean-up, and analyte properties (e.g., polarity, solubility). Combined with the ability of pairing various mass spectrometers such as QQQ (triple quadrupole), ToF (Time of Flight), and QToF (quadrupole ToF), RapidFire analysis can offer a versatile system capable of measuring HAT-relevant analytes. Note specific instrumentation and monitoring conditions (e.g., multiple reaction monitoring with triple quadrupoles, full-scan monitoring with ToF) will depend on multiple factors, including analyte, throughput, and mass accuracy specifications.

When performing a HTS run for small molecules or biological samples, minimizing cross contamination and run times is critical. Including blank injection(s) after each sample injection reduces cross contamination due to sample carryover, although this increases run times by at least two-fold. Hence, it is vital to ensure complete elution of the sample from the SPE cartridge by altering the RF method (flow and/or duration during each step) or by using appropriate mobile phases. The optimal solvent system will depend on the specific analytes being tested. Factors to consider include the solubility, chemical stability, and chromatographic properties of the specific analyte(s) in a given solvent system.

Compound-mediated assay interference in MS-based assays can manifest as ion suppression, but this phenomena is usually mitigated through sample purification, sample chromatography, the use of internal standards, and the aforementioned monitoring of orthogonal reactions (68). Chemical modification or adduct formation of the analyte by test compounds can also interfere with accurate analyte measurement by perturbing (a) analyte chromatographic and extraction behavior, or (b) measurement of parent ions due to mass shifts, especially when utilizing single or multiple reaction monitoring (69,70).

For additional details on MS-based assay development and optimization, refer to HPLC-MS/MS for hit generation.

The following is a sample protocol for a generic MS HAT assay. Specific reagents, concentrations, volumes, dispensing procedures, and time intervals should be optimized for a particular application.

Sample protocol

1. Dispense 1-2 µL enzyme mix (2X) into microplate using a liquid handling system such as Bioraptr. Centrifuge microplate briefly at 1000 rpm.
2. Dispense test compounds using a 384-head pin-tool or an acoustic dispenser
3. Dispense 1-2 µL substrate mix (2X) using a liquid handling system to initiate the reaction and centrifuge the plate at 1000 rpm for 1 min.
4. Incubate for desired time duration.
5. Add stop solution to quench the reaction using a large volume liquid dispenser; final volume should be at least 50 µL/well.
6. Briefly centrifuge and heat seal the plate(s) prior to RF-MS analysis. (Note: avoid using an adhesive sealer since the adhesive will clog the sipper tube in RF as well as leach on to the mass spectrometer, causing loss of signal).

In a representative RF method for a ~20-residue histone peptide, sample can be loaded on a C4 cartridge in 0.6 s, washed for 3 s with 100% dH_2O containing 0.1% (v/v) formic acid, eluted for 3 s with 80% acetonitrile containing 0.1% formic acid, and re-equilibrated for 5 s. The system can be programmed to perform a blank injection to minimize cross-contamination of subsequent samples.

Data processing

The Agilent RF mass spectrometry system is closely integrated with a proprietary data analysis software package (MassHunter Qualitative and Quantative Analysis) for measuring area under the curve (AUC) for each peak as well as converting the large data files into data for individual wells. Alternatively, RapidFire Integrator (Agilent) can be used for processing data from various mass spectrometer platforms (such as Sciex, Waters, and Agilent). These data can be processed further to calculate the amount of product (**Equation 1**).

Equation 1. $$\% \text{ Product conversion} = \frac{\text{Product}_{\text{AUC}}}{\text{Product}_{\text{AUC}} + \text{Substrate}_{\text{AUC}}}$$

Miscellaneous notes

- Due to the technical requirements of MS (e.g., instrumentation, chromatography/separation, troubleshooting), one may wish to consult with experienced mass spectrometrists when designing and optimizing an MS-based assay.
- The high sensitivity of many MS methods requires less product formation for detection relative to other technologies, potentially decreasing the amounts of required enzyme and substrate to complete a screening campaign.
- Polymeric detergents (e.g., Tween-20, Tween-80, Triton X-100, NP-40) are generally incompatible with MS assays, as they can broadly elude and saturate the assay signal. Monomeric detergents (e.g., CHAPS, octyl β-D-glucopyranoside, dodecyl β-D-glucopyranoside) are preferred, but can still interfere with MS assays.
- Multiple histone-based substrates have been reported for MS-based assays, including peptides and whole histone proteins (23).
- Like other detection methods, it is imperative to determine the limits of detection (LoD) and limits of quantitation (LoQ) for all analytes of interest, in presence and absence of IS. Determining the LoD and LoQ prevents detector saturation as well as determine the concentration of sample to be injected.

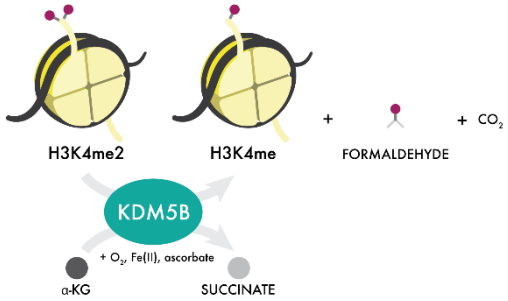

Figure 7. Measuring histone modifications by MS. Shown is a biochemical reaction demonstrating the KDM5B-catalyzed demethylation of H3K4 and the concurrent production of succinate. Similarly, HAT reactions can be monitored by measuring the production of acetylated histone products as well as the concurrent production of CoA/loss of acetyl-CoA (see **Figure 1**).

- Unlike LC-MS, RF-MS does not involve an elution gradient or prolonged retention times, which allows for cross contamination and carryover of samples. It is critical to establish optimal chromatography conditions for the analyte(s) of interest – appropriate SPE cartridge, alterations of load, wash and/or elute steps of RF method, along with the mass spectrometer detection method (positive or negative mode). If these manipulations fail to reduce carryover, it is advisable to incorporate blank injection(s) after each sample.
- Inclusion of an isotopically-labeled analyte (in stop solution) as an internal standard should also be considered to identify cases of incomplete sample injection, ion suppression, and matrix effects.
- Higher-throughput RF-MS can be achieved by minimizing the sample retention time on the system. This requires tubing with extremely small internal diameter combined with robust injection valves and LC-pumps. Thus, monitoring pump pressures facilitates the identification of clogs (if any), which might occur during longer runs using biological samples.
- Use of reverse-phase chromatography involving C4 or C18 cartridges requires sample preparation in 100% aqueous phase to prevent sample precipitation. In contrast, samples should be prepared in high organic (90 – 95% acetonitrile) when using HILIC cartridges (*see HPLC-MS/MS for hit generation for more details*).
- Arguably, RF-MS has lower throughput in comparison to a 1536-well biochemical assay read on a ViewLux. Multiplexing samples involving analytes that do not interfere in detection increases RF-MS throughput (71).

Non-Radiolabeled Proximity HAT Assays

There are several non-radioisotope, proximity-based technologies available to assay HAT activity, such as AlphaScreen (Amplified Luminescent Proximity Homogeneous Assay; **Figure 8**) and FRET (Fluorescent/Förster Resonance Electronic Transfer; **Figure 9**). Each of these technologies involves the excitation of a donor system by a light source, followed by signal transmission to an acceptor system that requires proximity for efficient transmission. The acceptor system, upon excitation by the donor system, then emits a signal which can be quantified. Alpha-based technologies (AlphaScreen, AlphaLISA) utilize singlet oxygen transfer, while FRET utilizes fluorescence resonance electronic transfer. Note that AlphaScreen acceptor beads contain a thioxene/anthracene/rubrene mixture, while AlphaLISA acceptor beads contain a thioxene/europium chelate mixture. The latter configuration creates a narrower emission band that is optimized for certain biological matrices. Time-resolved FRET (TR-FRET) adaptations using lanthanide fluorophore donors are common, and can enhance signal-to-noise by coupling an excitation pulse with delayed acquisition to allow for background fluorescence decay. For a well-designed example of a TR-FRET and AlphaLISA assay versus p300, we refer readers to a recent report by Lasko and colleagues (43).

Alpha- and FRET-based HAT assays share many advantages. Compared to conventional ELISA and Western blots, Alpha and FRET technologies are homogenous assays. This eliminates many assay steps such as washing, reducing assay time and simplifying the assay workflow. Both Alpha and FRET technologies require separate capture systems for the donor and acceptor components. Typically, this involves a combination of capture and affinity tags, and an acetylated histone recognition system (i.e., antibody or bromodomain). Both technologies are versatile, and allow for extensive customization of tags, substrates, and labeling strategies. For either technology, many reagent combinations are readily commercially available (so-called "off-the-shelf" assays), or are amenable to customization by relatively straightforward techniques or commercial services.

Alpha-based HAT assays have several potential advantages, including high sensitivity, low background, good dynamic range, and miniaturization (to 1536-well plates) (72). Additionally, singlet oxygen transfer can generally occur over longer distances compared to FRET. However, a disadvantage of Alpha technology can be reagent and instrumentation costs as well as light sensitivity. By contrast, TR-FRET assays may be less sensitive to DMSO (73). Both assay technologies are susceptible to specific modes of compound-mediated interference, including disruption of capture reagent systems and signal quenching (74,75).

Miscellaneous notes

- Optimization of the capture and affinity tags is advised for either technology. This includes experimenting with different tag combinations (e.g., 6xHis-Nickel, streptavidin-biotin, GST-glutathione) as well as the location of each tag on histone-based substrate.
- These technologies are dependent on the quality of the histone recognition motif. Characterize antibody specificity and optimize antibody titers. Specificity can also be assessed by titrating purified histone-based products.
- There have been reports of compounds interfering with antibody recognition of acetylated histone substrate (19). Consider a follow-up counter-screen with a second, independent antibody.
- As with fluorescence-based assays, avoid background light contamination when acquiring FRET and Alpha readouts.
- Perform titration experiments with the various assay components. Depending on the assay format and relative concentrations of each assay component, "hook effects" may be present (76). This can occur when a capture system is saturated by excess tagged substrate/product leading to an apparent signal plateau, followed by signal attenuation with further substrate/product titrations (e.g., excess biotinylated histone-based substrate/products for available streptavidin beads).
- The absolute concentration and ratio of donor:acceptor beads is critical for optimal assay performance. Start with manufacturer recommendations and slowly titrate.
- Because many of the Alpha- and FRET-based HAT assay formats rely on several binding events, it is recommended to determine the optimal order of reagent addition (e.g., binding of capture tag to affinity tag may interfere with the binding of another the antibody-histone pair, but not vice-versa).
- For Alpha-based technologies, the manufacturer typically recommends Tween 20 (0.01-0.1% v/v), Triton X-100 (0.01-0.1% v/v), CHAPS (0.1% v/v), and/or BSA (0.1% w/v) to mitigate nonspecific interactions.
- Certain assay components may interfere with Alpha-based technologies:
    - Residual azide (a common antimicrobial used for reagent storage) may interfere with singlet oxygen transmission.
    - Certain transition metals (Al^{2+}, Fe^{2+}, Fe^{3+}, Cu^{2+}, Ni^{2+}, Zn^{2+}) may quench singlet oxygen at low millimolar concentrations.
- To assess for assay interference:
    - Allow the reaction to go to completion, spike reaction with test compound, and then measure assay readout. If available, an alternative is to spike purified product and compound, then measure the assay readout.

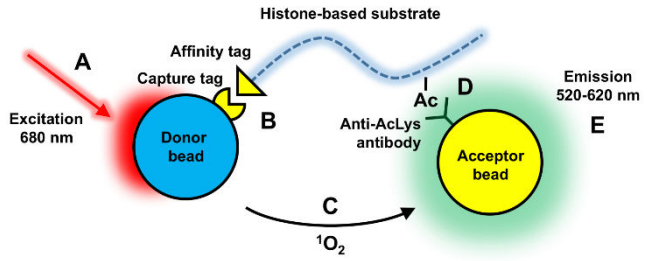

Figure 8. Example of an AlphaScreen-based HAT assay. A donor bead with a capture tag binds to a histone-based substrate with an affinity tag. An acceptor bead with an anti-acetyl lysine antibody binds to acetylated lysine on the histone-based substrate. Phthalocyanine from the donor bead is excited by a high-wavelength laser, which produces singlet oxygen ($^1O_2$). If in close proximity to the donor bead, thioxene, anthracene, and rubrene within the acceptor bead are excited by singlet oxygen to produce an emission at a lower wavelength. In the absence of interference, HAT activity is proportional to the emission intensity at this lower wavelength. There are five main potential areas of compound-mediated readout interference: (A) interference of excitation light source by test compound (quenching/absorbance/light-scattering); (B) disruption of donor bead-substrate interaction by test compound; (C) disruption of singlet oxygen transmission by test compound (quenching, chemical reaction); (D) disruption of acceptor fluorophore construct-product interaction by test compound; and (E) acceptor bead emission interference by test compounds (auto-fluorescence, quenching/absorbance/light-scattering).

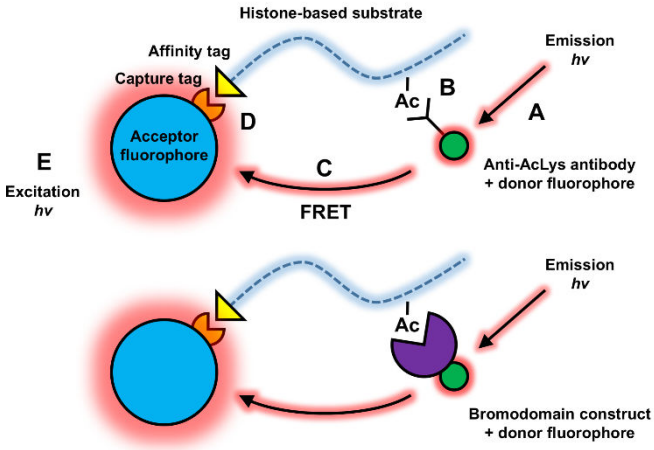

Figure 9. General schematic of (TR)-FRET HAT assays. A donor fluorophore conjugated to a recognition motif (top panel, antibody; bottom panel, bromodomain) binds to an acetylated lysine on the histone-based substrate. An acceptor fluorophore with a capture tag binds to the histone-based substrate with an affinity tag. The donor fluorophore is excited by a laser, which induces fluorescence. If in close proximity to the donor fluorophore, the acceptor fluorophore is excited by FRET. In the absence of interference, HAT activity is proportional to the emission intensity at this higher wavelength. There are five main potential areas of compound-mediated readout interference: (A) interference of excitation light source by test compound (quenching/absorbance/light-scattering); (B) disruption of donor fluorophore construct-substrate interaction by test compound; (C) disruption of FRET by test compound (quenching/absorbance/light-scattering); (D) disruption of acceptor fluorophore construct-product interaction by test compound; and (E) acceptor fluorophore emission interference by test compounds (auto-fluorescence, quenching/absorbance/light-scattering).

- For Alpha-based technologies, TruHit™ beads can also be used to identify compound-mediated readout interference.
- To assess interference with affinity tag systems, one can also test the effect of compounds on generic bead readouts that contain the affinity tag system of interest.

Enzyme-Coupled HAT Assays

Enzyme-coupled methods "indirectly" quantify HAT activity by measuring the product of a second, coupled enzymatic reaction **(Figure 10)**. This second enzyme system requires CoA substrate, which is produced from the primary HAT reaction. Additional substrates for this secondary enzyme are present in excess, so that the rate-limiting component of the final readout is the HAT reaction. Both α-ketoglutarate dehydrogenase or pyruvate dehydrogenase have been successfully used as the secondary enzyme (15,30). In both cases, α-ketoglutarate or pyruvate is oxidized, while NAD^+ is reduced to produce NADH. This latter product can be continuously monitored by spectrophotometry at 340 nm.

Enzyme-coupled assays have characteristic advantages and disadvantages. They are relatively inexpensive and amenable to higher-throughput set-ups. In the case of NADH readouts, these assays typically require larger amounts of product (low micromolar) for robust detection due to their absorbance-based readout. Like thiol-scavenging HAT assays, enzyme-coupled HAT assays are susceptible to multiple modes of compound-mediated assay interference. Compounds can react with free CoA, depleting substrate for the coupled reaction and producing either a false-negative or false-positive readout depending on the absorbance properties of the compound-CoA adduct. Compounds can also modulate the secondary enzyme. Finally, test compounds can interference with the absorbance readout.

The following are some considerations for enzyme-coupled HAT assays:

- The secondary enzyme reaction should not be rate-limiting, which can be verified by titrating each component of the secondary enzyme system. In many systems, the coupled enzyme is present in much higher concentrations than the primary (target) enzyme.
- Unlike thiol-scavenging HAT assays, DTT and other reducing agents do not typically interfere with the assay readout.
- Ensure each enzyme system components are compatible with one another, as certain HAT substrates (e.g., calf thymus histones) can interfere with previously described secondary reactions (15).
- Both α-ketoglutarate dehydrogenase or pyruvate dehydrogenase are available commercially.
- Reaction buffer should contain all of the necessary substrates and co-factors for the secondary enzyme (e.g., metals, NAD^+). Reaction buffer should be optimized for both the HAT activity and secondary enzyme activity.
- Cloudy solutions or precipitation may interfere with absorbance-based readouts.
- Background controls should be included. For instance, excluding HAT enzyme allows subtraction of non-enzymatic production of CoA. Additional controls can exclude secondary enzyme or various substrates to better characterize background.

Section Summary

There are a variety of technology platforms, each with signature advantages and disadvantages that must be carefully considered when choosing and subsequently optimizing a new HAT assay. Consideration should be given to the nature of the given HAT system being assayed, operator experience, available instrumentation, budget, project timeframe, as well as other factors. Regardless of the primary assay method, at least one orthogonal assay should be performed to confirm true compound-mediated HAT modulation.

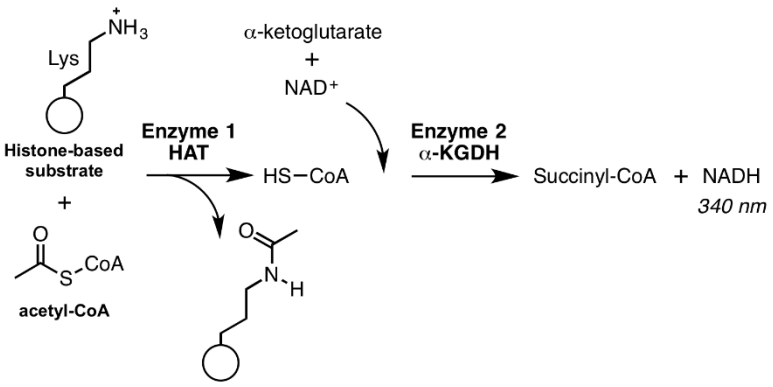

Figure 10. General schematic of enzyme-coupled HAT assays. Free coenzyme A produced by the HAT reaction serves as one of the substrates for a second enzymatic reaction. In the presence of excess co-substrate, the second enzymatic reaction produces a product that can be quantified. In absence of interference, HAT activity is proportional to the secondary enzyme product readout. In this example, the secondary enzyme α-ketoglutarate dehydrogenase (α-KGDH) catalyzes the conversion of free CoA and α-ketoglutarate to succinyl-CoA. The NAD^+ cofactor is reduced to NADH, which is monitored by absorbance at 340 nm. There are several potential areas of compound-mediated readout interference: (A) thiol-scavenging of CoA-SH by electrophilic test compounds; (B), modulation of secondary enzyme activity by test compounds; and (C), light-based interference by test compounds.

Cell-Based HAT Assays

Introduction

Several cell-based HAT assays have been reported, most of which quantify histone acetylation through antibodies targeted acetylated histone lysine products. This section briefly describes common approaches to assaying HAT activity in cellular systems, as well as recommendations for their interpretation.

Cell-Based HAT Assays

Cell-based HAT assays assess the effect of test compounds on HAT activity in the cellular context. Most cellular HAT assays involve treating cells with test compound, followed by either (a) fixing treated cells and measuring histone acetylation by immunohistochemistry, or (b) lysing treated cells and measuring histone acetylation by an antibody-based method (e.g., ELISA, Western blot, and now Alpha-based technology) (**Figure 11**). Histone acetylation is usually normalized to total histone content or cell number. More recent approaches involve live-cell imaging that links an acetylated histone recognition system (e.g., bromodomain) with a reporter-linked histone substrate (**Figure 11**). These latter approaches require transfection of engineered reporter constructs. In principle, analysis of cellular histone isolates can also be performed by MS, though such methods are generally not readily adaptable to quantitative or high-throughput analyses.

Unlike most biochemical HAT assays, histone acetylation in cellular systems is confounded by multiple variables, including HAT expression, histone deacetylase activity, histone chaperones, cell cycle effects, and rates of histone synthesis and degradation. Due to the complexities of these higher-order systems and the inherent properties of current detection technologies, many cell-based assays have smaller dynamic ranges and decreased precision than simpler biochemical assays. For these reasons, those performing cell-based HAT assays should carefully evaluate intra- and inter-assay precision and accuracy.

Interpretation of Cell-Based HAT Assays

Many well-characterized promiscuous compounds (including known thiol-reactive, redox-active, and/or aggregators) can disrupt cell proliferation and histone acetylation in cells at low-to-mid micromolar compound concentrations, raising the strong possibility that certain histone acetylation readouts are also susceptible to off-

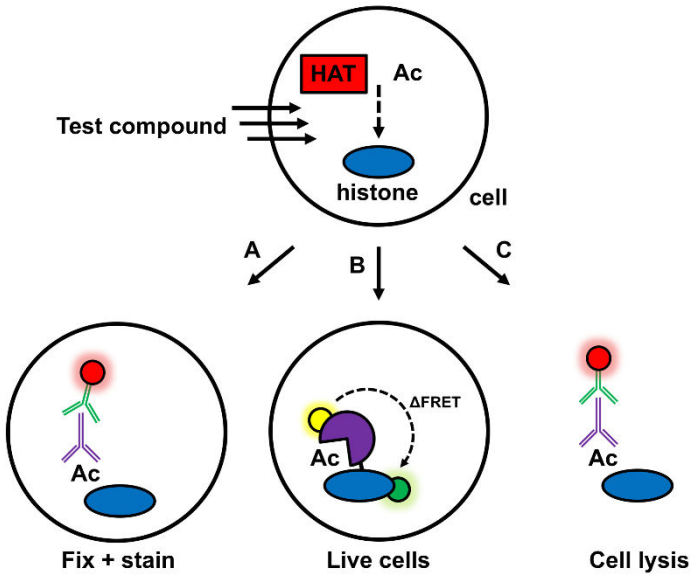

Figure 11. Schematic of representative cell-based HAT assays. Cells are incubated with test compound. (A) Cells can be fixed in preservative and analyzed by immunohistochemistry and related techniques. (B) HAT activity can be monitored in real-time with the introduction of special constructs, such as FRET-based systems. (C) Cells can be lysed, and histones can be probed for acetylation by antibody-based approaches, as well as mass spectrometry. Cell-based readouts should be interpreted with certain cautions (see main text).

targets (36). Therefore, caution is advised when interpreting such cell-based readouts, especially with chemical matter not sufficiently optimized or characterized for potency and selectivity. With nonspecific compounds, it is unclear whether changes in histone acetylation and other phenotypes are due to specific HAT engagement or off-target effects. It is likely that cellular HAT readouts are more interpretable with compounds possessing sufficient potency and selectivity (43).

The following are some cautions when interpreting cell-based HAT assay readouts:

- *HAT/substrate overlap*. HATs often have multiple substrates, and conversely, many histone modifications are catalyzed by more than one HAT. Changes in a particular histone acetylation after compound treatment may be due to simple engagement of the intended HAT. However, histone acetylation may be due to engagement of other HATs with overlapping substrate specificities.
- *Deacetylase activity*. Cellular histone acetylation exists in dynamic equilibrium between acetyltransferases and deacetylases. Histone acetylation can be reversed by HDACs and sitruins with deacetylase activity. One should carefully consider the effects of test compounds on HDAC/sirtuin activity in cellular systems.
- *Controlling for HDAC activity*. To control for HDAC activity, some researchers treat cells with HDAC inhibitors such as suberanilohydroxamic acid (SAHA) or trichostatin A (TSA). If employing this approach, one must consider the effects of HDAC inhibition in the context of the assay readout.
- *Sensitivity/acetylated histone content.* Depending on the experimental system including the specific histone acetylation, the concentration of analyte can be very low. One approach to increase measureable acetylated histones is to treat cells with HDAC inhibitors. As above, if employing this approach, again one must consider the effects of HDAC inhibition when interpreting the assay readout.
- *Cell cycle dependence*. Certain HATs and histone PTMs are cell-cycle dependent in their expression and activity. Furthermore, overall nucleosome content is cell-cycle dependent. Depending on the context, cell synchronization or cell cycle analyses may be necessary.

- *Cell proliferation*. Modulation of certain HATs can decrease cell proliferation and induce apoptosis. Decreases in cell proliferation or induction of apoptosis are not necessarily direct evidence of actual HAT engagement, and may be due to general compound toxicity.
- *Indirect readouts*. Due to complex cellular dynamics, histone acetylation is still an indirect marker of HAT engagement by a compound. Demonstrating direct target engagement in the cellular context generally requires sophisticated methodologies such as CETSA, radiolabeled compound, or chemical proteomics.

Section Summary

Compound modulation of HAT activity should be verified in a cell-based system. Due to the complex regulation of histone acetylation, changes in bulk as well as specific cellular histone acetylation may not always be attributable to a direct compound-HAT interaction. Subsequent efforts should be made to characterize direct target engagement and specificity in the cellular context using orthogonal methods (e.g. CETSA, compound-labeling).

Miscellaneous Considerations

The following are several miscellaneous considerations that may be especially useful in establishing and validating HAT assays:

- The relative order of compound and reagent addition may have significant effects on assay performance. It can affect enzymatic activity by altering HAT or substrate stability, for instance (40). Experiment with several configurations during assay development and even later mechanistic studies with promising lead compounds.
- For assays utilizing affinity tags, we recommend experimenting with several different tags, tag locations (i.e., *N*-terminal or *C*-terminal), and linkages. Often the optimal tag set-up is difficult to predict, and is best determined experimentally.
- Whenever possible use the highest quality reagents possible.

Conclusions

HATs are an emerging class of epigenetic targets in drug discovery and chemical probe development. Modulation of HAT activity by small molecules can be assayed by multiple orthogonal platforms, many of which are amenable to high-throughput formats. Designing robust and cost-effective HAT assays requires careful optimization of multiple experimental parameters. Identifying chemical matter capable of modulating HATs by tractable, useful mechanisms also requires well-designed orthogonal assays and counter-screens. Scientists investigating the effect of small molecules on HAT activity should incorporate the aforementioned strategies and principles into their assay design.

Acknowledgements

JLD acknowledges Dr. Thomas D. Chung for helpful discussions regarding enzyme kinetics.

Conflict of Interest Statement

The authors declare no financial conflicts of interest.

Suggesting Readings (alphabetical order)

1. Berndsen, C. E.; Denu, J. M. *Methods*, **2005**, *36*, 321.

A well-written walkthrough of filter-binding and enzyme-coupled HAT assays.

2. Dahlin, J.L., Nelson, K.M., Strasser, J.M., Barsyte-Lovejoy, D., Szewczyk, M.M., Organ, S., Cuellar, M., Singh, G., Shrimp, J.H., Nguyen, N., Meier, J.L., Arrowsmith, C.H., Brown, P.J., Baell, J.B., Walters, M.A. Assay interference and off-target liabilities of reported histone acetyltransferase inhibitors. Nat. Commun. **2017**;*8*:1527.

   Characterizes assay interference and off-target liabilities in many reported HAT inhibitors. Many widely used HAT inhibitors demonstrated nonspecific thiol reactivity, formed aggregates, and poor biochemical selectivity. Many also disrupted cell proliferation and histone acetylation similarly to several known promiscuous/interference compounds.

3. Dahlin, J. L.; Nissink, J. W. M.; Strasser, J. M.; Francis, S.; Zhou, H.; Zhang, Z.; Walters, M. *J. Med. Chem.* **2015**, *58*, 2091.

   Illustrative example regarding the limitations of fluorometric HAT assays. Describes the use of relevant counter-screens and other important concepts in HTS triage.

4. Falk, H.; Connor, T.; Yang, H.; Loft, K. J.; Alcindor, J. L.; Nikolakopoulos, G.; Surjadi, R. N.; Bentley, J. D.; Hattarki, M. K.; Dolezal, O.; Murphy, J. M.; Monahan, B. J.; Peat, T. S.; Thomas, T.; Baell, J. B.; Parisot, J. P.; Street, I.F. *J. Biomol. Screen.* **2011**, *16*, 1196.

   An excellent description on the adaptation of AlphaScreen technology to assay HATs in an HTS format, as well as describing assay-specific artifacts.

5. Lasko, L.M., Jakob, C.G., Edalji, R.P., Qiu, W., Montgomery, D., Digiammarino, E.L., Hansen, T.M., Risi, R.M., Frey, R., Manaves, V., Shaw, B., Algire, M., Hessler, P., Lam, L.T., Uziel, T., Faivre, E., Ferguson, D., Buchanan, F.G., Martin, R.L., Torrent, M., Chiang, G.G., Karukurichi, K., Langston, J.W., Weinert, B.T., Choudhary, C., de Vries, P., Van Drie, J.H., McElligott, D., Kesicki, E., Marmorstein, R., Sun, C., Cole, P.A., Rosenberg, S.H., Michaelides, M.R., Lai, A., Bromberg, K.D. Discovery of a selective catalytic p300/CBP inhibitor that targets lineage-specific tumours. Nature. **2017**;*550*:128–132.

   An elegant report of the discovery and optimization of A-485, a first-in-class potent, specific small-molecule inhibitor of p300/CBP with nanomolar cellular activity and *in vivo* activity.

6. Lopes da Rosa, J.; Bajaj, V.; Spoonamore, J.; Kaufman, P. D. *Bioorg. Med. Chem. Lett.* **2013**, *23*, 2853.

   Another example highlighting the challenges of fluorometric HAT assays. Describes several relevant orthogonal assays, counter-screens, and post-HTS mechanistic experiments.

7. Ngo, L.; Wu, J.; Yang, C.; Zheng, Y.G. *ASSAY Drug Dev. Technol.* **2015**, *13*, 210.

   An excellent example of SPA method development and troubleshooting.

8. Sorum, A. W.; Shrimp, J. H.; Roberts, A. M.; Montgomery, D. C.; Tiwari, N. K.; Lal-Nag, M.; Simeonov, A.; Jadhav, A.; Meier, J. L. *ACS Chem. Biol.* **2016**, *11*, 734.

   Describes the application of microfluidics to assay HAT activity.

References

1. Grunstein M. Histone acetylation in chromatin structure and transcription. Nature. 1997;389:349–352. PubMed PMID: 9311776.
2. Strahl B., Allis C. The language of covalent histone modifications. Nature. 2000;403:41–45. PubMed PMID: 10638745.

3. Roelfsema J., Peters D. Rubinstein-Taybi syndrome: clinical and molecular overview. Exp. Rev. Mol. Med. 2007;9:1–16. PubMed PMID: 17942008.
4. Furdas S., Kannan S., Sippl W., Jung M. Small molecule inhibitors of histone acetyltransferases as epigenetic tools and drug candidates. Arch. Pharm. (Weinheim). 2012;346:7–21. PubMed PMID: 22234972.
5. Simon R. P., Robaa D., Alhalabi Z., Sippl W., Jung M. KATching-up on small molecule modulators of lysine acetyltransferases. J. Med. Chem. 2016;59:1249–1270. PubMed PMID: 26701186.
6. Fiorentino F., Mai A., Rotili D. Lysine acetyltransferase inhibitors: structure-activity relationships and potential therapeutic implications. Future Med. Chem. 2018;10:1067–1091. PubMed PMID: 29676588.
7. Wapenaar H., Dekker F. Histone acetyltransferases: challenges in targeting bi-substrate enzymes. Clin. Epigenetics. 2016.:8. PubMed PMID: 27231488.
8. Karanam B., Jiang L., Wang L., Kelleher N., Cole P. Kinetic and mass spectrometric analysis of p300 histone acetyltransferase domain autoacetylation. J. Biol. Chem. 2006;281:40292–40301. PubMed PMID: 17065153.
9. Burgess R. J., Zhang Z. Histone chaperones in nucleosome assembly and human disease. Nat. Struct. Mol. Biol. 2013;20:14–22. PubMed PMID: 23288364.
10. Dahlin J. L., Sinville R., Solberg J., Zhou H., Francis S., Strasser J., John K., Hook D. J., Walters M. A., Zhang Z. A cell-free fluorometric high-throughput screen for inhibitors of Rtt109-catalyzed histone acetylation. PLOS ONE. 2013;8:e78877. PubMed PMID: 24260132.
11. Lopes da Rosa J., Bajaj V., Spoonamore J., Kaufman P. D. A small molecule inhibitor of fungal histone acetyltransferase Rtt109. Bioorg. Med. Chem. Lett. 2013;23:2853–2859. PubMed PMID: 23587423.
12. Gao T., Yang C., Zheng Y. G. Comparative studies of thiol-sensitive fluorogenic probes for HAT assays. Anal. Bioanal. Chem. 2012;405:1361–1371. PubMed PMID: 23138472.
13. Trievel R. C., Li F. Y., Marmorstein R. Application of a fluorescent histone acetyltransferase assay to probe the substrate specificity of the human p300/CBP-associated factor. Anal. Biochem. 2000;287:319–328. PubMed PMID: 11112280.
14. Chung C. C., Ohwaki K., Schneeweis J. E., Stec E., Varnerin J. P., Goudreau P. N., Chang A., Cassaday J., Yang L., Yamakawa T., Kornienko O., Hodder P., Inglese J., Ferrer M., Strulovici B., Kusunoki J., Tota M. R., Takagi T. A fluorescence-based thiol quantification assay for ultra-high-throughput screening for inhibitors of coenzyme A production. ASSAY Drug Dev. Technol. 2008;6:361–374. PubMed PMID: 18452391.
15. Kim Y., Tanner K. G., Denu J. M. A continuous, nonradioactive assay for histone acetyltransferases. Anal. Biochem. 2000;280:308–314. PubMed PMID: 10790315.
16. Dahlin J. L., Nissink J. W. M., Francis S., Strasser J., John K., Zhang Z., Walters M. A. Post-HTS case report and structural alert: promiscuous 4-aroyl-1,5-disubstituted-3-hydroxy-2*H*-pyrrol-2-one actives verified by ALARM NMR. Bioorg. Med. Chem. Lett. 2015;25:4740–4752. PubMed PMID: 26318992.
17. Dahlin J. L., Nissink J. W. M., Strasser J. M., Francis S., Zhou H., Zhang Z., Walters M. A. PAINS in the assay: chemical mechanisms of assay interference and promiscuous enzymatic inhibition observed during a sulfhydryl-scavenging HTS. J. Med. Chem. 2015;58:2091–2113. PubMed PMID: 25634295.
18. Ait-Si-Ali S., Ramirez S., Robin P., Trouche D., Harel-Bellan A. A rapid and sensitive assay for histone acetyl-transferase activity. Nucleic Acids Res. 1998;26:3869–3870. PubMed PMID: 9685509.
19. Falk H., Connor T., Yang H., Loft K. J., Alcindor J. L., Nikolakopoulos G., Surjadi R., Bentley J., Hattarki M., Dolezal O., Murphy J., Monahan B., Peat T., Thomas T., Baell J., Parisot J., Street I. An efficient high-throughput screening method for MYST family acetyltransferases, a new class of epigenetic drug targets. J. Biomol. Screen. 2011;16:1196–1205. PubMed PMID: 22086725.
20. Michaelides, M.; Hansen, T.; Dai, Y.; Zhu, G.; Frey, R.; Gong, J.; Penning, T.; Curtin, M.; McClellan, W.; Clark, R.; Torrent, M.; Mastracchio, A.; Kesicki, E. A.; Kluge, A. F.; Patane, M. A.; Van Drie, J. H., Jr.; Ji, Z.; Lai, C. C.; Wang, C. Spirocyclic compound as HAT inhibitors and their preparation. 2016.
21. Sorum A. W., Shrimp J. H., Roberts A. M., Montgomery D. C., Tiwari N. K., Lal-Nag M., Simeonov A., Jadhav A., Meier J. L. Microfluidic mobility shift profiling of lysine acetyltransferases enables screening and mechanistic analysis of cellular acetylation inhibitors. ACS Chem. Biol. 2015;11:734–741. PubMed PMID: 26428393.

22. Fanslau C., Pedicord D., Nagulapalli S., Gray H., Pang S., Jayaraman L., Lippy J., Blat Y. An electrophoretic mobility shift assay for the identification and kinetic analysis of acetyl transferase inhibitors. Anal. Biochem. 2010;402:65–68. PubMed PMID: 20338149.
23. Rye P. T., Frick L. E., Ozbal C. C., Lamarr W. A. Advances in label-free screening approaches for studying histone acetyltransferases. J. Biomol. Screen. 2011;16:1186–1195. PubMed PMID: 21908798.
24. Wu S., Liu B. Application of scintillation proximity assay in drug discovery. BioDrugs. 2005;19:383–392. PubMed PMID: 16392890.
25. Zheng W., Carroll S. S., Inglese J., Graves R., Howells L., Strulovici B. Miniaturization of a hepatitis C virus RNA polymerase assay using a −102°C cooled CCD camera-based imaging system. Anal. Biochem. 2001;290:214–220. PubMed PMID: 11237322.
26. Turlais F., Hardcastle A., Rowlands M., Newbatt Y., Bannister A., Kouzarides T., Workman P., Aherne G. W. High-throughput screening for identification of small molecule inhibitors of histone acetyltransferases using scintillating microplates (FlashPlate). Anal. Biochem. 2001;298:62–68. PubMed PMID: 11673896.
27. Kesicki, E. A.; Wang, C.; Patane, M. A.; Kluge, A. F.; Van Drie, J. H., Jr. HAT inhibitors and methods for their use. 2016.
28. Kesicki, E. A.; Kluge, A. F.; Patane, M. A.; Van Drie, J. H., Jr.; Wang, C. HAT inhibitors and methods for their use. 2016.
29. Marmorstein R. Biochemical and structural characterization of recombinant histone acetyltransferase proteins. Methods Enzymol. 2004;376:106–119. PubMed PMID: 14975301.
30. Berndsen C. E., Denu J. M. Assays for mechanistic investigations of protein/histone acetyltransferases. Methods. 2005;36:321–331. PubMed PMID: 16085424.
31. Dahlin J. L., Chen X., Walters M. A., Zhang Z. Histone-modifying enzymes, histone modifications and histone chaperones in nucleosome assembly: lessons learned from Rtt109 histone acetyltransferases. Crit. Rev. Biochem. Mol. Biol. 2015;50:31–53. PubMed PMID: 25365782.
32. Shechter D., Dormann H., Allis C., Hake S. Extraction, purification and analysis of histones. Nat. Protoc. 2007;2:1445–1457. PubMed PMID: 17545981.
33. Rodriguez-Collazo P., Leuba S. H., Zlatanova J. Robust methods for purification of histones from cultured mammalian cells with the preservation of their native modifications. Nucleic Acids Res. 2009;37:e81. PubMed PMID: 19443446.
34. Klinker H., Haas C., Harrer N., Becker P., Mueller-Planitz F. Rapid purification of recombinant histones. PLOS ONE. 2014;9:e104029. PubMed PMID: 25090252.
35. Tanaka Y., Tawaramoto-Sasanuma M., Kawaguchi S., Ohta T., Yoda K., Kurumizaka H., Yokoyama S. Expression and purification of recombinant human histones. Methods. 2004;33:3–11. PubMed PMID: 15039081.
36. Dahlin J. L., Nelson K. M., Strasser J. M., Barsyte-Lovejoy D., Szewczyk M. M., Organ S., Cuellar M., Singh G., Shrimp J. H., Nguyen N., Meier J. L., Arrowsmith C. H., Brown P. J., Baell J. B., Walters M. A. Assay interference and off-target liabilities of reported histone acetyltransferase inhibitors. Nat. Commun. 2017;8:1527. PubMed PMID: 29142305.
37. Johnston P. A., Soares K. M., Shinde S. N., Foster C. A., Shun T. Y., Takyi H. K., Wipf P., Lazo J. Development of a 384-well colorimetric assay to quantify hydrogen peroxide generated by the redox cycling of compounds in the presence of reducing agents. ASSAY Drug Dev. Technol. 2008;6:505–518. PubMed PMID: 18699726.
38. Soares K. M., Blackmon N., Shun T. Y., Shinde S. N., Takyi H. K., Wipf P., Lazo J., Johnston P. Profiling the NIH Small Molecule Repository for compounds that generate H_2O_2 by redox cycling in reducing environments. ASSAY Drug Dev. Technol. 2010;8:152–174. PubMed PMID: 20070233.
39. McGovern S. L., Caselli E., Grigorieff N., Shoichet B. K. A common mechanism underlying promiscuous inhibitors from virtual and high-throughput screening. J. Med. Chem. 2002;45:1712–1722. PubMed PMID: 11931626.
40. Copeland, R. *Evaluation of enzyme inhibitors in drug discovery*. John Wiley & Sons: Hoboken, NJ, 2005.

41. Balasubramanyam K., Swaminathan V., Ranganathan A., Kundu T. K. Small molecule modulators of histone acetyltransferase p300. J. Biol. Chem. 2003;278:19134–19140. PubMed PMID: 12624111.
42. Baell J., Miao W. Histone acetyltransferase inhibitors: where art thou? Future Med. Chem. 2016;8:1525–1528. PubMed PMID: 27557114.
43. Lasko L. M., Jakob C. G., Edalji R. P., Qiu W., Montgomery D., Digiammarino E. L., Hansen T. M., Risi R. M., Frey R., Manaves V., Shaw B., Algire M., Hessler P., Lam L. T., Uziel T., Faivre E., Ferguson D., Buchanan F. G., Martin R. L., Torrent M., Chiang G. G., Karukurichi K., Langston J. W., Weinert B. T., Choudhary C., de Vries P., Van Drie J. H., McElligott D., Kesicki E., Marmorstein R., Sun C., Cole P. A., Rosenberg S. H., Michaelides M. R., Lai A., Bromberg K. D. Discovery of a selective catalytic p300/CBP inhibitor that targets lineage-specific tumours. Nature. 2017;550:128–132. PubMed PMID: 28953875.
44. Jadhav A., Ferreira R. S., Klumpp C., Mott B. T., Austin C. P., Inglese J., Thomas C. J., Maloney D. J., Shoichet B. K., Simeonov A. Quantitative analyses of aggregation, autofluorescence, and reactivity artifacts in a screen for inhibitors of a thiol protease. J. Med. Chem. 2010;53:37–51. PubMed PMID: 19908840.
45. Thorne N., Auld D. S., Inglese J. Apparent activity in high-throughput screening: origins of compound-dependent assay interference. Curr. Opin. Chem. Biol. 2010;14:315–324. PubMed PMID: 20417149.
46. Lau O. D., Kundu T. K., Soccio R. E., Ait-Si-Ali S., Khalil E. M., Vassilev A., Wolffe A. P., Nakatani Y., Roeder R. G., Cole P. A. HATs off: selective synthetic inhibitors of the histone acetyltransferases p300 and PCAF. Mol. Cell. 2000;5:589–595. PubMed PMID: 10882143.
47. Zheng Y., Balasubramanyam K., Cebrat M., Buck D., Guidez F., Zelent A., Alani R. M., Cole P. A. Synthesis and evaluation of a potent and selective cell-permeable p300 histone acetyltransferase inhibitor. J. Am. Chem. Soc. 2005;127:17182–17183. PubMed PMID: 16332055.
48. Bowers E. M., Yan G., Mukherjee C., Orry A., Wang L., Holbert M. A., Crump N. T., Hazzalin C. A., Liszczak G., Yuan H., Larocca C., Saldanha S. A., Abagyan R., Sun Y., Meyers D. J., Marmorstein R., Mahadevan L. C., Alani R. M., Cole P. A. Virtual ligand screening of the p300/CBP histone acetyltransferase: identification of a selective small molecule inhibitor. Chem. Biol. 2010;17:471–482. PubMed PMID: 20534345.
49. Balasubramanyam K., Varier R. A., Altaf M., Swaminathan V., Siddappa N. B., Ranga U., Kundu T. K. Curcumin, a novel p300/CREB-binding protein-specific inhibitor of acetyltransferase, represses the acetylation of histone/nonhistone proteins and histone acetyltransferase-dependent chromatin transcription. J. Biol. Chem. 2004;279:51163–51171. PubMed PMID: 15383533.
50. Balasubramanyam K., Altaf M., Varier R., Swaminathan V., Ravindran A., Sadhale P., Kundu T. Polyisoprenylated benzophenone, garcinol, a natural histone acetyltransferase inhibitor, represses chromatin transcription and alters global gene expression. J. Biol. Chem. 2004;279:33716–33726. PubMed PMID: 15155757.
51. Yang H., Pinello C., Luo J., Li D., Wang Y., Zhao L., Jahn S., Saldanha S., Chase P., Planck J., Geary K., Ma H., Law B., Roush W., Hodder P., Liao D. Small-molecule inhibitors of acetyltransferase p300 identified by high-throughput screening are potent anticancer agents. Mol. Cancer. Ther. 2013;12:610–620. PubMed PMID: 23625935.
52. Biel M., Kretsovali A., Karatzali E., Papamatheakis J., Giannis A. Design, synthesis and biological evaluation of a small molecule inhibitor of the histone acetyltransferase Gcn5. Angew. Chem. Int. Ed. 2004;43:3974–3976. PubMed PMID: 15274229.
53. Coffey K., Blackburn T. J., Cook S., Golding B. T., Griffin R. J., Hardcastle I. R., Hewitt L., Huberman K., McNeill H. V., Newell D. R., Roche C., Ryan-Munden C. A., Watson A., Robson C. N. Characterisation of a Tip60 specific inhibitor, NU9056, in prostate cancer. PLOS ONE. 2012;7:e45539. PubMed PMID: 23056207.
54. Aldrich C., Bertozzi C., Georg G., Kiessling L., Lindsley C., Liotta D., Merz K. J., Schepartz A., Wang S. The ecstasy and agony of assay interference compounds. J. Med. Chem. 2017;60:2165–2168. PubMed PMID: 28244745.
55. Zhang J., Chung T., Oldenburg K. A simple statistical parameter for use in evaluation and validation of high throughput screening assays. J. Biomol. Screen. 1999;4:67–73. PubMed PMID: 10838414.

56. Eastwood, B.; Farmen, M.; Iversen, P.; Craft, T.; Smallwood, J.; Garbison, K.; Delapp, N.; Smith, G. The minimum significant ratio: a statistical parameter to characterize the reproducibility of potency estimates from concentration-response assays and estimation by replicate-experiment studies. *J. Biomol. Screen.* **2--6,** 11, 253-261.
57. Horiuchi K., Fujimoto D. Use of phospho-cellulose paper disks for the assay of histone acetyltransferase. Anal. Biochem. 1975;69:491–496. PubMed PMID: 1217715.
58. Ngo L., Wu J., Yang C., Zheng Y. G. Effective quenchers are required to eliminate the interference of substrate: cofactor binding in the HAT scintillation proximity assay. ASSAY Drug Dev. Technol. 2015;13:210–220. PubMed PMID: 26065557.
59. Glickman J., Schmid A., Ferrand S. Scintillation proximity assays in high-throughput screening. ASSAY Drug Dev. Technol. 2008;6:433–455. PubMed PMID: 18593378.
60. Poveda A., Sendra R. An easy assay for histone acetyltransferase activity using a PhosphorImager. Anal. Biochem. 2008;383:296–300. PubMed PMID: 18805389.
61. Han J., Zhou H., Horazdovsky B., Zhang K., Xu R.-M., Zhang Z. Rtt109 acetylates histone H3 lysine 56 and functions in DNA replication. Science. 2007;315:653–655. PubMed PMID: 17272723.
62. Allis C., Chicoine L., Glover C., White E., Gorovsky M. Enzyme activity dot blots: a rapid and convenient assay for acetyltransferase or protein kinase activity immobilized on nitrocellulose. Anal. Biochem. 1986;159:58–66. PubMed PMID: 3468811.
63. Pal S., Graves H., Ohsawa R., Huang T., Wang P., Harmacek L., Tyler J. The commercial antibodies widely used to measure H3 K56 acetylation are non-specific in human and drosophila cells. PLOS ONE. 2016;11:e0155409. PubMed PMID: 27187594.
64. Drogaris P., Villeneuve V., Pomies C., Lee E.-H., Bourdeau V., Bonneil E., Ferbeyre G., Verreault A., Thibaulta P. Histone deacetylase inhibitors globally enhance H3/H4 tail acetylation without affecting H3 lysine 56 acetylation. Sci. Rep. 2012;2:220. PubMed PMID: 22355734.
65. Shafer D. E., Inman J. K., Lees A. Reaction of Tris(2-carboxyethyl)phosphine (TCEP) with maleimide and alpha-haloacyl groups: anomalous elution of TCEP by gel filtration. Anal. Biochem. 2000;282:161–164. PubMed PMID: 10860517.
66. Khan M. Kinetics and mechanism of the alkaline hydrolysis of maleimide. J. Pharm. Sci. 1984;73:1767–1771. PubMed PMID: 6527252.
67. Shrimp J. H., Sorum A. W., Garlick J. M., Guasch L., Nicklaus M. C., Meier J. L. Characterizing the covalent targets of a small molecule inhibitor of the lysine acetyltransferase p300. ACS Med. Chem. Lett. 2015;7:151–155. PubMed PMID: 26985290.
68. Annesley T. Ion suppression in mass spectrometry. Clin Chem. 2003;49:1041–1044. PubMed PMID: 12816898.
69. Bernd O. K., Sui J., Youn A. B., Whittal R. M. Interferences and contaminants encountered in modern mass spectrometry. Anal. Chim. Acta. 2008;627:71–81. PubMed PMID: 18790129.
70. Kind T., Fiehn O. Advances in structure elucidation of small molecules using mass spectrometry. Bioanal. Rev. 2010;2:23–60. PubMed PMID: 21289855.
71. Leveridge M., Buxton R., Argyrou A., Francis P., Leavens B., West A., Rees M., Hardwicke P., Bridges A., Ratcliffe S., Chung C. W. Demonstrating enhanced throughput of RapidFire mass spectrometry through multiplexing using the JmjD2d demethylase as a model system. J Biomol Screen. 2014;19:278–286. PubMed PMID: 23896685.
72. Eglen R., Reisine T., Roby P., Rouleau N., Illy C., Bosse R., Bielefeld M. The use of AlphaScreen technology in HTS: current status. Curr. Chem. Genomics. 2008;1:2–10. PubMed PMID: 20161822.
73. Glickman J., Wu X., Mercuri R., Illy C., Bowen B., He Y., Sills M. A comparison of ALPHAScreen, TR-FRET, and TRF as assay methods for FXR nuclear receptors. J. Biomol. Screen. 2002;7:3–10. PubMed PMID: 11897050.
74. Schorpp K., Rothenaigner I., Salmina E., Reinshagen J., Low T., Brenke J. K., Gopalakrishnan J., Tetko I. V., Gul S., Hadian K. Identification of small-molecule frequent hitters from AlphaScreen high-throughput screens. J. Biomol. Screen. 2014;19:715–726. PubMed PMID: 24371213.

75. Brenke J., Salmina E., Ringelstetter L., Dornauer S., Kuzikov M., Rothenaigner I., Schorpp K., Giehler F., Gopalakrishnan J., Kieser A., Gul S., Tetko I., Hadian K. Identification of small-molecule frequent hitters of glutathione *S*-transferase-glutathione Interaction. J. Biomol. Screen. 2016;21:596–607. PubMed PMID: 27044684.
76. Acker M. G., Auld D. S. Considerations for the design and reporting of enzyme assays in high-throughput screening applications. Perspect Sci. 2014;1:56–73.

In Vitro Cell Based Assays

Marcie Glicksman, PhD, Zhuyin Li, PhD, Sarine Markossian, PhD, Terry Riss, PhD, G. Sitta Sittampalam, PhD, O. Joseph Trask, Jr., and Yueming Wang, PhD

Machine Learning and Assay Development for Image-based Phenotypic Profiling of Drug Treatments

Jonathan Z. Sexton, PhD,[1] Reid Fursmidt, MD,[1] Matthew J. O'Meara, PhD,[1] Wienand Omta, PhD,[2] Arvind Rao, PhD,[1] David A. Egan, PhD,[2] and Steven A. Haney, PhD✉

Created: March 15, 2023.

Abstract

High content imaging produces significant volumes of data on individual cells. The number of discrete measurements per cell can be in the thousands for highly multiplexed assays. Typically, one of these measurements is used as the assay metric (as examples: cell cycle phase, post-translational modification of a protein reporter expression, shape change), and one or a few others can be used as counter screen measures (frequently cell death or stress, sometimes activity of an orthogonal pathway). However, the rich data sets from high content studies can be combined using machine learning to integrate many features into an assay metric that can enhance assay performance and increase the information content in a screen, allowing a more judicious choice of hits. This chapter will review the potential benefits of implementing a machine learning approach in screening, including examples of where it provides more information or better hit selection than single metrics. Examples of machine learning in screening design that cover a few of the key methods, including regression analyses, decision trees, linear discriminant analyses and support vector machines are provided. This chapter will emphasize key elements of assay validation, including increasing general reproducibility and robustness through tracking algorithm performance, and linking feature measurements to the underlying biology. The basic role of an assay to identify perturbations that are most similar to a positive control are covered in depth. The ability to identify novel phenotypes, such as encountered in phenotypic profiling or "Cell Painting", are also presented.

Author Affiliations: 1 University of Michigan; Email: jzsexton@umich.edu. 2 Core Life Analytics.

✉ Corresponding author.

Flow Chart

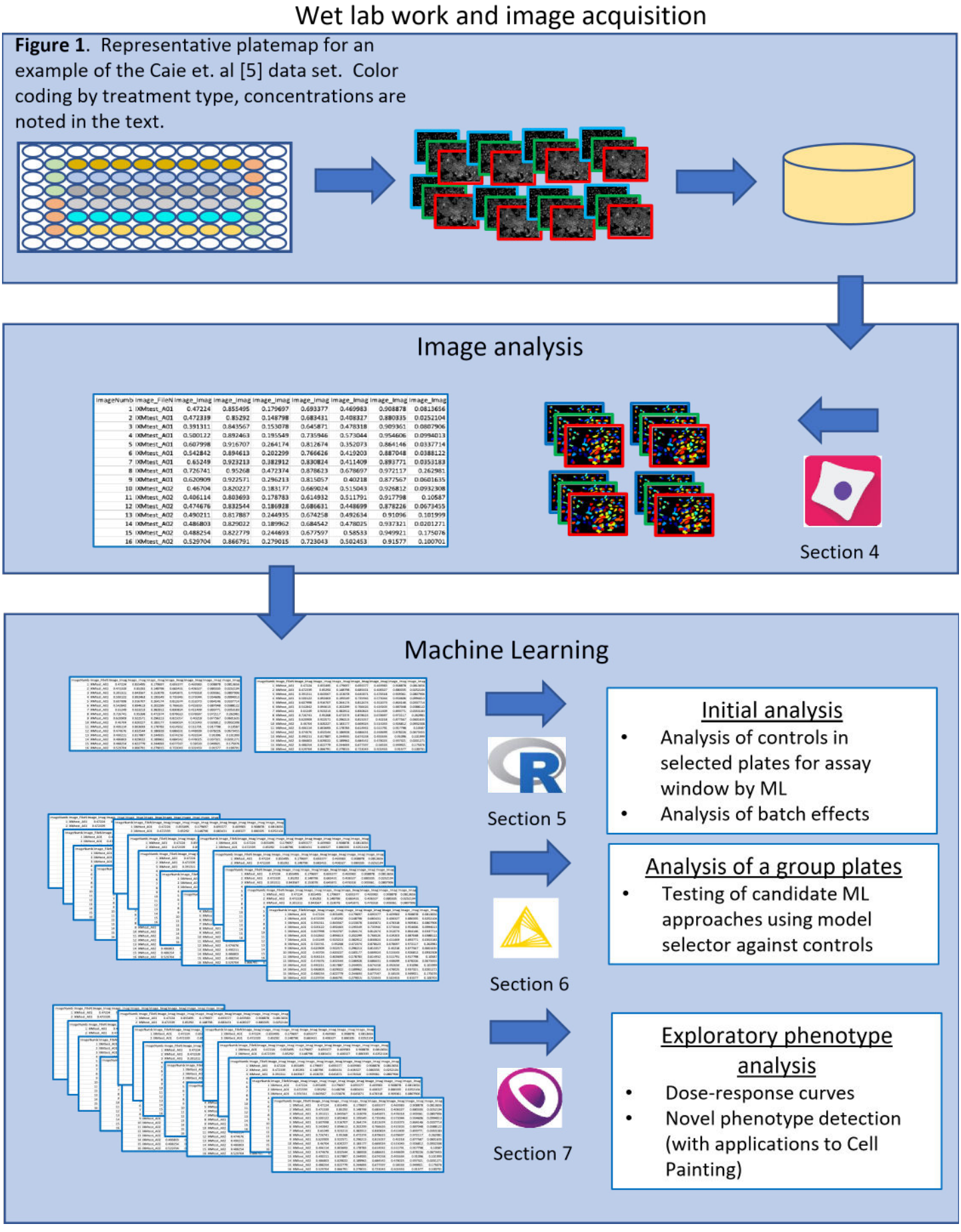
Wet lab work and image acquisition
Figure 1. Representative platemap for an example of the Caie et. al [5] data set. Color coding by treatment type, concentrations are noted in the text.
Image analysis
Section 4
Machine Learning
Section 5
Initial analysis
Analysis of controls in selected plates for assay window by ML
Analysis of batch effects
Section 6
Analysis of a group plates
Testing of candidate ML approaches using model selector against controls
Section 7
Exploratory phenotype analysis
Dose-response curves
Novel phenotype detection (with applications to Cell Painting)

Introduction

Image-based screening has continually challenged researchers by the immense wealth of data available that could be leveraged to learn about cellular responses to therapeutics, probe molecules, genetic perturbations and more (1). Until recently, the limitation has been on the computational side, developing multiple measurements into tractable metrics which elevates the computational burden by 10-1000 fold and can require the support of bioinformaticians. There are conceptual issues in considering the implementation of a machine learning algorithm as a screen, the most significant one being whether it brings enough value to the hit-selection process as opposed to a simple, yet definitive, metric such as nuclear area. In cases where a definitive cellular change can be identified, such as cell death, changes in any one of several features may be enough to differentiate living vs. dead cells (2). There are other cases where the phenotype may be less well summarized by a single feature. One example is cell motility, where protrusions and ruffling of the cell membrane may be a measure of motile index, but may need to be correlated with actin structure, cell size and nuclear morphology for motile cells to be differentiated from stressed or other irrelevant cells. Another example would be cytotoxic compounds that have diverse mechanisms of cell killing. One feature, such as nuclear size, may be common to many of them, but to distinguish between these mechanisms may require additional features. Despite conceptual issues, it is often worth using a machine learning algorithm to enhance the robustness because the performance of a single feature can vary while multivariate scoring systems are generally more stable (3). For example, a fluorescent compound can interfere in one channel and features derived from that channel may be spurious. In this case, a machine learning derived multivariate score that incorporates numerous features from independent fluorescent channels will be more tolerant of failures in single features. Lastly, differentiation (such as from iPSCs) is a morphologically complex process that typically can't be scored on the basis of one or two features.

Machine Learning (ML) is a subset of artificial intelligence (AI) that incorporates independent features to produce a measurement (or metric) for a sample that results from an aggregation of the input features. It is most frequently associated with Supervised Learning (SL) and is a prospective method that evaluates new samples based on an algorithm developed from historical (control) samples. These approaches are usually based on the premise that there is a definition of what the unperturbed and perturbed states look like, and the algorithm evaluates new samples based on these definitions. Since there is a definition of a positive response, ML can score cells as to how much they resemble cells in either the positive or negative controls. As such, this is a prospective analysis, essentially inferring if the next treatment condition will result in cells that look like the positive control. These approaches contrast with Unsupervised Learning (UL) which evaluates a set of samples and defines a number of groups based upon how the treatment phenotypes separate into classes or types. Clustering or principal component methods are generally used in this context as a retrospective analysis to assess how many distinct phenotypes exist in a screen. Clustering can be performed on new samples or the entire data set of old and new samples, but always after the samples have been collected, fixing the feature space before data reduction begins. For our purposes, we will limit ourselves to the approaches that best support screening and assay development, which are classical approaches, but we will also describe some of the hypothesis-free methods that are becoming common.

For this study, we chose a publicly-available data set of small molecule treatments on the MCF-7 breast cancer cell line (4), a widely used model for breast cancer. The study was performed by Neil Carragher and colleagues at AstraZeneca that use this and other cell lines to phenotypically characterize the range of cellular responses to a broad set of cancer drugs (5). They draw from several classes of chemotherapeutics, including DNA damaging agents, cytoskeletal perturbants, metabolic stressors, and other compounds that antagonize cancer cell growth. These drugs act on essential functions for proliferating cells and do so through actions on organelles such as the nucleus, actin and tubulin cytoskeleton networks, and energy metabolism. The cells were plated in the inner 60 wells of a 96 well plate, and an example is shown in Figure 1. The outer two columns are dedicated to positive controls treated with the microtubule stabilizer taxol and vehicle/negative controls. Cells treated with taxol and

the other agents undergo profound changes in morphology in addition to cell death, as shown in Figure 2. The list of compounds used in the 15-plate subset that we use in this chapter is listed in Table 1, the complete list of compounds is much larger.

The goals of this chapter are three-fold:

- Establish a machine learning workflow following image analysis. Software and data preprocessing of image data will be used to explore which features will be used to develop one or more machine learning algorithms. In general, machine learning algorithms benefit from standardization of the data where the means are set to zero (centering), the variance is scaled to 1 (scaling), distributions are corrected for skewness/kurtosis and redundant (highly correlated) features are eliminated. Preliminary algorithms will be trained on 80% of control data and are evaluated through the classification accuracy of a set of the remaining 20% control images. Implementation of the machine learning algorithm to evaluate wells of treated cells in standard assay description and validation procedures (such as assay window, Z' score, and robustness) will be described and demonstrated.
- Development of a conventional assay using machine learning. A conventional assay is one where clear positive and negative controls are used to define assay parameters. The assay described in this chapter is conventional, however, the critical difference is that the response metric is an aggregation of several phenotypic changes rather than a single measure of perturbant effect.
- Phenotypic exploration in the unperturbed and perturbed cellular population. This is an exploratory data analysis approach that can identify novel or unexpected cellular responses such as with the 'cell painting' methods defined by Carpenter and colleagues (6). There is a potential to incorporate a parallel unsupervised approach to identify novel effects in a screen to complement a supervised approach.

Methods and Resources

There are many excellent options for image analysis and algorithm development. For the examples in this chapter, we will focus on CellProfiler, R, Python, Knime, and Stratominer. There is a strong movement towards establishing transparency and rigor in the image analysis process, so the use of open-source applications is very common in the field and proprietary implementations routinely include processes to facilitate transparency and enable reanalysis and experimentation in the development of new image analysis algorithms. We will use both open-source and transparent proprietary platforms in this study. Resources for data and software used in this chapter are:

Image Sets for Method Development and Algorithm Evaluation

a. Broad Bioimage Benchmark Collection (BBBC): The BBBC is a collection of image sets, many from published studies, that can be downloaded and used as learning examples for researchers to gain familiarity with image analysis. Image sets include metadata to identify samples and frequently include model pipelines written in CellProfiler and ground truth assessments (7).
b. Image Data Resource (IDR): The IDR enables the review of large data sets, including raw images, ground truth and identified ROI's (where annotated) and is searchable by laboratory, study, cell type, perturbation, etc. It should be noted that image sets cannot be downloaded directly from the IDR, but contact information for the group uploading the images is available and the resource is used widely (8).

Software

a. CellProfiler and CellProfiler Analyst: Open-source software for image analysis. CellProfiler can accept images and metadata to segment and quantify intensity, shape and textural features of cells and produces output in csv files, sqlite files or can write results directly to a database. The output can be used by CellProfiler Analyst (CPA) or other data analysis software, including R and Python. CPA provides tools

DMSO	latruculin B_3000	latruculin B_1000	latruculin B_3000	latruculin B_1000	latruculin B_300	latruculin B_100	latruculin B_30	latruculin B_10	Taxol 300
DMSO	doxirubicin_1000(	doxirubicin_3000	doxirubicin_1000	doxirubicin_300	doxirubicin_100	doxirubicin_30	doxirubicin_10	doxirubicin_3	Taxol 300
DMSO	epothilone B_300	epothilone B_100	epothilone B_300	epothilone B_100	epothilone B_30	epothilone B_10	epothilone B_3	epothilone B_1	Taxol 300
Taxol 300	colchicine_3000	colchicine_1000	colchicine_300	colchicine_100	colchicine_30	colchicine_10	colchicine_3	colchicine_1	DMSO
Taxol 300	monastrol_30000	monastrol_10000	monastrol_3000	monastrol_1000	monastrol_300	monastrol_100	monastrol_30	monastrol_10	DMSO
Taxol 300	AZ-I_30000	AZ-I_10000	AZ-I_3000	AZ-I_1000	AZ-I_300	AZ-I_100	AZ-I_30	AZ-I_10	DMSO

Figure 1 Representative platemap for an example of the Caie et. al [5] data set. Color coding by treatment type, concentrations are noted in the text.

for classifying biological images and exploring and visualizing multidimensional data that has been extracted from CellProfiler. CPA can compare machine learning algorithms for a set of images. The algorithms are based on the Python scikit-learn package, described below (9-12).

b. Fiji/ImageJ: A wide suite of open-source image and file management tools that can analyze images and process data for downstream data analysis and modeling (13-15).
c. R: Open-source statistical software with many supplementary packages for data analysis (including machine learning) and graphic support for data and results. Historically a widely used platform for statisticians, its use has grown due to its expansion into various sciences (particularly biology and bioinformatics, through the Bioconductor platform for transcription profiling, genomics, RNAi screening and some image analysis). It is a command-line, interpreted language, but a GUIinterface that helps manage programming is available (RStudio).
d. Python and Scikit-learn: Open-source data analysis software; the scikit-learn package has become very popular due to the algorithms included and the generally simple nature of programming in Python.
e. Knime Analytics Platform and High Content Screening Tools: An open-source visual and intuitive data analysis software that requires no programming knowledge. The Knime analytics platform is a broadly useful tool for automating data munging and enables non-programmers to conduct sophisticated data analysis. Knime is a graphical data analysis interface that is built upon nodes, which are small, executable, and interchangeable 'boxes' that perform specific tasks. Knime has thousands of nodes covering a variety of fields and functions, allowing for any number of operations to be performed without programming in languages like python, or R (16). Additionally, the HCS-Tools package provides HCS specific tools for visualizing screening data, fitting dose response curves, data normalization and other utilities that is provided by the Max Planck Institute of Molecular Cell Biology and Genetics (MPI-CBG), Dresden, Germany (17).
f. StratoMineR is a cloud-based data analytics platform that guides the user through high content data mining workflows that can be used for phenotypic identification and classification of hits from high content chemical and functional genomic screens. HC StratoMineR is used herein for novel phenotype identification from Cell Painting style phenotypic screens.
g. Orange is an open-source visual data analytics, data mining, visualization and machine learning software from the University of Ljubljana.
h. RapidMiner and WEKALinks?: tools intended to provide a drag-and-drop interface for creating data mining workflows (ranging from feature preprocessing, plugins to permit more nuanced investigations including Bayesian networks, multi-task learning and anomaly detection via SMOTE.
i. Spotfire: A commercial platform for data visualization that is very flexible and robust. Some analysis options and programming capabilities are available but its strengths are in fast and versatile visualizations of large data sets, including grouping and labeling of subsets and integration of layered visualizations. Some HCS-specific functions (HCProfiler) have moved to the proprietary Signals Screening platform from Perkin Elmer.
j. Microsoft Excel (other paths based on region): Commercial but widely adopted software for spreadsheet visualization and analysis. Intended for finance, its statistical tools can be difficult to implement for distributional analyses that are common for image-based data analysis. However, it can be useful

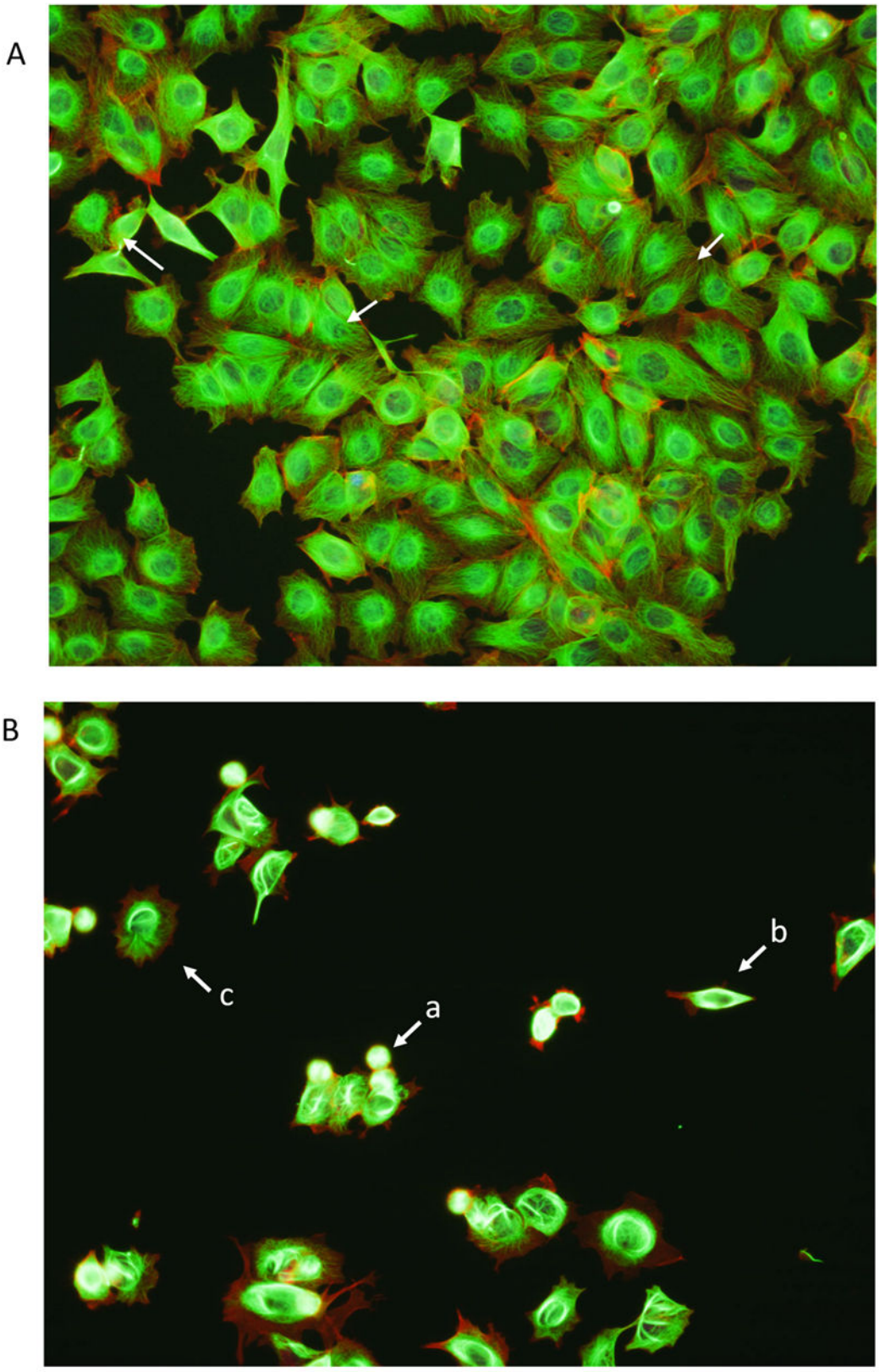

Figure 2 Images from the negative and positive control wells. Composite staining of cells. Wells are uniformly treated with a fixative, permeabilization and cellular staining procedure. In this study, DNA/chromatin is labeled with DAPI, tubulin with Alexa-488/anti b-tubulin IgG1 antibody and Alexa-568-conjugated phalloidin. One field from each of the 12 control wells per plate. Images are 3 color composites of DAPI-treated nuclei (blue), tubulin (green) and actin (red) **A**. Negative control (DMSO vehicle) treated cells. **B**. Positive control taxol treated cells. Multiple differences can be observed relative to the negative control treated cells. These include a reduced

cell number per field/well and abnormal phenotypes including small, rounded cells (a), elongated cells, and larger cells with atypical tubulin structures.

reformatting spreadsheets (e.g. feature selection, renaming columns, summarizing data with pivot tables). There are limits on the size of the spreadsheets that can be loaded, as such it can work well for individual plates and during assay development, but may be unsuitable for screen-level projects where preprocessing of data needs be done in R or Python.

Protocol Overview

Despite significant interest in high content phenotypic profiling and Cell Painting, utilizing the resulting data has presented a significant barrier and most notable publications have come from dedicated informatics groups or experimental groups with dedicated informatics support. An even greater challenge is to perform ML analysis on cell-level data where data tables can be routinely >100Gb, rather than the conventional analysis of well- or field-level averages where subpopulation effects and nuance is easily lost. The democratization of big data analysis has made several tools available so that non-programmers can approach high content phenotypic profiling. Importantly, these tools also allow for the automation of data analysis - a requirement in the screening setting. In this protocol, we present a comprehensive data workflow that uses 1) a publicly available data set, 2) the open-source CellProfiler to generate cell-level data, 3) open-source Knime Analytics Platform to construct the cell-level data table, associate metadata (compound ID and concentration) to each row, perform data centering and scaling, and perform supervised machine learning and model performance evaluation with several algorithms trained against the positive (Taxol) and negative control (DMSO-vehicle) classes, and 4) HC StratoMineR to explore novel phenotypes that are not captured by the machine learning models trained on Taxol treated cells.

The overarching goal of this protocol is to demonstrate a workflow that uses machine learning to build a predictive model that can detect other compounds with a similar mechanism of action to the positive control, Taxol. The publicly available subset of the Caie, et. al (5) data set consists of Hoechst-33342, Tubulin and Actin channels and is 55 plates total, ~40gb of images, 39,600 image files and 13,600 fields (https://bbbc.broadinstitute.org/BBBC021). 113 compounds were profiled at 8 concentrations for 24 hours and Taxol was used as the positive control. CellProfiler (9) was used in this example for segmentation, feature extraction and tabulation of object (nucleus, cell and cytoplasm) level data and the project file / image analysis pipeline is available in supplementary files. Focus scoring was performed prior to image analysis and entire images were rejected if the focus score (as described in Bray (18)) was three standard deviations below the mean focus score. Intensity, texture and granularity were measured for all three object types in their respective images. We then follow up this protocol with a discussion of batch effects and extend the analysis from a narrow detection of Taxol-like compound effects to broader investigation of pharmacologic perturbation using HC StratomineR.

Organization of the Protocol Sections

For this chapter, most methods and protocols involve adapting data processing workflows towards the specific set-up of the individual study. The text follows a tutorial format to describe how to set up each of the steps in the process but invokes specific segments of code to perform these steps. The code, with annotation for making adaptations that are necessary to make the protocols work for individual investigators, are included as supplemental files. The code for each of the segments are identified by protocol numbers. There are three sections to this part of the chapter. The first uses just two plates for the purposes of demonstrating the basic steps in data preprocessing, exploring methods for testing various machine learning algorithms and evaluating results with quality metrics. This is essentially exploratory data analysis for evaluating pilot screening data to inform a larger high content screening campaign. The next section develops the traditional assay that is based positive

and negative controls. It describes how to process multiple plates and track results. The third section introduces methods for evaluating the treatments with the control samples as well but incorporates methods for detecting novel phenotypes.

Image Analysis: Getting from Images to Numbers

All the data analysis in this chapter is based on the analysis of images using the CellProfiler platform (9, 12). The CellProfiler project file is provided in **Supplementary File 1**. Development of image analysis processes is well-documented in other resources, as noted in the Methods and Resources section above, we will describe how the pipeline was developed for this study, but these additional sources are essential for building a general understanding of CellProfiler. It functions to take image files and quantify cellular features, as diagramed in Figure 3.

In conventional high content screening, the goal is typically to answer a directed question (eg: NF-κB translocation to the nucleus) and only a few meaningful cellular features are reported. For more complex assays or assays with subtle phenotypes, the general strategy for developing a robust imaging-based assay is to extract/tabulate as many features as possible from each cell in each field, aggregate by well or treatment condition, and perform data mining. Future steps in data preprocessing will eliminate unimportant or redundant cellular features while maximizing the information content with respect to each cell. General guidelines for performing quantitative image analysis should be followed as described elsewhere. There are several key concerns for generating high-quality data sets for machine learning using image analysis software like CellProfiler for feature extraction.

High quality images lead to more robust image quantitation and the following considerations define high quality images and successful image analysis: **1) signal to noise ratio** – ensuring that images are not underexposed or saturated. **2) appropriate uncompressed image format** – lossy image compression files like JPG/GIFs should be avoided and uncompressed or lossless formats are preferred (TIFF/BMP). **3) Image quality control** – images should be scored for focus/saturation/artifacts and can be eliminated from analysis. Feature extraction from out-of-focus images injects noise into the data set and can lead to complication in analysis. A better approach is to measure the focus score on a per-cell basis with the goal of only extracting features from in-focus cells (18), or by collecting confocal images in 3D and using maximum intensity projection to ensure in-focus cells irrespective of their Z-position. **4) Illumination correction** – most images have some vignette due to the point-source of the illumination resulting in dim edges relative to the center of the image. This can be corrected on the microscope with flat-fielding algorithms using reference images derived from the microscope's specific illumination conditions or can be done after the fact using illumination correction algorithms that calculate and subtract/divide that illumination function from the original image. **5) Ensuring that image metadata is complete** (plateID, wellID, fieldID, treatment, etc) and is extracted directly from the source filename, folder name, and compound/treatment database.

With a high-quality image set, one can begin the image analysis process that starts with the organization of images into sets that emanate from a single location/field, then metadata is extracted and will be associated with the individual cell measurements in the output files. The complete process is described in **Supplementary File 1**. The general steps are:

- **Illumination correction** (if necessary) – there are many algorithms that can perform illumination correction with the goal of flattening the image so that thresholding produces evenly sized objects from the center to the edge of images. One good indication that images need illumination correction is if nuclei appear smaller at the edges than in the middle during object identification. Illumination correction is strongly suggested when measuring per-cell fluorescent intensity features to reduce the positional variability within a field due to inhomogeneous illumination, as small deviations from focus result in large decreases in excitation power density and emission.

- **Object identification** – define regions of interest (ROI) in the image. This typically starts with identifying the "primary object", usually nuclei that are well separated. The secondary object is typically the entire cell, and subtracting the nucleus from the cell yields the cytoplasm as the tertiary object. If subcellular features are necessary (spot identification), they can be handled as another primary object and can be related back to their parent cell.
- **Measurements** are made within regions of interest that are defined in the Object ID step. The general classes of measurements are: **Morphometric** – measure the object size/shape of the ROIs, **Intensity** – measuring the brightness of an image inside the region of interest (e.g., the integrated intensity inside the nuclear mask from a Hoechst/DAPI image is proportional to the DNA concentration), **Texture/ Granularity** – measures the spatial variation of a signal inside the ROI and can give general measurements relating to the smoothness or roughness of the signal, **Signal overlap/colocalization** – the amount to which two signals overlap spatially inside a cell can be tabulated and reported, **Radial Distribution** of signals inside ROIs can be used to gain insight into where a particular probe exists in the cell (e.g., as drug treatment causes the cytoskeleton to contract about the nucleus resulting in an inward shift in the radial distribution. Some terminology or functions are associated with Cell Profiler specifically, but other image analysis systems will make similar measurements.
- **Image analysis quality control** – during the development of an image processing algorithm, it is highly recommended to output an overlay image with the original multichannel color image and the identified objects for manual inspection. This allows for rapid identification of edge-cases where segmentation fails, and parameters must be adjusted for those conditions while maintaining high fidelity in the rest of the data. It is typical to observe spurious object identification in images with debris or with regions of out-of-focus cells.
- **Data Output** for machine learning is best done at the cell/object-level, and summaries/mean values can be easily generated by pivoting on metadata (like by PlateID/WellID to gain well-averaged means for reported features). An incredible amount of information is lost in the reduction of cellular data to mean values and subtleties of populations are lost. Cellular data can be directed to text output in CSV files or can be housed in a database. A typical three-channel data set with nuclei, cells and cytoplasm, and measurements of shape/size, intensity and texture/granularity can yield <500 measurement columns in the output and depending on the number of fields imaged and cell plating density; a single microplate can yield over a million cells/rows.

Supplementary File 1: Cell Profiler Project File

Supplementary File 2: Zipped example images folder

Supplementary File 3: Cell Profiler analysis instructions

Exploratory Data Analysis in Pilot Screening

Initial data review can be confusing and difficult to identify the key features from 100s-1000s of columns. Aside from the scale of imaging data, the data is heterogenous. Machine learning in other fields, such as transcriptomics, metabolomics, electronic health records, and business analytics typically results in homogenous data of a single type, such as the number of times a transcript or fragment is counted. Imaging has been developed to capture a varied set of data types that include intensity, area, shapes (such as ratios of length to width), textures, and counts, which present different scales and units of measure, making integration of these into a multivariate score challenging. There is also considerable redundancy in the data since many measurements are essentially the same thing (measurements that are inversely related with a correlation of -1) or highly correlated (e.g., the mean, median and maximal intensity or the length and area of an object). As such, fairly extensive preprocessing of imaging data is required. To the second point, assay development is firmly based on establishing strongly discriminating measurements between positive and negative controls, typically

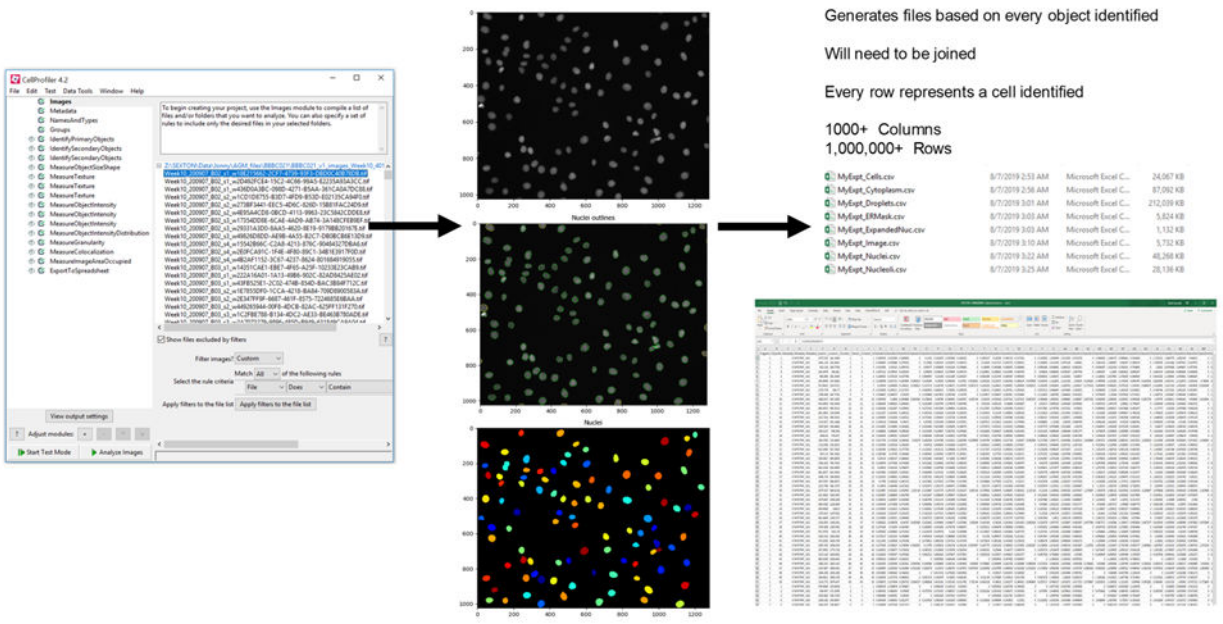

Figure 3 Schematic of using Cell Profiler to generate quantitative data for each of the cells and wells in the screen. From left to right, image sets are loaded into Cell Profiler and the algorithm developed to analyze each of the channels will identify and track each object in a field (center section) and output is tabulated in files (generally one for each channel, to be integrated later, see **Figure 4**).

based on a large signal window and low variance between the replicate measurements. Even in cases where a striking visual change exists (such as in Figure 2), the numerical data for the features at the cell level can be far less persuasive for researchers used to developing robust assays with Z' factors of 0.5 or greater. Despite this heterogeneity and overlap between the treatments, common summary statistics (the mean or median) or statistical tests (t-test or KS statistic) do show good discriminative power. The Z' factor is a different matter, as the overlap between samples typically results in negative scores. The Z' factor is used in this chapter in two contexts for exploratory data analysis and screening plate quality control. In exploratory data analysis, Z'-factor is used as a measurement of effect size between controls instead of its conventional usage for statistical power in calling hits, and negative values should not be interpreted as insufficient. Generally, Z'-factors are lower at cell-level resolution than for well-averaged features due to the reduction of cellular distributions to their simple means. After development of a machine learning scoring algorithm, the Z'-factor can be used to assess plate-to-plate data quality and suitability for hit-calling. This section will cover the steps of preprocessing and reviewing the data of a single plate, as would be performed during assay development and exploration of multivariate data analysis options.

Overview and Basic Preparation

Any image analysis and algorithm development process needs to be specifically adapted to the resources and computational architecture used by the individual laboratory. For the purposes at the pilot screen level (1-2 plates for basic assay development), we describe how these steps were performed and provide scripts (protocols) for reproducing them. All these steps can be performed on a reasonably recent laptop computer (16Gb memory, 2-4GHz processor with 2-4 cores, 256 Gb or more storage). All data is captured in one or more data files (usually comma separated value, or CSV, files). Data from a single plate can be opened in Excel for review, but as the screen progresses to several plates, automated data workflows using applications such as Knime/R/Python/Stratominer, etc., become required. Nevertheless, the first stages of reviewing data are typically performed at the single-plate level, so reviewing features in Excel is tractable. To prepare the pilot data set for this study, we have concatenated data from two plates into a single file. Each image is analyzed by three labels, so a total of six files need to be joined. A schematic for this is shown in Figure 4. Figure 4A represents staining of cells for each of the

three labels. In fact, all labels are captured in gray scale for each fluor individually, so Figure 4B is a more accurate representation of how image acquisition occurs. Image analysis results in the tables of data. Figure 4C highlights how the analysis generates files for each label and Figure 4D presents the organization of the files into a single table. For the pilot screen analysis, the actual dimensions are 510 columns by 56500 rows, so while this is still at the level that Excel can handle, it is clearly a daunting task to scroll through the table to look for patterns or feature names, so even at this stage exploratory data analysis is best performed using Knime/R/Python/ Stratominer, etc.

Preprocessing of Feature Data: Normalization and Feature Reduction

The next steps begin the process of machine learning in earnest. There are three key steps that each need to be performed: data cleaning, feature pruning, and assessment of effect size for leading phenotypic features.

Feature Pruning

In this step, the raw output from CellProfiler for each cell observed – referred to herein as the feature vector - must be constructed by joining measurements for each object type (e.g., nuclei, cell, cytoplasm) into a master csv data file. As noted above, the features reported for each cell are extensive, and many of the measurements are uninformative. These can include columns that are redundant with other features (e.g., integrated intensity vs mean intensity), measurements that are not useful in the current assay (e.g., X,Y locations of cells in the image), feature that do not vary in the current study (Z-distance in 2D experiments), or non-measurement metadata columns (e.g. wellID 'B02'). Feature reduction is critical to effective machine learning for several reasons, one is reducing the size of the data set to eliminate unnecessary computational time processing the data. A common example of data that is important for some studies, but perhaps not the current one is X,Y locations of cells in each field, which can be important for screens that that monitor changes in intracellular organization (e.g. organoids or T cell motility). Many additional features can be retained initially and evaluated during algorithm development before deciding whether they are important for the study. Features that may be retained initially include those that are correlated but not identical. For example, larger cells will have larger areas (by definition) but they generally will also have longer lengths and widths. These multiple measurements may seem redundant. Frequently they are, and they can be combined (such as through Principal Components Analysis), but it may happen that cells can become elongated under some treatment conditions, so it may be prudent to retain all three initially. Another important reason to prune highly redundant features is to avoid overfitting in the training data that can result in poor performance of the final model. These will be considered during data-driven feature reduction, discussed below.

Centering and Scaling the Data

Centering, the process of converting all the different measurement scales into a single range, is essential for machine learning on imaging data. Centering is simply subtracting the column mean value from each row value. To scale the features, the individual value is divided by the feature's standard deviation. The result of this process is to adjust the column means to zero and standard deviation=1 for all measurements. Most machine learning methods are designed for data where all of the measurement ranges are fairly similar (e.g. distances, shopping choices, etc.) and may not need to be rescaled. Imaging data includes broadly different feature types, some of which may be measurements of relationships in a scale of 0 to 1, while others such as integrated intensity may be as large as 10^6. The majority of ML algorithms assume that input data is similarly scaled, so features that change by orders of magnitude will carry more influence in the analysis. Therefore, it is necessary to rescale imaging data before any significant interrogation can begin. Scaling is actually very simple to perform, methods are available in R, Python, Knime and other data analysis packages. Normalization, defined here as adjusting normal variation between wells on a plate or between plates, also typically needs to be performed before analysis. There are several methods for performing this; the B score is common for screening campaigns and is also easily

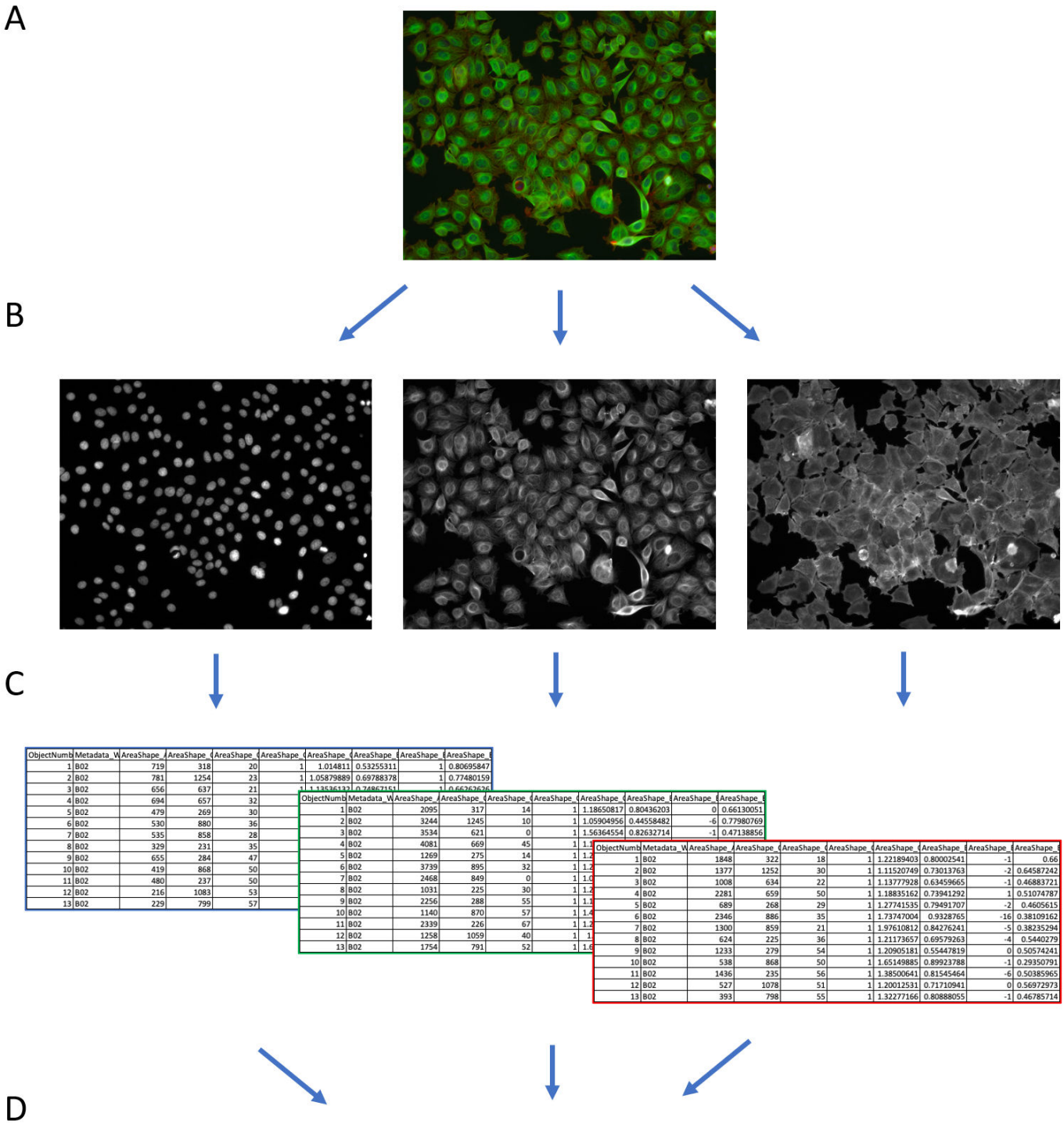

Figure 4 Image analysis and data-stitching process. **A**. False colored composite of cells as described in Figure 2. **B**. Actual mono-

chromatic images resulting from multiplex staining and wavelength-specific chromatic illumination/filtering. These are the images that are false colored to produce the images in **Figure 2** and **Figure 4A**. Image analysis of the images produce a set of cellular identifications and measurements that are captured in a csv file for each marker/image capture. **C**. the first step in experimental analysis and assay development is to link the individual data sets (by field and staining), resulting in the combined data set, exemplified by **D**.

performed (19). Note that a quality control step for each plate to identify significant deviations in feature means/variance between controls would be performed as part of the image analysis phase (discussed above) to eliminate plates that may have had material problems such as reagent preparation or pipetting errors should be eliminated and rerun.

Supplementary File 4: R-script - Data preprocessing

Supplementary File 5: Example Cell Profiler CSV output

Supplementary File 4 is an R script that completes all the following steps and reproduces the example below using the data file provided in **Supplementary File 5**. To reproduce this analysis, some minor edits to the script are necessary to redirect R to the location of the data file on your system and perhaps an additional redirect to the appropriate output folder. Instructions are included within the script. The data file requires a minimum of preprocessing to get two columns important for the analysis on the far-left side of the spreadsheet. This is also described in the file containing the R script. This exercise is set up to be performed by a scientist with general biological and screening training to evaluate a plate of treatments as would be performed during the initial screen development. That said, it introduces both an analytical process (through R) and exposure to imaging data that may be new to someone who has conducted experiments on an imager and used the vendor data analysis platform to analyze an experiment. Just getting used to these two areas may take a little bit of time but can be very valuable when larger scale machine learning is being used to analyze a screen. The data file itself is unwieldy, comprising 27046 rows and 506 columns for just one plate of the inner 60 wells! We will reduce this by about 50% in the next few steps and by 90% overall when we finally select the positive and negative control wells as we begin looking at Z' factors and related statistics. In this example, we have been able to delete several rows and columns in the data that make analysis difficult, less informative, or even cause an algorithm to crash altogether. These include:

- *Unneeded text columns*. A couple of columns of text are necessary to track the samples. These include the plate ID (which may in fact be numerical data, but function as an identifier rather than as data to be analyzed in the algorithm) and the well location (B02 to G11). These are set aside during this feature reduction step and reattached later, but there are additional columns of text that need to be eliminated. In this example, 23 columns were eliminated.
- *Features that do not change*. Some measurements do not change during the study. These features do not differentiate the effects of the compounds and therefore are eliminated to minimize the size of the data to reduce storage and computation time. 27 columns were eliminated at this stage.
- *Highly correlated features*. Features that covary also present data that does not differentiate samples but increase the size of the data. Testing for high correlations can identify these features and retaining only one of them helps to reduce the size of the data. Additionally, many algorithms assume the data is not correlated and can increase significance of correlated features in the analysis, such as clustering methods. The extent of correlation can be affected by the features themselves, where absolutely correlated features (Spearman correlation = 1.0) clearly should be reduced, but correlations of features that may be independent under some treatments may be retained. As an example, length and area will generally correlate as larger cells have longer lengths, but treatments that introduce elongation of cells will correlate less. In these cases, it may be valuable to retain them (at least initially). Setting the extent of correlation to coefficients of 0.95 or 0.90 is common at this stage. The correlation matrices of the initial and final data in

this example are shown in Figure 5. While some correlation between features exists in the final form, redundant features have been eliminated. 202 columns were eliminated at this stage.

- *Rows with non-numerical values*. The elimination of text columns above removed those with no numerical values. In addition, it happens that when trying to measure a feature for a cell, the image analysis algorithm is not able to assign a specific value. In these rare cases, a result of 'NA', 'NaN' or 'inf' may be returned. These values will cause some methods to fail, although it may be possible to instruct them to ignore such rows. In general, it is less trouble to simple eliminate them at this stage. The number of rows with such values is typically small, in this example, 50 rows were eliminated. If there is significant missing data, imputation of missing data is trivial in Python/R where the missing data is replaced by the mean or median value of the feature.

Feature Review and Importance

The next stage is to finally begin a review of the features. As this pilot stage follows the traditional process of assay development, to produce a robust assay based on the positive and negative controls, we will focus exclusively on the positive and negative control wells for the next couple of steps. The file to select data from these wells is provided in **Supplementary File 6**; the metadata needed for this phase is **Supplementary File 7**. This step greatly reduces the data to 5706 rows by 255 columns, about 10% of the initial data file.

Supplementary File 6: Example Metadata

Supplementary file 7: R-script - selection of control wells

The next step is to compare the features for their capacity to differentiate between the control wells. Currently, there is a consensus that selecting the mean or median values, and then calculating the Z' factors for wells is a generally effective method. There are several variations on this approach that have been described (summarized in Table 2 and discussed in some additional detail below). Most multivariate approaches either normalize the feature data first or employ a multivariate method that presumes normal data (such as using mean values for sample treatment features). That is not to say that there hasn't been considerable discussion about the best approach. This is because, as noted in the introduction to this section, the cell level data is highly heterogenous and frequently non-normally distributed. The mean value assumes that the data is normally distributed, and the median value assumes that skewing is the result of outliers. In fact, all image-based data sets have many examples of data that is fundamentally non-normally distributed and truly skewed (as opposed to including a fraction of outlier cells). For example, a simple Hoechst/Dapi intensity measurement across a population of cells will result in the convolution of distributions for 2N, S-phase and 4N cells and summarizing the entire distribution with a single mean value *can* exhibit meaningful differences but is far from optimal. Two groups have established working methods for selecting well values for cell level data: Ljosa (20) compared five methods: mean values, KS statistics, support vector machine (SVM)-generated hyperplanes, Gaussian mixed models and factor analysis.

References for Table 2:

- Young et. al (2008) (21)
- Kummel et. al (2011) (22)
- Kummel et. al (2012) (23)
- Hutz, et. al (2012) (24)
- Ljosa et.al (2013) (20)
- Reisen et. al (2013) (25)
- Warchal et. a. (2016) (26)
- Warchal et. al (2019) (27)

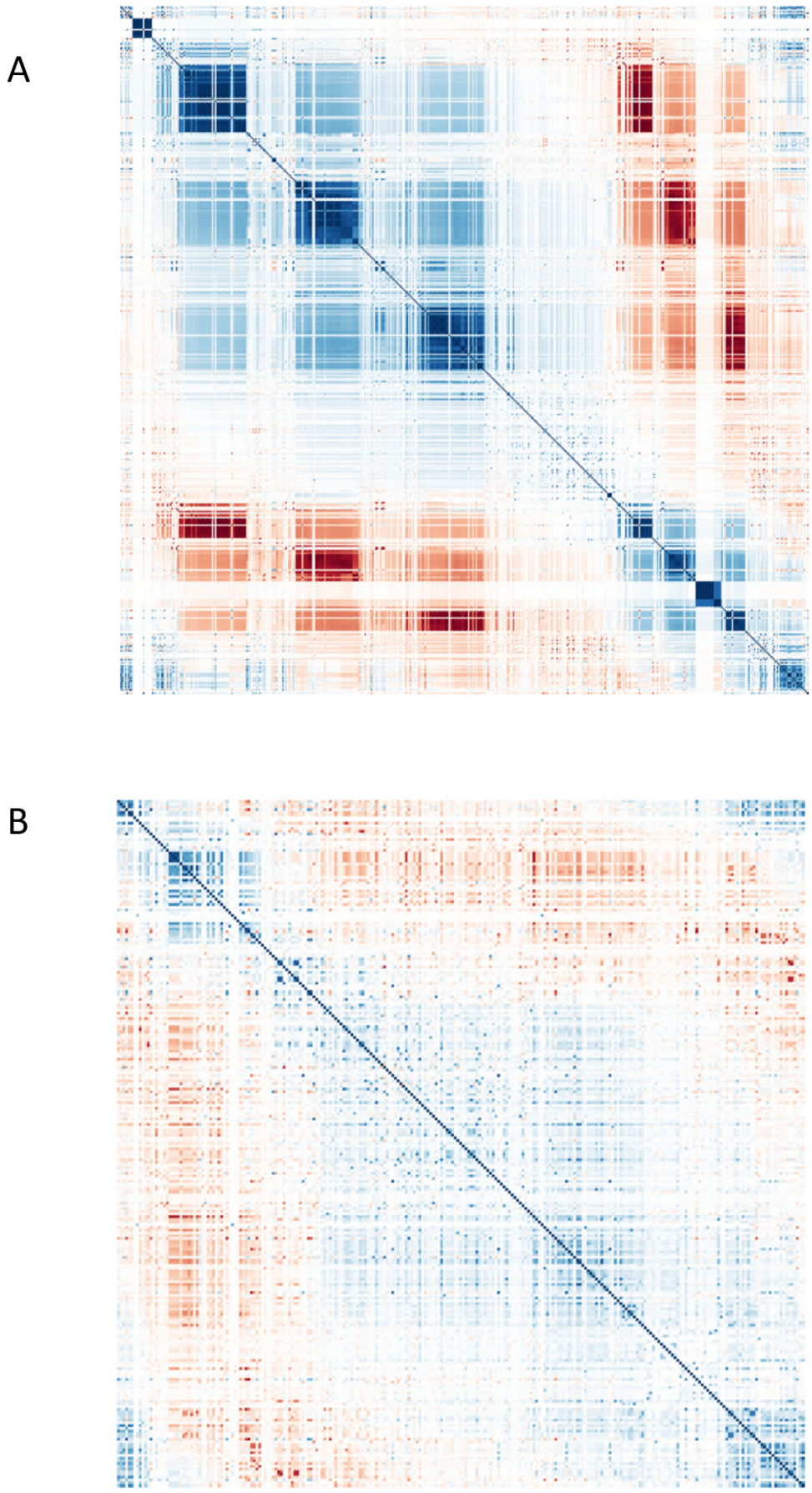

Figure 5 Correlation matrices of initial and correlation-reduced data sets. **A**. A correlation matrix of the initial data from the pilot plate

identifies many groups of strongly correlated features. **B**. Feature reduction through the elimination of strongly correlated features show some groupings of reasonably correlated features, but far less weighted for highly correlated features that add no additional information for data analysis.

The KS statistic is a common method for comparing two non-normal distributions, where atypical responses such as producing populations of both smaller and larger cells would effect the change in feature distributions but not the mean values. This approach was used by Perelman in a seminal study of phenotypic effects from various drugs (28). SVM hyperplanes was described by Loo (29), the Gaussian and factor analysis methods assume that heterogeneity results from discrete subpopulations and teases these out from the overall distribution of the data. Kummel (22) also looked at mean values and KS statistics, as well as sets of parametric summary statistics (mean, SD, skewness and kurtosis) as well as non-parametric percentiles (5^{th}, 25^{th}, 50^{th}, 72^{nd} and 95^{th} percentiles), creating sets of four and five parameters for each well, respectively. In both cases, the results did show a benefit from more complex approaches (factor analysis for Ljosa and the multi-parameter descriptions by Kummel), but the improvements were generally small, and the computationally simpler methods were still effective in the classification models.

However, there is a note of caution regarding considering the matter settled. One reason is that the image sets used to make these evaluations use agents that induce phenotypically striking perturbations. Ljosa uses the cytotoxic drug set described in Caie (5), the same image set used in this chapter, and Kummel evaluated a related subset of anticancer compounds on nuclear morphology and DNA replication markers. The profound effects these compounds have on cells may lead to a kind of 'methodological overfitting', where the conclusions discussed above may be genuinely settled for these kinds of studies, but subtler studies (iPSC differentiation, pancreatic β-cell stress and survival or 3D systems such as primary tumor organoids) may show stronger differentiation between methods. Towards that end, we provide methods for calculating Z' scores in both the pilot analysis and in the complete workflows, but we also provide KS and t-statistic evaluations to enable the scientist to make a more informed decision about how to quantify the cell level data. Even for these dramatic effects, the data still shows strong overlap between the treatment conditions and a high level of skewing for many features, as can be observed in Figure 6.

Measuring Effect Size – Multivariate Z', Related Approaches and KS Statistics

We present essentially two methods for comparing cell level data, the traditional Z' factor based on the means/standard deviations of the controls (we also include a t-test of the well mean values), and the KS statistic, which compares the cumulative distribution of the pooled cell data for the negative control wells with the individual cumulative values for both the positive and negative control wells. These KS statistics are then calculated as both Z' factors and t-statistics. The file to run these comparisons is **Supplementary File 8**.

The first approach is to calculate the mean values for the features and then calculate the Z' factors for the replicate wells. Results for a test plate are plotted in Figure 7. As expected for the taxol treatment as a positive control, many of the strongest discriminating features affect tubulin features, particularly texture features, which can be confirmed by inspecting the taxol treated cells in Figure 2B. The cell level data that is summarized by the mean or the median is shown for the highest scoring feature by Z' factor, the CorrelationRWCActinTubulin72 is shown in Figure 8A. The differences between the controls lacks the strong separation that is typical in robust screening assays, which has stimulated the interest in considering alternative metrics. The KS statistic is one such alternative that is easily calculated and very sensitive. It is calculated as the largest difference between the cumulative distribution functions (ECFs, essentially a running summation of the scaled rank ordered values for each sample. The ECFs are shown in Figure 8B, with the KS statistic being the length of the widest separation. The KS statistic is calculated by pooling the cell level data for the negative controls, and then calculating the KS

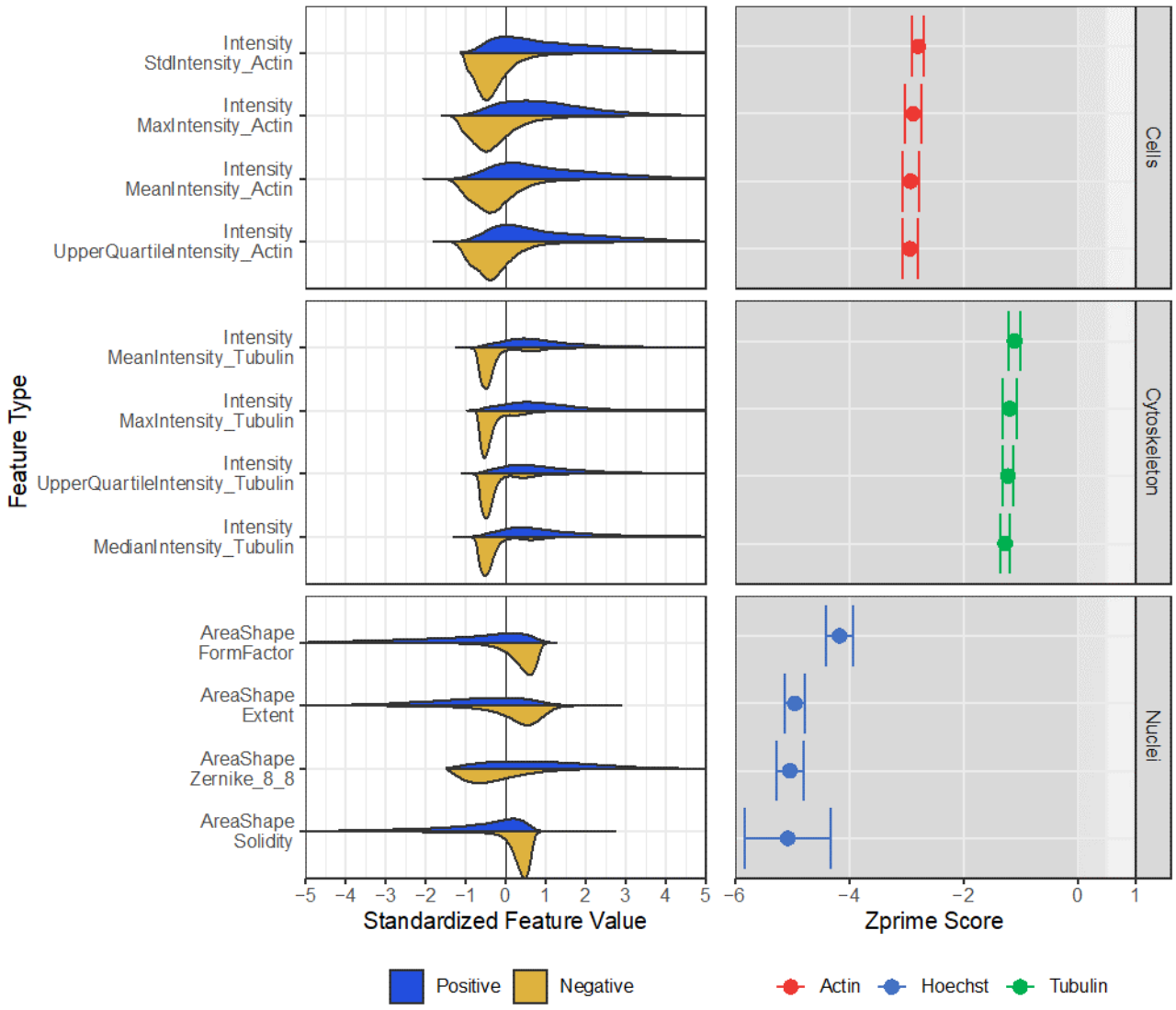

Figure 6 Split violin plots of features in the control wells. These plots allow a direct comparison for individual features across all of the channels. Note that Z' calculations in this figure are calculated for the cell level data directly, not the mean or median values from the cell level data per replicate.

statistics for all of the control wells. These values can then be evaluated by the Z' factor calculation. Figure 9A compares the two approaches. There is good correlation between the two methods, and for this study does support using the Z' factor to evaluate features. The points are colored by the p value, which makes an additional point, that features with low Z' factors are still statistically significant, with Z' factors of -5 or less still showing p values from a t test of less than 10^{-5}. There is no real disconnect between these two measures, the Z' factor was not developed or weighted to measure whether a treatment has an effect on a population of cells, the weighting towards the very high end (acceptable scores are generally greater than 0.5 on a scale of negative infinity to one) is to focus on the separation of controls necessary to enable single-point screening. The t-test is more common for the cell level comparisons made here. A related observation was made by Kummel (22), where they showed that features with very negative Z' factors were still effective in classifying treatment conditions.

To further explore the relationship between cell level distributions on the mean vs. KS statistic, the t-statistics were also calculated in the approach used to determine the KS statistics. As can be seen in Figure 9B, assuming parametric behavior of the cell level data did impose some variation, relative to the KS statistics, but overall,

there is good agreement between the two approaches. To conclude, we have evaluated the use of Z' factors to develop a machine learning algorithm for this study, as explored by others (20, 22, 30). We include these analyses to evaluate how they compare to a non-parametric approach. This accomplished most simply by plotting the cells using Principal Components Analysis (PCA). PCA is available in all data analysis platforms and can be used to show whether the final feature set after processing is in fact capable of differentiating the samples. An example is shown in Figure 10, using the process described in **Supplementary File 9**. The PCA analysis supports the idea that the feature data is strong enough to distinguish the positive and negative controls.

Supplementary File 8: R-script - statistical calculations

Supplementary File 9: R-script - PCA

Assessment of Batch Effects

A phenotypic, multiple endpoint screen needs to go through all of the rigor testing that any other screen requires (31), and many of these are operationally identical, such as testing for plate effects for the labels (intensity, localization, etc. that are a function of control treatments or dose), but since the metric in a machine learning screen is computationally intensive, the effect of normal variances in lab procedures, reagents, etc. needs to be tested as well. The most effective means to do this is to examine the data for batch effects using the calculated endpoint in addition to the individual features.

The aim of an experiment is the discovery mechanisms of a system through careful measurement of the response to treatments (32). In a screening experiment like BBBC021, the aim is to quantify which among a set of treatments are consistent with the positive control (taxol) or negative control (DMSO) (5). This multiple hypothesis testing setup can be confounded by factors that influence both the treatment and the response, which will not present in the biologically meaningful context, e.g., treatment of a patent in the clinic. These confounding factors are called batch effects and include factors such as the position of a well in the plate or the week that a compound is screened. If batch effects are not handled appropriately, this source of variation can lead to inappropriate selection of hits for follow-up screening that will fail in follow-up experiments, or it can lead to missing hits that would have been valid. Substantial methods have been developed in the context of high-throughput screening for experimental design (33) (34, 35), diagnosing (19, 36-41), and correcting for batch effects (40), many of which carry over to the morphological screening context . Here we will illustrate these statistical methods for BBBC021, discuss challenges and opportunities for handling batch effects in morphological profiling, and give examples of emerging methods to handle them.

The BBBC021 screen was designed to test 113 compounds for taxol-like response, modeled as the probability that a cell is classified as taxol-like (vs. DMSO-like) using the final cost-sensitive random-forest classifier trained using the model described in scripts and data provided in the link included in **Supplementary File 11**. Assuming cellular phenotypes are independently and identically distributed in each well, we can model the per-well number of taxol-like cells given the number of cells per well as a binomial distribution with per-well rate parameter θ. Figure 11 shows the relationship between taxol-like phenotype and cells across 10 weeks, testing two plates per week in triplicate. Each plate has 60 experimental wells and the edge wells are left empty, negative/vehicle control - DMSO is in B2-D2, E11-G11, positive control - taxol is in E2-G2 and B11-D11, and one treatment compound in each of the rows B-G in 8 descending half-log step doses in columns 3-10 (Figure 1). The top concentration for each compound ranged from 1 mM e.g., for hydroxyurea down to 10 nM for podophyllotoxin.

This experimental design allows for the evaluation of row, plate-in-week and week effects as batch variables that should not affect the score, which is defined as the fraction of cells in each well that are classified as taxol-like using the final cost-sensitive random-forest classifier trained over morphologic features. The MPStats package is used in this analysis and can be found here.

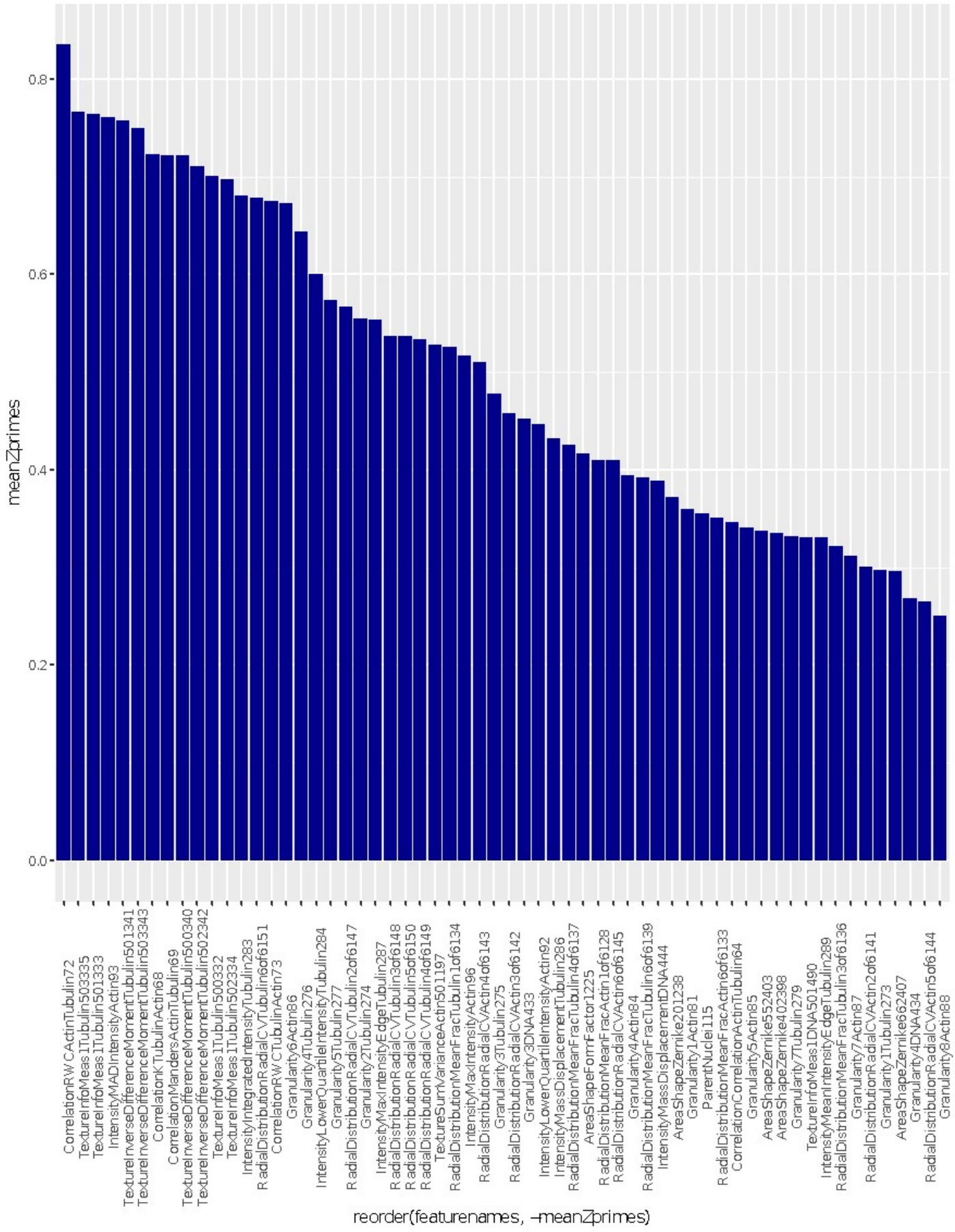

Figure 7 Initial analysis of features that differentiate positive and negative controls. Z' factors are plotted in the figure and listed along

the abscissa.

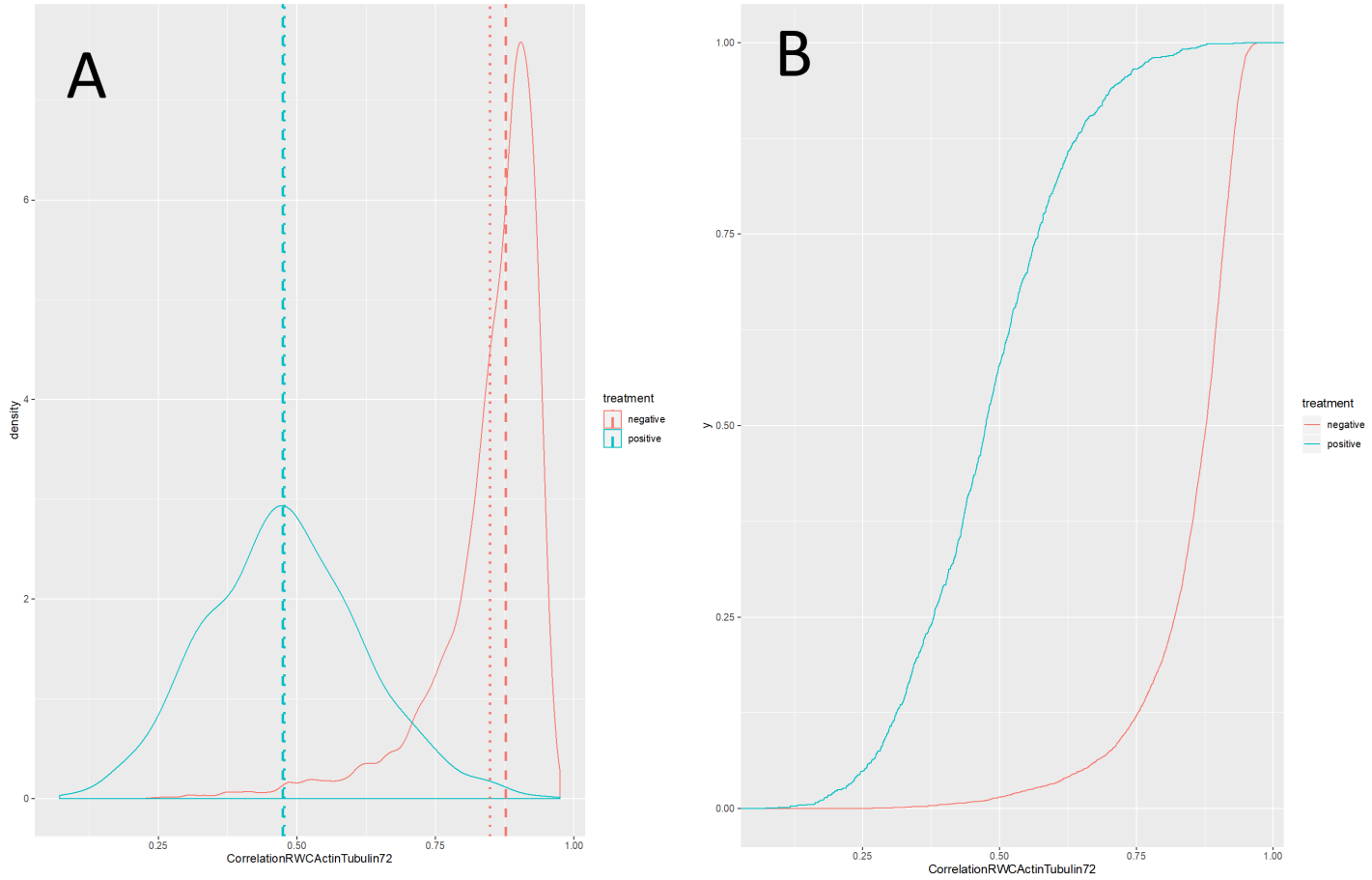

Figure 8 Cell level comparison of positive and negative controls for the top differentiating feature by Z' factor. **A**. Distribution plots of the positive and negative controls. Mean and median values are plotted by dotted and dashed lines, respectively. **B**. CDF plots of the same data. Rank ordered values (low-to-high) are plotted for their contribution to the total value for the data set (in this case, pooled for all positive and negative controls), from 0 to 1 (regardless of the total number of cells). The KS statistic is the length of the maximal difference between the two distributions, regardless of position along the abscissa (shown in dark blue; note that this is added to the figure to highlight the nature of the metric definition and was not specifically calculated for these data).

Assuming the probability of a taxol-like phenotype of each cell is independent, and identically distributed in each well, the number of taxol like cells will follow a binomial distribution. To test, we constructed a simple linear model as *score ~ row + plate + week* and found that the model is highly statistically significant, explaining over 6 percent of the score with each factor having a P-value less than 1e-10 and effect sizes ranging between 1-3%. Visualizing the per-well scores and linear trends across the batch variables (Figure 11), we can see a clear left-right trend in plate-scores and interestingly, an absence of wells in the upper-corners indicating that the outer wells may have a background set of cells that are artifactually called negative-control like. This indicates that the strategy of removing the outer wells to mitigate edge plate bias was not fully successful. Further because the concentration of cells varies across the columns, it is not possible to test if the column-batch effect is impacting the response. The plate-within-week batch variable indicates significantly more hits are found earlier rather than later each week, and similarly more hits are found in earlier weeks rather than later weeks, with a noticeable drop in hits around week-5. It is possible that the assortment of compounds across these batch variables are non-random and may simply favor more true-positive hits.

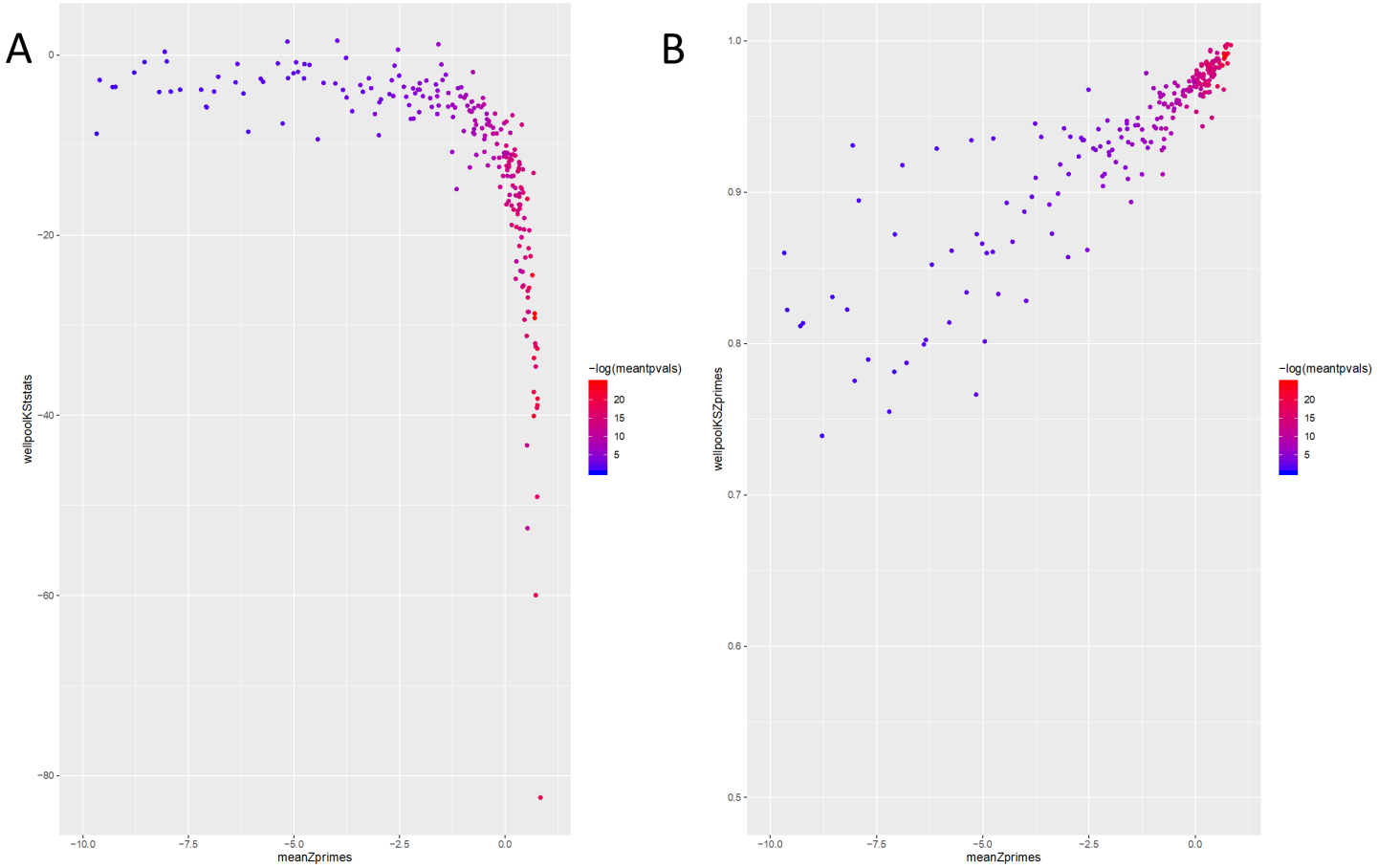

Figure 9 Analysis of metrics for feature differences between positive and negative controls. **A**. comparison between mean-Z' factors, and cell-level evaluations of positive and negative wells evaluated by KS statistics, with the resulting KS statistics evaluated by a t test between positive and negative controls. **B**. Evaluation of feature differences between positive and negative control wells by Z' factor for wells evaluated at the cell level by KS statistic and well level means. Color represents the -log of the p values for the t test as calculated in A.

Technical factors prior to image acquisition can affect measurements and subsequent statistical analysis. For example, cell density impacts the reliability of estimated response as low counts give higher-variance estimates and high-counts indicate possible cell crowding that may impact cellular behavior and morphology. Therefore, it is important to identify extreme cell counts and if these there are trends across batch effects, (Figure 12). The week-to-week variation is very high, indicating it should be handled explicitly. For the plate batch variable, there is an interesting split from a unimodal to bimodal distribution across over time, and there is a trend from left to right that is statistically significant.

Machine Learning for a Group of Plates

In this section we discuss the development and evaluation of a machine learning scoring system in a 15-plate subset that can be used to score a production screen. Several options for appropriate models are discussed, how to implement them and how to evaluate them. At the ML model training stage in assay development, one typically selects just data from the positive and negative controls, splits them randomly into an 80% training set and 20% test set where the model is naïve to assess model performance (commonly referred to as five-fold cross validation). When developing a multivariate assay metric for high throughput screening purposes, it is essential to understand the types of models and their caveats. Ultimately, the best practice is to evaluate several model types and inspect the performance of each and adhere to the principle of "reasonable force" in model selection.

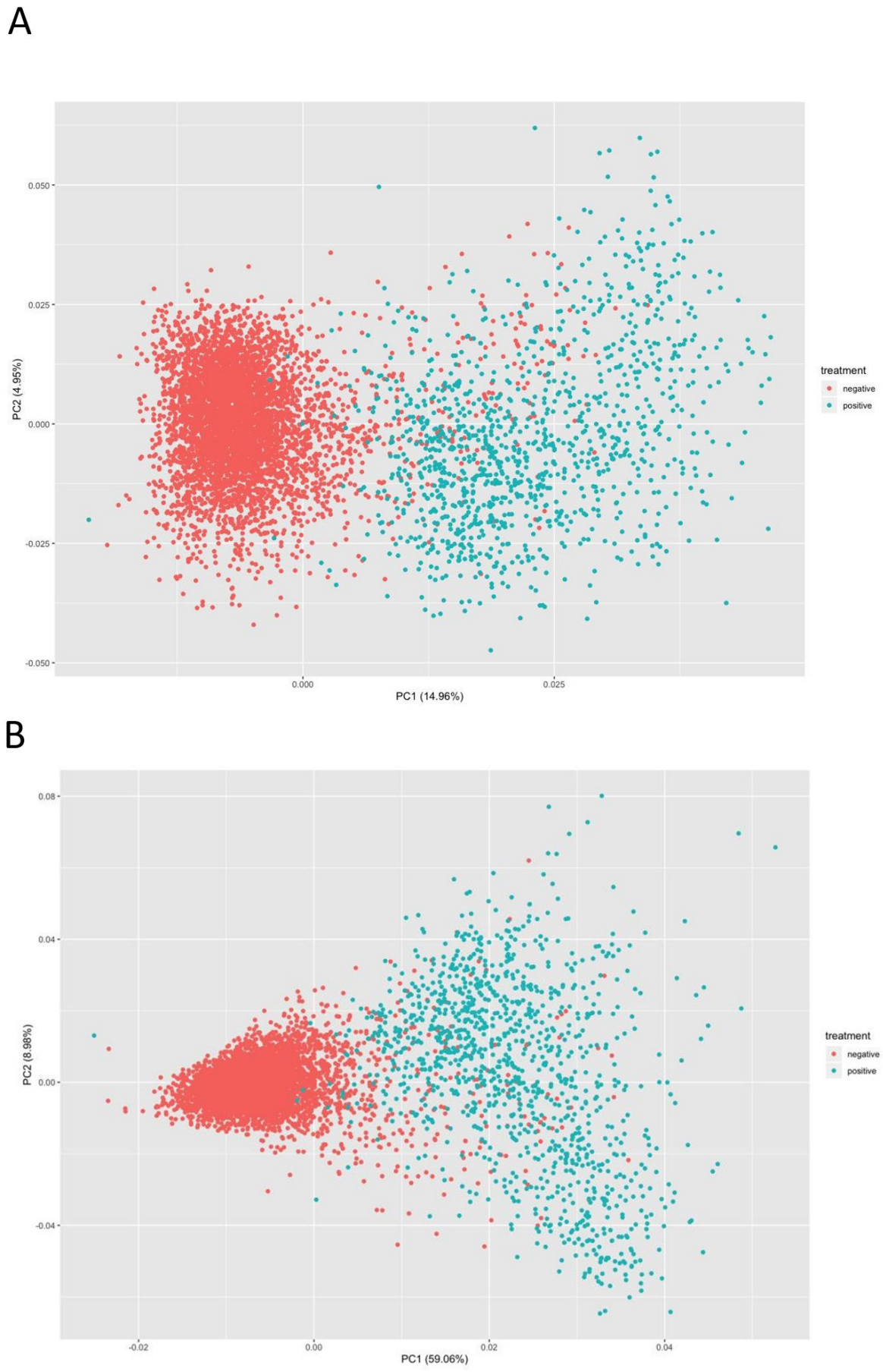

Figure 10 Separation of the positive and negative controls by Principal Components Analysis. Features after normalization, scaling and

redundancy removal are used to test their ability to robustly classify the control samples. **A.** PCA using the top 60 features by Z'. **B.** PCA using the top 25 features by Z'.

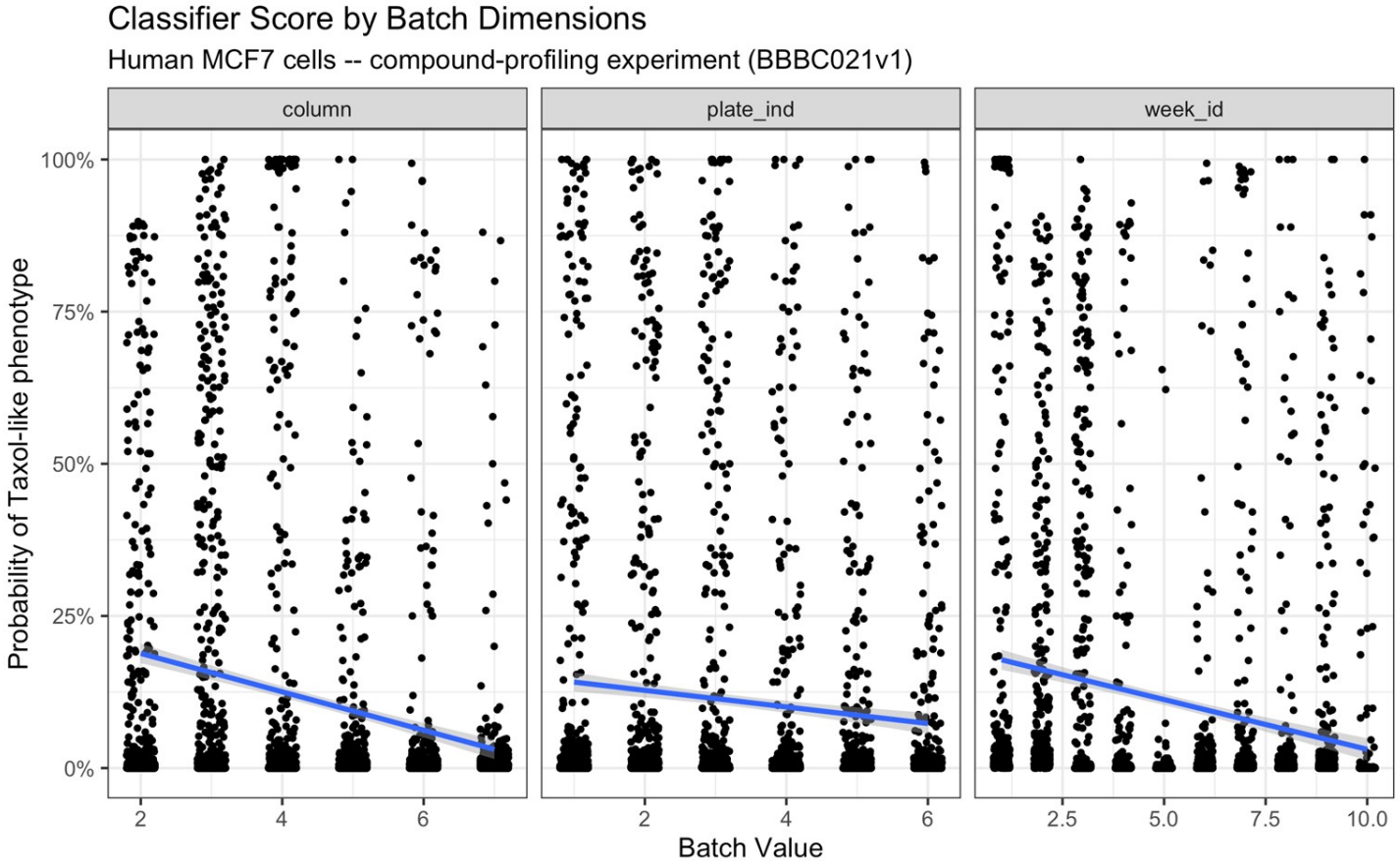

Figure 11 Classification Score by Batch Dimension. Each facet shows the distribution of average well scores by batch dimension: plate rows B-G (*row*), plate order for each week (*plate_ind*) and the assay week (*week_id*). The mean probability of cells classified as taxol-like are plotted as points with horizontal jitter. Linear trendlines show significant significant trends across each batch dimension with effect sizes [*row*: 3.1%, *plate_ind*: 1.7%, *week_id*: 1.7%] and P-values [*row*: p<2e-16, *plate_ind*: p<1e-10, *week_id*: p<2e-16].

This generally results in a workflow that: 1) identifies leading features – a machine learning model must substantially out-perform a univariate feature (single measurement like cell count for cytotoxicity) in terms of effect size and robustness. 2) Starts with simple discriminant/regression analysis (linear discriminant analysis or partial least squares regression). 3) Proceeds to nonparametric approaches like random forest and more complex models like convolutional neural networks. This process allows for the inspection of model performance from simple to more complex with the univariate feature as the comparator and will illustrate the benefits of one model type over another. When assessing model performance, Z'-factor indicates improvements over the single feature, the receiver-operating characteristics (ROC) curve and confusion matrix illustrate the performance of the model. A more conceptual and detailed discussion of model selection and performance is discussed below in discussion section 8.1. A random forest model was chosen for this example because 1) it is non-parametric and can detect nuance in the distributions, 2) RF performance was superior to other model types, and 3) RF allows for inspection of variable importance for features and indicates what cellular features drive the score. In this case, due to the extreme phenotypic differences between negative controls and taxol-treated positive controls, all model types chosen perform well. In assay systems with more subtle phenotypic shifts, the difference in model performance will be more apparent.

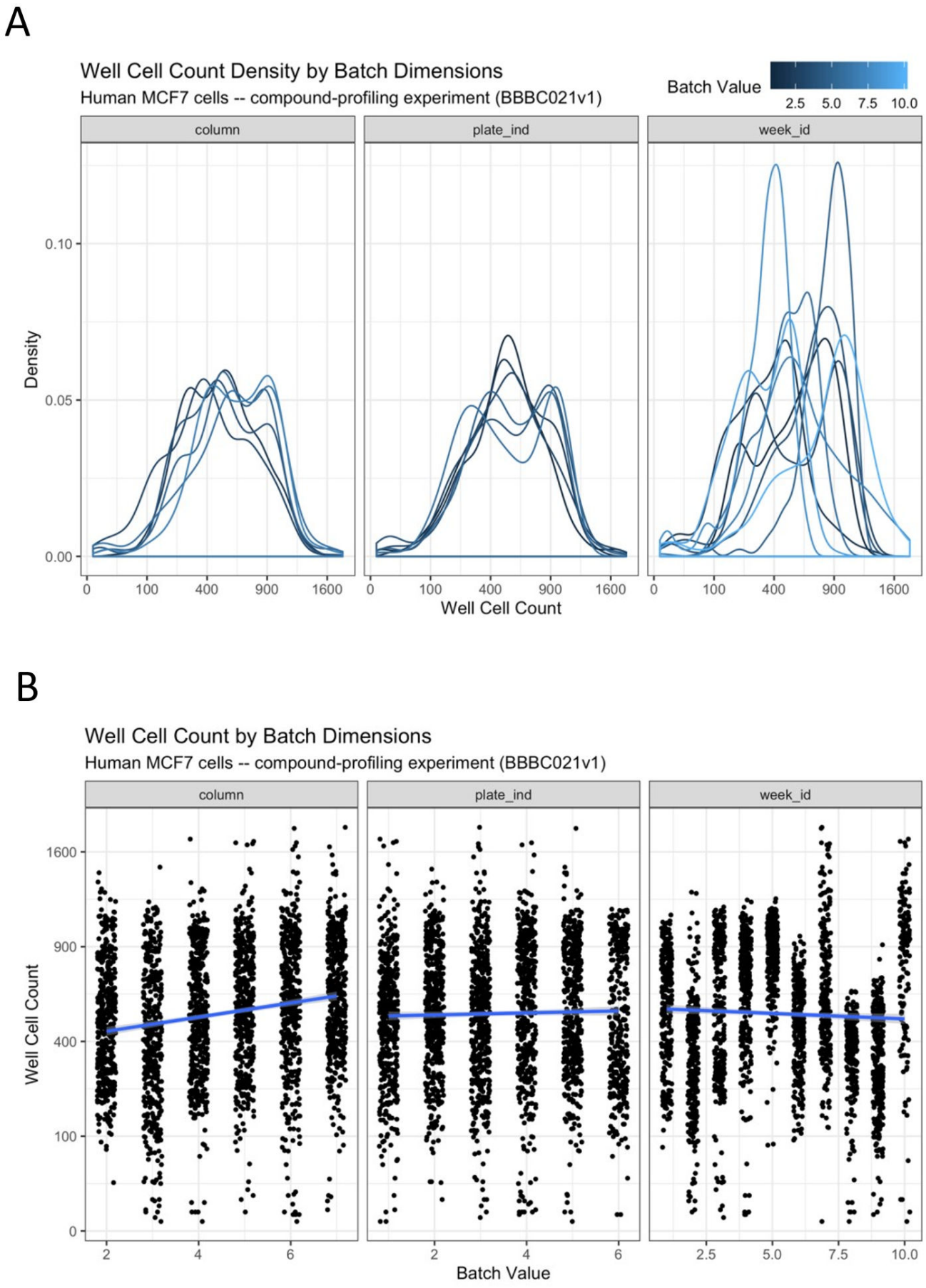

Figure 12 Distribution of Well Cell Counts by Batch variables. **A**. Each facet shows a kernel density estimate of the cell count for each

value of the batch value varying from black to blue. **B**. each facet shows the cell count for each well with horizontal jitter. Well counts have been square-root transformed to increase normality of variation. In B, Linear trend lines show significant variation in the *row* dimension with effect size .74 and p-value < 2e-16. The plate batch variable shows a trend from unimodal to bimodal distribution. An analysis of the between-week vs. within-week variance has an F-value of 115 and a P-value < 2e-16.

Machine Learning Model Evaluation

Model development should use more than a single plate of data to represent different batches and to allow for broader model applicability and isolation of batch effects, therefore at this stage, we analyzed a set of 15 plates using a Knime workflow and the "Model Selection" component that allows for simple head-to-head comparison of different models. The pipeline starts with data reading and imports CellProfiler output for the 15 plates, joins metadata to associate control conditions, compound treatments and compound concentration information with each cell/row. The "Data Preprocessing" step starts by subsetting the data to isolate the positive control taxol treated cells and the negative control vehicle treated cells. Imputation of missing values, low variance filtering and centering/scaling (Z-score normalization, not to be confused with Z'-factor) is performed and the resulting reduced data table is fed to the model inspector/model selection portion of the workflow. Once this final cell-level table is generated, any number of data analytics techniques including data reduction, model fitting, clustering can be performed. The overall structure of the Knime workflow is shown in Figure 13. The details are difficult to appreciate, but the overall structure of the data processing modules and how they connect to each can be seen. The data reading module, which integrates the data files for each of the channels into a single file, is highlighted in orange. An example of the output of the model selector is shown in Figure 14. The results for four common methods are shown, as well as performance metrics. The output is interactive, so the models can be examined by selecting tabs for each one, and the threshold for each model can be varied using the slider. Robustness, in the form of the ROC curve and accuracy, through the confusion matrix, are displayed in real time for four models chosen for this study: logistic regression learner, gradient boosted trees learner, random forest learner and cost sensitive random forest classifier. From this model evaluator, the complete dataset can be examined. The CellProfiler output CSV files for the 15-plate data set (selected from Caie et. al (5)), the Knime model selector workflow, and a guided tutorial are provided in **Supplementary File 11**.

Supplementary File 10: Knime ML instructions

Machine Learning Scoring: Identifcation of Positive Phenotypic Perturbation

The rationale for this section builds upon the identification of the optimal model from the previous section and uses a new Knime workflow located in **Supplementary File 12**. Once an optimal model has been trained on pilot screening data, a master workflow needs to be created to 1) perform plate quality control to determine suitability for inclusion into machine learning scoring, and 2) score the entire production screen (55 plates) for the purposes of hit selection to identify Taxol-like effects of the tested compounds.

Constructing the 55-plate master CSV

In this example, an entire screening campaign is scored using the random forest model that yields a well-level ProbPos. A single CSV file is built from the multiple CellProfiler object files that constitutes "cell-level" data from the Caie image data set. As in the model selection section, the final data table has one row per-cell and measured features and metadata are in columns. The tasks in these later stages require all the plate data to be joined before normalization, scaling and scoring can be performed. CellProfiler outputs individual CSV files based on PlateIDs and must be joined together alongside the metadata which contains the treatment information. This can result in large/cumbersome tables that are millions of rows and ~1,000-2,000 columns and ~15 gigabytes in size. The image analysis pipeline uses metadata to construct subfolders inside the default output folder for each

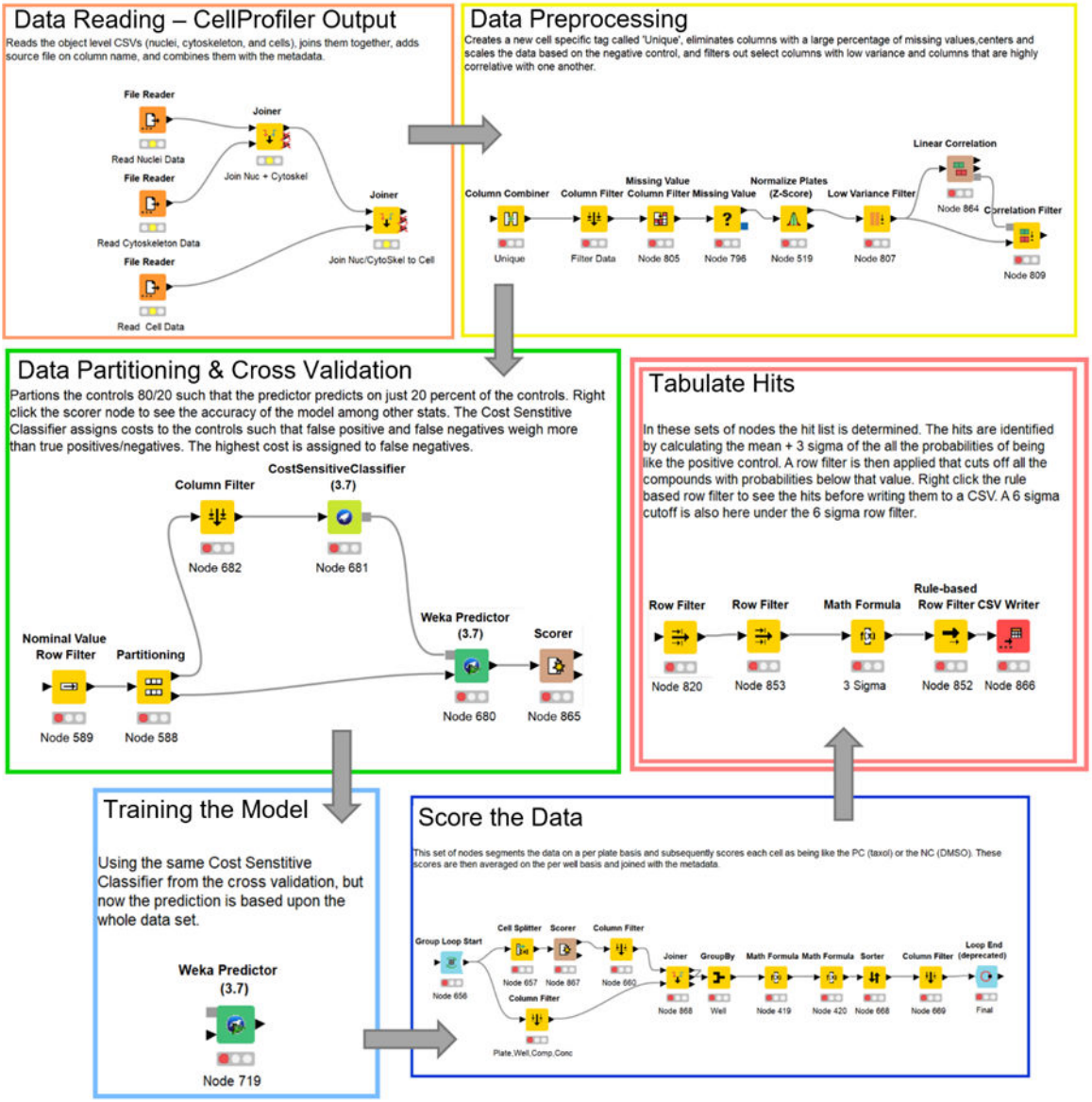

Figure 13 Knime workflow for data preprocessing and ML model development. Major segments of the workflow can be identified by colored boarders. The complete workflow is available in the supplementary files. The process links sequential steps for reading the data, preprocessing, cross validation, model training, data scoring and hit picking.

plates' data. Otherwise, the size of object-level data becomes too large and intractable for multi-plate runs. Three object-level CSV output files were written within the plate folder for Nuclei (MyExpt_Nuclei.csv), Cells (MyExpt_Cells.csv), and Cytoskeleton (MyExpt_CytoSkeleton.csv) and each are roughly 100 mb per plate. The three files were then joined to each other and joined to the plate metadata (compound, concentration, control class) using the provided knime workflow and a single file was generated that contains 512 features (the feature vector) and roughly 30,000 rows per assay plate where each cell identified is a row.

The object-level data table was built in Knime (16). The example workflow used for this data set are also provided in the **Supplementary File 10** and shown schematically in Figure 15. This machine learning KNIME workflow depicted in the figure integrates several discrete steps but allow for seamless data processing from object file to tabular and graphical results. The first step in building the object-level data table is to concatenate the individual object files for every plate. For example, each MyExpt_Cytoskeleton file will be read and then subsequently stacked on one another until all 55 MyExpt_Cytoskeleton files are contained in a single file by

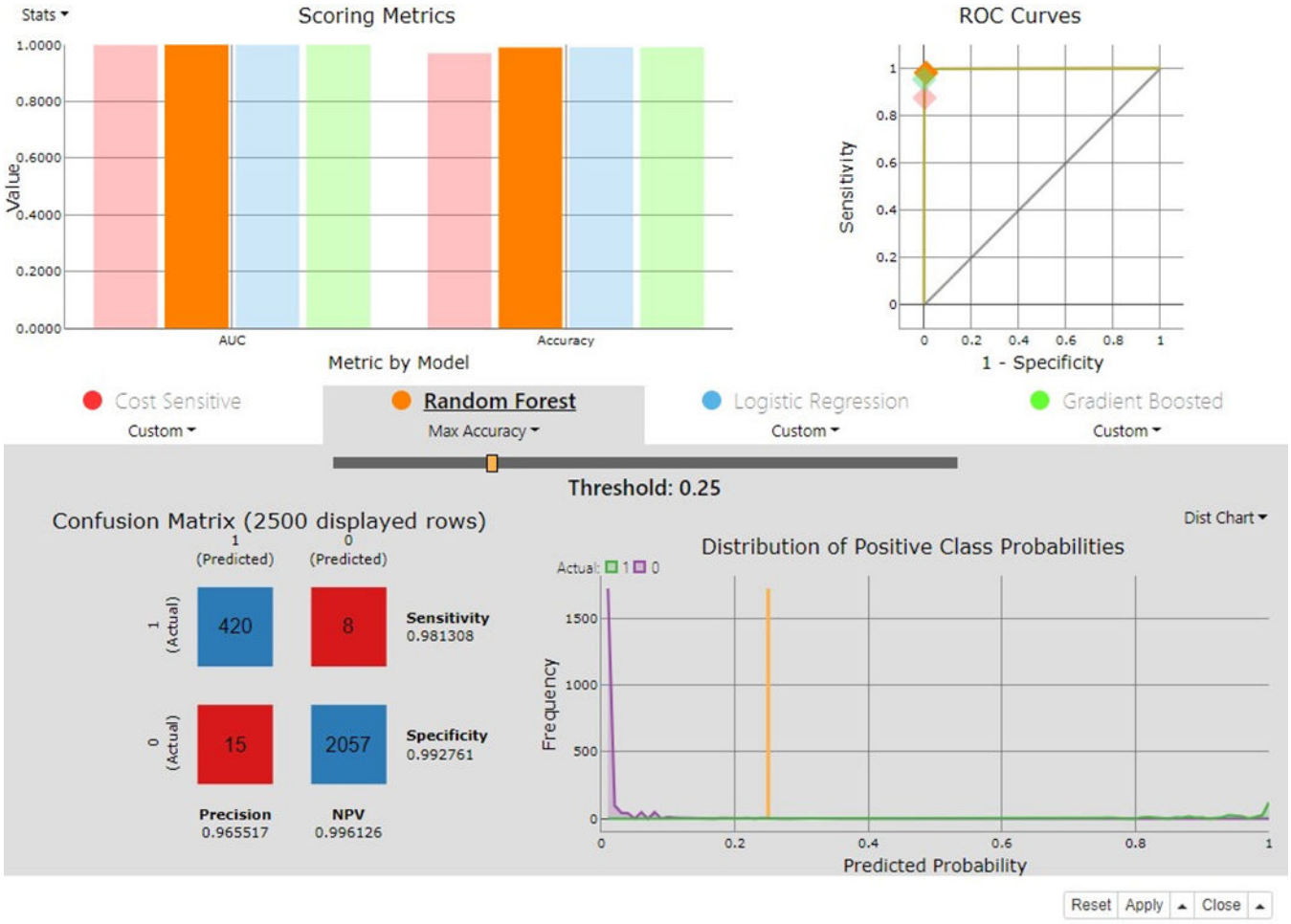

Figure 14 Dashboard for the model selector Knime workflow. The dashboard is a multi-panel output of results from each analysis. The top left displays the performance of each of the four models, the top right presents their ROC results. Each individual model can be considered individually through the tabs (the Random Forest model is highlighted). Within each tab for the models, the results.

looping the join operation. This table will then be joined to similarly constructed tables for the remaining objects. In this example, all the output files are contained in a single folder with each plate having its own sub-folder within. For constructing the object-level data table, the Random Forest Workflow was opened in Knime and the orange box titled 'data reading' (figure of data reading box) is where the object-level table is made. The workflow is already built for this example set; however, some nodes will require manual input. The first of these nodes is the list files node, which must be configured and point toward the folder that contains the screen. The rest of the loop is already configured, which converts the file location into a variable, reads the file, adds an identifier tag to each column, and then concatenates the files in the loop end node. For this data set, three individual object files will be used as were generated in the CellProfiler segmentation process. This method relies on the 1:1 correspondence of the primary object (nuclei) with the others (cell, cytoplasm). Other objects that do not have a 1:1 correspondence with the primary object (nuclei) must be summarized and associated with the primary object. For example, if multiple spots (e.g. mitochondria) are identified per-cell, then summary features (count, means for measurements) should be reported on a per-cell basis and then joined to the cell-level table.

Associating Metadata

Information about well-level treatment condition (compound ID, concentration and controls) was associated with each cell/row in a one-to-many joining operation. Metadata joining requires that the two data sources have matching unique fields and, in this case, the combination of PlateID and WellID designate unique conditions

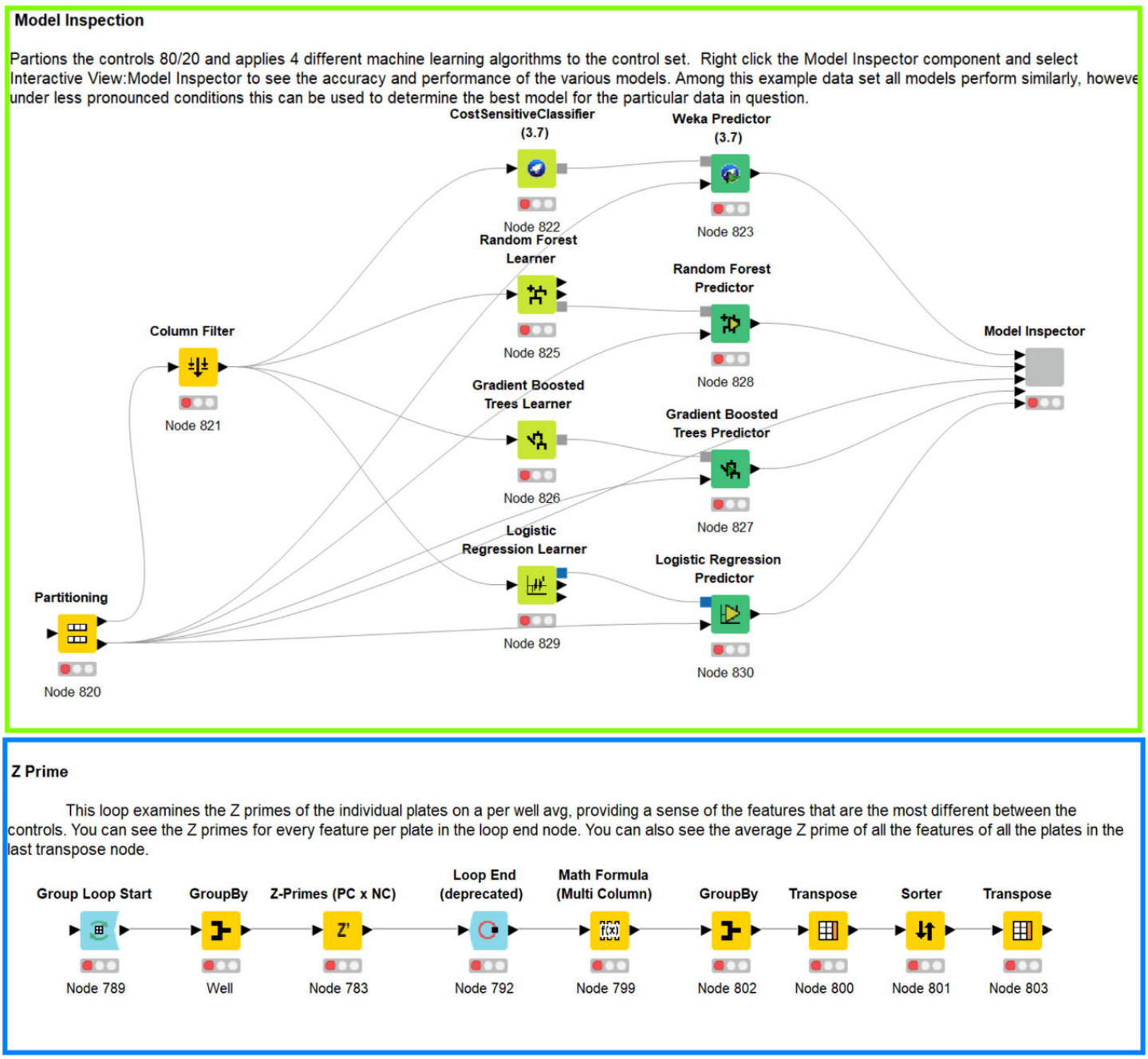

Figure 15 Knime workflow for Z' calculation and ML model selection. The complete workflow is available in supplementary files.

and are present in both the CellProfiler output and the plate map metadata file. The platemap was provided for download within the Broad Bioimage Benchmark Collection and was read by the csv reader node at the bottom of the workflow. Metadata in this example case will have the wellID of the compound, a plateID, as well as other information about each compound including concentration and condition (a marker for the controls). The metadata file for this screen is located within the supplemental information and the CSV reader must be configured to point to the file location. Once the document is read within Knime, it can be joined with one of the several files that Cellprofiler outputs. In the example workflow provided, metadata is joined with the myExpt_cytoskeleton file using plateID, wellID, and image number.

The remaining object files will need to be joined at the cell level. For these joins, PlateID, WellID, FieldID, ImageNumber, and ObjectNumber are all used, as these ensure every cell is matched to its respective cell level

feature. For example, nuclei 7 in field 4 in plate 33 is joined with cell 7 in field 4 in plate 33. Following the execution of the nodes, the master level object table is created with every row representing every cell in the screen with its respective objects. The single file created in this process represents the output of an entire screen or batch of screening plates and can routinely be 10s-100s of gigabytes in size. An alternative, and more efficient approach to constructing object-level data tables uses a relational SQL database (MySQL, Postgres) and CellProfiler can directly write to either a live SQL database or to a SQL file using the *ExportToDatabase* module.

Data Preprocessing

As highlighted earlier in this chapter, data preprocessing is a critical step to achieve robust statistical analysis and for building descriptive models using AI/ML methods in the context of high content screening. The same Knime workflow for creating the object-level data table will be used and this can be found in the supplemental Information section. The data centering and scaling takes place after data reading and is described graphically in the yellow box ('Data Preprocessing') in Figure 13. Data preprocessing in this workflow begins by removing empty columns and addressing missing values. Columns with missing values can result incorrect prediction or classification when the missing data is systematic (ie: small cells with zero cytoplasmic volume will result in missing values for some cellular features). Columns with substantial missing data can be removed or if chosen for inclusion, a method for imputing missing values must be used. In this example, columns with substantial missing data are removed. The threshold for this removal can be adjusted within the workflow under the missing column filter node. Following the removal of missing columns, the remaining missing values must be filled in. This is accomplished by the missing value node that applies the mean of the column in the missing cell. This can also be switched to median, but this process is more computationally expensive on a large set. The data is then centered and scaled using the normalization node which is based on the negative controls. The normalization node subtracts the mean of the negative control and divides by the standard deviation for every value in the particular column. This is a critical step in high content screening, as it allows each feature to represent the same magnitude and variance relative to one another. Without centering and scaling, integrated intensity features (>10^3) will dominate other measurements and will bias the machine learning algorithm towards those features. The final step in preprocessing is applying additional filters to remove columns with low variance, and columns that are highly correlated with one another. These columns do not offer new insight and again, could bias the machine learning toward a particular set of features that is overrepresented within the data set. In the context of high-content screening output, data preprocessing can often result in the elimination of >50% of all features. This is a critical data reduction step that will facilitate high quality modeling and analysis.

The order of operations is critical and was as follows: 1) removal of non-analytic variables (like pixel locations), 2) removal of empty columns (zero variance filter), 3) impute missing data – replacing missing data values with the column median values, 4) centering/scaling – subtraction of the negative control (DMSO) means from the entire data and scaling features to a Z-score=1, 5) feature pruning - remove low variance columns with less than 10% variance, and 6) remove highly correlated variables >90%. This process results in the "master" object-level data table that is suitable for analysis of data quality, pharmacologic effects and supervised and unsupervised machine learning. The impact on the data, particularly the effect on normalizing plates across the study, is shown in Figure 16.

Detecting Important Features and Computing Assay Statistics

Following data preprocessing, the centered and scaled data should be evaluated to ensure each plate is of acceptable quality for further analysis. Commonly used metrics in high throughput screening to assess plate quality are described elsewhere (25, 26) but include Z-prime, SSMD, and MSR. Z-prime is a simple signal-to-background statistic that shows separation in controls by examining the standard deviation and mean of the positive and negative control (41, 42). Z prime can also be used as a tool to assess the features that have the highest degree of difference between controls. For this reason, Z-primes are computed for each feature and are rank-ordered as an exploratory data analysis technique to indicate important features that are different between

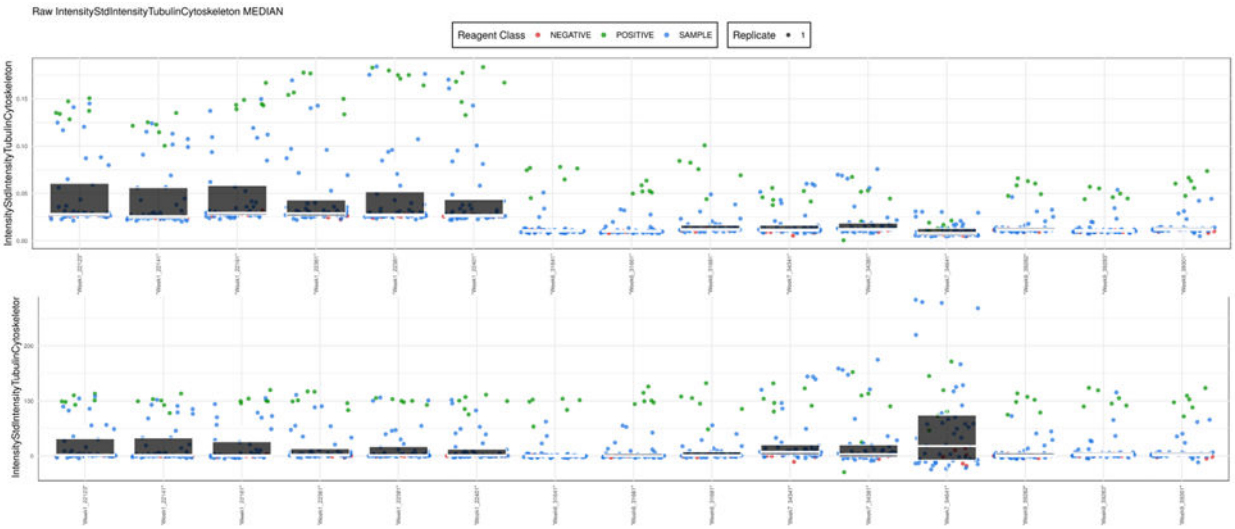

Figure 16 Pre and post centering/scaling for standard deviation of tubulin intensity in the cytoskeleton compartment.

control classes. The rank ordering Z prime calculation is found within the same workflow under the data preprocessing section, in the section aptly named Z prime. Since the Z-prime calculation is only computed based on the controls, the data is subset to include just the control wells. Z-primes are calculated based on the well-level average of every plate. The loop-end node, which concatenates the output of a loop, in this case contains the Z-primes for every feature of every plate and is accessible by rick-clicking on the node and selecting "Collected Results". Following this, the means of every feature are calculated, and the data is sorted from highest to lowest, which gives a sense of the most significant features in the entire screen.

Additionally, there is another approach for ML-based Z' factor that is calculated in the workflow under the section 'multivariate' Z prime. This utilizes a random forest model to determine the likelihood that each control well is correctly identified. In the case that the random forest cannot properly predict controls and there is a Z prime lower than 0.3 (or even perhaps negative), it is suggested that the plate is rejected. The ML Z' factor for each plate can be seen in the respective loop end node. There are other ways to obtain a multivariate Z prime that are not utilized in the workflow, but that can be beneficial depending on the particular screen. Importantly, the random forest model is well suited for feature selection in HCA.

Analysis of Z' factor for each feature was tabulated and rank ordered to identify important features in the data set. Once important features were identified, Z' factor for those features were inspected across individual microplates to ensure data quality. The feature with the maximum Z' factor for each of the 15 plates was tabulated resulting in an average of 0.6. Figure 17 shows the maximum Z' factor in the feature vector for each plate. Note – the maximum Z' factor feature can vary per-plate but was consistent among the global important features list. Important features emanating from this image analysis pipeline as distinguishing the positive versus negative controls are shown in Table 3 with brief descriptions.

Scoring for Taxol Similarity Using Random Forest

After centering and scaling and the plate has been validated for quality, machine learning techniques can be employed for hit selection or to detect outlier conditions. For model training purposes, the control data is partitioned into an 80% training and a 20% test set for prediction (standard 80/20 cross validation). This is performed in the workflow labeled 'Cross Validation'. Cross validation is essential, as it both generates the model and tests the performance and the accuracy of the model on new data.

The random forest used within this workflow is cost sensitive and is penalized more heavily for false negatives than false positives, meaning it has an asymmetric scoring system. In the context of high throughput screening,

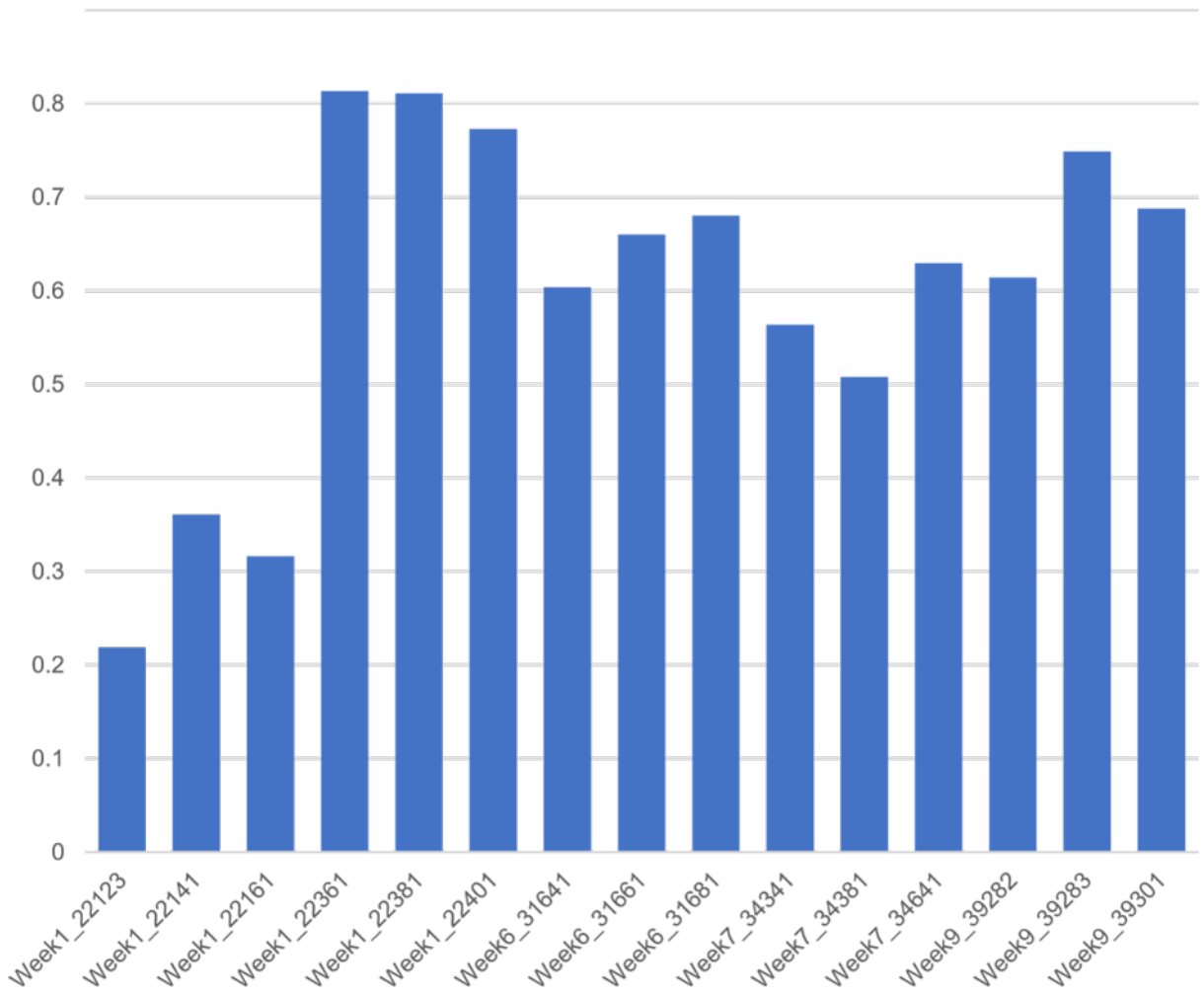

Figure 17 Maximum Z' in the feature vector for each plate. Z' scores were calculated based on mean values for each feature per well and subsequently analyzed by the Z' calculation for the groups of positive and negative control wells.

false negatives are indeed more expensive and can result in the loss of a valuable compound. Whereas false positives are less expensive because they can be easily identified and eliminated in confirmatory follow-up experiments. To assess the performance of the model, right click on the scorer node and click assess accuracy statistics. In the case of this example set, the predictor has about 99.97% accuracy. Once satisfied, the same cost sensitive classifier is applied to the rest of the data set. The cost sensitive random forest classifies every cell as being either like taxol (score=1) or like the vehicle/DMSO control (score=0). The well-level population statistics are computed by averaging the score to describe the aggregate probability of that well belonging to the positive or negative control classes. The data is broken up by plate and averaged at the well level in the section called, 'scoring the model'. It is here that another loop is utilized, allowing for fast scoring of each plate. Subsequently, the score is stored in the loop end and written out on a per-plate basis. To alter the location of the output, configure the csv writer in the section called output.

Following probability scoring, data can be visualized in a section of the workflow that separates the data in groups of 4-5 plates and shows the taxol-likeness on a scatter plot. Another can be seen in the section labeled 'hits' that removes the controls and filters the hits based on multiples of three and six standard deviations from the mean of the screening batch. The last section at the bottom of the workflow bins the data into ten bins based on the probabilities of taxol likeness and shows a histogram of the individual compounds and concentrations. This is especially important in determining dose-responsiveness. For this reason, a new column called 'treatment' is created, which is the compound @ concentration.

The Knime analytics platform was used to generate a supervised random forest classifier to detect "taxol-like" effects and then was used to score each cell treated with the 113 compounds at each concentration. The data was aggregated at the condition level (compound @ concentration) and a probability of "looking like taxol" was computed by simply averaging the individual classes. The example for this process is included in the supplementary data and is titled "Cross Validation" and "Developing an AI model and Hit Picking". The master cell table was used to generate a model trained on the positive (Taxol treated at 0.3uM) and negative control (DMSO Vehicle) classes. The control data was isolated with a row filter and was then partitioned with an 80/20 split. 80% of the data was fed to a cost sensitive classifier where 2X the cost was applied to false negatives versus 1X cost for false positives. The model was used to predict the residual 20% data and the ROC curve and confusion matrix are shown in Figure 18 with < 0.35% misclassification rate. The cost sensitive classifier was then used to score the entire data set for taxol likeliness and the highest-ranking compounds are shown in Figure 19. The model developed against the controls was used to classify each cell into the two control classes (Taxol=1 and Vehicle/DMSO=0) and the aggregate probability of Taxol-likeliness was calculated by averaging the scores for each cell under a particular treatment. The resulting probability of Taxol-likeliness (ProbPos) was used as a measure of efficacy and this method and successfully detected several taxanes and other drugs with similar cytoskeletal effects. Table 4 shows increasing positive probability for selected compounds. The positive probability was binned into 10 categories and a data bar is shown in the Bin column. This establishes the utility of the multivariate positive probability score for scoring cell-level high content data for similarity to the positive control in a supervised ML approach.

Evaluation of Effect Contribution from Each Channel

Figure 20 shows an UpSet plot to visualize the contribution of effect signal from each fluorescence channel and the intersection of each channel. The purpose of this analysis is to evaluate the contribution to the overall effect for each fluorescence channel to increase the understanding of their contributions to the machine learning scoring system. In short, the same procedure for training and deploying a model was performed on the 55-plate data set where the feature space was limited to just one channel (Hoechst, tubulin, actin), pairs of channels, and all three channels together. The random forest model scored each cell in the PC/NC data and then ProbPos scores were tabulated for each control condition and the Z' factor was calculated. The tubulin channel alone produced a Z' factor of 0.375, and the tublulin+Hoechst channel together yielded a Z' factor of 0.675. All three channels together performed equally well as the tubulin+Hoechst combination. For the purposes of scoring compound effects as taxol-similar, the actin channel can clearly be omitted. However, if unbiased phenotypic exploration (as is also done in Cell Painting assays) is important, then the actin channel may become important.

Analysis of Compound Dose-Responsiveness in qHTS

The aim of the study is to measure the dose-response effects of the treatment. To analyze these effects and categorize compounds as active/inactive and activity response type, we employ three alternative models to fit the ProbPos score - the fraction of taxol-like cells in each well of increasing complexity as described above. Morphological profiling based dose-response effects:

There are a wide range of potentially therapeutic effects that can be identified and categorized by the best-fit model:

- Flat-response (max < 50%) (not shown)
- Flat except for a few outlier wells (e.g., monastrol)
- Non-saturating in dose-range (e.g. cisplatin)
- steep dose response curves (e.g., anisomycin)
- gain-loss response (e.g. nocodazole)

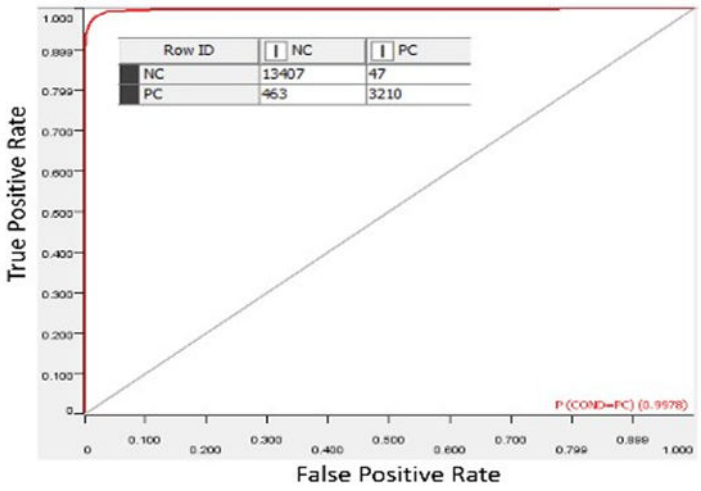

Figure 18 Receiver operating curve and confusion matrix (inset).

Compound	Max Score
AZ138	1.0000
filipin	1.0000
mevinolin/lovastatin	1.0000
staurosporine	1.0000
epothilone B	0.9954
docetaxel	0.9932
trichostatin	0.9813
AZ-C	0.9630
AZ-B	0.9412
cytochalasin D	0.9385
anisomycin	0.9343
tunicamycin	0.9200
vincristine	0.9041
brefeldin A	0.9000
MG-132	0.9000
AZ841	0.8947
mitoxantrone	0.8873
vinblastine	0.8776
cytochalasin B	0.8500
AZ235	0.8367

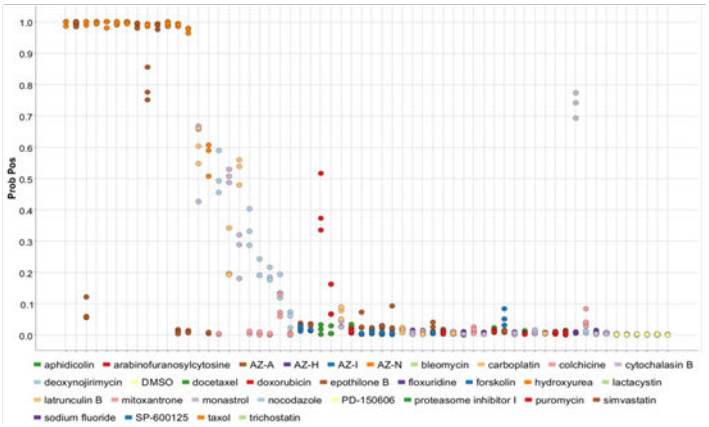

Figure 19 Compounds identified significantly similar to the taxol effect, and a probability scatter plot for compounds in a 15-plate subset.

Curves are fit using the tcpl R package(43). The statistical analysis methods are combined into the MPStats R package. This package consumes the well scores table generated in the Knime pipeline stage to produce batch effects, well cell count, and dose response analysis. Further, these methods are implemented a KNIME workflow using the R snippet KNIME nodes as shown in **Supplementary File 10**.

Figure 21 shows dose-response curves for the entire screen, in alphabetical order, where significant differential effects can be observed. The fit model is shown in blue and the cell count per field, (a direct measure of cytotoxicity) is shown in green. Interestingly, the green cell-count curves often decouple from the blue ProbPos score where compounds have pronounced cytotoxicity but do not resemble cells treated with taxol. This illustrates that the ML-derived ProbPos score is not a general cytotoxicity measure, rather specific to identifying taxol-similar effects.

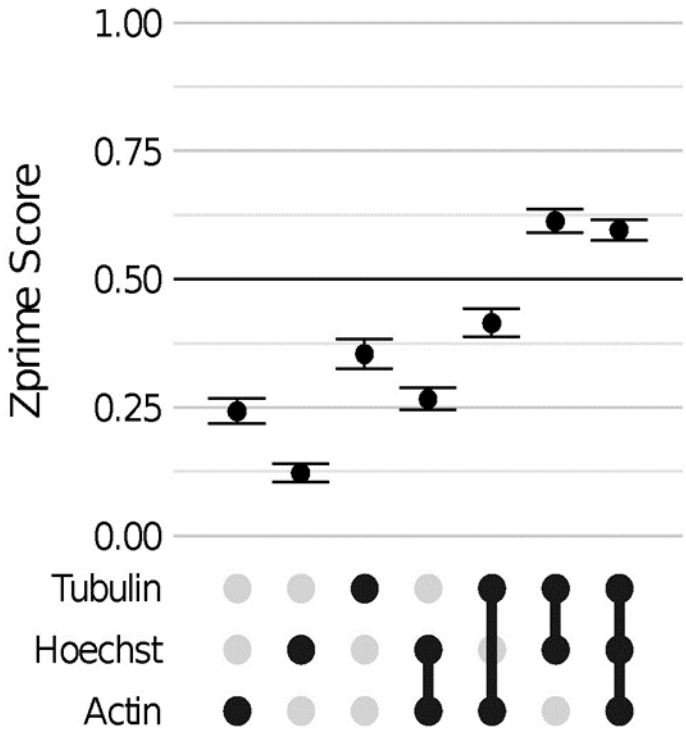

Figure 20 UpSet plot for channel-specific differentiation of control samples. Values are for all features after preprocessing. Zprime for cell-count across wells: -0.84.

Machine Learning, Incorporating Novel Phenotype Identification, With Applications to Cell Painting and Related Phenotypic Screens

In the previous example we have used machine learning implemented in KNIMEime to ask a very direct question: What wells in the screen are most similar to the Taxol positive controls? Here we show how machine learning can be used to augment a more exploratory analysis of the same data set. We use unsupervised multiparametric analysis methods to identify compounds that give a significantly different phenotype from the DMSO wells. With hierarchical clustering, we can determine if our assay and analysis method will allow us to separate compounds based on the mechanism of action. We can then identify wells that give strong phenotypes, and label them as classes for the building of robust machine learning models. These can then be applied to the larger data set. For this analysis, we have used StratoMineR 1.2.4, a commercial data analytics platform from Core Life Analytics but the same methods can be built in R or KNIME. The StratoMineR platform has these methods in a package that provides an integrated interface that streamlines many steps that enable biologists to make use of complex data analytics methods. The entire process can be replicated using a StratomineR guest account (follow the link in **Supplementary File 12**). Selected output from this workflow are included as additional supplementary files.

Supplementary File 11: Stratominer instructions

Data Preprocessing, Metadata and Quality Control

We used the same fifteen plate subset of the larger data set for this analysis, that encompassed 30 compounds. (**Table 1**). This data set was approximately 3.4 GB in size. The challenges of dealing with the large amounts of image data that are generated in high content screens has been long appreciated but recently the scale of the

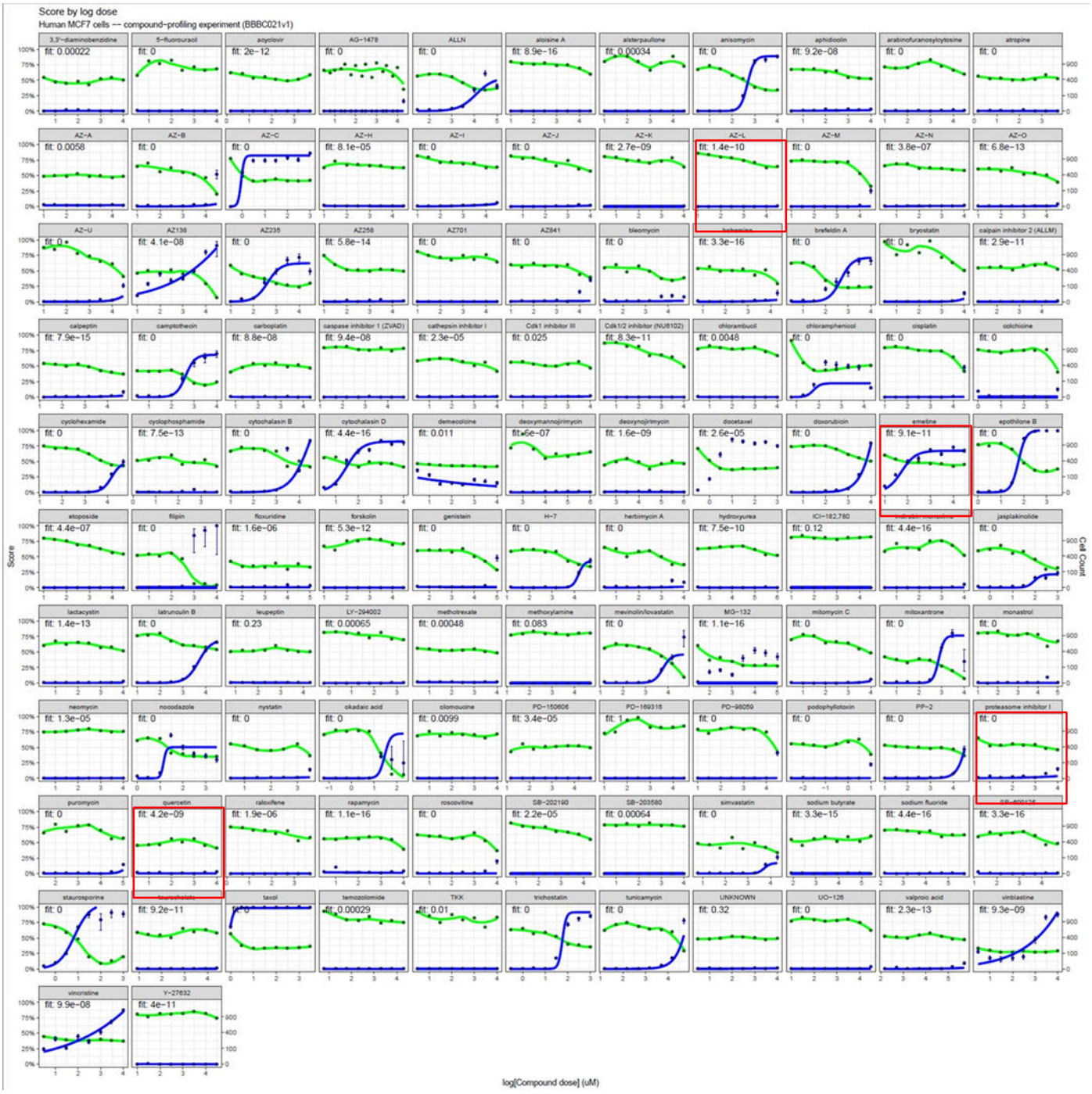

Figure 21 Dose-response curves for 112 compounds. The response of the taxol feature classifier is shown in blue, the cell (nuclear) counts per well are shown in green.

numeric data being generated is becoming a problem, especially for Cell Painting assays when the features are extracted at cellular resolution. In these cases a file for a single 384-well plate can be 10-100gb.

In our case fifteen files, one for each plate, were uploaded into the HC StratoMineR platform with the opportunity to select the number of plates and that it was run in triplicate. The system gives users an opportunity to easily preview the structure of the data to make sure that it is correct, with the same feature set across all the files. This is especially important if there has been manual manipulation of the data in spreadsheet programs. We recommend that this should be avoided if possible as errors are commonly introduced. In the Meta Settings section, the user can separate analytical features from metadata. The most important of these is a feature for well

identification but a unique plate identifier is also useful. Any other metadata that will be useful for enhancing the understanding of the analysis should also be identified. This includes information such as concentrations, the reagent class, (positive, negative controls; sample), reagent names; or annotations such as mechanism of action.

As well as giving users the option to isolate metadata from the raw data files, they also can add additional metadata. This is enormously beneficial for improving the analysis. This can be done in a text file but it does require, in addition to a well identifier, a common plate identifier feature that can be used to merge the metadata. Here we were able to merge compound names, reagent class, (POSITIVE, NEGATIVE, SAMPLE), the concentration, (nanomolar), and the mechanism of action of the compound as annotated in the original paper, **Supplementary File 12**. We recommend that the metadata be merged in this manner instead of manually adding it to raw data files with spreadsheet programs. As discussed previously this can lead to the introduction of errors. In corporate environments the metadata can frequently be generated from a LIMS platform.

A user can define a feature as a Default Feature. This gives the user a quick insight into whether the assay in a particular well worked. It is frequently one which gives a strong differential signal between positive and negative controls. Here, TextureEntropyTubulin503331 was identified as a Default Feature. The Default feature is prioritized at the top of the various data visualizations in the platform. The ObjectNumber2 feature was selected as the Cell Count feature. The median of this gives a relative indication of cell number.

Several data preprocessing steps were carried out similar to those outlined above. The platform automatically identifies and removes features that are not continuous, and eliminates those with a maximum Pearson Correlation coefficient of 0.99 or greater while keeping a single representative feature. This led to the removal of 117 features. Subsequently, the distributions of the remaining features were evaluated. Those that showed a uniform distribution, Figure 22A were automatically removed and others, Figure 22B (bottom), with distributions far from the normal distribution, Figure 22C; were flagged for attention. A further 7 features were removed at this point with 363 remaining.

One or more plate maps (Figure 23) from the experiment can be constructed in a visual manner or built based on a column from the raw data files, or merged metadata, that defines the reagent class. Previously defined plate maps can be reused or easily copied and modified for a new experiment. The management of plate maps can be quite challenging, especially at the assay development stage where they can be complex and change frequently.

Plate Normalization, Data Transformation and Scaling

Once the plate map was assigned the raw data for all features could be investigated using a variety of static plots, Figure 24A or with an interactive Visual Data Mining, (VDM) module, Figure 24B. VDM gives the user the ability to visualize up to three features simultaneously by reagent class, plate or replicate. Data points can be labelled with metadata and split by metadata into separate plots. Users can also eliminate outliers. Groups of wells can be annotated as new Reagent Classes. This allows for the easy tracking of a group of wells through subsequent analysis. This ability to be able to work more interactively with the data set is very powerful. It makes it possible to identify and investigate problems in the data set. It also makes it easier to gain a better understanding of the inner workings of the assay platform, especially for collaborators.

The median of all the plate Z-primes Figure 24C, SSMDs and Absolute Maximum Pearson Correlations were calculated for all features, **Supplementary File 13**. 20 features had a Z-prime greater than 0.5. Our default feature had a median Z' of 0.686. At this point features can also be easily removed.

Supplementary File 12. Stratominer metadata

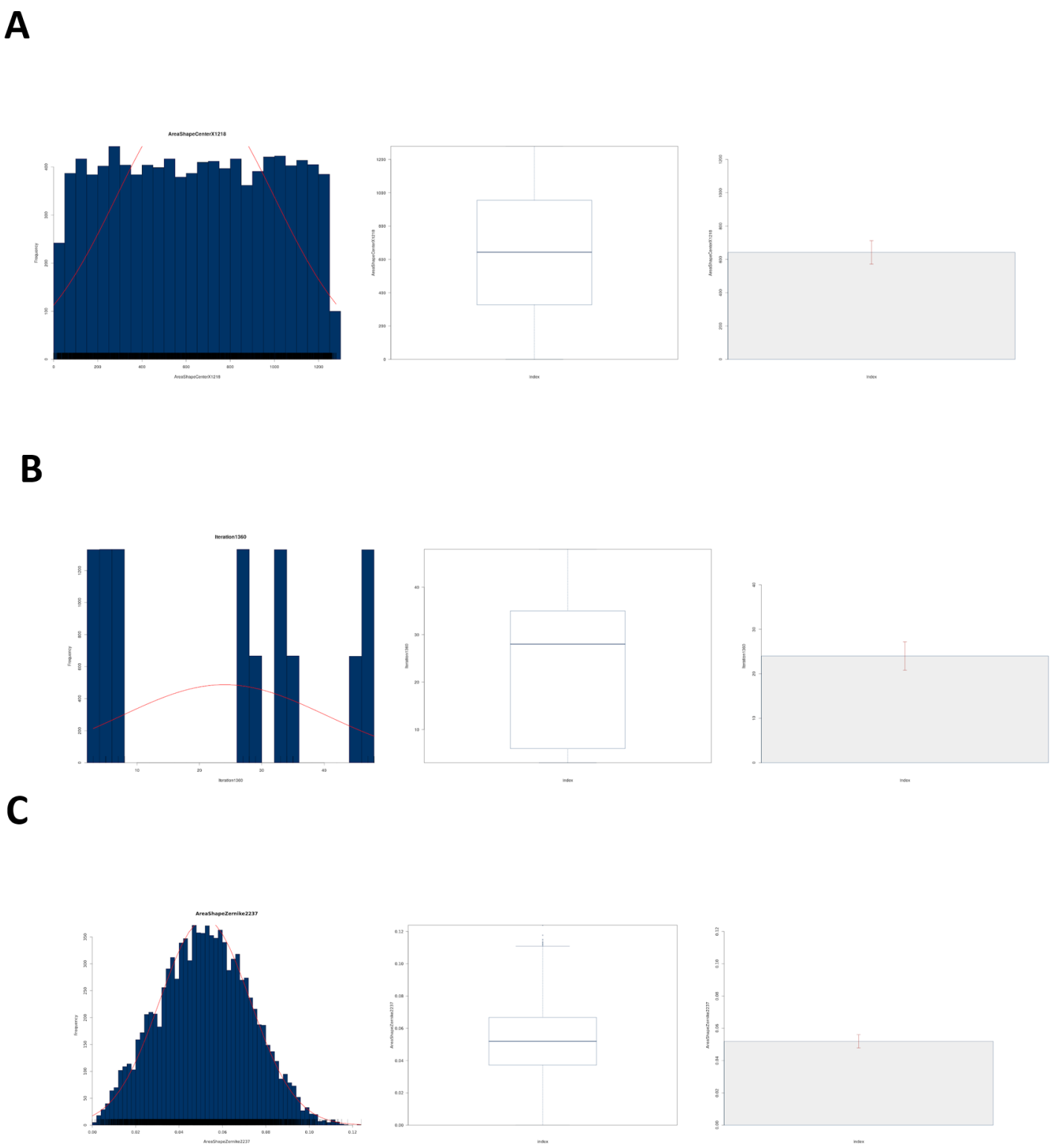

Figure 22 Data Preprocessing Examples of **A**. a feature with a uniform distribution, **B**. highly non-normal distribution and **C**. a normal distribution.

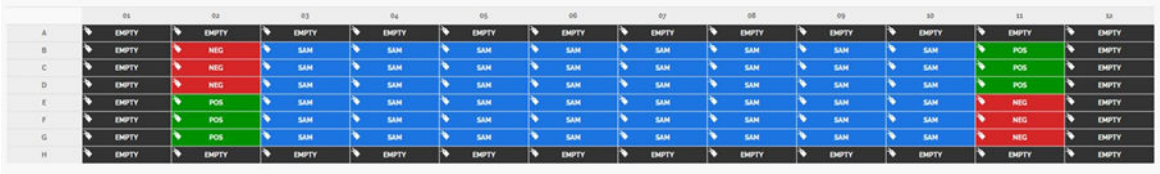

Figure 23 Plate Map Management. Template for assigning classifications to the compounds. This is developed in the StratomineR Plate Map Management tool. Users can differentiate between controls, screening perturbations and empty wells.

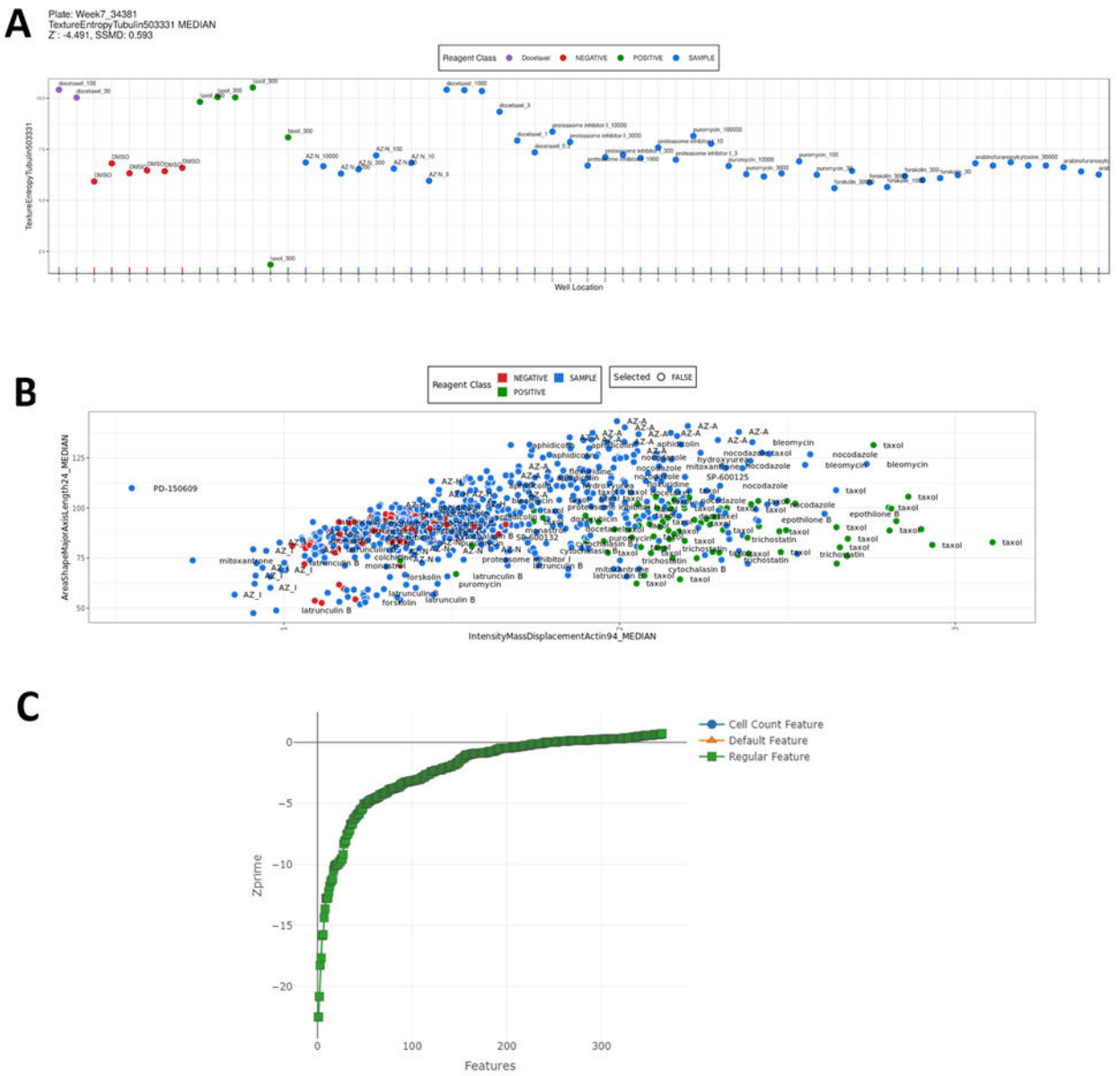

Figure 24 Quality Control. The visualization of raw data is critical for effective quality control. Effect of normalization on the data by plate. **A**. Static visualizations of data from a plate. **B**. Visualization of data for the complete experiment in VDM for the default and cell count features. **C**. A plot showing the median of the Z' scores for all features.

Data Imputation and Dimensionality Reduction Using Principal Components Analysis

All features were normalized at the plate level against the median of the negative DMSO control for that feature on that plate, Figure 24A. Other options here are to normalize against the median of all the samples or indeed the positive control. If a more traditional HTS approach was being taken the platform offers a Percent Inhibition, B-score and an option to normalize against the signal difference between the positive and negative controls that is termed Normalized % Control. All features are normalized in a similar fashion. The effect of the normalization is visualized using barplots and heatmaps.

Subsequent multiparametric analysis steps in the workflow are based on the mathematical assumptions that features have a normal distribution. To satisfy this, features that were heavily skewed from the normal distribution were identified and a transformation method was recommended. This resulted in 77 features being log-transformed, Figure 24B. Other options include square root and square and cube transformations. For similar reasons, a scaling method can be applied. A multiparametric analysis will be biased by features that have extreme scales. All features were then scaled using a robust z-score method on a plate basis, Figure 24C. Other options here include a standard z-score or a min-max method that scales all features from 0 to 1.

Supplementary File 13: Feature metrics

Missing data cannot be tolerated in certain methods used in our analysis. Missing data can result in dividing a value by zero which will result in errors. For this reason, it can be detected, and data imputation can be carried out with several options. The simplest method offered is to replace the missing value with the median of the other replicates. If this is not possible, the median of the column is used. More advanced regression and ML-based methods are also offered but these are computationally more intensive. In this case, no missing data was detected.

Cellular features are often not normally distributed and comparisons are best made on transformed and normalized features as shown in Figure 25.

For feature reduction users have the option of Common Factor Analysis, Principal Component Analysis or a form of non-linear reduction called Independent Component Analysis. In this case we chose principal component analysis (PCA). Figure 26A shows a correlation matrix of all the remaining features. It shows significant redundancy in the data set. A preview of the PCA generated a Scree plot which showed that the calculation of 9 would be appropriate, Figure 26B. 9 principal components were then calculated. The loadings of the features on the individual components were recorded, Supplementary File 14, shown in Figure 26C.

Supplementary File 14: Factor loadings

Hit and Novel Phenotype Identification Using Stratominer

In the analysis of traditional HTS data hits are identified based on a single score. In the case of high content data however doing this based on one feature or one component may neglect other phenotypic hits. For this reason, the StratoMineR platform allows for the quantification of phenotypic differences using a multidimensional distance score. The distance score is highly attractive in that it can provide a very simple answer to the very difficult question, “How different are these populations of cells?”. The number is always positive and in StratoMineR obvious differences generally lead to a distance score of 3 or more. The distance score, while a great measure of the strength of a phenotype does not give insight into the classification of different phenotypes (21). To do this, we can go back to the scores used and carry out clustering analysis to separate wells into groups of phenotypes (44).

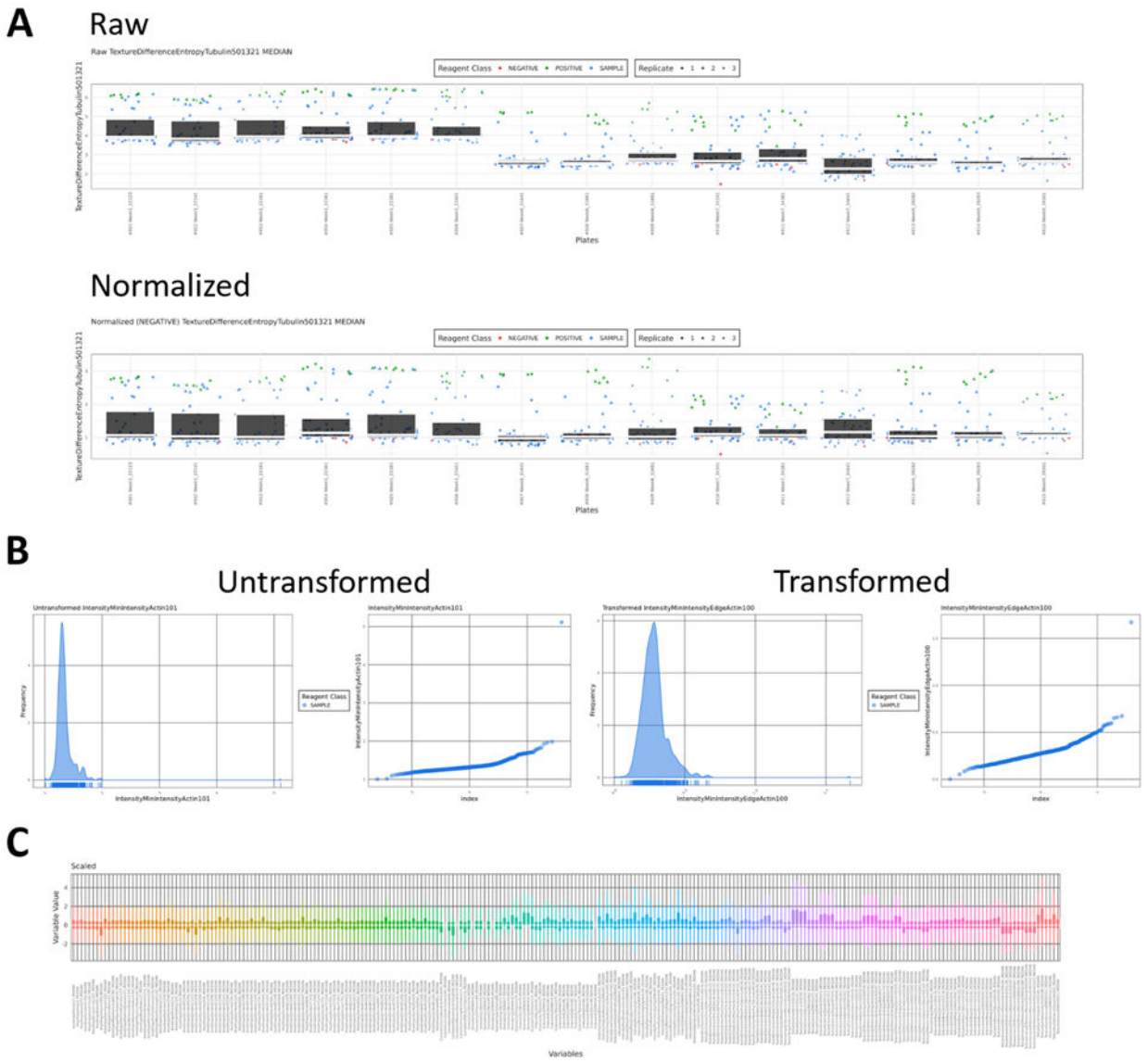

Figure 25 Normalization Transformation and Scaling. **A**. Normalization of plates across the screen. In this case, the feature, TextureEntropyTubulin503331, is one of many that show a strong differential between the positive and negative controls. This feature is used to monitor data normalization across the plates. **B**. Data transformation. Most features show skewing, as can be seen the top panel. If excessive, the data can be transformed (typically by a log transformation, but occasionally by a power transformation) to better fit a normal distribution. Q-Q plots for both, which give a stronger visual assessment of how well the data fits a normal distribution, are shown to the right of the density plots. **C**. Global assessment of skewing for all of the feature data. Box plots for the entire data set are shown, facilitating the identification of features that are strongly skewed and may need to be transformed or eliminated.

The distance score can be used to ask the very general question, "What wells look different from the Negative Controls?", by looking for wells that are distant from those controls, but if we have a robust positive control we can also ask a very specific question, "What wells look similar to our Positive Control" by looking for those that are close to the positives.

Here we use our 9 PCs to calculate a Euclidean distance score from the median of the Negative controls. For each well a p-value was also calculated based on the distribution of the negative Controls. A p-value cut-off of p,0.05 gave a hit rate of 36.25% with a false positive rate of 1.11% and a false negative rate of 0%. The. This high hit rate was expected, Figure 27A and Figure 27B. Full list is available in **Supplementary File 15.**

Supplementary File 15: Hit characterization

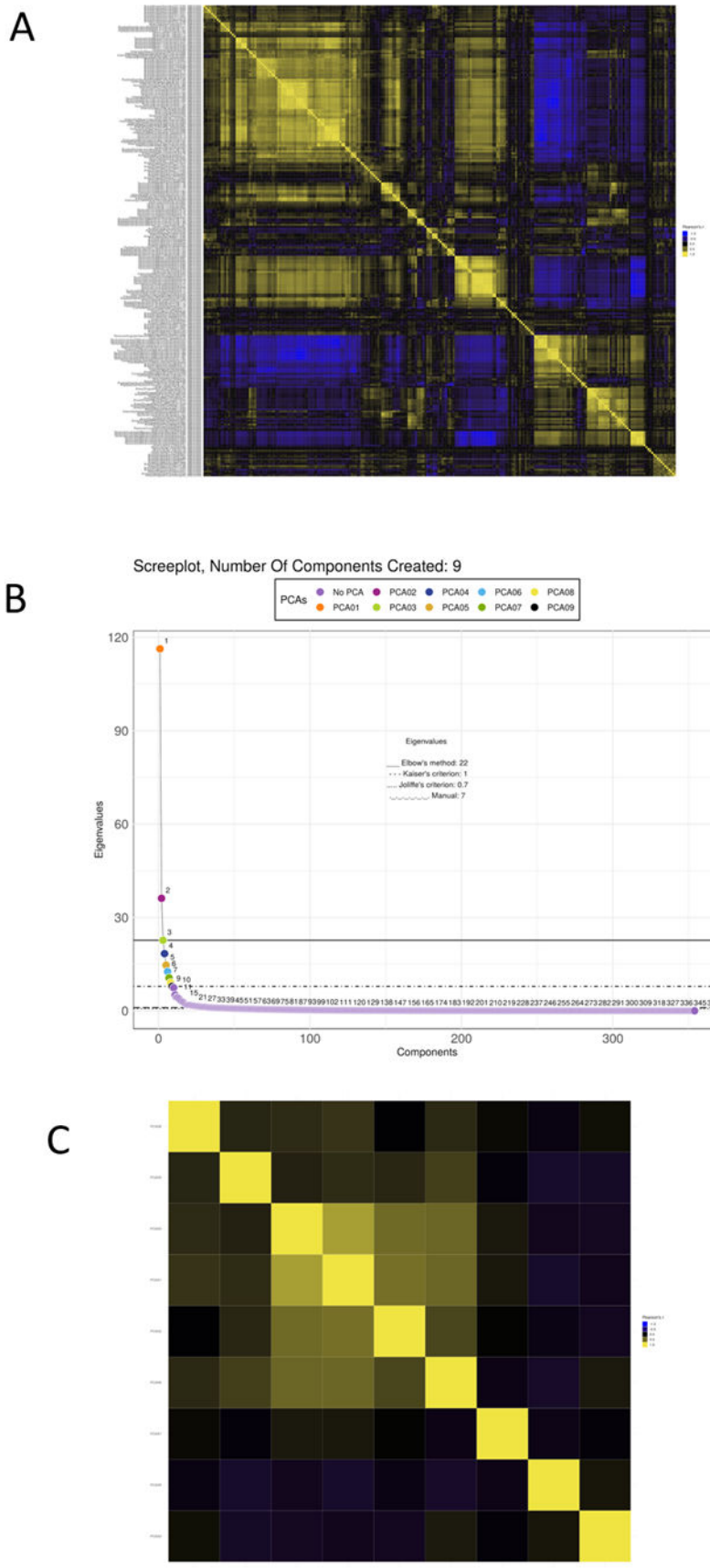

Figure 26 Feature reduction using Principal Components Analysis (PCA). **A**. Initial scoring of feature relationships by a correlation matrix. Correlations were scored by Spearman's ρ. **B**. PCA generates a set of new scales based on linear combinations of the initial features. The features are then rank ordered in a scree plot, which shows that only a small number of the components make significant

contributions to scoring the samples. **C.** The first nine components were shown to play appreciable roles in scoring the samples. The correlation matrix shows a high level of independence between them.

We took the hits and carried out hierarchical clustering using the 9 PC scores. Examination of the clusters showed that compounds that had the same annotated mechanism of action, (MOA), tended to cluster Figure 28, suggesting that the assay platform was indeed useful for separating phenotypes derived from different MOAs. We then adopted a more specific hit picking approach and calculated distance scores for all samples from the median of the taxol Positive controls. When we examined the top 20 hits that had the lowest distance scores, (closest to the Positives), 18/20 were taxol, docetaxel or epothilone B, all microtubule inhibitors, suggesting that the assay could be useful for identifying novels compounds with a similar MOA to a control.

We now tested a Machine Learning approach in which we used the Negative and Positive Controls to train a two-class Random Forest model. As in the KNIME workflow described above this model successfully identified taxol, docetaxel and epothilone B wells as being similar to the taxol Positive controls. The model was highly accurate with a well accuracy of 98.34% and a Kappa of 0.955. Unsurprisingly, 6 of the top 10 most important features were from the Tubulin channel. Interestingly, high concentrations of mitoxantrone were also picked up, a finding that was supported by a report that mitoxantrone has been found to be a tubulin inhibitor (27).

The success of the Machine Learning method for identifying phenotypes similar to that of the taxol Positive Control spurred us to test whether it could be used to classify compounds based on phenotypes identified in the screen. The fact that we could separate microtubule inhibitors, actin inhibitors and DNA damaging agents using the unsupervised methods suggested that this would be the case. We decided to identify suitable wells amongst the tested samples for the building of a machine learning model for phenotypes other than that of taxol.

Multi-Phenotype Machine Learning

As a first step we calculated distance scores for all the samples and generated dose-response curves for each of the 30 tested compounds. These curves made it very easy to identify compounds that gave strong dose-dependent phenotypic changes, Figure 29 and inspection of images from the data showed that the increased distance score did indeed correlate with visible changes in phenotype. Based on this analysis we chose Docetaxel, (microtubule inhibitor), Latrunculin B, (actin inhibitor), Doxorubicin, (DNA damage) and a compound AZ-I of unknown mechanism of action, for building our extended machine learning model, Figure 30. We chose two wells from each compound for building the model by defining these as new Reagent Classes in the StratoMineR plate map. We now built a five class Random Forest model and applied this to the whole data set. The resulting model was 96.3% accurate at the cell level and 95.7% accurate at well level, with a Kappa value of 0.949, Figure 31. Examination of the probability scores confirmed the accuracy of the model. The Docetaxel class pulled out taxol, a chemical analogue of docetaxel but also epothilone B, which is structurally quite different. This was a good validation of the power of High Content Screening to be able to identify chemically diverse compounds that give a similar phenotype. Latrunculin B pulled out the only other actin inhibitor in the data set, Cytochalasin B. Similarly, Doxorubicin pulled out multiple DNA damaging agents.

Conclusions

This analysis is another demonstration of the power of machine learning for phenotypic screening. One major benefit of the RF models is that they provide a feature importance plot which gives immediate insight into the biological differences between phenotypes. This is more difficult to discern in our Unsupervised analytics path. Our analysis also highlights the value of the combination of the Unsupervised analytics with Artificial Intelligence. Using the unsupervised path, we were able to identify robust phenotypes for training on a high-quality training set is essential for a high-quality ML model.

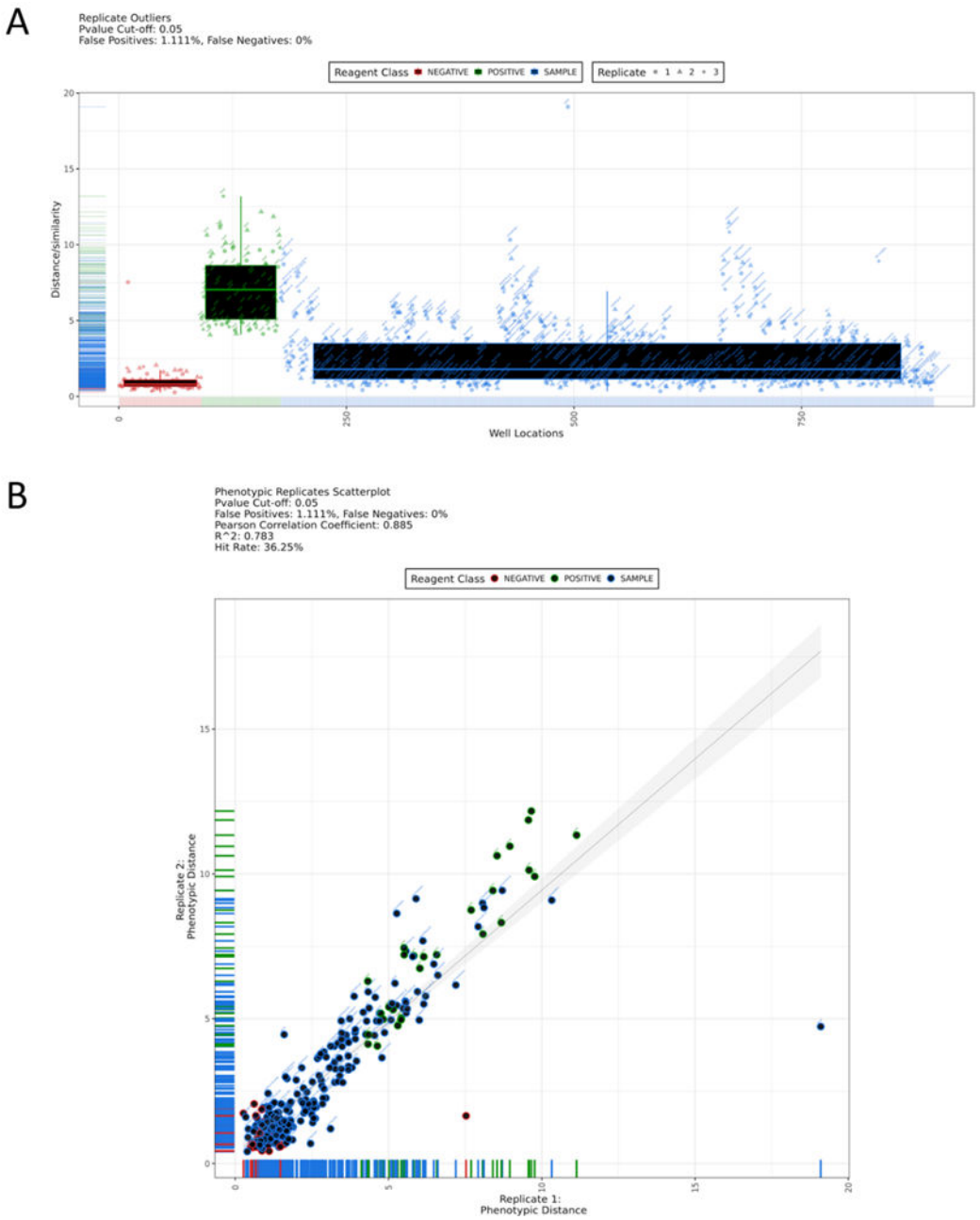

Figure 27 Hit Selection. **A**. The distance scores for each well in the screen grouped by reagent class. **B**. The correlation between the distance scores for the first two replicates across the complete experiment.

Fundamental to the notion of model deployment is the recognition of the parametric assumptions (if any) underlying the joint associations between input features and outputs. In most link-based regression models (such as linear regression, logistic regression), the data is assumed to arise from an exponential family (such as Gaussian, Poisson). Similarly, discriminant analyses (LDA/QDA) assume the feature space is multivariate Gaussian. While broadly applicable (and possibly inducible via appropriate transformations like Box-Cox or logarithm transformation), there may be scenarios where the model may not be applicable to the outcome we desire to model (i.e data many not be Gaussian). In such cases, it may be better to seek nonparametric approaches (like random forests) for regression or classifier modeling.

Similarly, unsupervised methods like clustering require several factors to be assessed before finding a reliable grouping strategy for deriving the most insight. Specifically, the choice of distance function (not all information

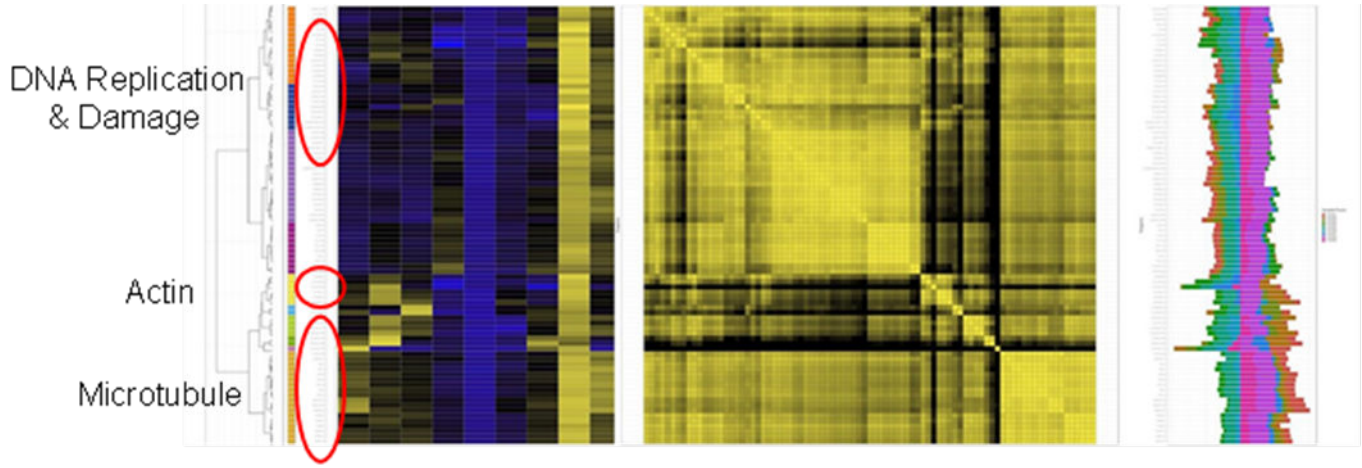

Figure 28 Clustering. Hierarchical clustering of the 9 principal component scores of hits reveals that samples with the same mechanism of action cluster together.

spaces obey Euclidean geometry) is fundamental to any downstream step involving clustering. Similarly, the choice of optimal cluster number is another important choice while model selection criteria like silhouette width, Akaike information criteria (AIC). The use of cluster validity statistics (45) is another potential way to assess the appropriate grouping structure in the data, using some relevant side information about the (potentially noisy) labels in the data. Several model-based clustering algorithms rely on multivariate Gaussian or convex assumption in the feature space that may not always be reasonable. We recommend an examination of multiple classes of clustering algorithms in order to most meaningfully query the structure in the data. Topological data analysis (46)techniques are another way to derive insight into the structure of the data to inform the clustering algorithm most likely to reveal insight.

Assessing heterogeneity: An oft-repeated observation about high content high throughput data is the enormous phenotypic heterogeneity in the imaging information. Specifically, the notion that imaging phenotypes from a single well may contain a mixture of phenotypes rather than a unique one. To deconvolve this, however, techniques are still in development. Rohban et.al (47) model the means and covariances in the observed data to discriminate mechanism of action for various drugs in the Cell Painting Assay. Kuthuru et.al (48) use a bag-of-visual words paradigm (routinely used in computer vision) to describe heterogeneity of morphometric phenotypes in an image. As has been described elsewhere (30) reduction of such morphologic heterogeneity into average/median/summary measurements overlooks heterogeneity that might be relevant to assessing the diversity of phenotypic consequences due to drug/perturbagen activity.

Appropriate assessment of model performance: While conventional metrics like AUROC, accuracy and null information rate are routinely used to assess the performance of machine learning models for discriminating phenotypes, it is essential to also examine the uncertainty associated with predictions; prediction intervals are one potential way to do this. Such measurements are essential before using these “out-of-the-box” models for downstream processes (such as for discriminating drug MoA). It is also essential to assess these prediction probabilities for biases due to “batch effects” (in contrast to biological variation) like imaging platform, pre-processing algorithms and acquisition settings before they can be used for other problems. Additionally, assessments of equivalence in feature distributions between “source” domain (the data set used to build the model) and “target” domain (the new data on which the model is to be applied) are essential to ensure appropriate model transferability/transportability so that these phenotype discrimination models are used in the right context. Batch effect assessments are also key to assess and mitigate before combining multiple data sets to create large metadata sets, before doing data analysis and model building.

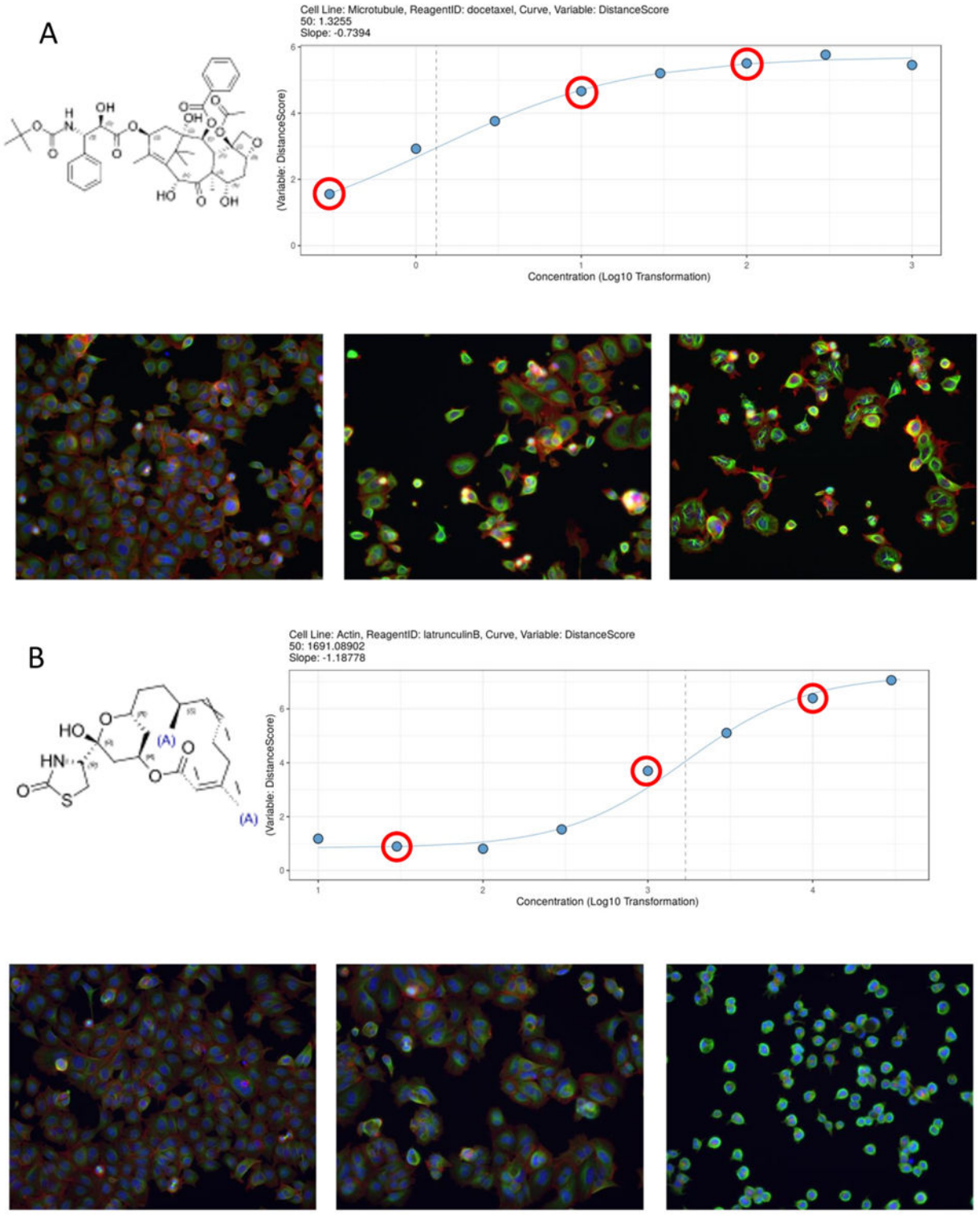
A
Cell Line: Microtubule, ReagentID: docetaxel, Curve, Variable: DistanceScore
50: 1.3255
Slope: -0.7394
(Variable: DistanceScore)
Concentration (Log10 Transformation)
B
Cell Line: Actin, ReagentID: latrunculinB, Curve, Variable: DistanceScore
50: 1691.08902
Slope: -1.18778
(Variable: DistanceScore)
Concentration (Log10 Transformation)

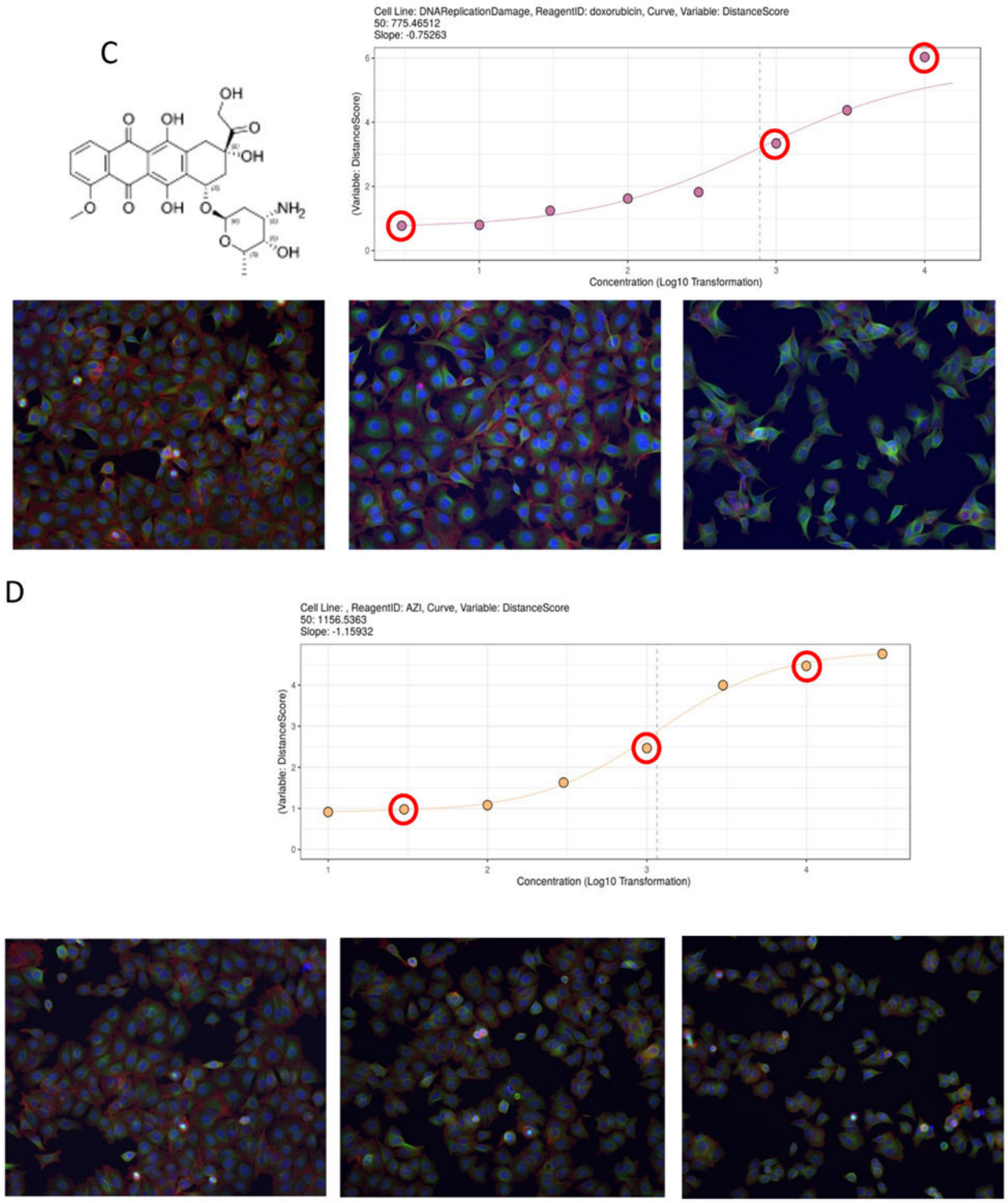

Figure 29 Novel Phenotype Identification. The distance scores all wells for **A**. Docetaxel, a tubulin inhibitor, **B**. Latrunculin B an actin inhibitor, **C**. Doxorubicin a DNA damaging agent, and **D**. AZ-I, with undisclosed mechanism of action; were plotted against dose. Low, intermediate and high distance score wells were chosen and representative images for these wells are shown.

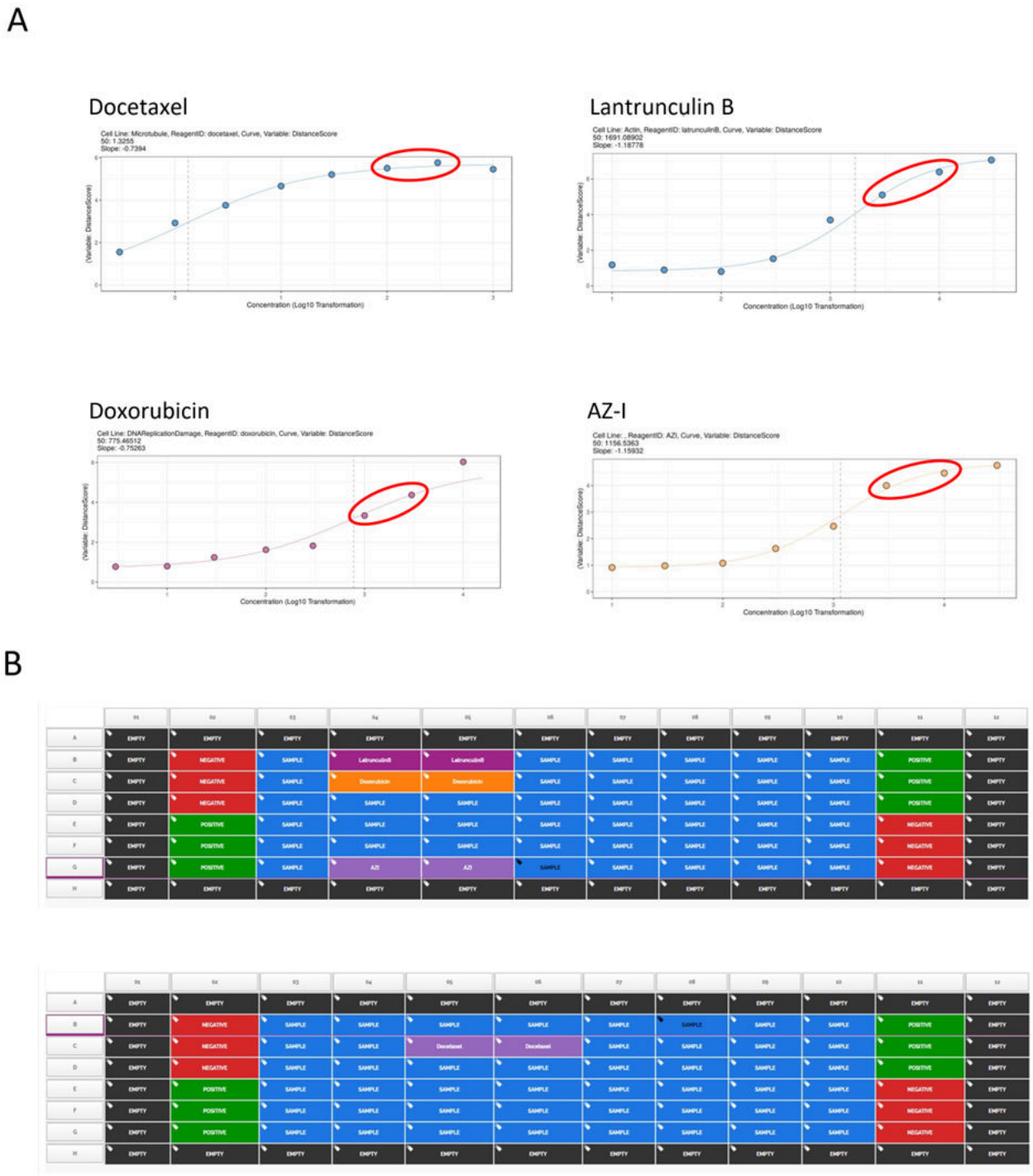

Figure 30 Selecting treatment conditions for training a classifier, based on the phenotype discovery in Figure 29. Identified wells were relabeled in the plate maps for the appropriate plates.

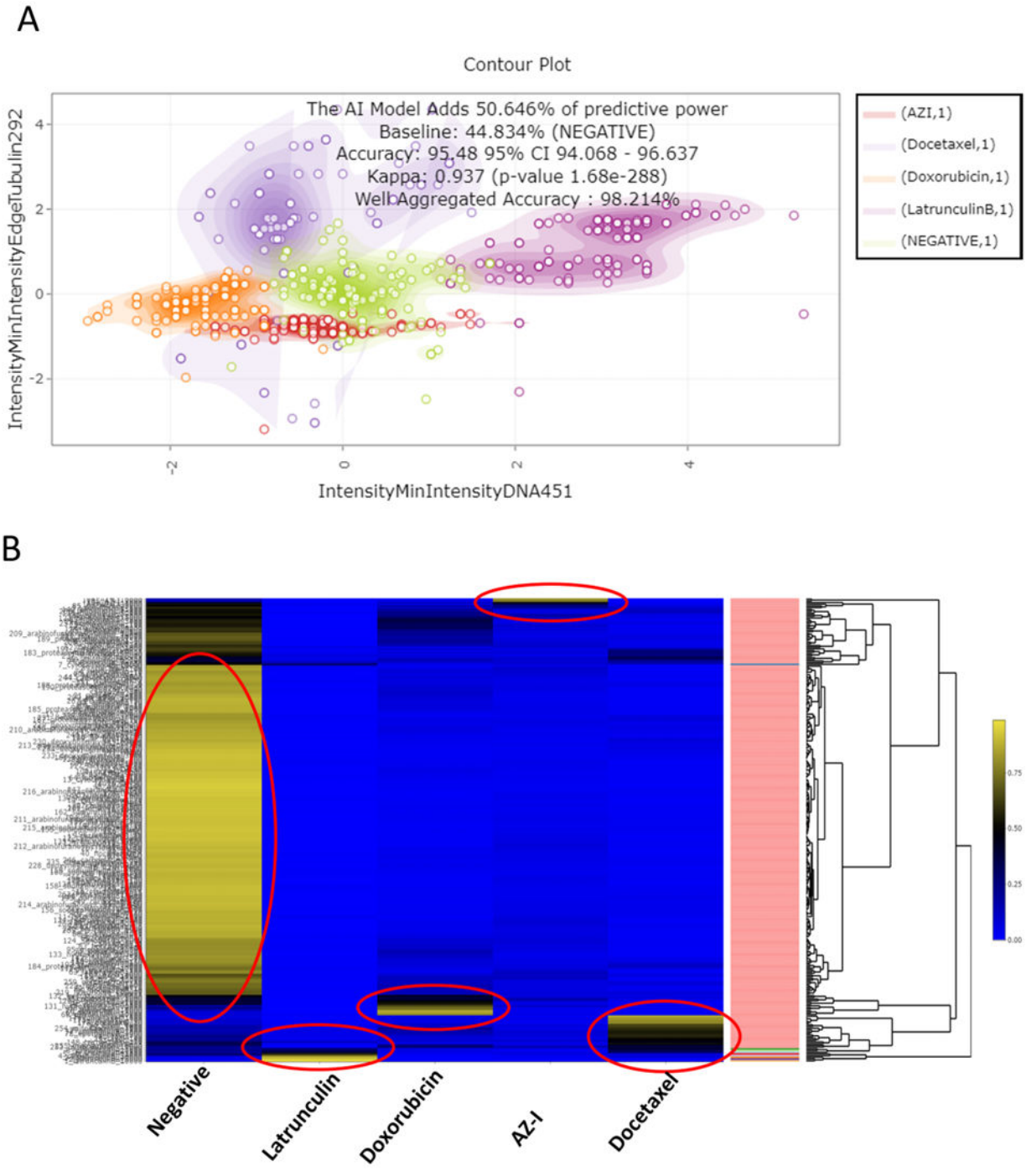

Figure 31 Results from the classification model based on novel phenotypes. **A**. 2D representation of the data showing differentiation of the samples into groups based on the scores of the two features with the highest importance in the machine learning model. **B**. Clustering of the probabilities of each sample being in each of the trained classes. Low probability ids blue, high probability is yellow.

References

1. Singh S., Carpenter A.E., Genovesio A. Increasing the Content of High-Content Screening: An Overview. J Biomol Screen. 2014;19(5):640–50.
2. Collins T.J., et al. A Versatile Cell Death Screening Assay Using Dye-Stained Cells and Multivariate Image Analysis. Assay Drug Dev Technol. 2015;13(9):547–57.

3. Law C.J., et al. Assay development and multivariate scoring for high-content discovery of chemoprotectants of endoplasmic-reticulum-stress-mediated amylin-induced cytotoxicity in pancreatic beta cells. Assay Drug Dev Technol. 2014;12(7):375–84.
4. Comsa S., Cimpean A.M., Raica M. The story of MCF-7 breast cancer cell line: 40 years of experience in research. Anticancer Research. 2015;35:3147–3154.
5. Caie P.D., et al. High-content phenotypic profiling of drug response signatures across distinct cancer cells. Mol Cancer Ther. 2010;9(6):1913–26.
6. Bray M.A., et al. Cell Painting, a high-content image-based assay for morphological profiling using multiplexed fluorescent dyes. Nat Protoc. 2016;11(9):1757–74.
7. Ljosa V., Sokolnicki K.L., Carpenter A.E. Annotated high-throughput microscopy image sets for validation. Nat Methods. 2012;9(7):637.
8. Williams E., et al. The Image Data Resource: A Bioimage Data Integration and Publication Platform. Nat Methods. 2017;14(8):775–781.
9. Carpenter A.E., et al. CellProfiler: image analysis software for identifying and quantifying cell phenotypes. Genome Biol. 2006;7(10):R100.
10. Dao D., et al. CellProfiler Analyst: interactive data exploration, analysis and classification of large biological image sets. Bioinformatics. 2016;32(20):3210–3212.
11. Jones T.R., et al. CellProfiler Analyst: data exploration and analysis software for complex image-based screens. BMC Bioinformatics. 2008;9:482.
12. McQuin C., et al. CellProfiler 3.0: Next-generation image processing for biology. PLoS Biol. 2018;16(7):e2005970. p.
13. Arena E.T., et al. Quantitating the cell: turning images into numbers with ImageJ. Wiley Interdiscip Rev Dev Biol. 2017;6(2)
14. Schindelin J., et al. Fiji: an open-source platform for biological-image analysis. Nat Methods. 2012;9(7):676–82.
15. Schindelin J., et al. The ImageJ ecosystem: An open platform for biomedical image analysis. Mol Reprod Dev. 2015;82(7-8):518–29.
16. Dietz C., Berthold M.R. KNIME for Open-Source Bioimage Analysis: A Tutorial. Adv Anat Embryol Cell Biol. 2016;219:179–97.
17. Stoter M., et al. CellProfiler and KNIME: Open-Source Tools for High-Content Screening. Methods Mol Biol. 2019;1953:43–60.
18. Bray M.A., Carpenter A.E. Quality Control for High-Throughput Imaging Experiments Using Machine Learning in Cellprofiler. Methods Mol Biol. 2018;1683:89–112.
19. Brideau C., et al. Improved statistical methods for hit selection in high-throughput screening. J Biomol Screen. 2003;8(6):634–47.
20. Ljosa V., et al. Comparison of methods for image-based profiling of cellular morphological responses to small-molecule treatment. J Biomol Screen. 2013;18(10):1321–9.
21. Young D.W., et al. Integrating high-content screening and ligand-target prediction to identify mechanism of action. Nat Chem Biol. 2008;4(1):59–68.
22. Kummel A., et al. Comparison of multivariate data analysis strategies for high-content screening. J Biomol Screen. 2011;16(3):338–47.
23. Kümmel A., et al. Integration of multiple readouts into the z' factor for assay quality assessment. J Biomol Screen. 2010;15(1):95–101.
24. Hutz J.E., et al. The multidimensional perturbation value: a single metric to measure similarity and activity of treatments in high-throughput multidimensional screens. J Biomol Screen. 2013;18(4):367–77.
25. Reisen F., et al. Benchmarking of multivariate similarity measures for high-content screening fingerprints in phenotypic drug discovery. J Biomol Screen. 2013;18(10):1284–97.
26. Warchal S.J., Dawson J.C., Carragher N.O. Development of the Theta Comparative Cell Scoring Method to Quantify Diverse Phenotypic Responses Between Distinct Cell Types. Assay Drug Dev Technol. 2016;14(7):395–406.

27. Warchal S.J., Dawson J.C., Carragher N.O. Evaluation of Machine Learning Classifiers to Predict Compound Mechanism of Action When Transferred across Distinct Cell Lines. SLAS Discov. 2019;24(3):224–233.
28. Perlman Z.E., et al. Multidimensional drug profiling by automated microscopy. Science. 2004;306(5699):1194–8.
29. Loo L.H., Wu L.F., Altschuler S.J. Image-based multivariate profiling of drug responses from single cells. Nat Methods. 2007;4(5):445–53.
30. Caicedo J.C., et al. Data-analysis strategies for image-based cell profiling. Nat Methods. 2017;14(9):849–863.
31. Iversen, P.W., et al., *HTS Assay Validation.*, in *Assay Guidance Manual*, G.S. Sittampalam, et al., Editors. 2012, Eli Lilly and Company and the National Center for Advancing Translational Sciences: Bethesda, MD.
32. Box, G.E.P., E.G. Hunter, and J.S. Hunter, *Statistics for experimenters : an introduction to design, data analysis, and model building*. 1978, New York: Wiley.
33. Lutz M.W., et al. Experimental design for high-throughput screening. Drug Discov Today. 1996;1:277–286.
34. Malo N., et al. Statistical practice in high-throughput screening data analysis. Nat Biotechnol. 2006;24(2):167–75.
35. Feng T., et al. Optimal design for high-throughput screening via false discovery rate control. Stat Med. 2019;38(15):2816–2827.
36. Makarenkov V., et al. HTS-Corrector: software for the statistical analysis and correction of experimental high-throughput screening data. Bioinformatics. 2006;22(11):1408–9.
37. Liu R., et al. HDAT: web-based high-throughput screening data analysis tools. Computational Science and Discovery. 2013;6(1):014006. p.
38. Murie C., et al. Improving detection of rare biological events in high-throughput screens. J Biomol Screen. 2015;20(2):230–41.
39. Zhai Y., et al. An Automatic Quality Control Pipeline for High-Throughput Screening Hit Identification. J Biomol Screen. 2016;21(8):832–41.
40. Wu Z., Liu D., Sui Y. Quantitative assessment of hit detection and confirmation in single and duplicate high-throughput screenings. J Biomol Screen. 2008;13(2):159–67.
41. Zhang J.H., Chung T.D., Oldenburg K.R. A Simple Statistical Parameter for Use in Evaluation and Validation of High Throughput Screening Assays. J Biomol Screen. 1999;4(2):67–73.
42. Zhang X.D. Illustration of SSMD, z score, SSMD*, z* score, and t statistic for hit selection in RNAi high-throughput screens. J Biomol Screen. 2011;16(7):775–85.
43. Filer D.L., et al. tcpl: the ToxCast pipeline for high-throughput screening data. Bioinformatics. 2017;33(4):618–620.
44. Omta W.A., et al. HC StratoMineR: A Web-Based Tool for the Rapid Analysis of High-Content Datasets. Assay Drug Dev Technol. 2016;14(8):439–452.
45. Brock G., et al. clValid, an R package for cluster validation. Journal of statistical Software. 2008;25(4)
46. Laubenbacher R., Hastings A. Topological Data Analysis. Bull Math Biol. 2019;81(7):2051.
47. Rohban M.H., et al. Capturing single-cell heterogeneity via data fusion improves image-based profiling. Nat Commun. 2019;10(1):2082.
48. Kuthuru S., et al. A Visually Interpretable, Dictionary-Based Approach to Imaging-Genomic Modeling, With Low-Grade Glioma as a Case Study. Cancer Inform. 2018;17:1176935118802796. p.

Biosensor Assays for Measuring the Kinetics of G-Protein and Arrestin-Mediated Signaling in Live Cells

Sam R.J. Hoare[1] and Thomas E. Hughes[2]

Created: September 1, 2021.

Abstract

G-protein-coupled receptors transmit signals through cascades of cellular signaling molecules to orchestrate physiological responses. Measuring the time course (kinetics or dynamics) of GPCR signaling is revealing new spatiotemporal paradigms of signaling with biological and therapeutic implications. Kinetics also impact drug activity measurements, for example biased agonism. Biosensors greatly facilitate the measurement of signaling kinetics by detecting signaling in live cells in real time; a ligand is applied to cells, the cells placed in a reader, and the change in light emission measured repeatedly over time. In this chapter, methods are presented for assaying signaling molecules using genetically-encoded fluorescent biosensors. Protocols are provided for the most common G-protein pathways (Gs and Gi, detecting cAMP; Gq, detecting diacylglycerol and Ca^{2+}), and also for arrestin recruitment. Methods for analyzing the time course data are required to obtain kinetic drug signaling parameters useful for lead optimization and large-scale receptor research. One such parameter is the initial rate of signaling by the ligand bound receptor (k_τ), a biologically-meaningful and familiar metric. Straightforward curve fitting methods are described for measuring the initial rate by analyzing the whole time course without the need to isolate the linear portion of the curve. Biased agonism is quantified using this approach, providing a simple metric that takes into account differential kinetics of signaling. These experimental and analysis methods enable investigators to routinely measure and quantify the kinetics of signaling in their receptor research and drug discovery projects.

Introduction

The superfamily of G-protein-coupled receptors comprise the largest family of signaling proteins in the human genome, transducing a remarkable diversity of extracellular stimuli into intracellular signaling networks that modulate and control physiological responses (1-3). Methods for measuring the intracellular signaling molecules have been evolving for sixty years. Laborious chemical methods were used in the discovery of second messengers and elucidation of their function, such as cAMP and inositol phospholipids (4,5). The development of immunoassays to quantify second messengers greatly improved throughput, enabling functional assays to be used routinely in drug screening (6). Biosensors are the latest advance in the measurement of GPCR signaling (7-12) (comprehensively reviewed in refs. (13,38)). These agents enable noninvasive detection of signaling molecules such as second messengers; the biosensor produces an optical signal on binding the target signaling molecule, which can be detected in plate readers. This technology provides three advances - the workflow for detecting the signal is minimal (Figure 1); signaling can be measured in live cells; and signaling can be measured routinely over time. Biosensors greatly facilitate time course assays because a single plate can be used for all the time points. In the workflow, ligands are applied to the cells, the plate placed in the plate reader, then the optical signal from the biosensor measured repeatedly in the same plate (Figure 1). This modality is referred to colloquially as “Real time” or “Continuous read” detection.

A genetically-encoded biosensor is a protein, transcribed from DNA delivered into cells, usually comprising two components (Figure 2) (13). First is a domain that binds the target molecule being detected, for example cAMP. The second is a fluorescent or luminescent reporter protein that produces a light signal. The biosensor is

Author Affiliations: 1 Pharmechanics, LLC. 2 Montana Molecular.

Corresponding author.

designed in such a way that the binding of the target molecule to the sensor causes a change in the optical properties of the reporter, e.g. emission of a photon or a change of fluorescence emission intensity (Figure 2) (13). In this way, a biological signal is converted to a light signal that can be easily detected. For GPCR signaling, numerous biosensors have been developed, the second messengers that can be detected including cAMP, Ca^{2+}, diacylglycerol (DAG) and phosphatidylinositol 4,5-bisphosphate (PIP_2) (see Table 2 of ref. (13)). In this chapter, the biosensors used are fluorescent - they are excited with an external light source at one wavelength and emit light at a second, longer wavelength. Binding of the target molecule causes a change of the intensity of the emitted light (Figure 2), which can be detected using a plate reader. The first goal of this chapter is to provide experimental protocols for employing the biosensors to measure GPCR signaling (see Measuring GPCR Signaling Using Genetically-Encoded Fluorescent Biosensors).

Measuring signaling over time is valuable for two reasons - discovering new signaling mechanisms and optimizing new therapeutics. Measuring the time course reveals new mechanisms of GPCR signaling and regulation. For example, in the late 1960's and 1970's it was discovered, by measuring cAMP over time, that the signal fades after reaching a peak (15-17). This phenomenon, termed desensitization, contributed to the discovery of the molecular machinery of GPCR regulation, including GPCR kinases and arrestins (reviewed in refs (14,18). More recently it was shown that some GPCR signals endure after the ligand has been washed out, evident from measuring the time course of signaling before and after washout (10,19-23). This led to the discovery of sustained signaling by internalized receptors, a new spatiotemporal dimension of GPCR signaling of potential therapeutic utility (24-26). From the perspective of optimizing new therapeutics, time course pharmacological studies have revealed that drug activity in signaling assays can change over time (27-30). For example, for the D2 dopamine receptor, the rank order of efficacy for a series of ligands was shown to change over time, which resulted in measurements of biased agonism changing over time (27). Biased agonism is the capacity of a ligand to stimulate selectively only some of the signaling pathways stimulated by the GPCR and is of considerable interest in development of next-generation GPCR therapeutics (see this section) (31-35). This time problem can be solved by using the rates of signaling activity in the bias calculation (29).

Data analysis methods are required for time course data to extract useful pharmacological parameters, of a form that can be used to guide medicinal chemistry and basic research on GPCR signaling. Specifically, curve-fitting methods are needed to reduce the raw data to useful parameter values. One such parameter is the initial rate of signaling by the ligand occupied receptor, termed k_τ (29,36,37). This parameter was developed by applying enzyme kinetics to GPCR signaling, and is analogous to the initial rate of enzyme activity. k_τ is determined as the initial rate of signaling produced by a maximally-stimulating concentration of ligand (37). First, the whole time course curve is fitted to an equation in familiar curve-fitting software (e.g. Prism from GraphPad Software). The fitted parameters are then used to calculate the initial rate using a simple formula. The initial rate is then used to determine k_τ.

In this chapter we describe the experimental methods for measuring signaling using biosensors (Measuring GPCR Signaling Using Genetically-Encoded Fluorescent Biosensors). Hundreds of biosensors have been developed by numerous laboratories, as comprehensively reviewed in refs (13,38). In this chapter we exemplify the methods for fluorescent biosensors using sensors developed and/or distributed by Montana Molecular. These sensors have been optimized to be simple and routine to use, with a high brightness enabling detection using plate readers, and employing the Bacmam viral vector to ensure consistent, reproducible expression from well to well and plate to plate in numerous cell types. Next, the data analysis methods for analyzing time course data are presented, by which the initial rate and k_τ are determined (Analyzing Signaling Time Course Data). Finally, the approach is applied to biased agonism (Simplifying Biased Agonism Assessment Using Signaling Kinetics) and it is shown how quantifying the initial rate simplifies bias quantification, enabling a simple ratio of signaling rates to be employed. By combining the biosensor assay protocols and initial rate analysis, we aim to provide investigators a straightforward, streamlined method to routinely measure the kinetics of GPCR signaling, facilitating research into GPCR signaling mechanisms and the kinetic optimization of new therapeutics.

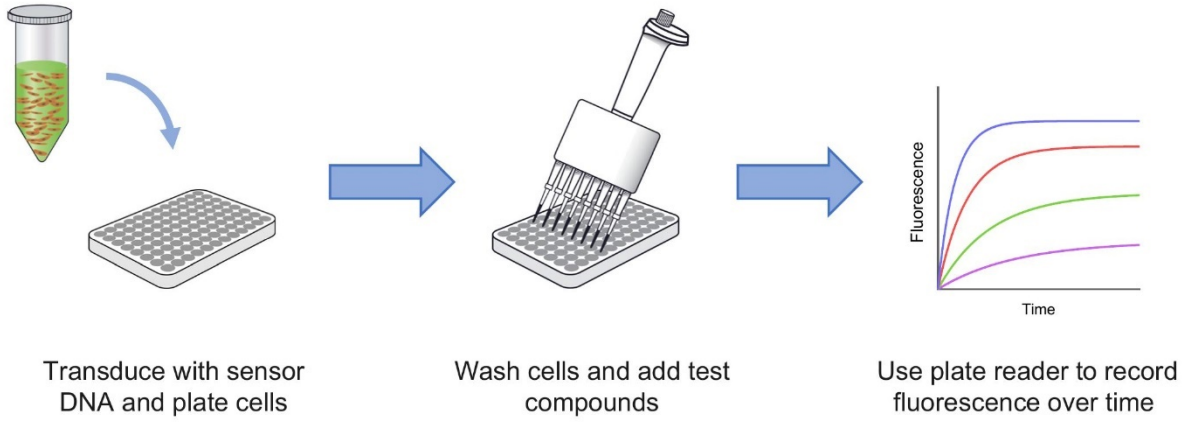

Figure 1. Assay overview of genetically-encoded fluorescent biosensors for measuring GPCR signaling. DNA for the biosensor is delivered into cells (left) and cells incubated for 24 hours to express the sensor. Medium is replaced with assay buffer and GPCR ligands added to the cells (center). The change in fluorescence resulting from activation of signaling is then measured in an automated plate reader (right).

Measuring GPCR Signaling Using Genetically-Encoded Fluorescent Biosensors

Biosensor Architecture

Genetically encoded, fluorescent biosensors offer many advantages. They provide real-time measurements of signaling dynamics, they can be genetically targeted to specific cell types, and these proteins can be directed to particular subcellular signaling domains. In this Chapter, we are focused on fluorescent biosensors, and to understand how the different types of fluorescent biosensors work, it is important to start with some basic photophysics. Imagine a fluorophore in solution in a cuvette. There are fundamentally only three ways in which the fluorescence intensity can change. The first is that the concentration of the fluorophore can increase or decrease. The second would be that the cross section of the fluorophore will change, and finally, it is always possible that the quantum efficiency will change (39).

Ratiometric, Two Color Sensors

The first fluorescent biosensors typically generated a change in Förster resonance energy transfer, or FRET, between two different fluorescent proteins (40). The chameleon Ca^{2+} sensor is an excellent example (41). In this sensor cyan and yellow fluorescent proteins were connected to one another by a linker that would change shape when bound to Ca^{2+}. Resonance energy transfer between two fluorophores is exquisitely sensitive to the distance between the fluorophores, and their relative orientation, so Ca^{2+} induced changes produced detectable changes in energy transfer. Here the underlying photophysics involves changes in the quantum efficiency of the donor fluorophore. This can be measured either by a change in the donor fluorescence intensity, or by the excited state lifetime of the donor, each of which will decrease as FRET efficiency increases. Many early sensors were created with the cyan/yellow pair of fluorescent proteins, but newer pairs of more efficient green and red proteins are being adopted (42,43). The fluorophore is buried in the middle of the fluorescent protein barrel, so FRET efficiency is quite limited. Indeed, the signal is so small that FRET-based sensors are not practical for use on automated fluorescence plate readers.

Beyond FRET sensors, two color ratiometric sensors have been designed to detect changes in the environment. For example, there is a chloride sensor in which the yellow fluorescent protein - venus - is halide sensitive while

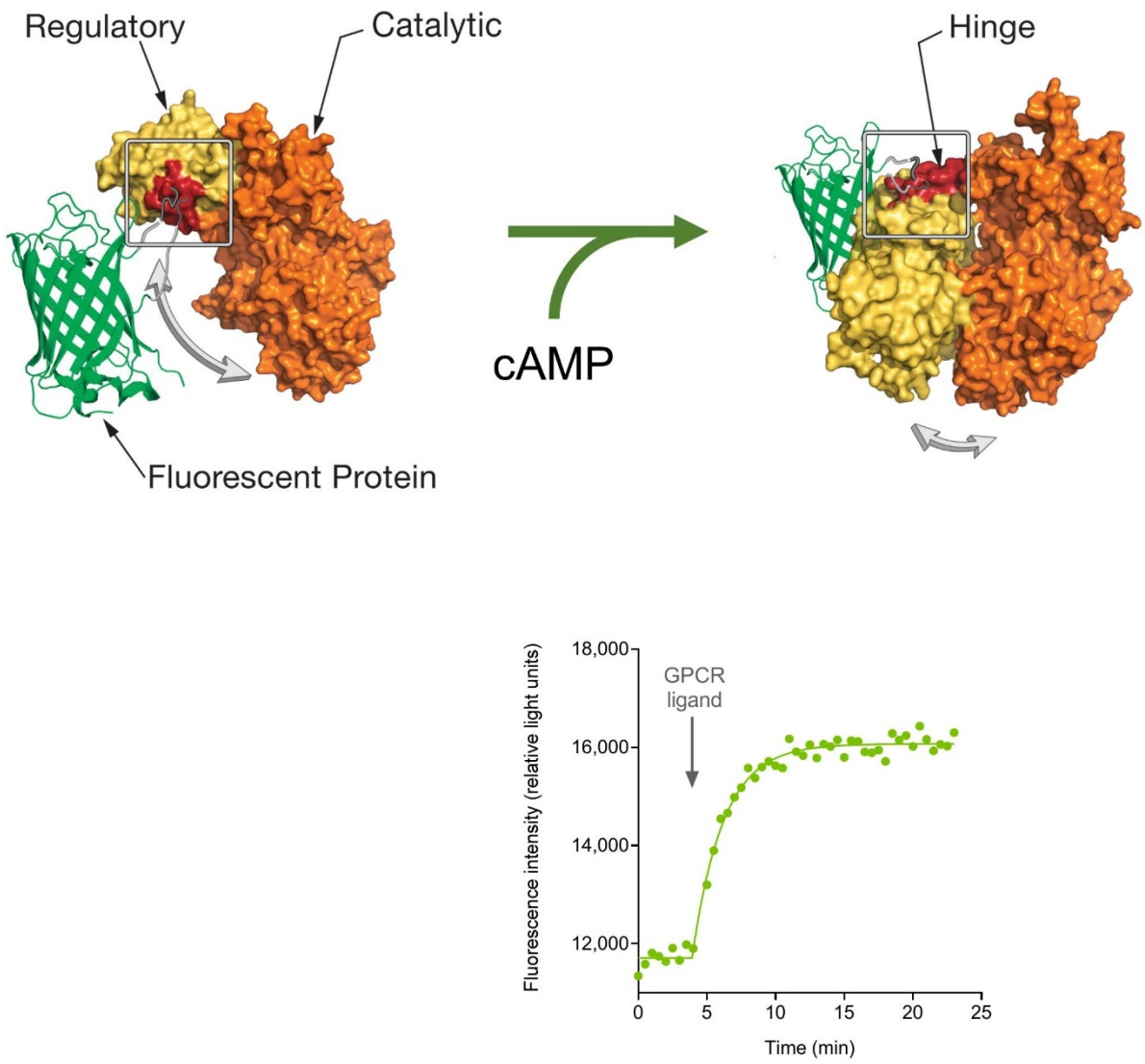

Figure 2. Biosensor architecture for cADDis cAMP sensor. The sensor comprises two components - a detector that binds the signaling molecule, and a fluorescent protein that reports when the signaling molecule binds the detector. In this case, the detector is EPAC2, a component of the cAMP signaling cascade. A green fluorescent protein (mNeon Green) is positioned between the signaling and catalytic domains of EPAC2. When cAMP binds, there is a global conformational rearrangement of the two domains and this results in a change in the conformation of the fluorescent protein. This changes the optical properties, in this case a change of the fluorescence intensity, i.e. the amount of light emitted. Thus, the amount of cAMP can be detected by the change of fluorescence intensity, which can be measured in a plate reader or fluorescence imaging system.

the cyan protein is not, so the ratio of fluorescence becomes a measurement of the chloride concentration (44). The Fucci biosensor beautifully reports the cell cycle by fusing different degradation signals to green and red proteins (45), and the unfolded protein response can be detected through color changes produced by mRNA splicing (46). The beauty of two color sensors, whether they work through changes in FRET, or simply through environmental sensitivity, is that the ratio of the two signals can be used to adjust for cell volume changes or differences in expression. The cost, however, of using two colors is that the absorption and emission bands of fluorescent proteins are quite broad, so using two different colors typically consumes much of the visible spectrum, making multiplex recordings with multiple sensors quite difficult.

BRET Sensors

Bioluminescent resonance energy transfer (BRET) biosensors have been introduced for quantifying GPCR signaling, including G-protein activation, arrestin recruitment and second messenger production (see for example refs (11,12)). GPCR signal transduction involves intermolecular interaction between signaling molecule proteins and BRET provides an ideal means to detect intermolecular interaction. One of the two interacting proteins is tagged with a luminescent protein (the donor) and the other tagged with a fluorescent protein (the acceptor). When the two proteins are in close enough proximity, the energy transfer between the donor and acceptor can be detected (8).

Single Fluorescent Protein, Intensiometric Sensors

Fusions to the original N- or C-termini of the fluorescent protein. The fluorescent proteins in use today are all barrel-shaped protein structures that are remarkably inert. The sequences, photophysical properties, and protein structures are easily viewed and analyzed in the fpbase database (47) (www.fpbase.org). Briefly, eleven staves of beta sheet create a warped barrel that contains the fluorophore. The N- and C- termini of the protein are the same end of the barrel, and these can readily be fused to other proteins. While these sorts of fusions have been used to "tag" proteins, they don't typically produce biosensors in the sense that the fusion partner doesn't produce a change in the photophysical properties of the fluorophore. There are two exceptions to this general rule. First, the dimeric and tetrameric forms of fluorescent proteins have larger cross sections and quantum yields than the monomeric forms. The dimerization-dependent fluorescent proteins take advantage of this phenomenon, and have been used to create a variety of sensors (48). The voltage sensors are another example of how fusing a single fluorescent protein to the end of another protein can create a sensor. In a seminal paper, Siegel and Isacoff showed that that a single fluorescent protein can be positioned in the C-terminus of a voltage-gated ion channel subunit to create a sensor that changes fluorescence intensity as transmembrane voltage was altered (49). This led to numerous voltage sensors, reviewed in ref. (50), that iteratively improved performance.

Fusions to circularly permuted fluorescent proteins. The interface of a dimer of fluorescent proteins is largely centered around the seventh barrel stave of the protein barrel. This stave is positioned close to one end of the fluorophore within the barrel, and it has important effects on the fluorophore. Baird and colleagues showed that protein domains can be successfully inserted into the seventh stave of the fluorescent protein barrel structure, close the fluorophore. The original N- and C-termini of the protein are connected and new N- and C-termini engineered into the seventh stave to create a circularly permuted fluorescent protein (51). Many different protein domains have been fused to the new termini of circularly permuted fluorescent proteins such that changes in the conformation of these proteins produce changes in fluorescence. A good example of this is the GCaMP6 Ca^{2+} sensor, which is widely used in neuroscience (52). In this case calmodulin is fused to one of the termini, and the M13 peptide is attached to the other. In the presence of Ca^{2+}, calmodulin binds to the M13 peptide and in some way influences the fluorescence intensity of the sensor. Recently, the photophysics of how this works has become clearer (53). In the case of GCaMP6, the cross section and quantum yield changes very little, but the concentration of the chromophore changes dramatically. The chromophore can exist in a protonated state where it absorbs light at 400 nm, or in an anionic state where it absorbs at 480 nm. The GCaMP6 sensor in the absence of Ca^{2+} is largely in the protonated state, so it doesn't absorb, or return fluorescence, when interrogated with 480 nm light. In the presence of Ca^{2+}, the chromophore is rapidly de-protonated and the concentration of anionic chromophore increases dramatically, producing a remarkable increase in 480 nm excited fluorescence. This increase is so large, and so rapid, that this remarkable biosensor has been used to image the activity of thousands of neurons in living brains at remarkable frame rates (54,55). The red fluorescent biosensors appear to work in much the same way (56). A significant advantage of this design is that in the absence of the second messenger, the chromophore resides in a different form that does not absorb the excitation light and does not photocycle or bleach.

Since the sensors constructed with circularly permuted fluorescent proteins work by shifting between the neutral and anionic states, it is also true that they can signal through either a decrease in fluorescence or an increase. Using GCaMP6 as an example, the Ca^{2+} binding causes an increase in the 480 nm excited fluorescence as the chromophore pool shifts to the anionic state. At the same time, the 400 nm excited fluorescence decreases as the pool of protonated fluorophore vanishes. Now there are numerous examples of biosensors that signal through either an increase or decrease in fluorescence excited at a particular wavelength, so it is worth considering the merits of each. Upward-going fluorescent biosensors are particularly useful in applications where photobleaching is anticipated, for example high content imaging or confocal microscopy applications. Downward going sensors offer the experimentalist the opportunity to adjust the acquisition parameters (gain, exposure time, slit width etc.) to place the baseline fluorescence in the most sensitive, or most linear, range of the instrument before beginning an experiment.

Choosing the Right Biosensor, Signal to Noise Considerations

Fluorescent biosensors can measure the amount of second messenger present in a living cell at any moment in real time. Ideally, the sensor fluorescence is bright, and the change in fluorescence intensity produces a large signal to noise ratio (SNR). There are different ways to calculate the SNR. Here we take a simple approach and define the signal as the amplitude of fluorescence change upon maximal stimulation, and the noise as the standard deviation of the baseline fluorescence before addition of a drug. With the latest generation of bright fluorescent proteins (57), and the large change in fluorescence produced in circularly permuted versions of these proteins, a SNR close to 80 can be observed on standard fluorescent plate readers. Many biosensors, however, are barely detectable on fluorescence plate readers. These can be detected on more sensitive microscopes, and produce SNR values of ~ 8 (58). In choosing a biosensor assay, SNR is one of the most important considerations, and there are several other important considerations that we will discuss in this Chapter.

Sources of Noise

In setting up an assay, there are several sources of noise. First, there are many ways of introducing genetically encoded, fluorescent biosensors. Transient transfection is often used, but this introduces a great deal of cell to cell variability in terms of expression. Cells overexpressing the sensor often do not respond, but they contribute to the baseline fluorescence. Viral expression, or stable cell lines, reduce cell to cell variability, thereby reducing noise and improving assay reproducibility.

Beyond the cells, fluorescence detection typically involves either a photomultiplier tube or a CCD/CMOS camera. In the green fluorescent emission part of the spectrum, these detectors work well, but green auto-fluorescence in many formulations of cell media often diminishes the size of the signal and raises the noise. Automated plate washers that carefully replace the media with a non-fluorescent buffer like PBS are often important in reducing this sort of noise. Red fluorescent sensors are less prone to autofluorescence artifacts, but many PMTs are insensitive in the red, so it is important to match the choice of fluorescent protein with the sensitivity of the detector. Near infrared sensors are currently being developed that may circumvent the problems associated with auto fluorescent media. However, they are not yet mature enough for deployment on automated plate readers, and their emission wavelengths will pose new problems for the PMT detectors on many instruments.

Applying Compounds and Collecting Kinetic Data, How Often Should You Sample, and with What Instrument?

Ultimately one would like to acquire time course data as quickly as possible, to capture rapid changes in second messenger levels. In practice, there are experimental trade-offs to consider. The more you sample fluorescent cells, the more the fluorophores will photocycle and eventually bleach irreversibly. In the case of Ca^{2+}, PIP_2 and DAG signaling, the events occur in seconds, so applying compounds and collecting kinetic data needs to occur

in that time scale. The FLIPR (59) and FDSS (Hamamatsu Photonics) plate readers can simultaneously add 384 different compounds and record from all of the wells at the 1 - 4 second intervals necessary to capture the salient features of rapid signaling events. The very transient nature of Ca^{2+}, PIP_2 and DAG signaling place constraints on which equipment can deliver the necessary kinetic information. Cyclic AMP and arrestin signaling occur on slower time scales that are well within the capabilities of most automated plate readers.

Photobleaching

Fluorescent proteins undergo both reversible and irreversible photobleaching. Some of the proteins visit long lived "dark" states only to return to a fluorescent state later. Irreversible photobleaching occurs as well, which can decrease the sensitivity of the assay. Every time the fluorophore within a fluorescent protein is excited, there is some chance that it will be damaged. Photobleaching can be minimized by: 1) expressing a great deal of the sensor, 2) using as little excitation light as possible, 3) collecting as much of the fluorescent emission as possible with optimized emission filters, and 4) using very sensitive detectors. Very bright, photo-stable fluorescent proteins used in the biosensor examples here, produce large signals and minimize bleaching. However, when they are used in the context of insensitive instruments, or very low expression levels, photobleaching will be significant.

Photobleaching is a particular concern when analyzing the time course of the response because it affects the curve shape of the time course. As described in Analyzing Signaling Time Course Data, the shape of the time course can be diagnostic of regulation of signaling mechanisms. If the shape is also affected by photobleaching this will cloud the interpretation of the data. Fortunately, photobleaching can be detected, if there is a sufficient baseline signal of the sensor (i.e. fluorescent signal in the absence of stimulating GPCR ligand). The approach is to run a vehicle control. If the response to the vehicle control falls over time, this indicates photobleaching. While photobleaching is best avoided, it can be accommodated within the kinetic data analysis – an example is shown in Example 2: Ca^{2+} Mobilization via the AT_1 Receptor.

Sample protocols

Numerous biosensors have been developed by many laboratories for measuring GPCR signaling (13,38). In this section we exemplify the measurement of GPCR second messengers using fluorescent biosensors developed and/or distributed by Montana Molecular. These sensors were developed to be straightforward to use by those investigators interested in GPCR signaling but not necessarily well-versed in optical biotechnologies. The sensors are bright, enabling detection using standard plate readers. The sensors are delivered using the viral vector Bacmam, which enables highly reproducible and robust expression in numerous cell types. The protocol described here is generally applicable to fluorescent biosensors developed by other laboratories, although the technical details specific to each sensor will vary. A generalized protocol is shown in Figure 3 and video presentations are at https://youtu.be/S-oHwesM37U and https://youtu.be/lTcOdi9wL9E . The protocols below are designed for rapidly-dividing, immortalized cell lines and work especially well in HEK293 cells. However these sensors are often used in primary cultures and iPSC-derived cell lines. The protocols described here are for 96-well assays and are scalable for 384-well format. The sensors are also compatible with detection by fluorescence microscopy and other imaging systems.

One common source of variability in live cell biosensor assays is gene expression. One solution to this issue is the BacMam viral expression system, which produces more consistent expression than a plasmid vector and is a good tool for delivering the biosensor to a wide variety of difficult to transfect cell types. The amount of BacMam used is determined from a preliminary titration experiment as described in Timeframe of Response Measurement. A troubleshooting guide is provided in the supplementary file Troubleshooting guide.

Materials

- Biosensor in BacMam vector (specific sensor for each second messenger specified in Table 1)

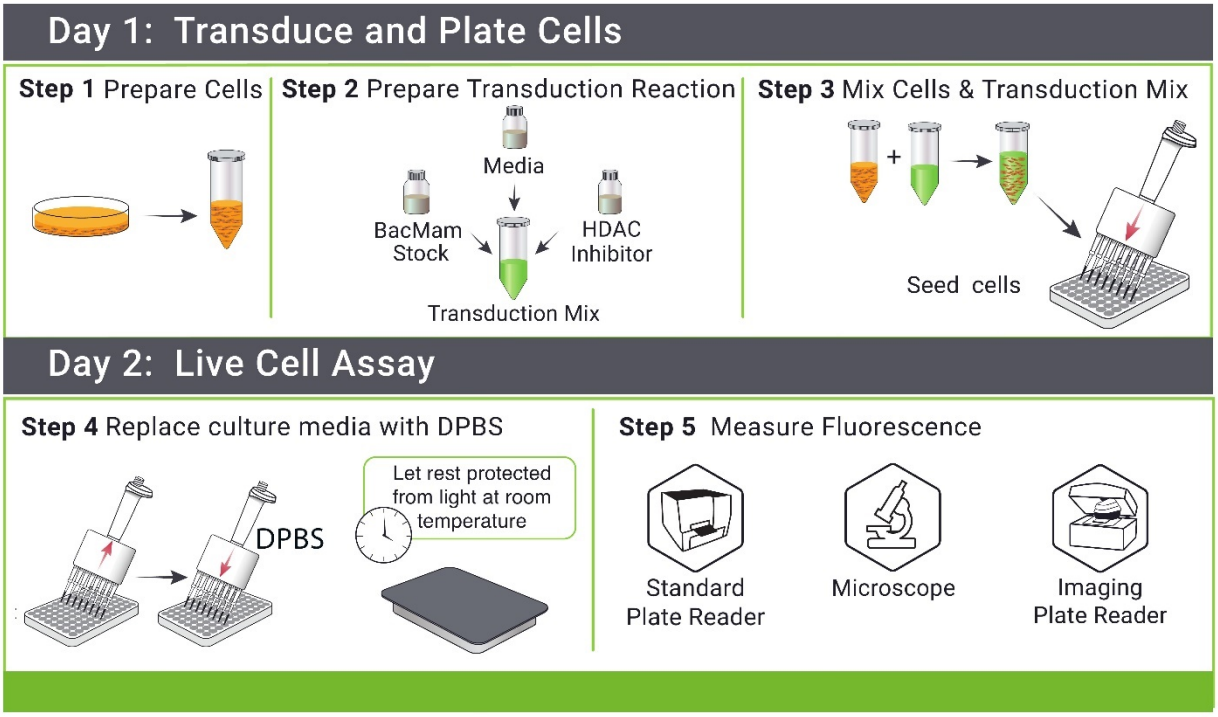

Figure 3. Workflow for GPCR biosensor assay employing sensors in the BacMam expression system. See also videos at https://youtu.be/S-oHwesM37U and https://youtu.be/lTcOdi9wL9E

- HEK293T cells
- Sodium butyrate (an HDAC inhibitor) (500 mM stock solution)
- Cell culture medium: Eagle's minimum essential media (EMEM) supplemented with 10% fetal bovine serum (FBS) and penicillin-streptomycin
- Assay buffer: Dulbecco's phosphate buffered saline (DPBS) supplemented with Ca^{2+} (0.9 mM) and Mg^{2+} (0.5 mM). (It is very important that the assay buffer is not autofluorescent, which precludes the use of colored tissue culture media which contain indicator dyes.)
- Microtiter tissue culture plate: Black, clear-bottom, with low autofluorescence, e.g. Greiner Cell Coat (#655946)

Table 1. Fluorescent biosensors for GPCR signaling employed in this chapter

Signal transduction molecule	Sensor name	Timeframe of signal	Protocol link
cAMP	Green Down cADDis	Usually rises to plateau. Sometimes peaks then plateaus. Duration varies, between 10 min and 60 min. See Figure 4.	www.montanamolecular.com/live-cell-camp-assay-caddis/green-caddis-camp-protocol/
cAMP	Green Up cADDis		
cAMP	Red Up cADDis		www.montanamolecular.com/live-cell-camp-assay-caddis/red-caddis-camp-protocol/

Table 1. continued from previous page.

Signal transduction molecule	Sensor name	Timeframe of signal	Protocol link
Diacylglycerol	Green Down DAG	Peaks then declines to zero or a lower plateau. Typical duration of 2-5 min. See Figures 6C & 11.	www.montanamolecular.com/dag-assay-kit/green-dag-protocol/
Diacylglycerol	Green Up DAG		
Diacylglycerol	Red Down DAG		www.montanamolecular.com/dag-assay-kit/red-dag-protocol/
Diacylglycerol	Red Up DAG		
Phosphatidylinositol 4,5-bisphosphate	Green PIP_2	Peaks then declines to zero or a lower plateau. Typical duration of 2-5 min. See Figure 6B.	www.montanamolecular.com/pip2-assay-kit/green-pip2-protocol/
Phosphatidylinositol 4,5-bisphosphate	Red PIP_2		www.montanamolecular.com/pip2-assay-kit/red-pip2-protocol/
Ca^{2+}	Green GECO	Peaks then declines to zero or a lower plateau. Typical duration of 2-5 min. See Figures 6D & 12.	www.montanamolecular.com/calcium-assay-kit-geco/green-geco-ca2-protocol/
Ca^{2+}	Red GECO		www.montanamolecular.com/calcium-assay-kit-geco/red-geco-ca2-protocol/

Plate Reader

Examples of automated fluorescence plate readers that are ideal for detecting the fluorescent biosensors discussed here include the Synergy MX and Cytation readers from BioTek Instruments (Winooski, VT); CLARIOStar from BMG Labtech (Cary, NC); Enspire from PerkinElmer (Waltham, MA); FDSS from Hamamatsu Photonics (Bridgewater Township, NJ); and Flexstation and FLIPR from Molecular Devices (San Jose, CA).

The green fluorescent sensors are best excited with light between 480 - 510 nm, and most of the emission occurs between 515 - 550 nm. The red fluorescent sensors are best excited at 560 nm (550 - 575) and the emission is captured with either 590 nm long pass filters, or very wide band pass emission filters (590 - 660).

Cell Culture and Viral Transduction

The transduction protocol below is for HEK293 cells. It can be modified for CHO cells (in which viral transduction efficiency is often lower) and a protocol is provided in the supplementary file CHO cell transduction.

1. Detach cells using standard trypsinization protocol. Re-suspend cells in cell culture medium and determine cell count.
2. Prepare a dilution of cells at your desired concentration. 100 µl of this cell re-suspension will be required for a single well in a 96-well plate, so prepare enough of the dilution to seed the desired number of wells in the plate. A typical cell number is 50,000 cells per well.
3. Prepare viral transduction reaction. Prepare the transduction solution by mixing the appropriate volume of the sensor BacMam stock (as determined from the titration experiment, see Box 1) with 0.6 µl of the sodium butyrate 500 mM stock solution and add cell culture medium for a total volume of 50 µl per well. Mix gently.
4. Mix the cells from Step 2 with the transduction mix from Step 3 in a 2:1 ratio, preparing sufficient volume for all the wells of the assay and the dead volume. Mix gently, then dispense 150 µl into the wells of the 96-well plate.